A STUDY OF THE BEHAVIOUR OF PARTIALLY PRESTRESSED BRICKWORK BEAMS

Peter John Walker, B. Sc.

A thesis submitted for the Degree

of Doctor of Philosophy

Department of Civil Engineering and Building Science,

The University of Edinburgh

September, 1987

To my mother and the memory of my father.

The Trowel

In a dream I stood on a building site. I was
A bricklayer. In my hand
I held a trowel. But when I bent down
For mortar, a shot rang out
That tore half the iron
Off my trowel.

B Brecht, 1953-1956

Declaration

This thesis is the result of research work undertaken in the Department of Civil Engineering and Building Science, University of Edinburgh, for the Degree of Doctor of Philosophy.

I declare that the work in this thesis has been, unless otherwise stated, carried out by myself under the supervision of Dr. B. P. Sinha.

Edinburgh, September 1987

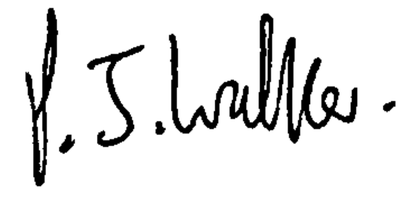

P. J. Walker

ACKNOWLEDGEMENTS

I should like to express my gratitude for the assistance given by the following people in the undertaking of this project.

To Dr B. P. Sinha, my supervisor, for his advice and assistance, to the departmental technicians especially Mr. N. Erskine and Mr. J. Hutchinson, and finally to Mrs S. M. Hartley for the typing of this thesis. I should also like to thank all of my friends for their encouragement, but especially Bob, Dave, Ian, Julie, Lorna, Marion, Mark, Pam and Sandra.

ABSTRACT

The thesis summarises the test results of 41 full-scale partially prestressed brickwork beams. These beams were tested to study the effect of:

(i) % area of steel

(ii) prestressing force

(iii) partial prestressing ratio

(iv) cover to non-tensioned steel

(v) brick strength

(vi) mortar strength or grade

upon the ultimate moment, deflection and cracking behaviour of partially prestressed brickwork beams.

The properties of the materials to be used in the theoretical analysis were obtained from experimental tests. The stress/strain relationship and the ultimate compressive strength of brickwork was obtained from a large number of tests carried out on both axially and eccentrically loaded prisms.

An interactive programme for use on a micro-computer was developed in conjunction with the experimental study. The programme predicts the ultimate moment, moment-curvature, deflection and crack widths of reinforced, fully and partially prestressed brickwork and concrete beams utilising the non-linear material characteristics. The programme also makes allowance for presence of a concrete cavity, composite section, and the tension-stiffening effect of the brickwork and concrete after cracking. The behaviour of the beams predicted by the analysis was compared with the experimental results.

The ultimate moment and deflection of the test beams were also compared with recommendations of the current limit state design code of practice for reinforced and prestressed masonry, BS 5628, Part 2.

C O N T E N T S

NOTATION

a	shear span
a_0	sum of perimeters of reinforcement
A	cross-sectional area of beam
A_e	effective area in tension
A_{ps}	area of tensioned reinforcement
A_s	area of non-tensioned reinforcement
A_{se}	effective area of tensile reinforcement
A_t	cross-sectional area of transformed section
b	breadth of section
b_c	breadth of concrete cavity
b_j	distance between vertical joints
c	cover to reinforcement
C	compressive force in section
C_0, C_1, C_2	tension-stiffening factors
d	effective depth of tensile reinforcement
d_{cr}	depth to level of cracking
d_e	effective depth of equivalant area of tensioned reinforcement
d_{ps}	effective depth of tensioned reinforcement
d_s	effective depth of non-tensioned reinforcement
e	eccentricity
E	modulus of elasticity
E'_c	initial modulus of elasticity of concrete
E_m	modulus of elasticity of brickwork
E'_m	initial modulus of elasticity of brickwork
E_0	modulus of elasticity of concrete
E_s	modulus of elasticity of steel
f	compressive stress in brickwork/concrete

f_{ct}	fictitious tensile stress
f_{cu}	compressive cube strength of concrete
f_k	characteristic compressive strength of masonry
f_m	average compressive strength of brickwork
f_{mt}	mean tensile stress in brickwork
f_{psy}	proof stress of tensioned reinforcement
f_{psu}	stress in tensioned reinforcement at ultimate
f_r	modulus of rupture of section
f_s	tensile stress in non-tensioned reinforcement at crack
f_{se}	tensile stress in equivalent area of tensioned reinforcement at crack
f'_{se}	stress in equivalent area of tensioned reinforcement away from crack
f_{scr}	stress in steel at crack at cracking moment
f_{secr}	stress in equivalent area of tensioned reinforcement at crack at cracking moment
f_{su}	stress in non-tensioned reinforcement at ultimate
f_{sy}	proof stress of non-tensioned reinforcement
$F_c(\varepsilon)$	stress/strain relationship of concrete
$F_m(\varepsilon)$	stress/strain relationship of brickwork
$F_{ps}(\varepsilon_{ps})$	stress/strain relationship of tensioned reinforcement
$F_s(\varepsilon_s)$	stress/strain relationship of non-tensioned reinforcement
h	total depth of section
h_c	depth to concrete cavity
h_{cr}	crack height
h_0	initial crack height
j_1, j_2, j_3	leverarm factors
K	tension-stiffening factor
K_1	coefficient for cracking
ℓ	span

ℓ_a	leverarm
m	modular ratio
M	moment
M_{cr}	cracking moment
M_u	ultimate moment
$(M_u)_p$	ultimate resisting moment due to tensioned steel
$(M_u)_{p+s}$	ultimate resisting moment due to total tensile steel
n	neutral axis depth
n_r	centroid of uncracked transformed secion
N_j	number of joints
P	prestressing force
P_e	ultimate load of eccentrically loaded brickwork
r_t	$\varepsilon_1'/\varepsilon_2'$
S_m	mean crack spacing
S_0	minimum crack spacing
t	thickness
T	tensile force
T_m	tensile force in brickwork
T_{ps}	tensile force in tensioned reinforcement
T_s	tensile force in non-tensioned reinforcement
V	shear force at ultimate
w, w_{av}	average crack width
w_{max}	maximum crack width
X_1, X_2, X_3	stress/strain coefficients
Z, Z_b, Z_t	section modulus
ε	strain in brickwork/concrete
ε_1 ε_2	strain in top and bottom fibre
$\varepsilon_{a1}, \varepsilon_{a2}$	applied strain in top and bottom fibre

ε_{cr}	strain to cause cracking
ε_{cu}	ultimate compressive strain of concrete
ε_{m}	ultimate compressive strain of brickwork
ε_{me}	ultimate compressive strain of eccentrically loaded brickwork
$\varepsilon_{p1}, \varepsilon_{p2}$	prestress strains
ε_{pe}	strain due to prestressing force in equivalent area of tensioned reinforcement
ε_{ps}	total strain in tensioned reinforcement
ε_{psa}	strain in tensioned reinforcement due to applied loading
ε_{psb}	strain due to precompression in brickwork at level of tendon
ε_{psp}	strain in tensioned reinforcement due to prestressing force
ε_{psy}	strain in tensioned reinforcement at proof stress
ε_{psu}	strain in tensioned reinforcement at ultimate
ε_{r}	ultimate tensile strain of brickwork
ε_{s}	total strain in non-tensioned reinforcement
ε_{sa}	strain in non-tensioned reinforcement due to applied loading
ε_{sb}	strain due to precompression in brickwork at level of non-tensioned reinforcement
ε_{sea}	strain in equivalent area of tensioned reinforcement due to applied loading at crack
ε'_{sea}	strain in equivalent area of tensioned reinforcement due to applied loading away from a crack
ε_{seam}	average additional strain in equivalent area of tensioned steel
ε_{sm}	average additional strain in non-tensioned reinforcement
ε_{smb}	average strain after cracking at any level of beam
ε_{sp}	strain in non-tensioned steel due to prestressing force
ε_{su}	strain in non-tensioned steel at ultimate
ε_{sy}	strain in non-tensioned steel at proof stress

$\lambda_1, \lambda_2, \lambda_3$	stress block factors
ρ, ρ_s	percentage of reinforcement
ρ_{bd}	percentage of reinforcement for balanced section
σ_1^1 σ_2^1	stresses in top and bottom fibres due to prestressing based on elastic stress distribution
σ_1, σ_2	stresses in top and bottom fibres due to prestressing
τ_b	bond stress
υ_u	ultimate shear stress
ϕ	curvature of beam
ϕ_{av}	average curvature of beam
ϕ_p	curvature due to prestress

CHAPTER 1

INTRODUCTION

1.1 HISTORICAL DEVELOPMENT

1.1.1 Plain Masonry

Humankinds use of masonry has been traced back 20 000 years[1]. One of the most vivid examples of the early use of masonry is Stonehenge in Wiltshire, England. The ancient civilisations of Egypt and Rome are recognised as being the first to widely utilise masonry as a building material, many fine examples of these early structures are still in existence; for example the Pyramid of Cheops, height 145 m, was built by the Egyptians[2] using stone blocks weighing up to 2 tonnes each. The standard of the workmanship was such that the joints were no more than 1 mm thick, a remarkable achievement even by present day standards. The manufacture of the first 'readily handled' sun-baked clay brick is credited to the Sumerians[1] some 5500 years ago.

Because of its very low tensile strength the use of plain masonry throughout history has been restricted to compression elements such as walls, columns and arches. Lateral stability against wind loading has been achieved through the massive self-weight of the load-bearing walls. This form of structure culminated in the construction of the Monadonack[1] building in Chicago in 1893; in modern terms the 16 storey building represented a grossly inefficient use of both space and materials. For example the external walls of the base of the building were 1.6 m thick so as to provide sufficient self-weight for lateral stability. The rising costs of natural resources prompted the construction industry to reject this form of structure in the late nineteenth and early

twentieth centuries, giving preference to steel and reinforced concrete framed buildings.

The post-war construction boom led to a renewed interest in the structural use of masonry[1]. Between 1951 and 1957 there was a departure from traditional forms of construction, developed by Swiss engineers, in which 18 storey buildings were built using brickwork bearing walls only 150 mm thick. Lateral stability was provided by a re-orientation of the brickwork panels as shear walls therefore eliminating the need for massive 'gravity' or framed type construction.

Brickwork is gradually being accepted as a structural material comparable with concrete. This is borne out by the publication of a code of practice for the structural use of unreinforced masonry[3]. The renewed interest in brickwork as a structural material has recently led research to consider the possibilities of both reinforced and prestressed masonry.

1.1.2 Reinforced brickwork

The development of reinforced brickwork is attributed to Marc Brunel[2,4]. In 1825, as part of the Thames river tunnel project, Brunel supervised the construction of two 15.2 m diameter brickwork shafts, 21.3 m high. They were reinforced both vertically and circumferentially with iron bolts and hoops. Although considerable settlement occurred later no cracks developed in the brickwork. Subsequently other engineers conducted tests on reinforced masonry. In 1837, Pasley[2] concluded that the addition

of tensile reinforcement significantly increased the flexural strength of brickwork.

Brebner's[4] work published in 1923 is seen as the beginning of modern reinforced brickwork technology. His report described results of a large number of tests on reinforced brickwork beams, columns and slabs. As a consequence reinforced brickwork was used extensively in countries subjected to earthquakes such as India and the USA in the 1920's and 30's. Reinforced brickwork still remains more popular in these countries than in Britain and the rest of Europe.

As an alternative to reinforced concrete, reinforced brickwork offers a number of advantages. Brickwork is a low energy input material which generally does not require items of sophisticated equipment. During the construction process formwork is normally not necessary, therefore providing a saving in resources. The amount of cement used is greatly reduced since bricks provide the greatest proportion of the total volume. Brickwork is aesthetically more pleasing than concrete and unlike reinforced concrete it does not stain with time. Recent cost comparisons[5] between reinforced concrete and brickwork retaining walls have shown that reinforced brickwork may prove to be considerably cheaper.

Like reinforced concrete reinforced brickwork also suffers from a number of disadvantages. As the tensile strength of brickwork is particularly low reinforced brickwork flexural members are generally cracked under the action of the service load. To provide adequate crack control the stress in the steel has to remain low, an

inefficient use of high grade steel reinforcement. A number of recent investigations[6-8] have shown that failure of reinforced brickwork beams generally to be in shear, consequently both the brickwork and steel are not fully utilised. Attempting to overcome the problem of premature shear failure has led researchers[6,9] to investigate the possibilities of prestressing the brickwork.

1.1.3 Prestressed brickwork

The techniques of prestressing are well established and have been successfully applied to concrete[10,11] for the last sixty years. The methods of prestressing are also equally applicable to brickwork and a number of investigations[9,12-14] have recently been conducted to establish the behaviour of post-tensioned brickwork beams. Prestressing offers a number of advantages, for example the application of a precompression to the brickwork beam allows the section to remain uncracked at service loading. Prestressing has also been proven to increase the effective shear resistance of the cross-section[9] and hence overcoming the problem of premature shear failure associated with reinforced brickwork beams.

In 1985 a limit state design code of practice for reinforced and prestressed masonry[15] was published. The code, BS 5628 Part 2, makes no allowance for cracking of the prestressed section and so implies that sufficient precompression should be applied to ensure the prestressed brickwork beam remains uncracked throughout its lifetime. Consequently, the introduction of a high level of precompression to the beam section may lead to a problem of excessive camber. From previous tests it has been noticed that during

application of high levels of prestress excessive tensile stresses may develop in the anchorage zone causing cracking[9]. The technique of partial prestressing, as applied to concrete, may overcome these problems.

1.2 PARTIAL PRESTRESSING

The term 'partial prestressing'[16] is used to define a beam section in which application of the prestress force is limited to counteract only part of the tensile stress developed at the working load. This can be done either by:

(1) reducing the level of initial prestress applied to all of the tensile reinforcement,

or (2) prestressing part of the tensile reinforcement to a maximum allowable stress and leaving the rest without prestress.

The first option may lead to an inefficient use of the expensive prestressing tendon and henceforth partial prestressing in this study refers to the later definition. Partial prestressing offers a number of advantages over the fully prestressed brickwork beam. The prestress force in a partially prestressed brickwork beam is less than for the equivalent fully prestressed brickwork beam and therefore problems of camber and excessive tensile stresses in the anchorage zone at transfer are avoided.

To avoid introducing tensile stresses into the brickwork beam section during the application of the prestress the prestressing steel must be located within the 'kern' limit. However, since part of the tensile reinforcement in the partially prestressed brickwork beam is non-tensioned it may be placed closer to the soffit of the section, and consequently improving crack width control compared to the fully prestressed brickwork beam.

No research work has been conducted to study the behaviour of partially prestressed brickwork beam and so this experimental study was undertaken.

CHAPTER 2

LITERATURE REVIEW

2.1 INTRODUCTION

As mentioned earlier, prior to this work no research had been conducted into the area of partially prestressed brickwork beams and so the review of literature covers the wider field of fully prestressed masonry. Recently a number of post-tensioned brickwork structures have been constructed, some of these projects are also briefly discussed.

2.2 RESEARCH WORK

Experimentally, the behaviour of prestressed masonry was first considered by Thomas[17] in 1963. He conducted tests on two post-tensioned brickwork beams constructed from perforated bricks using the cross-sections shown in figure 2.2.1. The tensile reinforcement in the first beam was passed through the bottom perforation of the bricks, tensioned to 67 kN and left unbonded. During the first loading cycle the beam, simply supported over a span of 2515 mm, sustained a central point load of 18.0 kN with little adverse affect and so the load was removed and the prestressing force increased to 107 kN. Upon re-application of the load failure occurred at only 17.2 kN, this was ascribed by Thomas to principal tensile stresses at the end of the beam exceeding the tensile strength of the bricks. Recent tests on prestressed concrete beams[18] have indicated that the transverse stresses in the anchorage zone increase with increasing shear force and so the explanation proposed would seem reasonable. Failure of the second beam, cross-section figure 2.2.1(b), occurred during the prestressing operation resulting from cracking along the mortar joints due to

BEAM SECTION OF K.THOMAS[17]

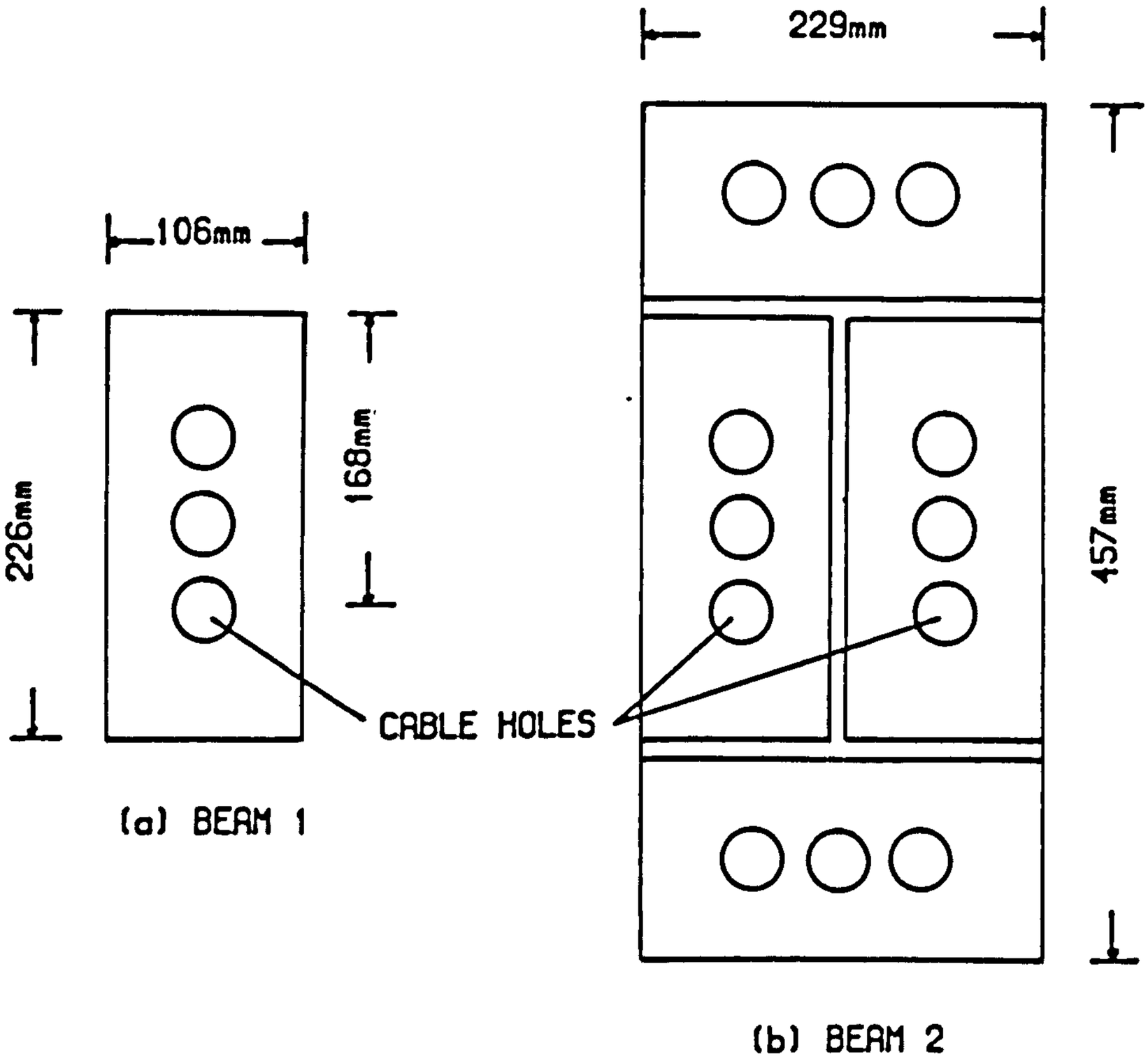

(a) BEAM 1

(b) BEAM 2

Figure 2.2.1

BEAM SECTION OF L.S.NG[17]

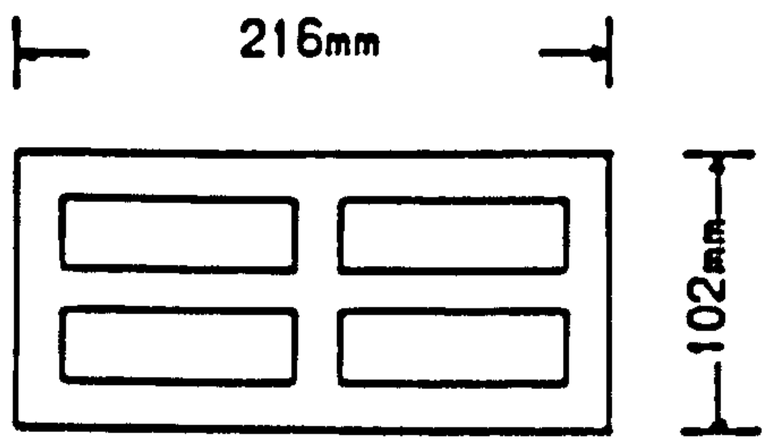

Figure 2.2.2

excessive tensile stresses developing behind the anchorage.

In 1965 Plowman[17] tested thirteen post-tensioned brickwork beams. The cross-section used was similar to figure 2.2.1(a) except that the prestressing reinforcement was placed within the lower 'kern' limit to avoid the introduction of tensile stresses into the section due to prestressing. Provision of the tendon within the 'kern' limit was made possible by using specially manufactured perforated bricks. The effects on the behaviour of the beams of varying brick strength, betwen 26.5 - 54.7 N/mm^2, and prestressing force, between 17.8 - 93.6 kN, were considered. Once prestressing was completed the tensile steel remained unbonded as grouting of the duct was not possible. The beams were tested simply supported, span 3048 mm, under central point loading. Eleven of the beams failed in flexure leading to crushing in the compression zone. The remaining beams failed during post-tensioning due to either failure of the anchorage plate or fracture of the tendon. Plowman calculated the factor of safety for each beam based on the load to cause decompression. The factor of safety for any beam, allowing for movement of the unbonded reinforcement, was not less than two.

The cross-sections adopted by both Thomas and Plowman introduced a number of limitations upon the design and construction of prestressed brickwork beams. Some difficulty was encountered during the construction process to ensure the perforations forming the duct for the reinforcement were perfectly aligned and free from mortar. Placing the tensile reinforcement in the perforations limited the amount and position of steel that was possible to introduce into the section. The amount of reinforcing bar or strand

was limited by the size of the perforations, the depth of the reinforcement was restricted by the position of the perforations relative to the section. It was also unlikely that non-tensioned steel could subsequently have been introduced to the section due to difficulty in grouting of the duct, since it was not possible to grout the duct there was little or no protection against corrosion of the steel. Finally, the manufacture of specialised masonry units to accommodate the reinforcement was likely to be an expensive solution.

In 1966 Ng[17] tested three post-tensioned masonry beams built using extruded clay bricks, section shown in figure 2.2.2. Epoxy resin was used, instead of a cement or lime mortar, to bond the blocks together in order to improve bond strength. This prevented the cracking problems encountered by earlier research[17] during transfer of prestress to the masonry. Two 5 mm diameter wires were placed in the perforations of each beam and tensioned to between 36 and 45 kN, the duct was grouted after prestressing. All three beams failed in flexure due to crushing of the masonry without sign of the tensile steel yielding. Based on the load to cause decompression of the prestress an average factor of safety of 3.5 was obtained. As a direct result of these preliminary tests a patent was taken out on a prestressed ceramic flooring system.

In 1970 Mehta and Fincher[19] reported on the testing of five pretensioned brick masonry beams. The bonding pattern, cross-section figure 2.2.3, and prestressing force were varied. 10 mm diameter seven wire strand was pretensioned in the cavity which was subsequently grouted, the prestressing force was approximately 187 kN in four of the beams and reduced to 94 kN in the remaining

TYPICAL SECTION OF MEHTA AND FINCHER[19]

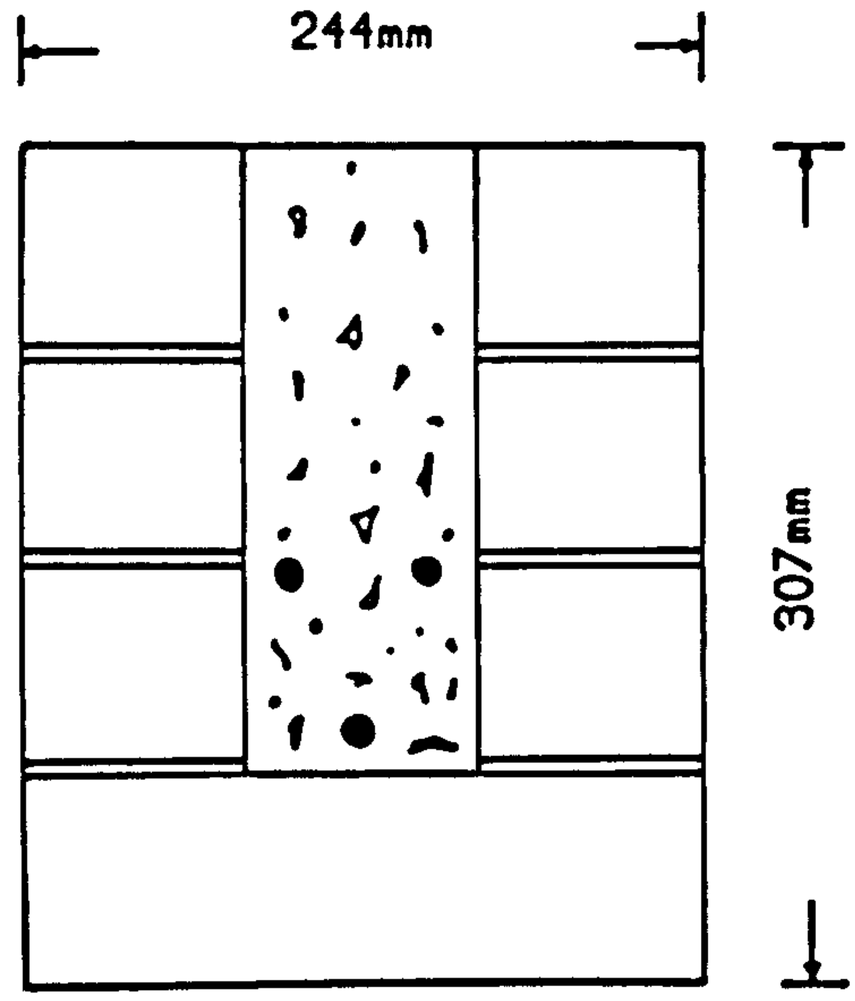

Figure 2.2.3

SECTION OF DIAPHRAGM WALL TESTED BY CURTIN AND PHIPPS[20]

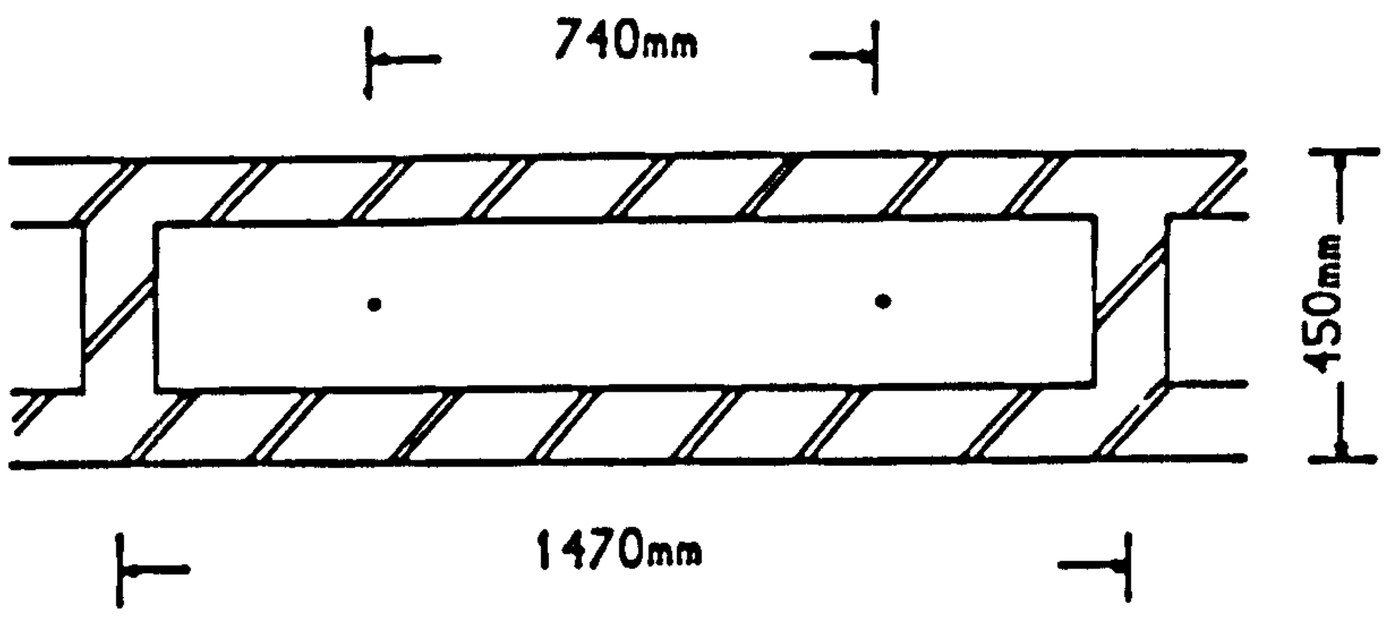

Figure 2.2.4

beam. The grout constituted at least 25% of the cross-sectional area, as a result the masonry was not used to its best advantage since only two thirds of the compression zone was brickwork.

All five beams failed in shear under a central point load, span 1830 mm. Mehta and Fincher did not comment on the effect of reducing the prestress upon the strength of the beams, but from tabulated results up to a 48% reduction in shear strength was observed for a 50% reduction in the prestressing force. Mehta and Fincher attempted to predict the deflection, shear strength and flexural strength of the beams. Deflection was calculated using a strength of materials approach, the elastic modulus for brickwork was derived from axially loaded brickwork prisms. The predicted values were between 1.46 and 2.36 times greater than the experimental results. In my opinion, although no explanation was offered, this discrepancy probably resulted from assuming the modulus of elasticity to be that derived from stack-bonded brickwork prisms which were not representative of the cross-section. Brickwork in the test beams was stressed in directions other than normal to the bed-joint, using results for stack-bonded prisms made no account for the orthotropic properties of masonry. It was also unlikely that the grout, forming 25% of the section, would have exhibited the same value for the modulus of elasticity as the brickwork. Using recommendations developed for prestressed concrete, Mehta and Fincher estimated the shear strength of the beams to within 20%. However, in three beams the experimental failure moment, corresponding to shear failure, was greater than the predicted ultimate flexural moment.

In 1982 Curtin and Phipps[20] reported on the construction

and testing of two prestressed brickwork diaphragm walls measuring 7.62 x 7.62 m, figure 2.2.4. The walls were built side by side onto a common concrete foundation into which the prestressing reinforcement, ten 40 mm Macalloy bars, was anchored. The walls, loaded laterally using air bags, were tied together at the top and so were assumed to act as propped cantilevers, however no attempt was made to verify this experimentally. At five different levels of precompression, ranging from 0 to 1.38 N/mm^2, lateral loading was applied to determine the influence of the prestressing force upon the flexural cracking load. As expected the cracking load was found to increase with the prestress. The cracking load was predicted with reasonable accuracy using a simple elastic analysis. Due to the scale of the walls, testing to collapse was considered too dangerous.

Consequently a number of investigations[12,21-23] have been conducted as a result of these tests in order to determine the ultimate moment of horizontal spanning beams using the diaphragm wall cross-section.

Williams and Phipps[12] tested six post-tensioned masonry box beams, figure 2.2.5. The beams were prestressed with one 40 mm diameter Macalloy bar passed through the cavity, the cavity was left ungrouted. In three beams cross-ribs were introduced to prevent movement relative to the section of the tensioned bar during loading. At three different levels of precompression ranging between 1.11 and 2.79 N/mm^2 two beams were tested, one with and one without the cross-ribs. Four brickwork prisms were also tested to ascertain the compressive strength of the section (h/t varying between 0.87 and 4.48). Five of the beams failed in flexure due to crushing of the brickwork in the compression zone, the sixth failed as a slender

BEAM SECTIONS OF WILLIAMS AND PHIPPS[12]

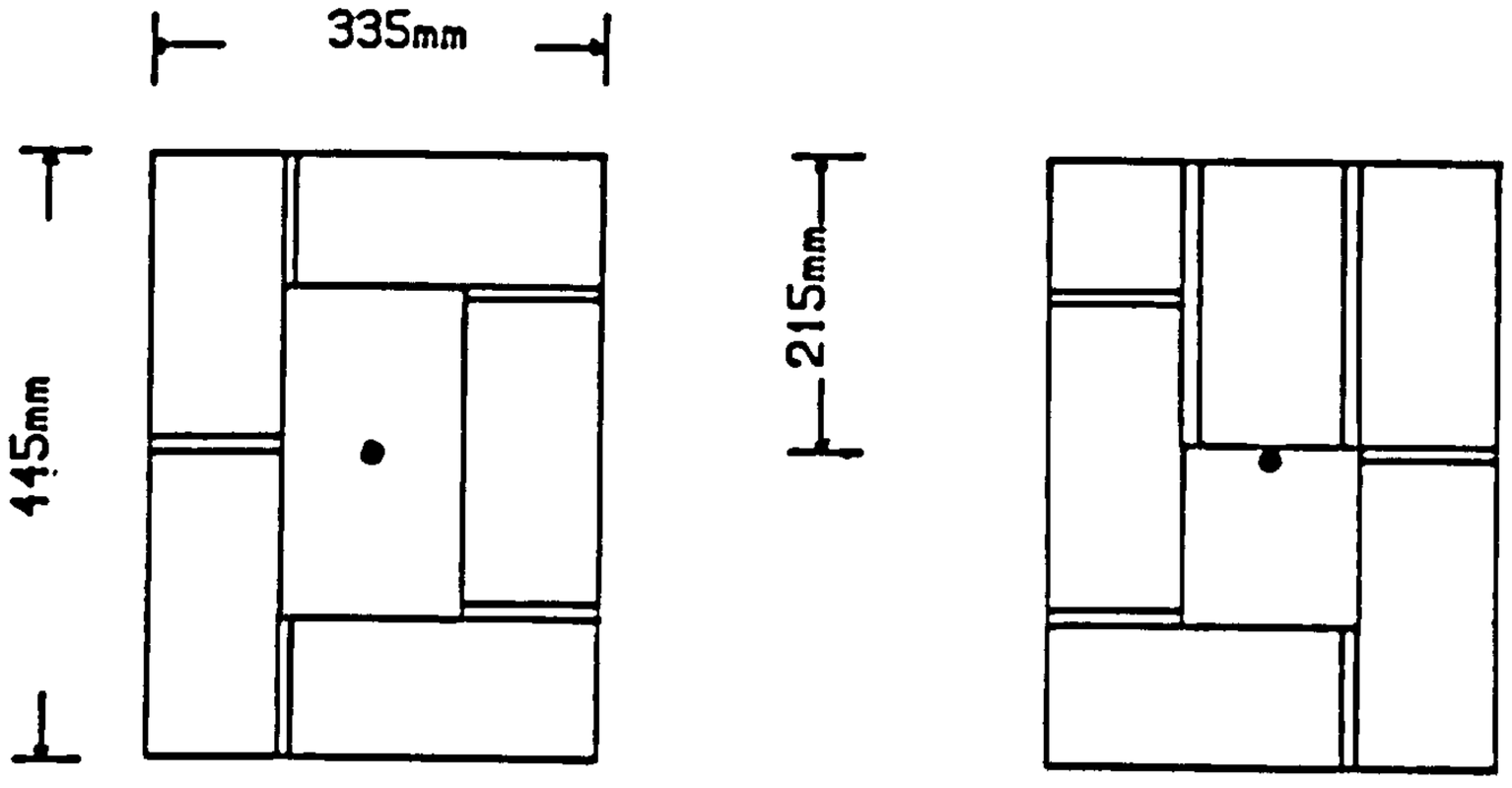

(a) WITHOUT CROSS-RIBS (b) WITH CROSS-RIBS

Figure 2.2.5

TYPICAL SECTION OF ROUMANI AND PHIPPS[21]

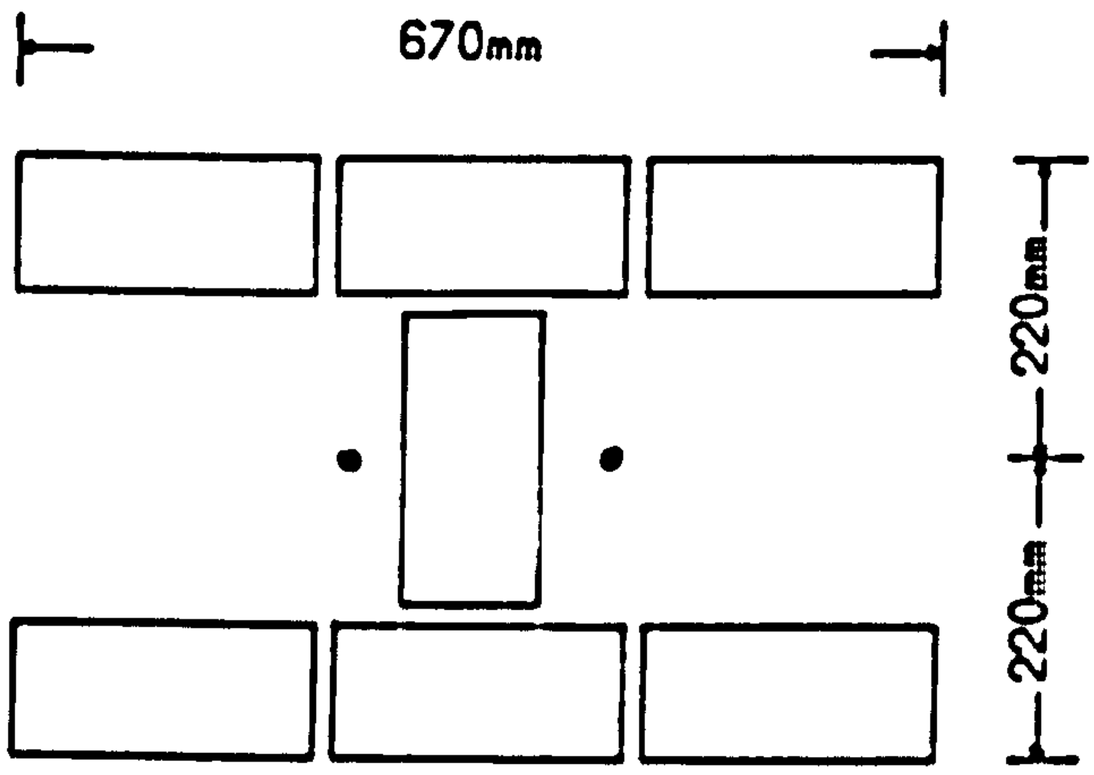

Figure 2.2.6

column resulting from the high level of prestress. The addition of cross-ribs increased the ultimate moment of the section by up to 300%.

A simple bending theory was developed by Williams and Phipps to predict the failure moment of the beams. The movement of the unrestrained tensioned steel was assumed to be equal to the deflection, but no attempt was made to verify this experimentally. Based upon the results of the six beams an empirical relationship between the steel stress and neutral axis depth at failure was derived, however, two of the six results indicated a significant variation with the average relationship. By considering the equilibrium of the tensile and compressive forces the neutral axis depth at failure was derived from the empirical relationship and hence the ultimate moment was calculated. There was reasonable agreement with experimental results.

Roumani and Phipps[21,22] in 1983 tested fifteen I and T section brickwork beams. The amount of precompression, a/d ratio, shape and depth were variables considered in their study of shear strength. A typical cross-section is shown in figure 2.2.6. All of the beams failed in shear, the results were used to derive an empirical relationship between the principal tensile strength of the brickwork and the a/d ratio. In 1984 Montague and Phipps[23] reported on the testing of twelve post-tensioned concrete blockwork box section beams in flexure, figure 2.2.7. The prestressing force provided by one 20 mm Macalloy bar was varied between 48 and 189 kN. The bonding pattern of the beams was also varied. The compressive strength of the masonry was determined from prism tests (h/t=1.5).

TYPICAL SECTION OF MONTAGUE AND PHIPSS[23]

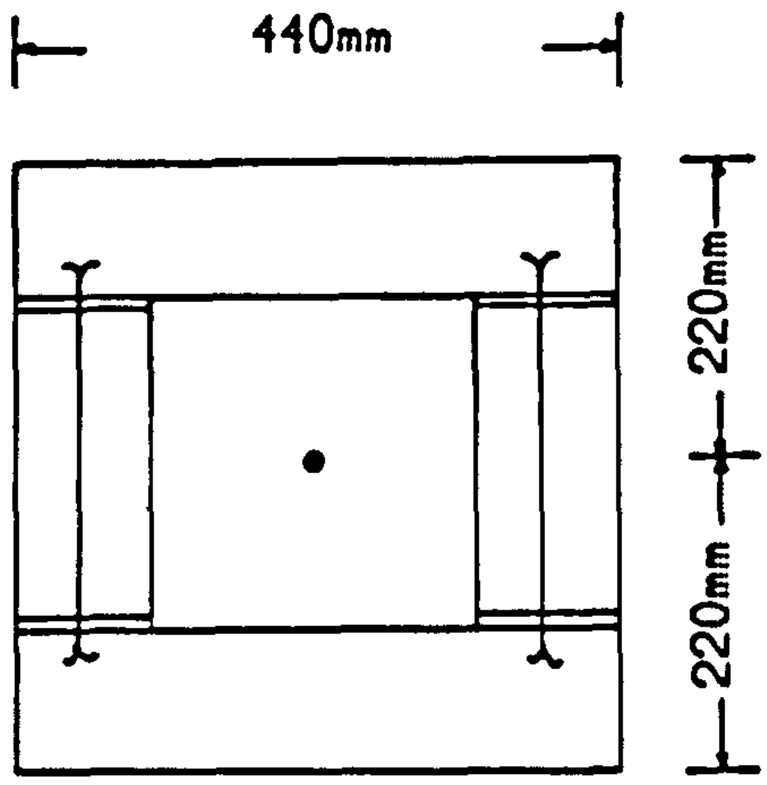

Figure 2.2.7

All beams failed in compression, that is the cross-section was over-reinforced. Ultimate moment was predicted to within on average 22%.

Robson et al[13,2] recently conducted a study into the behaviour of eighteen post-tensioned brickwork beams. The section used, figure 2.2.8, was post-tensioned after grouting of the cavity and so the tendons remained unbonded. This was an unnecessarily complicated construction procedure since provision was required for ducts for the steel involving three separate building operations. Three different percentages of steel and prestressing force were considered, six beams tested at each steel area at a/d ratios between 2.74 and 5.48. Five of the beams with the largest steel area failed due to crushing of the brickwork, an over-reinforced section, and the other failed in shear. All other beams with smaller steel area failed in tension, under-reinforced sections. Ten brickwork prisms (h/t=1.14), figure 2.2.9, were tested to determine the compressive strength and elastic properties of the masonry.

The experimental ultimate moments were compared with a theoretical method using the code[15] values for the compressive strength and stress block. The experimental values for the compressive strength of brickwork were also incorporated into the analysis. The best correlation with the experimental ultimate moments was achieved using the experimentally derived brickwork strength. However, in the case of the under-reinforced beams the predicted moments under-estimated the experimental values by as much as 23%, whereas the over-reinforced beams exhibited a much closer correlation. The brickwork prisms used, figure 2.2.9, represented

BEAM SECTION OF ROBSON ET AL[24]

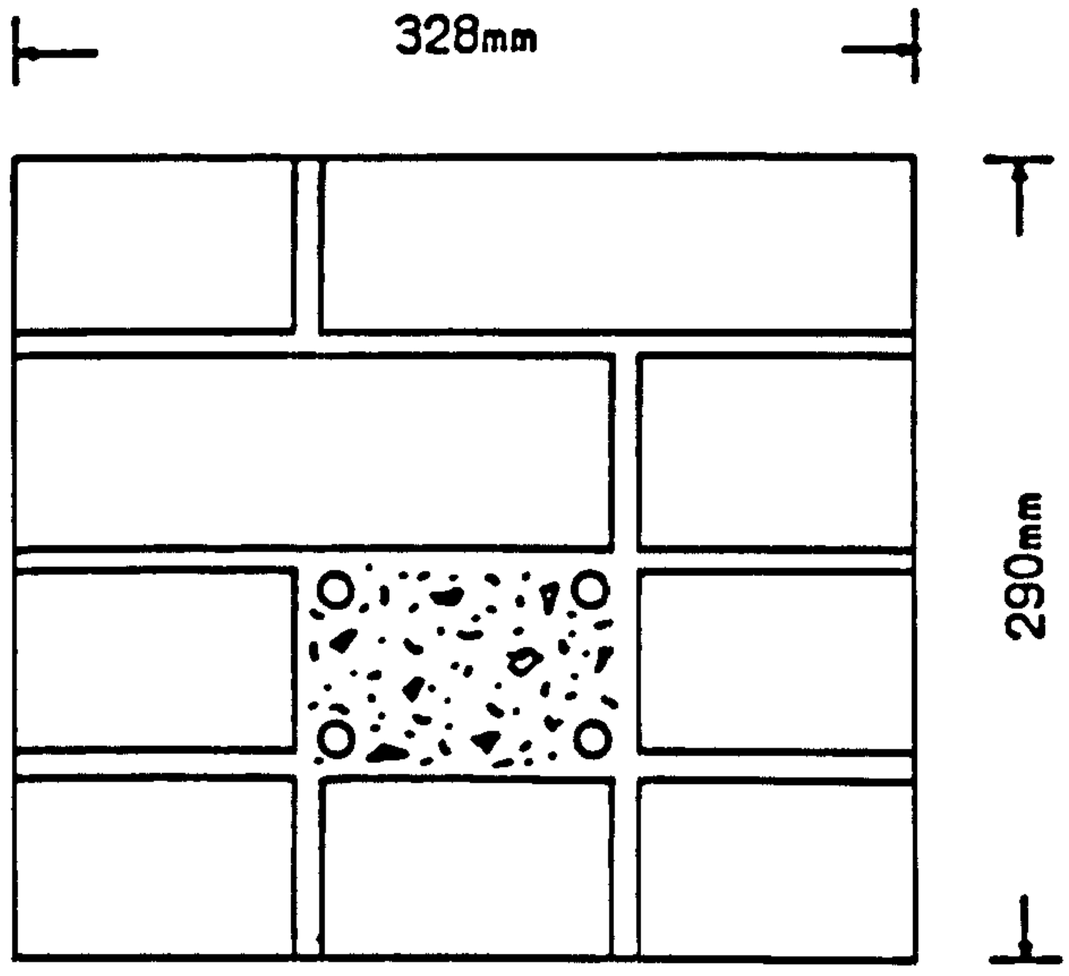

Figure 2.2.8

PRISMS OF ROBSON ET AL[24]

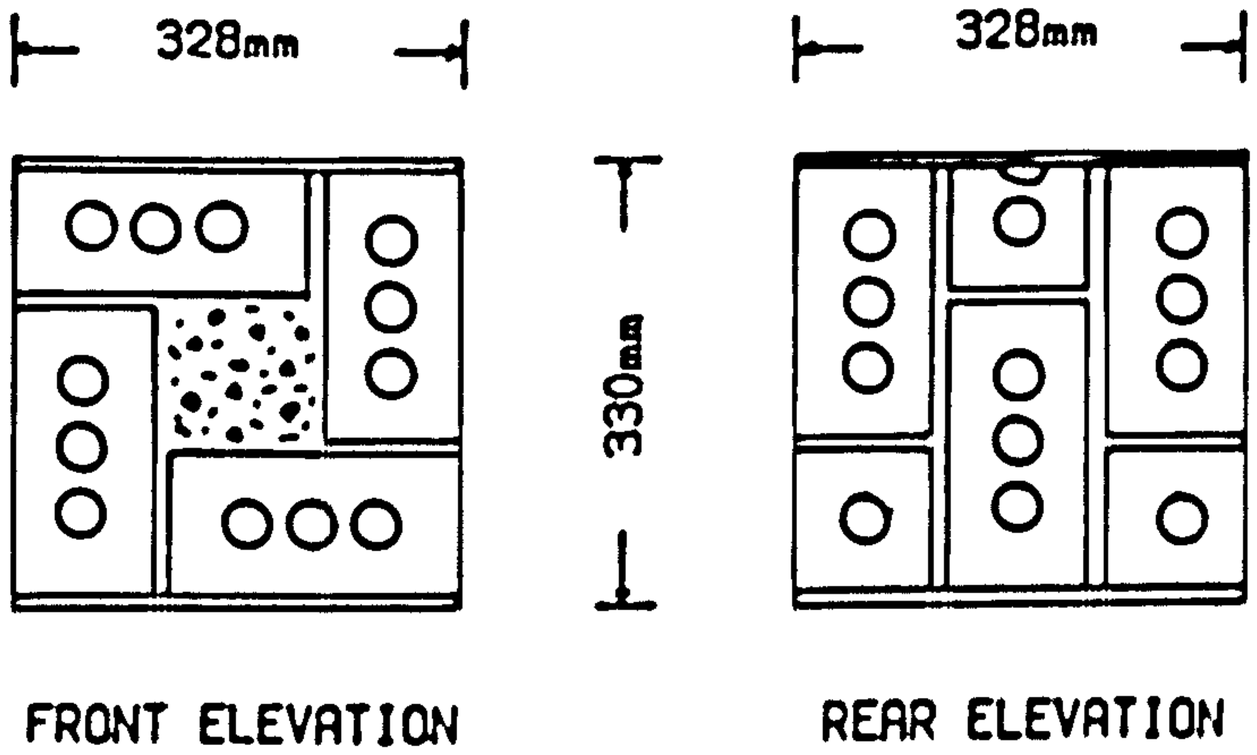

FRONT ELEVATION REAR ELEVATION

Figuro 2.2.9

the whole cross-section and so accurately represented the compressive behaviour of the beams only at prestressing. However, the prisms were more likely to model accurately the compression zone at failure in the over-reinforced beams where the neutral axis depth was much greater than in the under-reinforced beams the neutral axis depth at ultimate will be much smaller and therefore the compressive properties of the prisms were less likely to represent the compression zone properties of the beam. The predicted deflection, using the experimental values for elastic modulus of the section exhibited good agreement with experimental measurements. The deflection was greatly over-estimated when the code values for elastic modulus were used. The modulus of elasticity given by the code was taken from stack bonded prism loaded normal to the bed-joint, and therefore made no allowance for the orthotropic nature of the brickwork or for the presence of the concrete.

Between 1980 - 1983 an extensive research programme was undertaken by Pedreschi and Sinha[9,25] to study the behaviour of post-tensioned brickwork beams. A total of 51 post-tensioned brickwork beams with varying brick strength, mortar grade, steel area, prestressing force and a/d ratio were tested. The cross-sections used, shown in figure 2.2.10, represented an efficient use of the brickwork since the grouted cavity formed only 10% of the cross-sectional area. The grouted cavity also allowed full bond to develop after prestressing and provided adequate protection against corrosion. Each beam was prestressed with either two, three or four 10.9 mm diameter prestressing tendons located at the lower 'kern' limit. The effective prestressing force after all losses varied between 61 and 309 kN, tensile cracking was observed in the anchorage

BEAM SECTIONS OF PEDRESCHI AND SINHA[15]

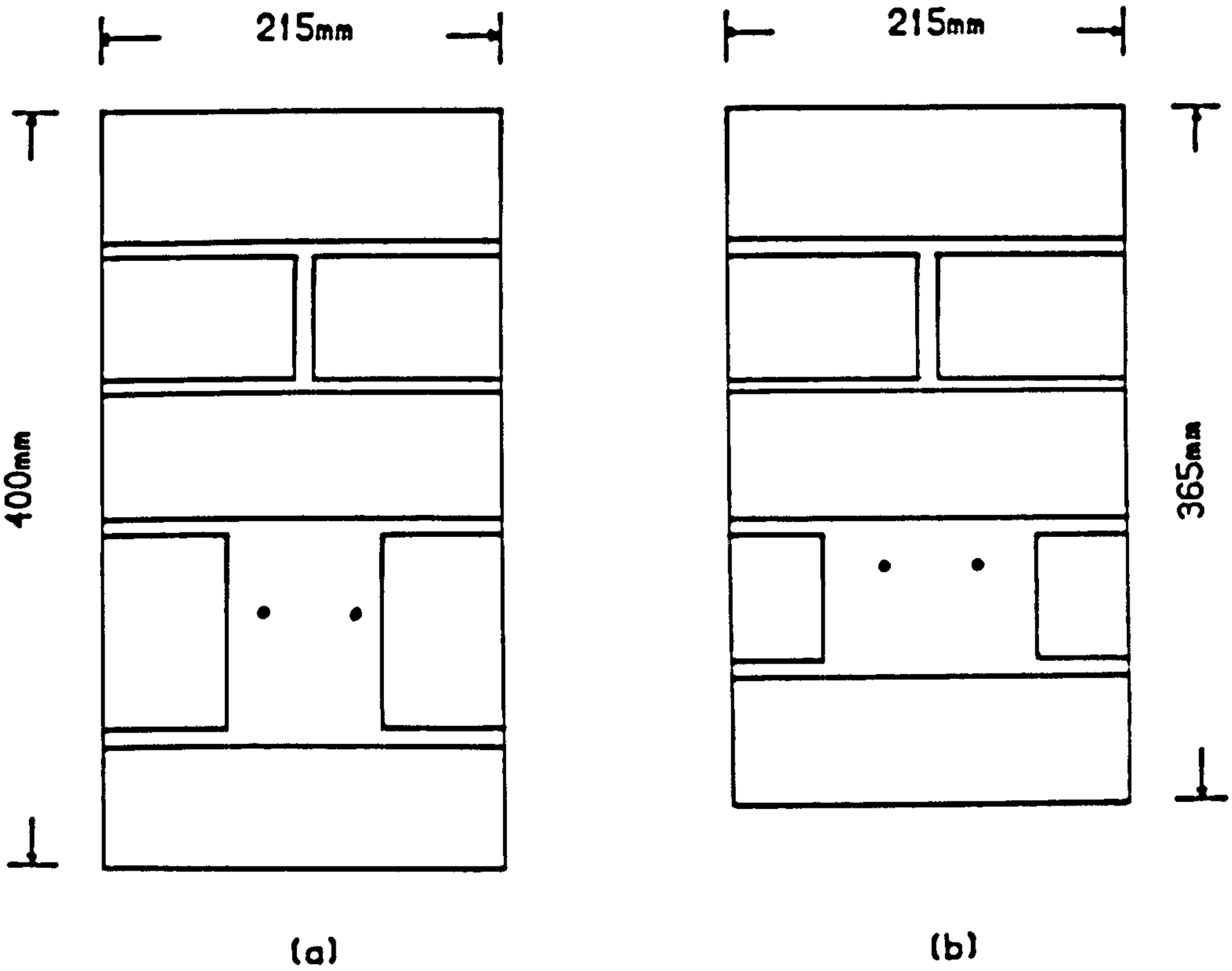

Figure 2.2.10

zone during prestressing of the beams with highest levels of prestress. The beams were tested under two point loads over spans up to 6200 mm, thirty of the beams failed in flexure. In conjunction with the beam tests sixty brickwork prisms, of the format shown in figure 3.6.1 (h/t =2 and 5), were tested in uniaxial compression to determine the compressive properties of the brickwork. As a result Pedreschi and Sinha proposed an expression for the stress/strain relationship of brickwork.

Pedreschi and Sinha undertook the first serious attempt to model the behaviour of post-tensioned brickwork beams using the actual non-linear material properties. Both deflection and ultimate moment were predicted accurately using properties for brickwork derived from the single course prisms, figure 3.6.1. The average crack widths were also estimated with reasonable accuracy using an equation based upon average crack spacing and average steel strain.

Prior to commencing this study on partially prestressed brickwork beams Garwood[14] had reported on the construction and testing of three fully prestressed brickwork beams in which the amount of tensile reinforcement and brickwork bonding pattern were varied. The first two beams were built using a section similar to that of Robson et al[13], figure 2.2.8. Due to the complexity of construction the section shown in figure 2.2.11 was adopted for the subsequent test. Brickwork prism tests were undertaken to determine the compressive properties of the beam section, figure 2.2.12 (h/t=5.0 and 6.8). All beams failed in flexure with crushing of the brickwork in compression. Although the steel strain was not measured Garwood estimated from a moment compatibility analysis that the

BEAM SECTION OF GARWOOD[28]

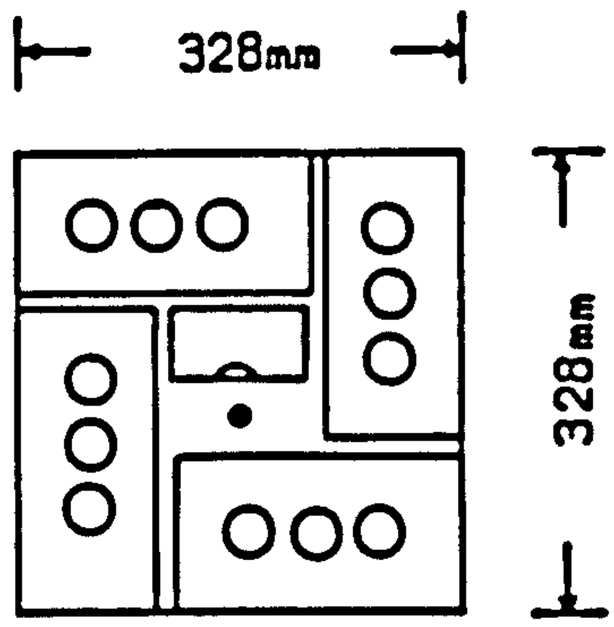

Figure 2.2.11

BRICKWORK PRISMS OF GARWOOD[17]

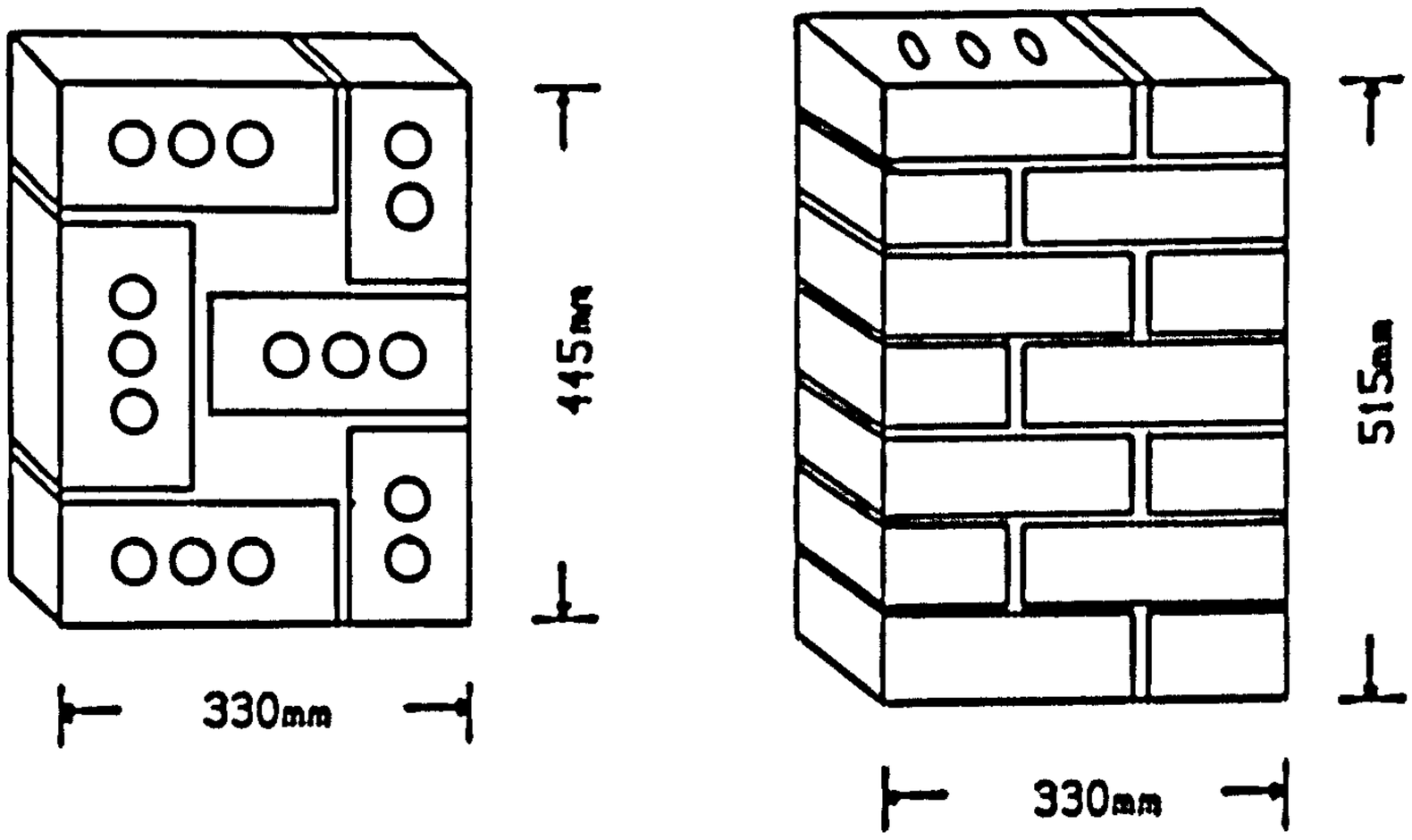

Figure 2.2.12

sections were under-reinforced.

After some of the preliminary results of the current investigation had been published[27] Garwood reported on the testing of nine partially prestressed brickwork beams[28]. Both of the cross-sections used earlier for the fully prestressed beams were adopted, figures 2.2.8 and 2.2.11. The beams were prestressed with either one 20 mm or 25 mm diameter Macalloy bar and reinforced with two 8 mm diameter mild steel bars. The degree of prestress was varied from a maximum to zero to study the influence of prestress on the behaviour. Due to the format of the cross-section the non-tensioned reinforcement was placed at the same depth as the tensioned steel. Any advantages to be gained in using non-tensioned bars by placing them closer to the soffit for improved cracking control was therefore lost. The behaviour of partially prestressed beams was compared with three similar reinforced brickwork beams.

The partially prestressed brickwork beams performed satisfactorily under load, the beams with higher prestress failed in flexure whereas those with lower and zero prestress shear failure predominated. The measured deflection and crack widths were greater in beams with least prestress, because of the reduction in cracking moment. Experimental results indicated a relationship between fictitious tensile stress in the brickwork and the maximum crack width. Prestressing was shown to enhance the shear strength and Garwood suggested that shear design for the length of the beam uncracked should be based on limiting principal tensile stresses. It is, however, surprising that no attempt was made to predict either the deflection or crack widths of the beams. As with the previous

experiments analysis of the results was somewhat restricted by the lack of instrumentation used during the testing. The measured brickwork strains were used in a moment compatability analysis to determine the steel stresses during loading. Garwood assumed a parabolic-rectangular stress/strain curve for brickwork, the transitional and ultimate brickwork strains were taken as 0.0022 and 0.0035 respectively. Apparently no attempt was made to confirm these assumptions, and consequently the steel stresses given to define the failure mode were approximate.

The renewed interest in prestressed brickwork has necessitated an investigation into the factors affecting prestress losses in brickwork. Lenczner[29-30] has conducted a number of such tests on post-tensioned walls and columns. A simplified theoretical approach to predict creep losses was proposed and shown to accurately estimate losses when compared with experimental results. Lenczner has also tested one post-tensioned brickwork beam[31], figure 2.2.13. Total losses in the beam over one year were 12%, unfortunately no attempt was made to apply the method suggested for vertical members to the prestress losses of the beam.

2.3 PRACTICAL APPLICATIONS OF POST-TENSIONED BRICKWORK

The last twenty years have seen a gradual increase in the use by the construction industry of prestressed brickwork. As yet, however, its use has generally been restricted to one of vertically stabilising laterally loaded walls in single storey buildings, such as factories and sports halls. The precompression has been used to

BEAM SECTION OF LENCZNER[31]

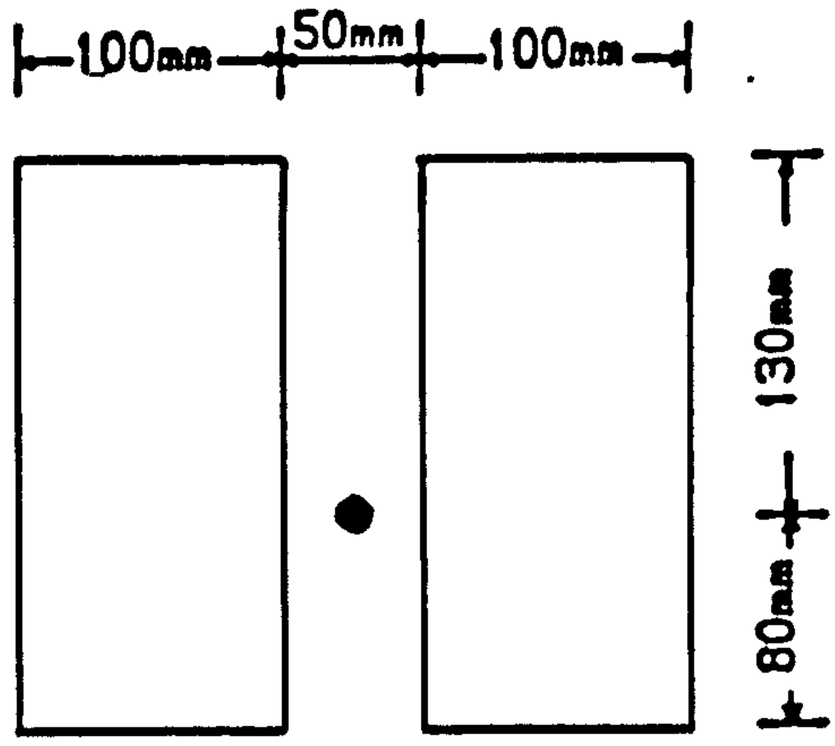

Figure 2.2.13

replace the load that would normally have been applied by the self weight of the structure above. The following with one exception[33], are examples of this technique.

Neil[32], in 1966, introduced a vertical precompression to stabilise 7.3 m high external walls of a factory in Darlington. High tensile steel rods were hung from high level fascia beams and then built into the foundations. The brickwork was built around the tensile bars and post-tensioned concentrically through the flange of the beam. Once prestressing was complete the steel fascia beams were welded to steel columns designed to carry the vertical loading. Prestressing of the brickwork allowed the width of the cavity wall to be kept to a minimum of only 280 mm instead of at least 460 mm. It also removed the need for intermediate framing or buttressing. Neil estimated the cost of the tensioning to be comparable to an additional 115 mm of brickwork.

Water storage facilities were required at a brick factory in case of fire. The solution adopted by Foster[33] was a prestressed brickwork cylindrical tank. The internal diameter of the tank was 12 m and the depth was 4.9 m. The tank was prestressed in both the horizontal and vertical directions. The walls of the tank were 225 mm thick built in flemish bond providing a vertical cavity for the prestressing reinforcement. High tensile wires, 7 mm diameter, were used. The vertical precompression was 1 N/mm^2 and circumferential compressive stress was 2 N/mm^2. After prestressing an external decorative skin of brickwork was built around the outside of the wall which provided a cavity for grouting of the horizontal reinforcement. The total width of the wall when completed was

380 mm.

In 1982 Curtin et al[34] reported on the construction of a religious assembly hall, 25 m x 15 m x 8.5 m. The architect required a clerestorey window and so the external walls were to be designed as free cantilevers. A post-tensioned brickwork diaphragm wall stressed with two 32 mm diameter Macalloy bars, 665 mm wide, was chosen. Prestressing provided the necessary lateral stability while keeping the construction costs to a minimum. A prestressing force of 100 kN was applied concentrically introducing a compressive stress of 0.5 N/mm^2 at transfer.

The design and construction of a post-tensioned brickwork wall was described by Bradshaw et al[35] in 1982. To retain crops, as part of a steel portal frame farm building, a post-tensioned retaining wall 2.4 m high designed as a cantilever was selected. The wall provided no support for the portal frame. The wall was 777 mm wide, an eccentric prestress of 45 kN was applied inducing a maximum precompression of 0.3 N/mm^2. The tensile reinforcement was accommodated in pockets provided within the web of the wall.

2.4 SUMMARY AND SCOPE OF THE PRESENT INVESTIGATION

The research undertaken to date to study prestressed brickwork has concentrated on beams which have contained tensioned reinforcement only. The tensile reinforcement has remained unbonded in approximately half of the beams tested. It seems likely that this form of construction has been adopted not because of any behavioural

advantages but as a result of practical difficulties in grouting of the cross-section. Adverse effects of high levels of prestress, such as tensile cracking in the anchorage zone at transfer of prestress, were reported in a number of the previous investigations[9,17].

Until recently little attempt was made to predict the behaviour of prestressed brickwork beams. Even so, with the exception of Pedreschi and Sinha[26], calculations have been limited to the predictions of ultimate strength and elastic deformation. The beams have tended to be regarded as similar to class 1 or 2 prestressed concrete beams[36] and consequently little attention has been given to cracking. This was reflected in the code of practice[15] where no recommendations were given for the cracking in prestressed brickwork.

The level of prestress has been proven to be an important factor in the shear strength of prestressed brickwork beams. However, very little work has been conducted to study the influence of partial prestressing upon the flexural behaviour. The only investigation[28] to be published concerning partial prestressing did not fully utilise the possibilities of the non-tensioned steel due to practical restrictions imposed by the choice of cross-section. Analysis of the experimental behaviour was approximated by the limited test instrumentation. No attempt was made to predict either the elastic or post-cracking behaviour of the beams. Prior to this current work there was no understanding of the behaviour of partially prestressed brickwork beams.

In practice prestressed brickwork has with a few exceptions

been limited to the introduction of a vertical precompression as a means of providing stability for laterally loaded walls. This form of construction uses the prestress to increase the effective dead weight of the structure and therefore provides no major alternative to more conventional forms of construction using the brickwork solely as a compression element.

As outlined in chapter 1 partially prestressed brickwork offers a number of advantages over both reinforced and fully prestressed brickwork. A reduction in the prestress will reduce the camber of the beam and may prevent tensile cracking of the anchorage zone in post-tensioned beams. The combination of prestressed and non-tensioned steel close to the soffit of the section offers improved crack control characteristics. Application of a precompression will increase the effective shear strength and therefore may prevent premature shear failure as associated with reinforced brickwork.

Due to the current lack of knowledge concerning the behaviour of partially prestressed brickwork beams this experimental study was undertaken. As part of the investigation the influence of the following variables upon ultimate moment, deflection and cracking of partially prestressed brickwork beams were considered in detail:

(i) percentage area of steel

(ii) prestressing force

(iii) partial prestressing ratio[37]

(iv) cover to the non-tensioned steel

(v) brick strength

(vi) mortar grade.

A total of 41 partially prestressed brickwork beams were tested. An interactive computer programme to predict the flexural behaviour of the beams was developed in conjunction with the experimental work. The computations allowed for the presence of a concrete cavity and the tension-stiffening effect of the brickwork and concrete after cracking. The non-linear material properties derived from experimental tests were used to predict the behaviour. The compressive properties of the brickwork were determined from a comprehensive series of tests carried out on both axially and eccentrically loaded brickwork prisms (h/t=5).

CHAPTER 3

MATERIAL PROPERTIES, CONSTRUCTION AND TEST PROCEDURE

3.1 INTRODUCTION

For the theoretical analysis, computer programming, the mechanical properties of the materials were required. Therefore a comprehensive series of tests were undertaken to determine the compressive and tensile properties and stress/strain characteristics of the materials used in the investigation. This chapter presents and discusses the results of those tests.

Conventionally brickwork is used for compression members in which the compressive stresses develop in a direction normal to the bed-joint. Consequently the tests developed to determine the compressive strength of the brick units require the bricks to be tested flat. In the partially prestressed brickwork beams compressive stresses were to develop parallel to the bed-joint direction and hence it was also necessary for the bricks to be tested in this manner.

The compressive strength and stress/strain properties of the brickwork were determined from a series of small-scale axially loaded prism tests. However, the compression zone in a flexural member is subjected to a linear variation of strain with depth, or strain gradient. Research[51] on eccentrically loaded brickwork has reported an apparent increase in the compressive strength of brickwork due to the strain gradient. A programme of tests were therefore also undertaken on prisms loaded at an eccentricity of t/6 to determine the influence of the strain gradient on the compressive properties of the brickwork used in this investigation.

The modulus of rupture of the beam section was determined from plain unreinforced brickwork/concrete composite prisms tested in flexure.

Both the tensioned and non-tensioned reinforcements were tested in uni-axial tension to determine the stress/strain relationship, ultimate tensile strength and proof stress.

Finally the chapter describes in detail the development, construction, prestressing, concreting and reinforcement details of the partially prestressed brickwork beams. Particulars are also given of the procedure and instrumentation used in the testing of the beams.

3.2 PROPERTIES OF THE BRICKS

Three different strengths of extruded 3-hole perforated clay bricks (figure 3.2.1) were used; designated as high, medium and low strength. The average percentage area of perforations was approximately 10.4%, 13.3% and 11.7% for the high, medium and low strength bricks respectively.

The compressive strength test was carried out in accordance with BS 3921[38] in three orthogonal directions, figure 3.2.1. The results are presented in table 3.2.1. The compressive strength was calculated based on both the gross and net cross-sectional areas.

In all three types of bricks the compressive strength was

PERFORATED CLAY BRICK AND LOADING DIRECTIONS

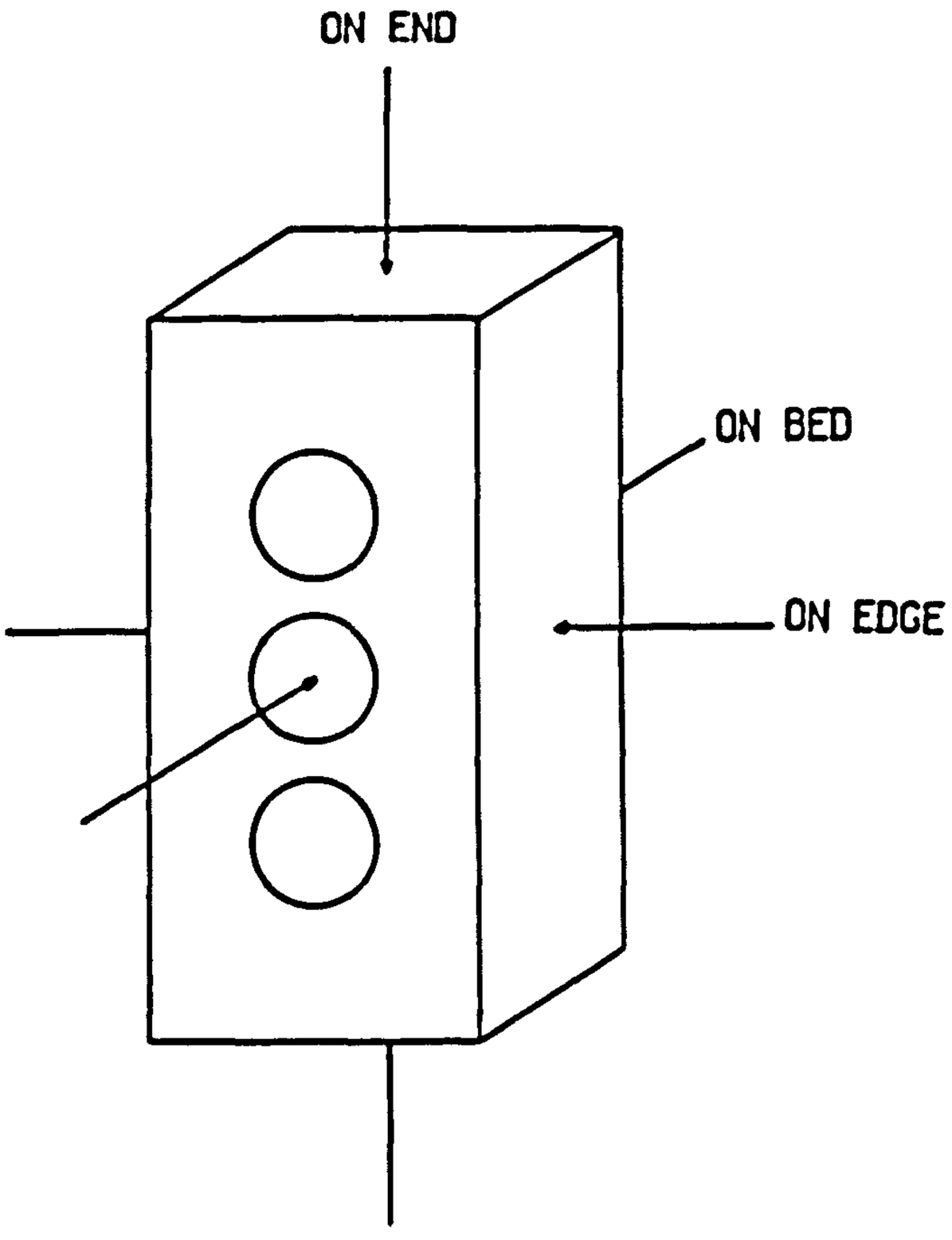

Figure 3.2.1

Table 3.2.1 Properties of bricks

Brick Type	Compressive Strength					Water Absorption % by weight (5 hr)	Initial rate of suction Kg/(m³/min)
	Loading Direction	Average N/mm²	Range N/mm²	Std Deviation N/mm²	Coeff of Variation %		
High	Bed	96.58 (107.87)	78.57 - 107.60	11.39	11.79	4.40	0.26
	Edge	53.52 (94.87)	45.52 - 61.40	5.39	10.07		
	End	32.74 (48.32)	27.07 - 40.84	4.67	14.26		
Medium	Bed	72.25 (83.66)	60.08 - 88.26	9.96	13.79	8.77	1.11
	Edge	23.51 (46.50)	18.65 - 27.27	2.65	11.27		
	End	15.11 (23.21)	12.03 - 17.54	1.92	12.71		
Low	Bed	19.69 (22.20)	16.01 - 25.78	2.98	15.13	26.34	3.06
	Edge	7.05 (13.14)	5.23 - 10.12	1.74	24.68		
	End	6.48 (9.58)	4.33 - 10.58	2.40	37.04		

Note: Value in brackets is the average compressive strength based upon net area

highest when loaded normal to the bed-joint and least when tested on-end. The trend is similar if the net cross-sectional area is used for the calculation. In table 3.2.2 the compressive strength on-edge and on-end is compared as a fraction of the bed-joint compressive strength for each brick type. Based on the gross cross-sectional area the strength on-edge varies between 32.5% and 55.4% of the on-bed strength. The strength when on-end was between 20.9% and 33.9% of the on-bed strength. Using the net cross-sectional areas to calculate the compressive strength increased the relative on-edge and on-end strengths, since the perforations formed a greater proportion of the cross-section. The on-edge and on-end strengths were increased to 55.6% - 87.9% and 27.7% - 44.8% of the on-bed strength respectively.

The failure mode of the bricks differed depending upon the direction of loading. For bricks tested on-bed and on-edge (aspect ratios[1] 0.63 and 1.58 respectively), failure occurred by spalling of the brick leading to eventual crushing. In the bricks tested on-edge the spalling occurred in the region of the perforations. Failure of the bricks tested on-end (aspect ratio 3.31) occurred by vertical tensile splitting along the centre line of the bricks. The failure mode will significantly influence the value for compressive strength. The mode of failure will be influenced by the aspect ratio, 'platen' restraint, and the orientation of the perforations with respect to loading direction[39].

---

[1] Aspect ratio = ratio of height to least lateral dimension (h/t).

Table 3.2.2

Comparison of brick strength in three directions

		Ratio of bedjoint strength		
Area	Brick Type	Bed	Edge	End
Gross	High	1.0	0.554	0.339
	Medium	1.0	0.325	0.209
	Low	1.0	0.358	0.329
Net	High	1.0	0.879	0.448
	Medium	1.0	0.556	0.277
	Low	1.0	0.592	0.432

For bricks tested on-bed the effect of the platen restraint will be more significant than for the other two directions and hence the compressive strength may be higher. Tested on-end the platen restraint will be reduced and therefore the compressive strength is reduced. Page and Marshall[40] have tested solid bricks with varying aspect ratios, 0.36 to 3.03, under both confined and unconfined compression to study the influence of the platen restraint upon the compressive strength. At low values of aspect ratio the confined strength was as much as twice that of the unconfined test. There was no difference in compressive strength under similar test conditions for specimens having an aspect ratio of 3.03.

Orientation of the perforations will influence the compressive strength, the reduction in strength caused by stress concentrations in the vicinity of the perforations[39]. This is supported by the experimental observation of crushing in the region of the perforations for bricks tested on-edge.

The difference in compressive strength for the three directions may therefore be attributed to platen restraint and the stress concentrations in the region of the holes as well as to the orthotropic properties of the bricks.

Other researchers[39-42] have tested perforated bricks in compression in three directions. There is, however, no distinct general relationship between the bed-joint strength and the strength in the other two directions. The ratios between bed to edge strength and bed to end strength vary from 0.290 to 0.809 and 0.110 to 0.535 respectively, and so the general trend is similar to that of the

bricks used in this investigation.

Results of the water absorption and initial rate of suction tests, carried out in accordance with BS 3921[38], are presented in table 3.2.1.

3.3 MORTAR

3.3.1 Cement

Ordinary Portland cement to BS 12[43] was used throughout for both the mortar and the concrete infill.

3.3.2 Lime

Lime conforming to BS 890[44] was used in the mortar.

3.3.3 Aggregates

A sand, from Edzill Fife, conforming to BS 1200[45], sieve analysis table 3.3.1, was used throughout in the mortar mix.

Concrete sand, from Helville quarry Lothian, sieve analysis table 3.3.2, and 10 mm coarse aggregate both conforming to BS 892[46] were used throughout in the concrete infill mix.

Table 3.3.1

Sieve analysis of mortar sand

Test Sieve	% by weight passing through sieve	
	Test result	BS 1200 limit (Table 2)
5.00 mm	100	100
2.36 mm	100	90 - 100
1.18 mm	96	70 - 100
600 µm	62	40 - 80
300 µm	24	5 - 40
150 µm	9	0 - 10

Table 3.3.2

Sieve analysis of concrete sand

Test Sieve	% by weight passing through sieve	
	Test result	BS 882 limit (Table 5)
10.00 mm	100	100
5.00 mm	97	90 - 100
2.36 mm	87	60 - 100
1.18 mm	81	30 - 100
600 µm	73	15 - 100
300 µm	47	5 - 70
150 µm	11	0 - 15

3.3.4 Mortar

Grade I, 1:¼:3 (cement:lime:sand), and grade II, 1:½:4½ (cement:lime:sand), mixes were used. The mortar mix was proportioned by volume using gauging boxes, the sand was dried prior to mixing. Water/cement ratios of 0.9 for the grade I mortar and 1.3 for the grade II mortar were used. Three 100 mm control cubes were taken from each batch immediately after mixing and tested at 28 days. The average compressive strength of the mortar used in the brickwork prisms and in the beams is given in tables 3.6.1 and 5.2.1 respectively.

3.4 CONCRETE

3.4.1 Mix proportion and compressive strength

A 1:2½:2 (cement:sand:coarse aggregate) concrete mix by volume was used for all beams. A plasticiser, 'conbex' was added to reduce the effects of shrinkage and to shorten the setting time. The water content was adjusted to achieve a slump of betwen 200 and 250 mm. Three 100 mm cubes were cast during the concreting operation and tested at 7 days. The average compressive strength of the concrete for each beam is given in table 5.2.1.

3.4.2 Stress/strain relationship

The partially prestressed brickwork beam section was a composite consisting of approximately 82% brickwork and 18% concrete

infilling. Accurate prediction of the moment-curvature and load/deflection relationshps, section 4.2.1, requires a knowledge of the stress/strain relationship of concrete. The expression proposed by BS 8110 Part 2[47] for rigorous analysis, as illustrated in figure 3.4.1, was adopted for this work.

The equation of the curve is defined by the following:

$$f = 0.8f_{cu}\left(\frac{K\eta-\eta^2}{1+(K-2)}\right) \qquad (3.4.1)$$

where $$\eta = \frac{\varepsilon}{\varepsilon_{c,1}} = \frac{\varepsilon}{0.0022} \qquad (3.4.2)$$

and $$K = \frac{1.4\varepsilon_{c,1}\ E_o}{f_{cu}} = \frac{3E_o}{f_{cu}} \qquad (3.4.3)$$

3.5 PROPERTIES OF THE TENSIONED AND NON-TENSIONED REINFORCEMENT

3.5.1 Prestressing strand

Seven-wire stabilised strand conforming to BS 5896[48] was used throughout. Two sizes of strand were used , a 10.9 mm diameter having nominal cross-sectional area 72 mm^2 and 7.9 mm diameter with nominal cross-sectional area 38.8 mm^2.

3.5.2 Reinforcing bars

The non-tensioned reinforcement used throughout was composed of 10, 12 and 16 mm diameter hot rolled deformed high yield steel bars conforming to BS 4449[49].

STRESS/STRAIN RELATIONSHIP FOR CONCRETE

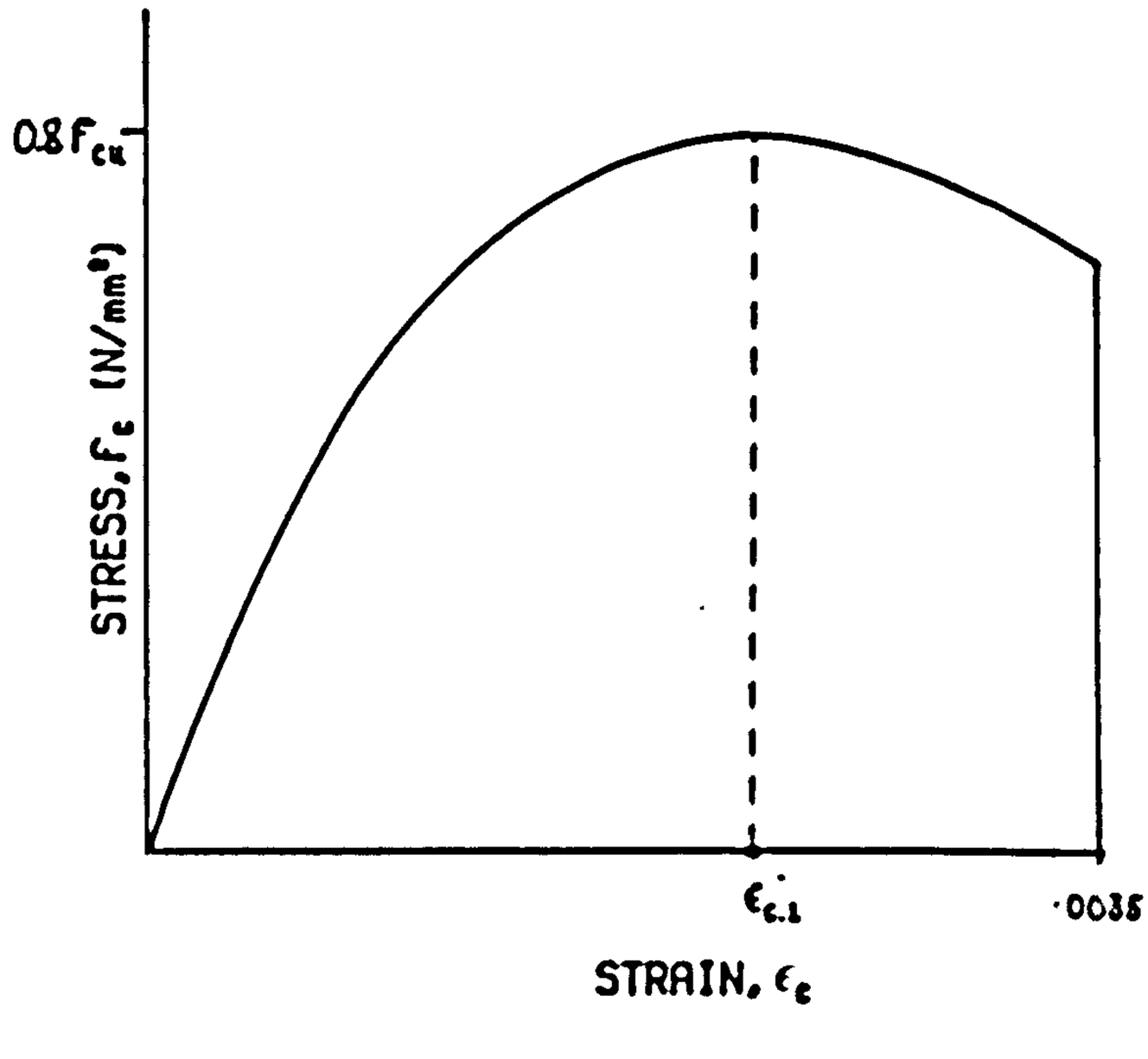

Figure 3.4.1

3.5.3 Idealised stress/strain relationship

A total of three samples for each type of reinforcement were tested in uniaxial tension, in accordance with BS 18[50], to determine the stress/strain relationship of the steel. The strain was measured using electrical resistance strain gauges fixed to the steel. Values of the ultimate tensile strength, 0.2% proof stress and elastic modulus are given in table 3.5.1. In order to utilise the stress/strain relationships in the computerised theoretical analysis the experimental stress/strain curves were idealised into tri-linear relationships, figures 3.5.1 to 3.5.5.

3.6 PROPERTIES OF BRICKWORK

3.6.1 Compressive strength and stress/strain relationship

3.6.1.1 Prism type and test method

From preliminary tests of the partially prestressed brickwork beams it was observed that the neutral axis depth at failure was located within the top three courses of brickwork. The three course prism, type A in figure 3.6.1, was selected to represent the compression zone of the test beams. However, in a number of these tests it was noticed that the tensile cracking progressed sufficiently deep into the section from the soffit of the beam and as a result only the top course of brickwork resisted the compressive stresses at ultimate load. Therefore a single course prism, type B in figure 3.6.1, was also tested in axial compression.

Table 3.5.1

Properties of tensioned and non-tensioned reinforcement

Designation	Nominal diameter	Ultimate tensile strength, N/mm^2	0.2% proof stress N/mm^2	Youngs modulus kN/mm^2
Seven wire stabilised steel strand	7.9 mm	1813	1660	202
	10.9 mm	1708	1642	214
Hot rolled deformed high yield steel bars	10.0 mm	654	500	187
	12.0 mm	670	470	200
	16.0 mm	670	465	194

IDEALISED TRI-LINEAR STRESS/STRAIN
RELATIONSHIP FOR 7.9mm DIAMETER STRAND

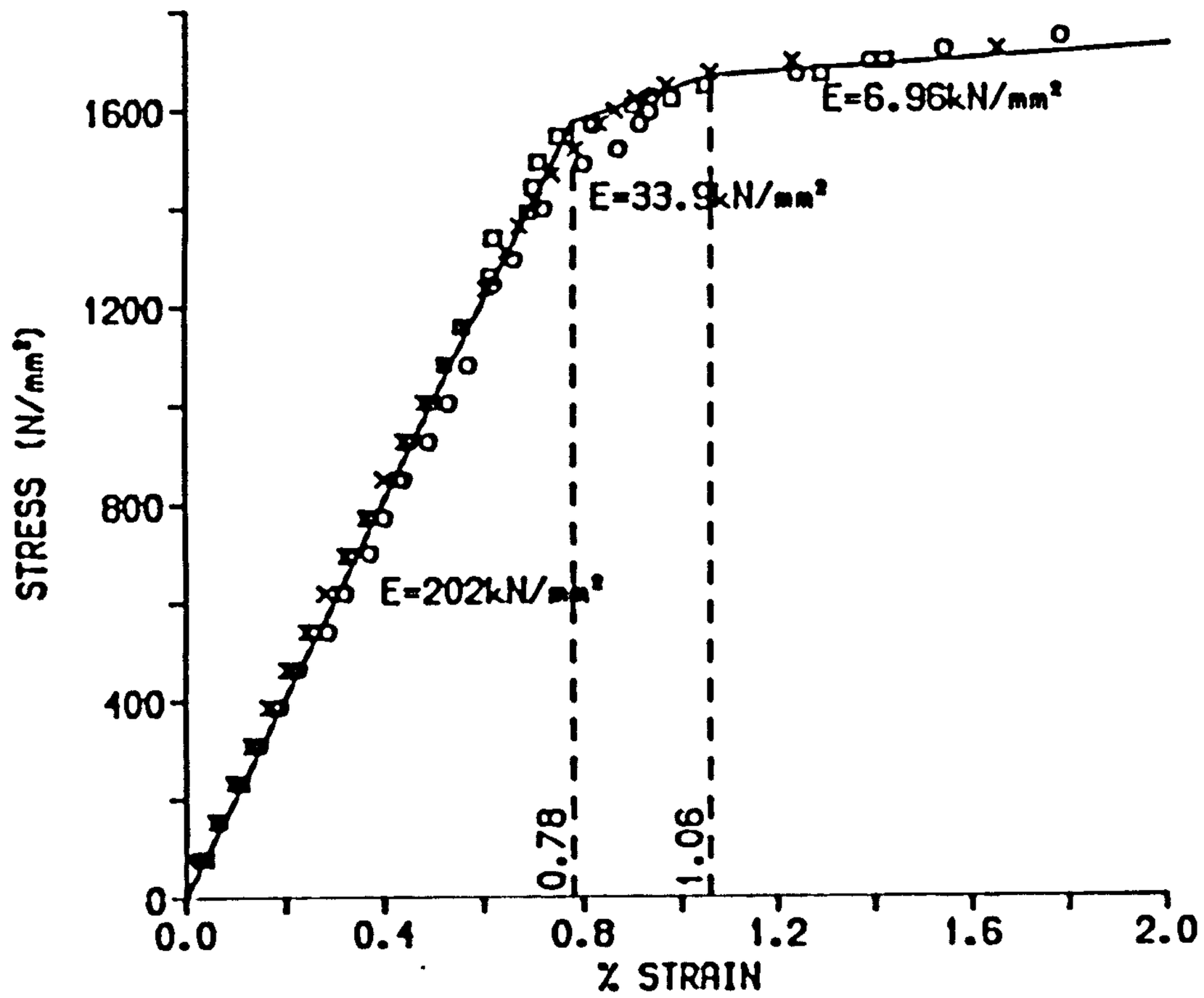

Figure 3.5.1

IDEALISED TRI-LINEAR STRESS/STRAIN
RELATIONSHIP FOR 10.9mm DIA. STRAND

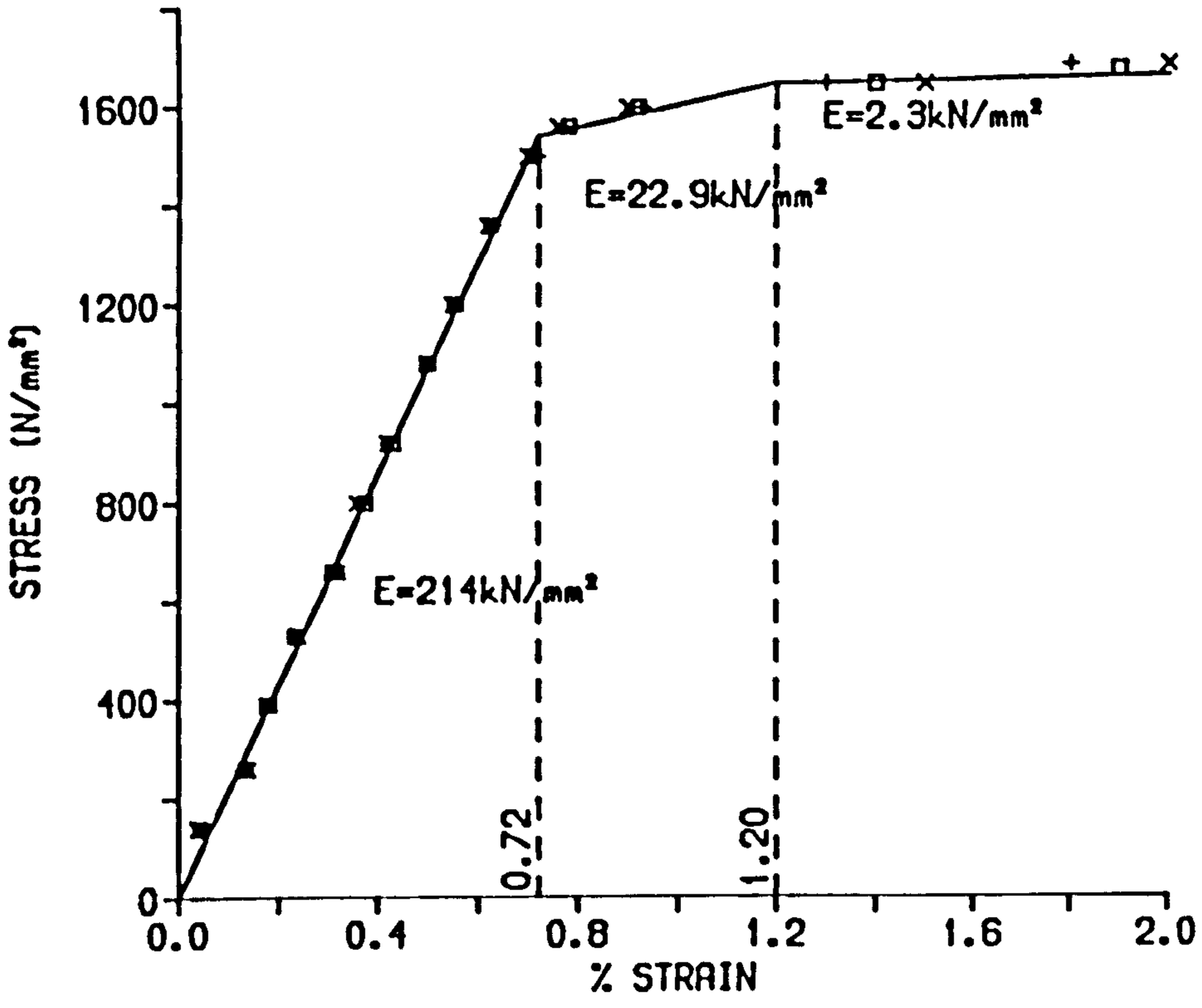

Figure 3.5.2

IDEALISED TRI-LINEAR STRESS/STRAIN RELATIONSHIP FOR 10mm DIAMETER DEFORMED BAR

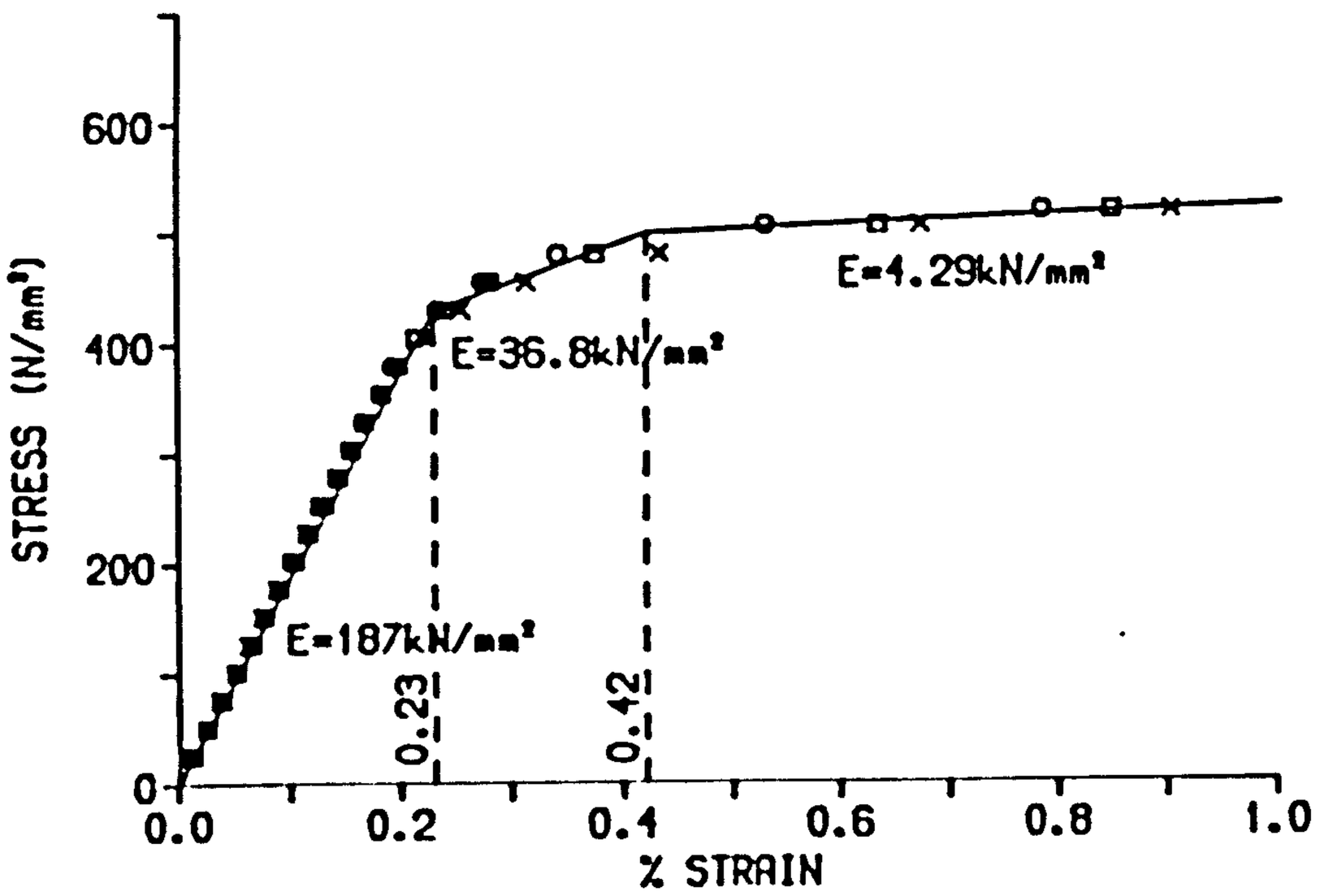

Figure 3.5.3

IDEALISED TRI-LINEAR STRESS/STRAIN RELATIONSHIP FOR 12mm DIAMETER DEFORMED BAR

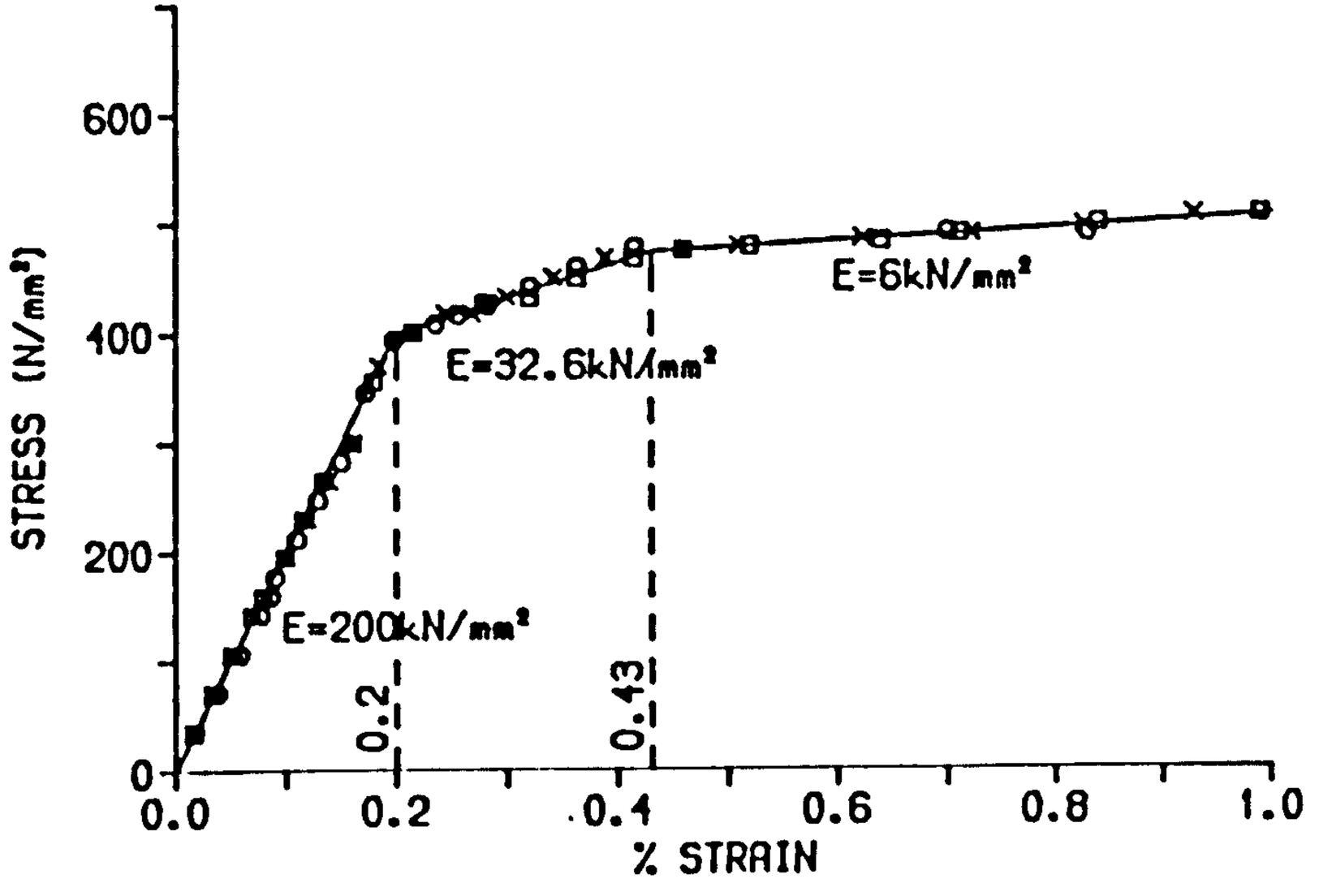

Figure 3.5.4

IDEALISED TRI-LINEAR STRESS/STRAIN RELATIONSHIP FOR 16mm DIAMETER DEFORMED BAR

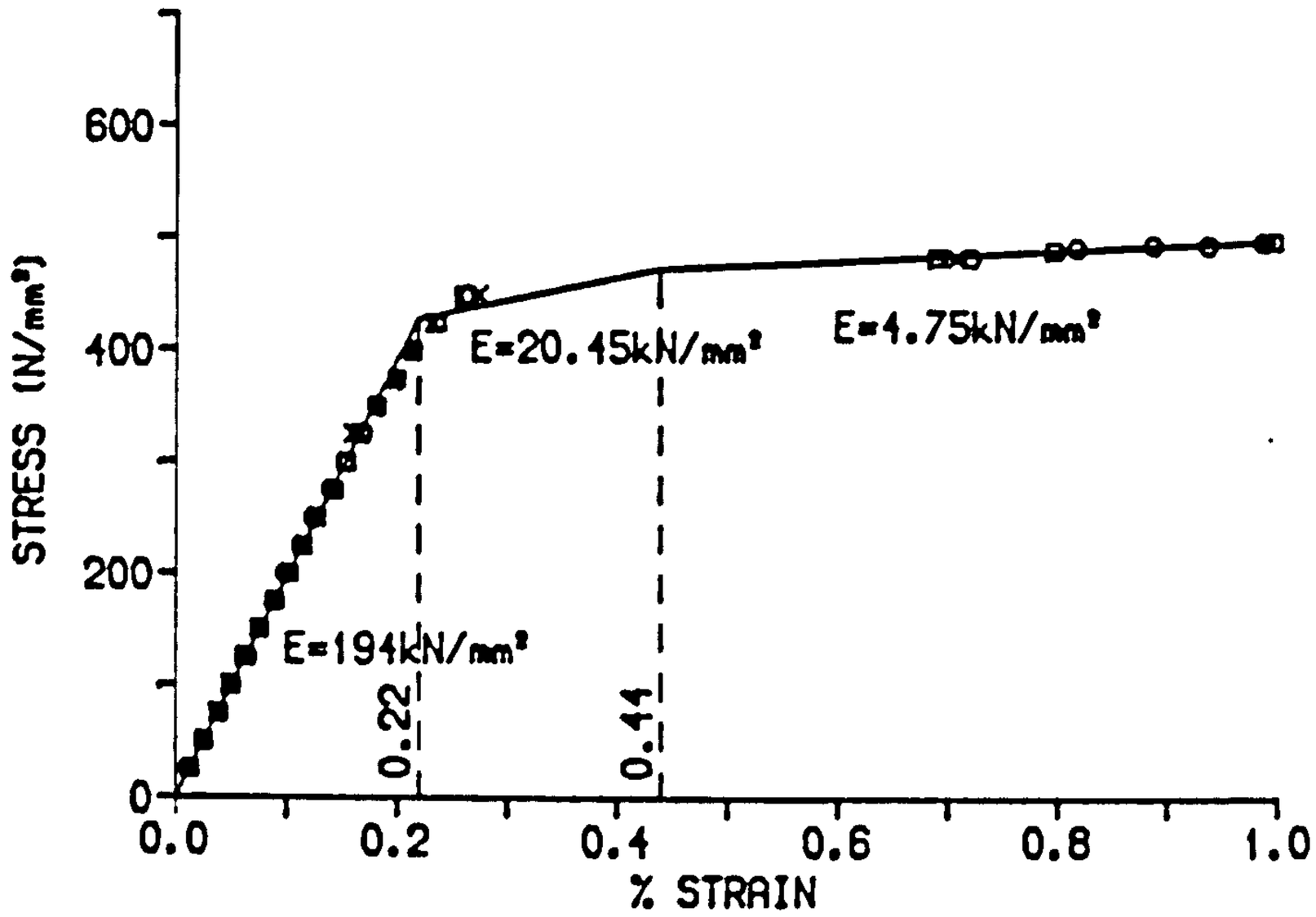

Figure 3.5.5

BRICKWORK PRISMS

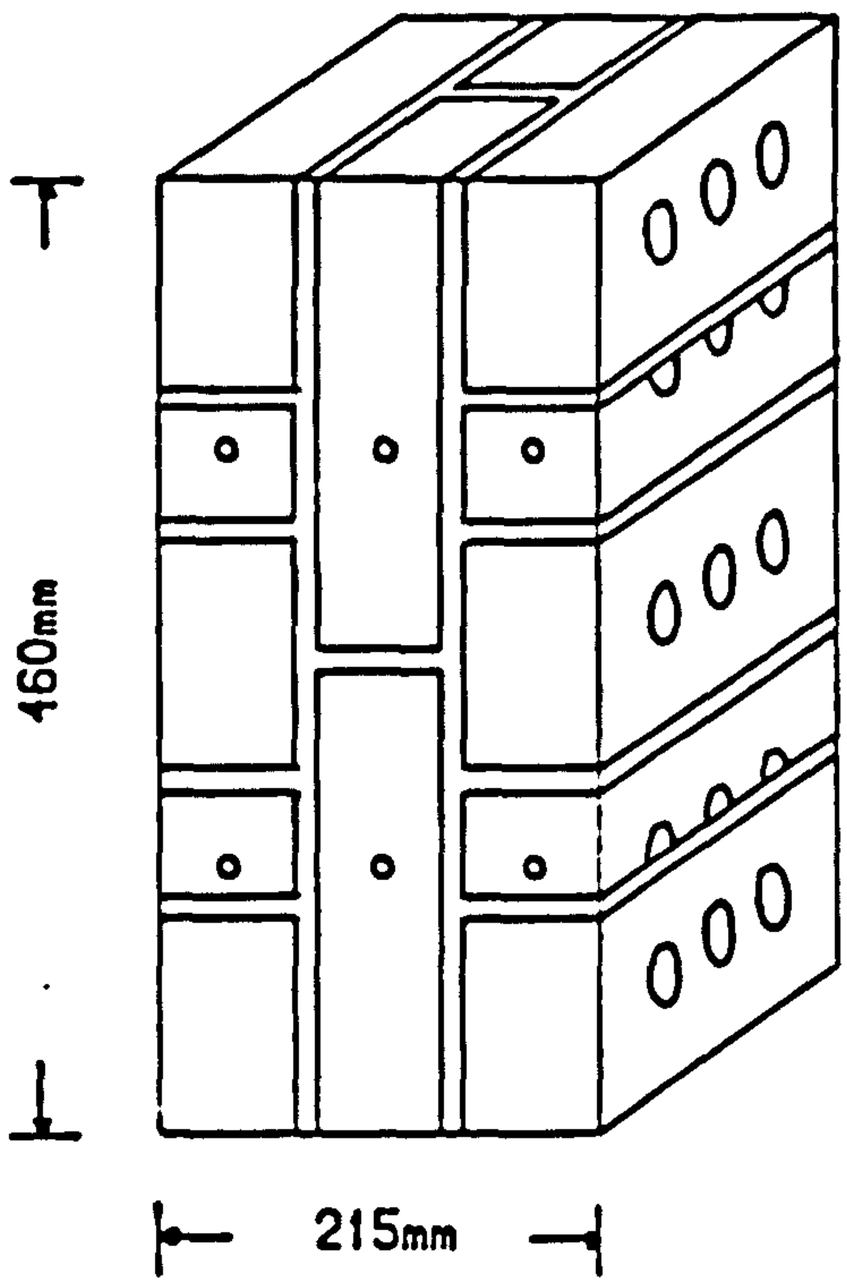

PRISM TYPE A
THREE COURSE

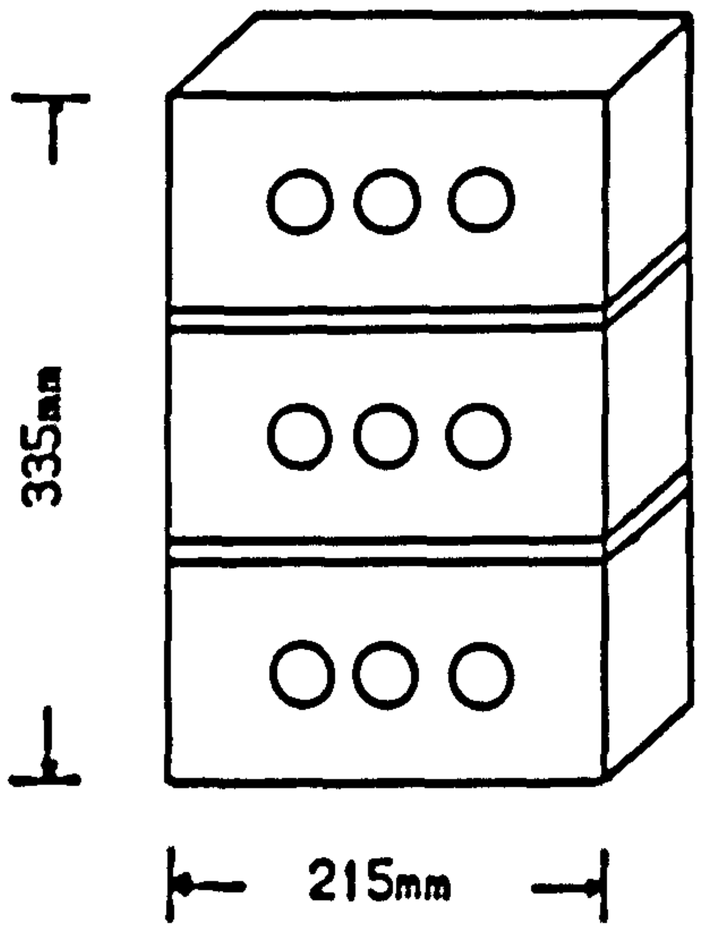

PRISM TYPE B
SINGLE COURSE

Figure 3.6.1

The distribution of strain within the compression zone of the partially prestressed brickwork beams was well defined, varying linearly with depth from zero at the level of the neutral axis depth to a maximum at the outermost compression fibre, chapter 5. The type of the strain distribution was identical to that obtained for a prism loaded at an eccentricity of t/6. Previously researchers[51] testing eccentrically loaded brickwork prisms have noted an apparent increase in the compressive strength of brickwork compared with an equivalent axially loaded prism. This increase has been attributed to the variation of strain across the breadth of the brickwork, the strain gradient. However, more recently research[52] has indicated that this may not be the case and that the ultimate compressive strength and strain remain unchanged with an eccentricity of loading. In order to determine the effect of the strain gradient and obtain the compressive properties of the beams compression zone a number of single course prisms loaded at an eccentricity of t/6 were tested. Preliminary comparisons of the flexural behaviour of the test beams with predicted values using both the three and single course axially loaded prism properties indicated that the single course prisms provided the best representation of the compression zone[27]. Subsequently prism tests concentrated on the single course prisms and so only the single course brickwork prisms were tested under eccentric loading.

Prior to testing the axially loaded prisms were capped and levelled using a rich mortar mix. To ensure an even distribution of the applied load 3 mm plywood sheets were placed between the test specimen and loading platens. Strain measurements were taken at a number of positions across the breadth of the prism, figure 3.6.1,

using either a 150 mm or 200 mm 'demec' gauge. Initially axial load was ensured by adjusting the platen such that the increase in strain for the first load increment was equal at all points of measurement. The brickwork strain was recorded at regular intervals of loading up to 95% of the ultimate load.

The test set-up for the eccentrically loaded prisms is shown in figure 3.6.2. The loading platens were so arranged that the line of action of the load was at an eccentricity of t/6. The prisms were bedded onto the platens using dental plaster to ensure a proper distribution of load to the brickwork. Strain measurements were taken at regular intervals across the breadth of the prism using a 'demec' gauge at increments of load up to failure.

3.6.1.2 Mode of failure and compressive strength of brickwork prisms

Failure of the axially loaded three course prisms was preceeded by splitting of the vertical mortar bed-joints. Once splitting had occurred, at a loading between 53% and 72% of the failure load, the prism ceased to behave monolithically but acted as three independent prisms. This is apparent from the strain distribution measured across the breadth of the section prior to and after separation of the courses, figure 3.6.3. Before cracking the strain distribution was uniform indicating that the prism was under a uniform compressive stress. After splitting at the mortar joints the uneven distribution may have been caused by a re-distribution of the load that had taken place upon splitting due to the differential movement of the three courses of brickwork. It was impossible to re-adjust the loading to achieve a state of uniform stress and so

TEST SET-UP FOR ECCENTRICALLY LOADED PRISMS

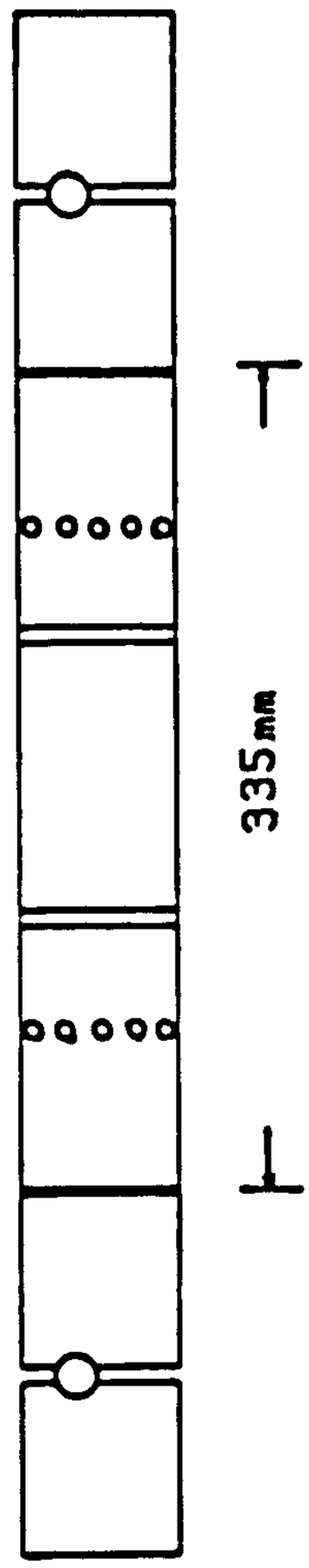

Figure 3.6.2

TYPICAL DISTRIBUTION OF STRAIN FOR THREE COURSE PRISM

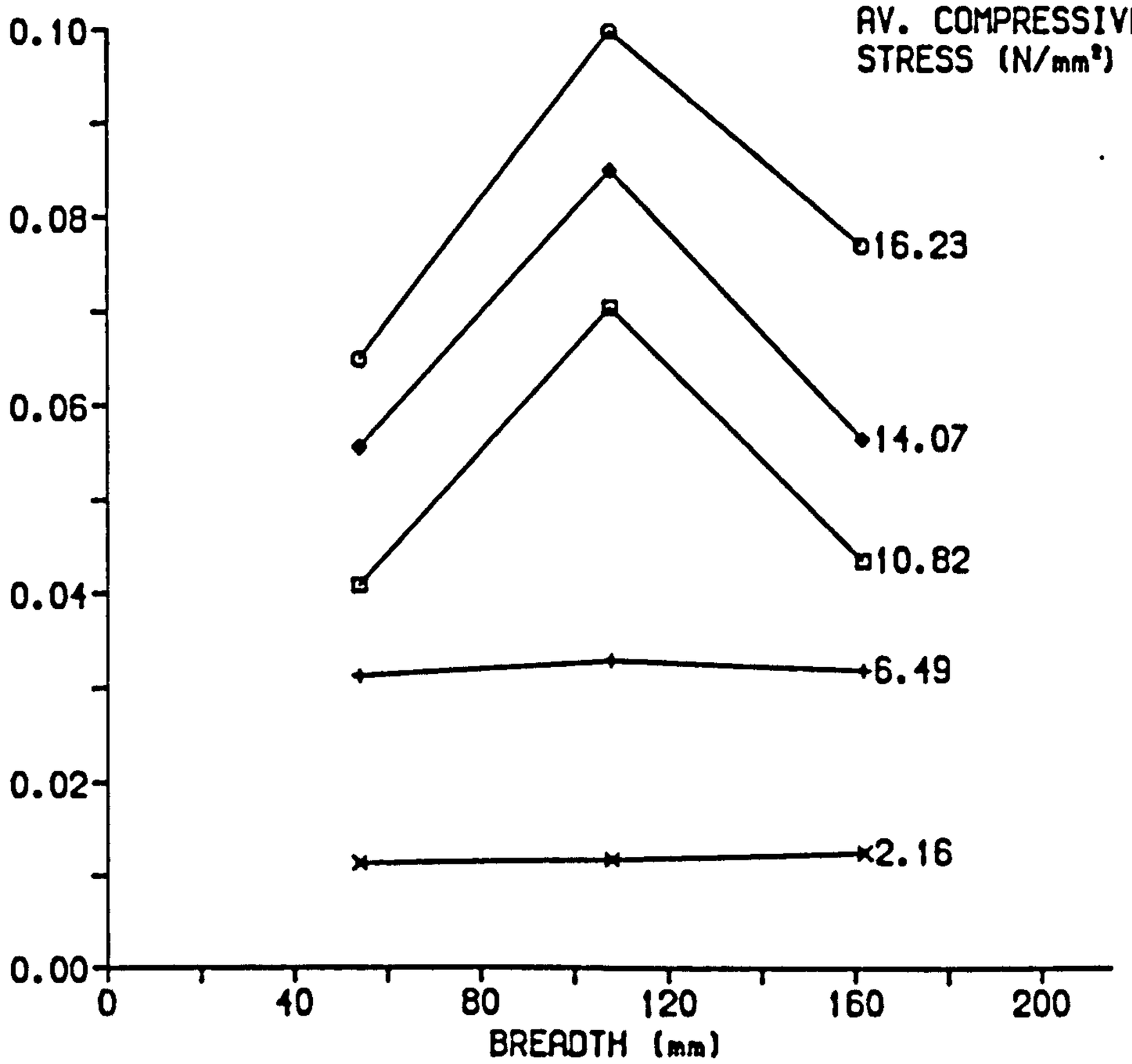

Figure 3.6.3

ultimate load corresponded to the collapse due to crushing of either one or two of the courses. In none of the prisms did all three courses fail simultaneously, Plate 3.2.

The single course prisms subject to axial loading failed as a result of vertical tensile cracks developing along the centre-line of the prism parallel to the axis of loading. Cracking of the brickwork occurred at between 75% and 95% of the ultimate load. In figure 3.6.4 the distribution of strain across the section before and after cracking is presented. Although cracking had taken place, at a stress level of 25.09 N/mm^2 (76% of the average compressive strength), the strain distribution remained approximately uniform and hence the prism was considered to be under a state of uniform stress until failure. Collapse of the single course prisms was caused by explosive spalling of the brickwork, Plate 3.1.

The eccentrically loaded single course prisms failed as a result of crushing of the brickwork at the maximum compression stress face. No vertical splitting of the materials was observed as with similar axially loaded prisms. Once crushing of the brickwork occurred that part of the section was no longer resisting the compressive stresses and so the effective width of the cross-section was reduced. In the revised section the load was no longer applied at t/6 but outside the 'kern' limit and therefore introduced tensile stresses to the face opposite to that at which the crushing occurred. The tensile stresses were sufficient with increasing load to cause cracking at the mortar bed-joint opposite to the crushed face of the prism. Further loading reduced the effective cross-sectional area in compression until the eccentricity of the load was sufficient to

TYPICAL DISTRIBUTION OF STRAIN FOR SINGLE COURSE PRISM

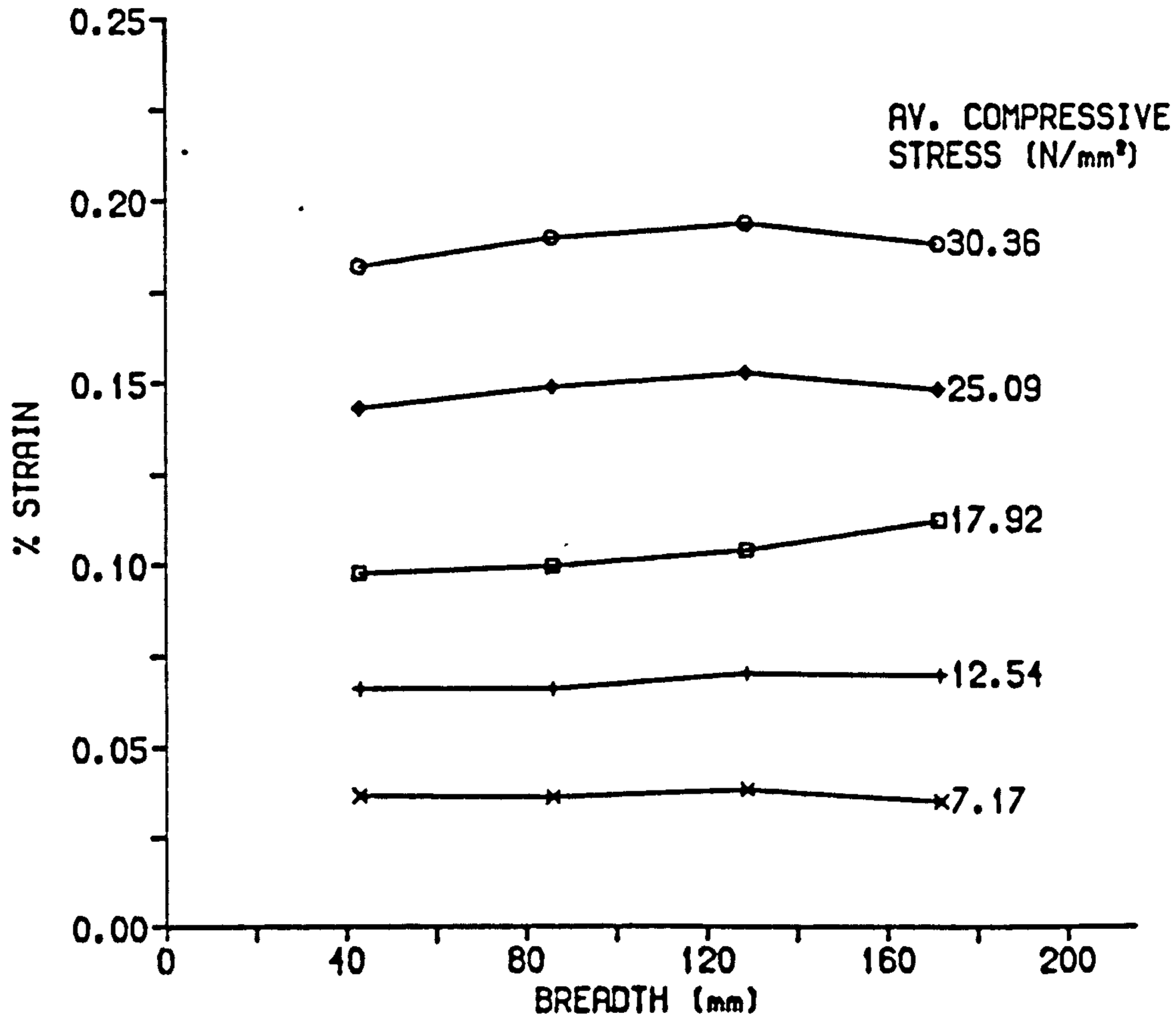

Figure 3.6.4

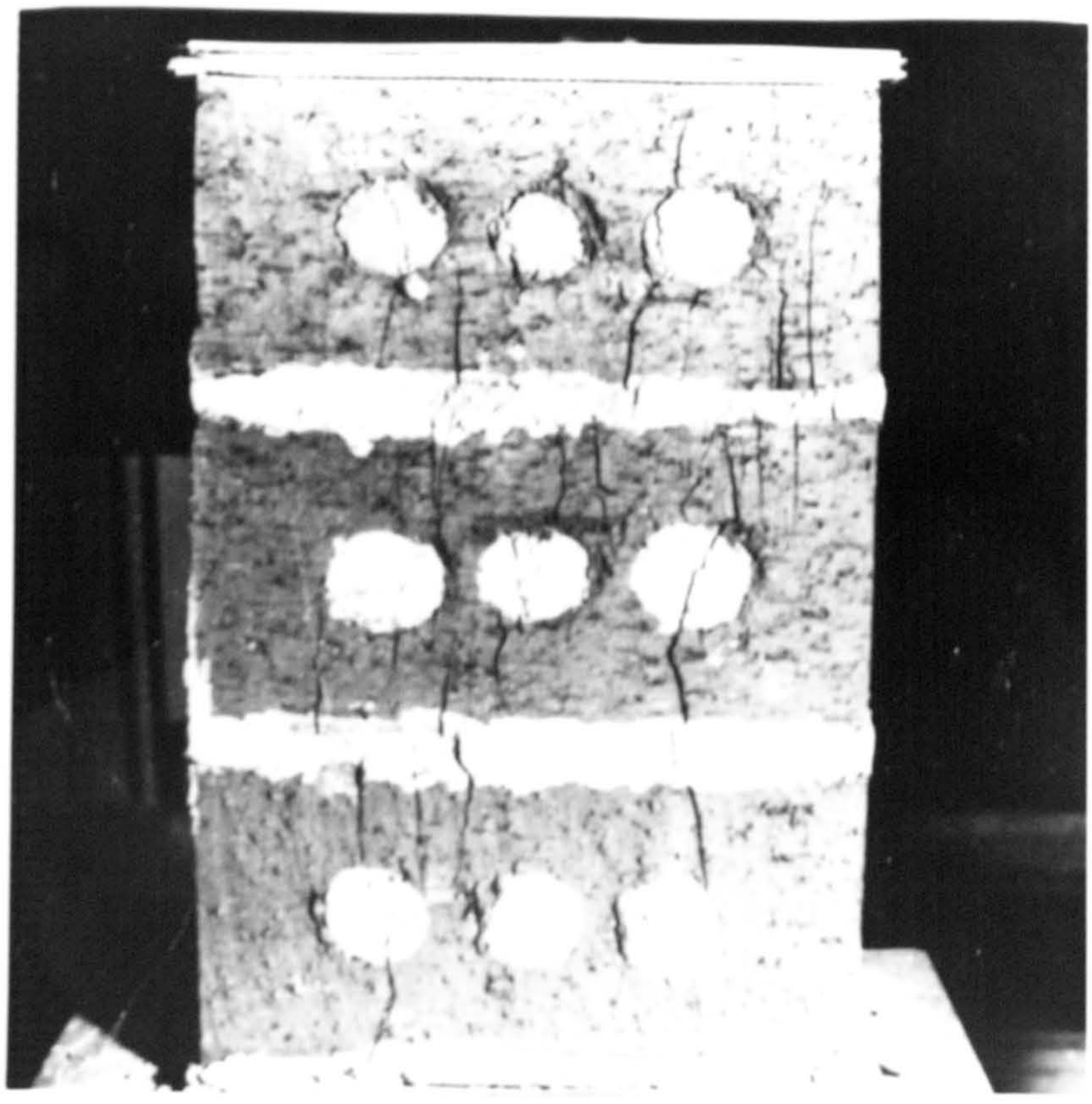

Plate 3.1

Typical failure of single course prism

Plate 3.2

Typical failure of three course prism

cause a 'buckling type' collapse of the prism.

Values for compressive strength of brickwork were derived from the axial compression tests. Table 3.6.1 summarises the test results obtained based on ultimate load and gross cross-sectional area.

For all types of brickwork the value of the average compressive strength for the single course prisms exceeds that of the three course prism. The average strength of all the single course prisms was 61% higher than the three course prisms, table 3.6.1. In the case of low strength brick prisms the difference was only 24%. Previous work[39,42] has shown that prisms built with a continuous mortar joint parallel to the direction of the applied load have a compressive strength lower than brickwork without the joint. In the past this reduction has been ascribed to the orthotropic nature of brickwork since comparisons were made with conventional stack-bonded prisms. This was not the case for the single and three course prisms since the bricks were stressed in the same direction and therefore the reduction must have been due to the vertical mortar joint. As discussed earlier upon separation of the courses the load may have been re-distributed unevenly in the three course prism. Failure of all three courses simultaneously did not occur and thus the average compressive strength of the three course prism was less than that for the individual course.

Recent tests[9] conducted on brickwork prisms of the same format built with similar bricks produced values for compressive strength similar to those in table 3.6.1. Pedreschi argued that the

Table 3.6.1

Compressive strength of brickwork prisms

Brick Type	Mortar		Prism Type	Compressive Strength				Sample Size
	Mix	Average Compr. Strength, N/mm²		Average (N/mm²)	Range (N/mm²)	Std. Dev. (N/mm²)	Coeff. of Variation %	
High Strength	1:¼:3	19.3	Single	33.10	24.67-47.90	5.75	17.39	23
			Three	20.55	13.80-28.84	3.72	18.08	16
High Strength	1:½:4½	7.6	Single	27.41	18.73-33.18	4.03	14.69	21
			Three	15.98	12.51-18.31	1.94	12.13	6
Medium Strength	1:¼:3	19.9	Single	19.43	15.77-24.99	2.59	13.32	9
			Three	11.80	10.63-13.00	0.99	8.42	6
Low Strength	1:¼:3	20.0	Single	7.27	6.17- 8.81	0.85	11.76	9
			Three	5.56	4.61- 6.73	0.90	16.12	6

brickwork properties of the three course prism were unlikely to provide an accurate estimate of the flexural capacity of a prestressed brickwork beam since the stress distribution at failure of the prism was non-uniform. The linear strain profile in the beams up to failure suggests that a re-distribution of stresses after splitting did not occur and therefore the average compressive strength of the three courses will be less than the brickwork strength at the outermost face at failure. Theoretically predicted ultimate moments for the full prestressed test beams supported this view point as the single course prisms were found to be inherently more accurate. The neutral axis depth at ultimate in the under-reinforced brickwork beams was observed to be within the top course, suggesting that the single course prisms were likely to provide the more accurate estimates for the flexural compressive strength of the partially prestressed brickwork beam section.

3.6.1.3 Stress/strain relationship for brickwork

The experimental stress/strain curves are presented in figures 3.6.5 - 3.6.8. The values for strain were calculated from the average of up to ten 'demec' strain readings at each load increment.

All of the stress/strain relationships show similar characteristics. Initially the relationships are linear at low levels of stress where the brickwork can be considered to be elastic. As the stress level increases the strain increases more rapidly until failure. It was not possible to measure the strain at or beyond the maximum compressive stress and hence there was no falling branch as

STRESS/STRAIN RELATIONSHIPS FOR HIGH STRENGTH BRICK, GRADE I MORTAR, THREE COURSE PRISMS

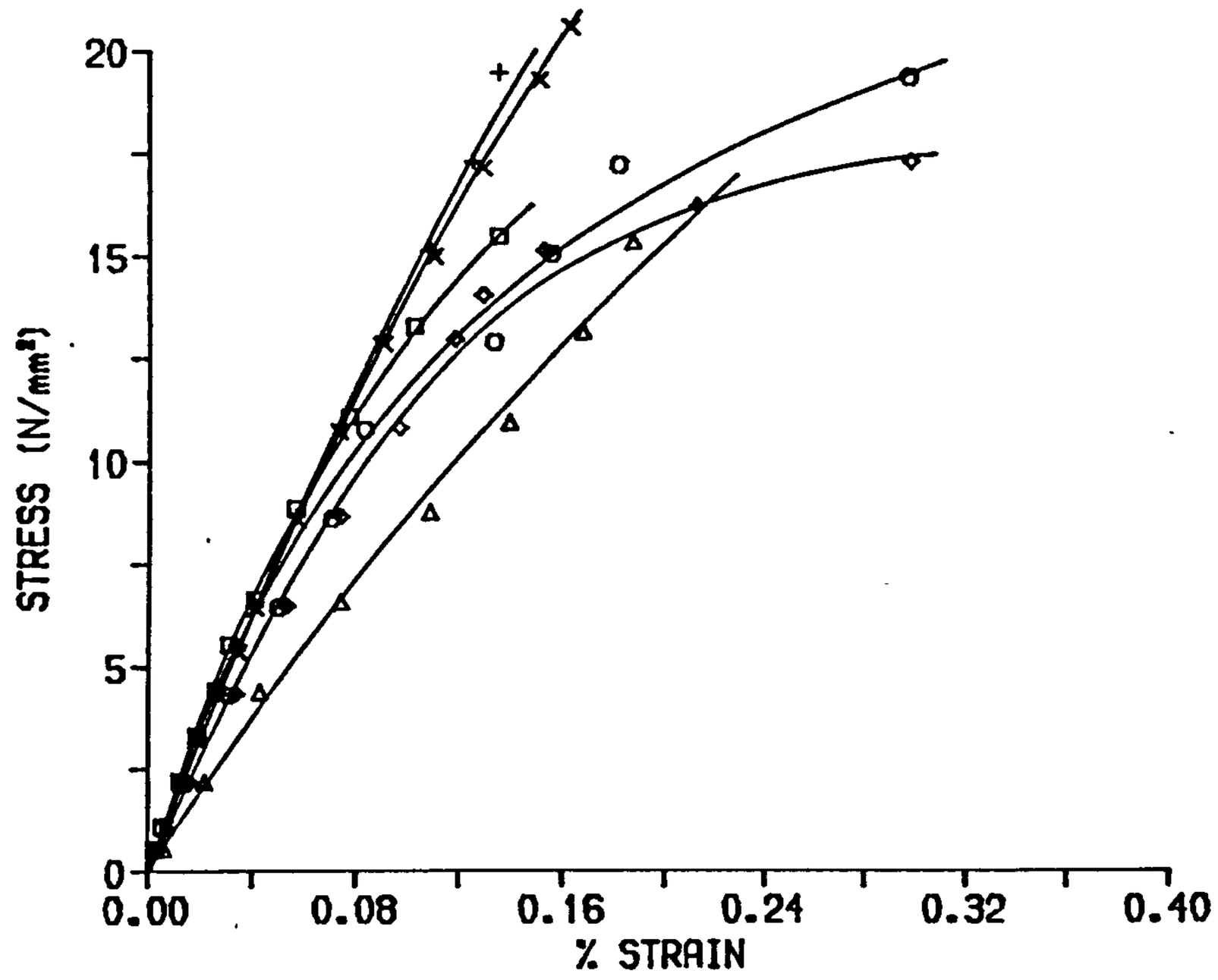

(a)

STRESS/STRAIN RELATIONSHIPS FOR HIGH STRENGTH BRICK, GRADE I MORTAR, SINGLE COURSE PRISMS

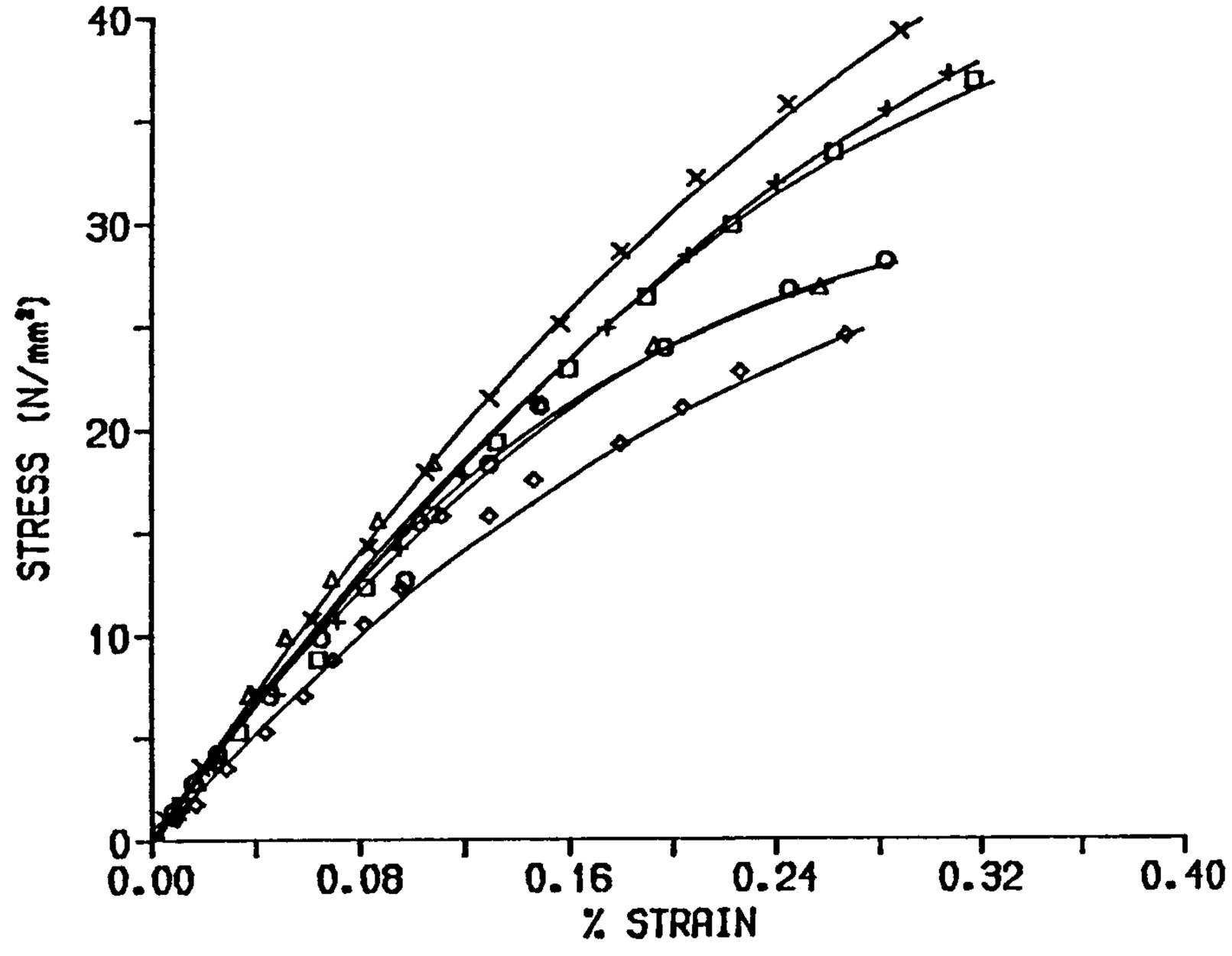

(b)

Figure 3.6.5

STRESS/STRAIN RELATIONSHIPS FOR HIGH STRENGTH BRICK, GRADE II MORTAR, THREE COURSE PRISMS

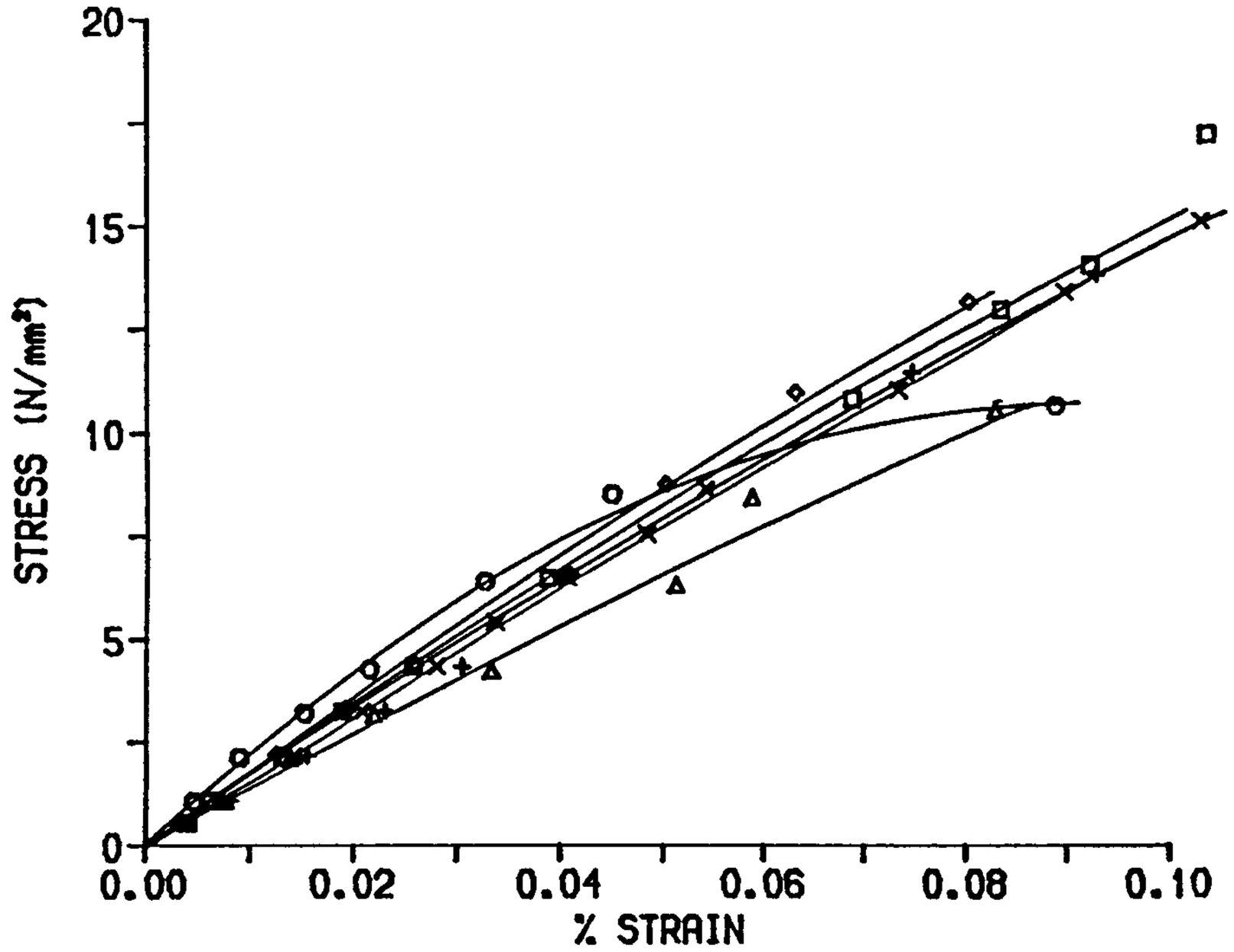

(a)

STRESS/STRAIN RELATIONSHIPS FOR HIGH STRENGTH BRICK, GRADE II MORTAR, SINGLE COURSE PRISMS

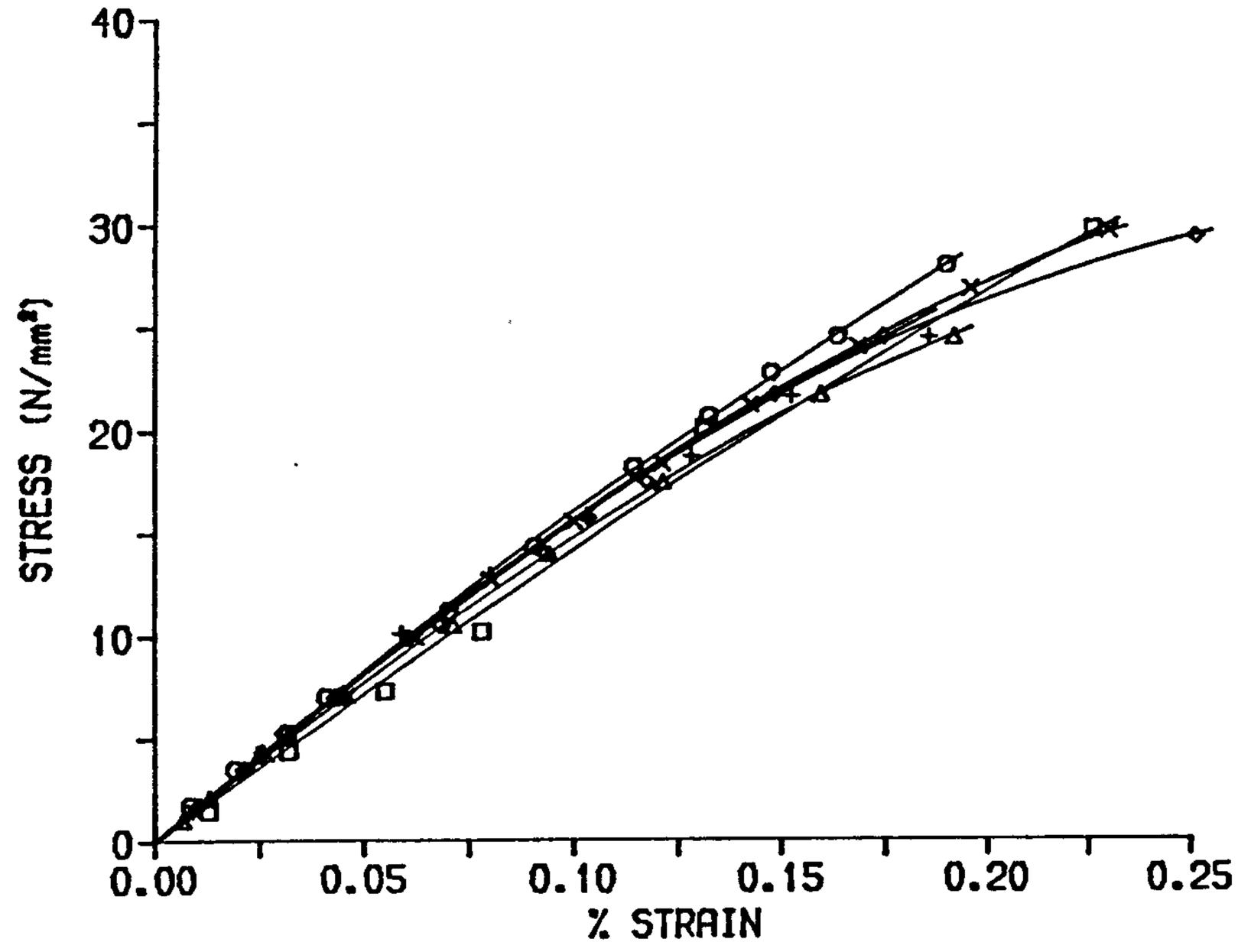

(b)

Figure 3.6.6

STRESS/STRAIN RELATIONSHIPS FOR MEDIUM STRENGTH BRICK, THREE COURSE PRISMS

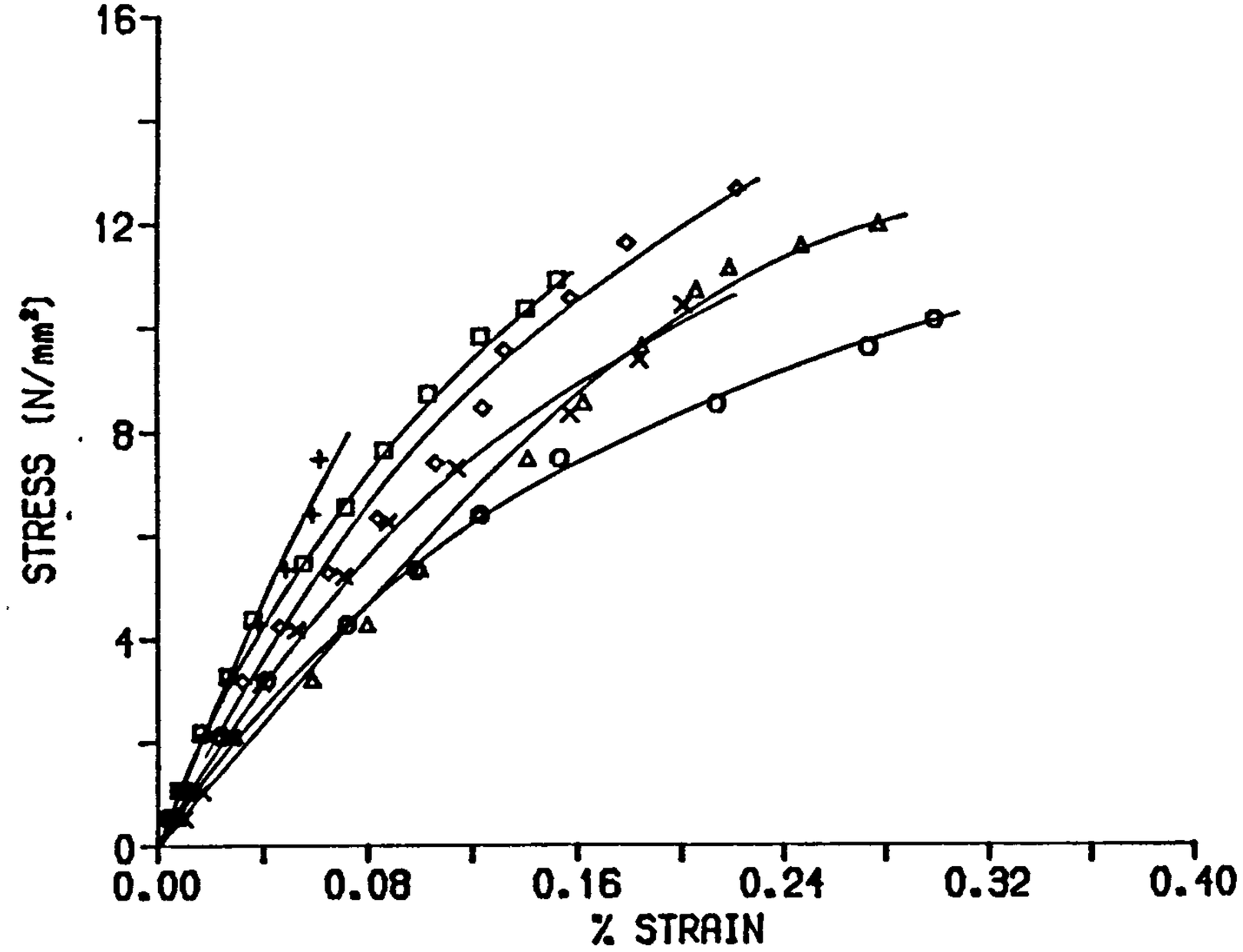

(a)

STRESS/STRAIN RELATIONSHIPS FOR MEDIUM STRENGTH BRICK, SINGLE COURSE PRISMS

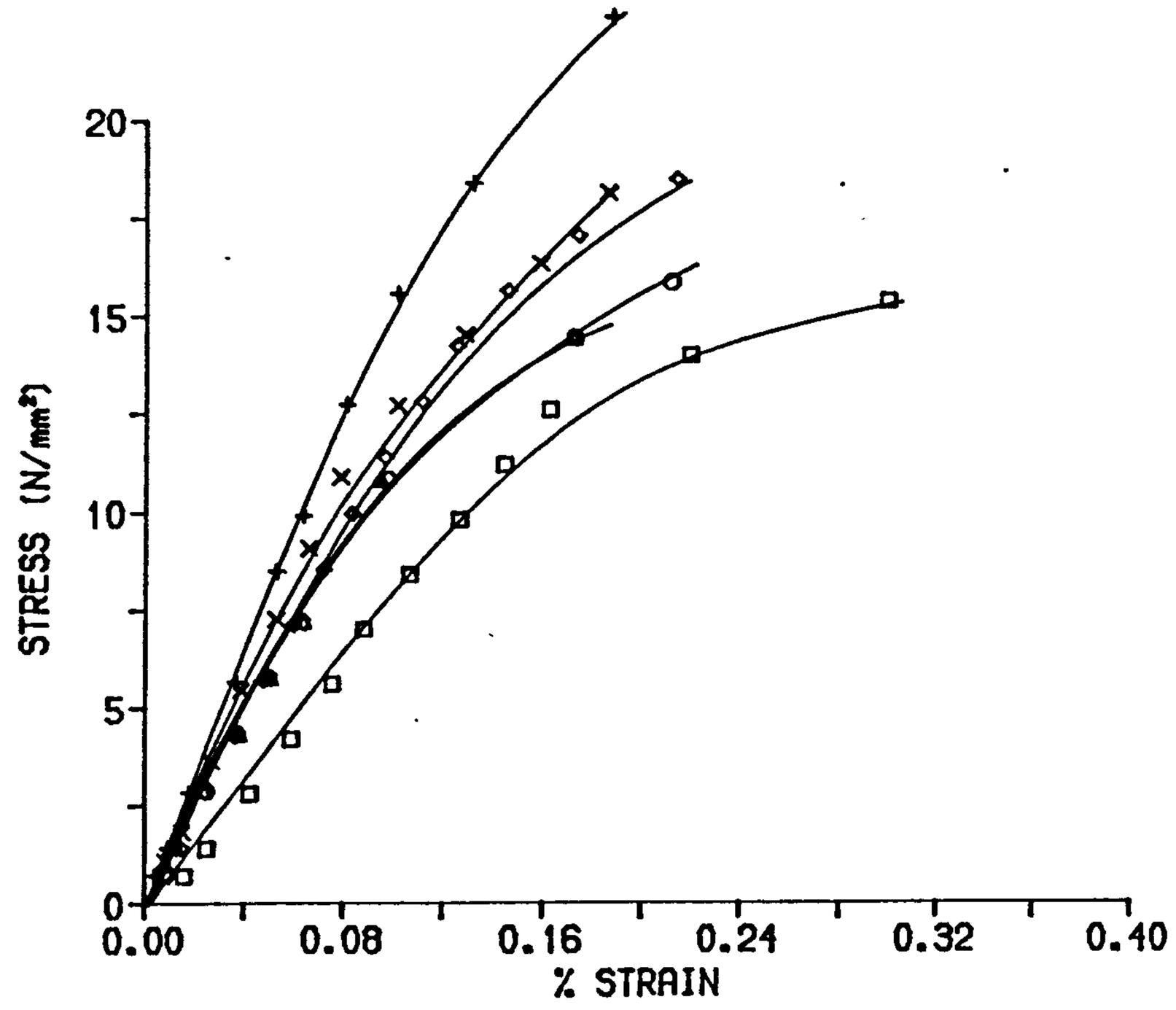

(b)

Figure 3.6.7

STRESS/STRAIN RELATIONSHIPS FOR LOW STRENGTH BRICK, THREE COURSE PRISMS

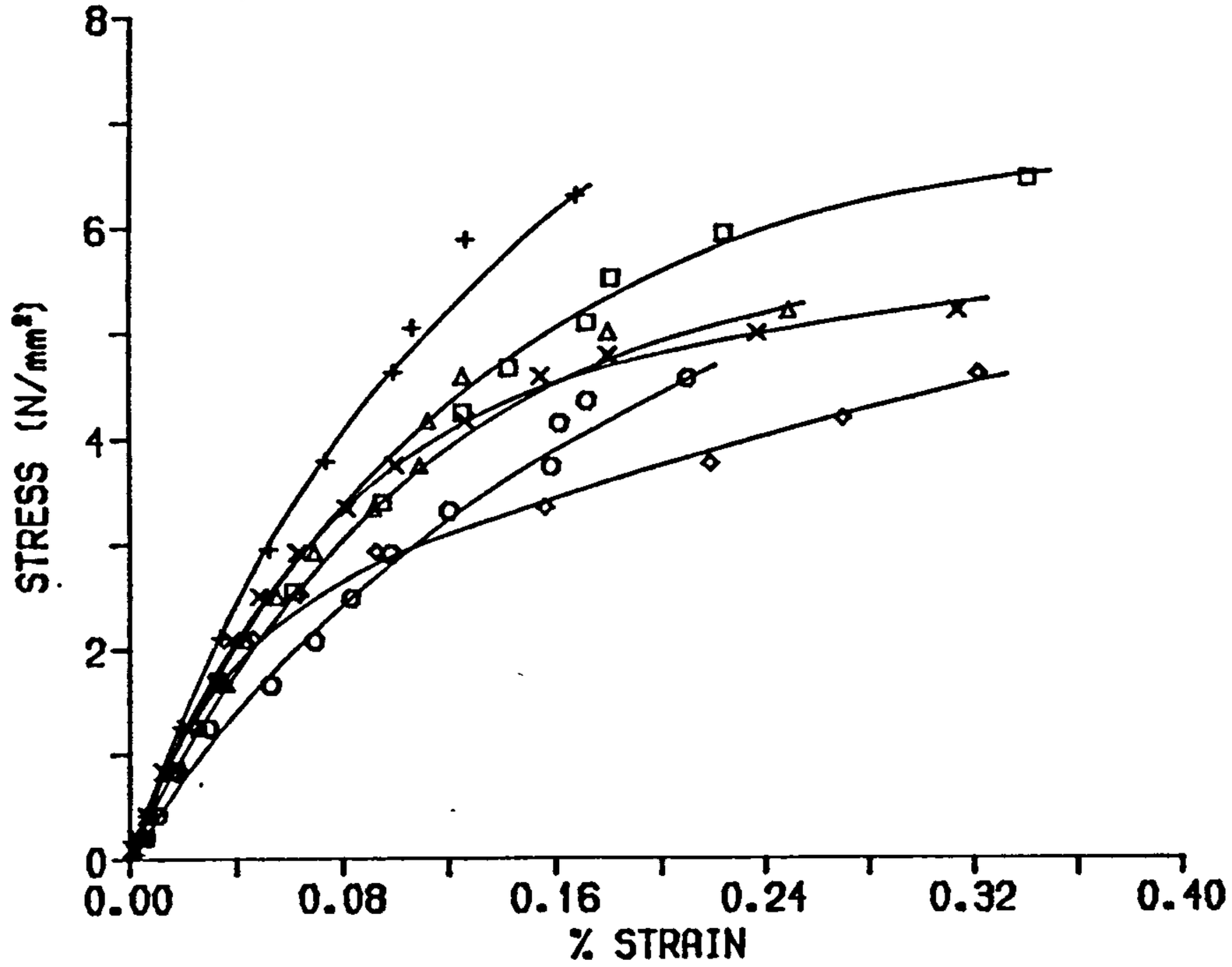

(a)

STRESS/STRAIN RELATIONSHIPS FOR LOW STRENGTH BRICK, SINGLE COURSEPRISMS

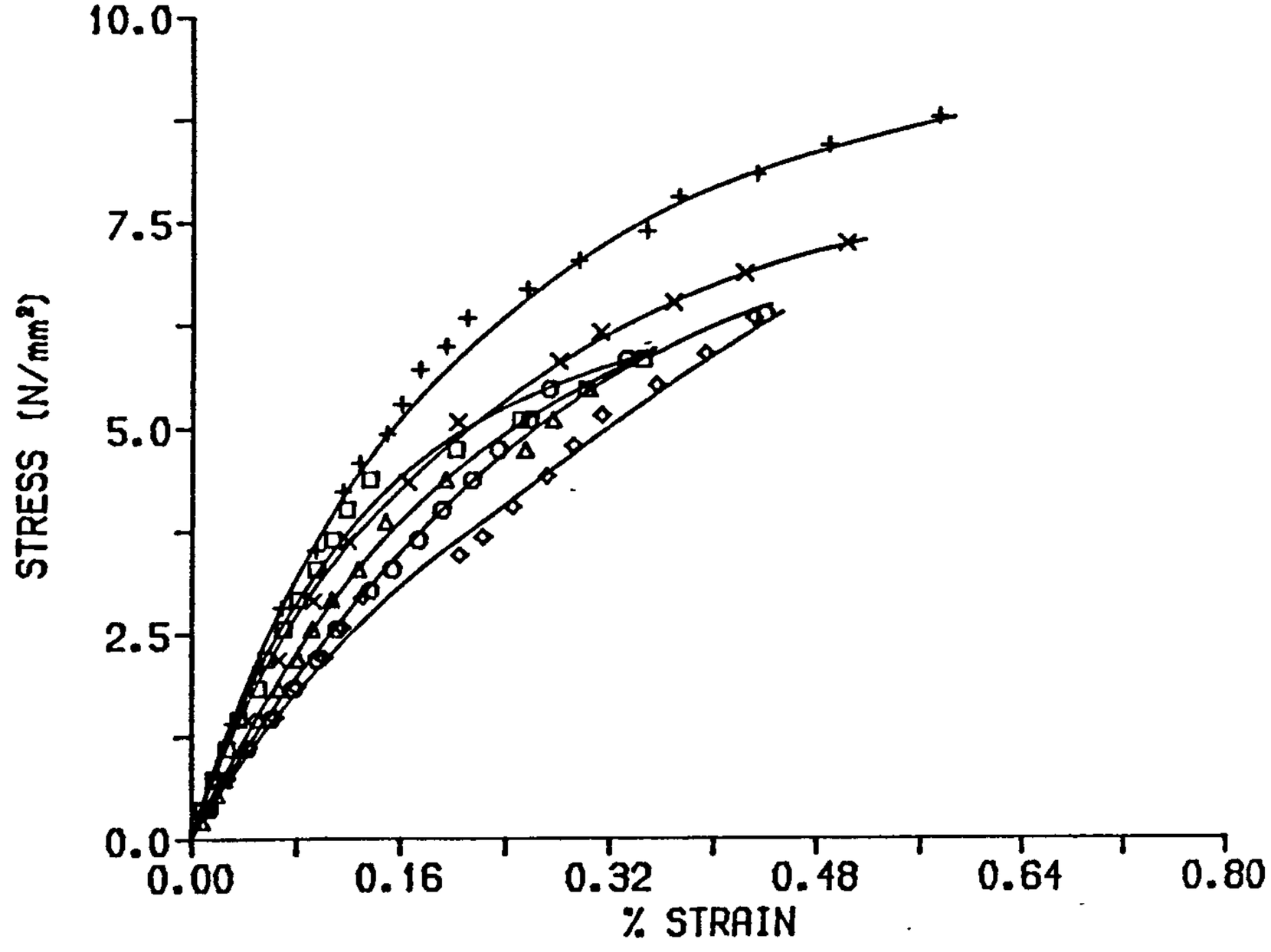

(b)

Figure 3.6.8

in brickwork loaded normal to the bed-joint[53]. Work carried out by Hodgkinson and Davies[42], and Pedreschi[9] indicated that the falling branch was absent for brickwork prisms when stressed in a direction other than normal to the bed-joint. Since failure of the prisms was very explosive it is reasonable to assume that there is no falling branch for the brickwork tested in this work.

It was not possible to measure the strain at failure and therefore the values of ultimate strain, table 3.6.2, were mathematically extrapolated from the experimental stress/strain relationship for each prism, figures 3.6.5 - 3.6.8.

The ultimate strain varied between 0.00111 and 0.00476, table 3.6.2. In all cases the average ultimate strain in the single course prisms was greater than the value for the corresponding three course prisms. The average ultimate compressive strain for all of the single and three course prisms was 0.00366 and 0.00224 respectively. The value from the single course prisms agrees well with that recommended by the British standard code of practice[15], ε_m = 0.00350.

The experimental stress/strain relationships of the axially loaded prisms exhibited some variation between individual prisms of the same material and format, figures 3.6.5 - 3.6.8. To overcome the experimental variation research carried out in the past has expressed stress/strain relationships of concrete[54] and brickwork[55] in a non-dimensional form. Theoretical prediction of the flexural behaviour required the stress/strain properties of the brickwork to be expressed in a mathematical form. Using a least squares

Table 3.6.2

Ultimate compressive strain of brickwork prisms

Brick Type	Mortar	Prism Type	Average Compressive Strength N/mm²	Ultimate compressive strain			
				Average	Range	Standard Deviation	Coeff of Variation %
High Strength	1:¼:3	Single	33.10	0.00353	0.00250 - 0.00472	0.00045	12.7
		Three	20.55	0.00254	0.00160 - 0.00452	0.00086	33.8
High Strength	1:½:4½	Single	27.41	0.00332	0.00211 - 0.00470	0.00079	23.8
		Three	15.98	0.00111	0.00093 - 0.00149	0.00024	21.6
Medium Strength	1:¼:3	Single	19.43	0.00303	0.00252 - 0.00370	0.00043	14.1
		Three	11.80	0.00243	0.00164 - 0.00344	0.00068	28.1
Low Strength	1:¼:3	Single	7.27	0.00476	0.00273 - 0.00651	0.00105	22.1
		Three	5.56	0.00287	0.00191 - 0.00399	0.00069	24.0

approximation it was possible to combine the experimental results of each brick and prism type to derive the non-dimensional stress/strain relationship as a third degree polynomial, figure 3.6.9, such that:

$$f/f_m = X_1(\varepsilon/\varepsilon_m) - X_2(\varepsilon/\varepsilon_m)^2 + X_3(\varepsilon/\varepsilon_m)^3 \qquad (3.6.1)$$

Values for X_1, X_2 and X_3 are given in table 3.6.3 and the average curves are presented in figures 3.6.10 - 3.6.13. The individual results were used in the calculation of the behaviour of the beams and prediction of the stress blocks of the eccentrically loaded brickwork. The experimental variation associated with the individual stress/strain curves was reduced by expressing the relationships non-dimensionally.

The values for X_1, X_2 and X_3 were very similar for all types of brickwork with the exception of the low strength brick prisms. Combining results of all the axially loaded prisms the following general expression was derived, figure 3.6.14:

$$f/f_m = 2.12(\varepsilon/\varepsilon_m) - 1.78(\varepsilon/\varepsilon_m)^2 + 0.66(\varepsilon/\varepsilon_m)^3 \qquad (3.6.2)$$

3.6.1.4 Stress distributions in eccentrically loaded brickwork

The eccentrically loaded prisms were tested to model the compression zone behaviour of the partially prestressed beams and so ascertain the influence of the strain gradient upon the development of the compressive stress distribution. Brickwork stresses cannot be directly measured and therefore the stress distribution in each of the eccentrically loaded prisms was derived from the measured strain profiles using the stress/strain relationship for brickwork given by

NON-DIMENSIONAL STRESS/STRAIN RELATIONSHIP

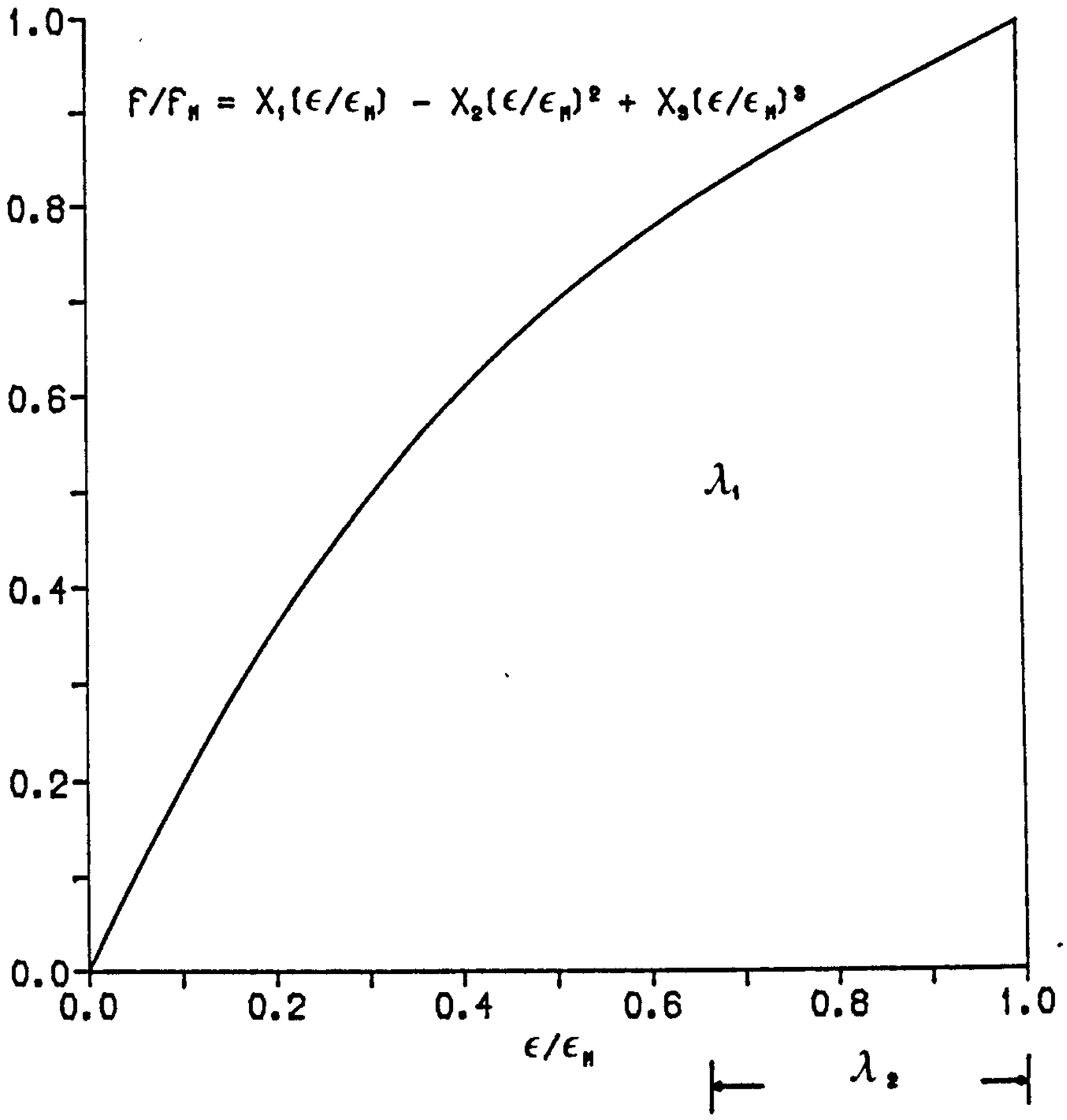

Figure 3.6.9

Table 3.6.3

Stress/strain relationship coefficients and stress block factors

Brick Type	Mortar	Prism Type	Stress/strain relationship coefficients			Stress block factors	
			X_1	X_2	X_3	λ_1	λ_2
High Strength	1:¼:3	Single	1.958	1.596	0.636	0.606	0.372
		Three	1.956	1.548	0.599	0.612	0.371
High Strength	1:½:4½	Single	2.005	1.566	0.565	0.622	0.373
		Three	1.739	1.040	0.276	0.592	0.375
Medium Strength	1:¼:3	Single	2.094	1.556	0.466	0.645	0.376
		Three	1.965	1.586	0.621	0.609	0.372
Low Strength	1:¼:3	Single	2.868	3.655	1.804	0.663	0.396
		Three	2.663	2.840	1.171	0.678	0.393

NON-DIMENSIONAL STRESS/STRAIN RELATIONSHIP FOR HIGH STRENGTH BRICK, GRADE I MORTAR, THREE COURSE PRISM

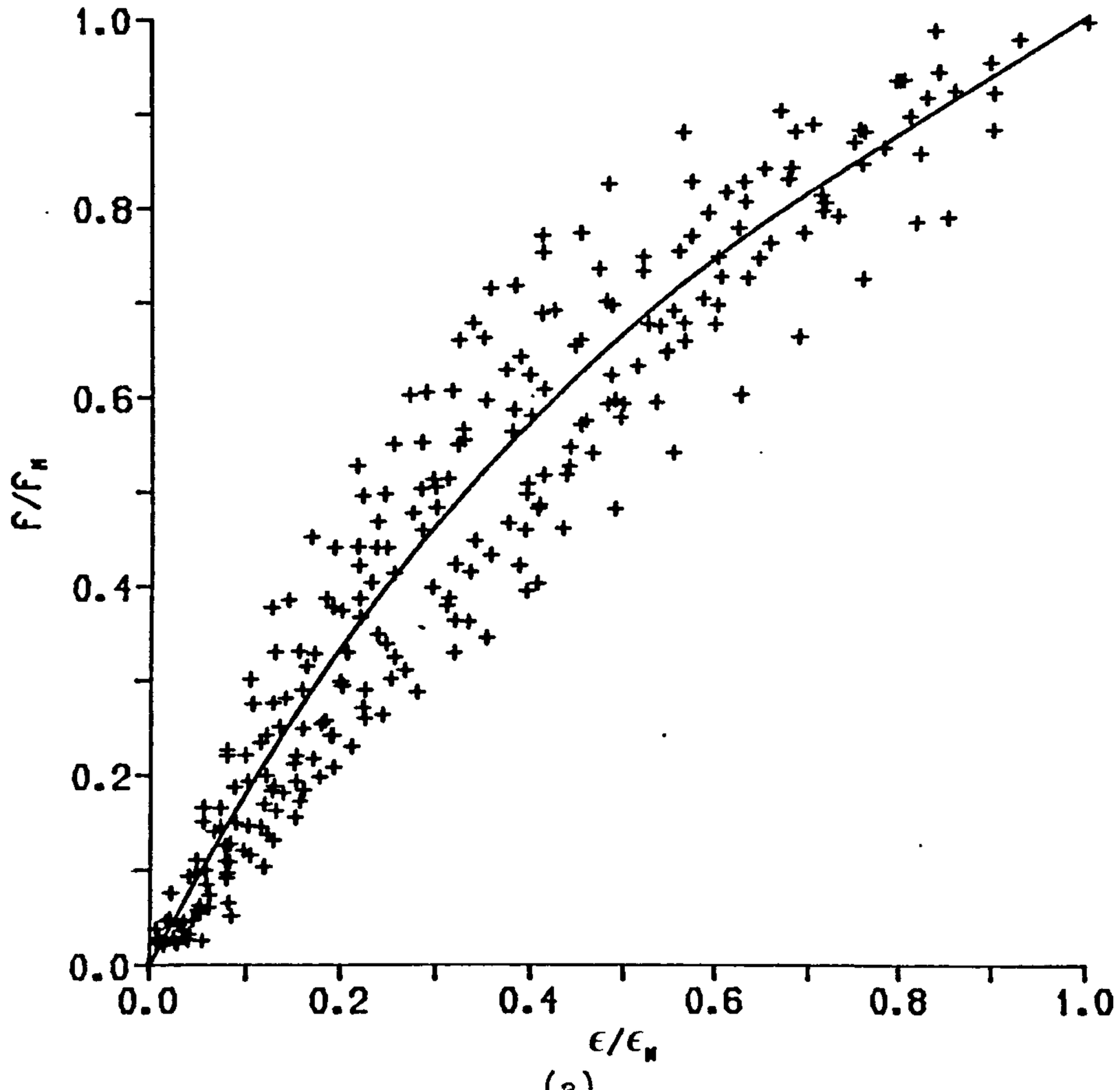

(a)

NON-DIMENSIONAL STRESS/STRAIN RELATIONSHIP FOR HIGH STRENGTH BRICK, GRADE I MORTAR, SINGLE COURSE PRISM

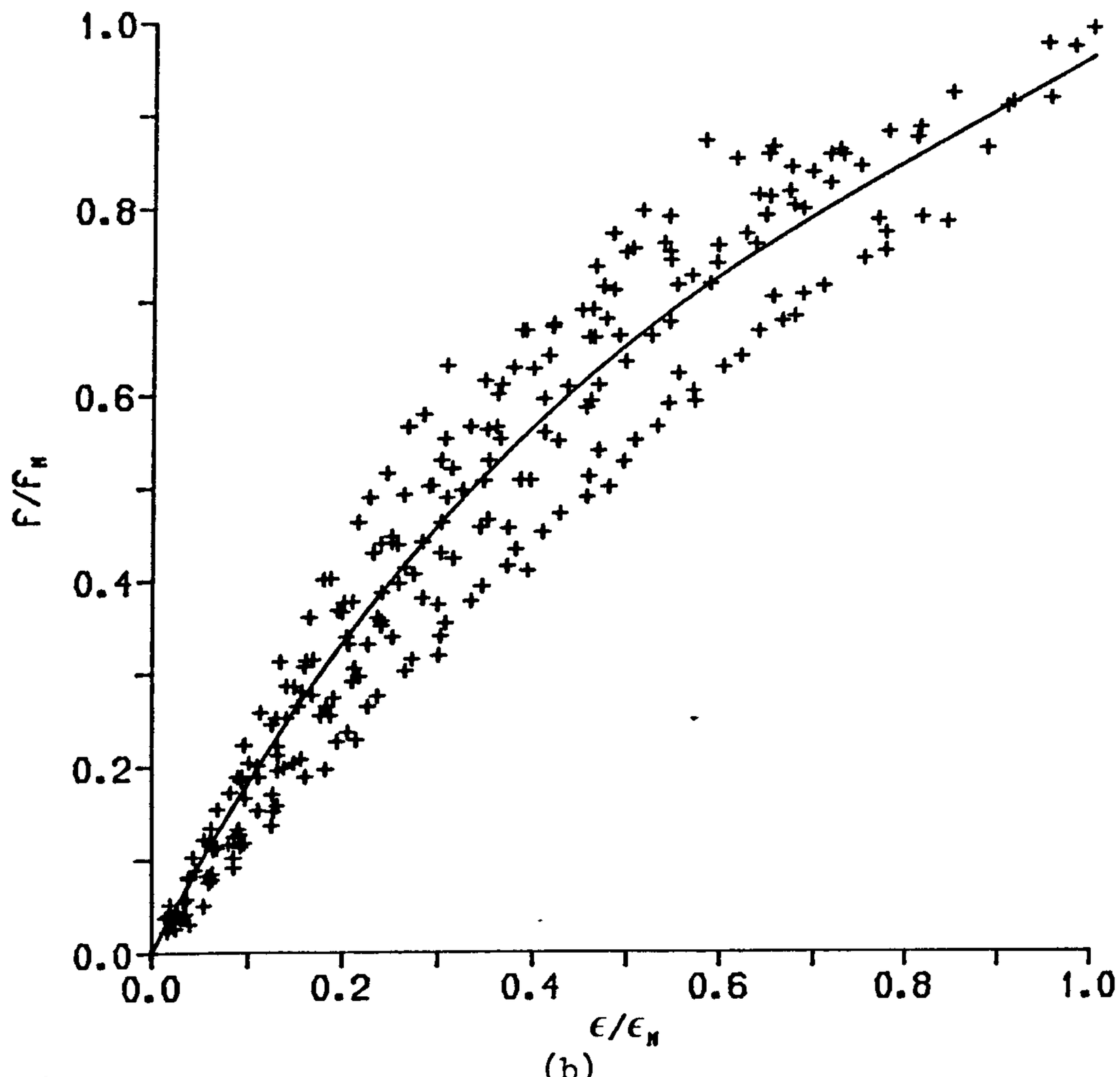

(b)

Figure 3.6.10

NON-DIMENSIONAL STRESS/STRAIN RELATIONSHIP FOR HIGH STRENGTH BRICK, GRADE II MORTAR, THREE COURSE PRISM

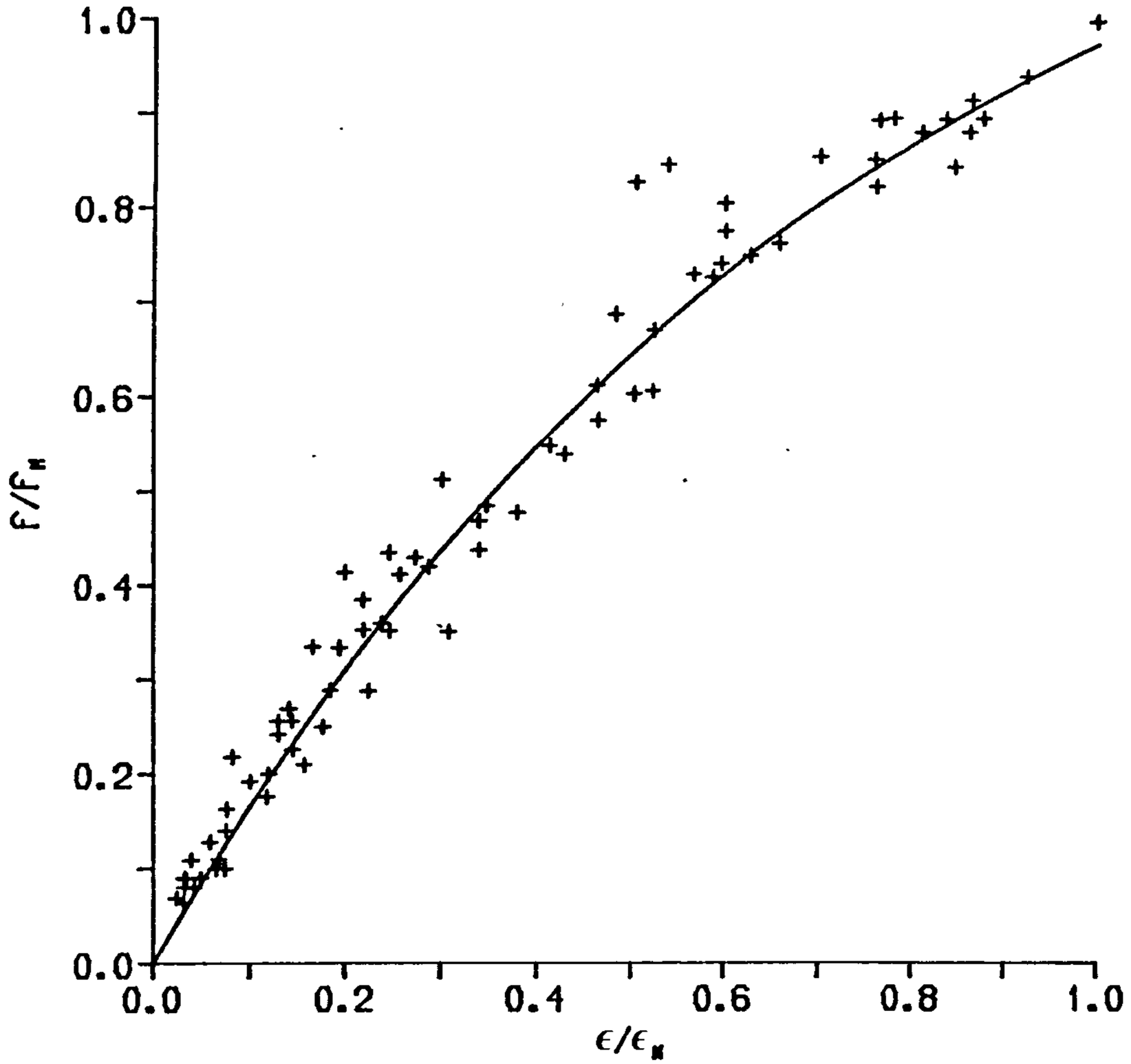

(a)

NON-DIMENSIONAL STRESS/STRAIN RELATIONSHIP FOR HIGH STRENGTH BRICK, GRADE II MORTAR, SINGLE COURSE PRISM

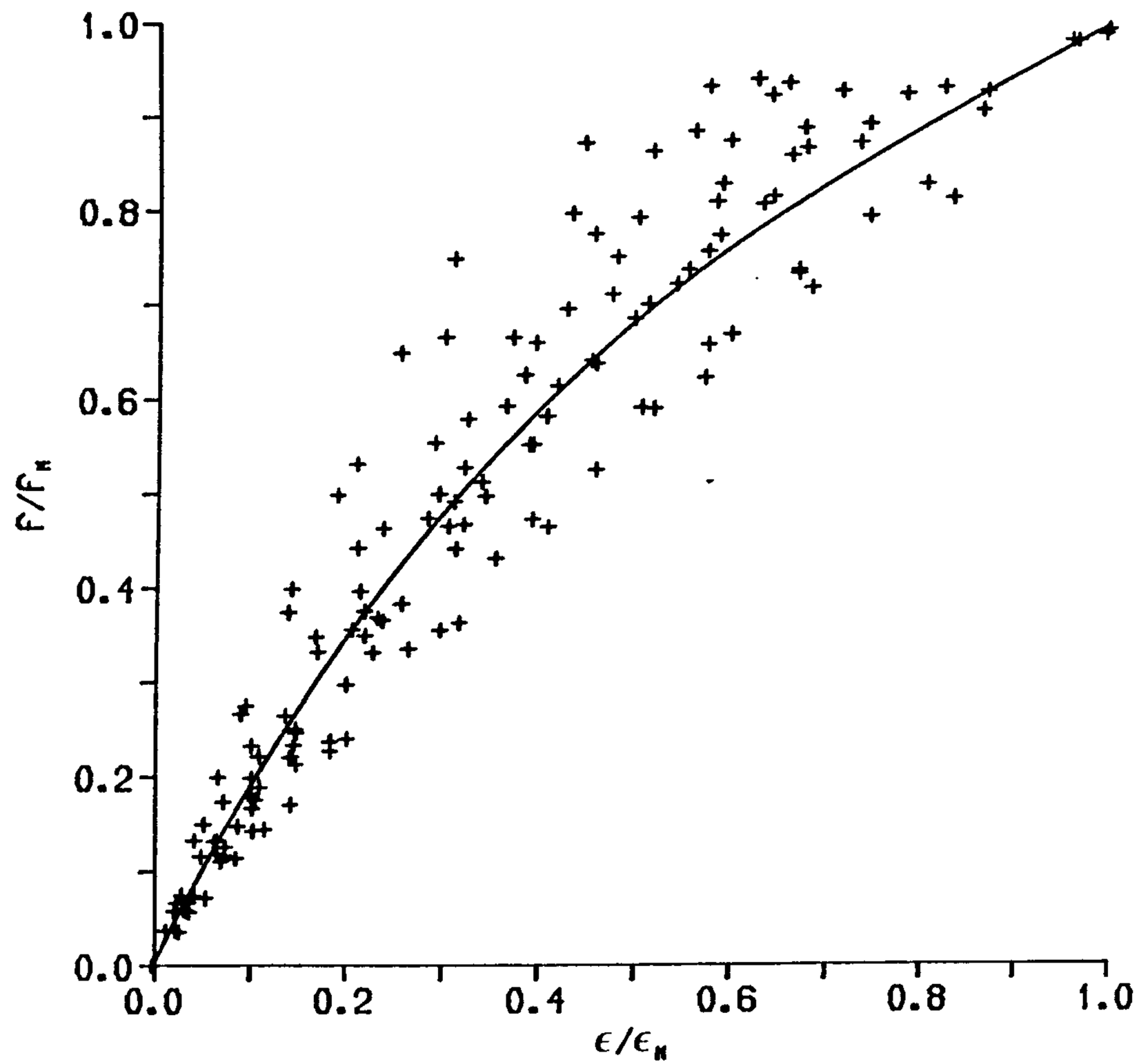

(b)

Figure 3.6.11

NON-DIMENSIONAL STRESS/STRAIN
RELATIONSHIP FOR MEDIUM STRENGTH BRICK
THREE COURSE PRISM

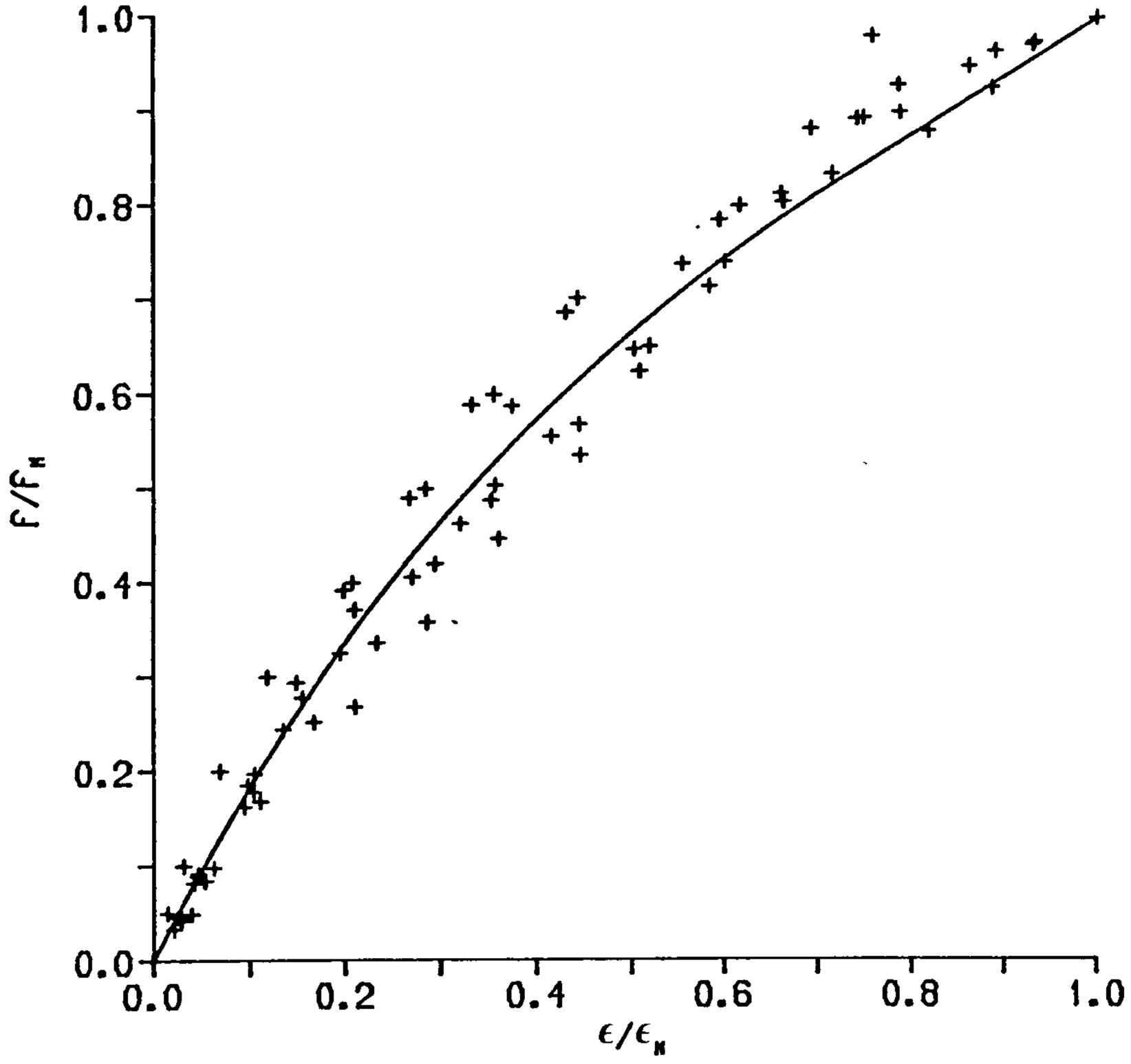

(a)

NON-DIMENSIONAL STRESS/STRAIN
RELATIONSHIP FOR MEDIUM STRENGTH BRICK
SINGLE COURSE PRISM

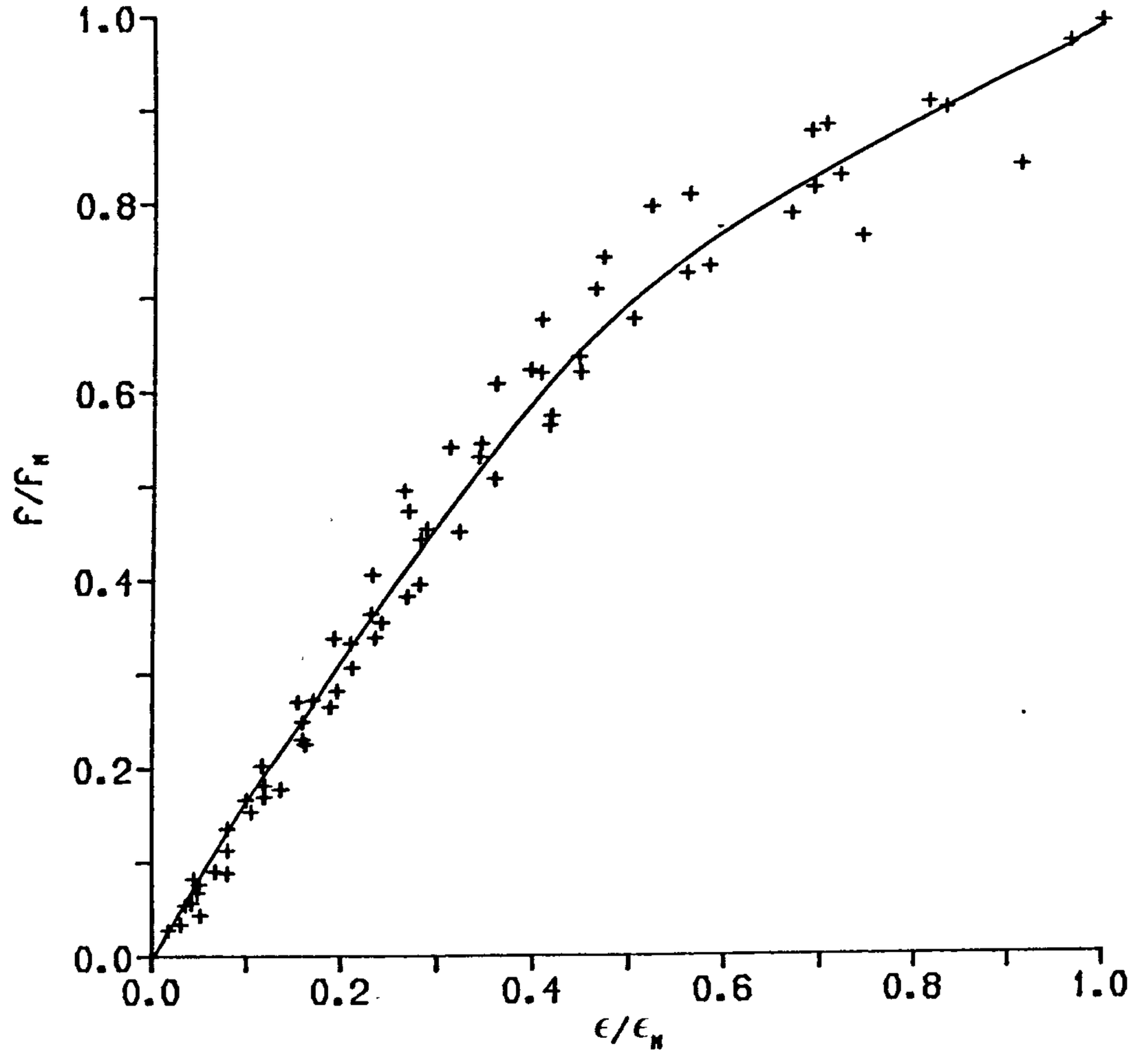

(b)

Figure 3.6.12

NON-DIMENSIONAL STRESS/STRAIN RELATIONSHIP FOR LOW STRENGTH BRICK, THREE COURSE PRISM

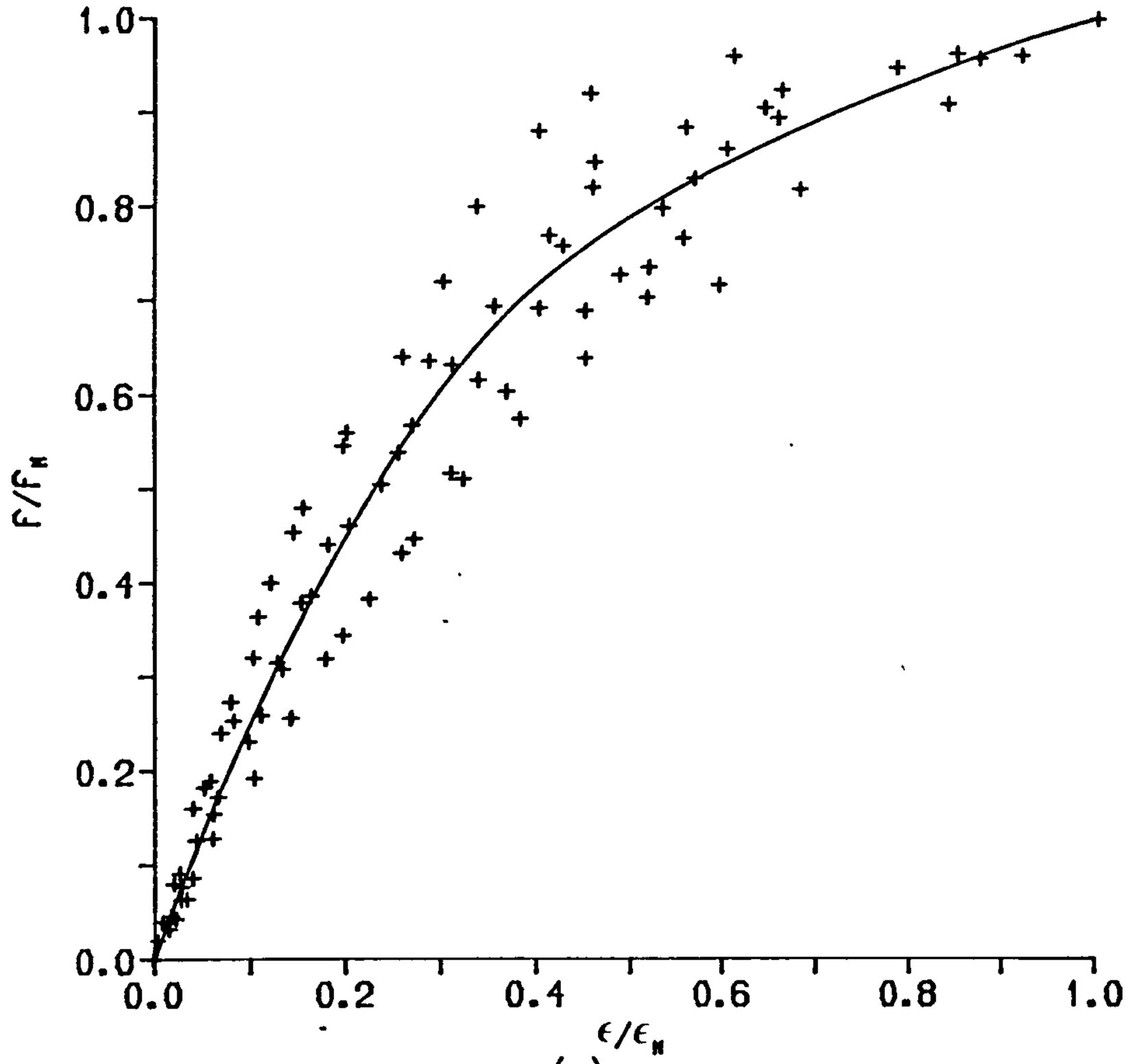

(a)

NON-DIMENSIONAL STRESS/STRAIN RELATIONSHIP FOR LOW STRENGTH BRICK, SINGLE COURSE PRISM

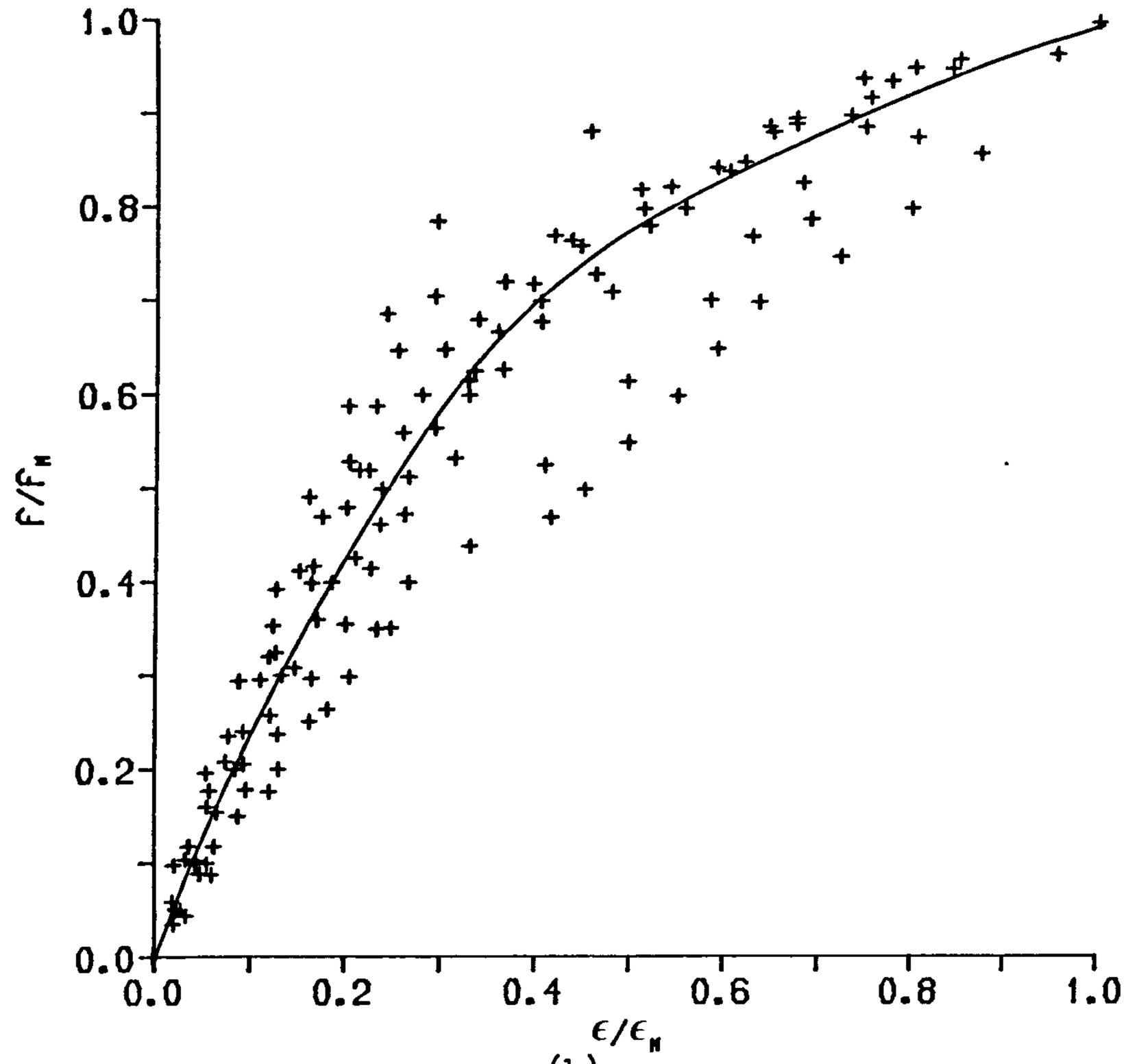

(b)

Figure 3.6.13

NON-DIMENSIONAL STRESS/STRAIN
RELATIONSHIP FOR BRICKWORK

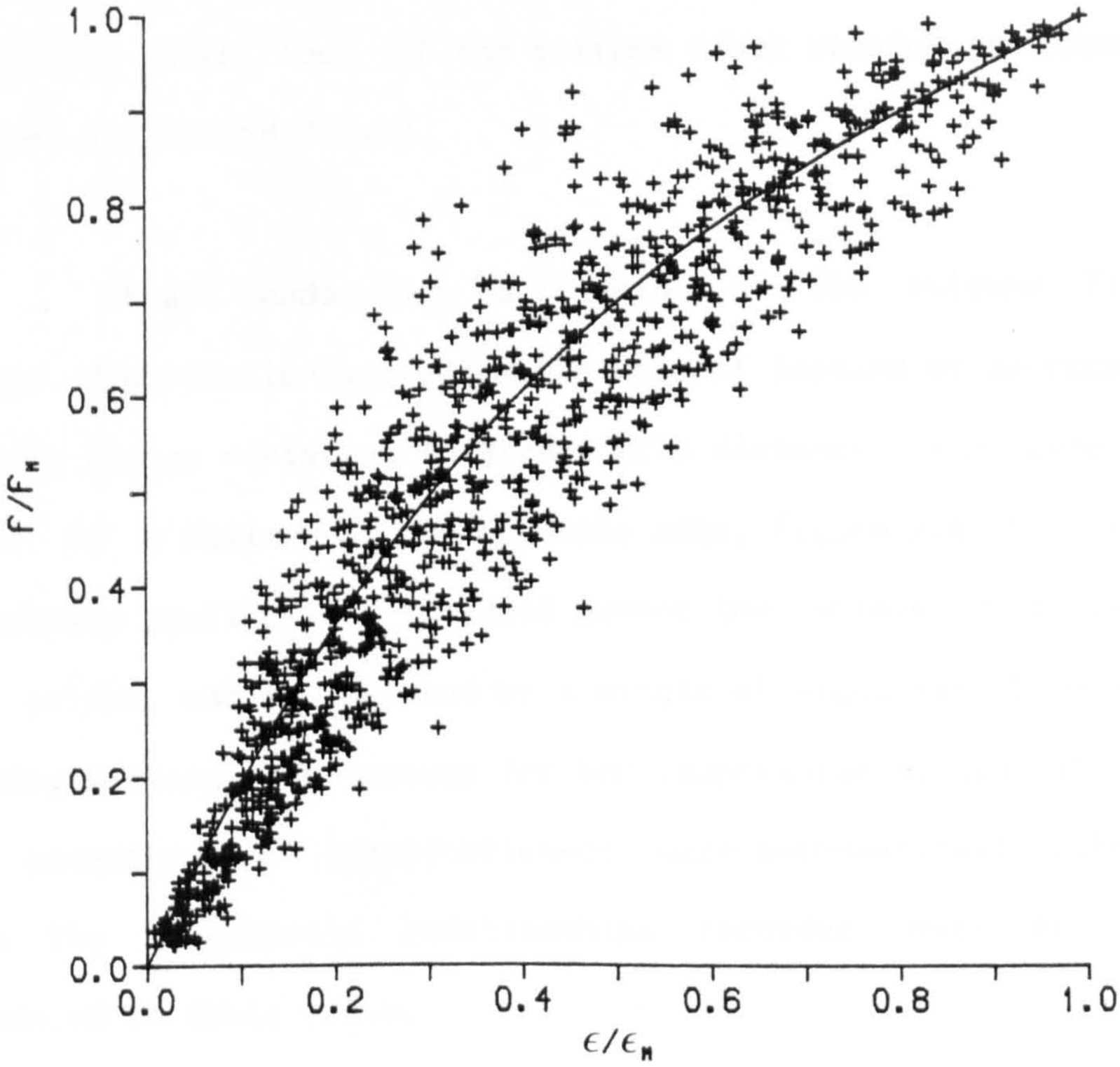

Figure 3.6.14

the axially loaded single course prism tests, section 3.6.1.3.

Strain was measured across the breadth of each prism up to approximately 95% of the ultimate load, a typical strain distribution for the eccentricaly loaded brickwork is shown in figure 3.6.15. Variations with load of the extreme fibre strains are presented in figures 3.6.16 and 3.6.17.

At all loads prior to crushing of the extreme fibre the strain distribution was characteristic of loading at an eccentricity of t/6; linear variation in strain with distance from zero at one fibre to a maximum at the opposite edge, figure 3.6.15. Similar to the strain profile in a flexural member the strain distribution in the prisms was represented by a single straight line throughout the loading history. The values for the compressive strain at ultimate for eccentrically loaded brickwork were mathematically extrapolated from the load/strain relationships recorded prior to failure, presented in table 3.6.4.

Crushing of the brickwork was observed at between 75% and 90% of the ultimate load. After crushing the effective width of the section resisting the compressive stresses was reduced and as a result the line of action of the load was applied outside of the 'kern' limit and consequently tensile strains were recorded at the fibre opposite to crushing, figures 3.6.15 - 3.6.17. The compressive strains at ultimate derived from the eccentrically loaded tests exceeded the corresponding values from axial tests by up to 42% and 300% for grade I and II mortar brickwork respectively. Values derived from the eccentrically loaded tests were influenced by local

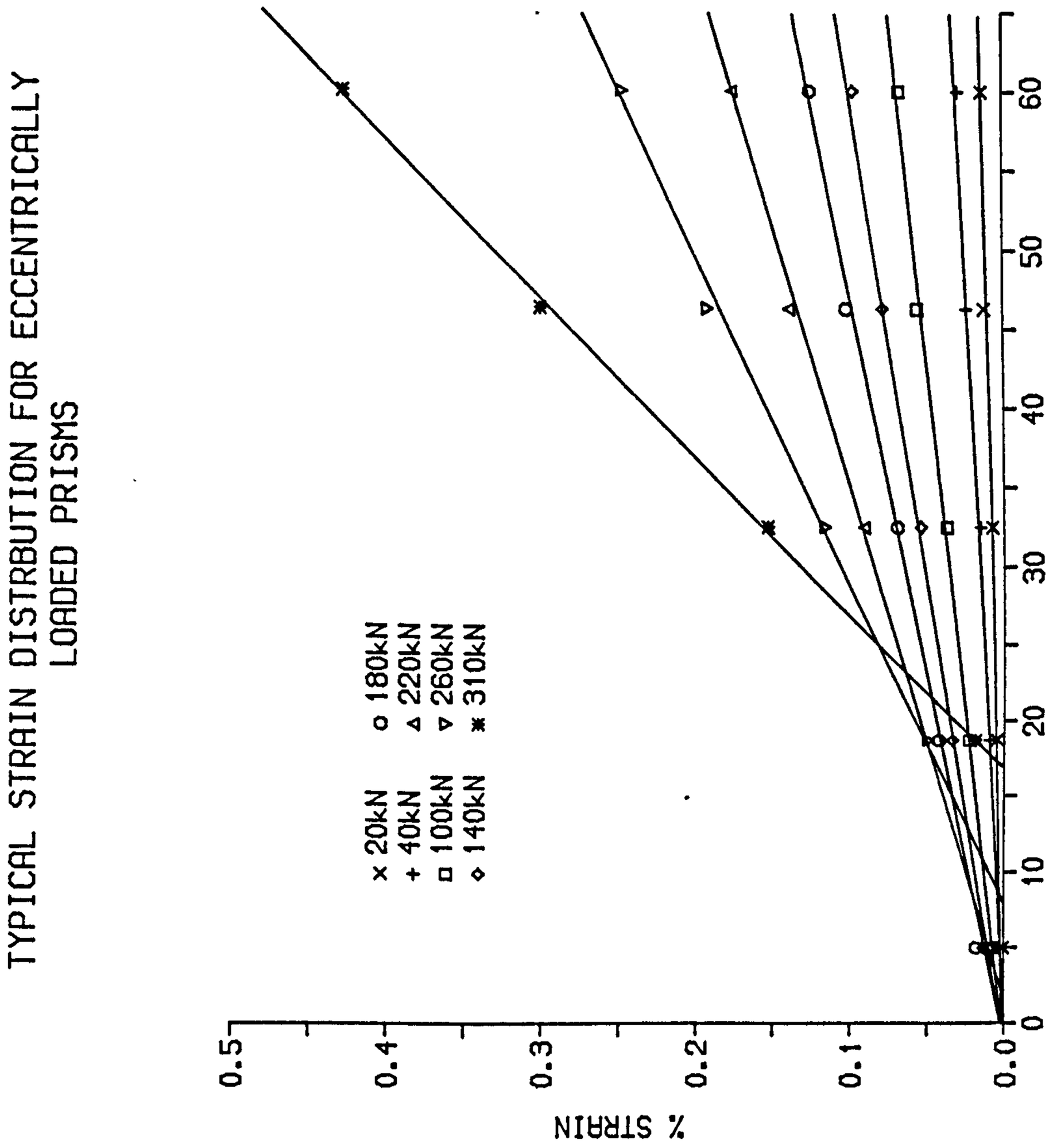
TYPICAL STRAIN DISTRBUTION FOR ECCENTRICALLY
LOADED PRISMS
o 180kN
▲ 220kN
▽ 260kN
* 310kN
× 20kN
+ 40kN
□ 100kN
◇ 140kN
% STRAIN
0.5
0.4
0.3
0.2
0.1
0.0
0
10
20
30
40
50
60
BREADTH (mm)

Figure 3.6.15

LOAD/STRAIN RELATIONSHIPS FOR ECCENTRICALLY LOADED PRISMS, HIGH STRENGTH BRICK, GRADE I MORTAR

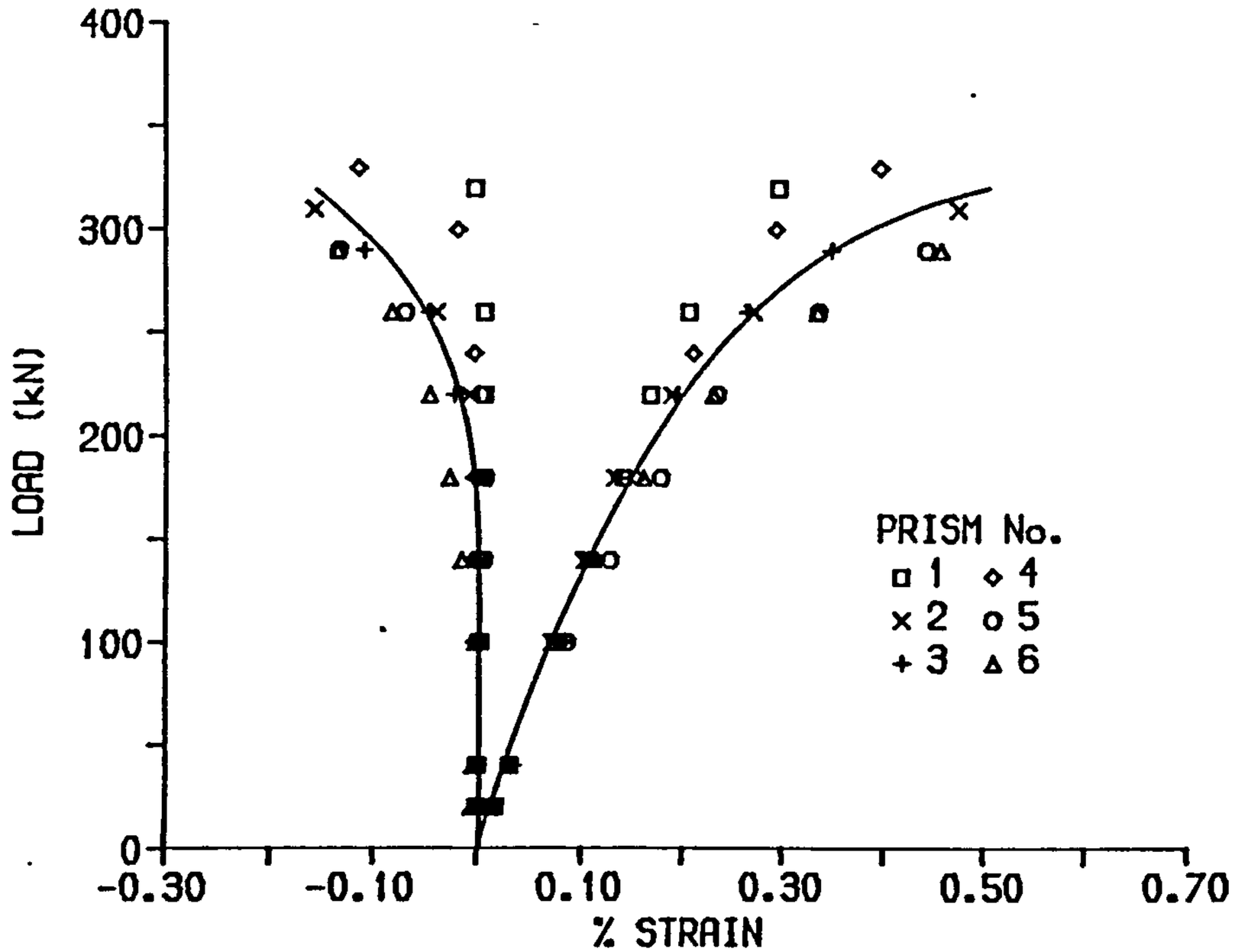

Figure 3.6.16

LOAD/STRAIN RELATIONSHIPS FOR ECCENTRICALLY LOADED PRISMS, HIGH STRENGTH BRICK, GRADE II MORTAR

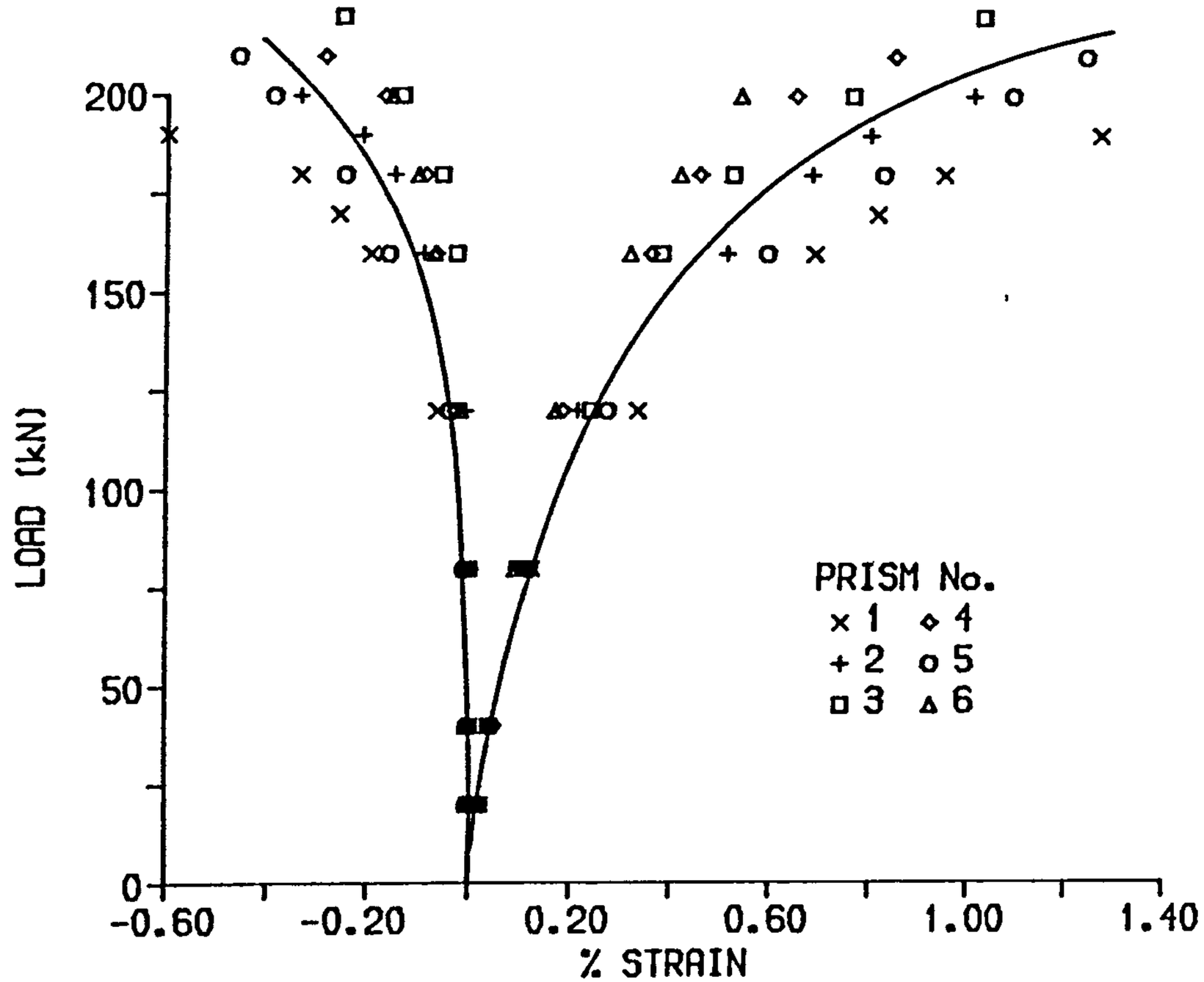

Figure 3.6.17

Table 3.6.4

Summary of Eccentrically loaded prism tests

Brick Strength	Mortar Strength N/mm^2	Prism Number	Ultimate Load kN	Ult. Compr. Strain
High	23.8	1	294	0.00454
		2	400	0.00428
		3	325	0.00477
		4	340	0.00420
		5	302	0.00500
		6	300	0.00460
		Average:	327	0.00450
		Coeff of Var	12.2%	6.6%
High	7.6	1	190	0.0127
		2	211	0.0116
		3	231	0.0133
		4	214	0.00856
		5	210	0.0124
		6	230	0.00880
		Average:	214	0.0112
		Coeff of Var	7.1%	182%

effects at the point of measurement such as crushing and spalling of the brickwork, the strains measured were due to the continued deformation of the prism after the initial crushing. It is therefore reasonable to propose that the values in table 3.6.4 do not represent the actual ultimate compressive strain for eccentrically loaded brickwork. Crushing of the brickwork and the introduction of tension into the section occurred once the compression strain exceeded the ultimate compressive strain derived from axial prism tests, ε_m, figure 3.6.15 and 3.6.17. Crushing occurs immediately the brickwork has exceeded its compressive strength. The compressive strain recorded at the time of crushing was equal to the ultimate strain from the axial single course prism, table 3.6.2. By inference the ultimate compressive strain in the axial and eccentrically loaded prisms was equal. The presence of a strain gradient across the width of the prism has had no effect upon the magnitude of the ultimate compressive strain for brickwork.

The experimental stress/strain relationships for brickwork, section 3.6.1.3, were used together with the measured strain distributions of the eccentrically loaded prisms to determine the compressive stress distributions at ultimate. The stress was calculated at a number of positions across the breadth of each prism using the single course prism stress/strain relationships. The stress distributions thus plotted, are illustrated in figures 3.6.18 and 3.6.19. The stress distributions were plotted non-dimensionally to minimise the experimental variation between individual results. As the ultimate compressive strain was unchanged by the eccentric loading the compressive strength will also remain the same by use of the non-dimensional stress/strain relationship. Initially the

AVERAGE STRESS BLOCK AT FAILURE
FOR HIGH STRENGTH BRICK, GRADE I MORTAR

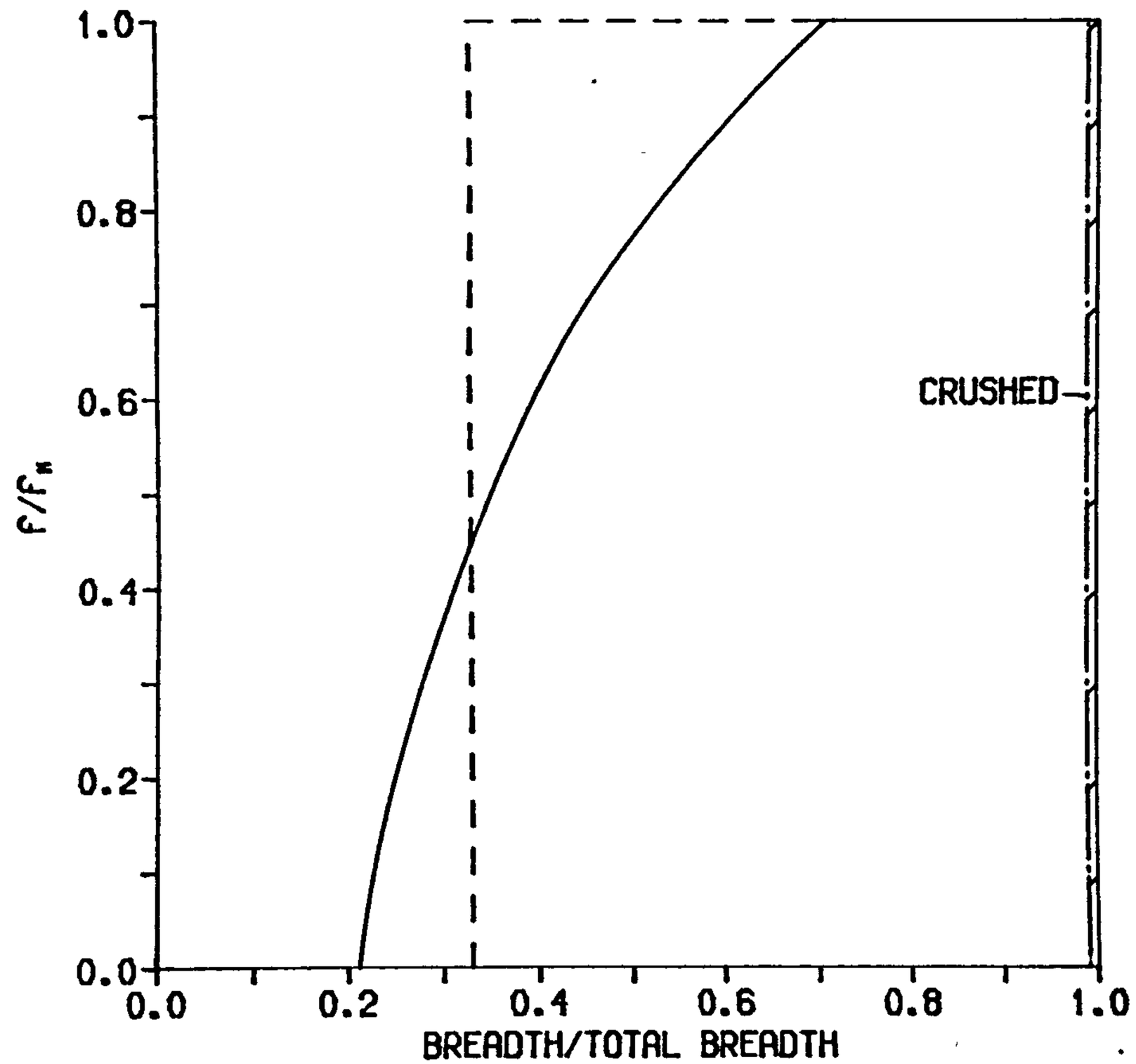

Figure 3.6.18

AVERAGE STRESS BLOCK AT FAILURE FOR
HIGH STRENGTH BRICK, GRADE II MORTAR

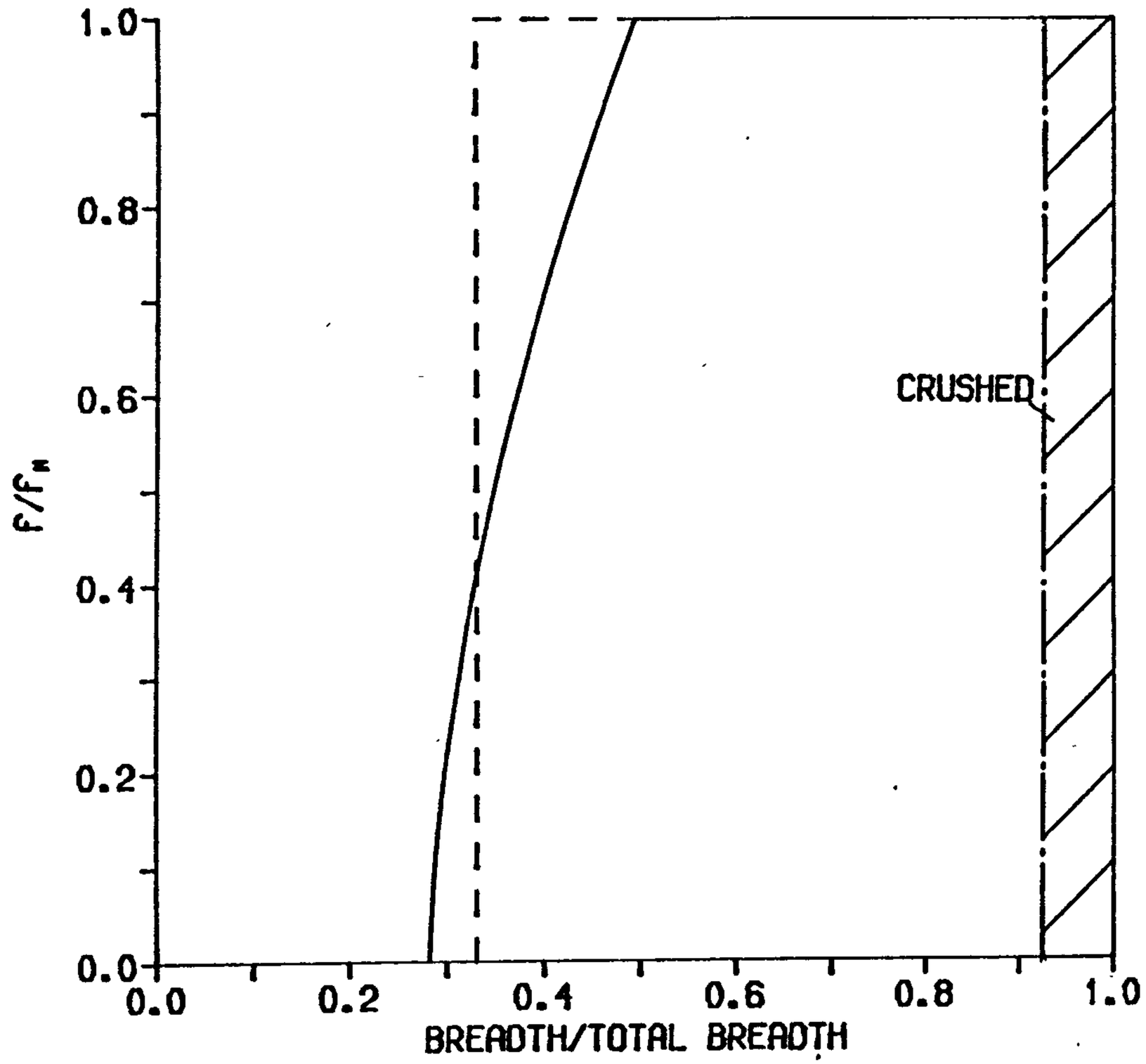

Figure 3.6.19

development of the stress distributions the ultimate stress was assumed to remain constant at f_m once the strain had exceeded ε_m. The stress distributions were later modified for the proportion of the section that had crushed.

At failure only approximately 75% of the section was resisting the compressive stresses, the remaining part of the section was in tension due to the revised eccentricity of the load. Between zero and maximum compressive strength the equation of the curve representing the stress distribution was equal to that of the stress/strain relationship. Compressive strains were measured up to 1.33% and clearly the brickwork at that point had crushed. By taking moments about the line of action of the load, i.e. at the centre of gravity of the stress distribution, it was possible to determine the width of cross-section that was no longer effective in resisting the compression. The width of the prism thus calculated and so assumed to be crushed is shown as a shaded region in figures 3.6.18 and 3.6.19.

Experimentally it was not possible to determine whether the stress/strain relationship exhibited a falling branch, section 3.6.1.3. Although throughout this work the falling branch has been assumed not to be present it is of interest to determine the influence of assuming a falling branch on deriving the stress distribution for the eccentric prisms. The stress/strain relationship used by Beard[56] suggests a falling branch with a cut-off point of $1.5\varepsilon_m$. However, if this limit is applied to the eccentric prism tests the centre of gravity of the calculated stress distribution is no longer in equilibrium with the line of action of

the load. This was due to the reduction in stress beyond f_m and also cut-off of the stress/strain relationship at $1.5\varepsilon_m$. This would suggest that the parabolic stress/strain relationship with a falling branch is not applicable to the brickwork used in this investigation.

The calculated stress distributions may be back substituted to predict the corresponding ultimate load, table 3.6.5. The process was repeated for approximately 80% of the ultimate load, the load corresponding to the commencement of crushing of the brickwork. Excellent agreement is shown for both of the loading levels which demonstrates the accuracy and validity of the technique to determine the stress distributions in eccentrically loaded brickwork. The experimental ultimate loads are also compared in table 3.6.5 with values predicted using the rectangular stress distribution as suggested by BS 5628, Part 1[3] for eccentrically loaded masonry. A very good correlation was illustrated when using the rectangular stress block with the experimental value for average compressive strength of brickwork, f_m, from the single course prisms.

Summarising, the results of the eccentrically loaded prism tests indicate that the ultimate compressive strength and strain remain unchanged by the presence of the strain gradient and therefore the axial single course prisms are likely to provide accurate estimates for the compressive properties of the brickwork beam section. Since the axial and eccentric prism tests provide the same value for compressive stength it is necessary to test only the axial prisms as the experimental procedure and data processing for axial prisms is more simplified and not dependent upon the results of other tests.

Table 3.6.5

Comparison of experimental and predicted loading

for eccentrically loaded prisms

Mortar Strength N/mm²	Ultimate load			Approximately 0.8 x Ultimate load	
	Experimental Load kN	Non-linear stress block kN	Rectangular stress block kN	Average Expt. load kN	Non-linear kN
23.8	327	311	308	277	282
7.6	214	219	255	171	193

3.6.2 Stress block characteristics

An understanding of the magnitude and relative position of the resultant forces in the compression zone of a brickwork beam is necessary to predict the ultimate flexural strength. This section considers firstly the experimentally derived stress block characteristics and then compares the results with previous research[9,56-58] and also with the recommendations of the British standard code of practice for reinforced and prestressed masonry[15].

The distribution of compressive stresses and therefore the resultant forces are defined by the stress block factors λ_1 and λ_2, as defined in figure 3.6.9.

λ_1 is equivalent to the area under the non-dimensional stress/strain curve and is the ratio of the compressive strength to the average compressive stress in the compression zone, given by:

$$\lambda_1 = \int_0^1 \left[X_1(\varepsilon/\varepsilon_m) - X_2(\varepsilon/\varepsilon_m)^2 + X_3(\varepsilon/\varepsilon_m)^3 \right] d(\varepsilon/\varepsilon_m) \qquad (3.6.3)$$

λ_2 defines the position of the centroid of the area under the non-dimensional stress block, stress/strain curve, measured from $\varepsilon/\varepsilon_m = 1$, figure 3.6.9, and therefore defines the line of action of the resultant compressive force in the compression zone, given by:

$$\lambda_2 = 1 - \frac{\int_0^1 \left[(\varepsilon/\varepsilon_m)(X_1(\varepsilon/\varepsilon_m) - X_2(\varepsilon/\varepsilon_m)^2 + X_3(\varepsilon/\varepsilon_m)^3) \right] d(\varepsilon/\varepsilon_m)}{\lambda_1} \qquad (3.6.4)$$

Experimental values for λ_1 and λ_2 were determined from the non-dimensional stress/strain curves of the axially loaded single and

three course prisms, table 3.6.4. Results for λ_1 vary between 0.592 and 0.678 and for λ_2 between 0.371 and 0.396. The stress block factors may be considered independent of the brickwork properties and prism format since there was little variation. Average values for λ_1 and λ_2, derived from equation 3.6.2. may be taken as 0.629 and 0.376 respectively.

The stress distributions for the eccentrically loaded brickwork were used to derive stress block factors λ_1 and λ_2. Results are presented in table 3.6.6 and are also compared with the corresponding stress block factors for the axial prism tests. Although superficially the shape of the stress block differs significantly between the axial prisms, figures 3.6.10 - 3.6.13, and eccentric prisms, figures 3.6.18 and 3.6.19, the magnitudes of the stress block factors remain comparatively unchanged.

The recent renewal of interest in brickwork as a structural material has seen a number of authors[9,56-58] propose stress blocks for brickwork. Sinha[58] has used successfuly a cubic parabolic stress/strain relationship for brickwork to predict the ultimate moment of reinforced brickwork beams, stress block factors $\lambda_1 = 0.75$ and $\lambda_2 = 0.40$, figure 3.6.20. Later Sinha[57] also used a curve-linear stress block obtained from axial prism tests, the predicted ultimate moment using the properties of stress block were similar to those using the parabolic stress/strain relationship. Beard[56] adopted a parabolic stress/strain relationship for brickwork, figure 3.6.20, showed that for a reinforced beam with a rectangular section the compressive face was maximum when $\varepsilon/\varepsilon_m = 1.5$, the stress block factors $\lambda_1 = 0.75$ and $\lambda_2 = 0.417$ were very similar

Table 3.6.6

Comparison of stress block characteristics

Mortar Grade	Axial, single course prisms		Eccentric prisms	
	λ_1	λ_2	λ_1	λ_2
I	0.606	0.372	0.672	0.333
II	0.622	0.373	0.572	0.333

TYPICAL STRESS BLOCKS

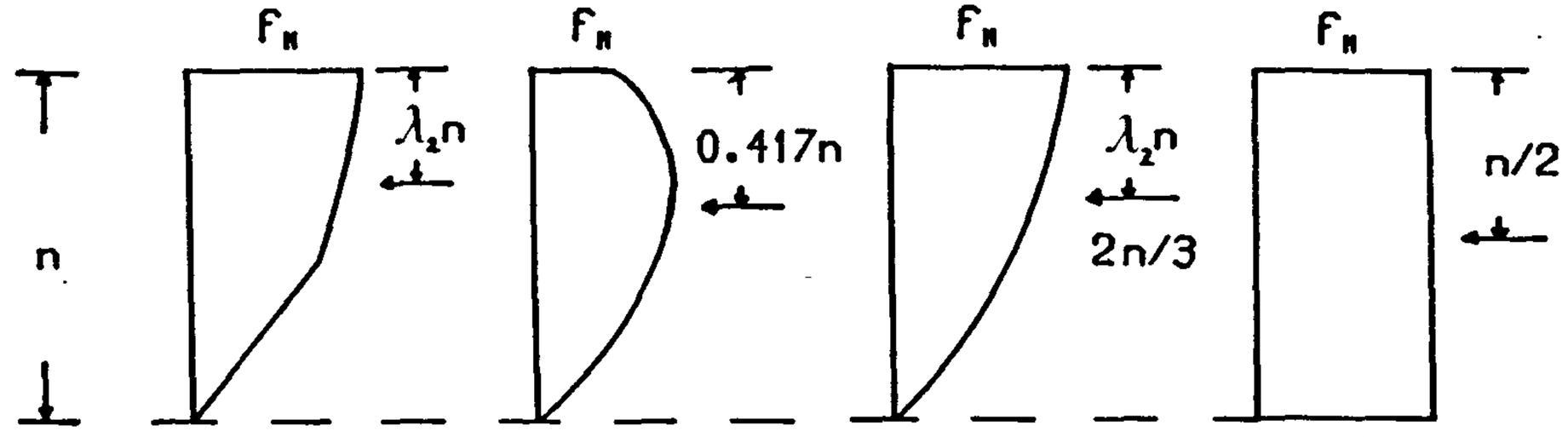

Figure 3.6.20

to those proposed by Sinha[58]. In comparison with the average stress block characteristics derived from the axial prism tests λ_1 and λ_2 for Sinha[57] and Beard[56] showed a 19% and 6-11% increase respectively.

Attempting to model the behaviour of fully prestressed brickwork beams Pedreschi[9] developed a cubic polynomial stress/strain relationship for brickwork based on axially loaded prism tests. The stress block factors, average $\lambda_1 = 0.64$ and $\lambda_2 = 0.38$, were found to be independent of brick strength, mortar grade and prism format. The present test results described in section 3.6.1 confirm the results of Pedreschi[9].

In 1985 BS 5628, Part 2[15], the code of practice for reinforced and prestressed masonry, was published. Although the code makes no recommendations for the stress/strain relationship for brickwork it suggests a rectangular stress block, $\lambda_1 = 1$ and $\lambda_2 = 0.5$, figure 3.6.20. The compressive strength, f_k, is assumed to develop over the whole neutral axis depth. Compared with the axial prism test results λ_1 has increased by 59% and λ_2 by 33%. Although λ_1 has increased significantly in calculating the ultimate moment this may be offset by the increase in λ_2, due to a reduction in the leverarm.

The theoretical ultimate moments were calculated using the stress block factors from the axially loaded prism tests, since there appears to be no advantage in using eccentrically loaded prisms.

3.6.3 Modulus of Elasticity

A knowledge of the elastic modulus for brickwork is required for the prediction of curvature due to prestress of partially prestressed brickwork beams , section 4.2.2.1. Previously research[55] has developed empirical relationships between compressive strength and elastic modulus for brickwork loaded normal to the bed-joint. Recently an expression[59] was proposed for prisms loaded both normal and parallel to the bed-joint. Because of the orthotropic nature of brickwork the expression covered a wide range of values and as yet no expression has been developed specifically for brickwork loaded parallel to the bed-joint.

The initial tangent modulus of elasticity of each test prism was obtained using a linear regression analysis on the experimental stress/strain relationships up to 25% of the ultimate load. In figure 3.6.21 the resultant values are plotted against compressive strength. Although there is some considerable experimental scatter a distinct relationship between elastic modulus and compressive strength is apparent. Applying a least squares analysis to the test results the following general expression to derive an approximate value for the elastic modulus was developed:

$$E_m = 1308\ f_m^{0.74} \qquad (3.6.5)$$

3.6.4 Modulus of rupture

Adopting an omniscient view of the flexural behaviour of

RELATIONSHIP BETWEEN COMPRESSIVE STRENGTH AND ELASTIC MODULUS

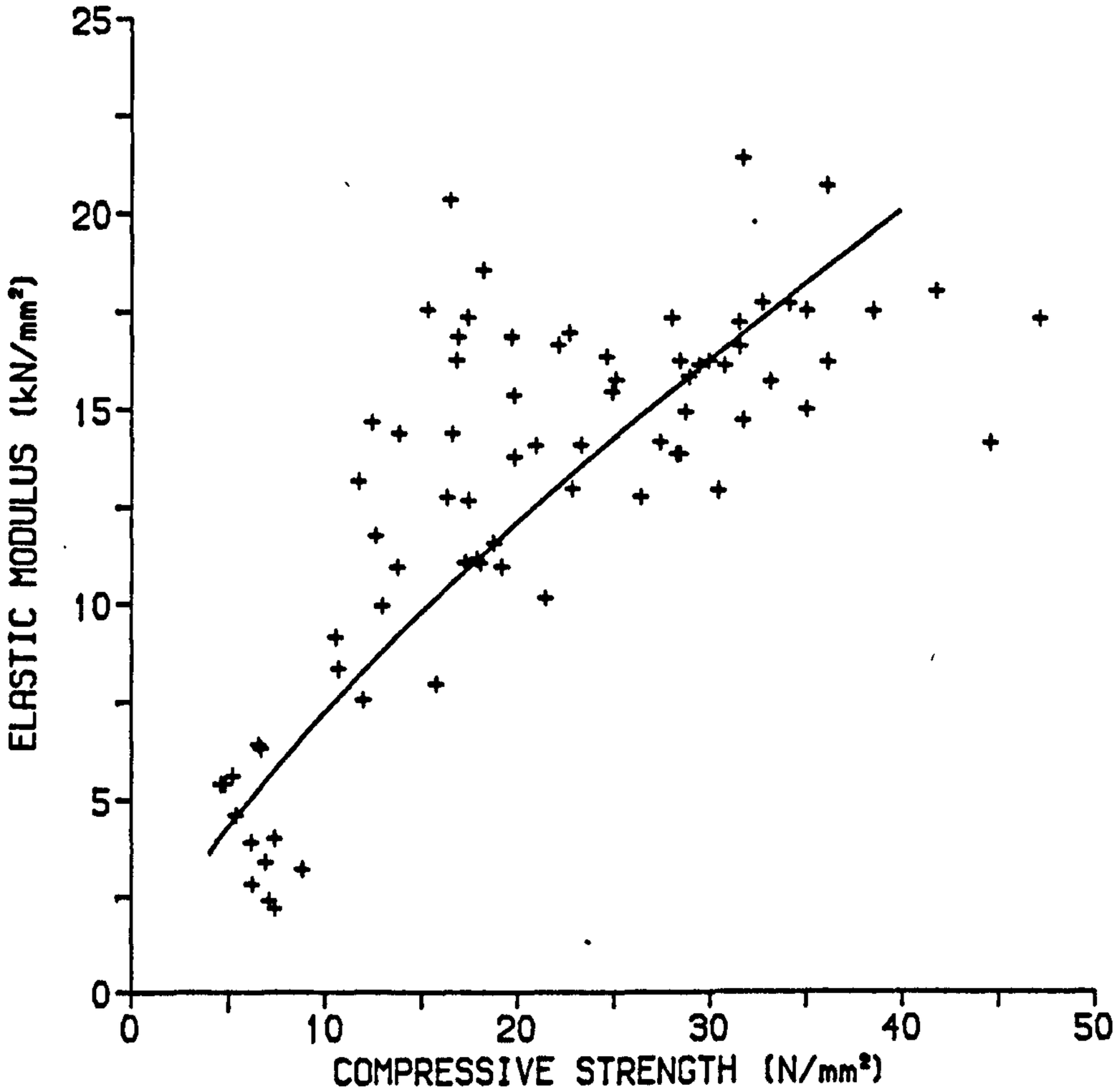

Figure 3.6.21

partially prestressed brickwork beams requires not only a knowledge of the compressive properties of brickwork but also the flexural tensile strength or modulus of rupture. Failure in tension of brickwork occurs at the joint since the tensile strength is dependent upon the strength of the brick/mortar interface and not on the tensile strength of either the brick unit or the mortar. Factors influencing the strength of the brick/mortar bond are mortar grade and suction rate of the bricks. However, the soffit of the beam section, figure 3.7.1, was a composite of brickwork and concrete, consequently the modulus of rupture will also be influenced by the properties of the concrete. Unreinforced prisms, figure 3.6.22, representing the bottom two courses of the beam section were tested in flexure under four point loading over a span of 750 mm. Test specimens were built using both grade I and II mortar mixes. Once cracking occurred the section was unable to withstand further loading and the specimens collapsed, Plate 3.3. The modulus of rupture, based on the gross cross-section, was determined from the failure moment, table 3.6.7. Tests were also conducted on three unreinforced concrete members of similar dimensions to the brickwork specimens. An average modulus of rupture for the concrete equal to 2.26 N/mm^2 was obtained.

It is clear from table 3.6.7 that the modulus of rupture of the test specimens was the same irrespective of the mortar grade. An average modulus of rupture for all eighteen test specimens may be taken as 1.83 N/mm^2. Compared to the flexural tensile strength of similar plain masonry members[9] an increase of 23% for grade I mortar, from 1.49 N/mm^2, and 62% for grade II mortar, from 1.13 N/mm^2, was obtained. Since the modulus of rupture was unaffected by

TEST SPECIMEN FOR MODULUS OF RUPTURE OF SECTION

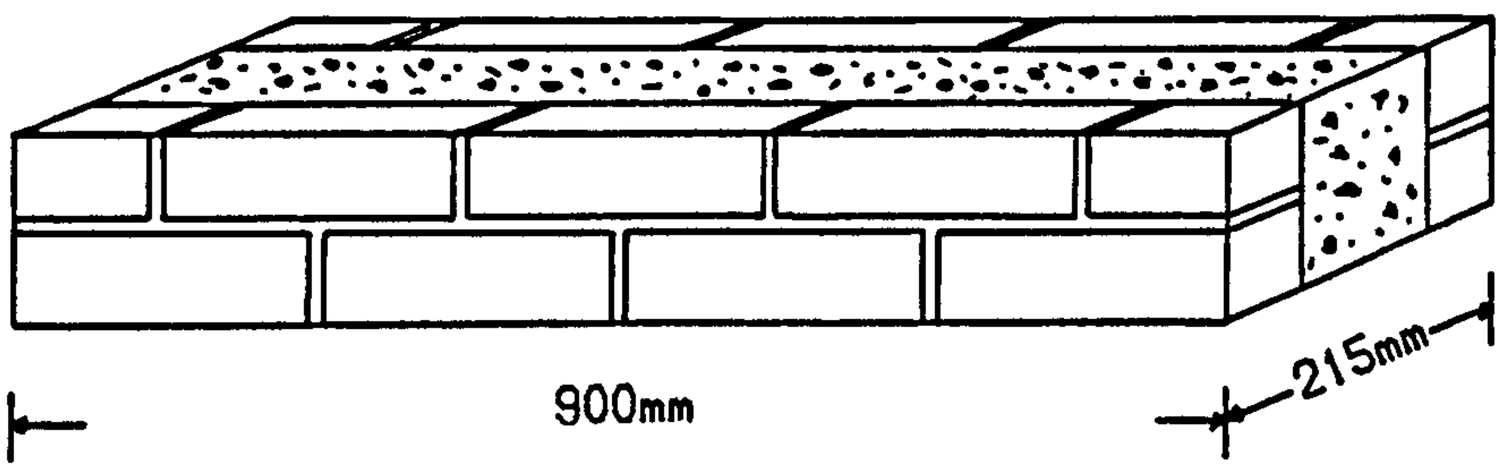

Figure 3.6.22

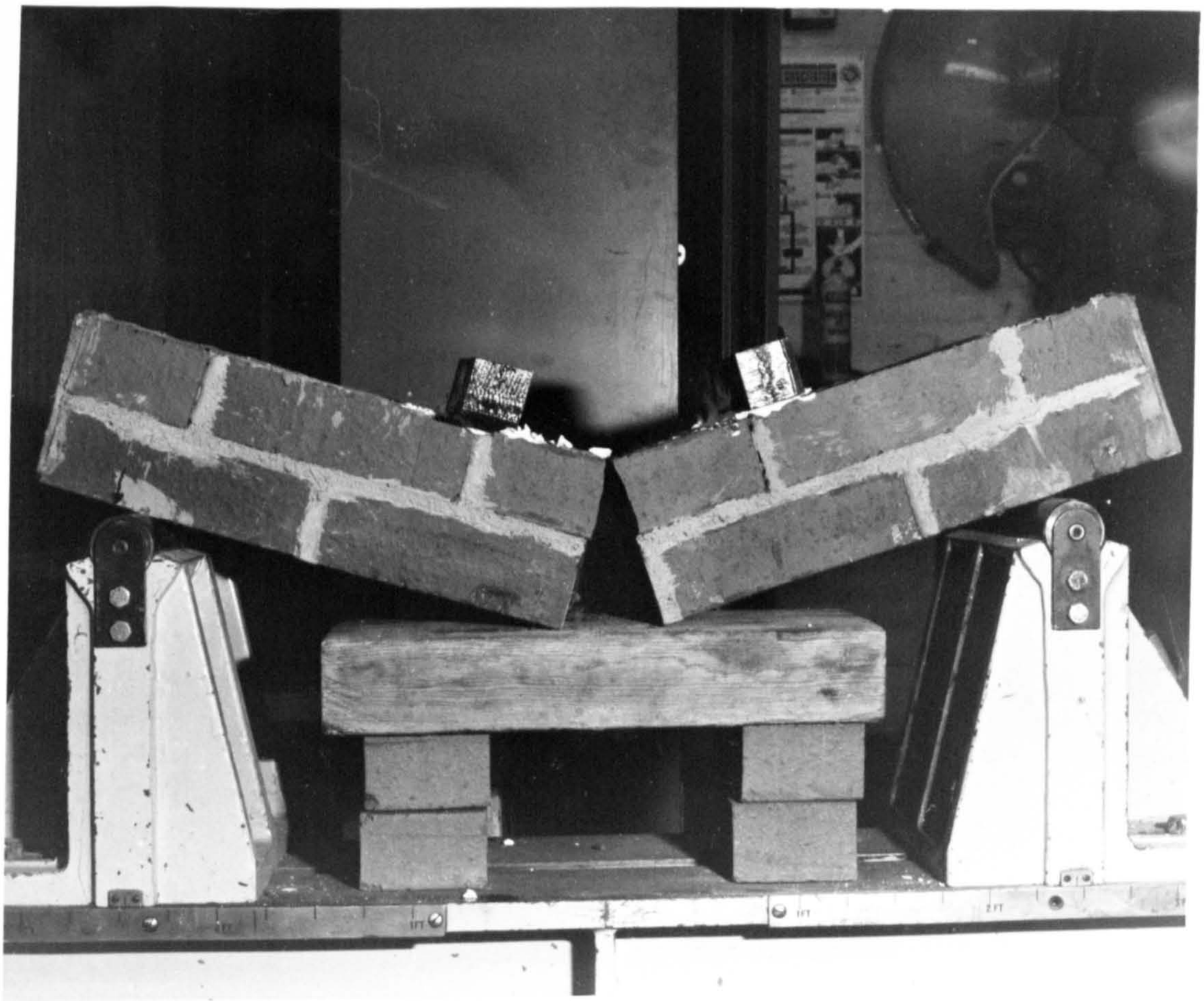

Plate 3.3

Typical failure of modulus of rupture specimen

Table 3.6.7 Modulus of rupture of test specimens

Specimen Number	1:¼:3			1:½:4½		
	Mortar Strength (N/mm^2)	Concrete Strength (N/mm^2)	Modulus of Rupture (N/mm^2)	Mortar Strength (N/mm^2)	Concrete Strength (N/mm^2)	Modulus of Rupture (N/mm^2)
1	19.9	18.7	1.8	8.0	18.7	1.6
2	19.9	18.7	1.8	8.0	20.1	2.0
3	19.9	18.7	2.1	8.0	21.4	1.8
4	19.9	17.4	1.7	8.0	21.4	2.0
5	19.9	17.4	1.6	8.0	20.2	2.0
6	19.9	18.7	1.8	8.0	20.2	2.2
7	17.9	15.8	1.7	7.7	15.8	1.7
8	17.9	16.8	1.9	7.7	16.8	1.8
9	17.9	17.5	1.6	7.7	17.5	1.6
Average	19.2	17.7	1.80	7.9	19.1	1.96
Std Dvtn	0.93	0.99	0.14	0.16	2.01	0.20
Coeff of Vartn. %	4.8	5.6	7.7	2.0	10.5	10.8

the mortar grade it may be reasonable to assume that it will also be independent of the brick strength. The flexural tensile strength of the composite section was 19% lower than for the plain unreinforced concrete specimen.

3.7 CONSTRUCTION DETAILS AND TEST PROCEDURE

This section describes in detail the development, construction, instrumentation and testing of the partially prestressed brickwork beams

3.7.1 Details of the beam section and construction

The cross-section used throughout the test programme for the reinforced and partially prestressed brickwork beams is shown in figure 3.7.1. The section was similar to that previously used for fully prestressed brickwork beams[9,25], figure 2.2.10. The location of the cavity in the fully prestressed brickwork beams allowed the tensioned reinforcement to be placed within the 'kern' of the cross-section and so avoiding the introduction of tensile stresses into the section during the post-tensioning operation. Additional to this requirement it was felt necessary that the cavity in the partially prestressed beams must extend to the soffit of the beam to allow the non-tensioned steel to be placed closer to the bottom of the section for improved cracking control.

The section, figure 3.7.1, comprised of the top three courses of brickwork laid in standard 'English' bond. The final

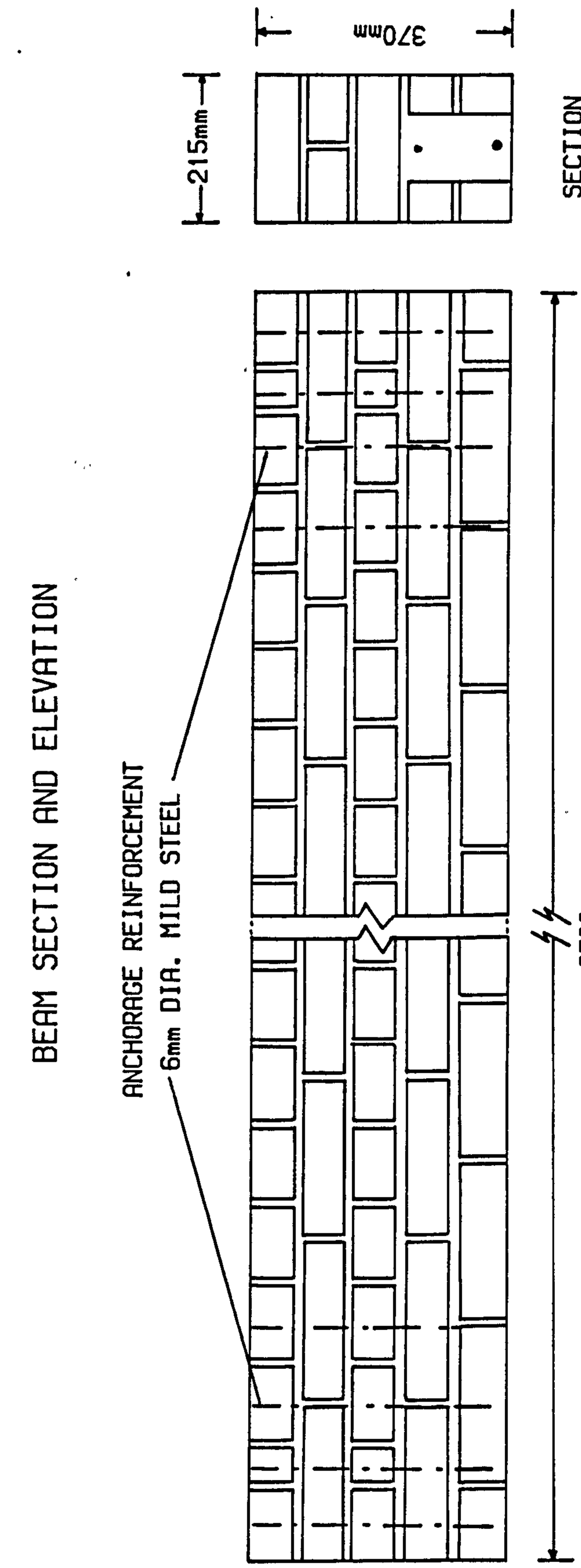
370mm
215mm
SECTION
BEAM SECTION AND ELEVATION
ANCHORAGE REINFORCEMENT
6mm DIA. MILD STEEL
6500mm
ELEVATION

Figure 3.7.1

bottom two courses which formed the sides of the cavity consisted of bricks split lengthwise laid flush with the face of the beam. To prevent separation of the sides of the cavity during prestressing galvanised twist iron wall ties were placed at spacings of approximately 500 mm along the bed-joint between the bottom two courses of brickwork. In the completed section the concrete filled cavity formed only 18% of the gross cross-sectional area.

All test beams were built on the floor of the laboratory by an experienced bricklayer and generally the standard of workmanship was good, Plate 3.4. The beams were built upside down allowing access to the cavity for the positioning of the reinforcement and later concreting. During the prestressing operation transverse tensile forces, which may have caused cracking along the bed-joints, developed in the 'lead in length' of the beams as a result of anchorage zone stresses. To prevent horizontal splitting of the bed joints the end zones of the beams were reinforced with 6 mm diameter mild steel rods placed vertically at 100 mm centres either side of the cavity. The rods were passed through the perforations in the bricks, figure 3.7.1.

The 'lead in length' of the beams fabricated with low strength bricks was concreted prior to prestressing. The prism strength in the case of the low strength bricks was particularly low and therefore it was necessary to distribute the prestress over a greater proportion of the cross-section. The tensioned and non-tensioned reinforcement within the concreted end zone were sheathed in 25 mm diameter plastic piping. This allowed tensioning of the tendon and prevented the introduction of compressive stresses

Plate 3.4

Construction of brickwork beams

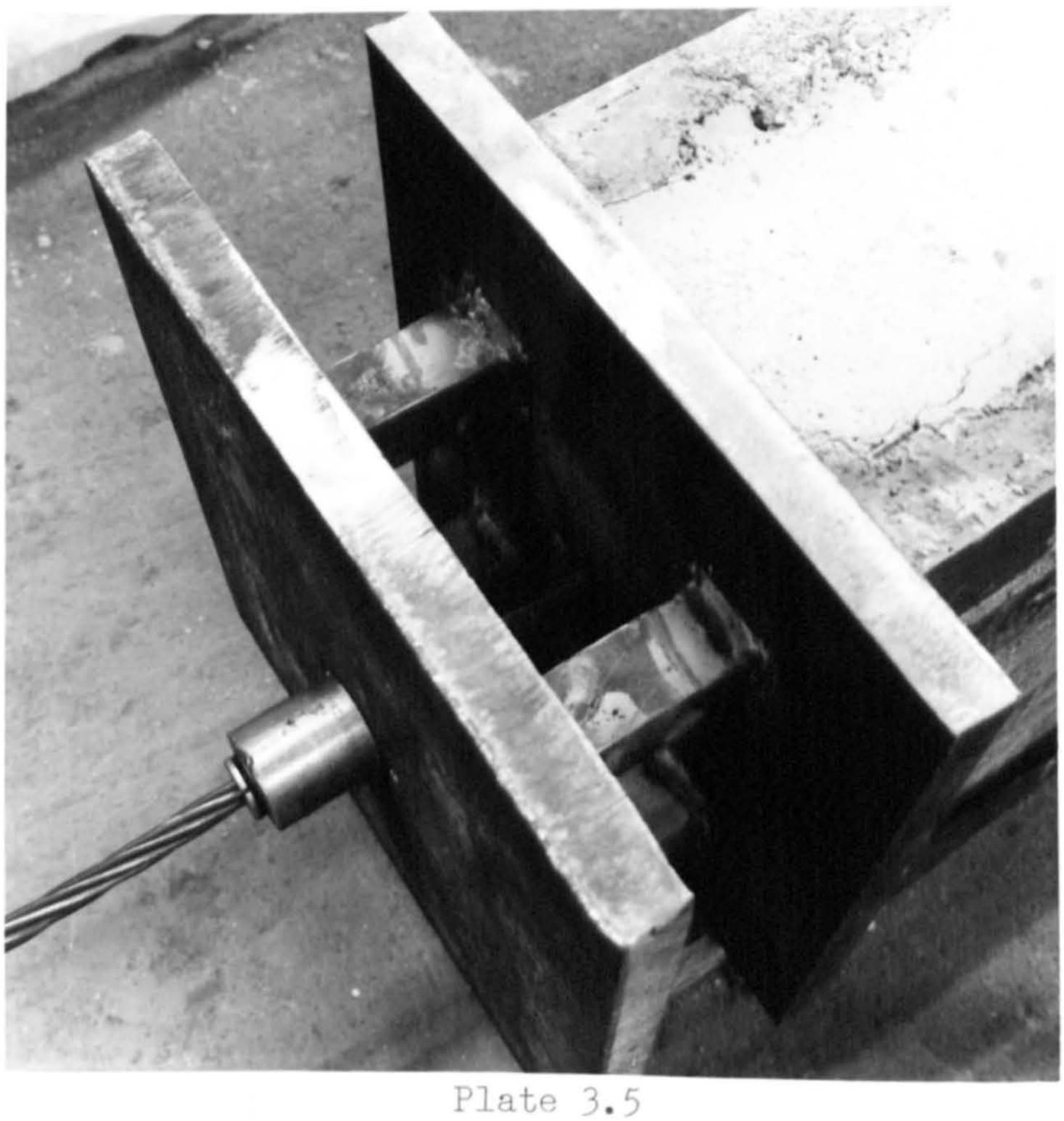

Plate 3.5

Removable anchorage plates

into the non-tensioned reinforcement at the transfer of prestress.

Figure 3.7.2 shows the amounts of tensioned and non-tensioned steel used in each of the test beams. Each beam was cured under polythene for a minimum of 21 days before prestressing. Prior to stressing the tensioned and non-tensioned steel were set to the required depths, the non-tensioned deformed bars were suspended from a frame placed over the beam and were therefore independent of the section until concreting of the cavity. To transfer the prestress at the anchorage zone of the beams mild steel anchor plates were bedded into the ends of the beams using a rich mortar mix or dental plaster. The plates were removed and re-used after testing. As an alternative to the permanently fixed plates removable anchor plates, Plate 3.5, were used in three of the beams, C6 - C8. Each end anchorage plate consisted of two mild steel plates 300 x 300 x 20 mm welded together at a spacing of 70 mm. This arrangement allowed a length of 70 mm of stressed tendon to remain outside of the prestressed beam at either end. Seven days after concreting, allowing adequate time for sufficient bond to develop between the steel and concrete, the tensioned reinforcement outside of the section was cut manually and the plates removed. A 6 mm diameter mild steel helix, designed to satisfy to the recommendations of BS 8110[36], was installed prior to concreting to resist any possible bursting forces in the anchor zone once the plates were removed.

Prestressing was carried out using a C.C.L. 'stress-o-matic' pump with a type 300 manual control stressing head capable of applying prestress forces up to 300 kN. Throughout stressing the tendon was held by C.C.L. XL open grips, which were barrel and wedge

BEAM SECTIONS

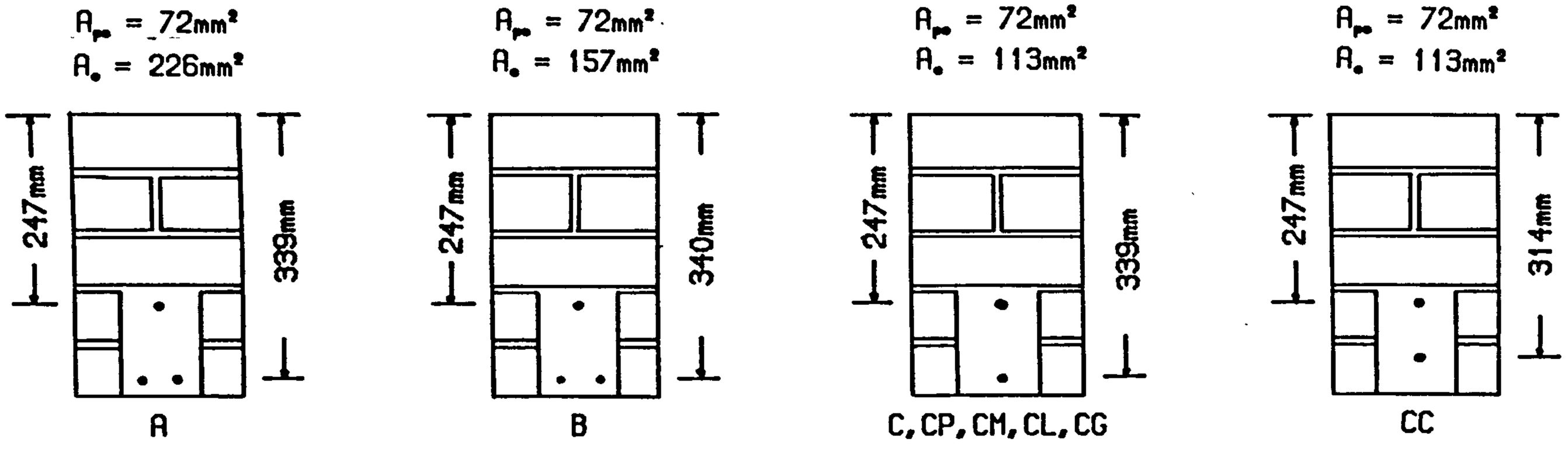

Figure 3.7.2

type. Except in beam series AB, CP and CL the tendon was stressed to a maximum allowable 70%[15] of the breaking load. The tendons were stressed to only 50% of the breaking load in beams CL because of the low compressive strength of the brickwork prisms.

Electrical resistance strain gauges attached to the prestressing steel were used in conjunction with the meter contained within the prestressing system to monitor the prestressing force. The meter was only able to measure the force applied at prestressing and so the effective prestress after losses due to lock off (slip between the tendon and the wedge) and elastic shortening of the brickwork were measured by the electrical resistance strain gauges. Results for the prestressing force are given in table 5.2.1 and discussed in chapter 5.

Concreting of the cavity was carried out manually, the mix was compacted using a tamping rod. In all beams, except series A, a neat slurry was poured into the cavity prior to the concrete to ensure a good bond between the concrete and brickwork. All beams were allowed to cure for at least seven days before testing.

3.7.2 **Instrumentation**

3.7.2.1 Brickwork strain

Strains were measured on the surface of the brickwork in the constant moment zone throughout the loading history of each beam using 'demec' gauges of lengths 150 and 200 mm. The strain was measured at various depths, as shown in figure 3.7.3, to obtain the

POSITION OF 'DEMEC' POINTS ON SIDE OF BEAM IN CONSTANT MOMENT ZONE

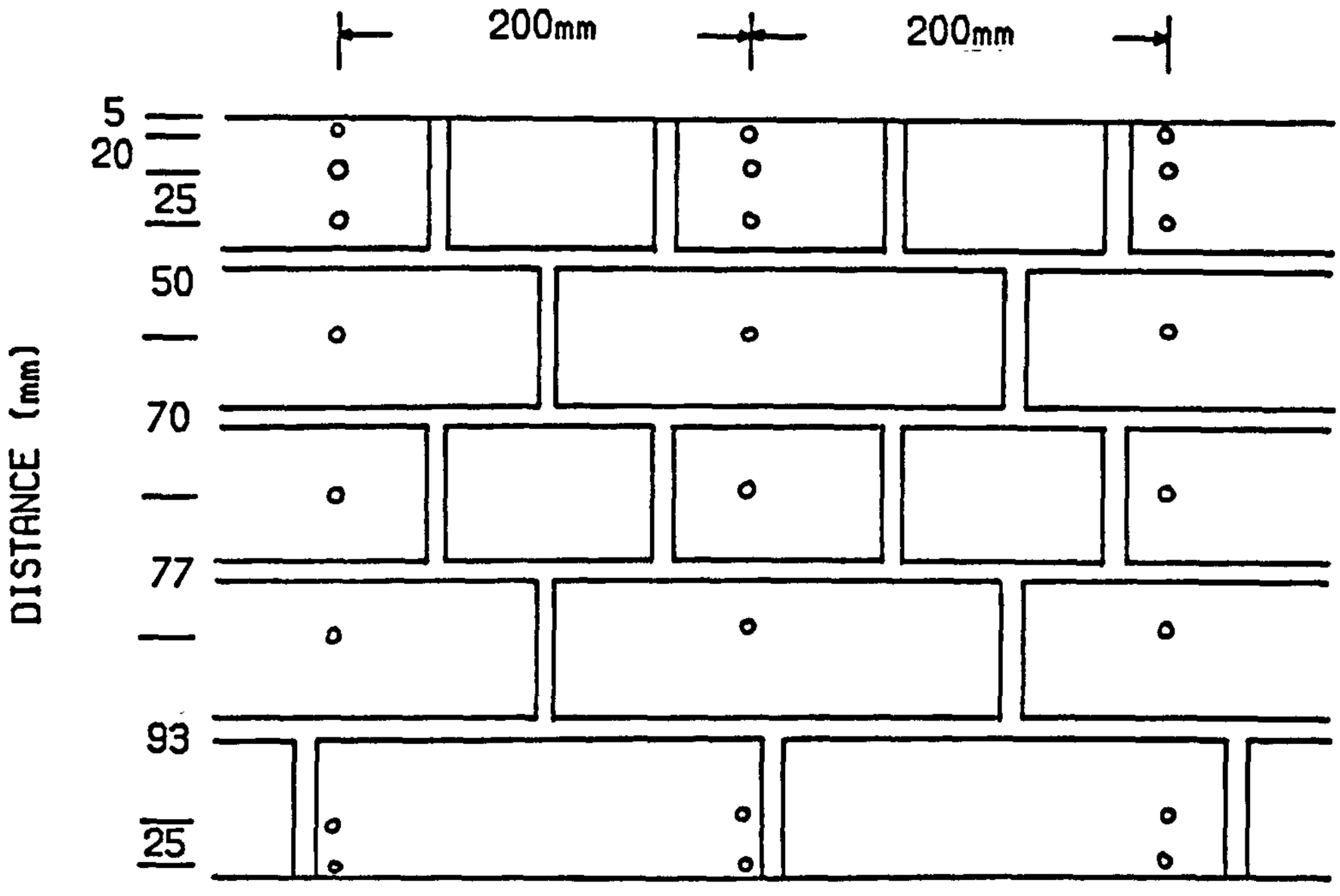

Figure 3.7.3

strain profile at each loading increment. The strain was also measured at different vertical sections within the constant moment zone to monitor the strain across and away from the flexural cracks and to obtain the variation in neutral axis depth along the beam.

3.7.2.2 Steel strain

Electrical resistance strain gauges were used to measure strain in both the tensioned and non-tensioned reinforcement. 'Post-yield' type foil strain gauges with a gauge length of 5 mm , capable of recording strains up to 20%, were bonded to the reinforcement in all test beams. Additionally embeddment strain gauges (gauge length 60 mm) were used in a number of beams and placed in the concrete adjacent to the steel. A 'Gauge Technique' data logging system was used to monitor the output from the strain gauges.

The strain gauges were positioned on the reinforcement to record steel strain in the constant moment zone. From the onset of cracking the strain in the reinforcement varies greatly between cracks and across cracks. Since in brickwork flexural cracking will commence at the mortar joints along the soffit of the beam the strain gauges were positioned on the non-tensioned reinforcement to coincide with the joints and therefore to measure the maximum tensile strain at that level. Gauges in a number of beams were also placed on the reinforcement between the mortar joints to study the distribution of tensile strain.

3.7.2.3 Deflection

Deflection of the beams due to applied load were measured at the mid-span and quarter points. Dial gauges reading to 0.01 mm were used throughout. Gauges reading to 0.002 mm were used to measure any settlement of the beam at the supports due to the applied load. When the beams approached failure, where deflections were large, the dial gauges were removed from underneath the beam and the deflection was measured using a ruler reading to 1 mm.

3.7.2.4 Crack widths

Flexural crack widths were measured in the constant moment zone using an 'ultra lomara' microscope and a vernier gauge reading to 0.02 mm. The hand held microscope directly read the crack widths, but the format of the instrument only allowed measurements to within 25 mm of the soffit of the beam. The vernier gauge measured distance between two demec points placed either side of the crack. As cracking will initiate at the mortar joints along the soffit of the beam all demec points were placed 50 mm apart either side of the mortar joints and at 5 mm above the soffit.

3.7.2.5 Load measurement

The load applied by each jack was measured using 100 kN load cells positioned above the jacks in the testing rig . The output was monitored by a digital voltmeter, each reading was automatically transferred onto a pen-chart recorder.

3.7.3 Test procedure

All beams were tested under a four point loading system in a 'self-straining' rig, figure 3.7.4. The distance between loading points remained constant throughout the investigation at 750 mm. Each test beam was placed onto the supports at a pre-set span, the supports consisting of one roller and one pin support (simply supported). The load was applied through hydraulic jacks connected in a single feed to a hydraulic pump. The test set-up is shown in Plate 3.6.

The minimum age of all beams at testing was 28 days, allowing 21 days before prestressing and a further 7 days for curing of the concrete. Since all test beams were built upside down on the floor of the laboratory it was necessary for each beam to be turned upright using an overhead crane. During the turning operation tensile stresses may have been introduced into the section due to the self-weight of the beam. In the reinforced beams an external prestress force was applied concentrically to the section to prevent premature failure. Once the beam was turned the prestress was removed.

All beams were weighed using two 30 kN load cells. The average weight for the high strength brick beams was 1.78 kN/m, medium strength 1.70 kN/m and low strength 1.53 kN/m.

The load was applied in equal increments, numbering between twelve and fifteen, up to the expected failure load. At each increment the load was held constant and readings of deflection,

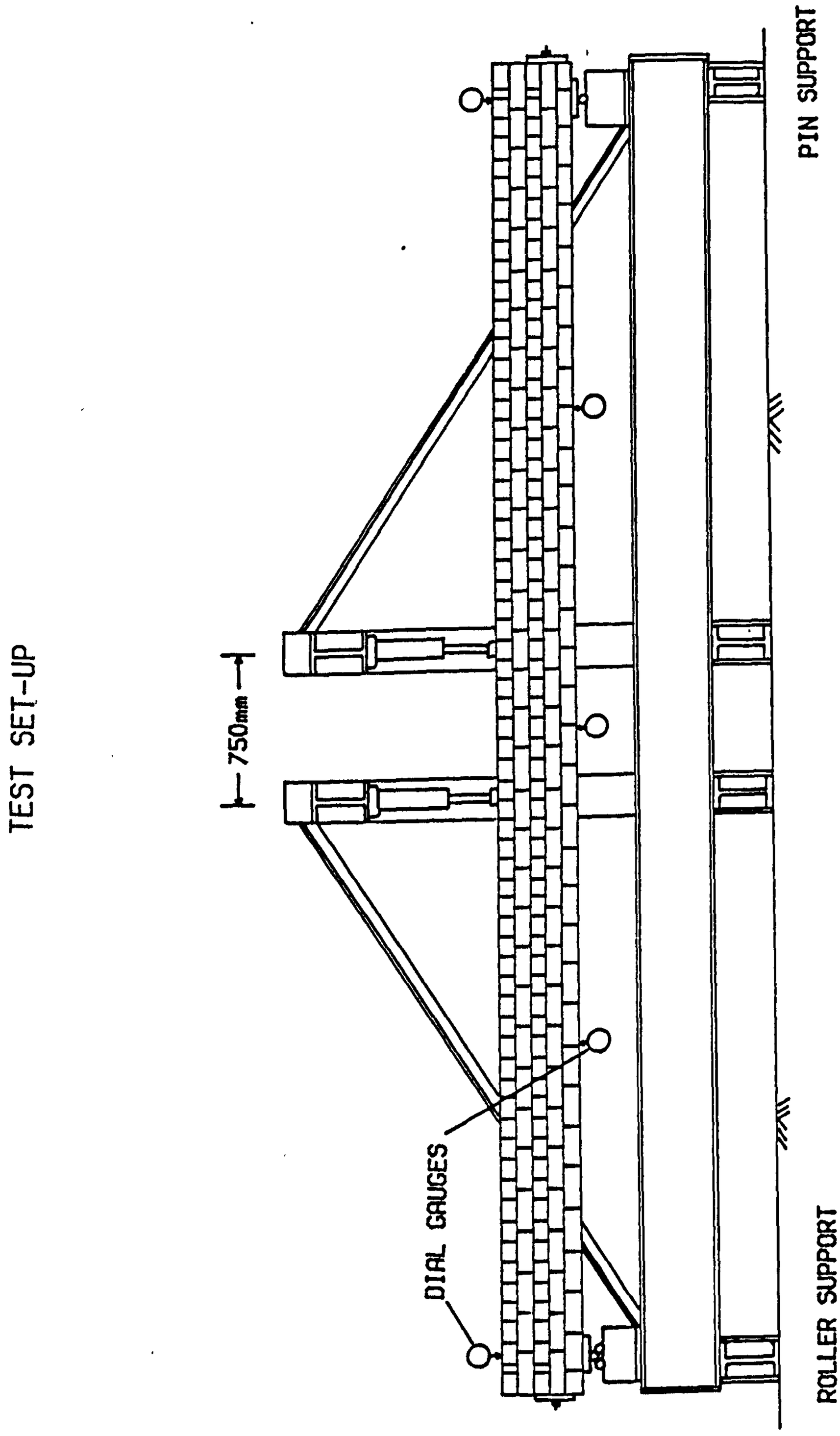

Figure 3.7.4

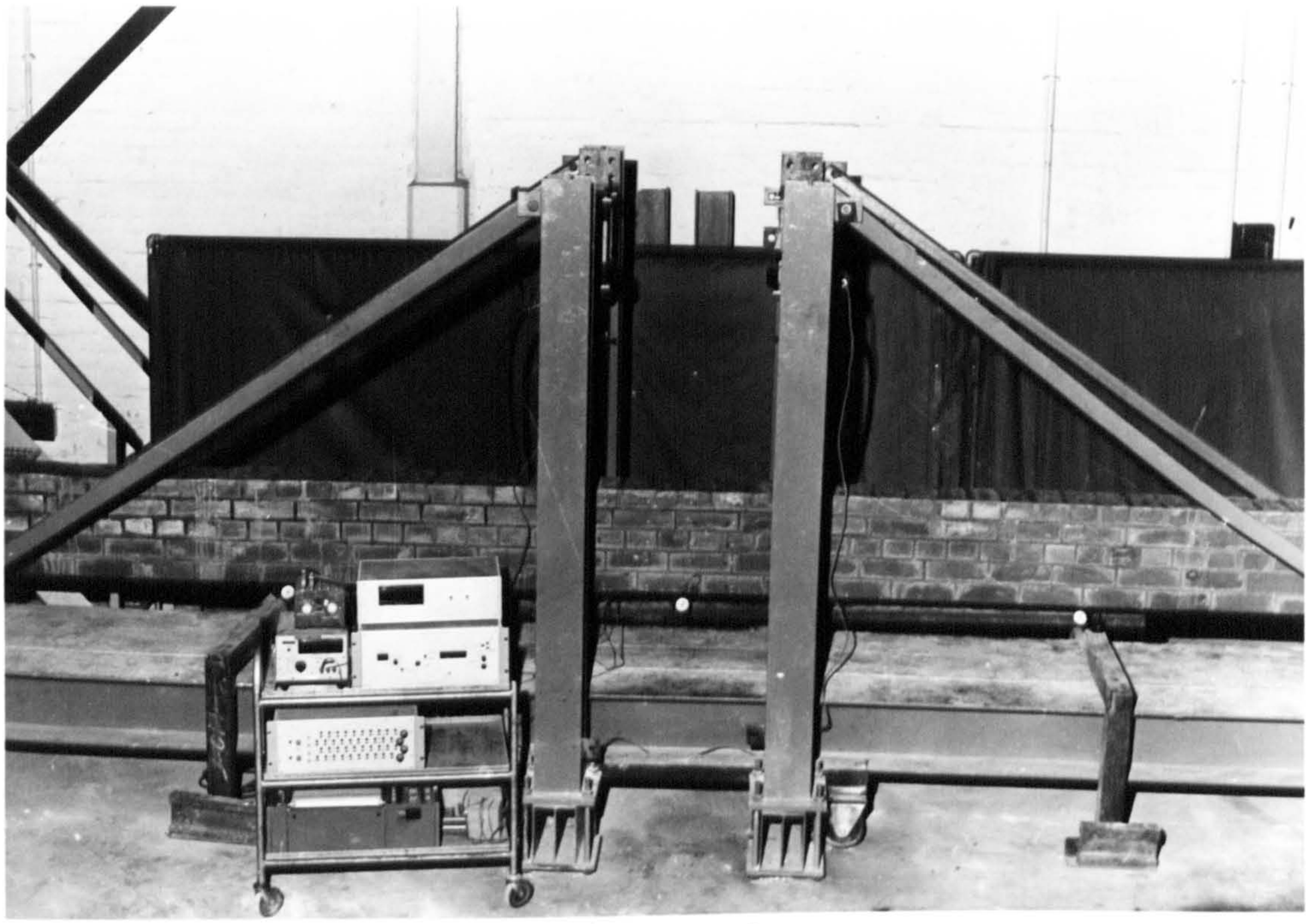

Plate 3.6

Test set-up

brickwork strain and steel strain were taken. After the onset of cracking the crack widths were measured in the constant moment zone and the cracking pattern marked on the face of the beam. Approaching failure the load increment was decreased. Readings of deflection, strain and crack widths were taken as near to failure as possible. Once failure occurred the applied load was removed and the recovery of the beam was noted.

3.8 SUMMARY AND CONCLUSIONS

1. The compressive strength of the brick unit seems highest when tested on the bed and least when on-end. Platen restraint, the orientation of the perforations with respect to loading direction, and the orthotropic material properties were responsible for the difference in compressive strength.

2. The compressive strength and ultimate compressive strain of the single course prisms were consistently higher than the corresponding values of the three course prisms. Experimental observations suggest that the single course prisms may provide a better representation of the beams compressive properties.

3. When the stress/strain relationship for brickwork was presented non-dimensionally the brick strength, mortar grade or prism type had little significant effect upon its stress/strain characteristics.

4. Values for ultimate compressive strength and strain were the same under both axial and eccentric loading. The strain gradient has no effect upon the compressive properties of the brickwork. The stress block factors λ_1 and λ_2 are similar under both axial and eccentric loading.

5. The modulus of rupture of the brickwork/concrete composite section used in this investigation was independent of the mortar grade.

CHAPTER 4

THEORETICAL ANALYSIS OF PARTIALLY PRESTRESSED BRICKWORK BEAMS

4.1 INTRODUCTION

The limit state design philosophy requires a partially prestressed brickwork beam to satisfy both the ultimate and serviceability limit states. Economical design necessitates accurate methods with which to predict the ultimate moment capacity of a beam section and the deflection of a beam under service loading.

In this chapter a method to predict both ultimate moment and deflection of partially prestressed beams using the actual stress/strain properties and strength of the constituent materials is presented. An alternative simplified version of the method to predict the ultimate moment, more suitable for design, is also outlined.

4.2 THEORETICAL PREDICTION OF MOMENT-CURVATURE, ULTIMATE MOMENT AND DEFLECTION

4.2.1 General

The direct method of analysis, as previously used for prestressed concrete beams[60,61], was developed to predict the flexural behaviour of partially prestressed brickwork beams. Utilising the actual stress/strain relationships of the composite materials the method was used to predict the moment-curvature relationship from prestressing to ultimate.

At given values of either the extreme tensile or compressive

fibre strain the shape of the strain profile was found iteratively by equating the internal compressive and tensile forces. Once the shape of the strain profile was known the curvature and moment were calculated. The ultimate moment was predicted when the extreme compressive fibre strain was equal to the ultimate compressive strain, ε_m. Deflection was determined from double integration of the moment-curvature relationship along the length of the beam.

The bottom two courses of the partially prestressed beams were a composite of brickwork and concrete, the concrete forming approximately 18% of the cross-sectional area, figure 3.7.1. In previous theoretical investigations[9,19] the concrete infill has been assumed to exhibit the same properties as the brickwork. Experimentally the values for the modulus of rupture indicated that the concrete significantly influenced the properties of the beam soffit, section 3.6.4. An accurate analysis required the brickwork and concrete to be considered as having different material properties. The direct method was further developed to incorporate a concrete cavity into the section, the concrete having the non-linear stress/strain properties as outlined in section 3.4. The stress/strain characteristics of the brickwork and steel used in the investigation were discussed in sections 3.6.1 and 3.5 respectively.

Calculation of the moment-curvature and load/deflection relationships involved a large number of iterative computations, and hence an interactive BASIC language computer programme was developed. A listing of the programme and details of the data input requirements are presented in Appendix A.

4.2.2 Moment-curvature relationship

The following assumptions have been made during the prediction of the moment-curvature relationship:

(i) The strain distribution at all loading increments is linear throughout the depth of the section.

(ii) Full bond exists between the concrete and the tensioned reinforcement, non-tensioned reinforcement and brickwork.

(iii) Stress/strain relationships for the brickwork and concrete in compression and steel reinforcement in tension are known.

(iv) The stress/strain behaviour of the brickwork and concrete in tension is linear and the initial tangent modulus is equal to that in compression.

(v) Maximum strain at the outermost compression fibre at ultimate is equal to the ultimate compressive strain, ε_m derived from the brickwork prism tests. Failure is assumed to occur once the ultimate compressive strain is reached irrespective of whether the tensile reinforcement has yielded.

The moment-curvature relationship was determined by considering the behaviour of the beam in three stages:

(i) at prestressing

(ii) from prestressing to cracking

(iii) post-cracking to ultimate.

4.2.2.1 Prestressing

The stress and strain distributions in a rectangular partially prestressed brickwork beam with a concrete cavity are shown in figure 4.2.1. Initially assuming linear elastic behaviour the stresses in the extreme fibres can be found using the properties of the transformed section, thus:

$$\sigma_1' = \frac{P}{A_t} - \frac{P.e}{Z_t} \qquad (4.2.1)$$

$$\sigma_2' = \frac{P}{A_t} + \frac{P.e}{Z_b} \qquad (4.2.2)$$

From these the extreme fibre strains are determined assuming a value for the initial tangent modulus of brickwork, E_m', thus:

$$\varepsilon_{p1(2)} = \frac{\sigma_{1(2)}'}{E_m'} \qquad (4.2.3)$$

Throughout the analysis the ratio of the top fibre and bottom fibre strains, r_t, and the modular ratio, m, are assumed to remain constant, where:

CONDITIONS IN PARTIALLY PRESTRESSED BRICKWORK BEAM DUE TO APPLIED PRESTRESS

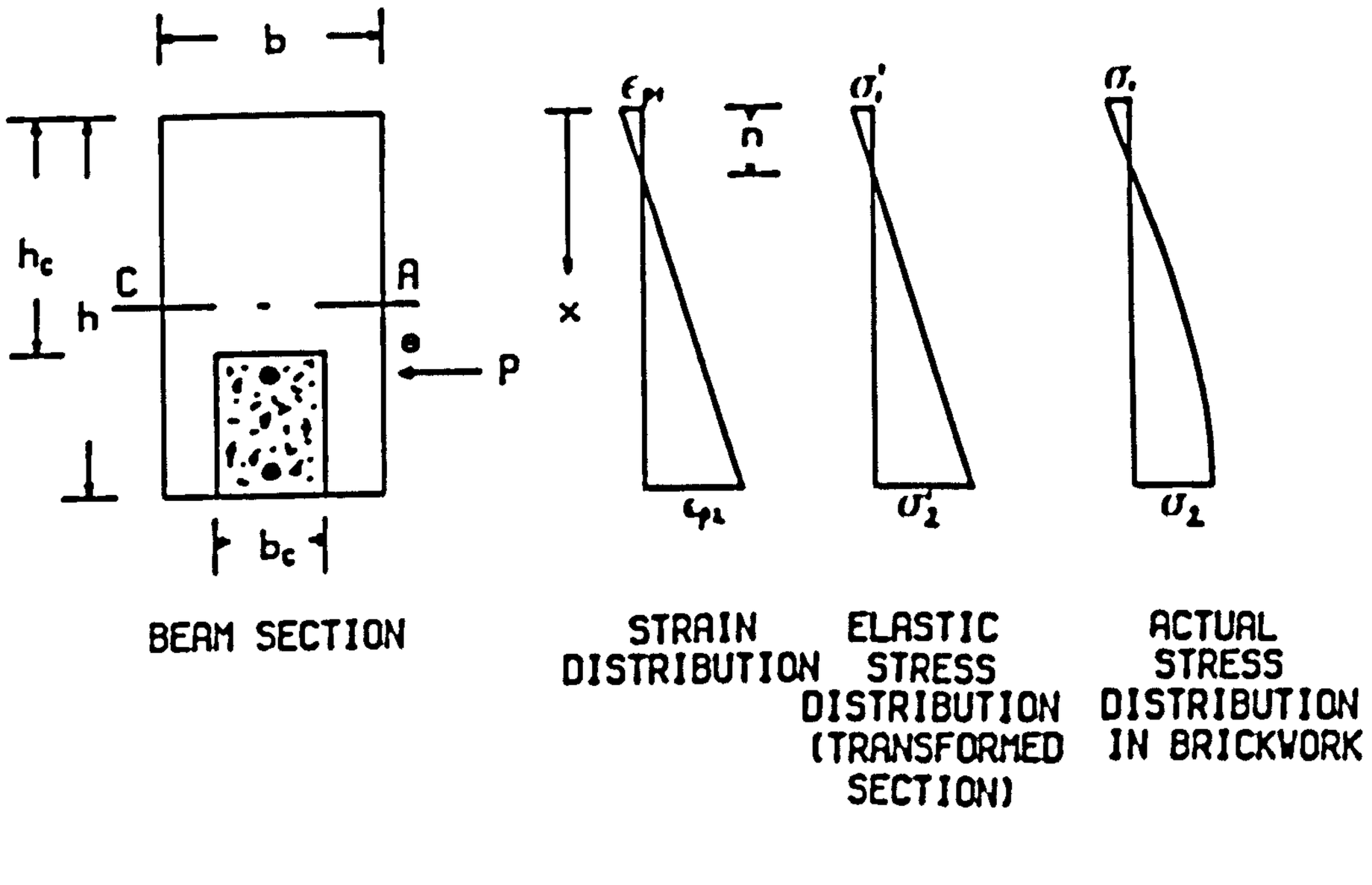

Figure 4.2.1

$$r_t = \frac{\varepsilon_{p1}}{\varepsilon_{p2}} \qquad (4.2.4)$$

and, $$m = \frac{E'_c}{E'_m} \qquad (4.2.5)$$

The resultant compression force in the section is found and equated to the applied prestressing force, thus:

$$C = b\int_n^{h_c} F_m(\varepsilon)dx + (b-b_c)\int_{h_c}^{h} F_m(\varepsilon)dx + b_c\int_{h_c}^{h} F_c(\varepsilon)dx \qquad (4.2.6)$$

where,

$$\varepsilon = \varepsilon_{p_1} + (\varepsilon_{p_2} - \varepsilon_{p_1})\frac{x}{h} \qquad (4.2.7)$$

For equilibrium:

$$C = P \qquad (4.2.8)$$

If, however, equation 4.2.8 is not satisfied then the value for E'_m is modified, thus:

$$E_m = E'_m(C/P) \qquad (4.2.9)$$

The values of ε_{p_1} and ε_{p_2} are calculated using E_m and equations 4.2.6, 4.2.8 and 4.2.9 are applied until equilibrium is satisfied.

The curvature due to prestress is therefore:

$$\phi_p = \frac{\varepsilon_{p_1} - \varepsilon_{p_2}}{h} \qquad (4.2.10)$$

4.2.2.2 Moment-curvature up to cracking

The stress distribution just prior to cracking is shown in figure 4.2.2. Once decompression of the prestress has taken place and the flexural tensile strength has been exceeded cracking will occur.

The magnitude of strain at any particular loading is a sum of the strain distribution due to prestress and applied load, figure 4.2.3. The strain necessary to decompress the prestress will be equal and opposite to ε_{p_2} and so the strain necessary for cracking is:

$$\varepsilon_{cr} = \varepsilon_r + \varepsilon_{p_2} \qquad (4.2.11)$$

where, $$\varepsilon_r = \frac{f_r}{E'_n} \quad \frac{b}{[(b-b_c)+b_c\, n\,]} \qquad (4.2.12)$$

f_r = modulus of rupture of section

$$n = \frac{E'_c}{E'_n}$$

CONDITIONS IMMEADATELY PRIOR TO CRACKING

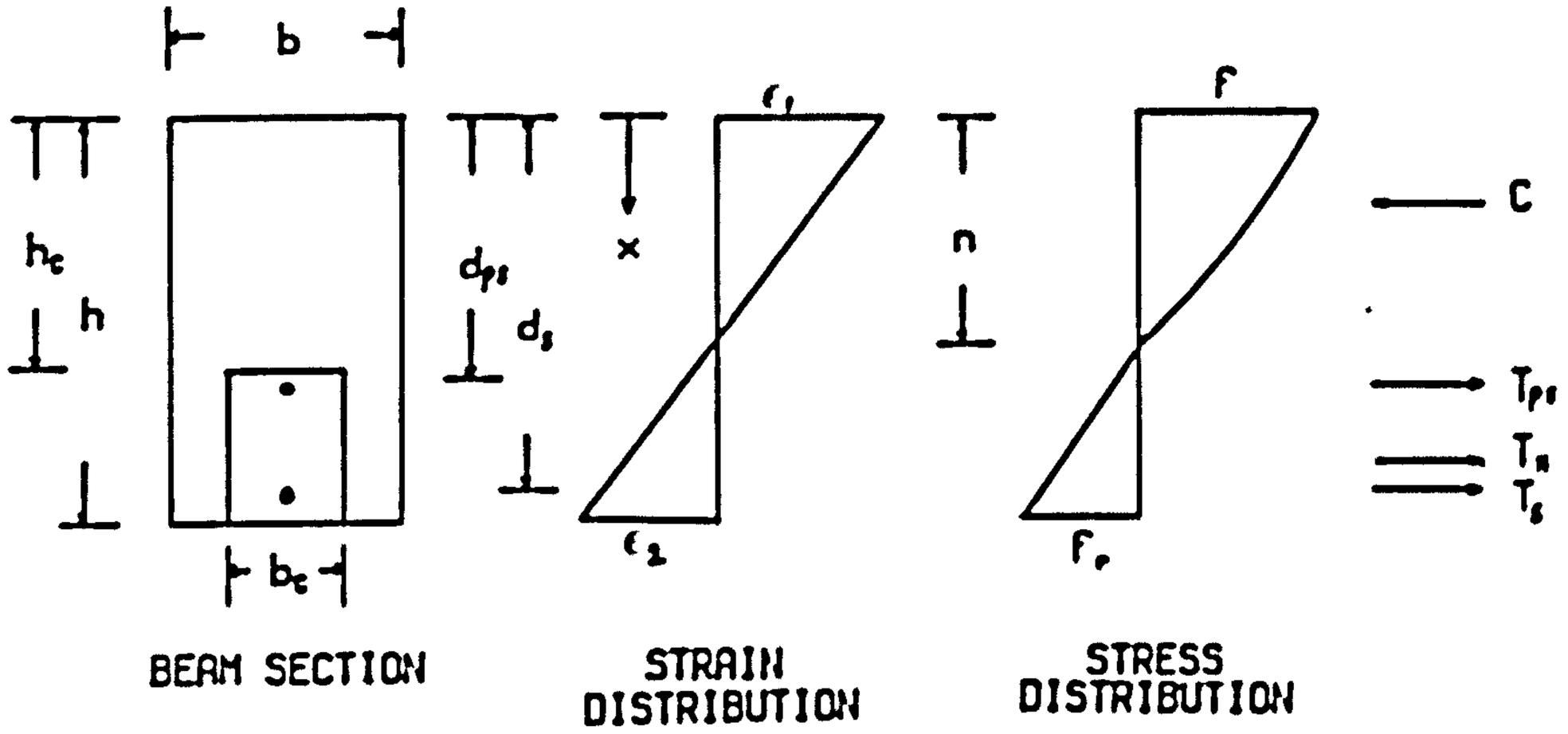

Figure 4.2.2

STRAIN PROFILES

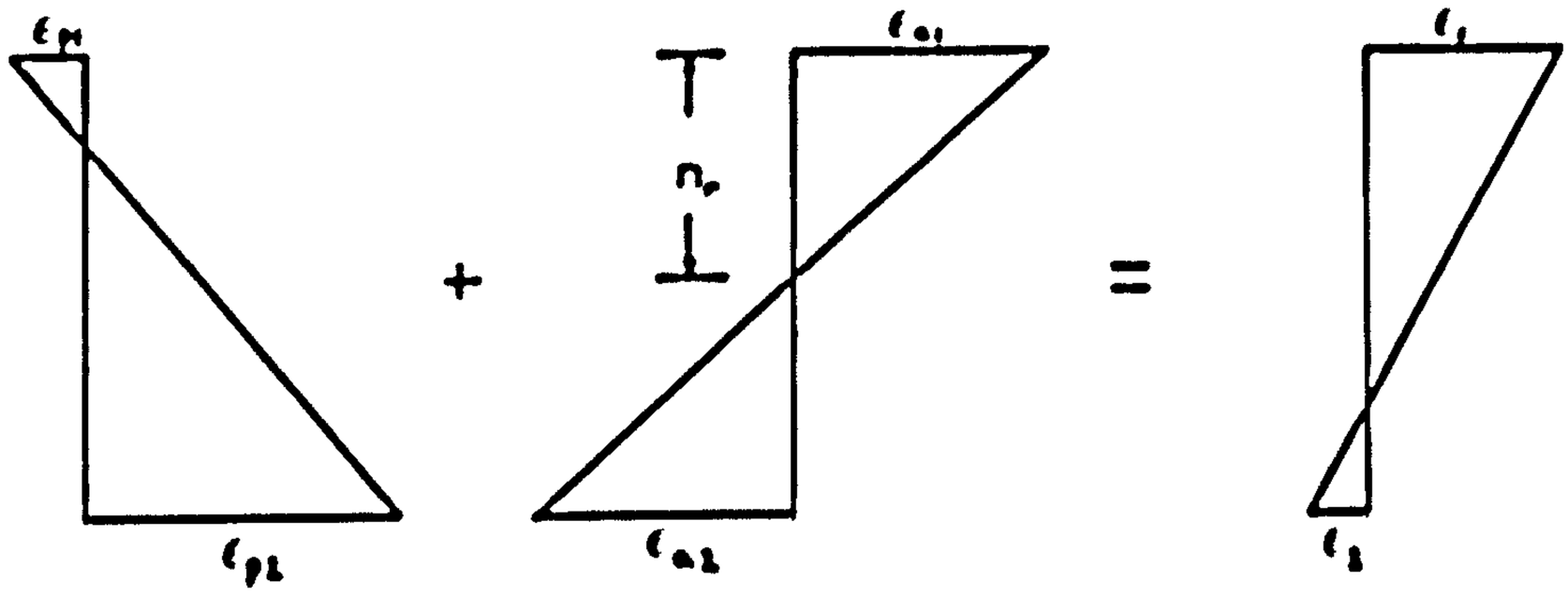

Figure 4.2.3

The cracking moment is found by equating the internal forces and taking moments about the soffit of the beam. The total compressive force in the section is given by:

$$C = b\int_{(n-h_c)}^{n} F_m(\varepsilon)dx + (b-b_c)\int_{0}^{(n-h_c)} F_m(\varepsilon)dx + b_c\int_{0}^{(n-h_c)} F_c(\varepsilon)dx \qquad (4.2.13a)$$

if, however, the neutral axis depth is less than h_c then equation 4.2.13a simplifies to:

$$C = b\int_{0}^{n} F_m(\varepsilon)dx \qquad (4.2.13b)$$

where $$\varepsilon = \varepsilon_1 - (\varepsilon_1 \frac{x}{n}) \qquad (4.2.14)$$

$$n = \left(\frac{\varepsilon_1}{\varepsilon_1+\varepsilon_2}\right) h \qquad (4.2.15)$$

The strain in the tensioned reinforcement is the sum of the strain due to prestress, ε_{psp}, prestrain in the brickwork at the level of the tensioned steel, ε_{psb}, and the strain due to applied loading, ε_{psa}. Before tensile strains occur in the brickwork at the level of the tendon the precompression at that level must be overcome, assuming full bond an equal strain will be induced into the tensioned steel, ε_{psb}. The strain due to applied loading is given by:

$$\varepsilon_{psa} = \varepsilon_{a_2} \frac{(d_{ps}-n_r)}{(h-n_r)} \qquad (4.2.16)$$

and therefore the total strain in the tensioned steel is:

$$\varepsilon_{ps} = \varepsilon_{psa} + \varepsilon_{psb} + \varepsilon_{psp} \qquad (4.2.17)$$

and, hence the tensile force:

$$T_{ps} = A_{ps}\, F_{ps}(\varepsilon_{ps}) \qquad (4.2.18)$$

The strain in the non-tensioned reinforcement due to applied load, ε_{sa}, is given by equation 4.2.16, except d_{ps} is substituted by d_s. Total strain in the non-tensioned steel is the sum of strain due to applied load and precompression at the level of the non-tensioned reinforcement, thus:

$$\varepsilon_s = \varepsilon_{sa} + \varepsilon_{sb} \qquad (4.2.19)$$

and so:

$$T_s = A_s\, F_s(\varepsilon_s) \qquad (4.2.20)$$

The tensile force in the brickwork, assuming linear elastic behaviour is:

$$T_m = fr\, \frac{b}{2}(h-n) \qquad (4.2.21)$$

If $n < h_c$ then a small error is introduced since f_r, the modulus of rupture for the composite section, is greater than the flexural tensile strength of brickwork, section 3.6.4. The difference, however, is sufficiently small not to influence the accuracy.

For equilibrium:

$$C = T_{ps} + T_s + T_c \qquad (4.2.22)$$

or $$0.98 < \frac{C}{T} < 1.02 \qquad (4.2.23)$$

The cracking moment is found by taking moments of forces about the soffit of the beam. The distance to the centroid of the compression zone with respect to the soffit is given by either:

$$\ell_a = \frac{\left[b\int_{(n-h_c)}^{n} F_c(\varepsilon)(h-x)dx + (b-b_c)\int_{0}^{(n-h_c)} F_c(\varepsilon)(h-x)dx + bc\int_{0}^{(n-h_c)} F_c(\varepsilon)(h-x)dx\right]}{C} \qquad (4.2.24)$$

or if $n<h_c$ then,

$$\ell_a = \frac{b\int_{0}^{n} F_c(\varepsilon)(h-x)dx}{C} \qquad (4.2.25)$$

Thus the cracking moment:

$$M_{cr} = C\,\ell_a - \left[T_{ps}(h-d_{ps}) + T_s(h-d_s) + T_c\left(\frac{h-n}{3}\right)\right] \qquad (4.2.26)$$

Curvature is given by:

$$\phi = \left(\frac{\varepsilon_1 - \varepsilon_2}{h}\right) \qquad (4.2.27)$$

The moment-curvature relationship up to cracking is found by applying increments of ε_{cr} to the bottom fibre strain. An initial neutral axis depth, n_r, is assumed for the strain profile due to applied loading, either h/2 or the depth of the centroidal axis of the transformed section. From this the applied loading strains in the brickwork and steel are found. The internal forces are found from equations 4.2.13, 4.2.18, 4.2.20 and 4.2.21. If equation 4.2.23 is not satisfied the process is repeated with a revised value for n_r until equilibrium is obtained. Moments and curvatures are found from equations 4.2.26 and 4.2.27.

4.2.2.3 Moment-curvature from cracking to ultimate

Once cracking has occurred the crack is assumed to extend up to the neutral axis depth, however, this is not strictly correct because of the tensile strength of the brickwork. Since the tensile strength of the brickwork is very small the validity of the analysis is not altered. The moment-curvature is calculated from cracking moment to ultimate. There are two possible states at cracking, the uncracked, section 4.2.2.2 and the cracked. Once the tensile strength has been exceeded the steel stress and strain increases and there is a decrease in neutral axis depth causing an increase in compressive strain and stresses in the brickwork. The equation of equilibrium becomes:

$$b\int_{(n-h_c)}^{n} F_m(\varepsilon)dx + (b-b_c)\int_{0}^{(n-h_c)} F_m(\varepsilon)dx + b_c\int_{0}^{(n-h_c)} F_c(\varepsilon)dx = A_{ps}F_{ps}(\varepsilon_{ps}) + A_sF_s(\varepsilon_s) \qquad (4.2.28)$$

where $\varepsilon = \varepsilon_1 - (\varepsilon_1\, x/n)$ (4.2.29)

if $n < h_c$ then equation 4.2.28 becomes:

$$b\int_0^h F_m(\varepsilon)dx = A_{ps}F_{ps}(\varepsilon_{ps}) + A_sF_s(\varepsilon_s) \qquad (4.2.30)$$

Thus the cracking moment is defined by:

$$M_{cr} = C\,\ell_a - \left[T_{ps}(h-d_{ps}) + T_s(h-d_s)\right] \qquad (4.2.31)$$

As values for tensile and compressive strains are not known, figure 4.2.4, they are found by simultaneous solution of equations 4.2.28, 4.2.30 and 4.2.31.

The moment-curvature relationship up to ultimate is found by applying increments of strain to the top fibre up to ε_m. The internal forces are equated using equation 4.2.28 and the moment is found thus:

$$M = C\,\ell_a - T_{ps}(h-d_{ps}) + T_s(h-d_s) \qquad (4.2.32)$$

and so the curvature:

$$\phi = \frac{\varepsilon_s + \varepsilon_c}{d_s} \qquad (4.2.33)$$

The ultimate moment is given by the equation above when the top fibre strain equals the ultimate compressive strain, ε_m.

4.2.3 Deflection

The moment-curvature relationship from prestressing to ultimate is now known and hence the curvature at any point along the

CONDITIONS AT CRACKED SECTION

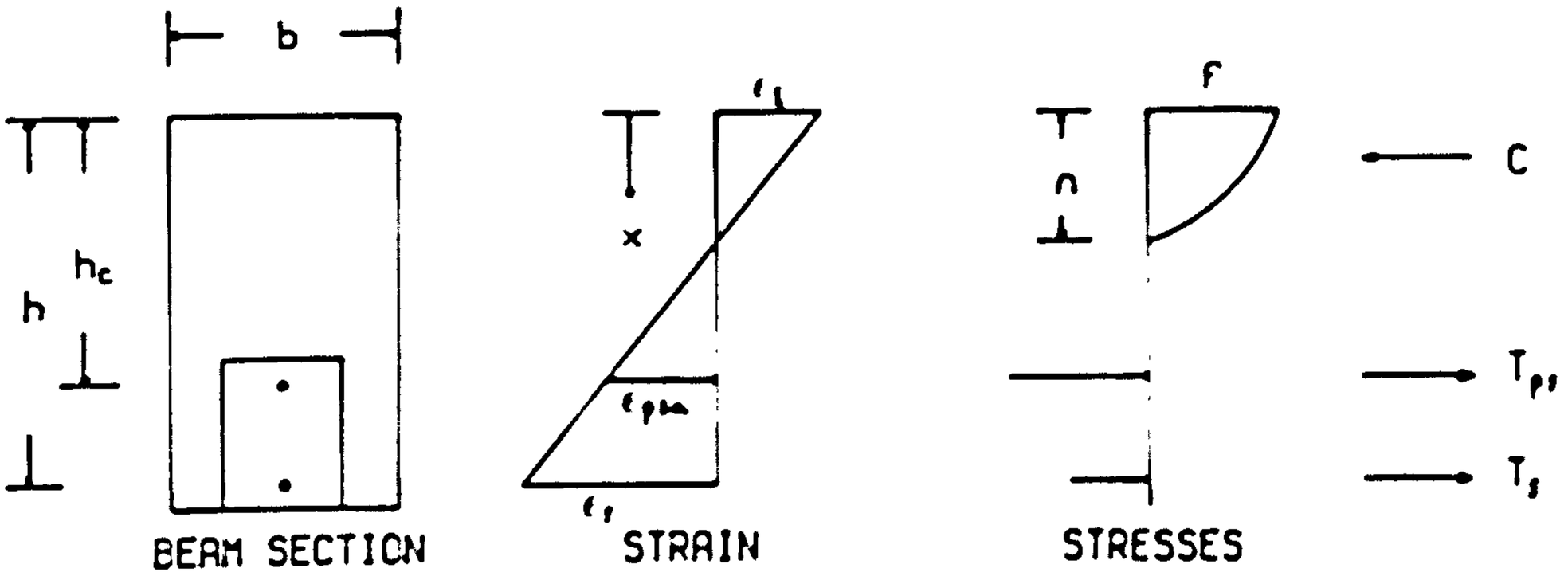

Figure 4.2.4

span of the beam can be determined if the shape and magnitude of the bending moment diagram is also known. The calculation of deflection becomes a simple problem of double integration of the average moment-curvature relationship, chapter 6, along the span of the beam, ie:

$$\phi = \frac{d^2y}{dx^2} \qquad (4.2.34)$$

The technique of finite differences[62] was used to obtain the deflections. A series of simultaneous equations are generated which are solved using standard mathematical techniques. A large number of computations are involved to derive the load/deflection response, the numerical method adopted was readily incorporated into the computer programme, Appendix A.

4.3 ULTIMATE MOMENT IN DESIGN

4.3.1 Ultimate moment

Using the direct method the ultimate moment is predicted in the process of calculating the complete moment-curvature relationship, involving a large number of calculations. For design a more simplified method to estimate the ultimate moment of resistance of a section may be required, an alternative method is presented in this section.

Conditions at the ultimate limit state of flexure for a

rectangular partially prestressed brickwork beam are shown in figure 4.3.1. The assumptions made for the direct method, section 4.2, apply also in the following derivation.

At the time of flexural failure the prestress has been completely neutralised and so conditions are very similar to those in a reinforced beam. Ultimate moment is determined by initially balancing the internal forces, for the general case:

$$C = \lambda_1 \lambda_2 b n f_m \qquad (4.3.1)$$

$$T = A_{ps} f_{psu} + A_s f_{su} \qquad (4.3.2)$$

$$C = T \qquad (4.3.3)$$

$$\varepsilon_{psu} = \varepsilon_{psp} + \varepsilon_{psa} + \varepsilon_{psb} \qquad (4.3.4)$$

where ε_{psp} = strain due to prestress

ε_{psa} = strain due to applied load

ε_{psb} = strain due to precompression in brickwork at level of tendons

$$\varepsilon_{su} = \varepsilon_{sp} + \varepsilon_{sa} + \varepsilon_{sb} \qquad (4.3.5)$$

where ε_{sp} = strain induced into non-tensioned steel due to prestress. Assumed to be zero.

ε_{sa} = strain due to applied load.

ε_{sb} = strain due to precompression in brickwork at level of non-tensioned steel.

CONDTIONS AT ULTIMATE MOMENT IN PARTIALLY PRESTRESSED BRICKWORK BEAM

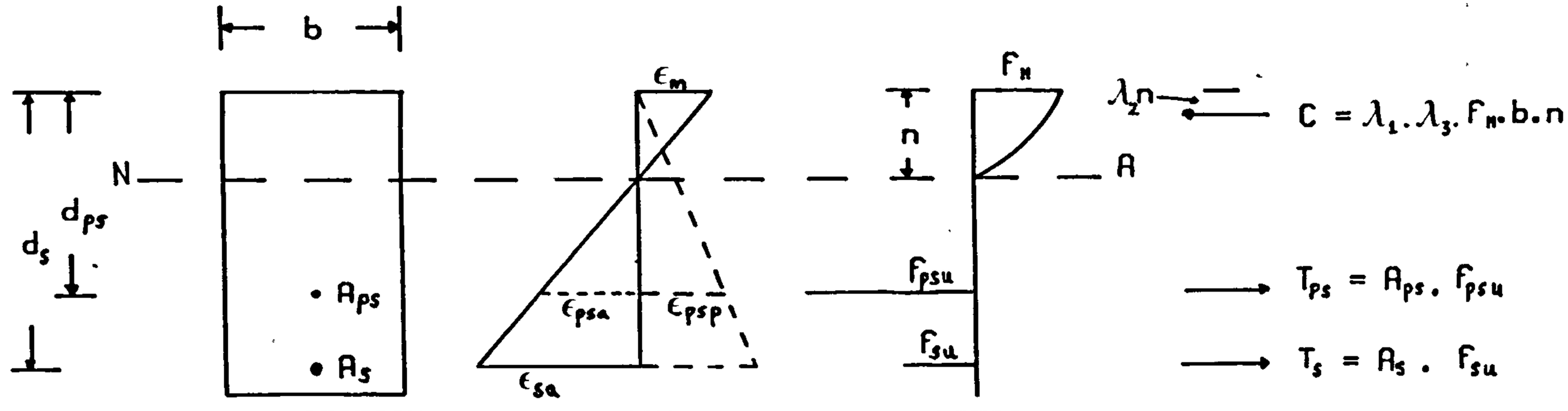

Figure 4.3.1

The strains due to applied load are given by:

$$\varepsilon_{psa} = \frac{\varepsilon_m (d_{ps} - n)}{n} \qquad (4.3.6)$$

$$\varepsilon_{sa} = \frac{\varepsilon_m (d_s - n)}{n} \qquad (4.3.7)$$

f_{psu} and f_{su} are there obtained by substituting ε_{psu} and ε_{su} into their respective stress/strain relationships. By a process of trial and error the neutral axis depth, n, is adjusted until equation 4.3.3 is satisfied.

Once this is achieved the ultimate moment is given by:

$$M_u = f_{psu}\, A_{ps} \left[d_{ps} - \lambda_2 n\right] + f_{su}\, A_s \left[d_s - \lambda_2 n\right] \qquad (4.3.8)$$

Equation 4.3.8 represents the ultimate moment for a general case. Design of reinforced and prestressed brickwork beams will be carried out in accordance with the recommendations of BS 5628, Part 2[15]. A rectangular stress block is assumed to develop at ultimate, compressive strength equal to f_k, $\lambda_1 = 1$, $\lambda_2 = 0.5$, and $\lambda_3 = 1$.

Therefore equation 4.3.1 becomes:

$$C = b\, n\, f_k \qquad (4.3.9)$$

and equation 4.3.8 simplifies to:

$$M_u = f_{psu}\, A_{ps} \left[d_{ps} - n/2\right] + f_{su}\, A_s \left[d_s - n/2\right] \qquad (4.3.10)$$

4.3.2 Balanced section

Accurate prediction of the ultmate moment is possible only when all the likely failure modes and their characteristics have been considered. The possible failure modes are tensile, an under-reinforced section, compression, an over-reinforced section, and shear or a combination of these. Failure of an under-reinforced section, yielding of the tensile steel, is associated with large deflections and cracking thereby giving adequate warning of the inevitable collapse. Conversely a primary compression failure, no yielding of the tensile steel, generally occurs without warning and also leads to inefficient use of the materials. Whether a design solution is under or over-reinforced is therefore of some considerable practical interest. The adequate warning of collapse and economy of materials makes the under-reinforced section the preferable design solution. Ideally, however, the section would be balanced, where failure of the tensile reinforcement and brickwork in compression takes place simultaneously.

In conventionally reinforced brickwork or concrete beams calculation of the balanced section is a simple procedure[63], the steel area for balanced conditions are given by:

$$\rho_{bal} = \lambda_1 \lambda_3 \frac{f_m}{f_{sy}} \left(\frac{\varepsilon_m}{\varepsilon_m + \varepsilon_{sy}}\right) \qquad (4.3.11)$$

Fully prestressed brickwork[9] presents a more complicated problem since the steel stress at failure and hence the balanced steel area wil be influenced by the prestrain in the tensioned steel. The balanced section steel area is given by:

$$\rho_{bd} = \lambda_1 \lambda_3 \frac{f_m}{f_{psy}} \frac{\varepsilon_m}{\varepsilon_m + \varepsilon_{psy} - (\varepsilon_e + \varepsilon_{psp})} \qquad (4.3.12).$$

In a partially prestressed beam section the problem is made more complex by the presence of both tensioned and non-tensioned steel. If all the steel, tensioned and non-tensioned, is placed at one level, Thurlimann[64] showed that for both reinforcements to achieve their full capacity the prestress should equal the difference between proof stress of the tensioned and non-tensioned steel. Applying this criteria to the reinforcement type used in this investigation, $f_{psy} = 1650\ N/mm^2$ and $f_{sy} = 475\ N/mm^2$, the prestress would equal $1175\ N/mm^2$ or approximately 70% of the tendons breaking load. For a balanced section the combined area of tensile reinforcement must yield simultaneously with crushing of the brickwork. This may be found from equation 4.3.12 by incorporating the area of non-tensioned steel into an effective area of tensioned steel.

The conditions at a balanced failure are shown in figure 4.3.2 for a partially prestressed brickwork beam in which the non-tensioned steel is placed closer to the soffit. For simultaneous yielding of the tensile reinforcement, strain in the tensioned reinforcement due to prestress must equal:

$$\varepsilon_{psp} = \varepsilon_{psy} - \frac{(d_{ps} - n)}{(d_s - n)} \varepsilon_{sy} \qquad (4.3.13)$$

From equation 4.2.13 above it is apparent that as the depth to the non-tensioned steel increases compared to the depth of the

CONDITIONS AT BALANCED FAILURE

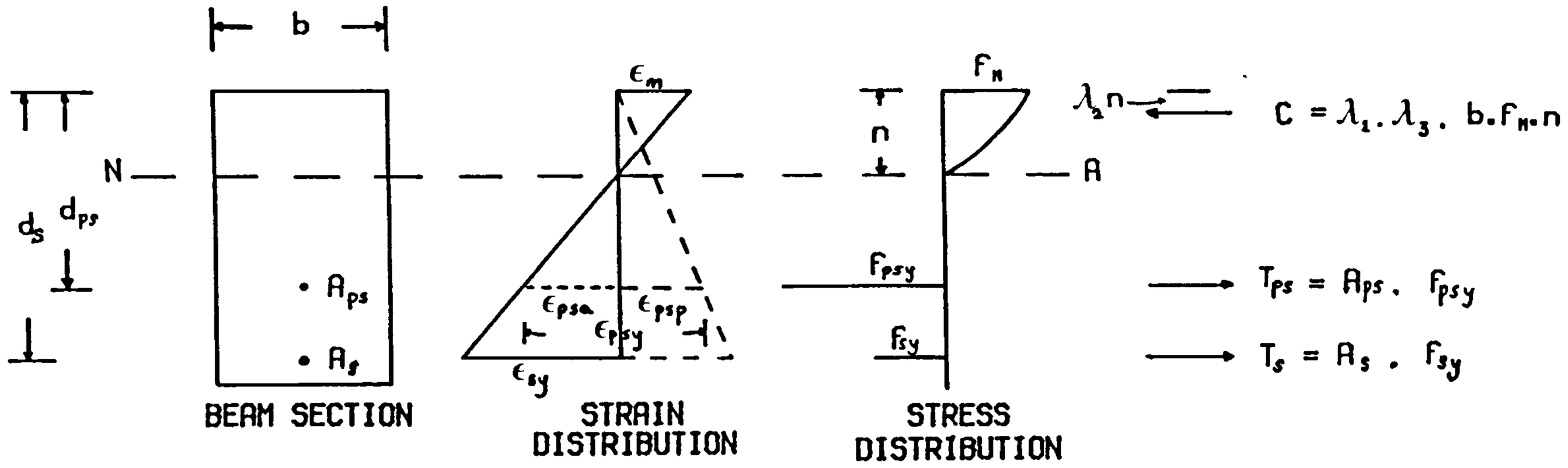

Figure 4.3.2

tensioned the prestress necessary for balanced behaviour must increase. However since the maximum allowable prestressing force is not greater than 80%[36] of the tendons breaking load balanced behaviour is not likely for most practical applications.

The effective steel area may be found from equation 4.3.12, however, this does not ensure simultaneous yielding of the reinforcement. It is possible for the beam section to be under-reinforced for the non-tensioned steel and over-reinforced with respect to the tensioned. Accurate prediction of the ultimate moment and hence steel stresses using the direct method will ensure in design whether or not the member is under-reinforced.

CHAPTER 5

EXPERIMENTAL RESULTS AND COMPARISON WITH THEORY

5.1 INTRODUCTION

This chapter presents and discusses in detail the experimental results for ultimate moment, moment-curvature and load/deflection responses of the 41 full-scale partially prestressed brickwork beams tested as part of this study. The cross-sectional details of each of the beam series reported below were given in section 3.7.1.

The primary aims of this investigation were to study the effect of the following variables:

(i) % area of steel

(ii) prestressing force

(iii) partial prestressing ratio

(iv) cover to non-tensioned steel

(v) brick strength

(vi) mortar grade or strength

on the ultimate moment and load/deflection of partially prestressed brickwork beams.

The influence of the % area of steel on the behaviour of partially prestressed brickwork beams was investigated by comparing behaviour of beam series A (0.47% steel area), with the results of beam series B (0.37% steel area) and the results of beam series C (0.31% steel area). The brick strength, mortar grade and prestressing force were kept constant in all three series of beams.

The effect of varying the prestressing force was studied by the comparing behaviour of beam series AA with the behaviour of beam series AB. All of the variables mentioned earlier were kept constant except for a reduction in the average prestressing force in beams AB1 - AB3 compared to the average prestressing force of beams AA1 - AA3. The effect of varying the prestressing force was also briefly considered by comparing the behaviour of beam series C and beam series CP. Details of the beams are given in figure 3.7.2 and table 5.2.1.

In chapter 1 partially prestressed sections were defined as containing both tensioned and non-tensioned reinforcement. Clearly partially prestressed beams occupy a whole spectrum of possible beam sections between the extremes of reinforced and fully prestressed beams. In order to quantify the amount of prestressing in a partially prestressed brickwork beam the term 'partial prestressing ratio' [37] was adopted for this work. The partial prestressing ratio (PPR) is defined as the ratio of ultimate moment due to the prestressing steel to ultimate resisting moment due to the total tensile steel, i.e.

$$PPR = \frac{(Mu)_p}{(Mu)_{p+s}} \qquad (5.1.1)$$

The partial prestressing ratio varies between zero, a reinforced beam, and unity, represented by a fully prestressed beam. Between these two extremes lie any number of possible partially prestressed sections.

To study the effect of PPR on the load/deflection response

of partially prestressed brickwork beams four different beam series were tested. The ultimate moment of all four beam series was maintained constant. The PPR was experimentally varied between zero, reinforced brickwork beams R1-R3, and unity, the results for fully prestressed brickwork beams were taken from a previous experimental study[9]. Two series of intermediate partially prestressed brickwork beams were also tested, PPR = 0.56 (beams C1 - C8) and PPR = 0.33 (beams P1 - P3), figure 3.7.2. The partial prestressing ratio of the two partially prestressed beams were calculated on basis of the theoretical calculations of ultimate moment using the properties of brickwork given by the single course prisms.

The influence of cover to the non-tensioned steel on the ultimate moment and moment-curvature of partially prestressed brickwork beams was also briefly considered by comparing the experimental results for beam series C, cover equal to 25 mm, with the results of beam series CC, cover equal to 50 mm.

The effect of brick strength was considered by comparing the behaviour beam series C, built of high strength bricks, with the ultimate moment and load/deflection response of beam series CM, built using medium strength bricks, and beam series CL, built using low strength bricks. The influence of mortar grade was found by comparing the behaviour of beam series C, built with grade I mortar, with that of beam series CG, built with grade II mortar, whilst brick strength was kept constant.

The experimental results are compared with theoretical values for ultimate moment, moment-curvature and load/deflection

predicted using the theory developed in chapter 4 and the experimentally derived material properties as outlined in chapter 3. Computations were carried out using the computer programme listed in Appendix A. The ultimate moment and deflection was also predicted in accordance with the recommendations of BS 5628 Part 2[15] and compared with a number of the experimental test results.

5.2 EXPERIMENTAL RESULTS

The results for effective prestressing force, ultimate moment, ultimate shear stress and mode of failure for all beams tested in this study are presented in table 5.2.1.

In this section the results for prestressing force are considered. Also the results for the top fibre brickwork strain, additional strain in the tensioned steel, strain in the non-tensioned steel and neutral axis depth plotted against moment are presented and briefly discussed.

5.2.1 Prestressing force

The prestressing forces for each beam at transfer, at lock-off and at the time of testing are shown in table 5.2.1.

Comparison of the prestressing forces at transfer and after lock-off show that the losses due to lock-off varied between 2.3% (beam CP3) and 16.1% (beams AA2 and CL2). The average reduction in the prestressing force as a result of lock-off losses was 11.4%.

Table 5.2.1

Summary of Experimental results

Beam No	Brick Strength N/mm²	Mortar Strength N/mm²	Concrete Strength N/mm²	Span mm	Prestress Force					Ult. Moment kNm	Shear Stress[1] N/mm²	Mode of failure
					At transfer kN	At lock-off kN	% loss at lock-off	At test kN	Total % loss			
A1	96.6	16.9	19.8	6200	83.6	72.1	13.8	68.5	18.1	61.3	0.393	Shear
A2	96.6	19.8	21.7	6200	84.2	71.5	15.1	67.8	19.5	58.1	0.374	Shear
A3	96.6	16.3	23.2	6200	85.2	73.2	14.1	68.7	19.4	73.4	0.462	Tension[2]
AA1	96.6	19.0	22.1	6200	154.0	137.0	11.0	127.7	17.1	81.5	0.542	Tension[2]
AA2	96.6	18.4	20.4	6200	155.8	130.7	16.1	124.1	20.3	88.6	0.586	Tension
AA3	96.6	21.3	18.2	6200	160.1	142.4	11.1	132.7	17.1	87.5	0.579	Tension
AB1	96.6	18.5	18.8	6200	112.3	106.9	4.8	100.1	10.9	60.7	0.537	Tension[2]
AB2	96.6	17.5	17.1	6200	106.4	98.2	7.7	94.7	11.0	79.4	0.535	Tension[2]
AB3	96.6	19.0	20.2	6200	111.7	105.8	5.3	90.1	19.3	70.6	0.474	Tension[2]
B1	96.6	17.9	23.6	6200	85.4	72.4	15.2	68.8	19.4	62.0	0.404	Tension
B2	96.6	18.6	20.9	6200	80.4	71.5	11.1	68.3	15.1	70.6	0.415	Tension
B3	96.6	19.1	18.8	6200	83.8	74.7	10.9	66.2	21.0	63.4	0.412	Tension
C1	96.6	19.2	21.5	6200	81.6	71.6	12.3	67.4	17.4	52.8	0.357	Tension
C2	96.6	19.9	20.0	6200	82.7	73.6	11.0	66.7	19.4	53.2	0.359	Tension
C3	96.6	16.4	21.1	6200	83.1	73.3	11.8	61.4	26.1	54.6	0.368	Tension
C4	96.6	19.5	18.1	6200	82.4	70.6	14.3	64.8	21.4	51.5	0.349	Tension
C5	96.6	22.3	18.9	6200	85.1	72.9	14.3	69.2	18.7	51.5	0.349	Tension
C6	96.6	20.6	32.4	6200	85.2	75.0	12.0	57.7	32.3	57.5	0.386	Tension
C7	96.6	16.1	27.0	6200	89.1	78.5	11.9	70.8	11.5	54.3	0.367	Tension
C8	96.6	21.4	23.6	6200	82.8	71.8	13.3	66.7	19.5	52.2	0.353	Tension
CC1	96.6	22.1	16.9	5927	82.1	73.5	10.5	66.2	19.4	52.8	0.387	Tension
CC2	96.6	17.8	19.1	5927	77.0	67.4	12.5	64.4	16.4	52.5	0.386	Tension
CC3	96.6	21.4	20.2	5927	92.6	80.5	13.1	78.0	15.7	50.3	0.371	Tension
CP1	96.6	20.4	17.7	6200	65.5	57.0	13.0	51.4	21.5	52.0	0.353	Tension[2]
CP2	96.6	16.6	15.5	6200	62.4	54.4	12.8	51.1	18.1	53.6	0.362	Tension
CP3	96.6	17.0	16.6	6200	61.1	59.7	2.3	52.5	14.1	49.3	0.336	Tension[2]
P1	96.6	19.9	20.3	6200	46.1	42.6	7.6	36.6	19.5	56.6	0.356	Tension
P2	96.6	20.1	25.2	6200	51.1	45.7	10.6	35.3	30.9	55.3	0.349	Tension
P3	96.6	17.4	20.6	6200	48.7	43.2	11.3	41.6	14.7	52.9	0.336	Tension
R1	96.6	16.9	23.0	6200	-	-	-	-	-	52.2	0.304	Tension[2]
R2	96.6	19.7	18.8	6200	-	-	-	-	-	48.9	0.287	Tension[2]
R3	96.6	21.8	17.5	6200	-	-	-	-	-	48.9	0.299	Tension[2]
CG1	96.6	7.3	23.0	6200	95.2	85.8	9.9	76.8	19.4	54.5	0.363	Tension
CG2	96.6	8.6	20.9	6200	84.6	77.7	8.2	66.1	21.7	54.5	0.364	Tension
CG3	96.6	6.6	22.3	6200	80.8	71.4	11.6	70.7	12.4	54.5	0.368	Tension
CM1	72.3	19.6	23.6	6200	82.1	71.9	12.4	66.9	18.5	51.8	0.351	Tension[2]
CM2	72.3	21.3	21.3	6200	71.4	61.6	13.7	57.5	19.4	53.0	0.359	Tension
CM3	72.3	18.9	23.9	6200	83.2	73.0	11.3	64.1	23.0	48.5	0.331	Tension[2]
CL1	19.7	19.9	19.3	6200	67.3	57.4	14.7	55.9	16.9	26.4	0.195	Shear
CL2	19.7	17.2	23.7	6200	58.4	49.0	16.1	44.2	24.3	31.6	0.227	Shear
CL3	19.7	17.5	30.3	6200	65.1	63.0	3.2	52.6	19.3	41.4	0.287	Tension

[1] Shear stress calculated as V/b.d irrespective of failure mode

[2] Secondary shear failure

Lock-off losses were due to slip between the tendon and the wedge once the prestressing jack was released and consequently the losses were subject to a large amount of variation due to the random nature of the slippage. A proportion of the reduction in prestressing force ascribed to lock-off losses in beams AA1-AA3 and AB1-AB3 were in fact due to elastic shortening of the brickwork as these beams were post-tensioned with two tendons. After tensioning of the first tendon was completed the reduction in the length of the beam due to tensioning of the second tendon caused a relaxtion of the stress in the first tendon and hence a prestress loss. This loss was in the order of 1-2%.

Further losses in the prestressing force during the minimum of seven days between lock-off and testing varied between 0.8% (beam CG3) and 20.3% (beams C6 and P2), the average loss recorded was 7.5%. The significantly larger losses recorded in beams C6 and P2, table 5.2.1, were because testing of these beams was delayed by up to 28 days after concreting and so allowing greater time for loss of the prestressing force. The additional losses in the prestress after lock-off may have been caused by creep and shrinkage of the brickwork and concrete and relaxtion of the tendon. However, it was not possible to ascertain the exact nature of the prestress losses due to the complex nature of the composite section and also it was outside the scope of this work.

The total losses in prestressing force between transfer and testing varied between 10.9% (beam AB1) and 32.3% (beam C6), the average total prestress loss was 18.9%.

5.2.2 Variation of strain with depth

Throughout the loading history of each beam the surface strain distribution was measured. Typical variations of strain with depth are shown for high and medium strength brick beams in figures 5.2.1 and 5.2.2 respectively. As expected the strain distribution at all load increments from prestressing to ultimate varied linearly with depth. Strain in the brickwork was therefore directly proportional to the distance from the neutral axis, confirming the assumption made in the theory in section 4.2. Initially the strain at the soffit of the beam was compressive due to the prestress. With loading the compressive brickwork strains reduced at the soffit and increased at the top of the section. Eventually there was a change in the sign of the slope (curvature) of the strain distribution and with further loading the strain at the soffit of the beam became tensile after decompression of the prestress. Between prestressing and decompression the neutral axis depth remained outside of the section. Once cracking occurred the neutral axis depth from the top fibre of the beam decreased rapidly resulting in the increase of strain at the extreme fibres and with further loading the neutral axis depth moved up the beam. In the high and medium strength brick beams the neutral axis at the time of flexural failure was observed as being within the top course of brickwork, i.e. the neutral axis depth was less than 65 mm.

During the theoretical calculations it was assumed that full bond existed between the brickwork/concrete and steel reinforcement. This assumption was supported by observation during testing since in none of the beams was an anchorage bond failure seen to occur. In

TYPICAL STRAIN DISTRIBUTION FOR BEAM SERIES C

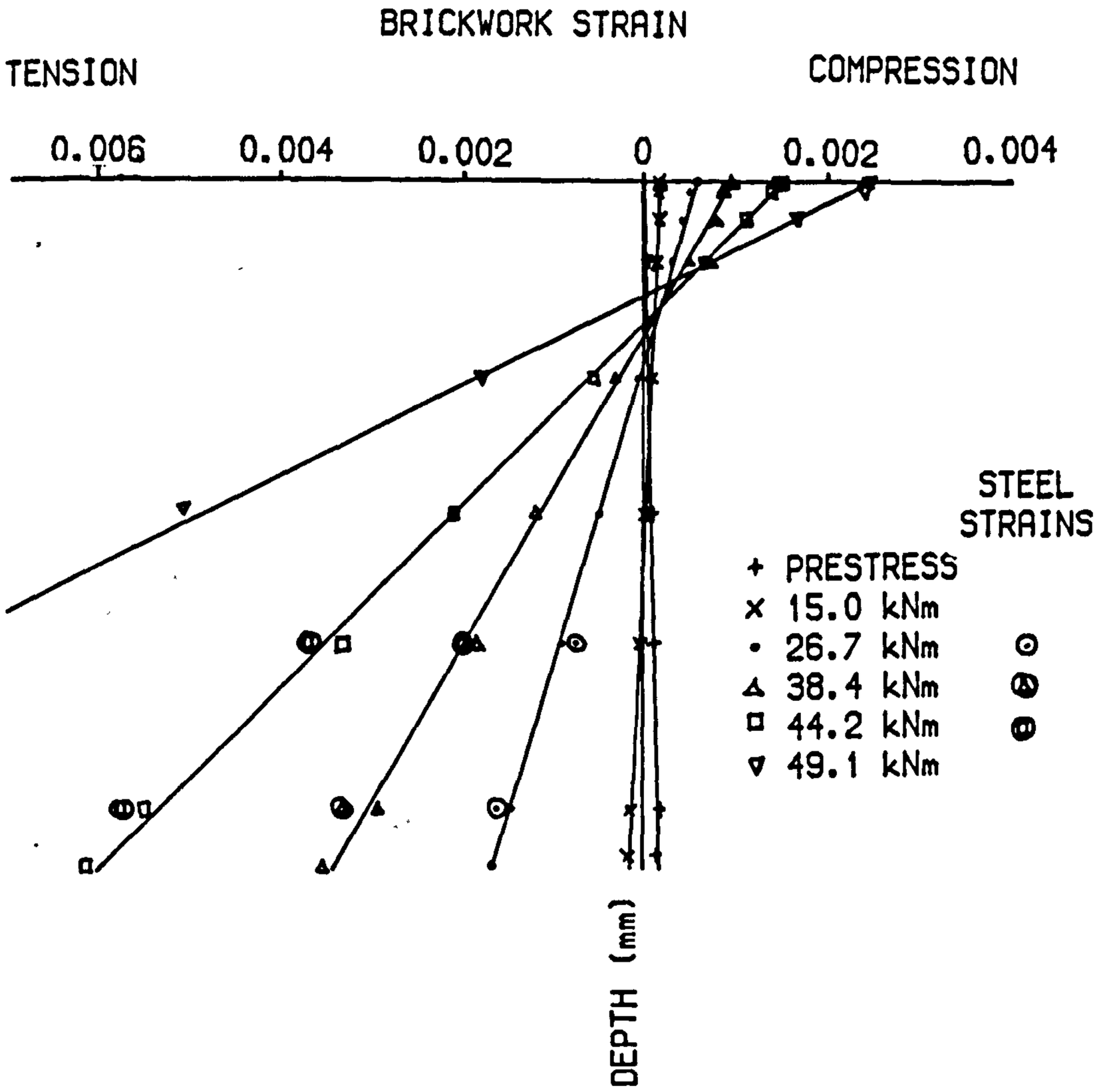

Figure 5.2.1

TYPICAL STRAIN DISTRIBUTION FOR BEAM SERIES CM

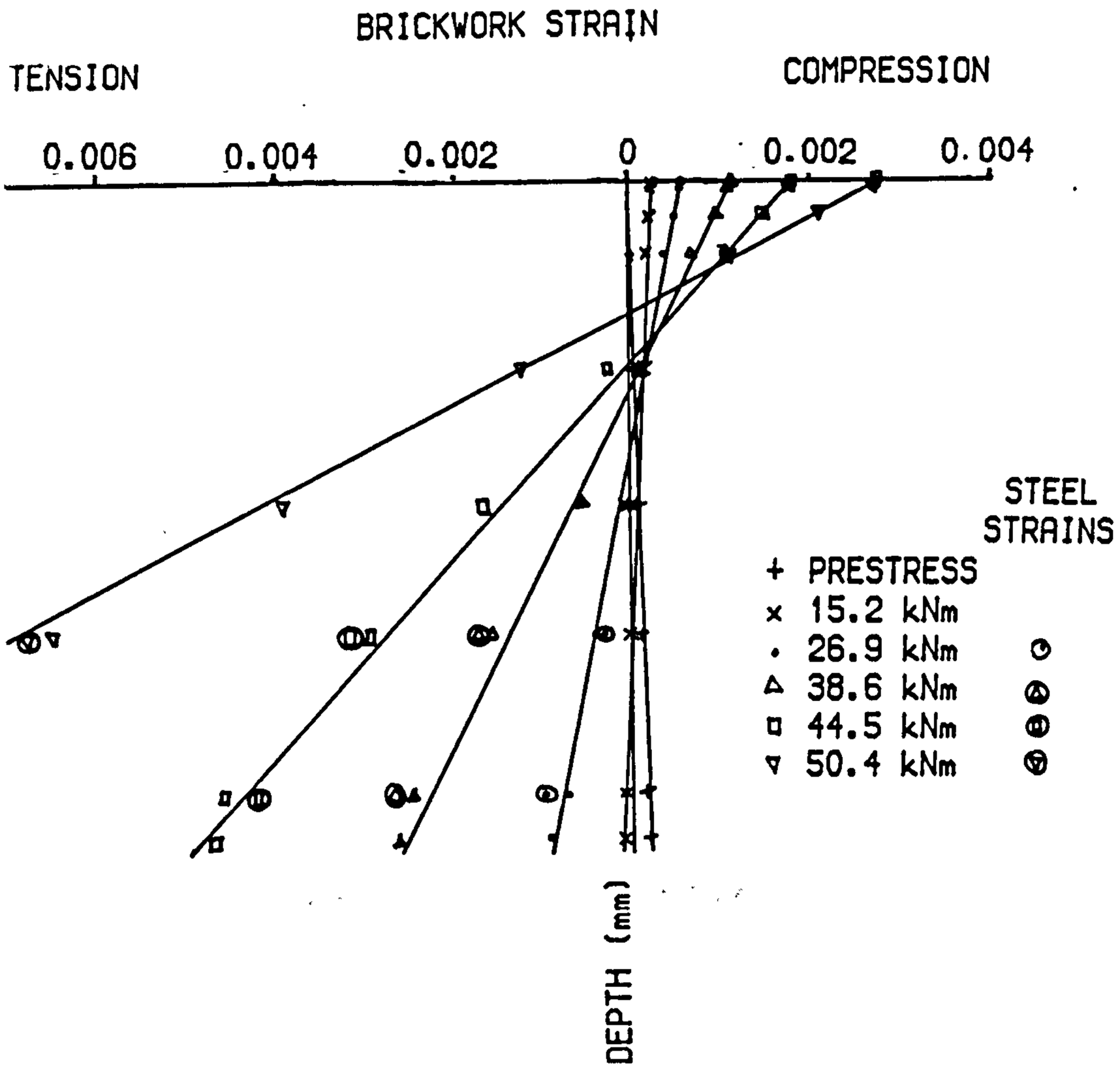

Figure 5.2.2

beams C6 - C8 removable anchorage plates were used, Plate 3.5, and consequently the tendon was no longer fixed to the end of the beam by the mild steel anchorage plates. No loss of prestress was recorded during removal of the plates at seven days after concreting, and during the testing no slip between the tensioned steel and the concrete was measured by dial gauges at each end of the beam.

Typical results of the strain measurements taken by electrical resistance gauges fixed to the steel and demec surface strain gauges on the beam at the same level are given in figures 5.2.1 and 5.2.2. There was close agreement between both the brickwork 'demec' strain and steel strain measurements between prestress and ultimate load which would indicate that full bond existed between the brickwork/concrete and steel.

5.2.3 Relationship between steel strain and moment

The experimental relationships between moment and strain in the tensioned and non-tensioned steel are given in figures 5.2.3a - 5.2.14a and 5.2.3b - 5.2.14b respectively. The values for strain given for the tensioned steel are the additional strains, over and above the initial prestrain, due to the applied moment. As the steel strains were measured at a number of positions in the constant moment zone, the results presented are those corresponding to maximum tensile strain, i.e. across a crack.

In the partially prestressed brickwork beams the compressive strain measured in the non-tensioned steel between prestressing and testing, caused by shrinkage and creep of the concrete and prestress

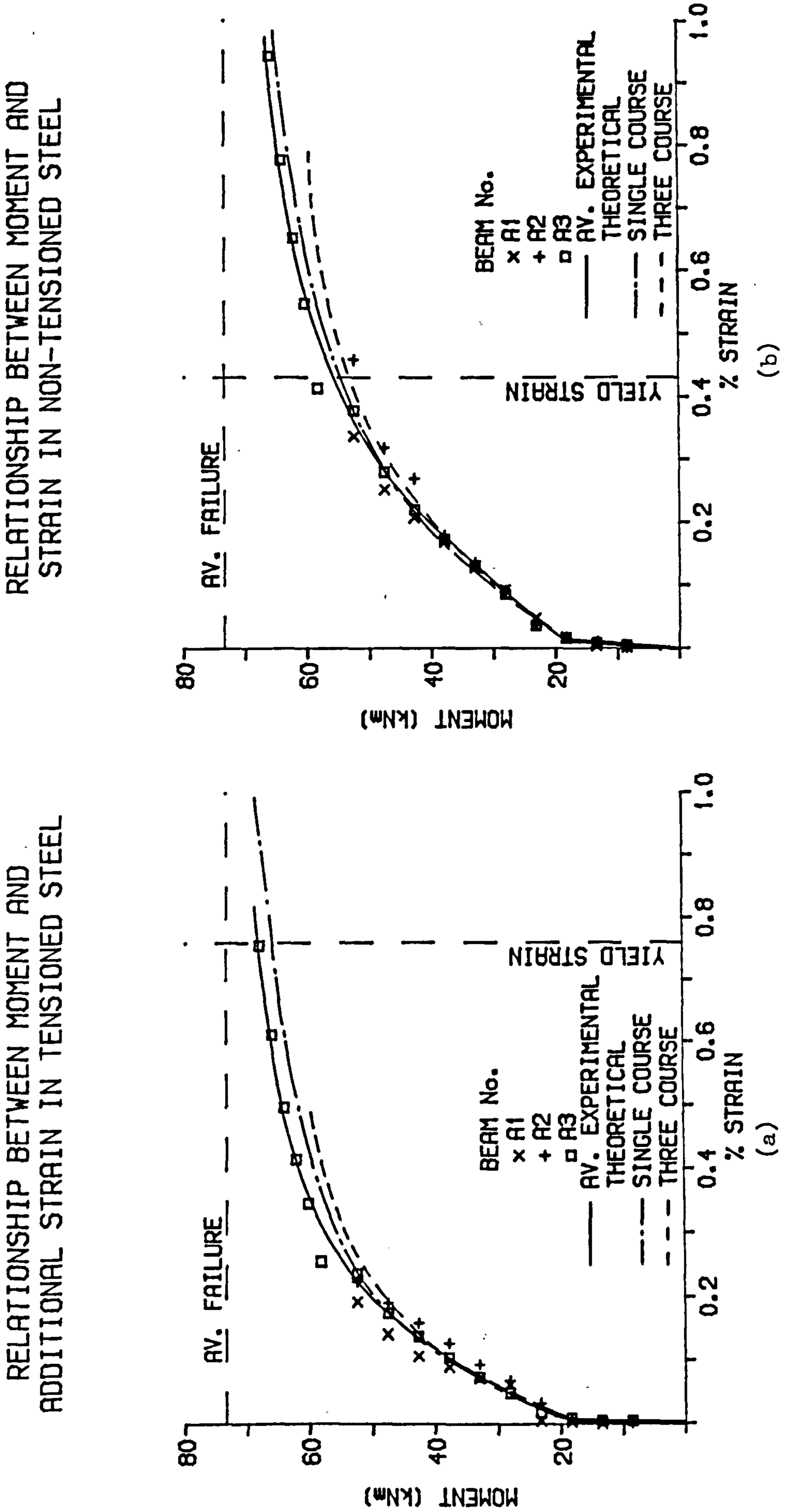
RELATIONSHIP BETWEEN MOMENT AND
STRAIN IN NON-TENSIONED STEEL
AV. FAILURE
MOMENT (kNm)
80
60
40
20
0
0.2
0.4
0.6
0.8
1.0
% STRAIN
YIELD STRAIN
BEAM No.
× A1
+ A2
□ A3
AV. EXPERIMENTAL
THEORETICAL
SINGLE COURSE
THREE COURSE
(b)
RELATIONSHIP BETWEEN MOMENT AND
ADDITIONAL STRAIN IN TENSIONED STEEL
AV. FAILURE
MOMENT (kNm)
80
60
40
20
0
0.2
0.4
0.6
0.8
1.0
% STRAIN
YIELD STRAIN
BEAM No.
× A1
+ A2
□ A3
AV. EXPERIMENTAL
THEORETICAL
SINGLE COURSE
THREE COURSE
(a)

Figure 5.2.3

RELATIONSHIP BETWEEN MOMENT AND TOP FIBRE STRAIN

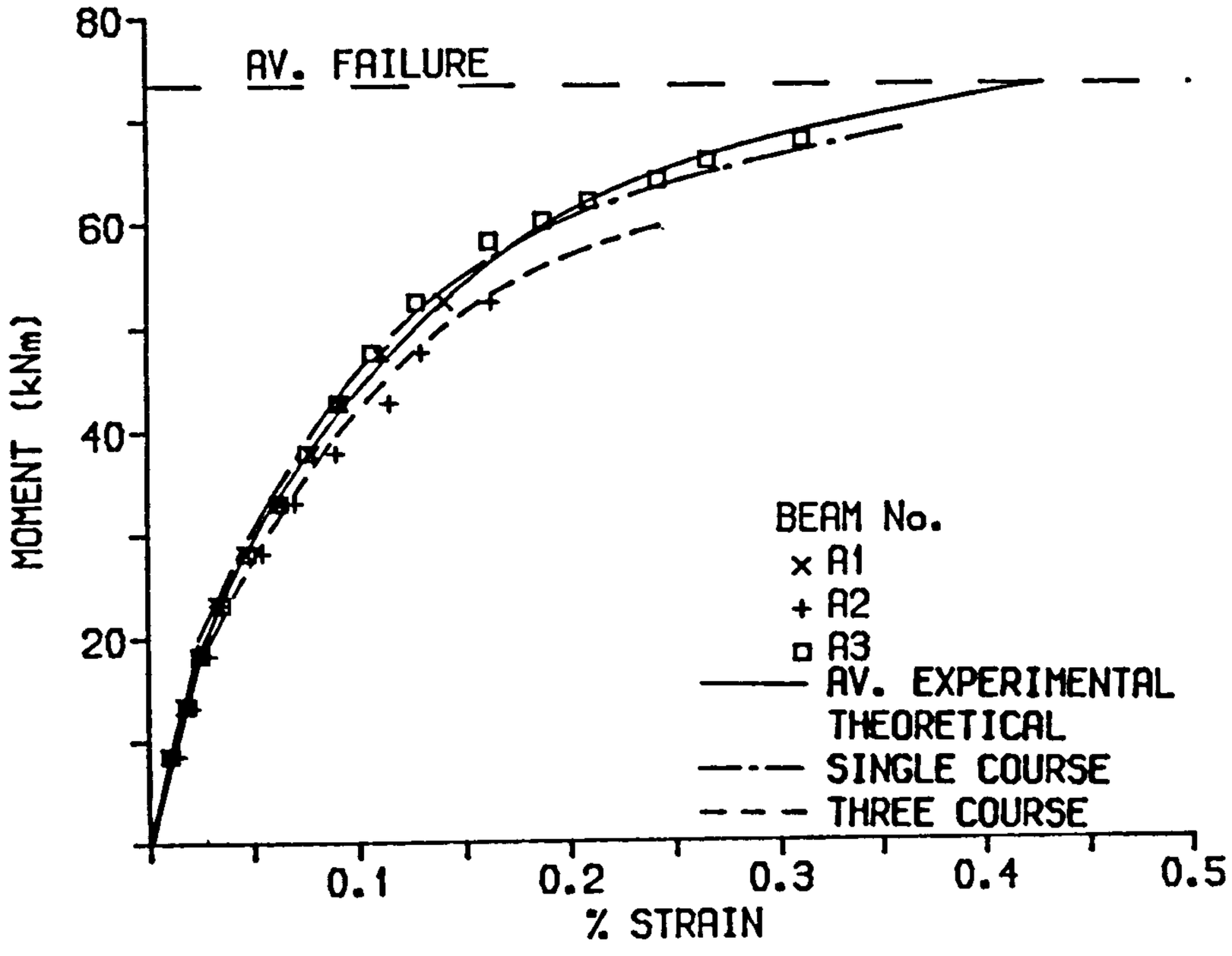

(c)

RELATIONSHIP BETWEEN MOMENT AND NEUTRAL AXIS DEPTH

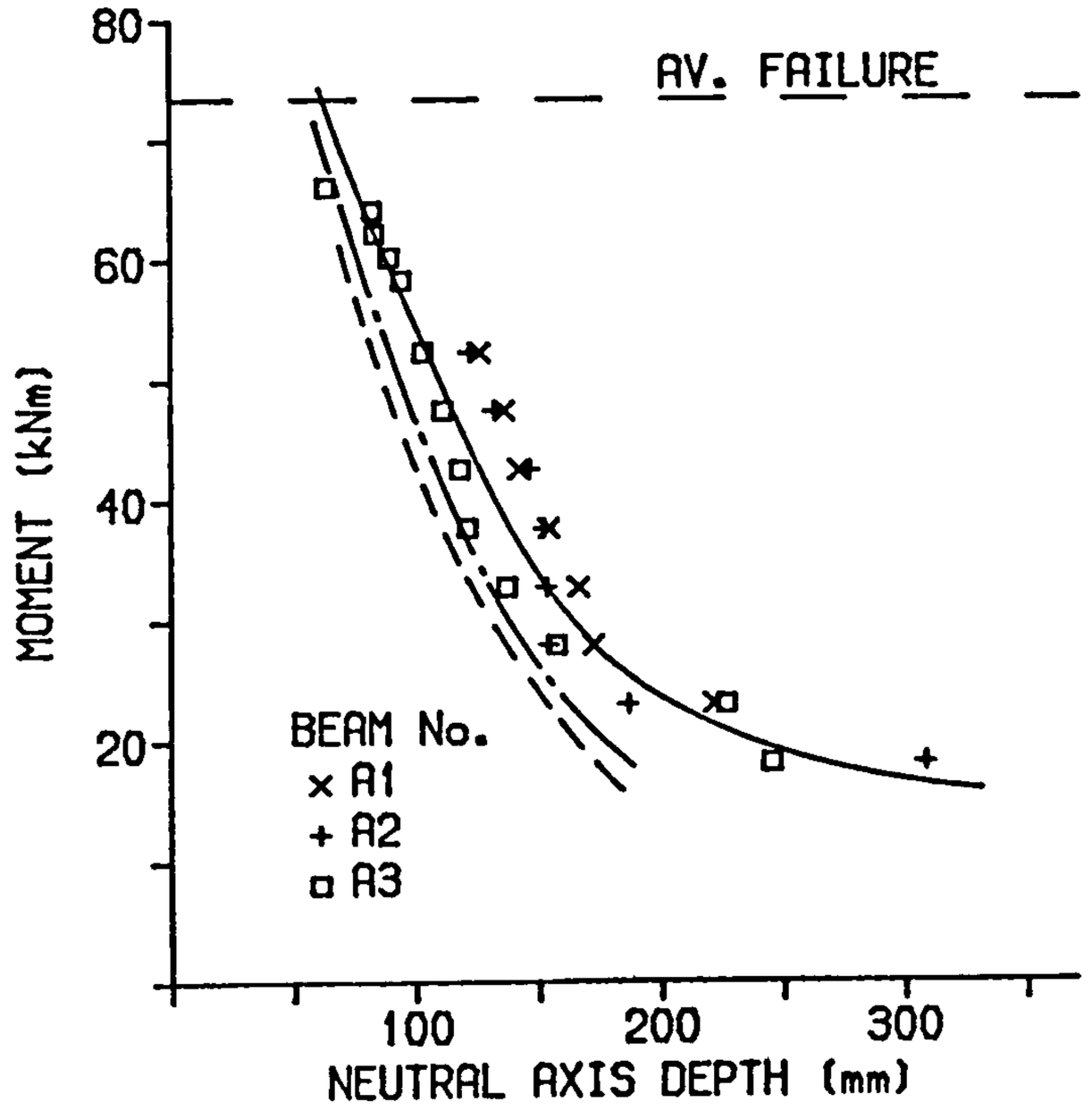

(d)

Figure 5.2.3 (Cont.)

RELATIONSHIP BETWEEN MOMENT AND ADDITIONAL STRAIN IN TENSIONED STEEL

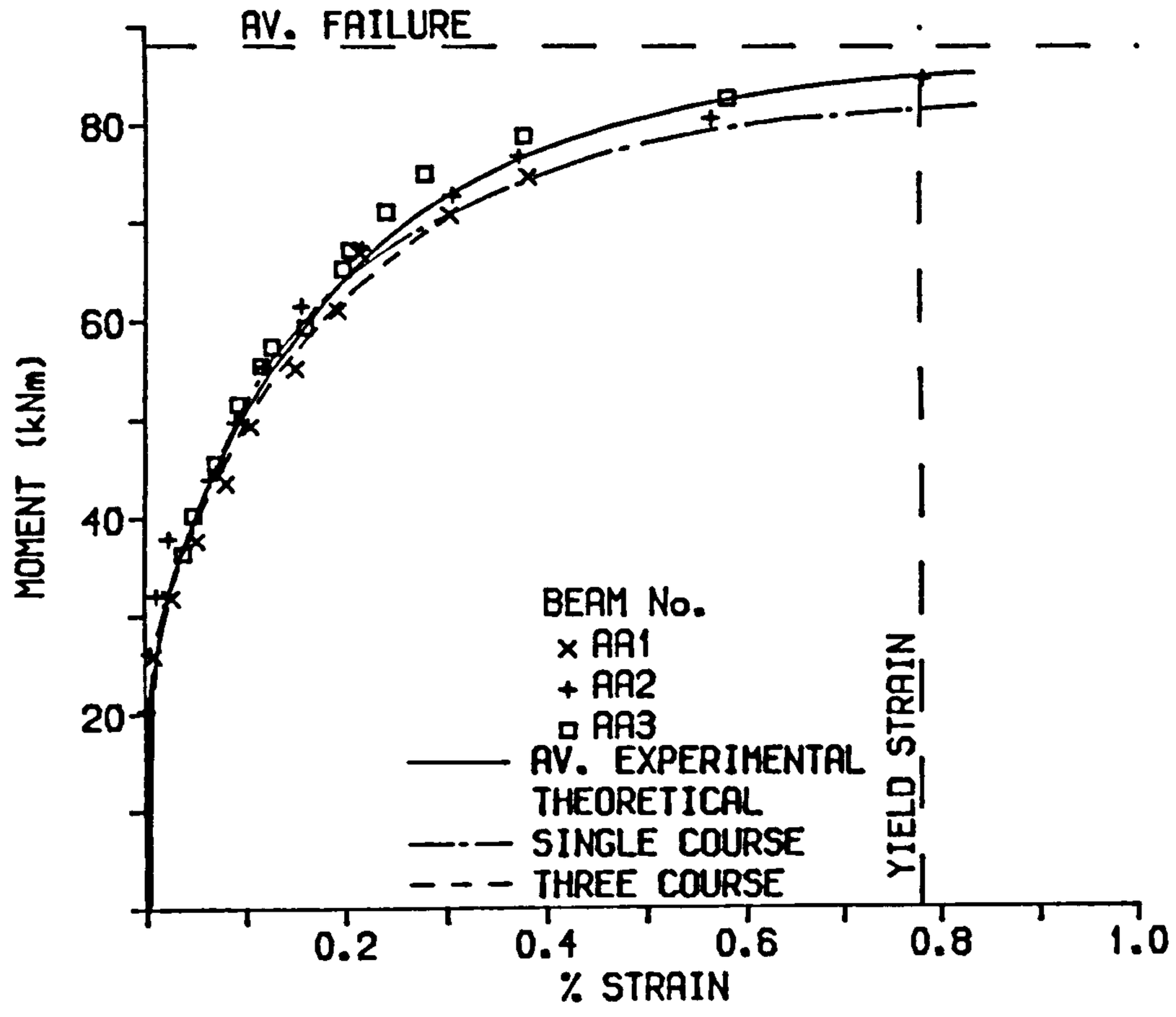

(a)

RELATIONSHIP BETWEEN MOMENT AND STRAIN IN NON-TENSIONED STEEL

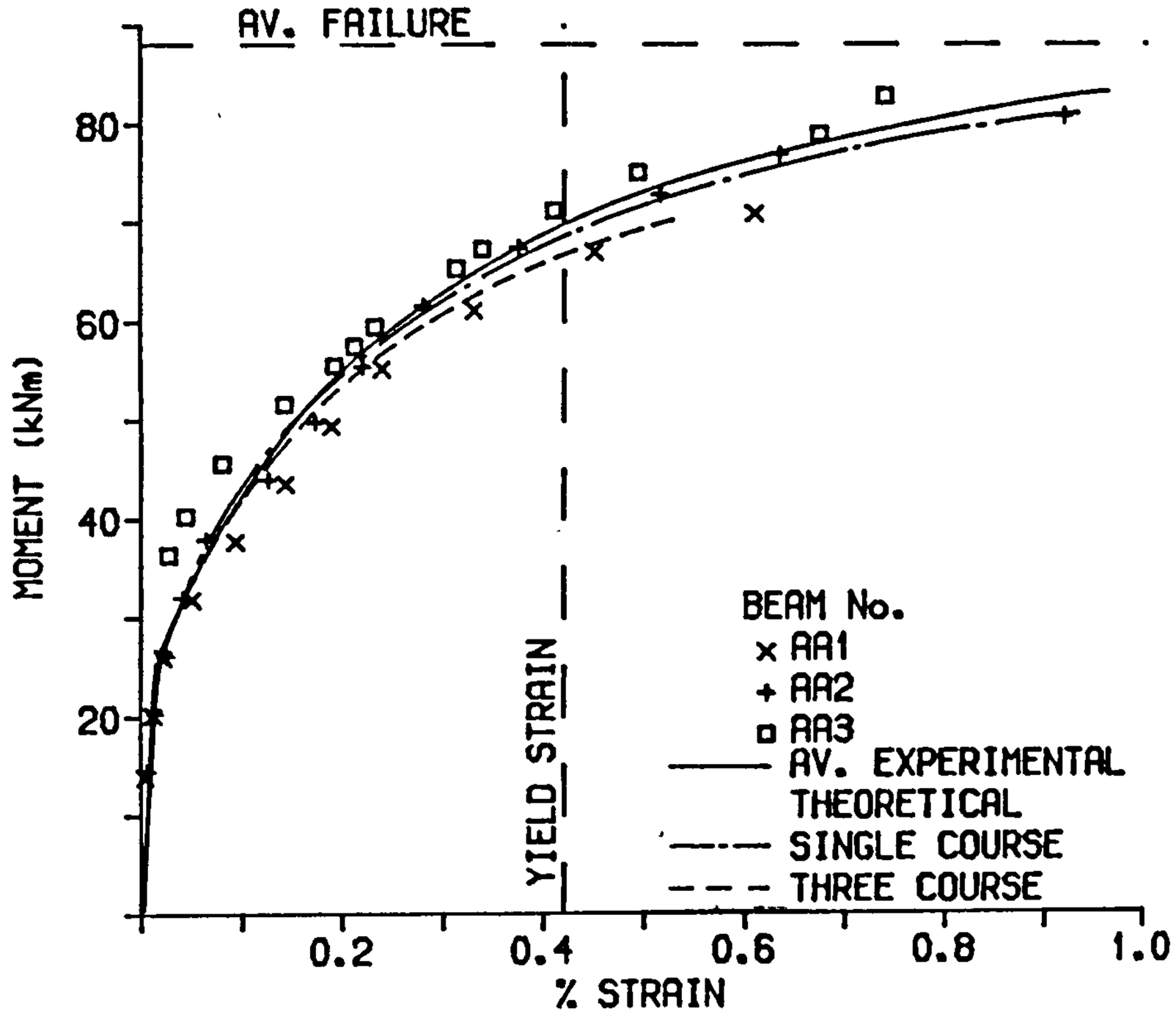

(b)

Figure 5.2.4

RELATIONSHIP BETWEEN MOMENT AND TOP FIBRE STRAIN

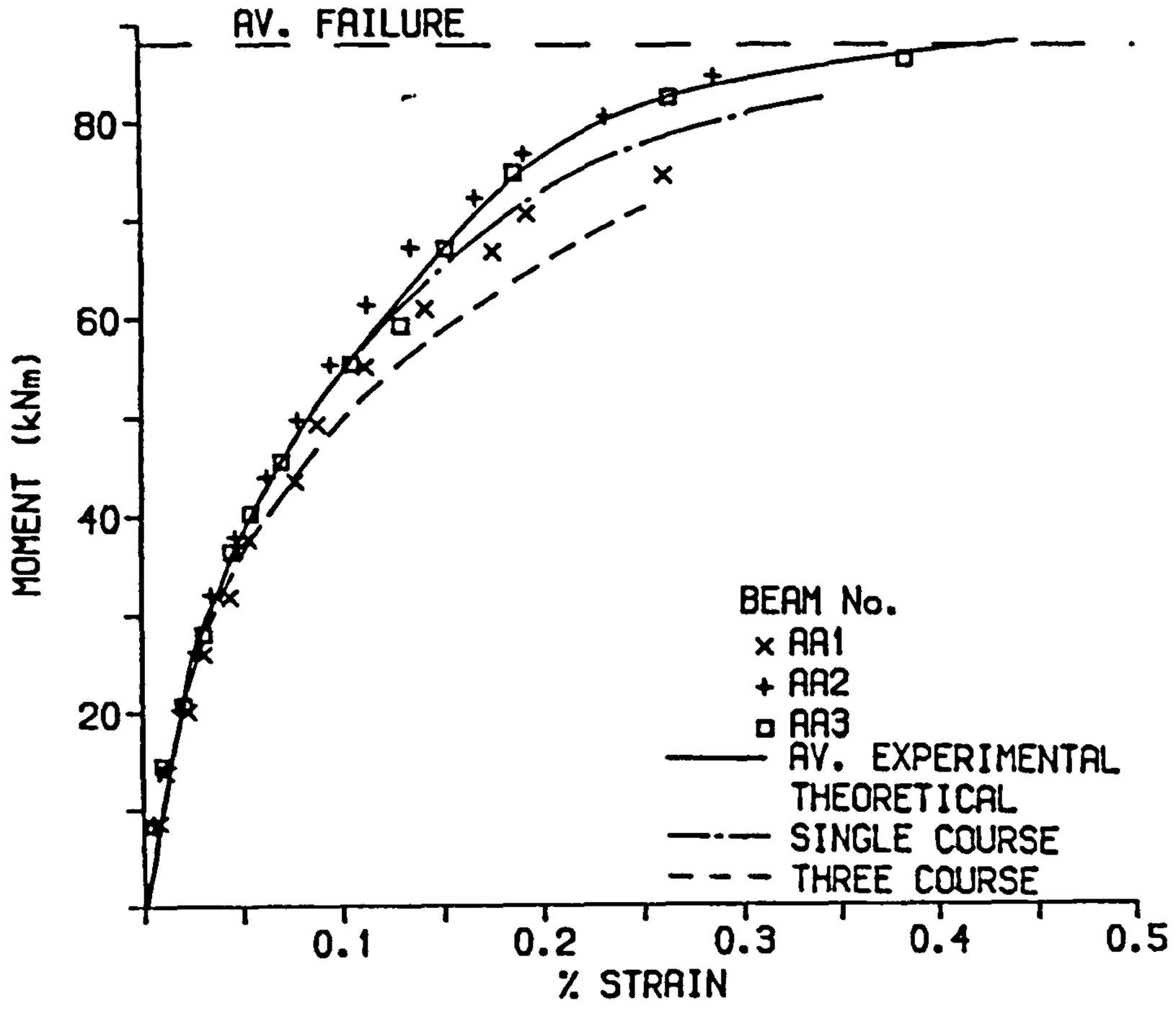

(c)

RELATIONSHIP BETWEEN MOMENT AND NEUTRAL AXIS DEPTH

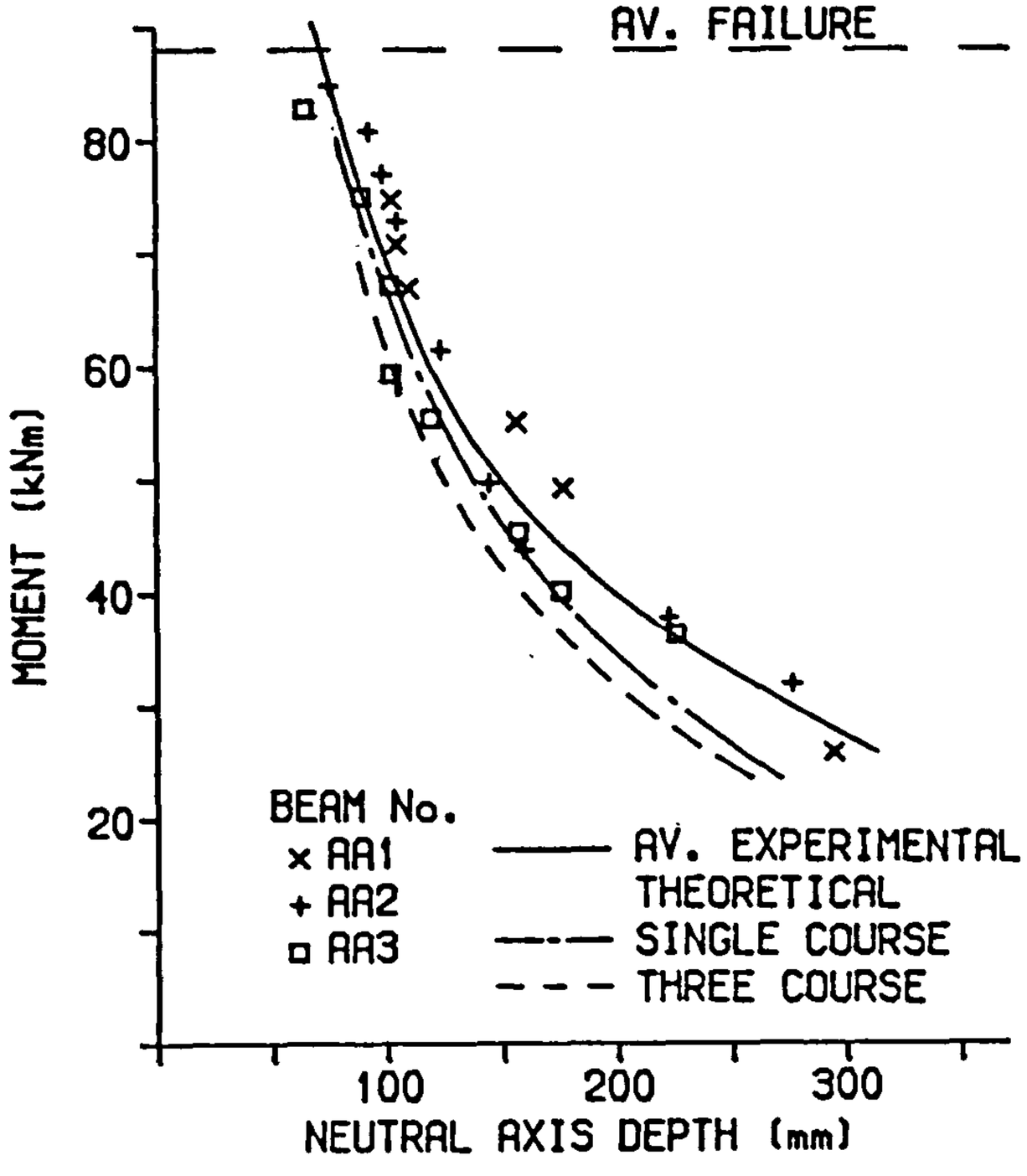

(d)

Figure 5.2.4 (Cont.)

RELATIONSHIP BETWEEN MOMENT AND ADDITIONAL STRAIN IN TENSIONED STEEL

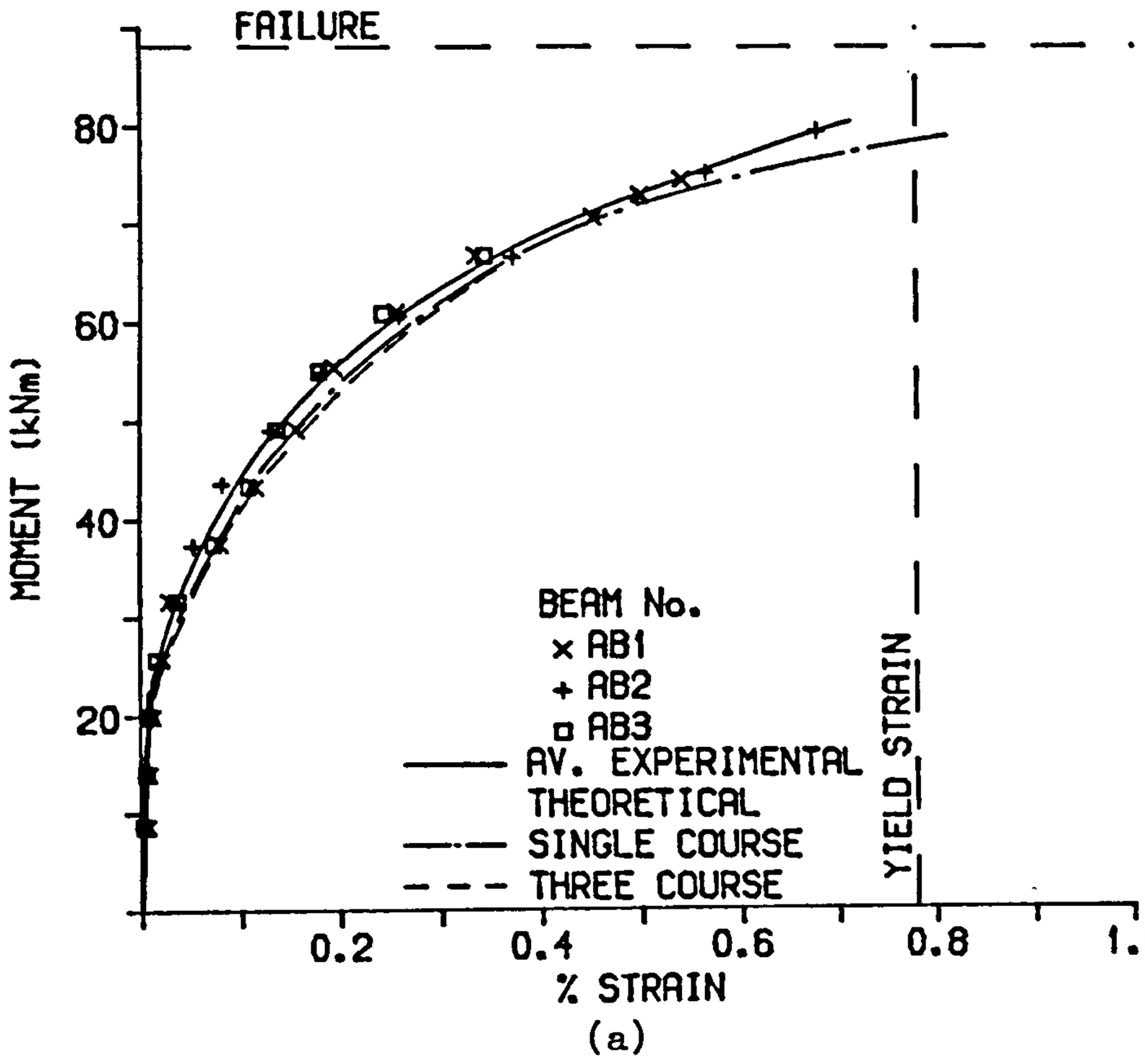

(a)

RELATIONSHIP BETWEEN MOMENT AND STRAIN IN NON-TENSIONED STEEL

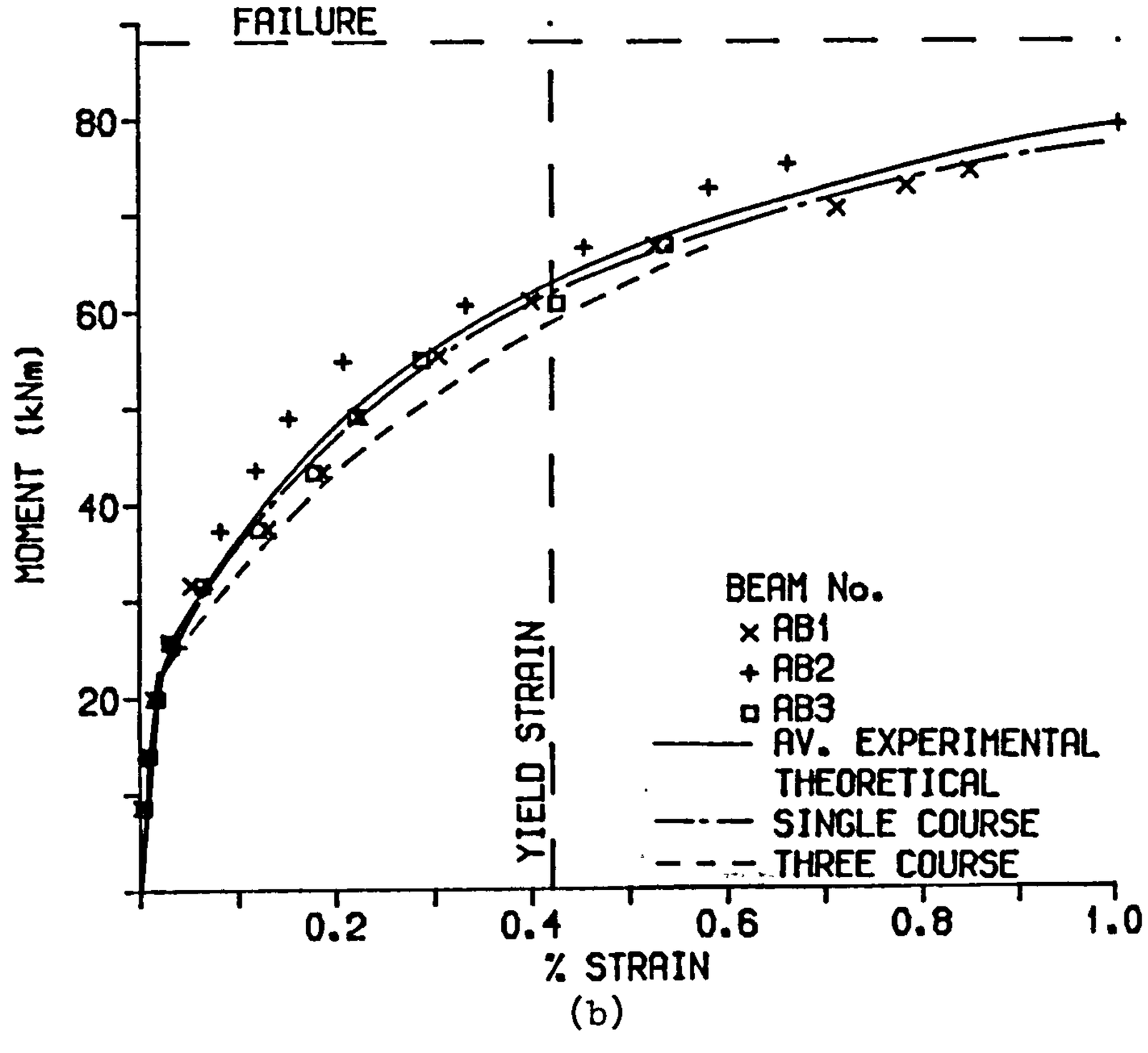

(b)

Figure 5.2.5

RELATIONSHIP BETWEEN MOMENT AND TOP FIBRE STRAIN

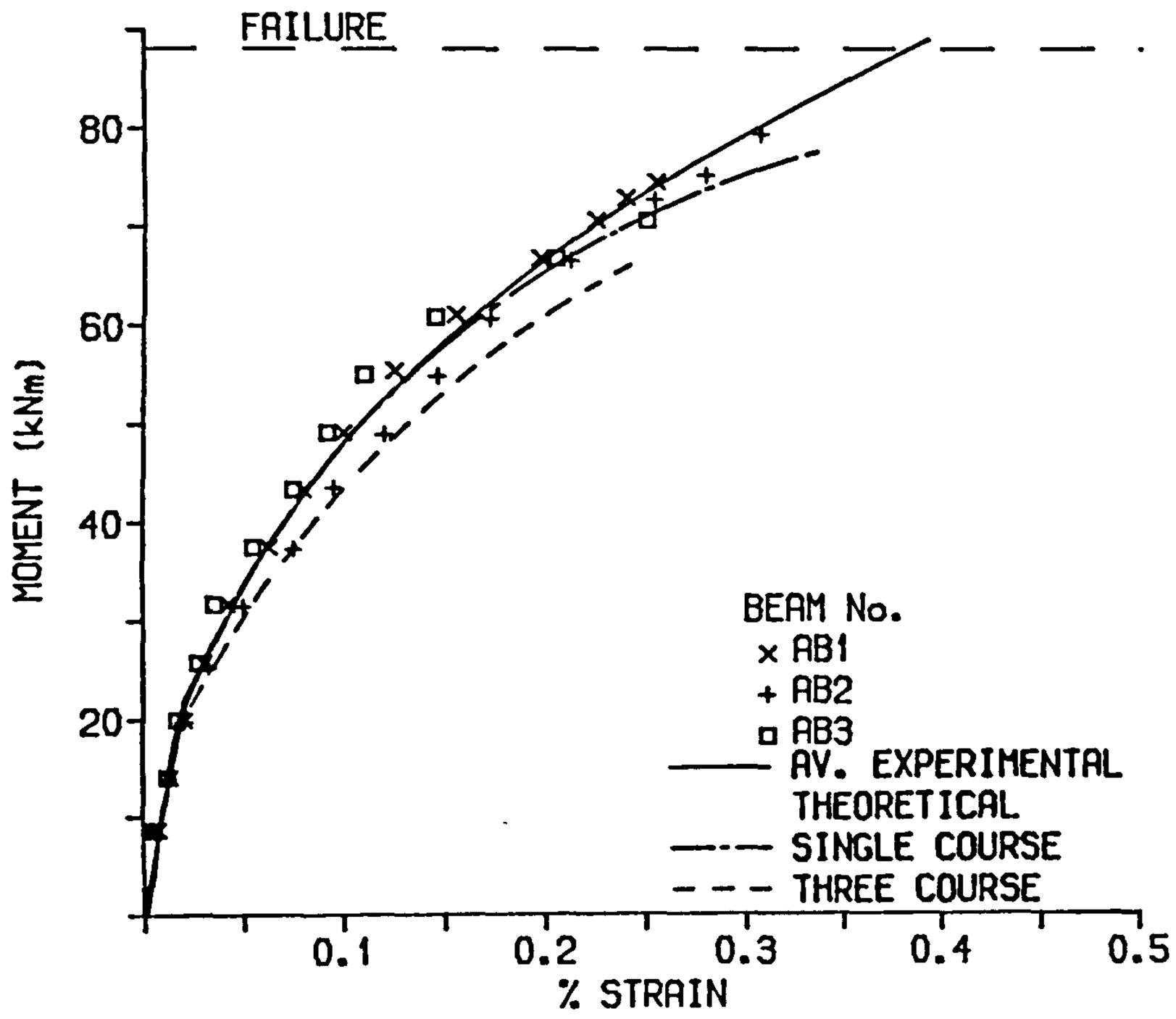

(c)

RELATIONSHIP BETWEEN MOMENT AND NEUTRAL AXIS DEPTH

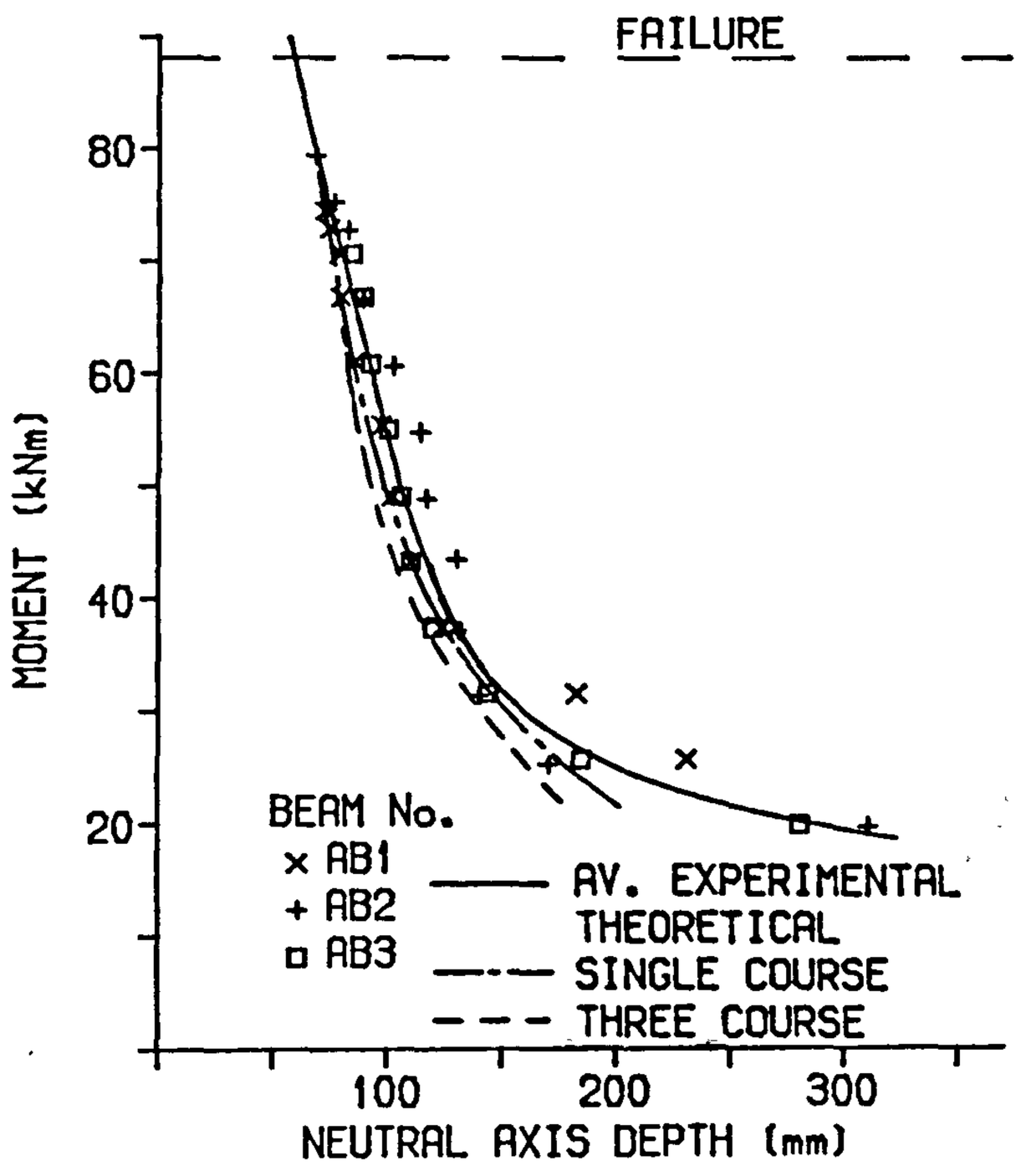

(d)

Figure 5.2.5 (Cont.)

RELATIONSHIP BETWEEN MOMENT AND ADDITIONAL STRAIN IN TENSIONED STEEL

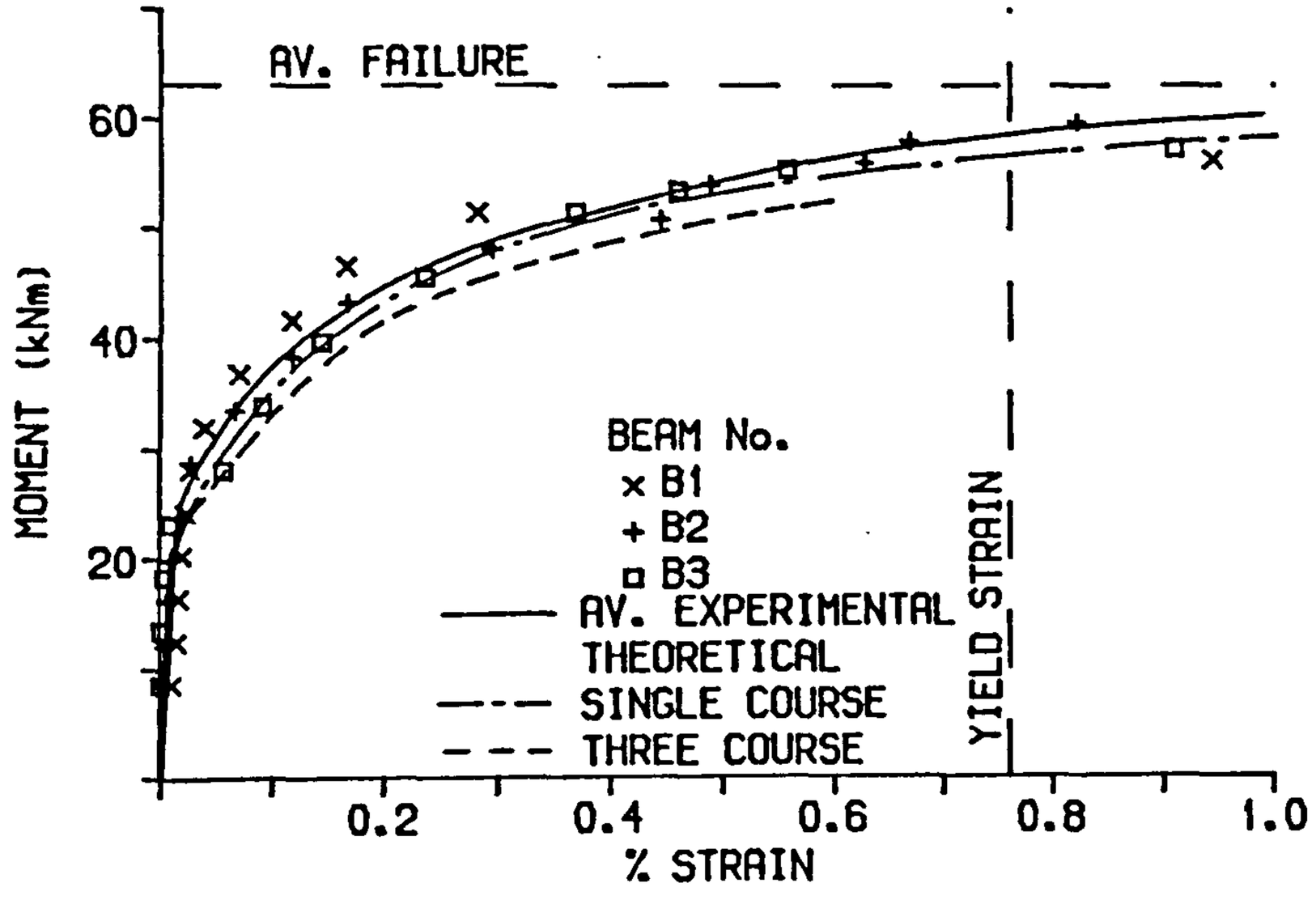

(a)

RELATIONSHIP BETWEEN MOMENT AND STRAIN IN NON-TENSIONED STEEL

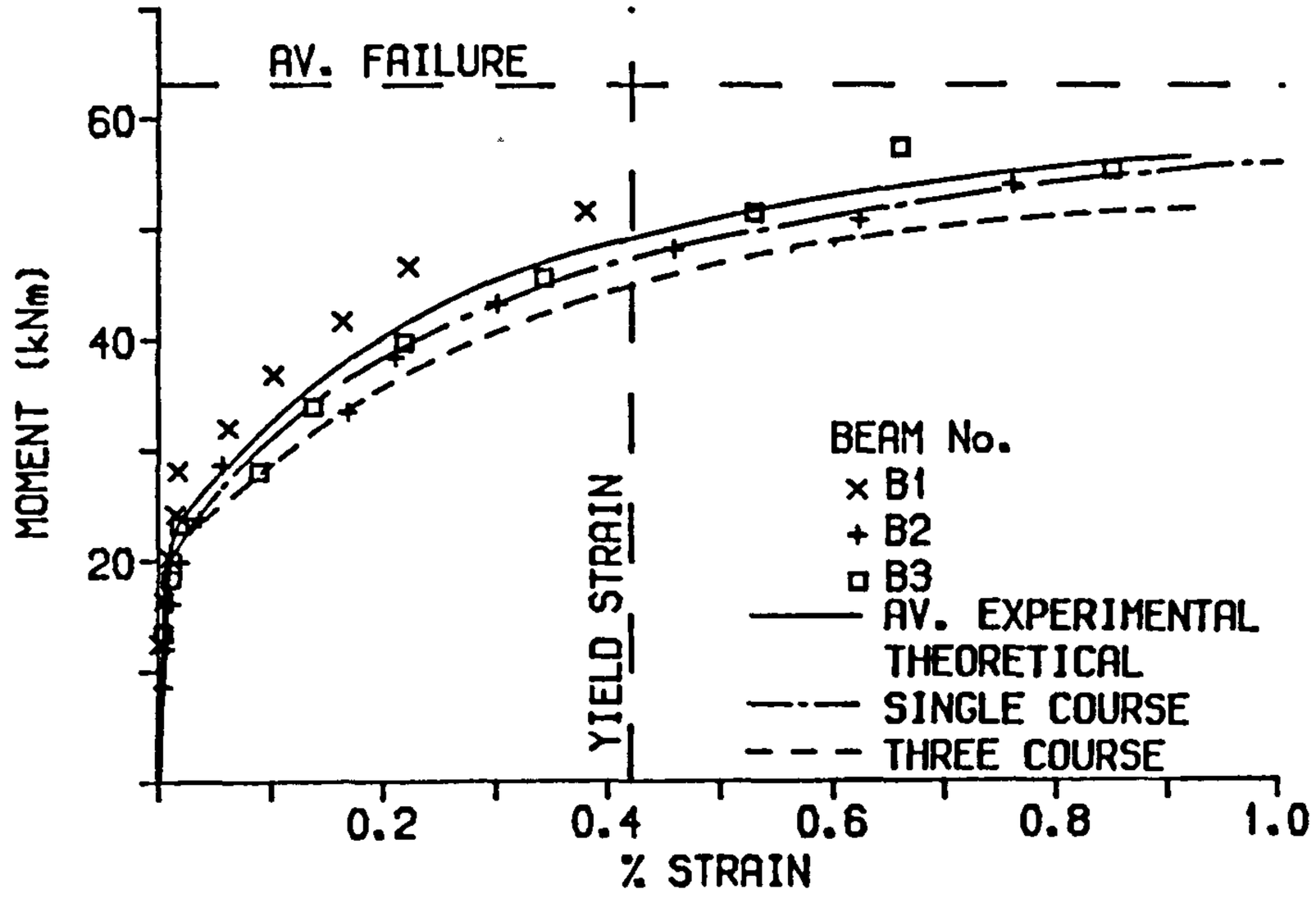

(b)

Figure 5.2.6

RELATIONSHIP BETWEEN MOMENT AND TOP FIBRE STRAIN

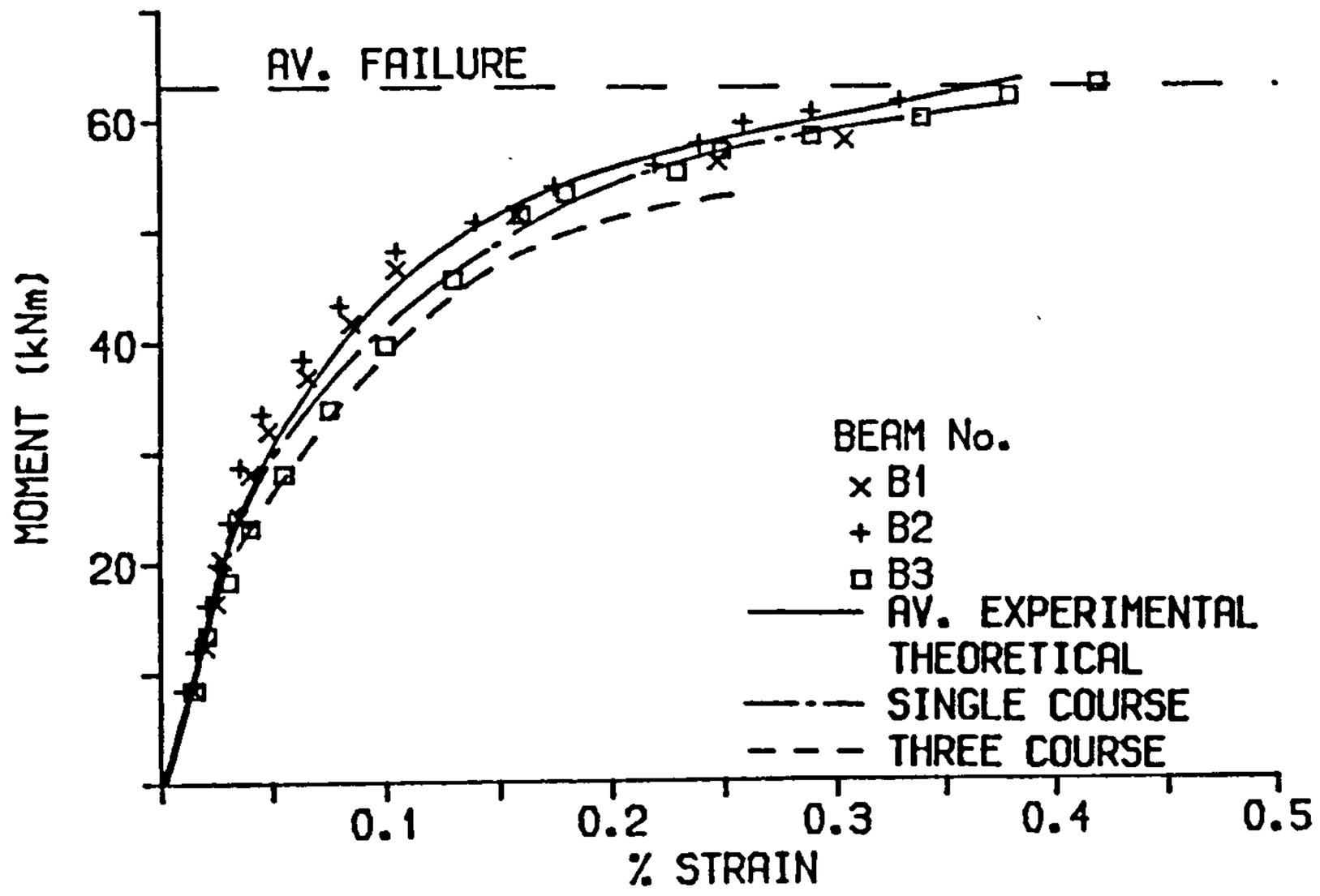

(c)

RELATIONSHIP BETWEEN MOMENT AND NEUTRAL AXIS DEPTH

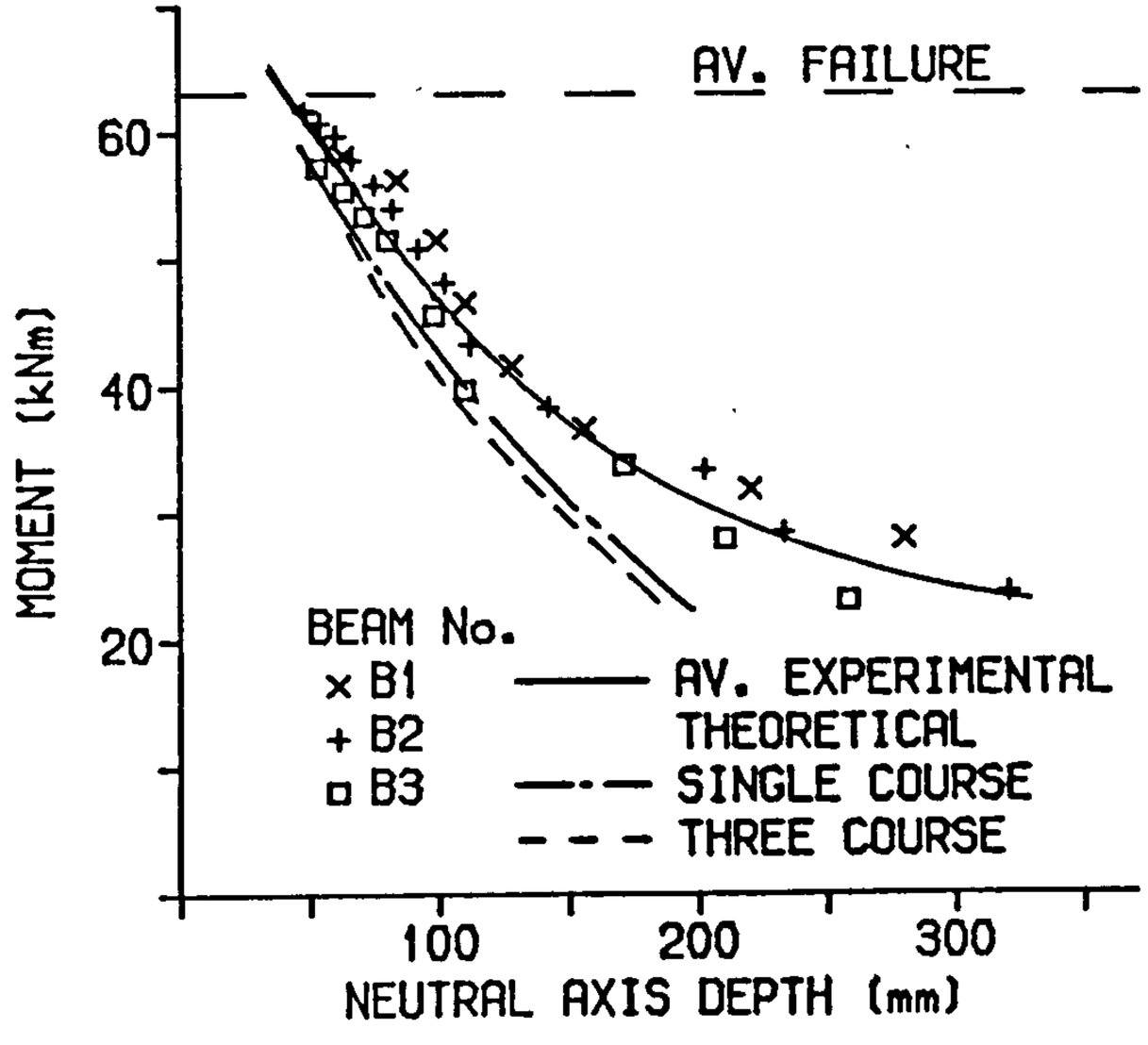

(d)

Figure 5.2.6 (Cont.)

RELATIONSHIP BETWEEN MOMENT AND ADDITIONAL STRAIN IN TENSIONED STEEL

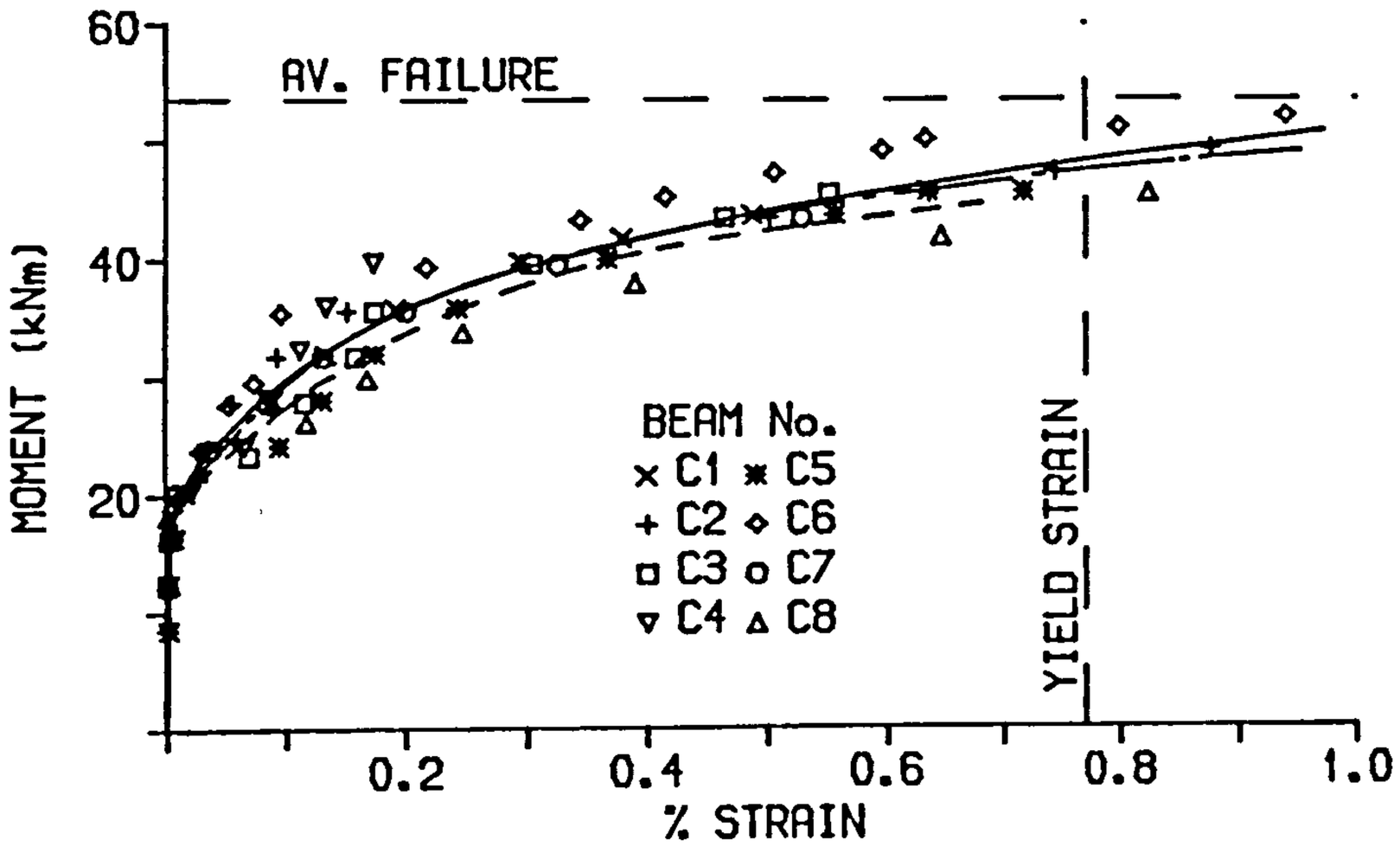

(a)

RELATIONSHIP BETWEEN MOMENT AND STRAIN IN NON-TENSIONED STEEL

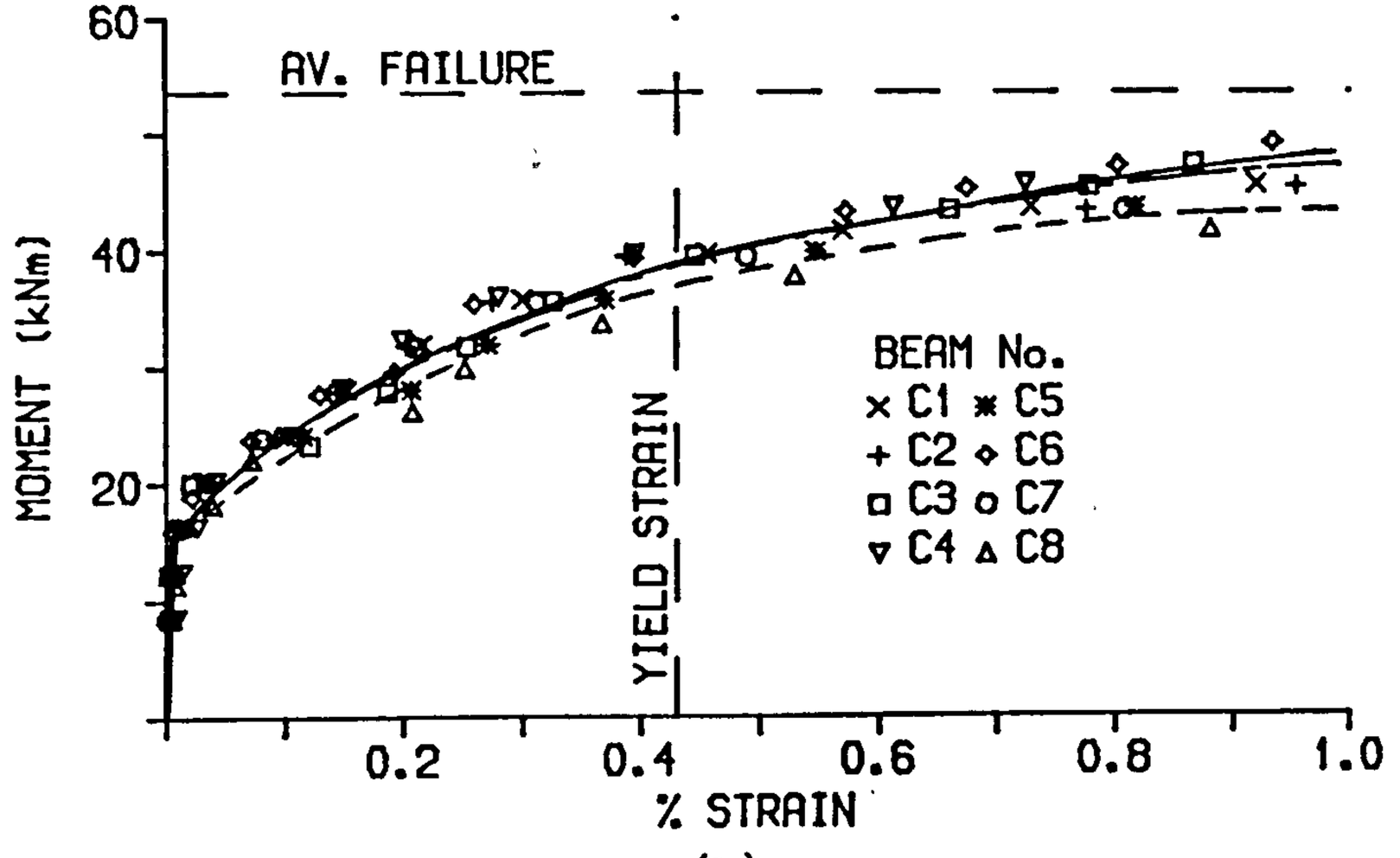

(b)

Figure 5.2.7

RELATIONSHIP BETWEEN MOMENT AND
TOP FIBRE STRAIN

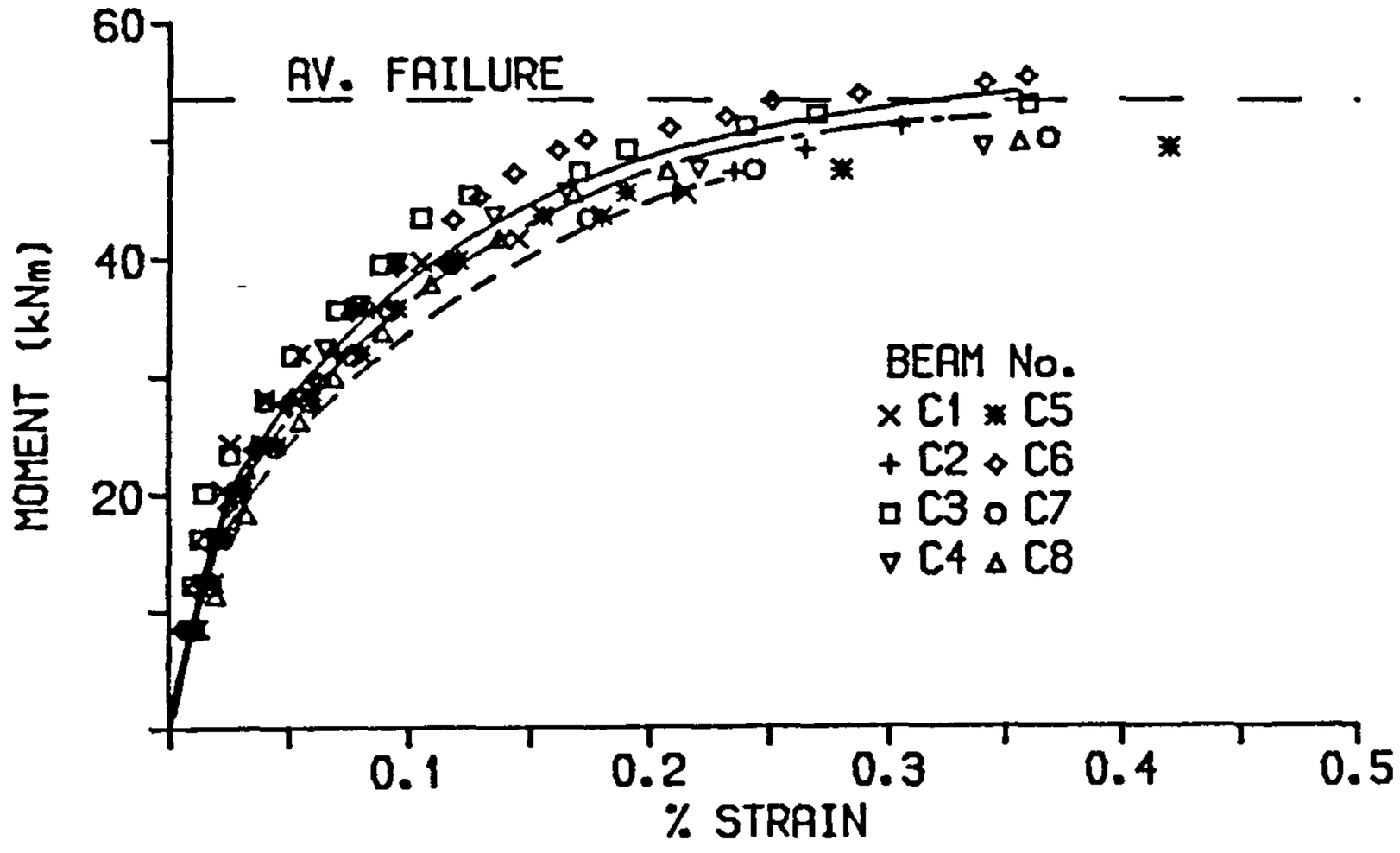

(c)

RELATIONSHIP BETWEEN MOMENT
AND NEUTRAL AXIS DEPTH

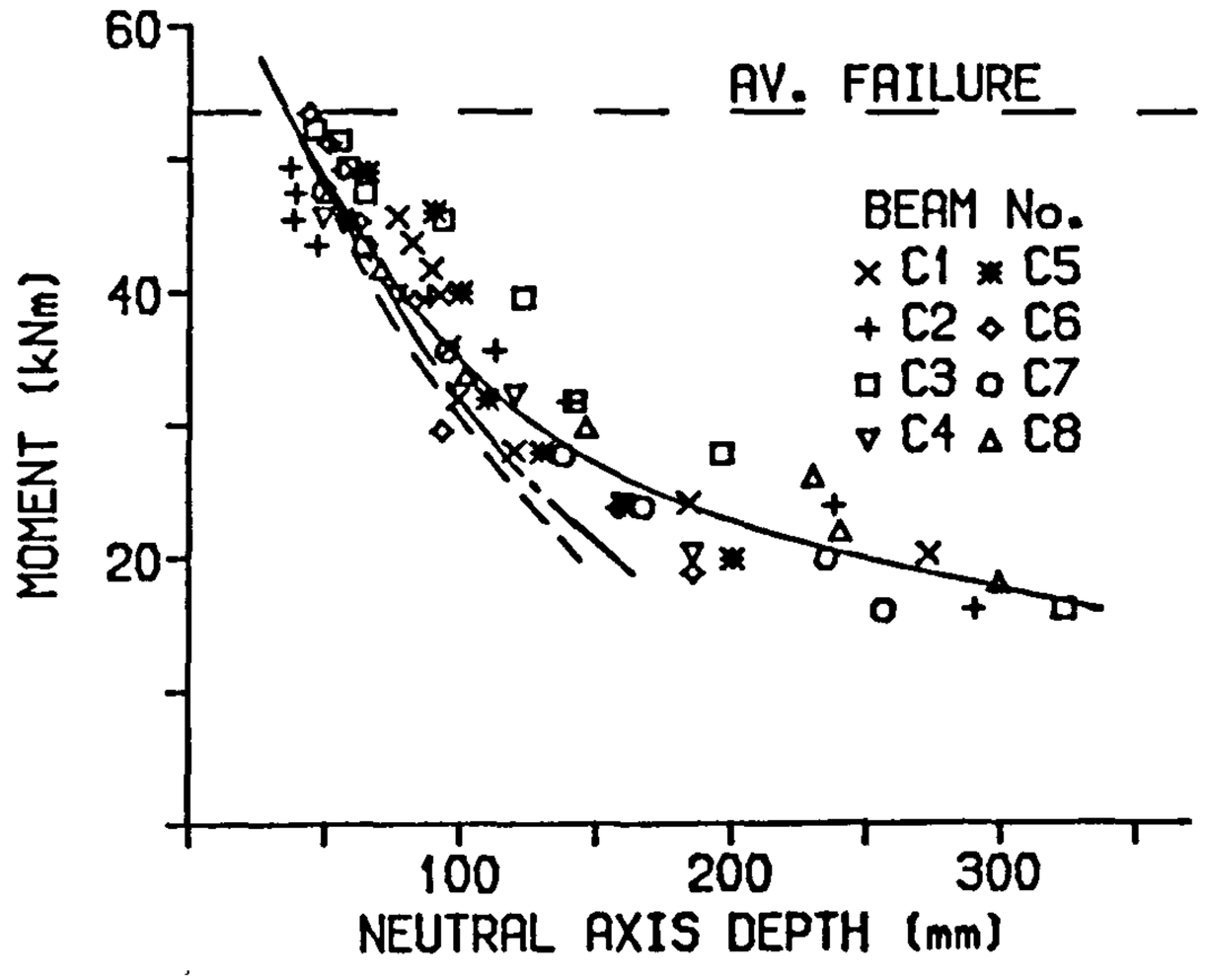

(d)

Figure 5.2.7 (Cont.)

RELATIONSHIP BETWEEN MOMENT AND ADDITIONAL STRAIN IN TENSIONED STEEL

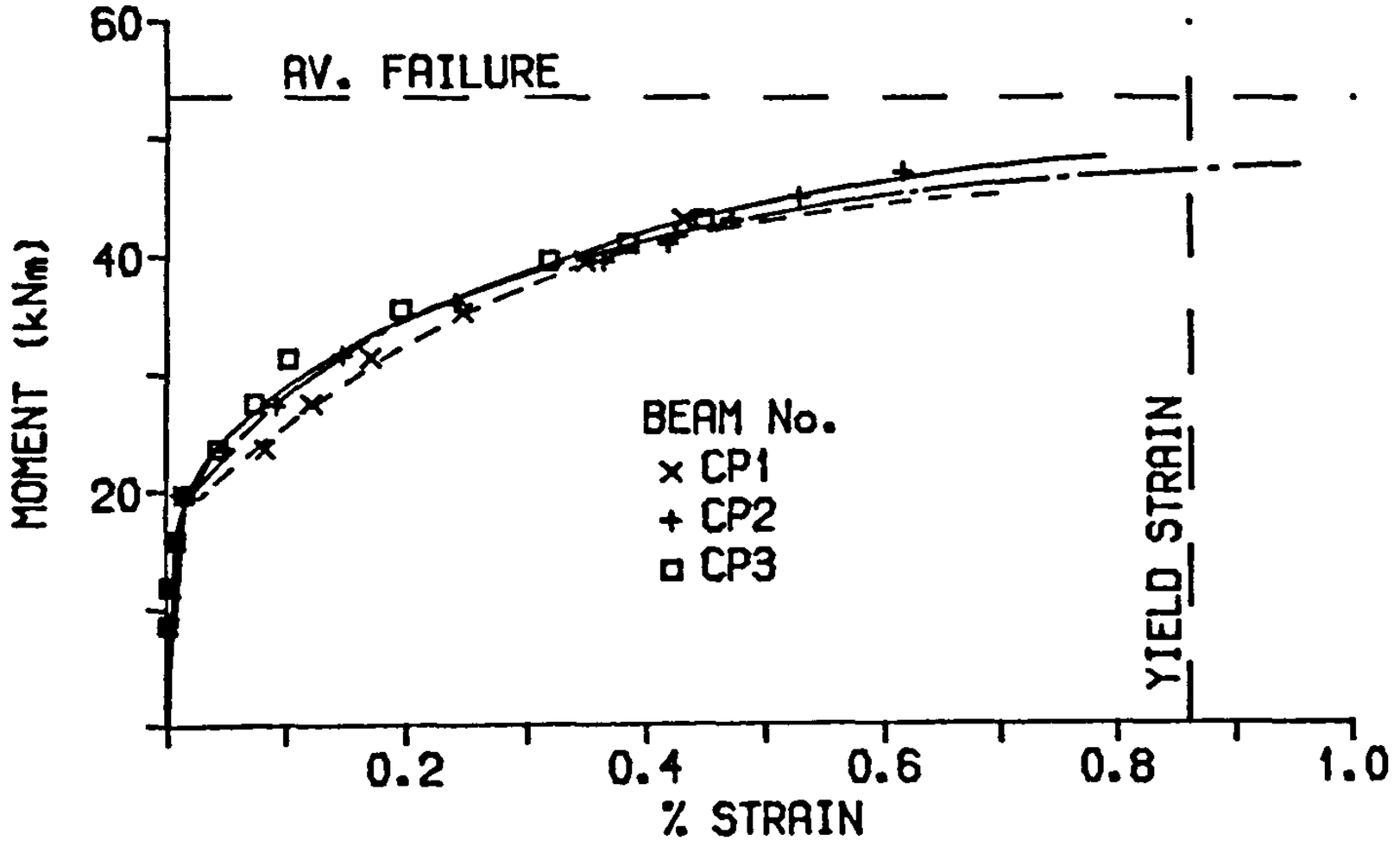

(a)

RELATIONSHIP BETWEEN MOMENT AND STRAIN IN NON-TENSIONED STEEL

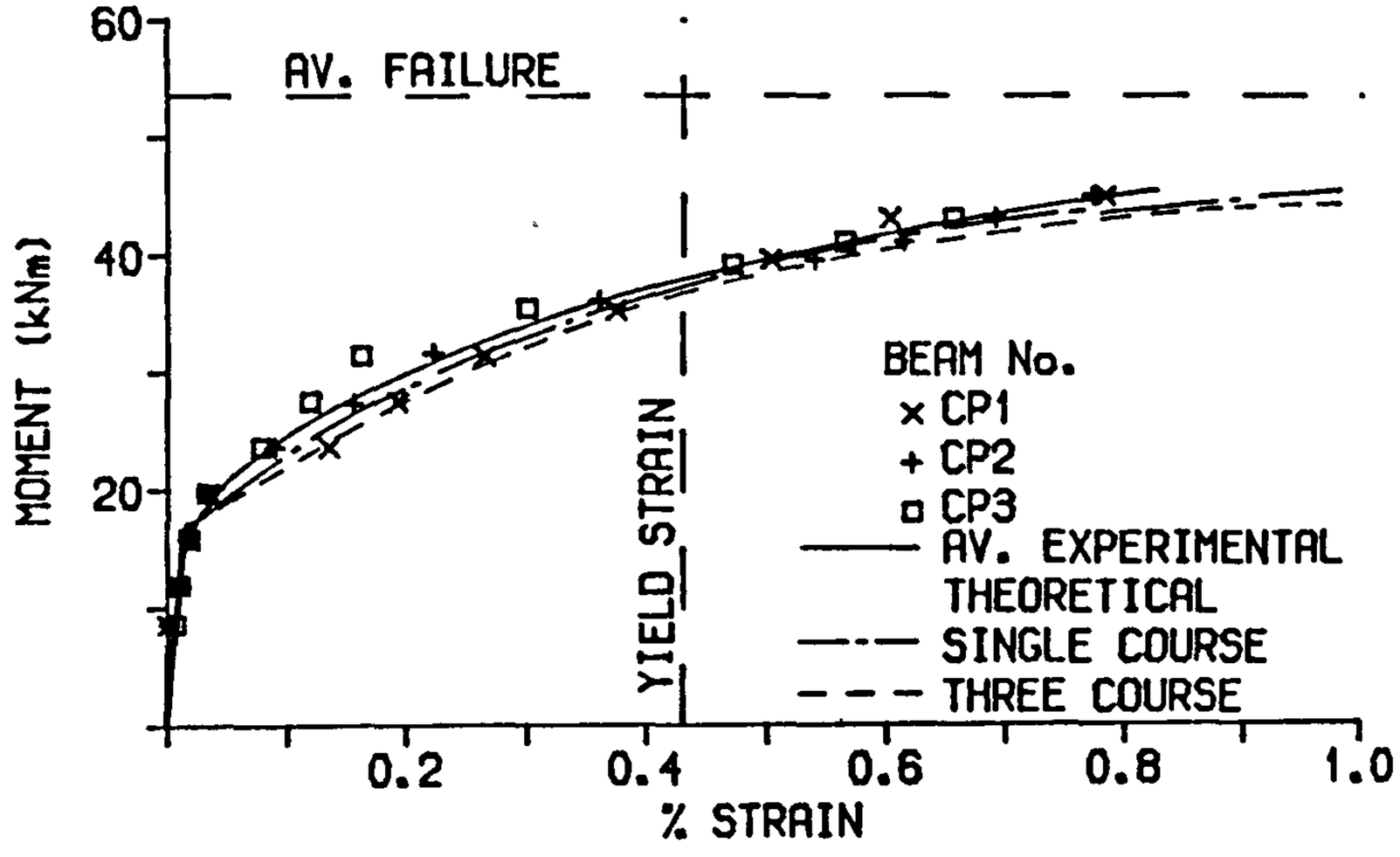

(b)

Figure 5.2.8

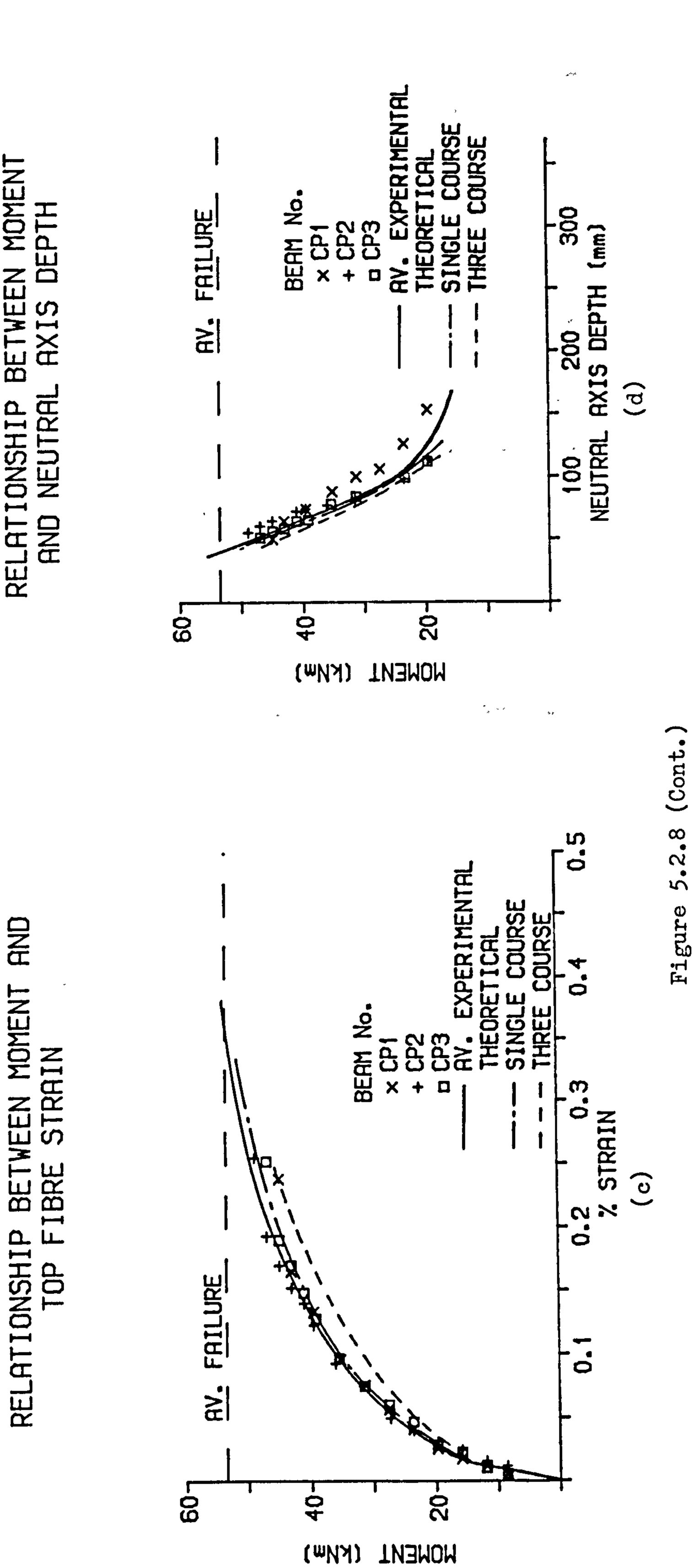

(Cont.)

Figure 5.2.8

RELATIONSHIP BETWEEN MOMENT AND ADDITIONAL STRAIN IN TENSIONED STEEL

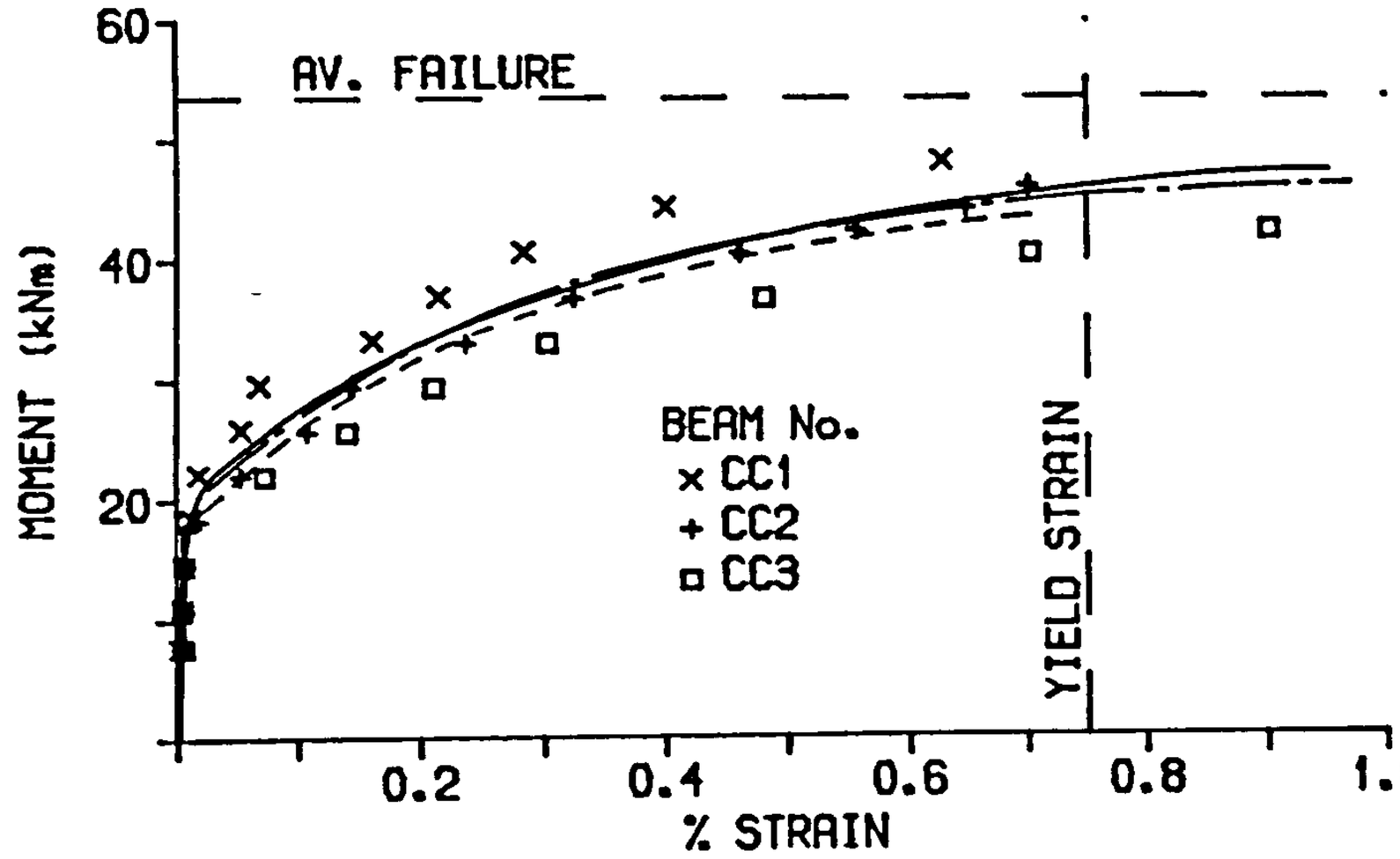

(a)

RELATIONSHIP BETWEEN MOMENT AND STRAIN IN NON-TENSIONED STEEL

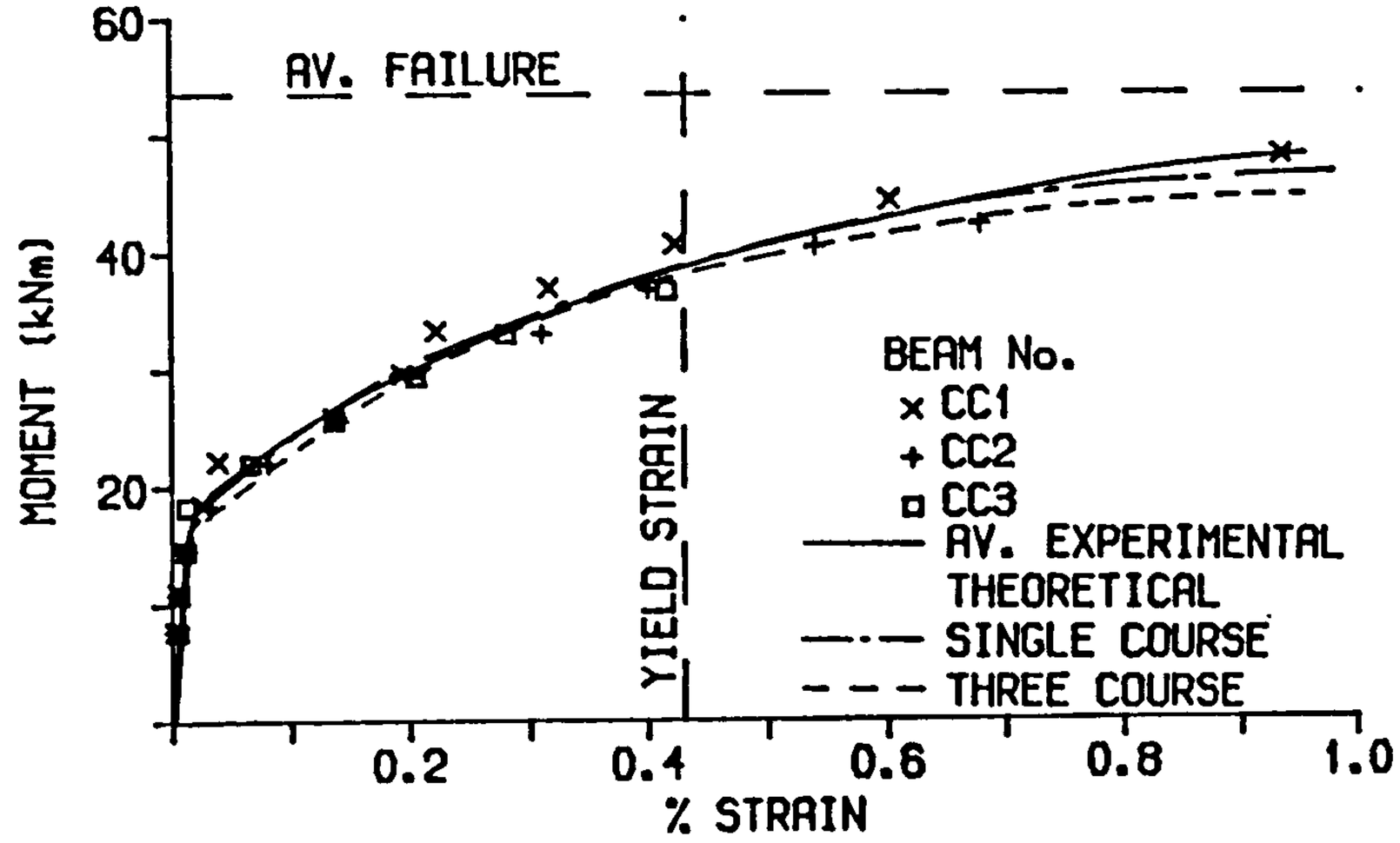

(b)

Figure 5.2.9

RELATIONSHIP BETWEEN MOMENT AND TOP FIBRE STRAIN

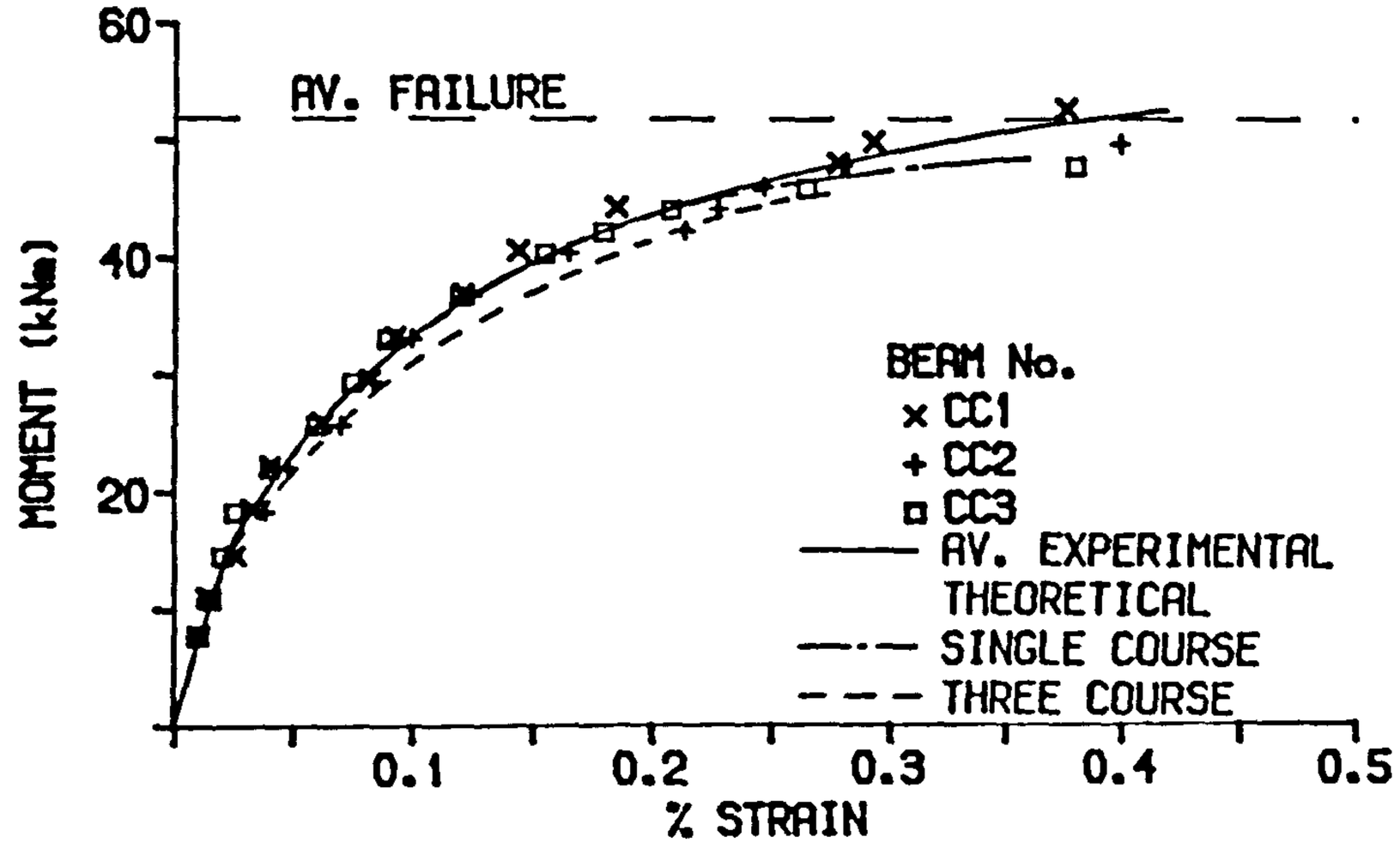

(c)

RELATIONSHIP BETWEEN MOMENT AND NEUTRAL AXIS DEPTH

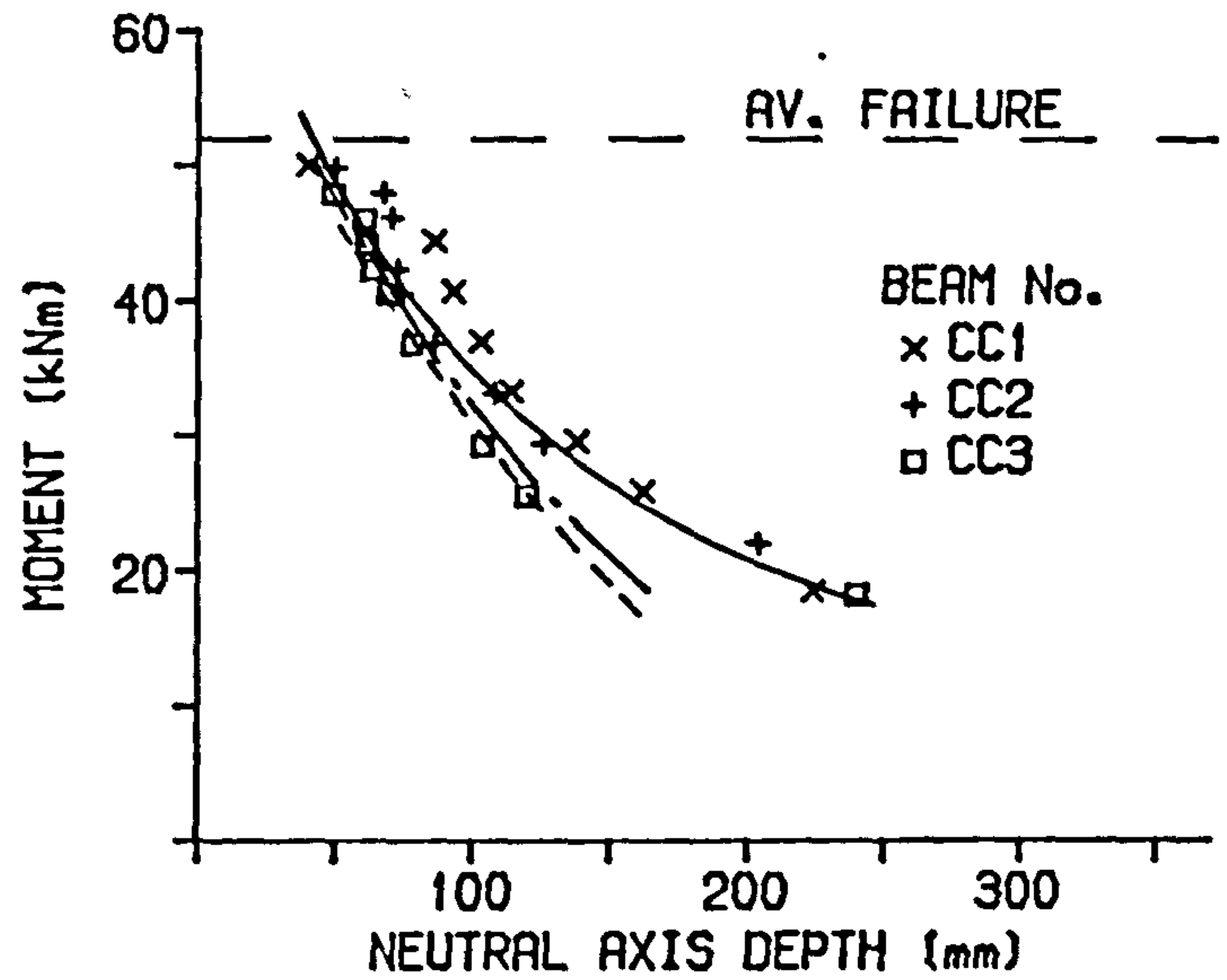

(d)

Figure 5.2.9 (Cont.)

RELATIONSHIP BETWEEN MOMENT AND ADDITIONAL STRAIN IN TENSIONED STEEL

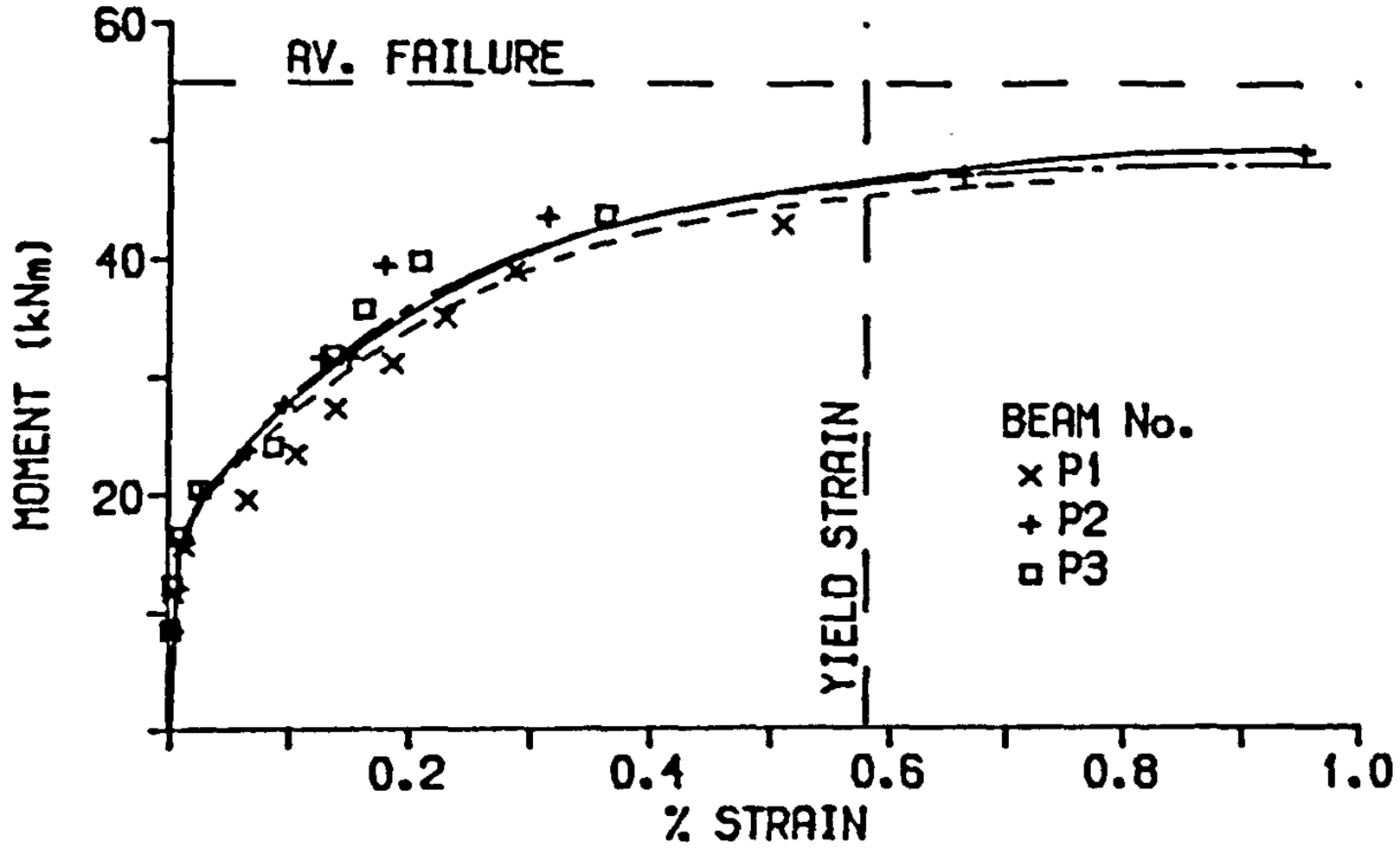

(a)

RELATIONSHIP BETWEEN MOMENT AND STRAIN IN NON-TENSIONED STEEL

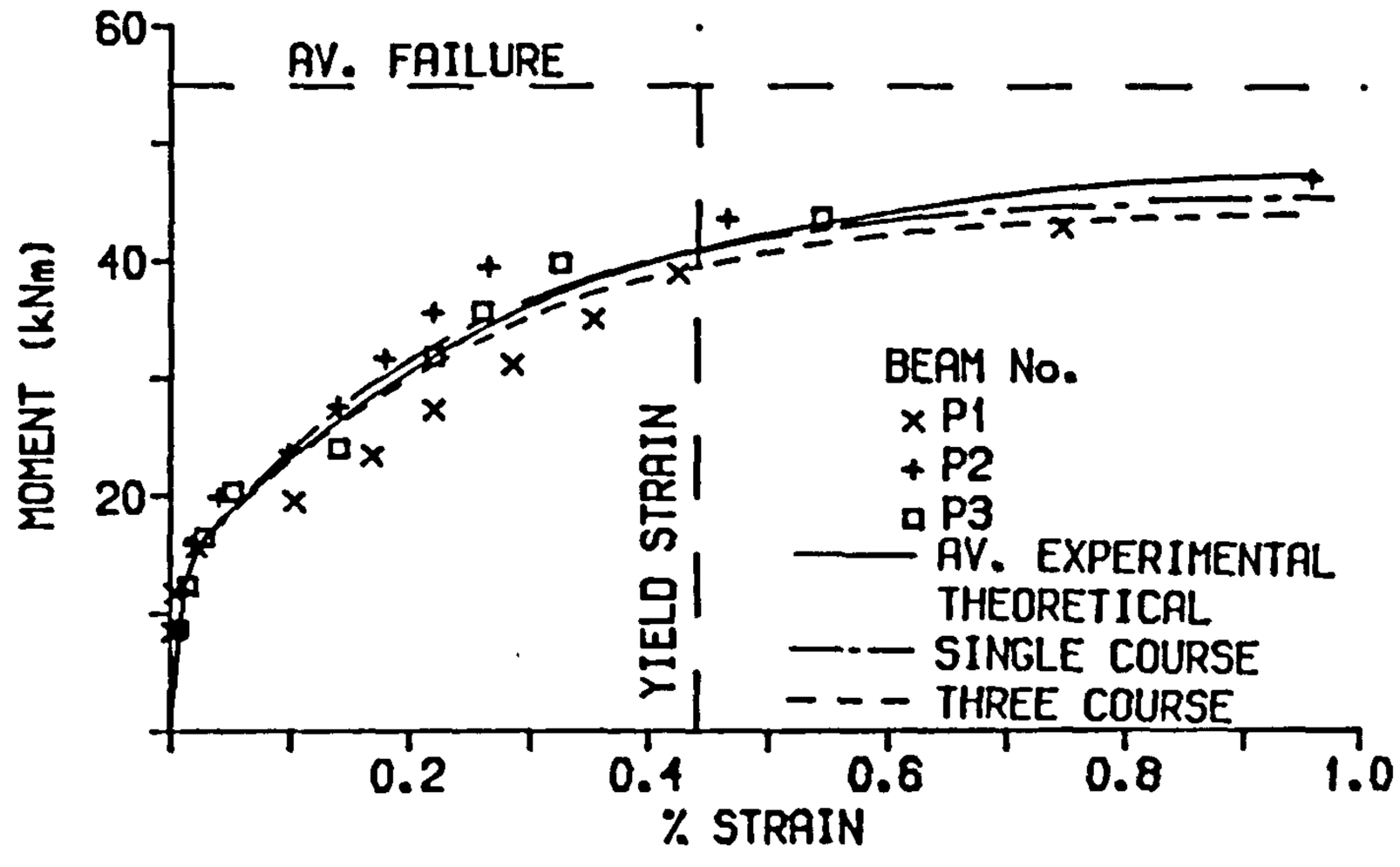

(b)

Figure 5.2.10

RELATIONSHIP BETWEEN MOMENT AND TOP FIBRE STRAIN

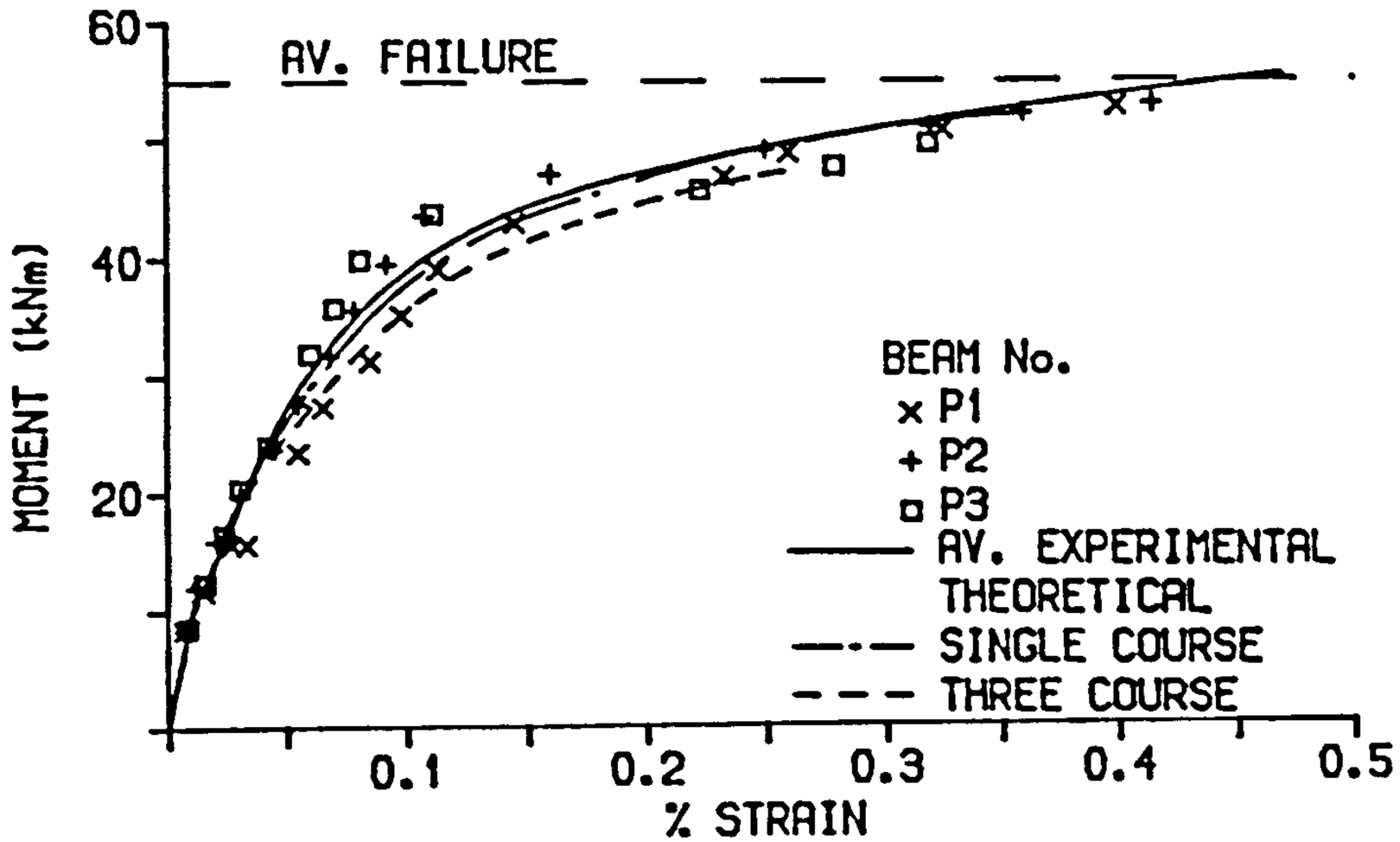

(c)

RELATIONSHIP BETWEEN MOMENT AND NEUTRAL AXIS DEPTH

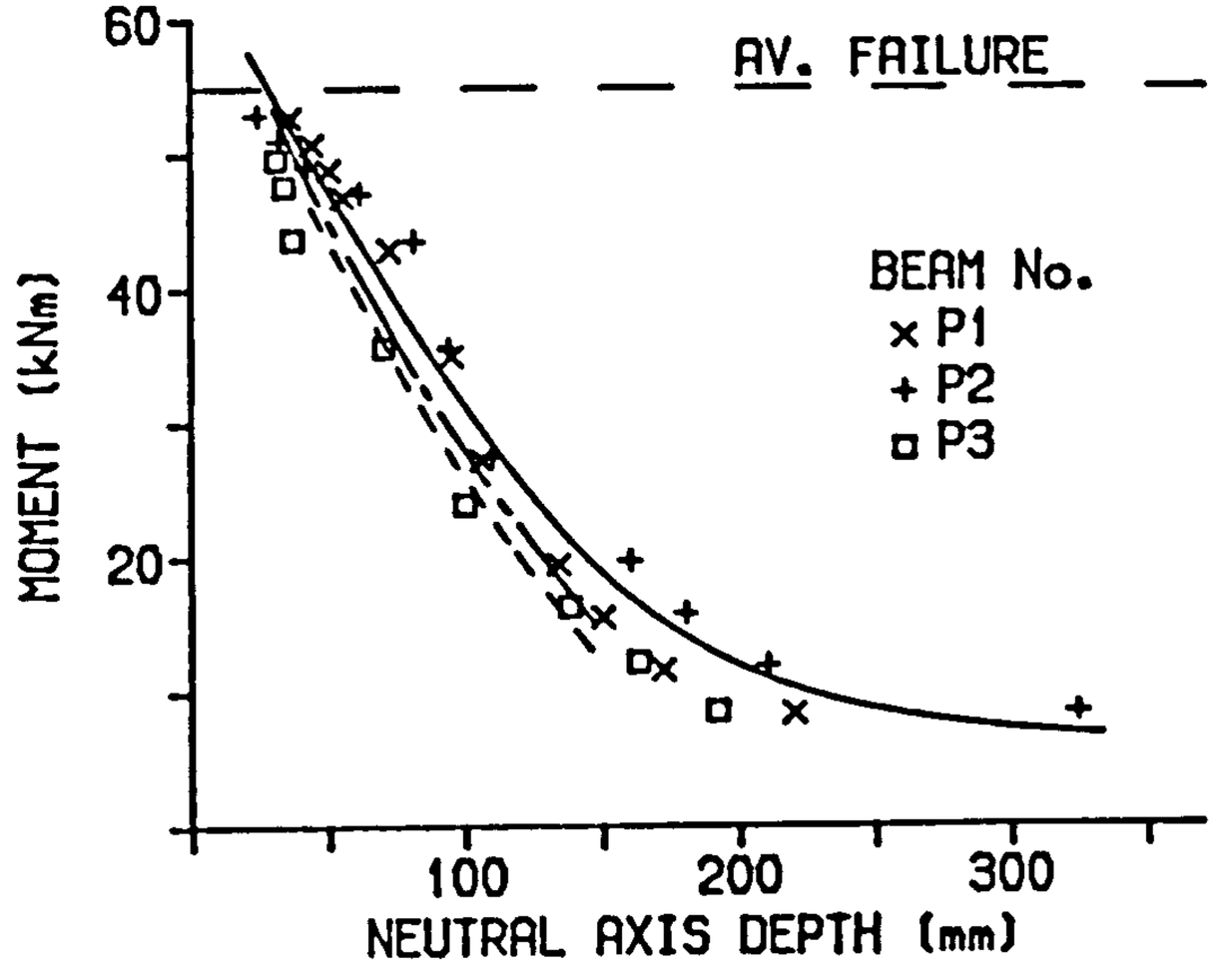

(d)

Figure 5.2.10 (Cont.)

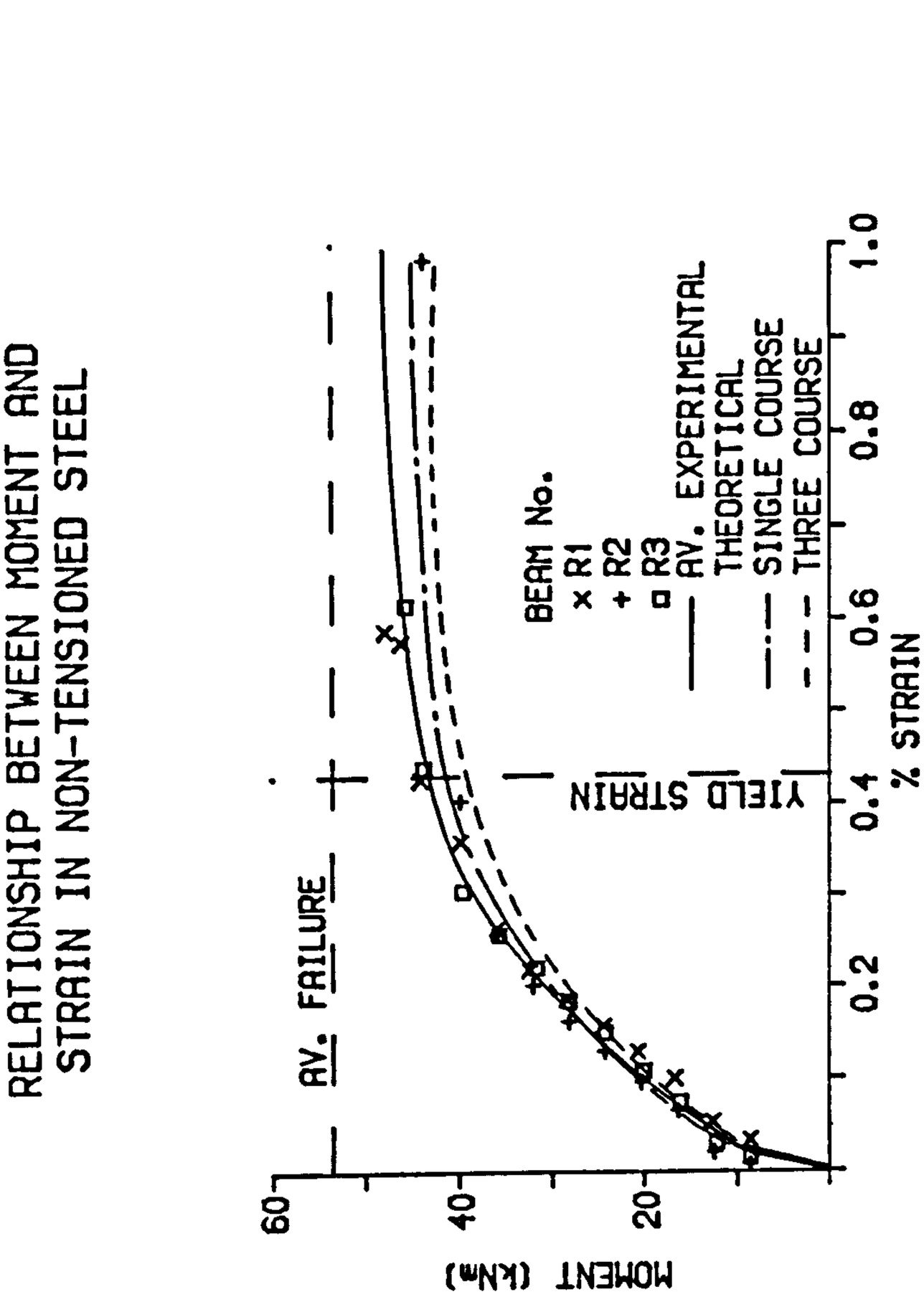

(b)

Figure 5.2.11

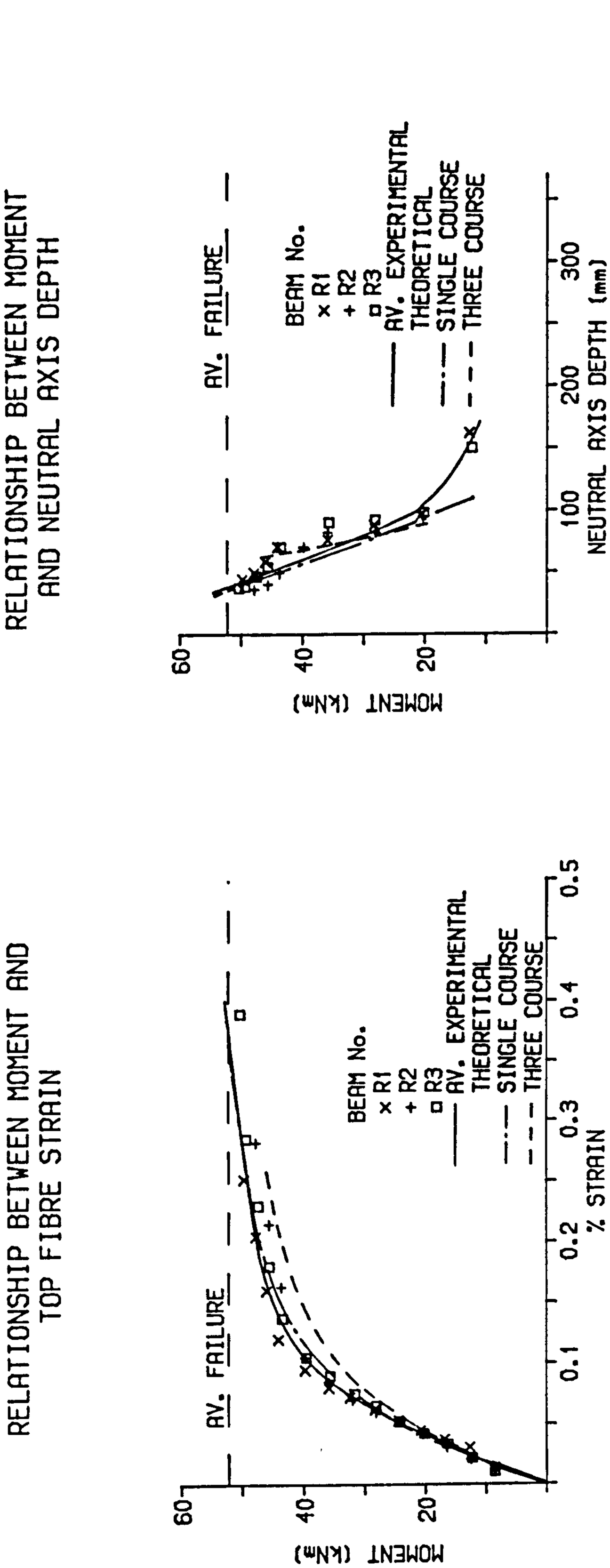

Figure 5.2.11 (Cont.)

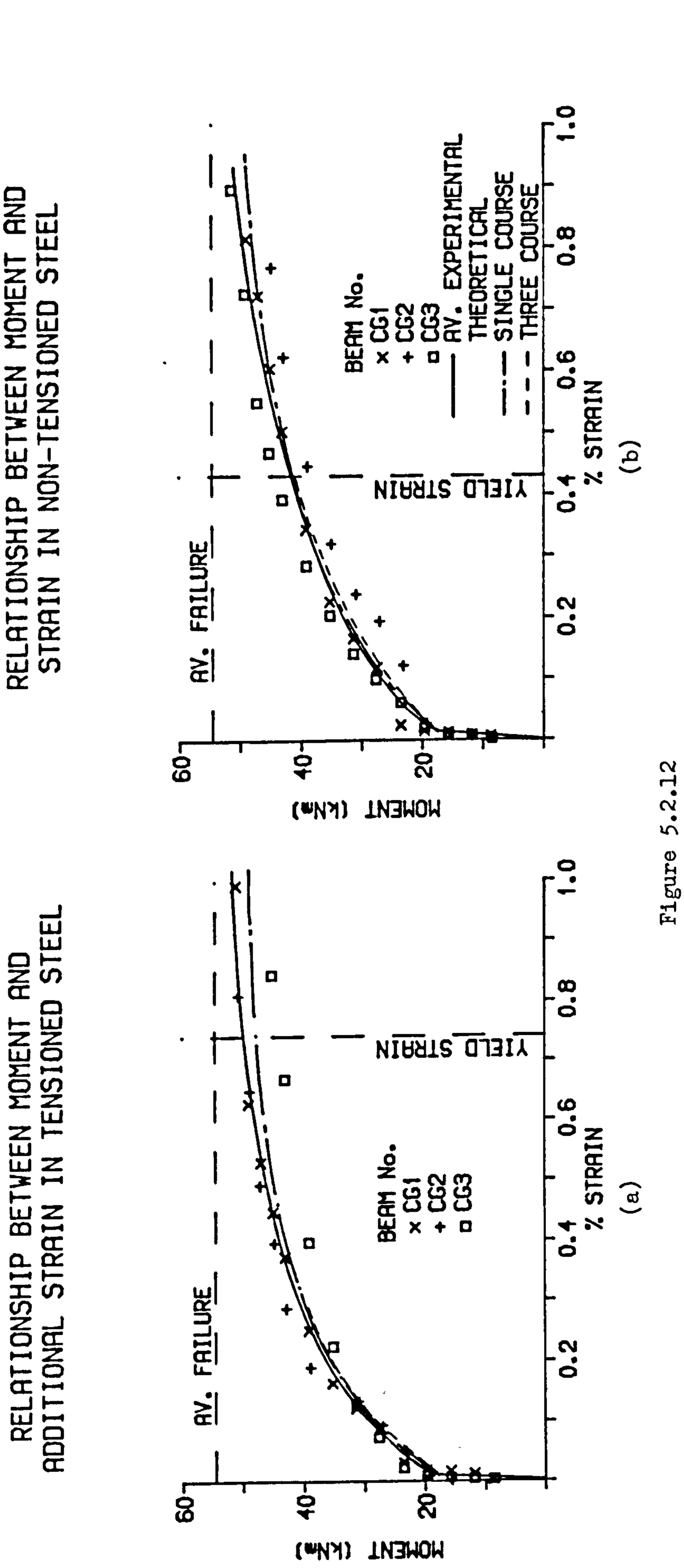
RELATIONSHIP BETWEEN MOMENT AND
STRAIN IN NON-TENSIONED STEEL
AV. FAILURE
YIELD STRAIN
BEAM No.
× CG1
+ CG2
□ CG3
AV. EXPERIMENTAL
THEORETICAL
SINGLE COURSE
THREE COURSE
MOMENT (kNm)
60
40
20
0.2
0.4
0.6
0.8
1.0
% STRAIN
(b)
RELATIONSHIP BETWEEN MOMENT AND
ADDITIONAL STRAIN IN TENSIONED STEEL
AV. FAILURE
YIELD STRAIN
BEAM No.
× CG1
+ CG2
□ CG3
MOMENT (kNm)
60
40
20
0.2
0.4
0.6
0.8
1.0
% STRAIN
(a)

Figure 5.2.12

RELATIONSHIP BETWEEN MOMENT AND TOP FIBRE STRAIN

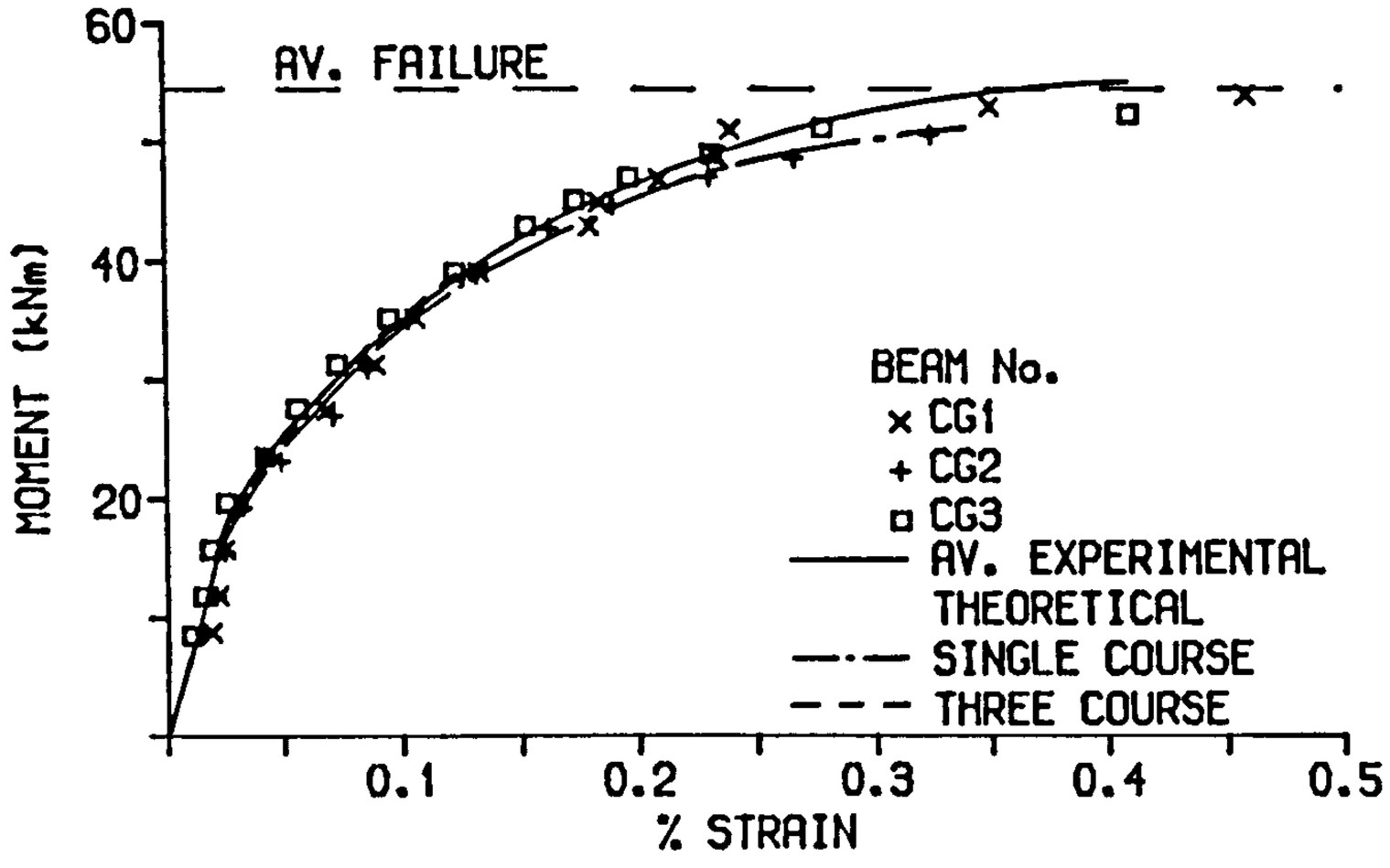

(c)

RELATIONSHIP BETWEEN MOMENT AND NEUTRAL AXIS DEPTH

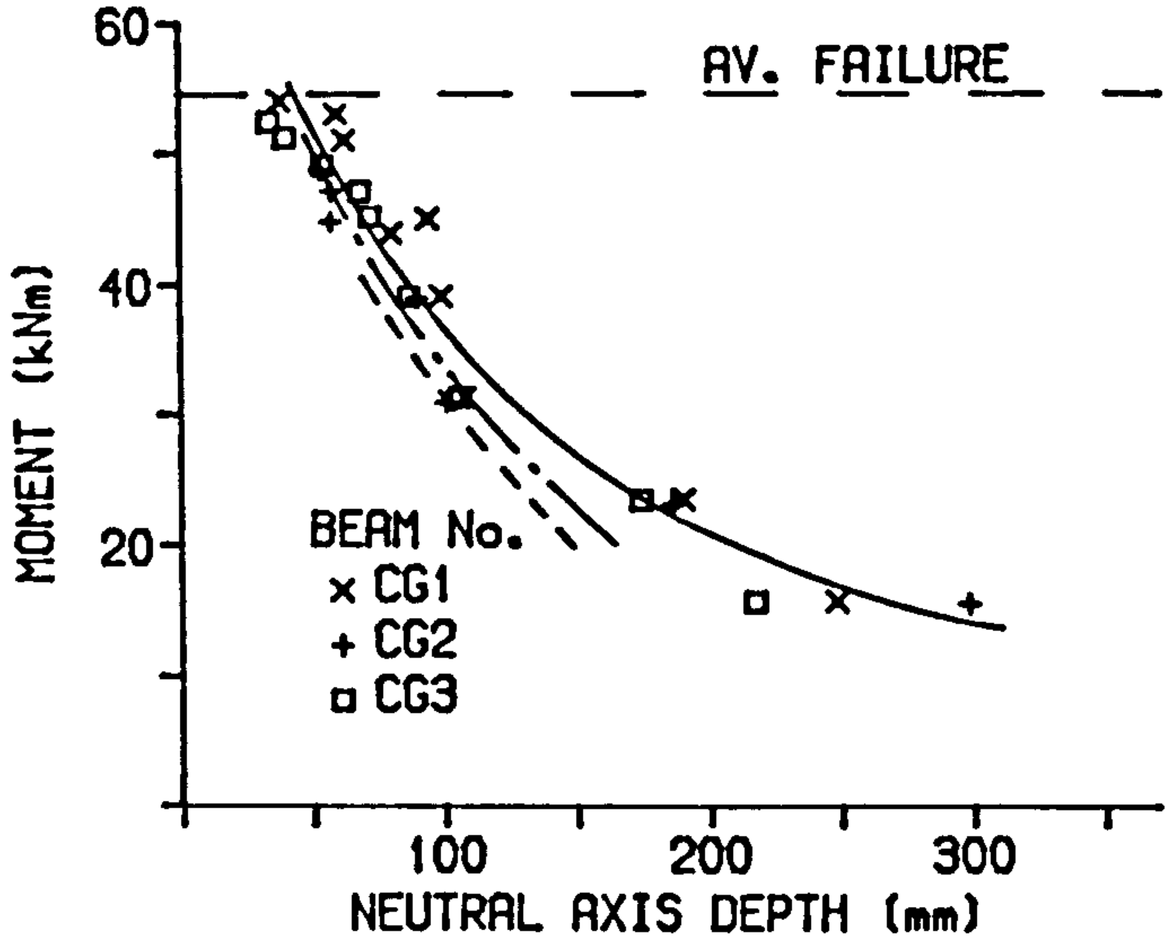

(d)

Figure 5.2.12 (Cont.)

RELATIONSHIP BETWEEN MOMENT AND ADDITIONAL STRAIN IN TENSIONED STEEL

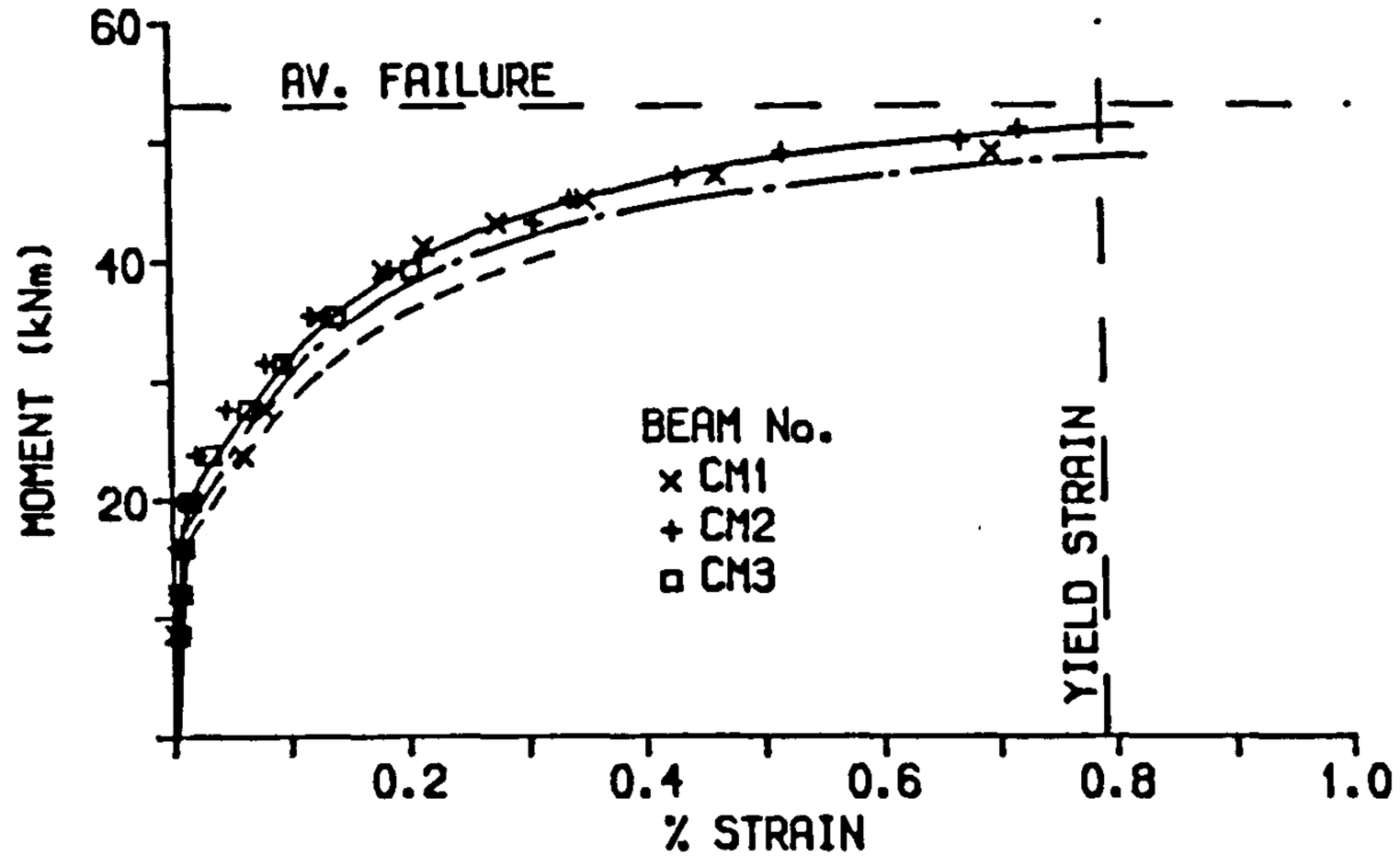

(a)

RELATIONSHIP BETWEEN MOMENT AND STRAIN IN NON-TENSIONED STEEL

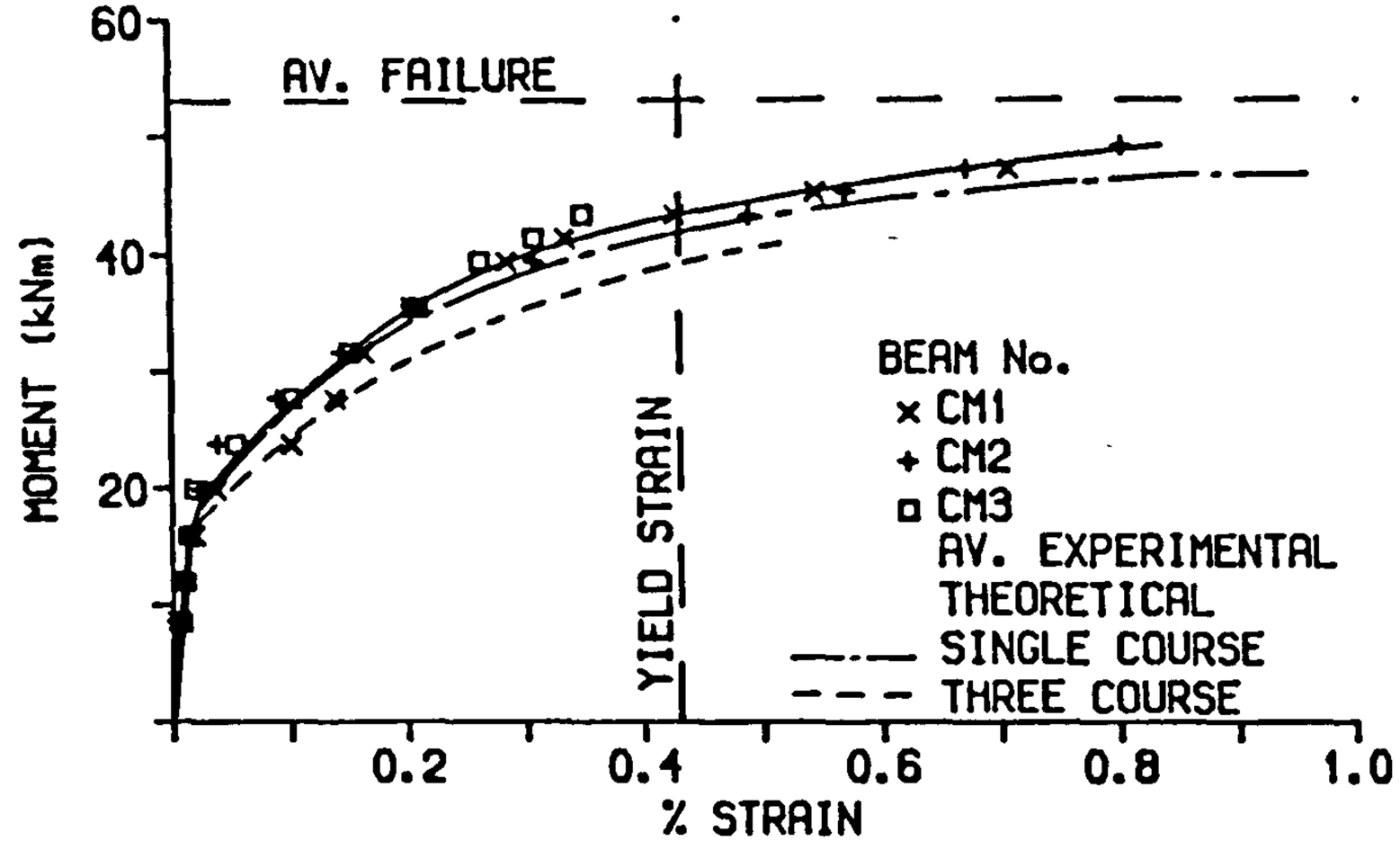

(b)

Figure 5.2.13

RELATIONSHIP BETWEEN MOMENT AND TOP FIBRE STRAIN

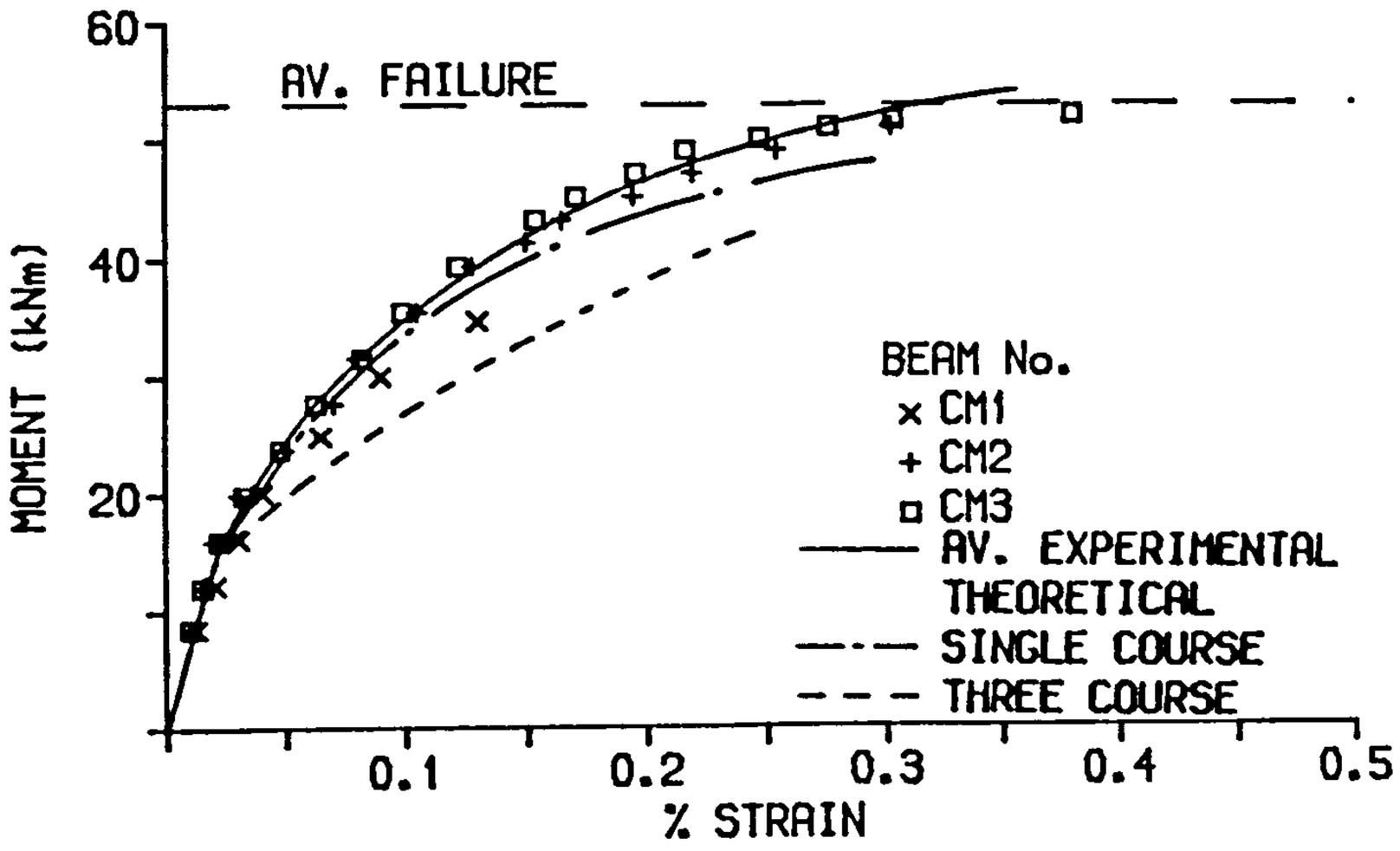

(c)

RELATIONSHIP BETWEEN MOMENT AND NEUTRAL AXIS DEPTH

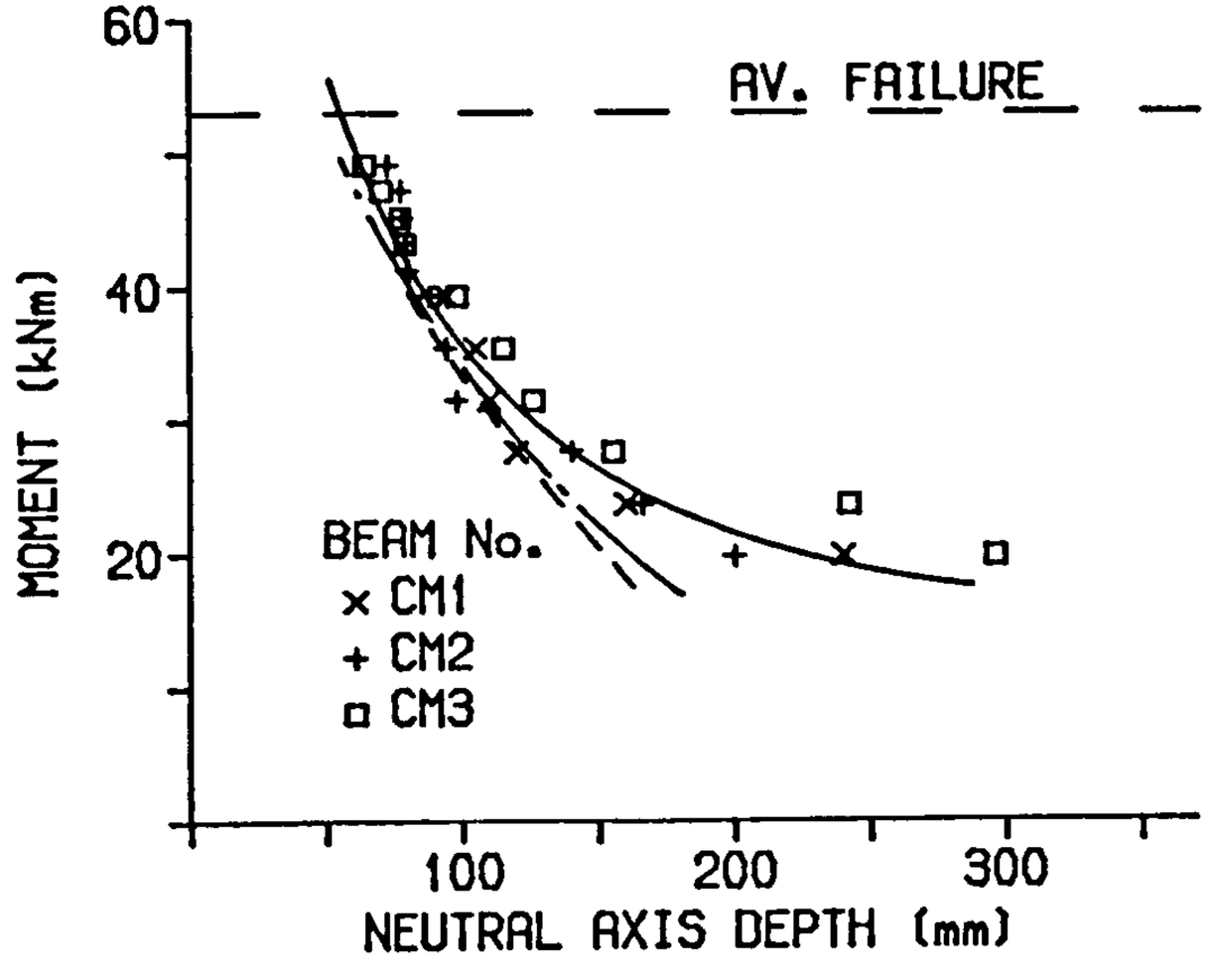

(d)

Figure 5.2.13 (Cont.)

RELATIONSHIP BETWEEN MOMENT AND ADDITIONAL STRAIN IN TENSIONED STEEL

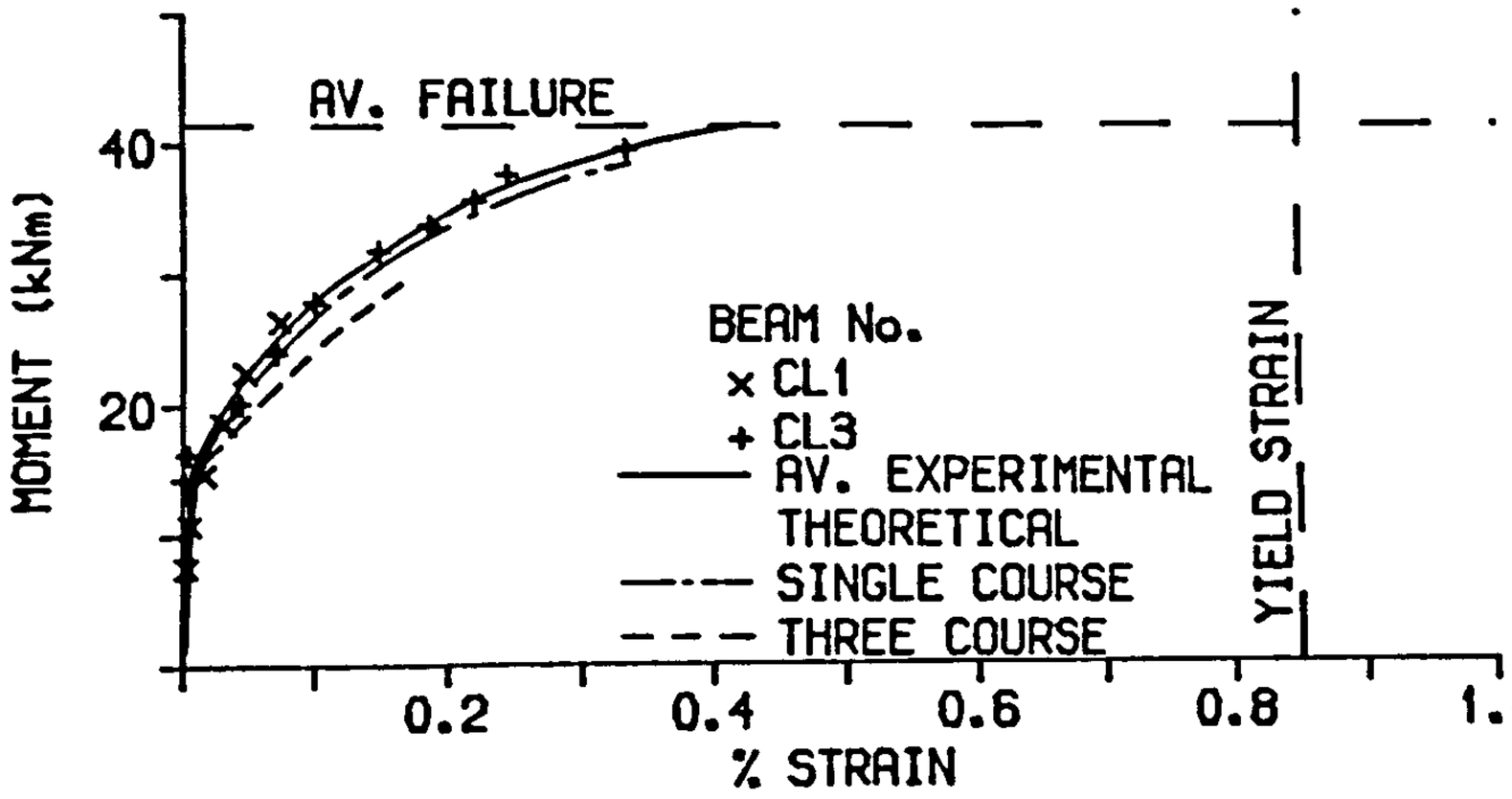

(a)

RELATIONSHIP BETWEEN MOMENT AND STRAIN IN NON-TENSIONED STEEL

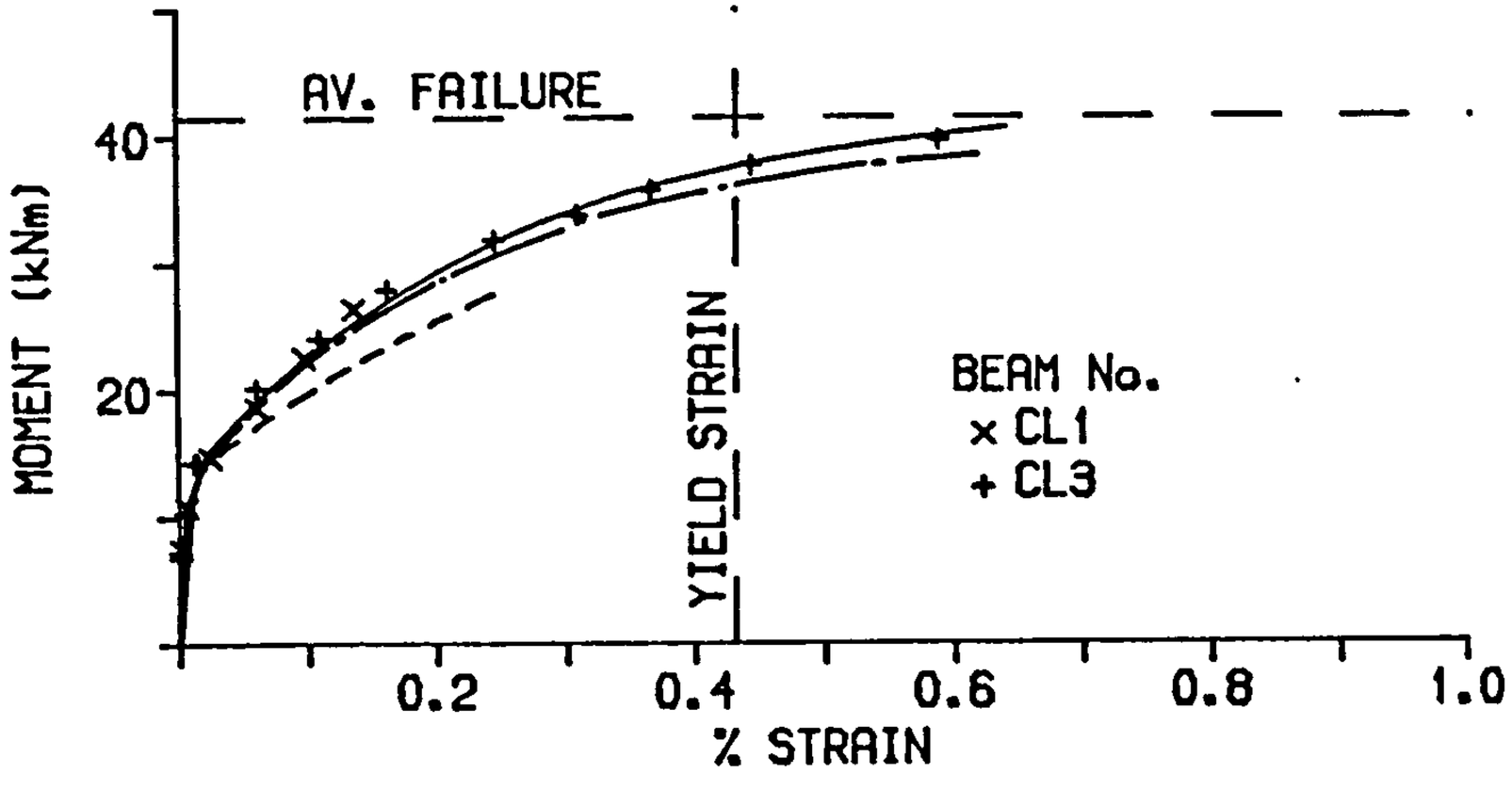

(b)

Figure 5.2.14

RELATIONSHIP BETWEEN MOMENT AND TOP FIBRE STRAIN

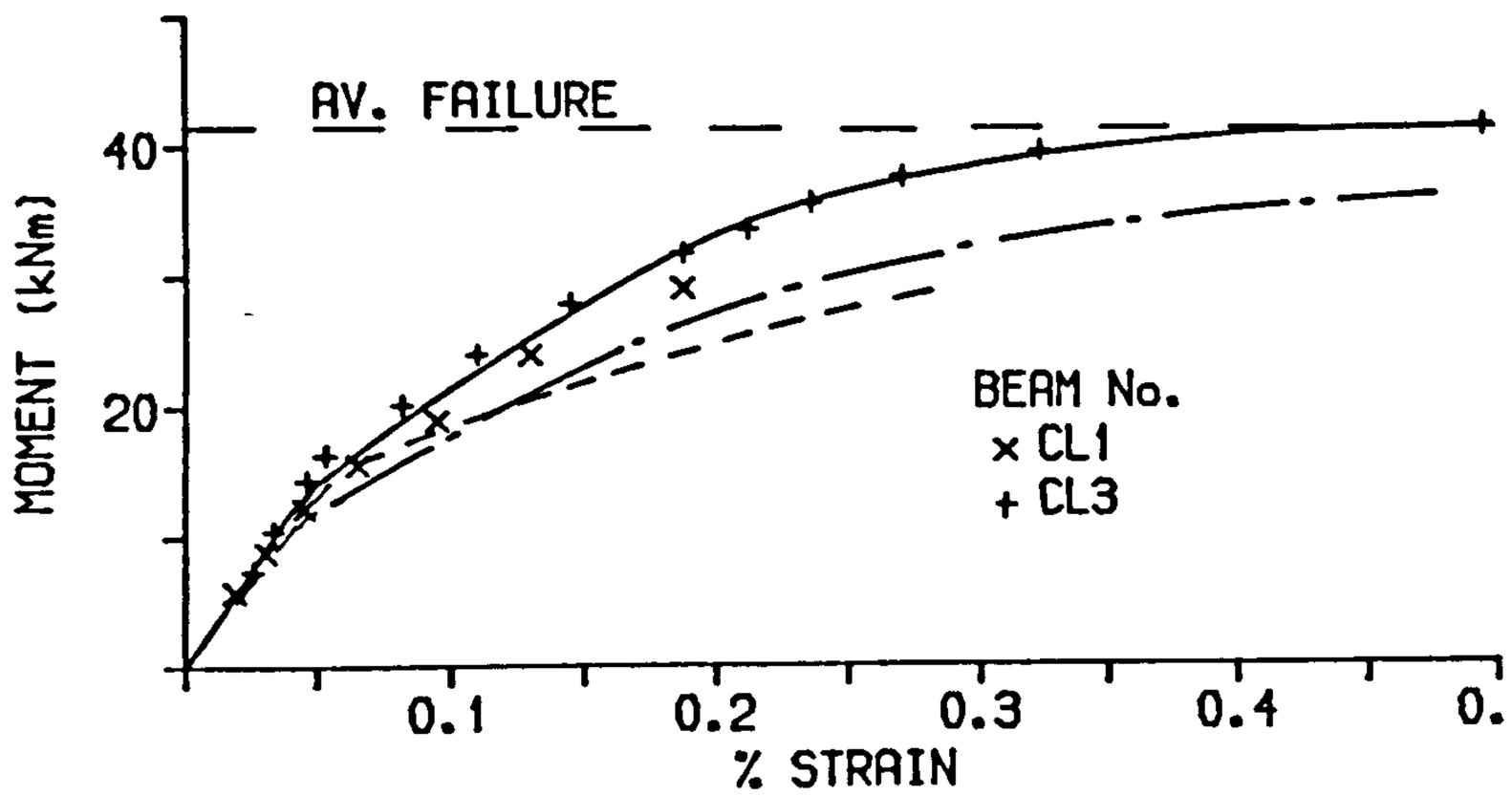

(c)

RELATIONSHIP BETWEEN MOMENT AND NEUTRAL AXIS DEPTH

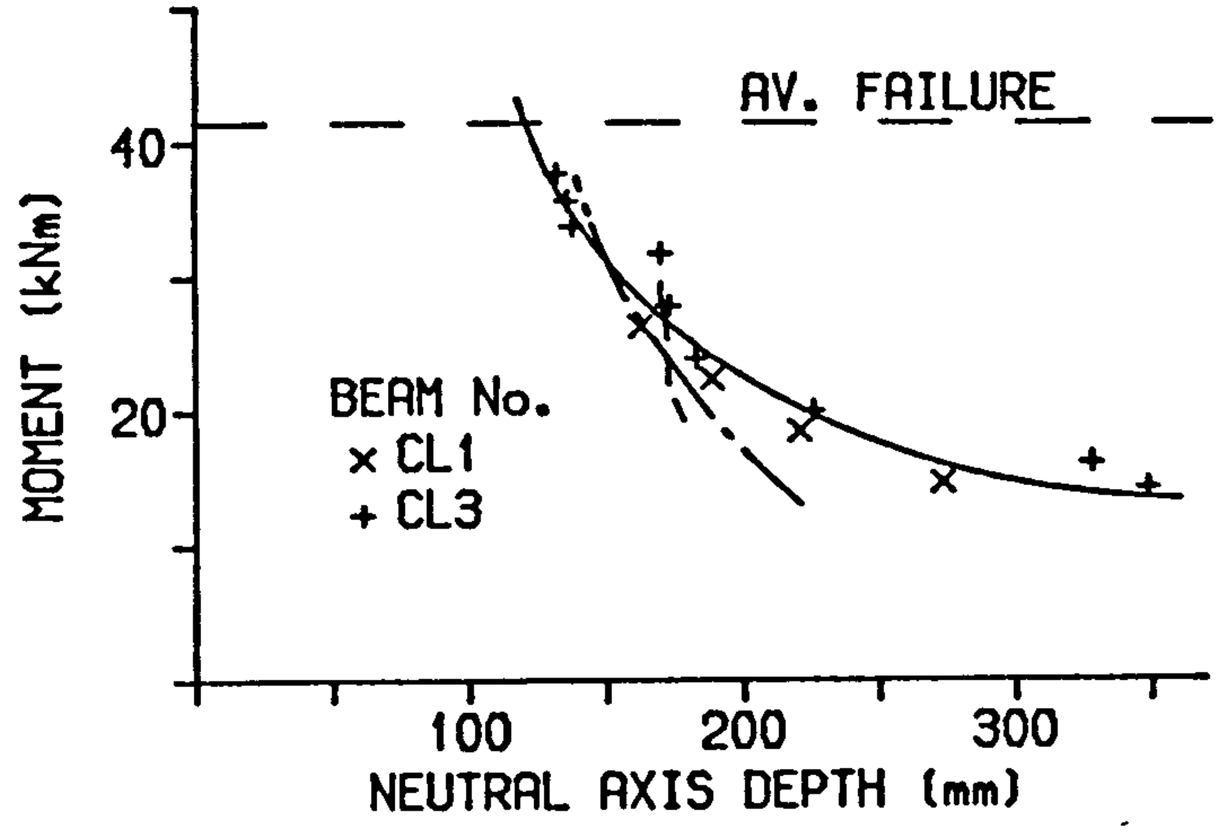

(d)

Figure 5.2.14 (Cont.)

of the beam at the level of the steel, was less than 0.001%. Compared with subsequent levels of strain due to the applied moment, figures 5.2.3b - 5.2.14b, the compressive strain introduced may be considered as being insignificant and consequently the compressive strains have been ignored in the construction of the curves and so all of the graphs commence at the origin.

The curves for additional strain in the tensioned steel and total strain the non-tensioned steel plotted against moment show similar characteristics, figures 5.2.3 - 5.2.14. Initially there was a linear elastic relationship between moment and steel strain up to cracking. After cracking the strain increased more rapidly until failure, the strain due to the applied moment was always greatest in the non-tensioned steel due to its larger distance from the neutral axis. After exceeding the proof stress the curves for the steel strain became parallel to the x-axis.

Shown in each figure is the strain necessary for yielding and the average ultimate flexural moment. From extrapolation of the average experimental curves the failure modes as given in table 5.2.1 were derived, discussion of the failure mode in section 5.3.

5.2.4 Relationship between top fibre brickwork strain and moment

The variation of the maximum compressive brickwork strain at the top fibre with respect to moment for each beam is presented in figures 5.2.3c - 5.2.14c. Each curve was initially linear up to cracking at which point the beam was behaving elastically. After cracking the strain increased more rapidly with moment until it

'flattened off' after yielding of the tensile reinforcement. Values for the ultimate compressive strain of brickwork were obtained from the intersection of the curve representing the average experimental results with the average ultimate flexural moment. In a beam series where a number of the beams failed in shear before crushing of all the brickwork the ultimate moment represents the maximum moment of the beams in that group.

The average ultimate compressive strain, ε_m , for all of the high strength brick beams, grade I mortar, varied between 0.003 and 0.0045. An average value for all the high strength brick beams of 0.0036 shows close agreement with the corresponding value derived from the axially loaded single course prisms, ε_m = 0.00353. It was noticeable that the compressive brickwork strain measured in a number of beams built of differing brick strengths was in excess of 0.005. This was due to local effects at the point of measurement such as spalling of the brickwork after the ultimate strain had been exceeded.

The average ultimate strain for the high strength brick, grade II mortar, beams (series CG) was 0.0038, figure 5.3.12c. This corresponds to a value of 0.00332 from the axially loaded single course brickwork prisms chapter 3. The average values for ultimate compressive strain for the medium and high strength brick beams was 0.0033 and 0.0042, figures 5.3.13c and 5.3.14c respectively. There appears to be good agreement with the corresponding values from the axially loaded single course prisms of 0.0030 (medium strength) and 0.00476 (low strength), chapter 3.

5.2.5 Relationship between neutral axis depth and moment

Presented in figures 5.2.3d - 5.2.14d are the experimental results for the variation in neutral axis depth with moment for each beam series. The values for the neutral axis depth from the top fibre, although not directly measured, were derived from the brickwork strain profiles measured on each beam at every load increment, section 5.2.2.

Initially the relationships indicated a rapid decrease in the neutral axis depth with increasing moment. Approaching failure, after yielding of the tensile reinforcement, the curves started to 'level off' until reaching a minimum value at the ultimate moment at which point crushing of the brickwork occurred.

In the high strength brick beams which developed full flexural moment typical neutral axis depths at failure were between 40-60 mm, figures 5.2.3d - 5.2.12d. The magnitude of the neutral axis depths at ultimate were dependant upon the steel area. The larger the steel area the greater the neutral axis depth necessary for the compression force to equate with the increased tensile force. The results for neutral axis depth support the preliminary experimental observation (Plate 5.1) that the compressive forces at ultimate were carried solely by the top course of brickwork, and hence the single course prism was most likely the best representation of the compression zone of the partially prestressed brickwork beams.

The neutral axis depths measured in the medium and low strength brick beams, figure 5.2.11 and 5.2.12, at ultimate were

increased in comparison with the equivalent high strength brick beams, figure 5.3.5. This was due to the reduction in compressive strength and hence the section required an increase in the depth of the compression zone in order to equate with similar tensile forces after yielding of the reinforcement.

5.3 FAILURE MODE

The likely failure modes for the partially prestressed brickwork beams tested in this study were as follows;

(i) Tension (flexural) : a tensile failure of the non-tensioned and tensioned reinforcement occurs, leading to large increase in both the tensile and compressive strains with a rise in the neutral axis and resulting in crushing of the brickwork.

(ii) Compression : the strain in the compression zone reaches ultimate prior to yielding of either the non-tensioned or tensioned steel and crushing of the brickwork occurs.

(iii) Shear.

As each failure mode has distinct characteristics the behaviour of each beam at ultimate and consequently its mode of failure generally may be discerned from experimental observation. However, since the mode of failure is defined by the level of strain

in the steel and brickwork at the time of failure moment a more complete discussion requires that the experimental values for steel strain and brickwork strain at ultimate are considered. Measurement of the steel strain and brickwork strain at ultimate was not always possible and so the values for steel and brickwork strain at ultimate were extrapolated from the experimental relationships recorded prior to failure, figures 5.2.3 - 5.2.14.

5.3.1 Experimental observation

The observed flexural behaviour of each beam under the action of the applied load was similar up to failure, irrespective of whether the eventual failure was due to shear or in flexure. Initially the soffit of the beam was in compression due to the prestress, with increasing moment the prestress was neutralised and eventually sufficient tensile stresses developed to cause cracking. The cracks were observed to progress up through the section with further loading, the extent of the cracking at each load increment was dependant upon the individual details of each beam section.

Plate 5.1 shows a typical flexural, tension, failure. The failure was characterised by excessive tensile cracking and gross deflections indicating that the tensile reinforcement had yielded, leading to crushing of the extreme brickwork compression fibre. In many of the high strength brick beams which failed in tension, although no increase in the applied moment was possible, excessive deflection was observed as it was possible to deflect the beam under load sufficiently for the soffit to touch the test rig, approximately 280 mm or span/22, with little visible distress to the

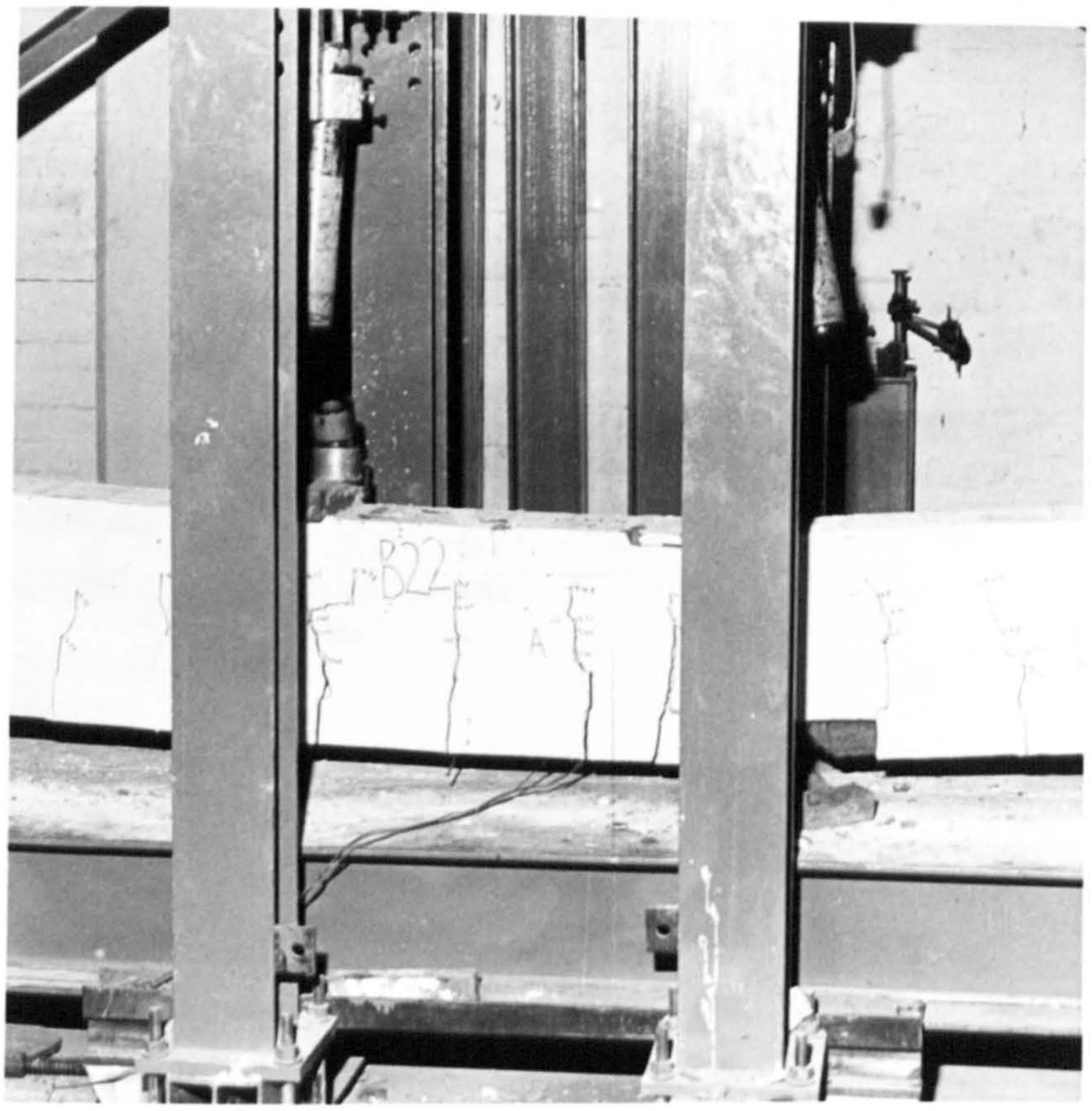

Plate 5.1

Typical tensile failure

Plate 5.2

Typical secondary shear failure

top course of brickwork. With unloading the beams recovered up to 35% in deflection eventhough the tensioned steel had clearly exceeded its proof stress. It was possible to repeatedly re-load the beam up to 95% of the ultimate moment without crushing of the top course of brickwork.

In a number of beams although clearly the steel had yielded, indicated by large deformations, a secondary shear failure occurred before crushing of the brickwork. A typical secondary shear failure is shown in Plate 5.2. The failure mechanism was similar to that of a conventional shear failure with the exception that all or part of the tensile reinforcement had yielded. Eventual failure occurred suddenly along the inclined cracks in the shear span and also along the brickwork/concrete interface of the third and fourth courses of brickwork to the support, Plate 5.2. A total collapse of the beams did not occur and upon removal of the load a number of these beams displayed considerable recovery of both deflection and cracking.

A primary shear failure was observed in four of the test beams, a typical failure shown in Plate 5.3. Experimental observation suggests that the shear failures were due to a weak bond between either the brickwork and concrete, beams A1 and A2, or the bricks and mortar, beams CL1 and CL2. The shear cracks travelled longitudinally in the shear span along the interface between the third and fourth courses, brickwork and concrete cavity, from the load point to the support in beams A1 and A2, Plate 5.3. Beams A1 and A2 were the first to be built and tested as part of this work, in all subsequent beams the cavity was slurried with a neat cement/water mixture prior to concreting in order to improve bond between the

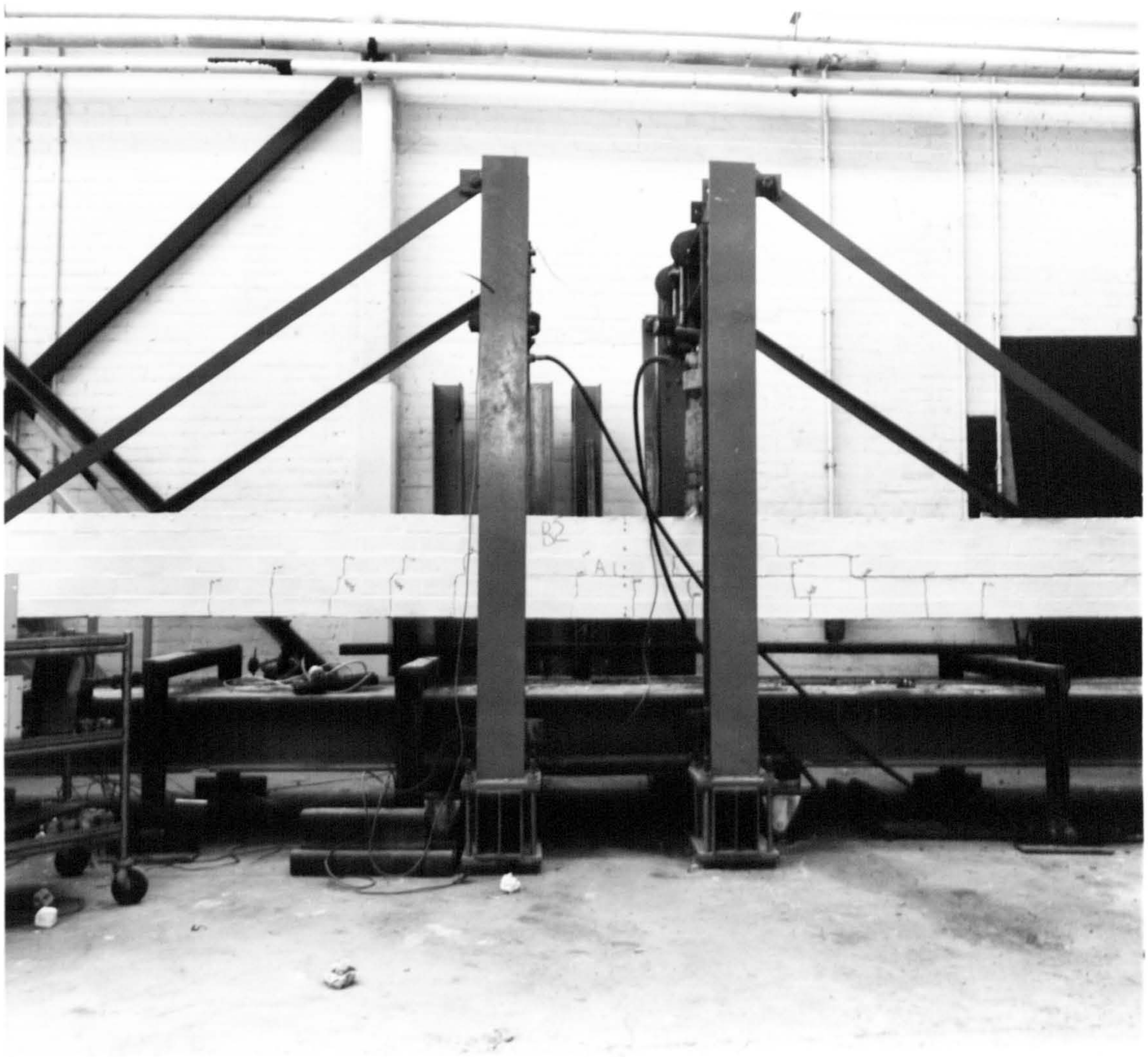

Plate 5.3

Typical primary shear failure

brickwork and concrete. This type of failure was not observed in any of the further tests. The shear failures in the low strength brick beams were characterised by longitudinal cracking along the bed-joints in the shear span. Observation of the weak bond between the bricks and the mortar, caused by the very high suction rate of the bricks (table 3.2.1), was the reason for the shear failures and hence the very low shear strength, table 5.2.1.

5.3.2 Steel strain

The strain measured in both the tensioned and non-tensioned steel near to failure is shown for all beams in figure 5.2.3 - 5.2.14. From these figures the failure modes as given in table 5.2.1 were derived. Of the 41 beams tested a total of 37 beams failed in tension of which 12 subsequently exhibited secondary shear failures. Four beams failed due to primary shear. All of the beams tested in this study were under-reinforced.

The non-tensioned reinforcement yielded before the tensioned steel in all 37 beams which exhibited a flexural failure, figure 5.2.3 - 5.2.14. This is not surprising due to the greater distance from the neutral axis and the lower yield strain of the reinforcing bars. Although in figures 5.2.3 - 5.2.14 strain in the steel is not shown beyond 1.0%, since the steel had long since yielded, strains were in fact measured up to 2.0% using the post-yield type strain gauges. Subsequent to the yielding of the non-tensioned steel the tensioned steel yielded at an increased moment in all beams which full flexural capacity with the exception of beam CL3. From figure 5.2.14a it is clear that although the non-tensioned steel had yielded

at approximatley 85% of the ultimate moment the tensioned steel did not. Hence beam CL3 was over-reinforced with respect to the tendon as crushing occurred before yielding of the steel, i.e. the brickwork strength was insufficient to allow yielding of the tensioned steel.

Twelve test beams exhibited secondary shear failures, of which these may be split into two groups, those in which all of the tensile steel yielded and those in which only part of the reinforcement yielded. Those beams in which all of the steel had yielded, namely beams A3, CP1, CP3, R1-R3 and CM1-CM3 it was clear from comparison of the results that the reduction in ultimate moment was minimal, figures 5.2.4 - 5.2.13 and table 5.2.1. Crushing of the brickwork was observed in a number of beams and hence it was likely that shear failure coincided with the development of full flexural capacity. Since there was little increase in moment after the tendon yielded (figures 5.2.3 - 5.2.13), secondary shear failure was not significant to cause a reduction in moment capacity. However, comparison of beams AB1-AB3 with AA1-AA3 indicates a significant reduction in ultimate moment due to secondary shear failure resulting from the reduction in prestress. The additional strain measured in the tendon at the time of the secondary shear failure of beams AB1-AB3 varied between approximately 0.4% (beam AB3) and 0.7% (beams AB1 and AB2), figure 5.2.5a. The strain necessary for yielding was 0.78% and, beams AB1 and AB2 were close to achieving this.

Beams A1 and A2 in which a shear failure was recorded figure 5.2.3b indicates that shear failure was coincident with yielding of non-tensioned steel. However, the strain in the non-tensioned steel in beams CL1 and CL2 at failure was only between 0.15-0.2%, clearly

well below the necessary yield strain of 0.43%, figure 5.2.14b.

5.3.3 Brickwork strain at failure

In section 5.2.3 discussion of the top fibre brickwork strain at failure in those which showed flexural failures suggested that the ultimate compressive strain for brickwork derived from the single course prisms was an accurate indication of the value which developed in the beams at failure. Therefore by comparison of the compressive strain recorded at failure in the beams which showed secondary shear failure with the ultimate strain for the single course prisms it was possible to determine exactly how near to a flexural failure each beam was.

The top fibre brickwork strain measured in beam AA1 at the time of the secondary shear failure was 0.0028, figure 5.2.4c. Clearly the strain in the top fibre was less than the ultimate strain of 0.00353 and hence the failure was secondary shear. However, the strain measured in beams AB1 and AB2 of 0.0031 would indicate that these beams were nearer to achieving their full flexural capacity at the time of secondary shear. Likewise the strain in the top fibre of beams CP1 and CP3 was in excess of 0.003 at failure and therefore the secondary shear failure in these beams was coincident with crushing of the brickwork. This is further supported by the ultimate moment of beams CP1 and CP3, 52.0 and 49.3 kNm respectively, was very close to the ultimate moment of beam CP2, 53.6 kNm, in which secondary shear was absent, table 5.2.1.

In the reinforced brickwork beams, R1-R3, the average top

brickwork strain at secondary shear failure was 0.0032, figure 5.2.11c. Clearly the reinforced beams were at the point of achieving full flexural capacity, as the steel had yielded. Therefore the flexural capacities and shear capacities of the reinforced brickwork beam section tested in the project were very similar.

5.4 ULTIMATE MOMENT

In this section the experimental results for ultimate moment of the partially prestressed brickwork beams are discussed and compared with theoretical predictions.

5.4.1 Effect of % area of steel

All eight beams with 0.31% steel area, beams C1-C8, and the three beams with 0.37% steel area, beams B1-B3, failed in flexure. From table 5.4.1 it can be seen that the increase in steel area significantly increased the ultimate moment. The average ultimate moment of beams B1-B3 was 63.1 kNm which shows an 18% increase in moment capacity when compared to average ultimate moment of 53.5 kNm for beams C1-C8.

Two of the beams with 0.47% steel area failed in shear, beams A1 and A2 in table 5.2.1. The shear failures were most likely due to the weak bond that developed between the brickwork and concrete although the increase in steel area will have influenced the failure mode. The ultimate moment for beam A3, 73.4 kNm, shows an increase of 27% compared to the average ultimate moment of beam

Table 5.4.1

Effect of % area of steel on ultimate moment

Beam Nº	% area of steel	Effective Prestress kN	Average Effective Prestress kN	Ultimate Moment kNm	Average Ultimate Moment kNm
A3	0.47	68.7		73.4	
B1		68.8		62.0	
B2	0.37	68.3	67.8	63.9	63.1
B3		66.2		63.4	
C1		67.4		52.8	
C2		66.7		53.2	
C3		61.4		54.6	
C4	0.31	64.8	65.6	51.5	53.5
C5		69.2		51.5	
C6		57.7		57.5	
C7		70.8		54.3	
C8		66.7		52.2	

series C, table 5.4.1. Whilst the shear capacity was sufficient to allow a flexural failure an increase in steel area directly led to an increase in ultimate moment. However, if the increase in steel area was such that the applied loads required to yield the steel were greater than the shear capacity of the section then the increase in ultimate moment capacity would have been limited by the shear capacity of the section.

5.4.2 Effect of prestressing force

The effect of prestressing force upon the development of full flexural capacity of partially prestressed brickwork beams can be obtained by comparing the results of beams AA1-AA3 with beams AB1-AB3, table 5.4.2. Although the beams failed in tension, table 5.2.1, beams AA1 and AB1-AB3 also indicated secondary shear failures prior to crushing of the brickwork compression zone, figures 5.2.4c and 5.2.5c.

The average ultimate moment of beams AA2 and AA3 was 88.1 kNm, which shows an increase of 13% compared with the average ultimate moment of beams AB1-AB3 of only 76.9 kNm. This corresponds to an increase in the average prestressing force for beams AA2 and AA3 of 26% compared to the average prestressing force of beams AB1-AB3, table 5.4.2. The difference in ultimate moments was most likely due to the reduction in prestress leading to a reduction in the effective shear strength and hence causing a secondary shear failure. In beams AA2 and AA3 the prestressing force was sufficient for crushing of the brickwork to occur after yielding of both layers of steel, figure 5.2.4. However, the prestressing force was only

Table 5.4.2

Effect of prestressing force on ultimate moment

Beam Nº	Effective Prestress kN	Average Effective Prestress kN	Ultimate Moment kNm	Average Ultimate Moment kNm
AA2	124.7	128.4	88.6	88.1
AA3	132.7		87.5	
AB1	100.1		80.7	
AB2	94.7	94.5	79.4	76.9
AB3	90.1		70.6	
C1-C8	-	65.6	-	53.5
CP1	51.4		52.0	
CP2	51.1	51.7	53.6	51.6
CP3	52.5		49.3	

sufficient for yielding of the non-tensioned steel in beams AB1-AB3, figures 5.2.5, before secondary shear occurred. The average ultimate shear strength of beams AA2 and AA3 was 0.58 N/mm² (failure corresponded to flexure). For beams AB1-AB3 the ultimate shear strength only 0.52 N/mm², a reduction in shear capacity of 11.7% most likely due to the reduction in prestressing force. In conclusion if the reduction in prestressing force is sufficient to alter the failure mode from flexure to shear the reduction in ultimate moment may be significant.

The influence of prestressing force was also studied by comparing the results of beams C1-C8 and beams CP1-CP3. For a 21% decrease in prestressing force the ultimate moment decreased by only 3% (table 5.4.2) although beams CP1 and CP3 both indicated secondary shear failures similar to beams AB1-AB3 (table 5.2.1). However, unlike the secondary shear failure of beams AB1-AB3 the secodary shear failures in beams CP1 and CP3 occurred after yielding of both layers of steel, figure 5.2.8, whereas in the case AB1-AB3 only the non-tensioned steel had yielded. Once both layers of steel had yielded the subsequent increase in moment was very small. Thus if the prestressing force was sufficient for yielding of both layers of steel a reduction in prestressing force will not have a significant effect on the ultimate moment as long as the failure was tensile.

5.4.3 Effect of cover to non-tensioned steel

Failure of all three beams CC1-CC3, in which the cover to the non-tensioned steel was 50 mm, was in flexure. Compared to beams C1-C8 the ultimate moment decreased by 3% for an corresponding

increase in cover to the non-tensioned steel of 100%, table 5.4.3.

Since all of the material properties and prestressing forces were constant the neutral axis depth at failure will also remain unchanged, at approximately 43 mm (figures 5.2.7 and 5.2.9). The decrease in ultimate moment was due to the reduction in the leverarm to the non-tensioned steel. Therefore, as long as the non-tensioned bars were placed at a sufficient depth to allow yielding the decrease in the moment capacity was a direct function of the change in the effective depth.

5.4.4 Effect of brick strength

All eight of the high strength brick beam series C failed in flexure, average ultimate moment 53.5 kNm. The medium strength brick beam series CM failed in secondary shear, however, figure 5.2.13 indicates that both layers of reinforcement had yielded and therefore the reduction in ultimate moment due to the secondary shear was not likely to be significant. The average ultimate moment for the medium strength brick beams was 51.1 kNm, table 5.4.4, and therefore a reduction of only 4% in ultimate moment occurred for a reduction in the on-bed brick strength of 25%.

Only one of the low strength brick beams failed in flexure, beam CL3 in table 5.2.1. Although the non-tensioned steel yielded prior to ultimate, figure 5.2.14, the brick strength was insufficient to allow the tendon to yield and crushing of the brickwork occurred. Compared with high strength brick beams CP1-CP3 beam CL3 showed a reduction in ultimate moment of 20% for a reduction in the on-bed

Table 5.4.3

Effect of cover to non-tensioned steel on ultimate moment

Beam N°	Cover mm	Effective Prestress kN	Average Effective Prestress kN	Ultimate Moment kNm	Average Ultimate Moment kNm
C1-C8	25	-	65.6	-	53.5
CC1		66.2		52.8	
CC2	50	64.4	69.5	52.5	51.9
CC3		78.0		50.3	

Table 5.4.4

Effect of brick strength on ultimate moment

Beam N°	Brick Strength N/mm²	Effective Prestress kN	Average Effective Prestress kN	Ultimate Moment kNm	Average Ultimate Moment kNm
C1-C8	96.6	-	65.6	-	53.5
CM1		66.9		51.8	
CM2	72.3	57.5	62.8	53.0	51.1
CM3		64.1		48.5	
CP1-CP3	96.6	-	51.7	-	51.6
CL3	19.7	52.6	-	41.4	-

brick strength of 78%, table 5.4.4. It was noticeable that two of the low strength brick beams failed in primary shear, beams CL1 and CL2. The reduced shear strength was caused by the weak bond that developed between the brick and mortar as a result of the high suction rate of the bricks, table 3.2.1.

At ultimate flexural moment sufficient compressive forces need to develop to allow the tensile steel to yield. Consequently the neutral axis depth at ultimate will be greatest for the weakest brickwork strength in order that the necessary compressive forces may develop. As the stress block shape was unchanged for all brickwork strengths, section 3.6.1, an increase in the neutral axis depth will lead to a proportionate decrease in the leverarm to the tensile reinforcement and consequently a decrease in the ultimate moment. For example the neutral axis depths at failure in the high and medium strength brick beams were approximately 43 mm and 67 mm respectively, figure 5.2.7d and 5.2.13d. In the low strength brick beams the brickwork strength was insufficient to allow the tendon to yield, the neutral axis depth at failure in beam CL3 at ultimate was 120 mm, figure 5.2.14d. A combination of a reduction in leverarm and tensile force caused a reduction in ultimate moment of 20%.

Whilst the compressive strength of the brickwork was sufficient to allow the tensile steel to yield the ultimate moment is governed by the properties of the steel and the brickwork influences the neutral axis depth and leverarm. Therefore for an under-reinforced section the brick strength does not significantly influence the ultimate moment. However, if the brickwork strength is insufficient to allow all or part of the tensile steel to yield, the

strength of the brick may influence the ultimate moment to a much greater extent.

5.4.5 Effect of mortar grade

All of the grade I mortar beam series C and grade II mortar beam series CG failed in flexure. The results are summarised and compared in table 5.4.5. For a 61% decrease in mortar strength there was in fact a 2% increase in the ultimate moment. This may be attributed to experimental variation and the slightly increased average prestressing force.

It has long been known that the compressive strength of brickwork is influenced by a change in the mortar strength by only a third or fourth root relationship[54]. This was apparent from the brickwork prism tests where there was only a 17% and 22% decrease in brickwork strength for single and three course prisms respectively, for a change in mortar grade from I to II, table 3.6.1. As the brickwork strength was sufficient to allow the tensile steel to yield, an under-reinforced section, the ultimate moment was not significantly influenced.

5.4.6 Comparison of experimental results and theoretical predictions of ultimate moment

The theoretical approach outlined in section 4.2 was used to predict the ultimate moment of the test beams. The material properties used for the analysis are given in tables 3.6.1 and 3.6.2 and figures 3.5.1 - 3.5.5. The experimental and theoretical ultimate

Table 5.4.5

Effect of mortar grade on ultimate moment

Beam Nº	Mortar Grade / Strength N/mm²	Effective Prestress kN	Average Effective Prestress kN	Ultimate Moment kNm	Average Ultimate Moment kNm
C1-C8	I / 19.4	-	65.6	-	53.5
CG1		7.3	76.8	54.5	
CG2	II / 8.6	8.6	66.3	54.5	54.5
CG3		6.6	70.7	54.5	

moments were compared only for those beams which exhibited flexural failure. The prestressing forces used for the analysis were those measured after all losses, table 5.2.1.

In chapter 3 it was confirmed that the shape of the stress block for brickwork derived from the axially loaded prism tests was independent of the brick strength, mortar grade and prism type. Although initial results suggest that the single course prisms provided the best representation of the compression zone the experimental ultimate moments were compared with both the single and three course prism properties, table 5.4.6. The results are also compared with the predicted values using the recommendations of BS 5628 Part 2[15].

From table 5.4.6 it can be seen that the single and three course prism brickwork properties generally under-predicted the ultimate moment of the high strength brick beams, by on average 6% and 21% respectively. The ratio of experimental to theoretical ultimate moment varied between 0.91 and 1.14 using the single course prism properties and between 1.05 and 1.29 when using the three course, table 5.4.6. In nearly all of the high strength brick beams the single course prisms consistently provided the best estimate of the flexural capacity.

In the medium and low strength brick beams the single course prisms under-estimated the ultimate moments by on average 14% and 21% respectively. Similarly the three course prisms under-predicted the moment by 32% and 43% for the medium strength and low strength brick beams respectively. From this it appears that the single course

Table 5.4.6

Comparison of experimental and theoretical ultimate moments

Beam N°	Expt Ultm Moment kNm	Single Course		Three Course		BS 5628 Part 2			
						γ_{mm}, γ_{ms}=1		γ_{mm}=2, γ_{ms}=1.15	
		kNm	$\frac{\text{Expt}}{\text{Theory}}$	kNm	$\frac{\text{Expt}}{\text{Theory}}$	kNm	$\frac{\text{Expt}}{\text{Code}}$	kNm	$\frac{\text{Expt}}{\text{Code}}$
A3	73.4	69.4	1.06	63.0	1.17	48.1	1.53	32.0	2.29
AA2	88.6	78.5	1.13	69.6	1.27	50.3	1.76	30.4	2.91
AA3	87.5	78.6	1.11	69.8	1.25	50.5	1.73	30.4	2.88
B1	62.0	56.6	1.10	51.4	1.21	41.6	1.49	28.8	2.15
B2	63.9	56.6	1.13	51.4	1.24	41.6	1.54	28.8	2.22
B3	63.4	56.6	1.12	51.4	1.23	41.6	1.52	29.1	2.18
C1	52.8	50.5	1.05	44.8	1.18	37.2	1.42	26.6	1.98
C2	53.2	50.5	1.05	44.7	1.19	37.2	1.43	26.6	2.00
C3	54.6	50.5	1.08	44.6	1.22	37.0	1.48	26.5	2.06
C4	51.5	50.5	1.02	44.7	1.15	36.8	1.40	26.5	1.94
C5	51.5	50.5	1.02	44.8	1.15	37.3	1.38	26.7	1.93
C6	57.5	50.5	1.14	44.5	1.29	37.2	1.55	26.6	2.16
C7	54.3	50.5	1.08	44.8	1.21	37.1	1.46	26.6	2.04
C8	52.2	50.5	1.03	44.7	1.17	37.2	1.40	26.6	1.96
CC1	52.8	48.1	1.10	43.1	1.23	35.8	1.48	25.1	2.10
CC2	52.5	48.1	1.09	43.0	1.22	35.8	1.47	25.1	2.09
CC3	50.3	48.2	1.05	43.2	1.16	36.2	1.39	25.1	1.98
CP1	52.0	50.2	1.04	44.4	1.17	36.6	1.42	26.1	1.99
CP2	53.6	50.2	1.07	44.4	1.21	36.6	1.46	26.1	2.05
CP3	49.3	50.2	0.98	44.4	1.11	36.6	1.35	26.1	1.89
P1	56.6	54.9	1.03	46.6	1.21	39.2	1.44	29.1	1.95
P2	55.3	54.9	1.01	46.6	1.19	39.9	1.41	29.1	1.90
P3	52.9	54.9	0.96	46.6	1.14	39.3	1.35	29.2	1.81
R1	52.2	53.9	0.97	46.4	1.13	37.6	1.39	29.8	1.75
R2	48.9	53.9	0.91	46.4	1.05	37.6	1.30	29.8	1.64
R3	57.3	53.9	0.95	46.4	1.11	37.6	1.36	29.8	1.72
CG1	54.5	48.3	1.13	40.2	1.36	34.1	1.60	22.3	2.44
CG2	54.5	48.3	1.13	39.7	1.37	33.8	1.61	22.3	2.44
CG3	54.5	48.3	1.13	39.1	1.39	34.0	1.60	22.4	2.43
CM1	51.8	45.1	1.15	38.9	1.33	35.0	1.48	23.8	2.18
CM2	53.0	44.9	1.18	38.8	1.37	34.7	1.53	23.2	2.28
CM3	48.5	45.1	1.08	38.9	1.25	34.9	1.39	23.7	2.05
CL3	41.4	34.1	1.21	29.0	1.43	16.3	2.54	8.17	8.08

prisms provided the best estimate of ultimate moment in both the medium and low strength brick beams, table 5.4.6.

As mentioned previously the stress block factors λ_1 and λ_2 were equal for the single and three course prisms. The ultimate compressive strengths and strains were significantly higher for the single course prisms than the three course in all types of brickwork, section 3.6. Measurements taken of the ultimate top fibre brickwork strain on the beams indicate much closer agreement with the single course prism values of ultimate compressive strain, figures 5.2.3c - 5.2.14c and section 5.3.

In table 5.4.6 the experimental ultimate moments are also compared with estimates of ultimate moment using the code recommendations. The code allows the characteristic compressive strength for masonry, f_k, to be determined from either experimental tests or from table 3 of the code. The design engineer is more likely to use the values given by the table in the code, as opposed to an expensive testing programme, and hence these values have been used in this comparison. The ultimate moment has been calculated with and without applying the partial safety factors, $\gamma_{mm} = 2.0$ and $\gamma_{ms} = 1.15$, to the material properties. Values of compressive strength of brickwork obtained from the single course prisms are compared with the characteritic compressive strength, f_k, given by the code in table 5.4.7.

Comparison of the experimental and predicted values for high strength brick, grade I mortar, beams show the code to under-predict the moment by on average 46% if the partial safety factors are taken

Table 5.4.7

Comparison of the compressive properties of brickwork

Brick Type	Mortar Grade	f_k N/mm²	$\lambda_1 f_k$ N/mm²	Single course f_m N/mm²	Single course $\lambda_1 f_m$ N/mm²	f_k / f_m	$\lambda_1 f_k / \lambda_1 f_m$
High	I	7.8	7.8	33.1	20.2	0.24	0.39
High	II	6.0	6.0	27.4	17.0	0.22	0.35
Medium	I	6.5	6.5	19.4	12.5	0.34	0.52
Low	I	2.4	2.4	7.3	4.8	0.19	0.50

as unity and 106% if the partial safety factors $\gamma_{mm} = 2$ and $\gamma_{ms} = 1.15$ are incorporated into the calculations, table 5.4.6.

Comparison between the code and experimental results for high strength brick, grade II mortar, show the code to under-predict the ultimate moment by 60%. Similarly for the medium and low strength brick beams the code under-estimates the ultimate moment by on average 47% and 154% respectively. The ratio between the theoretical and code predictions (using the partial safety factors) for all beams was not less than 1.64, table 5.4.6.

From table 5.4.7 it is clear that the code values for compressive strength of brickwork were conservative estimates compared with the compressive strength of the single course brickwork prisms, f_m. The ratio f_k/f_m varies between 0.19 and 0.34. At ultimate the compressive force is controlled by the product $\lambda_1 f_m$ or $\lambda_1 f_k$, the ratio $\lambda_1 f_k/\lambda_1 f_m$ varies between 0.35 and 0.52. The compressive force as proposed by the code, was insufficient to allow all or part of the tensile reinforcement to yield in nearly all of the beams. Hence the beams will be classified as over-reinforced according to the code, whereas test confirms that they were under-reinforced. Consequently the predicted compression failures under-estimate the actual flexural ultimate moment. Due to the lower compressive strength the neutral axis depth at ultimate will be greater and hence the leverarm will be smaller, this will further contribute to the reduced ultimate moment. In the rectangular stress block $\lambda_2 = 0.5$ will also cause the leverarm to be reduced.

In figures 5.4.1 and 5.4.2 typical experimental

COMPARISON OF EXPERIMENTAL AND CODE STRESS/STRAIN RELATIONSHIPS FOR TENSIONED STEEL

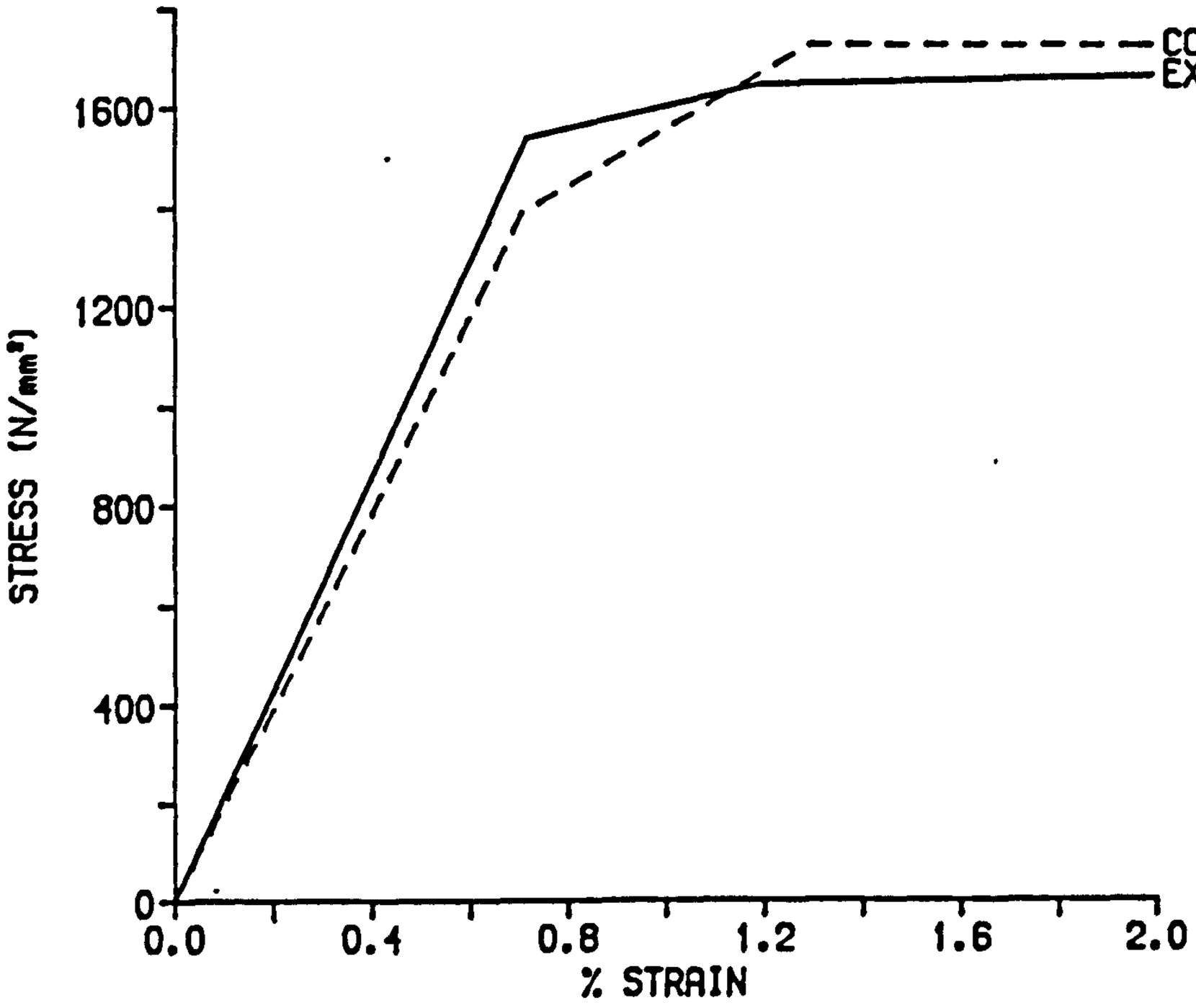

Figure 5.4.1

COMPARISON OF EXPERIMENTAL AND CODE STRESS/STRAIN RELATIONSHIPS FOR NON-TENSIONED STEEL

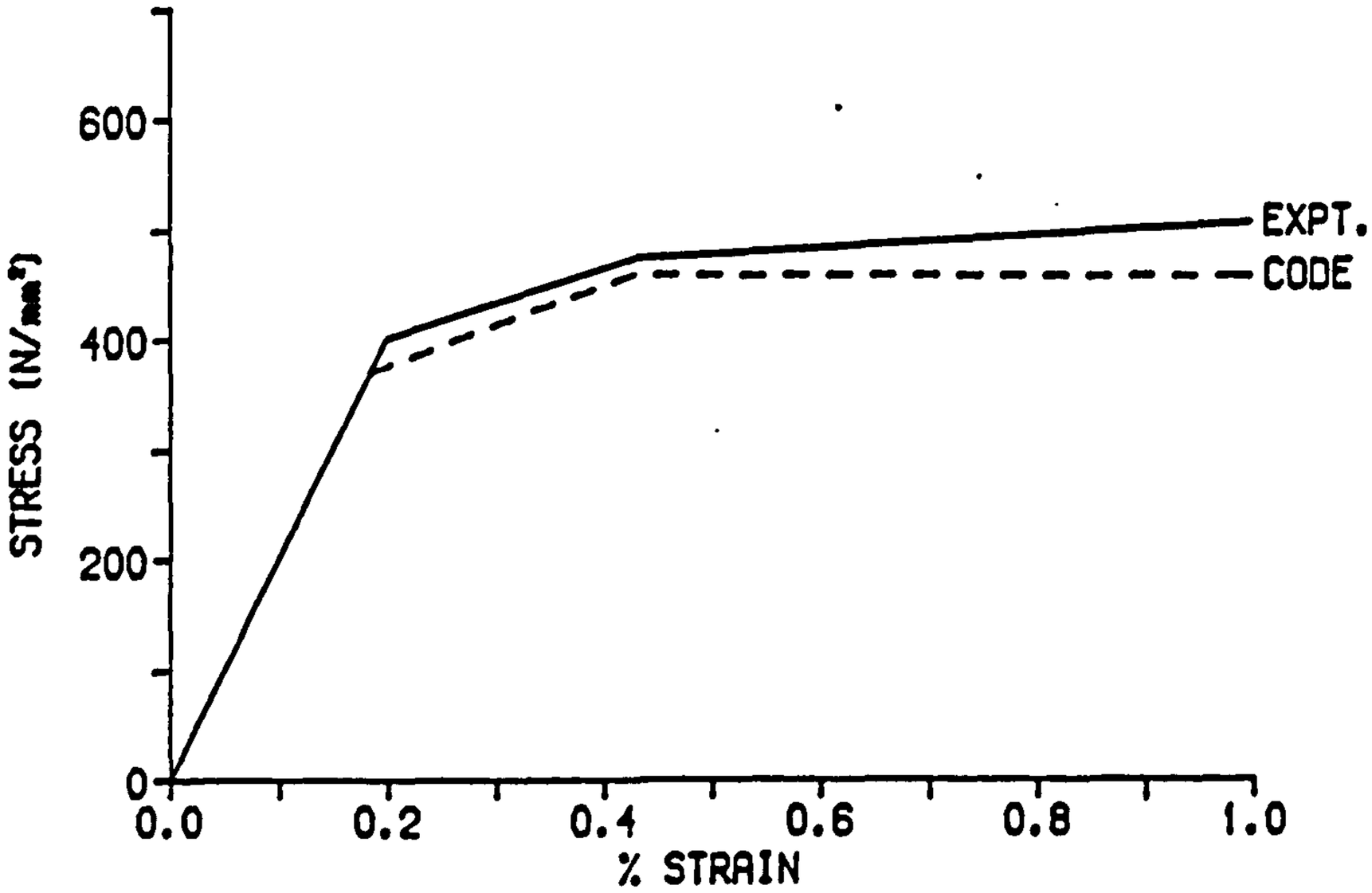

Figure 5.4.2

stress/strain relationships for tensioned, 10.9 mm diameter tendon, and non-tensioned, 12 mm diameter deformed bar, are presented. Also shown are the corresponding code stress/strain relationships. The two stress/strain relationships for the prestressing tendon, figure 5.4.1, were very similar between zero and ultimate tensile strength, and therefore use of the code stress/strain curve for the tendon will not introduce any difference with the predicted ultimate moment using the experimental stress/strain properties. From zero up to the proof stress the stress/strain relationships for non-tensioned deformed bars were very similar, beyond yielding the stress/strain reltionship of the code estimated a significantly lower stress than the experimental curve. After exceeding the proof stress the reduced stresses in the non-tensioned steel predicted by the code stress/strain relationship may reduce the ultimate moment.

Summarising, the code predictions under-estimate the experimental ultimate moment by on average 47%. The under-estimation was due to, for the most part, the very low values of compressive strength proposed by the code. The ultimate moments calculated when using the partial safety factors were safe and proved acceptable for design.

5.5 MOMENT-CURVATURE RELATIONSHIPS ACROSS A CRACK FOR PARTIALLY PRESTRESSED BRICKWORK BEAMS

The experimental results for the moment-curvature relationships across a crack are presented in figures 5.5.1 - 5.5.12. The experimental values for curvature were derived from strain

MOMENT-CURVATURE RELATIONSHIP ACROSS CRACKS FOR BEAM SERIES A

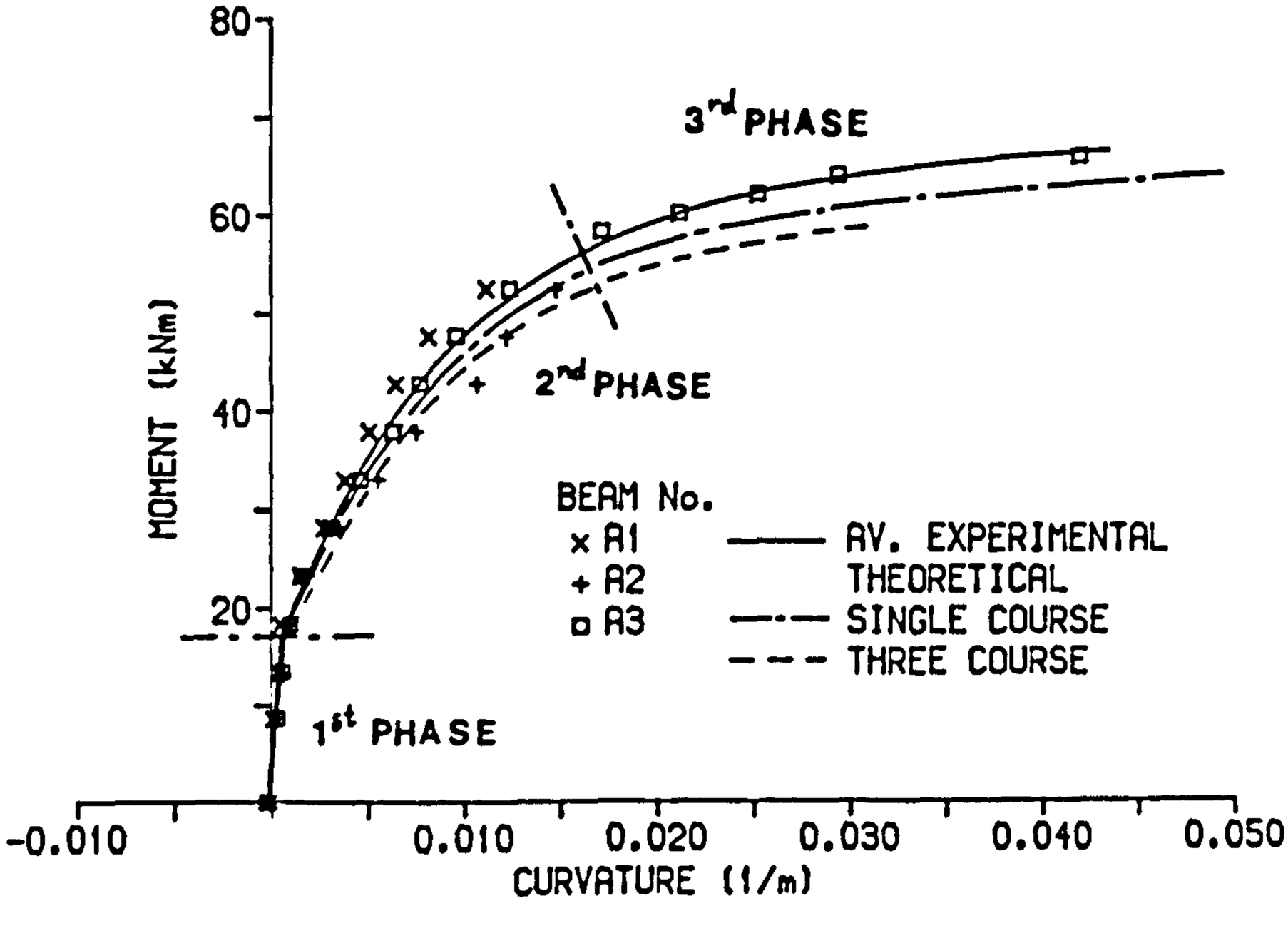

Figure 5.5.1

MOMENT-CURVATURE RELATIONSHIP ACROSS CRACKS FOR BEAM SERIES B

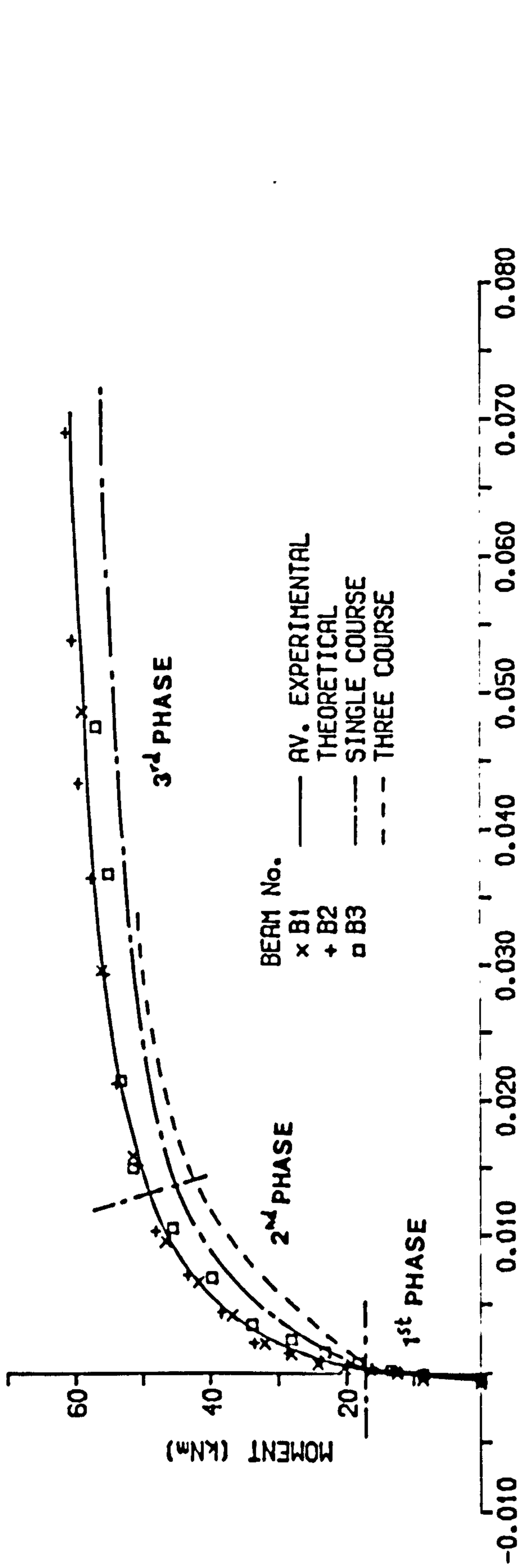

Figure 5.5.2

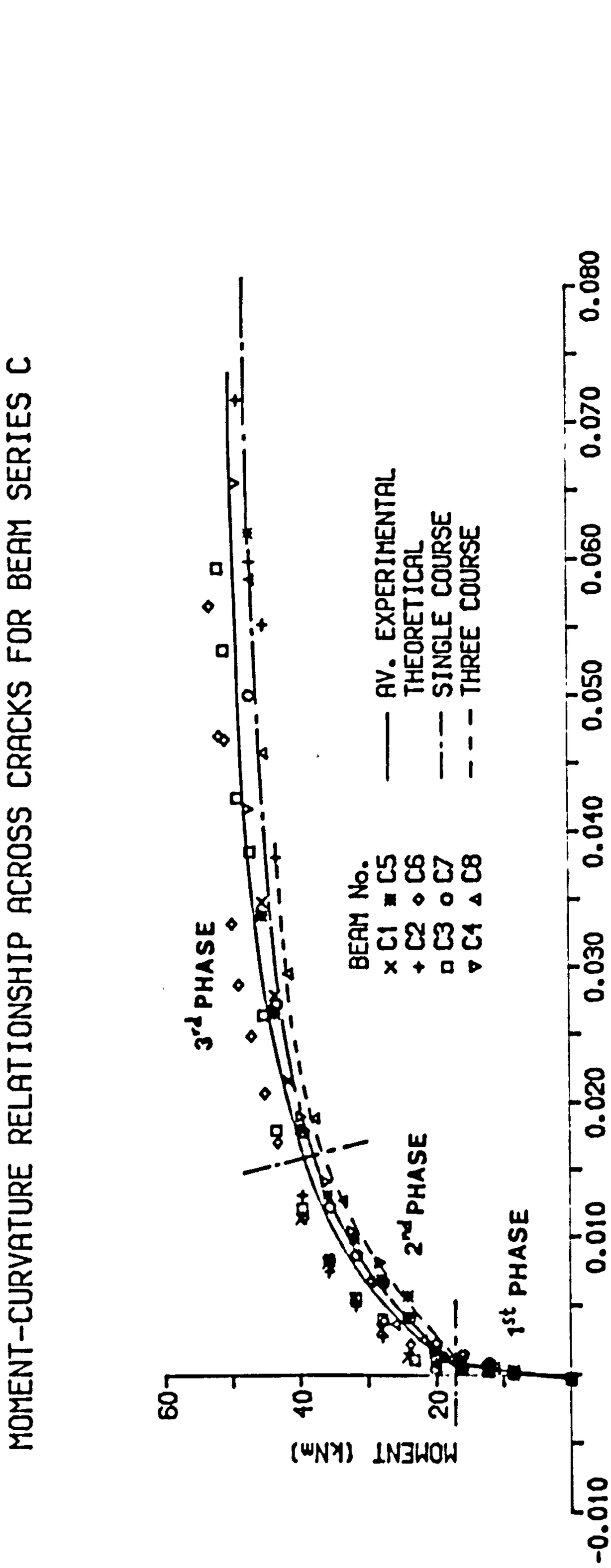
MOMENT-CURVATURE RELATIONSHIP ACROSS CRACKS FOR BEAM SERIES C
MOMENT (kNm)
CURVATURE (1/m)
1st PHASE
2nd PHASE
3rd PHASE
BEAM No.
× C1 ■ C5
+ C2 ◆ C6
□ C3 ○ C7
▽ C4 △ C8
AV. EXPERIMENTAL
THEORETICAL
SINGLE COURSE
THREE COURSE
60
40
20
0.030
0.040
0.050
0.060
0.080
0.070
0.020
0.010
-0.010

Figure 5.5.3

MOMENT-CURVATURE RELATIONSHIP ACROSS CRACKS FOR BEAM SERIES AA

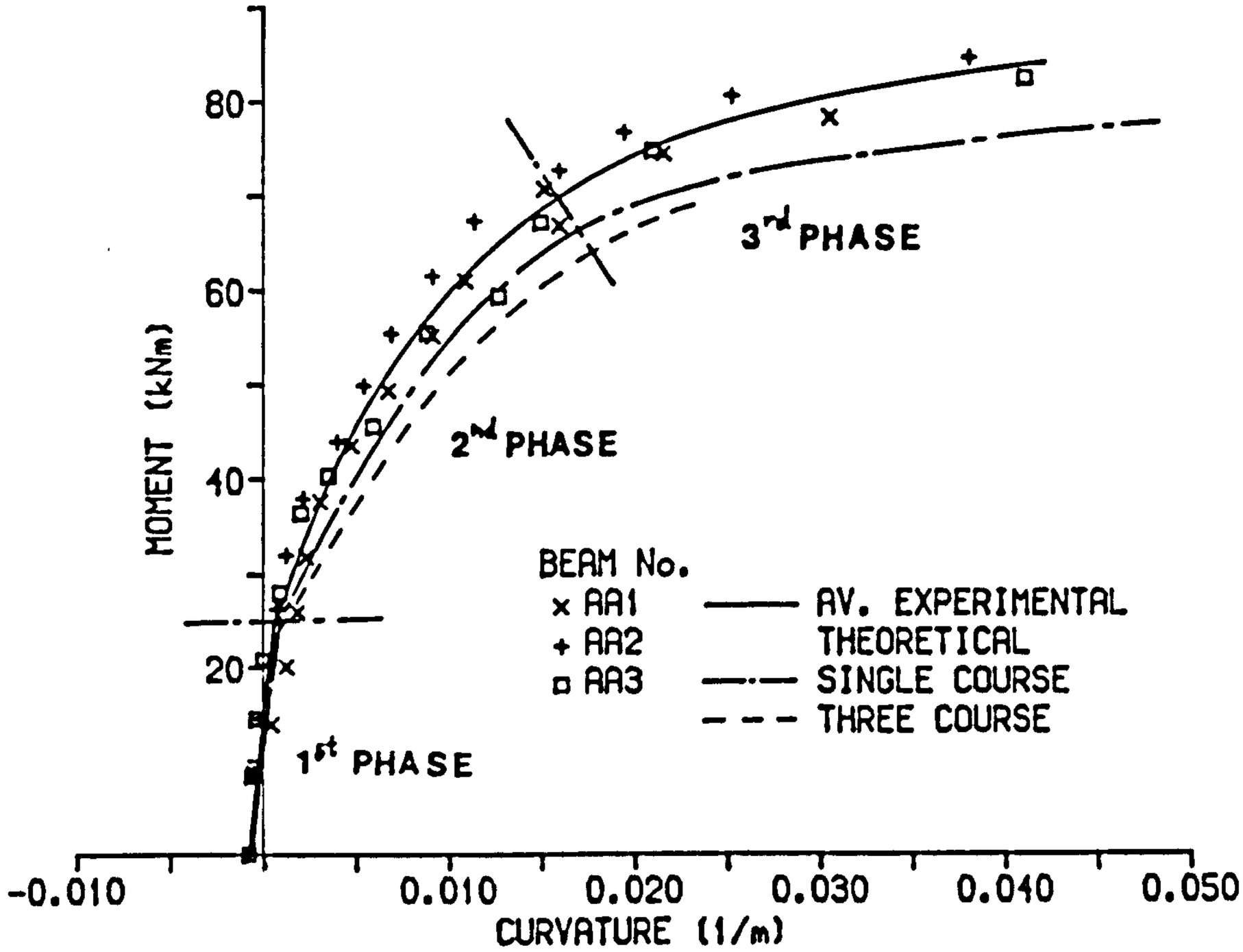

Figure 5.5.4

MOMENT-CURVATURE RELATIONSHIP ACROSS CRACKS FOR BEAM SERIES AB

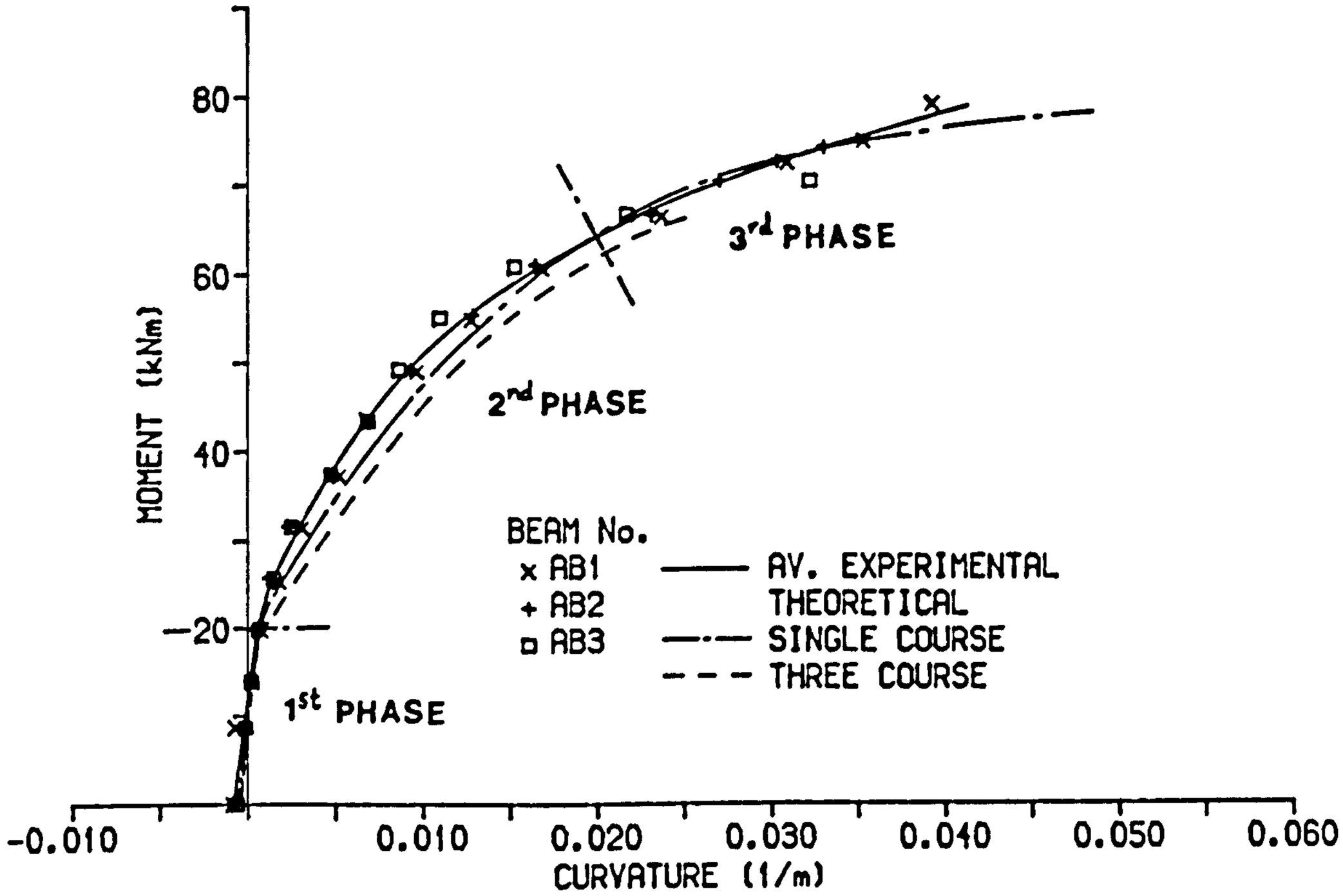

Figure 5.5.5

MOMENT-CURVATURE RELATIONSHIP ACROSS CRACKS FOR BEAM SERIES CP

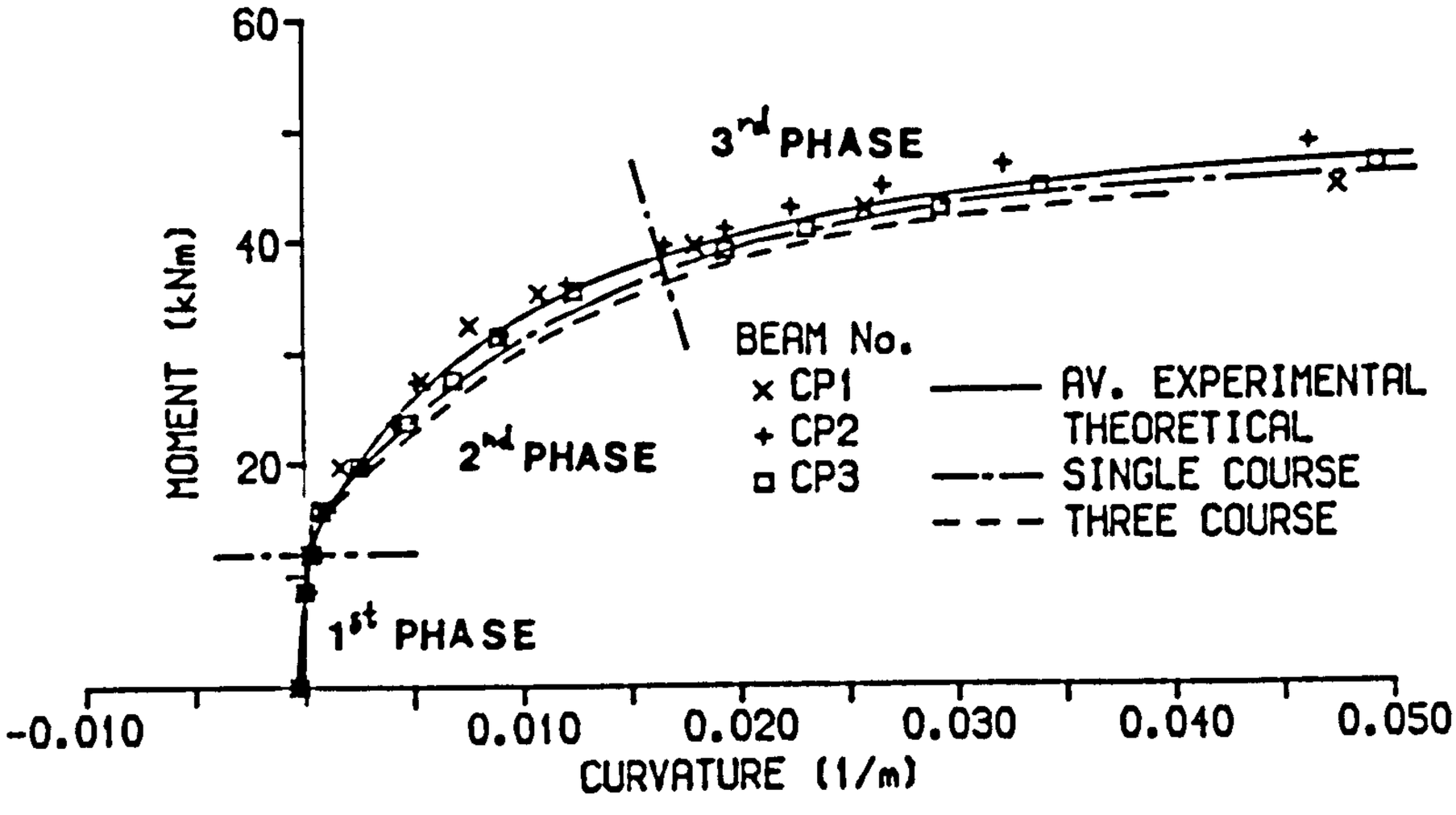

Figure 5.5.6

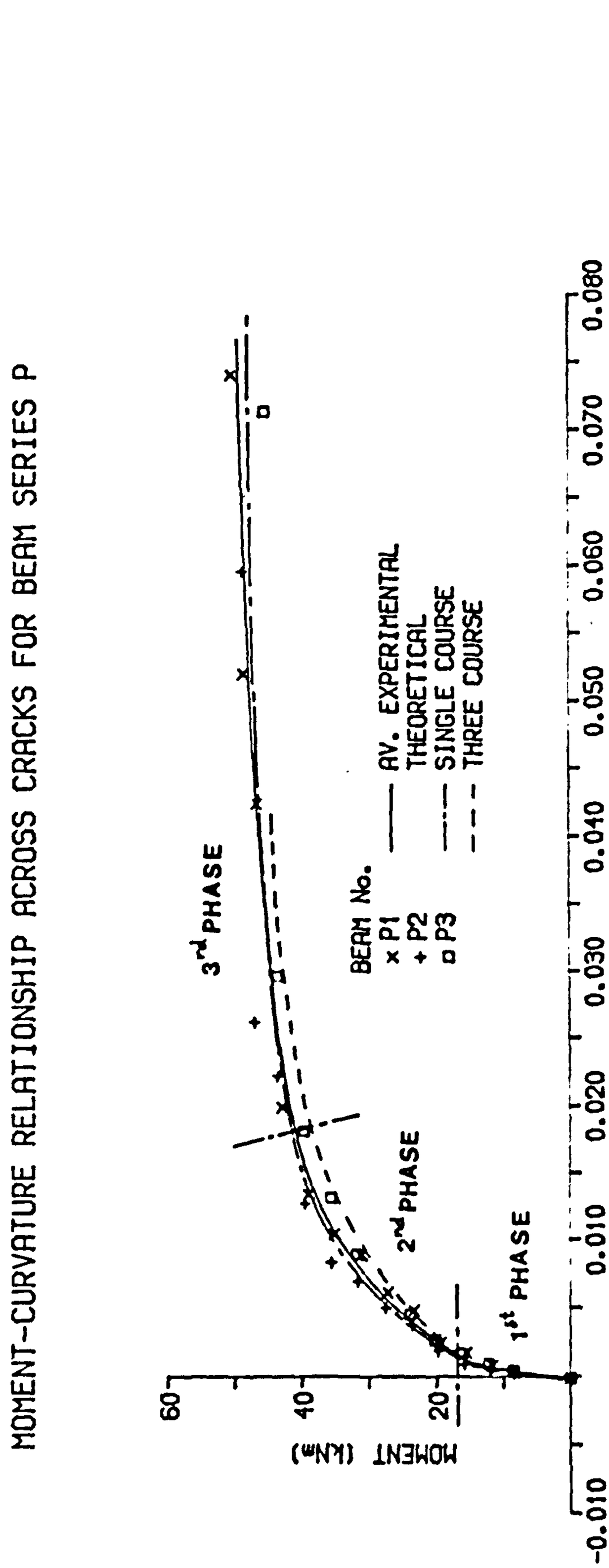
MOMENT-CURVATURE RELATIONSHIP ACROSS CRACKS FOR BEAM SERIES P
MOMENT (kNm)
60
40
20
0.030
0.040
0.050
0.060
0.070
0.080
0.010
0.020
-0.010
CURVATURE (1/m)
1st PHASE
2nd PHASE
3rd PHASE
BEAM No.
× P1
+ P2
□ P3
AV. EXPERIMENTAL
THEORETICAL
SINGLE COURSE
THREE COURSE

Figure 5.5.7

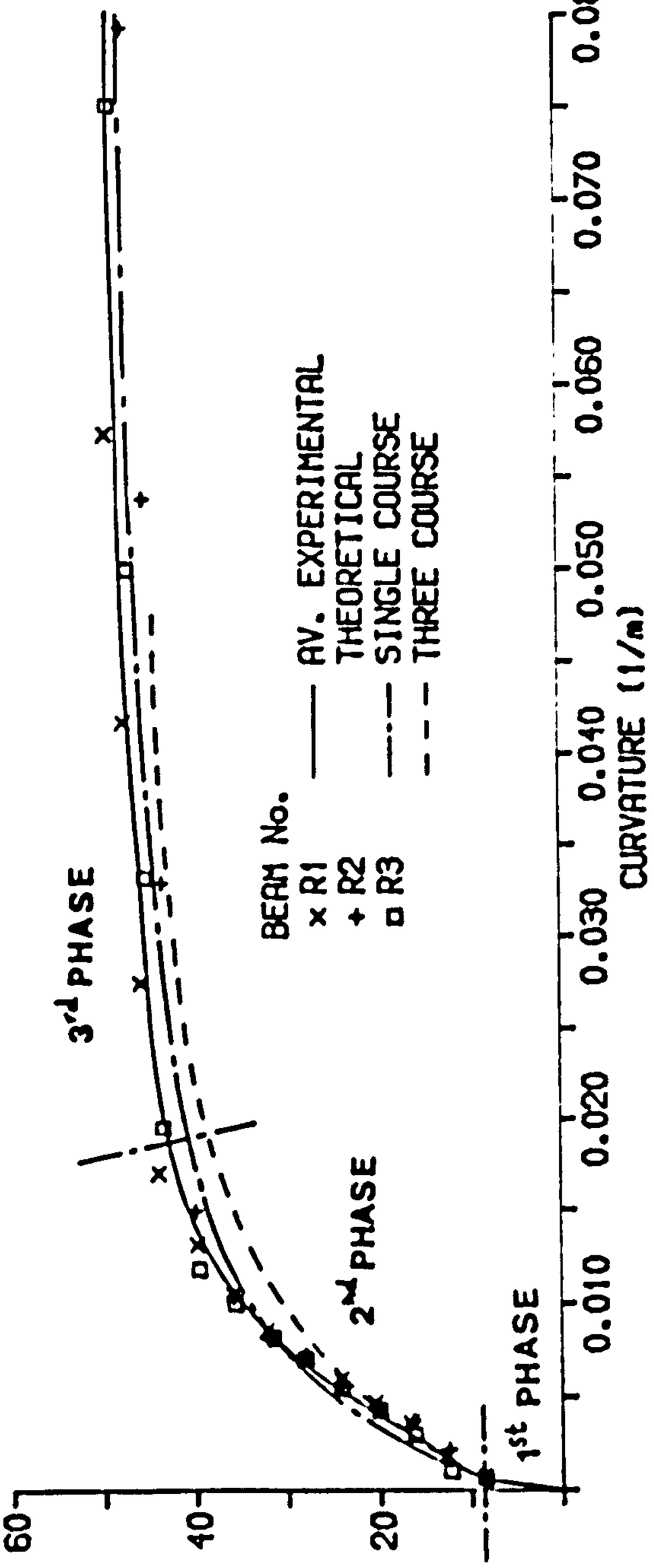
MOMENT-CURVATURE RELATIONSHIP ACROSS CRACKS
FOR BEAM SERIES R
MOMENT (kNm)
60
40
20
0.010
0.020
0.030
0.040
0.050
0.060
0.070
0.080
CURVATURE (1/m)
1st PHASE
2nd PHASE
3rd PHASE
BEAM No.
× R1
+ R2
□ R3
AV. EXPERIMENTAL
THEORETICAL
SINGLE COURSE
THREE COURSE

Figure 5.5.8

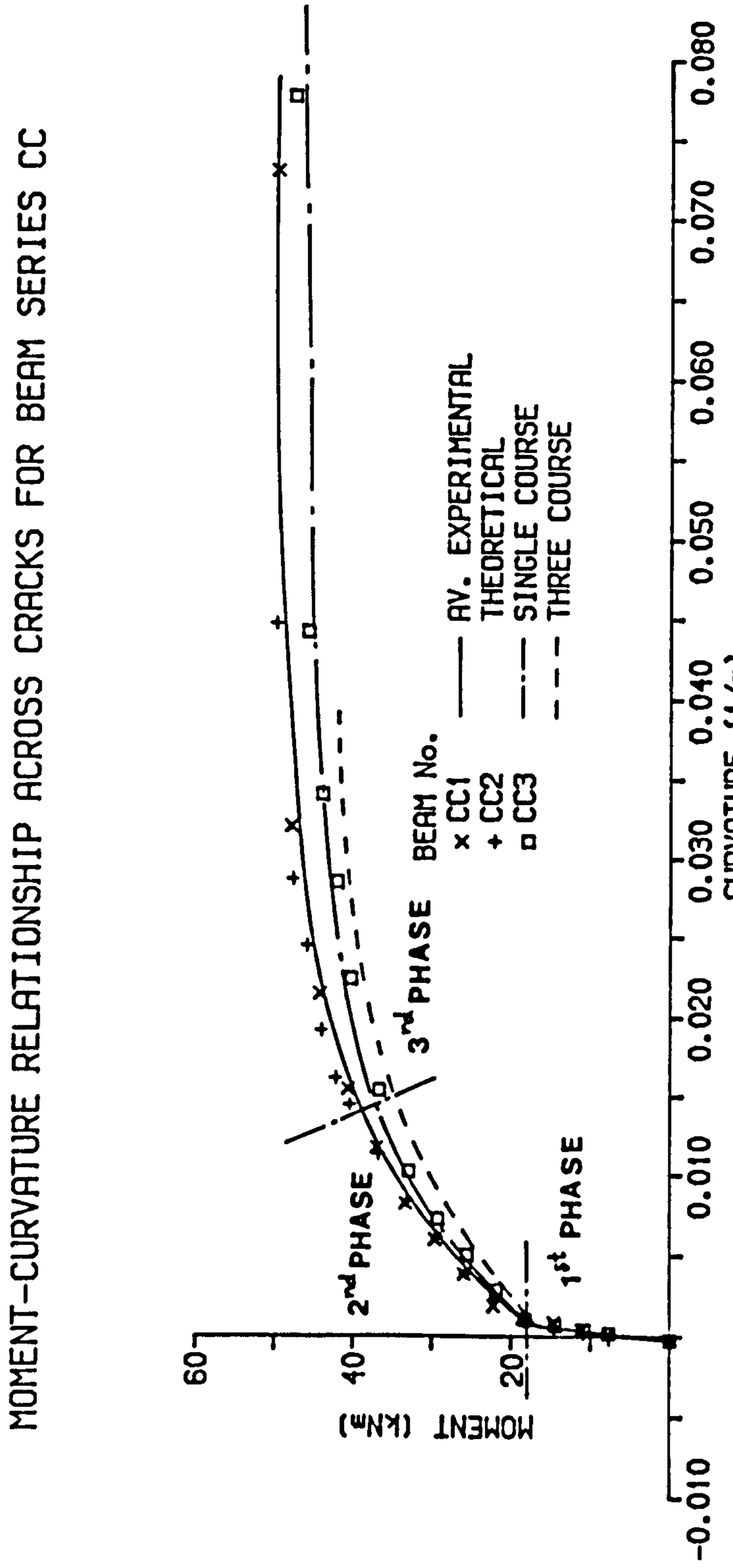
MOMENT-CURVATURE RELATIONSHIP ACROSS CRACKS FOR BEAM SERIES CC
BEAM No.
× CC1
+ CC2
□ CC3
AV. EXPERIMENTAL
THEORETICAL
SINGLE COURSE
THREE COURSE
1st PHASE
2nd PHASE
3rd PHASE
MOMENT (KNm)
CURVATURE (1/m)
0.030
0.040
0.050
0.060
0.070
0.080
0.020
0.010
60
40
20

Figure 5.5.9

MOMENT-CURVATURE RELATIONSHIP ACROSS CRACKS FOR BEAM SERIES CM

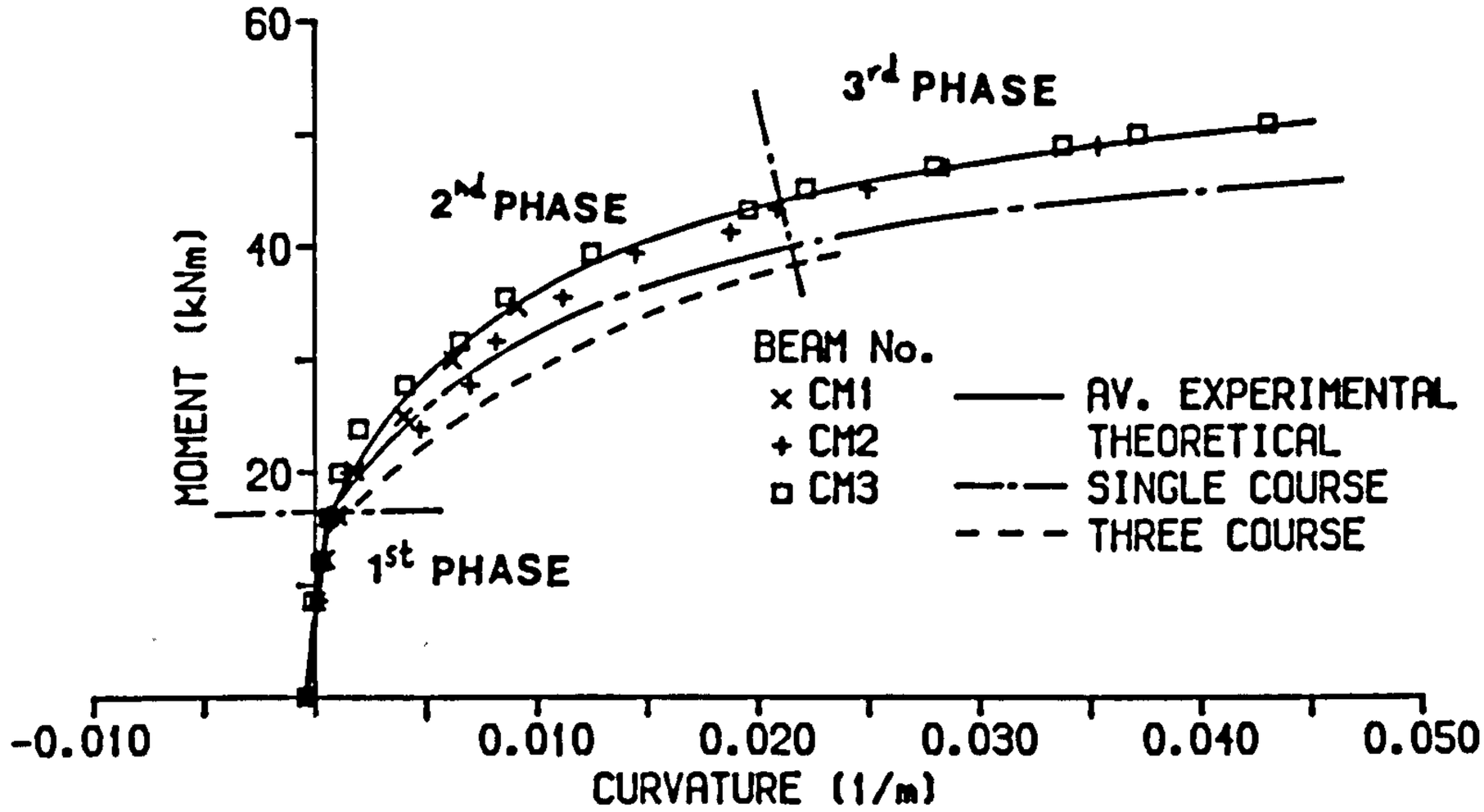

Figure 5.5.10

MOMENT-CURVATURE RELATIONSHIP ACROSS CRACKS FOR BEAM SERIES CL

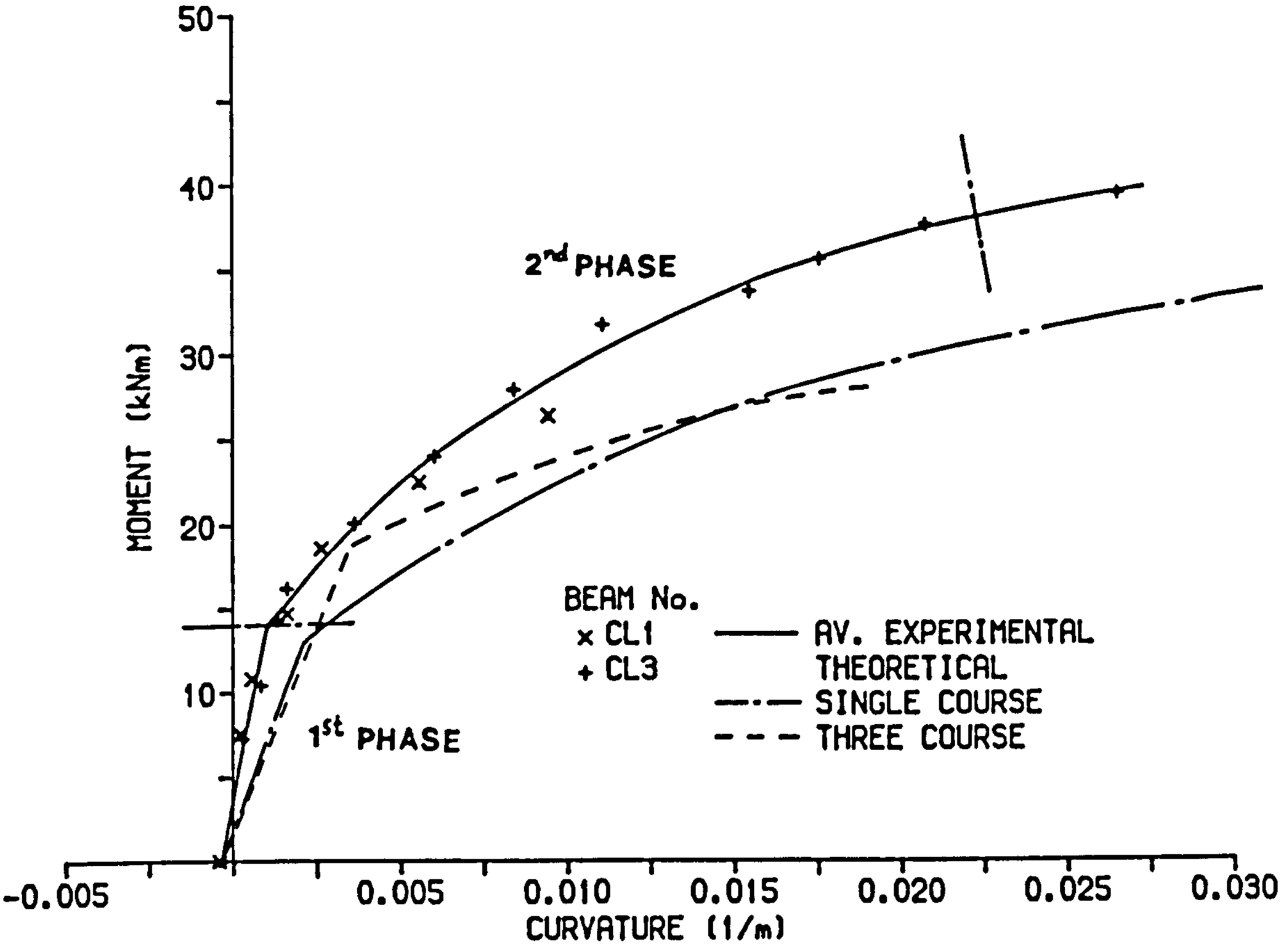

Figure 5.5.11

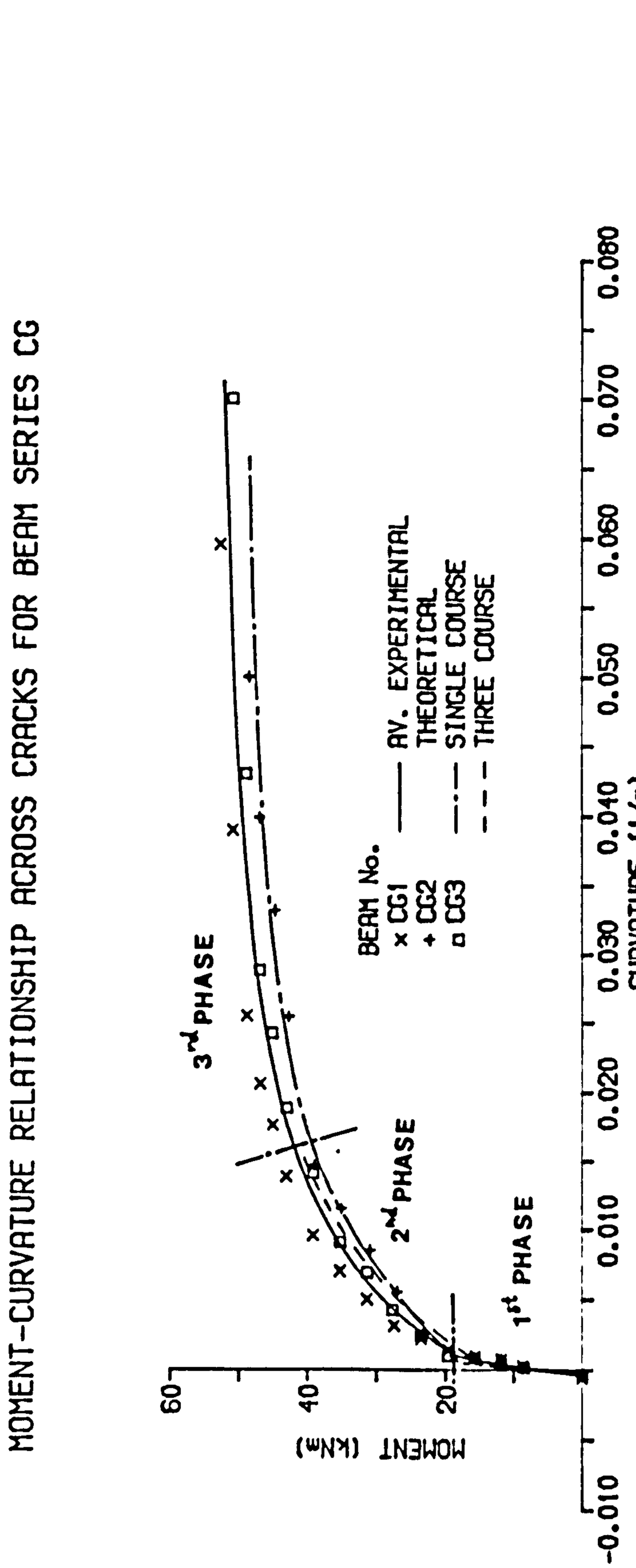
MOMENT-CURVATURE RELATIONSHIP ACROSS CRACKS FOR BEAM SERIES CG
MOMENT (kNm)
60
40
20
0.010
0.020
0.030
0.040
0.050
0.060
0.070
0.080
CURVATURE (1/m)
1st PHASE
2nd PHASE
3rd PHASE
BEAM No.
× CG1
+ CG2
□ CG3
—— AV. EXPERIMENTAL
THEORETICAL
—·— SINGLE COURSE
– – – THREE COURSE

Figure 5.5.12

measurements taken on the brickwork, the curvature at a section equal to the slope of the strain profile at each loading increment. Typical strain distributions are shown in figures 5.2.1 and 5.2.2. When the curvature was measured across more than one crack the average of all the results was presented.

All of the partially prestressed brickwork beams tested were under-reinforced, table 5.2.1, and consequently the moment-curvature relationships exhibit well defined three phase format normally associated with more conventional under-reinforced reinforced and prestressed concrete beams[60].

Prior to the application of the moment there was an initial negative curvature, camber, caused by the eccentrically applied prestressing force. The first phase of the relationship corresponds to a linear increase in curvature with moment from zero up to cracking, during which the whole section was resisting the applied moment.

Once cracking occurred the stiffness of the section was significantly reduced, causing large increases in the internal stresses and strains combined with a reduction in the neutral axis depth causing the curvature to increase more rapidly. Both the tensioned steel and non-tensioned reinforcement were behaving elastically at this stage.

The third phase corresponded to yielding of the tensile reinforcement and hence 'plastic' behaviour. After the tensile failure a flattening of the moment-curvature curve occurred,

corresponding to large increases in curvature with little increase in moment. This phase was absent for those beams failing in shear since a tensile failure of the steel did not occur. Transition to the third phase in the partially prestressed brickwork beams was less distinct than for previously tested fully prestressed brickwork[9] or concrete[60]. This was due to the relatively large distance between the two layers of tensile reinforcement, tensioned and non-tensioned, resulting in yielding of the reinforcement in two stages. Firstly the non-tensioned reinforcement close to the soffit reached its proof stress followed by the tensioned at an increased moment. A change of slope in the moment-curvature curve was coincident with each type of reinforcement yielding and the curve eventually became parallel to the x-axis once all of the tensile steel had yielded, figures 5.5.1 - 5.5.12.

In figures 5.5.1 - 5.5.9 the moment-curvature relationships for the beams built from high strength bricks and grade I mortar are presented. With the exception of beams AB1-AB3, figure 5.5.5, where eventual failure was due to secondary shear, the average experimental results illustrate clearly the full development of all three phases of the moment-curvature relationships. From figure 5.5.5 the moment-curvature curve for beam series AB, it was apparent that the beam had entered the third phase of the moment-curvature relationship since, yielding of the non-tensioned reinforcement had occurred. However, the flattening of the curve was not fully defined up to the full flexural capacity due to the secondary shear failure of the beams.

The average moment-curvature relationships for the high

strength brick beams built with grade II mortar, beams CG1-CG3, figure 5.5.12, and the medium strength brick beams, figure 5.5.10, show characteristics very similar to those of the equivalent high strength brick beams C1-C8 (grade I mortar), figure 5.5.3. Full development of the moment-curvature relationships was observed with flattening of the curve leading up to ultimate moment. Of the low strength brick beams tested only beam CL3 failed in flexure. Although the third phase of the moment-curvature curve was present, since the non-tensioned steel yielded, the flattening of the curve was not as well defined as in the tests on the equivalent high and medium strength brick beams as a compressive failure of the brickwork occurred prior to yielding of the tendon, figure 5.5.11.

A study of the effect of the cover to the non-tensioned steel on the load/deflection behaviour was not possible since the span of the beam series C and beam series CC were different, table 5.2.1, in order to maintain the a/d ratio constant. Therefore for the purposes of determining the effect of the cover upon the deformation characteristics of partially prestressed brickwork beams the experimental moment-curvature relationships were considered. The moment-curvature relationships for beam series C and CC are shown in figures 5.5.3 and 5.5.9 respectively. The average experimental curves are compared in figure 5.5.13.

It can be seen from figure 5.5.13 that an increase in the cover caused an increase in the curvature of up to 10%. The behaviour of the two beam series prior to cracking was similar since the stiffness of the uncracked sections were not significantly altered. After cracking the increase in curvature for beams CC1-CC3

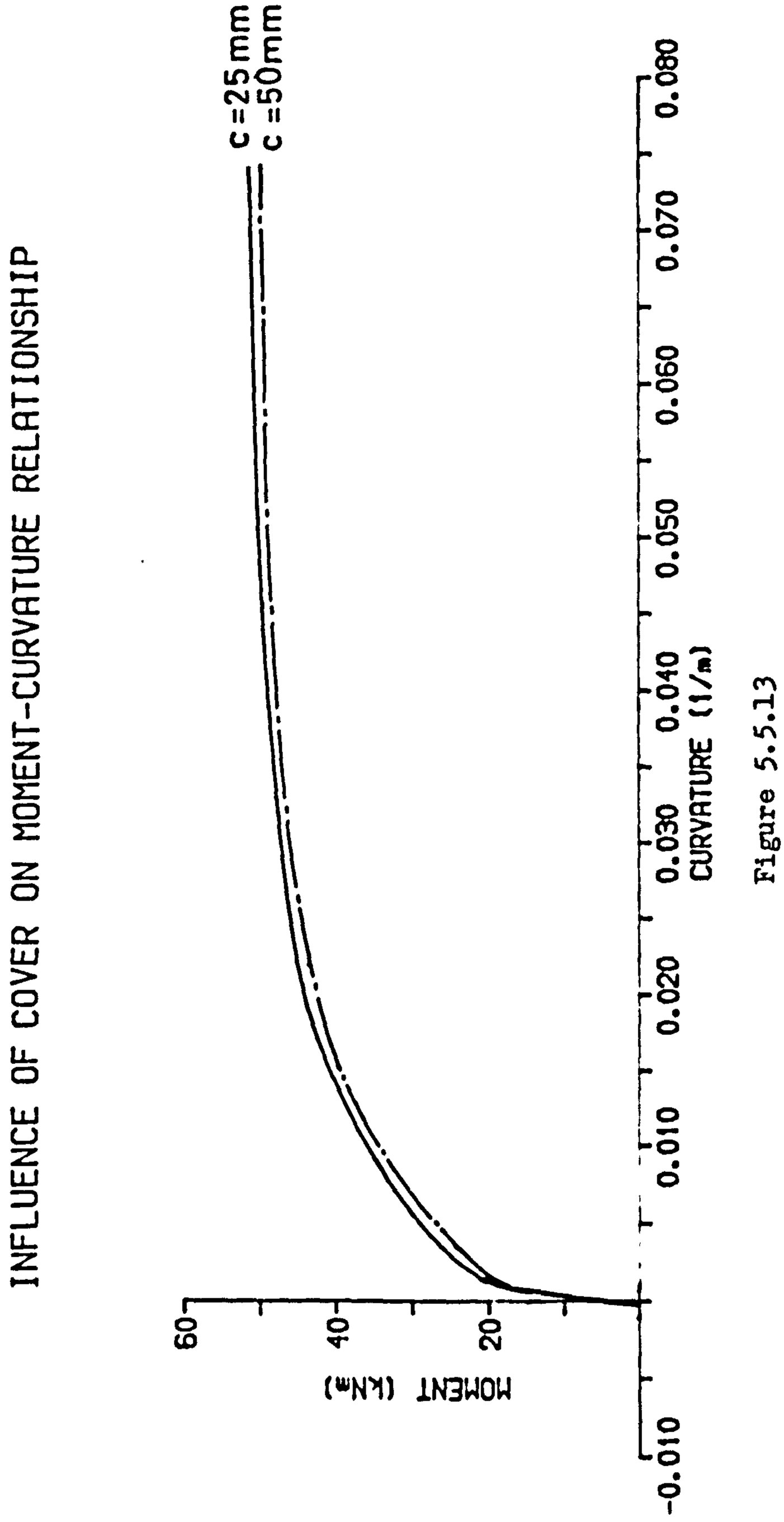
INFLUENCE OF COVER ON MOMENT-CURVATURE RELATIONSHIP
c=25mm
c=50mm
MOMENT (kNm)
60
40
20
0
0.010
0.020
0.030
0.040
0.050
0.060
0.070
0.080
CURVATURE (1/m)

Figure 5.5.13

was due to the reduction in the stiffness of the cracked section resulting from the decrease in the effective depth to the non-tensioned steel.

A comparison of the experimental results show the theoretical estimations, with the exception of the low strength brick beam series CL (figure 5.5.11), to exhibit close agreement up to between 80-90% of the average experimental ultimate moment. Beyond this point the theory over-estimated the moment-curvature relationship due to an under-estimation of the ultimate moment (section 5.4), figures 5.5.1 - 5.5.12. The curvatures predicted by the three and single course prisms were initially in close agreement. The three course prism properties tended to predict slightly larger curvatures than the curvature given by the single course prism brickwork properties. With further increase in the moment the predicted moment-curvature relationship was cut short of the experimental result due to the under-estimated ultimate moment. Predictions of the curvature using the single course prism brickwork properties generally showed excellent agreement with the experimental results.

Initially the curvature predicted by the three course prisms indicated good agreement with the average experimental results. During the early stages of behaviour the neutral axis depth, from the top fibre, was compartively large, figures 5.2.3d - 5.2.14d, and therefore at this stage the three course prisms were more likely to accurately represent the compression zone behaviour of the beams, and hence the good correlation between the average experimental and theoretical curvature. Since the curvature is a representation of

the variation in the strain and neutral axis depth in the beam section it is therefore relevant to briefly consider the comparison between the experimental and theoretical results for the variation of strain and neutral axis depth with moment illustrated figures in 5.2.3 - 5.2.14.

The theoretically predicted results were obtained by using the direct method outlined in chapter 4. The compressive properties for brickwork given by both the single and three course prisms were used for the analysis. Generally the predicted behaviour (figures 5.2.3 - 5.2.14) using the single course prism properties was in good agreement with the experimental results up to and including the ultimate moment. The theory tended to slightly to over-estimate the strains in the steel and brickwork and under-estimate the neutral axis depth. It was possible to conclude from the comparison that the single course prism brickwork properties provide an accurate representation of the compressive properties of the brickwork beams.

Initially the three course prism proeprties provided good indications of the beams behaviour, figures 5.2.3 - 5.2.14. However, approaching failure the average behaviour was no longer accurately modelled by the three course prisms because of the significant under-estimation of the ultimate moment. During the early stages of loading, whilst the neutral axis depth was nearest to the soffit of the beam, the three course prism brickwork properties gave a good approximation of the compressive properties and so there was good agreement between the experimental results and the theory. Once the neutral axis depth decreased sufficiently, such that the compression zone was confined to less than the top three courses of brickwork, it

was likely that the three course prism brickwork properties would no longer represent the compression zone and therefore the correlation between theory and experiment was poor.

With increasing bending moment the neutral axis depth progressively decreased, figures 5.2.3d - 5.3.14d. In the high strength brick beams developing flexural failure the neutral axis eventually was located within the top two courses of brickwork and with further moment eventually in the top course of brickwork. Once the neutral axis depth had decreased to such an extent it was unlikely that the three course prism properties would continue to accurately represent the compressive zone of the beam. The values for compressive stress and ultimate compressive strain for brickwork given by the three course prisms was shown to be consistently less than the corresponding values from the single course prisms, chapter 3. Therefore applying these values to the theoretical analysis the three course prisms provided higher curvatures than the single course prisms due to the reduction in stiffness as a result of the reduced compressive strength. Once the compression zone was restricted to within the top three courses of brickwork in the beam it was clear that the properties of the three course prisms no longer represented the compressive behaviour of the beams and hence the reduced compressive strength of the three course prism led to the significant over-estimation of curvature at failure.

The single course prisms throughout the investigation provided the best estimate for the moment-curvature relationship, with the exception of the low strength brick beams the predicted values were generally to within 10% of the average experimental

curves. The single course prisms clearly provide the most accurate representation of the compression zone in the partially prestressed brickwork beams, this confirms previous observations, section 5.2, and earlier studies[9].

5.6 LOAD/DEFLECTION RELATIONSHIPS

The experimental and predicted load/deflection curves for the mid-span are presented in figures 5.6.1 - 5.6.12. The load/deflection curves exhibit the same three phase characteristics as the moment-curvature curves. The curves were initially linear up to cracking, followed by the second phase of post-cracking with the steel elastic followed by post-yield flattening of the curve and excessive deflection with little increase in load. The load in figures 5.6.1 - 5.6.12 corrseponds to applied load only since it was not possible to determine the deflection due to self weight of the beam and so the load/deflection curves commence at the origin and do not show the initial negative camber due to the prestressing force.

Until now the moment-curvature and load/deflection have been considered only for increasing moment or load from zero up to failure. However, three beams were tested in which the load was removed after each increment to study the recovery of the beam. The results for beams B3, C4 and AB3 are presented in figures 5.6.13, 5.6.14 and 5.6.15 respectively.

The unloading-reloading cycle clearly illustrates the hysterisis loop normally associated with reinforced and prestressed

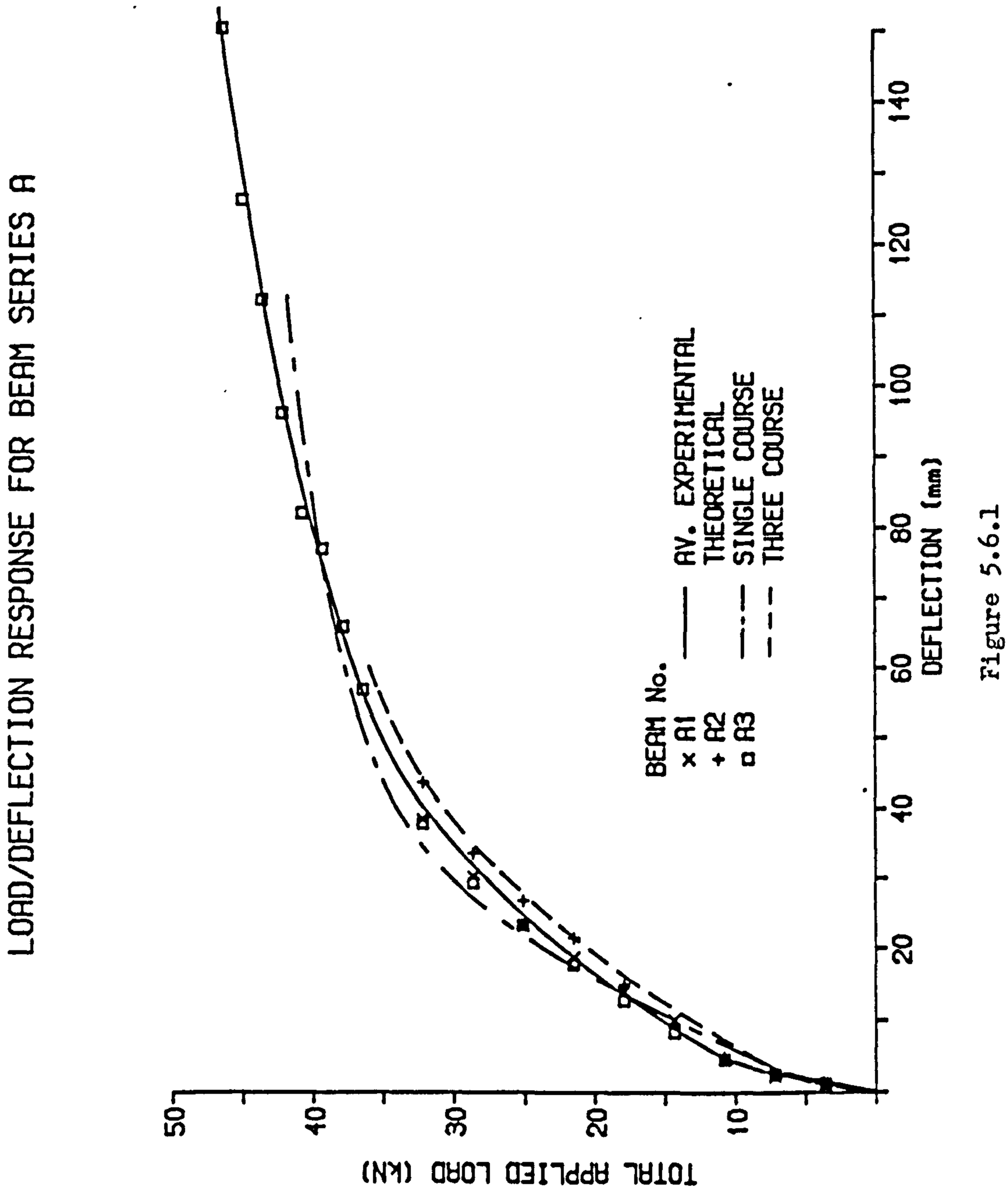
LOAD/DEFLECTION RESPONSE FOR BEAM SERIES A
TOTAL APPLIED LOAD (kN)
DEFLECTION (mm)
0
20
40
60
80
100
120
140
10
20
30
40
50
BEAM No.
× A1
+ A2
□ A3
— AV. EXPERIMENTAL
— THEORETICAL
— SINGLE COURSE
— THREE COURSE

Figure 5.6.1

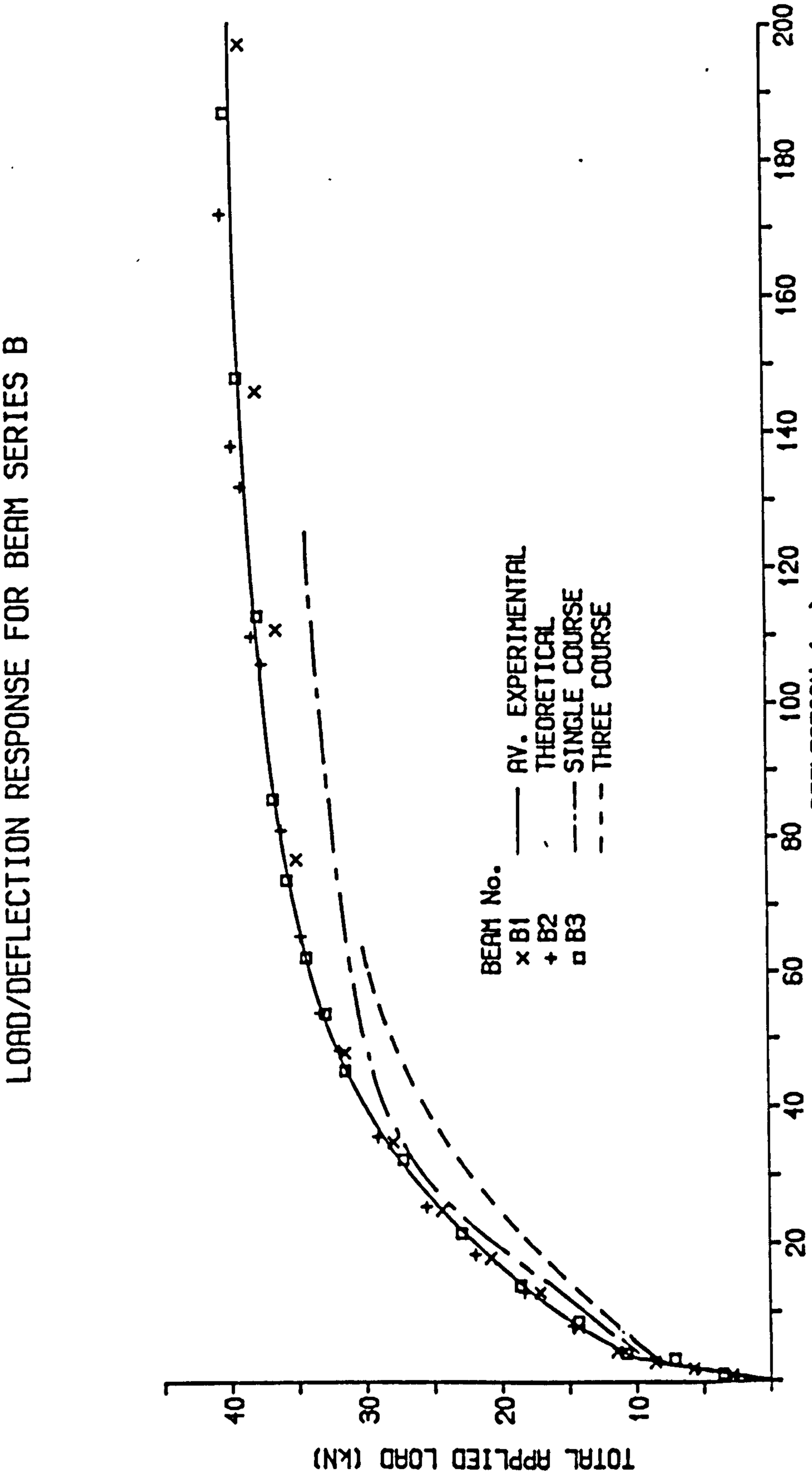
LOAD/DEFLECTION RESPONSE FOR BEAM SERIES B
TOTAL APPLIED LOAD (kN)
DEFLECTION (mm)
BEAM No.
× B1
+ B2
□ B3
— AV. EXPERIMENTAL
THEORETICAL
—·— SINGLE COURSE
– – THREE COURSE
10
20
30
40
20
40
60
80
100
120
140
160
180
200

Figure 5.6.2

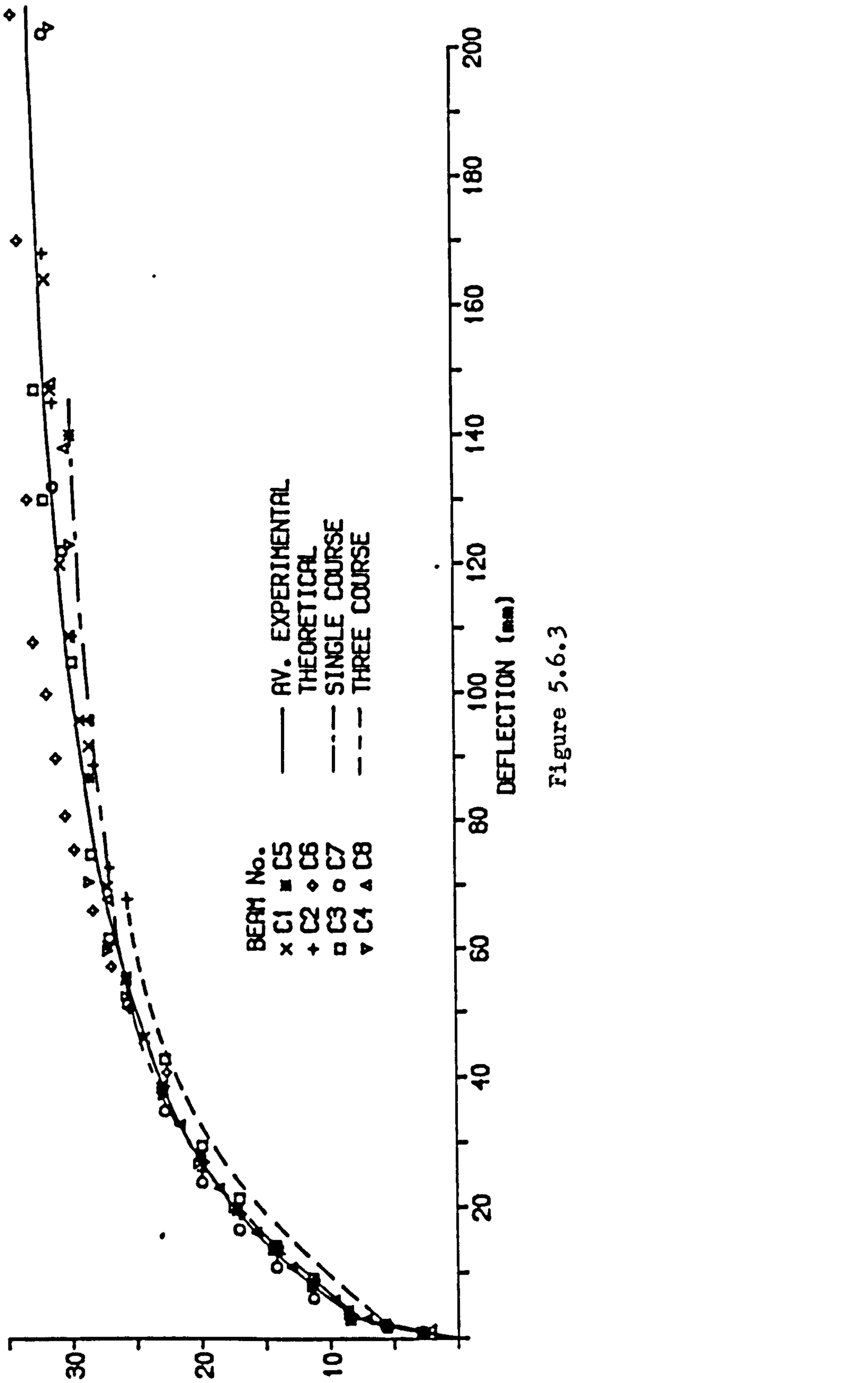
LOAD/DEFLECTION RESPONSE FOR BEAM SERIES C
TOTAL APPLIED LOAD (kN)
DEFLECTION (mm)
BEAM No.
C1 C5
C2 C6
C3 C7
C4 C8
AV. EXPERIMENTAL
THEORETICAL
SINGLE COURSE
THREE COURSE

Figure 5.6.3

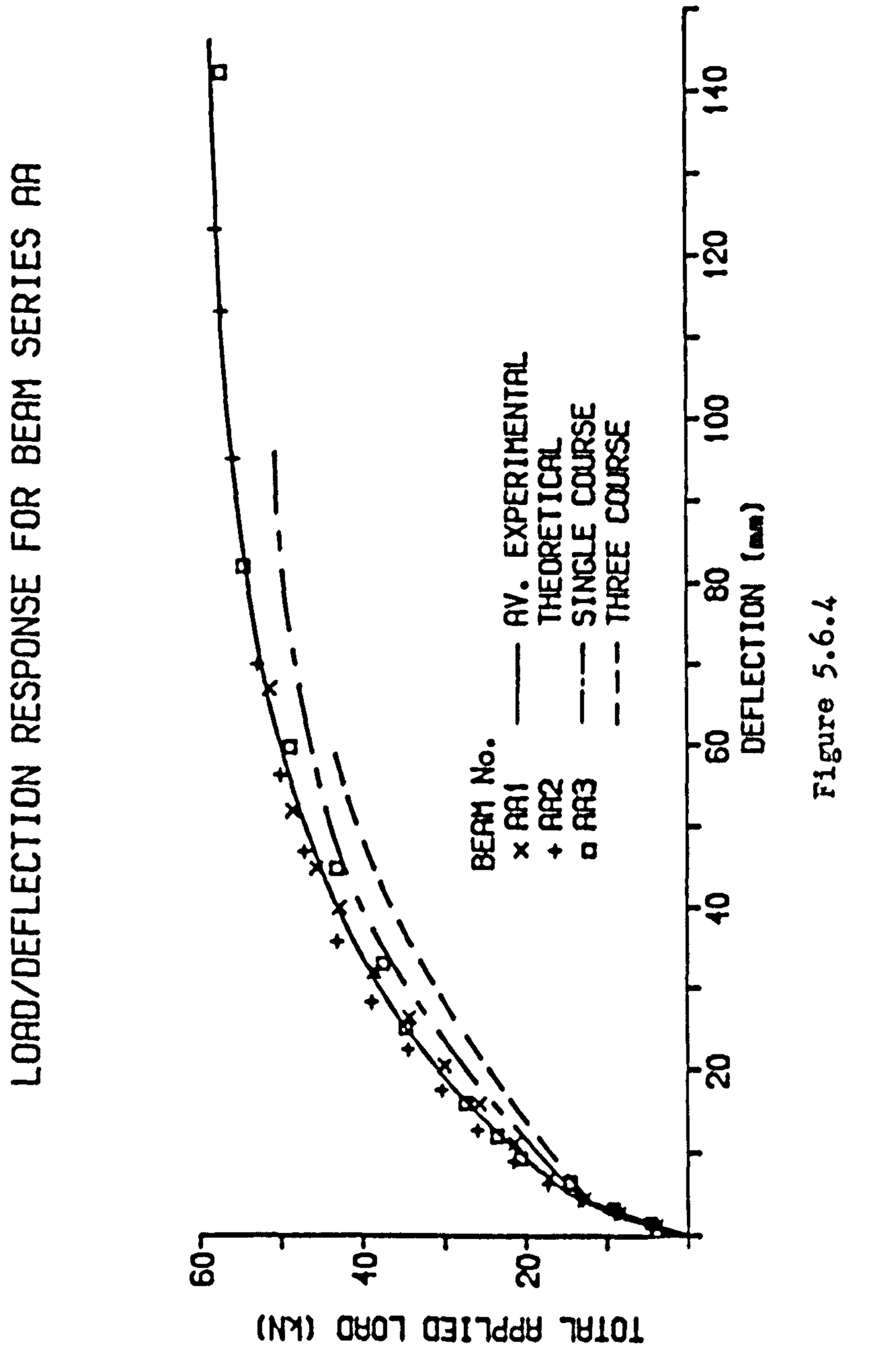
LOAD/DEFLECTION RESPONSE FOR BEAM SERIES AA
TOTAL APPLIED LOAD (kN)
DEFLECTION (mm)
BEAM No.
× AA1
+ AA2
□ AA3
—— AV. EXPERIMENTAL
—— THEORETICAL
—·— SINGLE COURSE
— — THREE COURSE
0
20
40
60
80
100
120
140

Figure 5.6.4

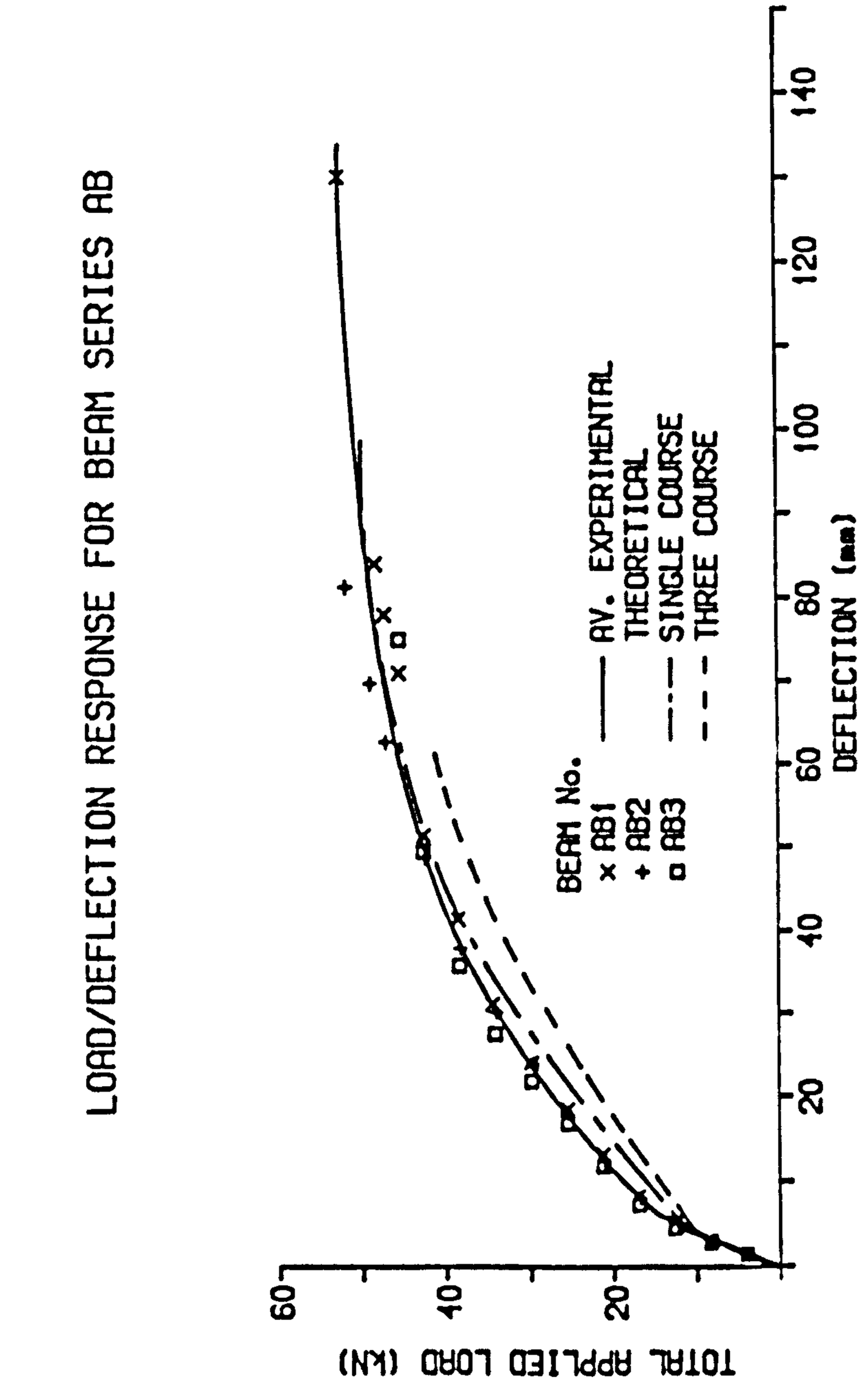
LOAD/DEFLECTION RESPONSE FOR BEAM SERIES AB
TOTAL APPLIED LOAD (kN)
DEFLECTION (mm)
0
20
40
60
80
100
120
140
BEAM No.
× AB1
+ AB2
□ AB3
— AV. EXPERIMENTAL
THEORETICAL
— SINGLE COURSE
— THREE COURSE

Figure 5.6.5

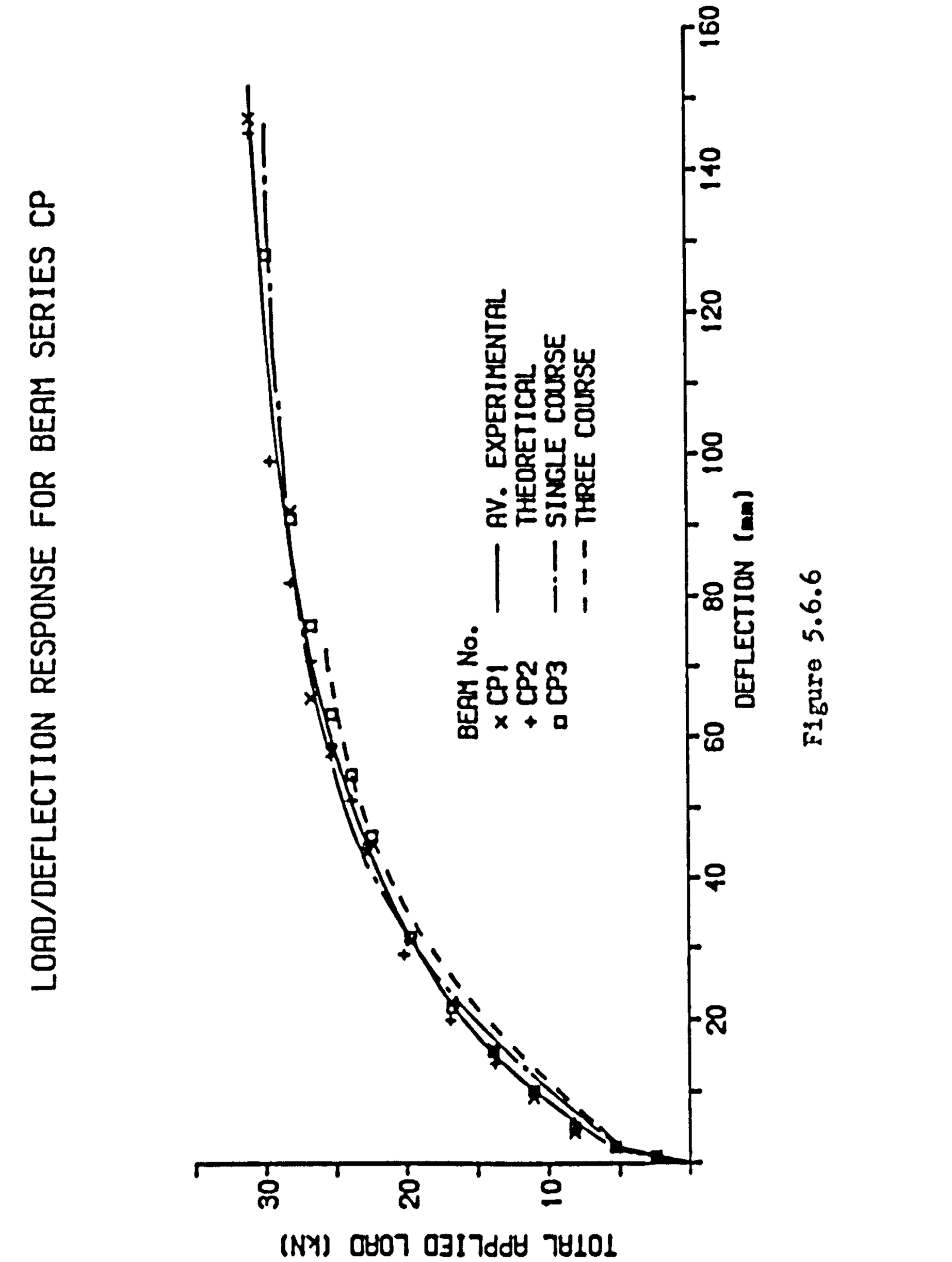
LOAD/DEFLECTION RESPONSE FOR BEAM SERIES CP
TOTAL APPLIED LOAD (kN)
DEFLECTION (mm)
BEAM No.
× CP1
✦ CP2
□ CP3
—— AV. EXPERIMENTAL
THEORETICAL
—·— SINGLE COURSE
- - - THREE COURSE
0
10
20
30
40
60
80
100
120
140
160

Figure 5.6.6

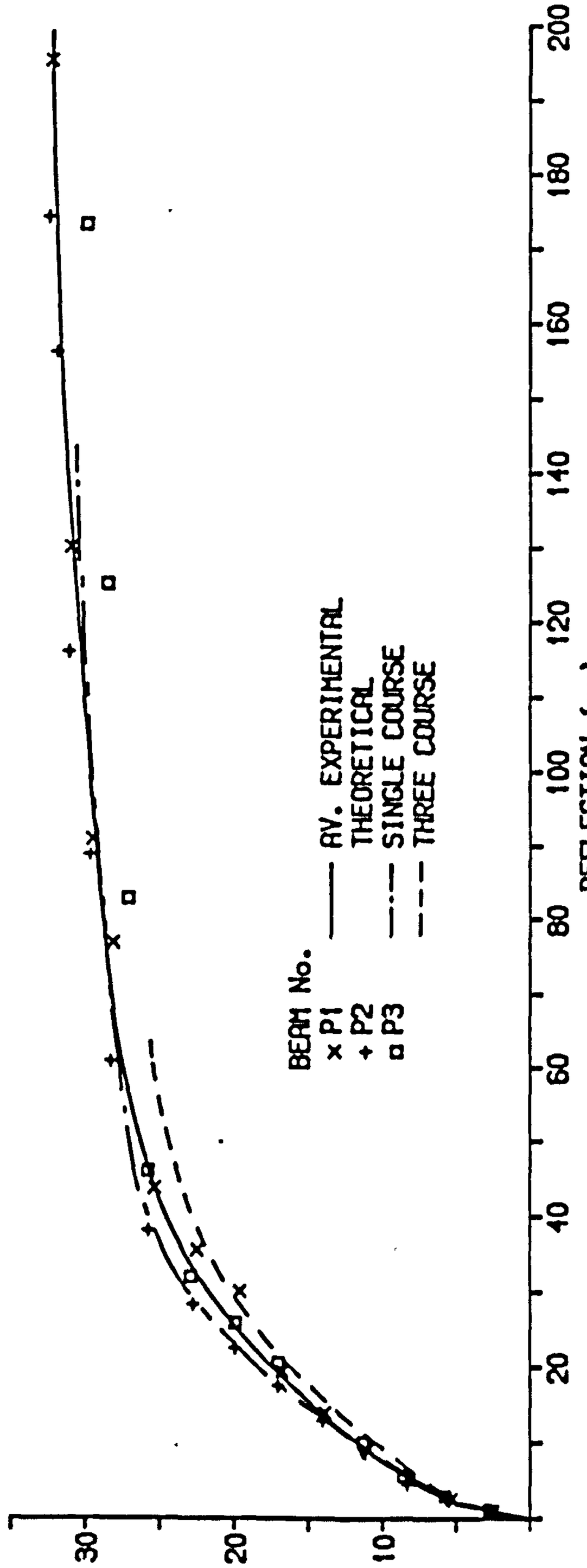
LOAD/DEFLECTION RESPONSE FOR BEAM SERIES P
TOTAL APPLIED LOAD (kN)
DEFLECTION (mm)
BEAM No.
× P1
+ P2
□ P3
— AV. EXPERIMENTAL
— THEORETICAL
-·- SINGLE COURSE
-·- THREE COURSE
10
20
30
40
60
80
100
120
140
160
180
200

Figure 5.6.7

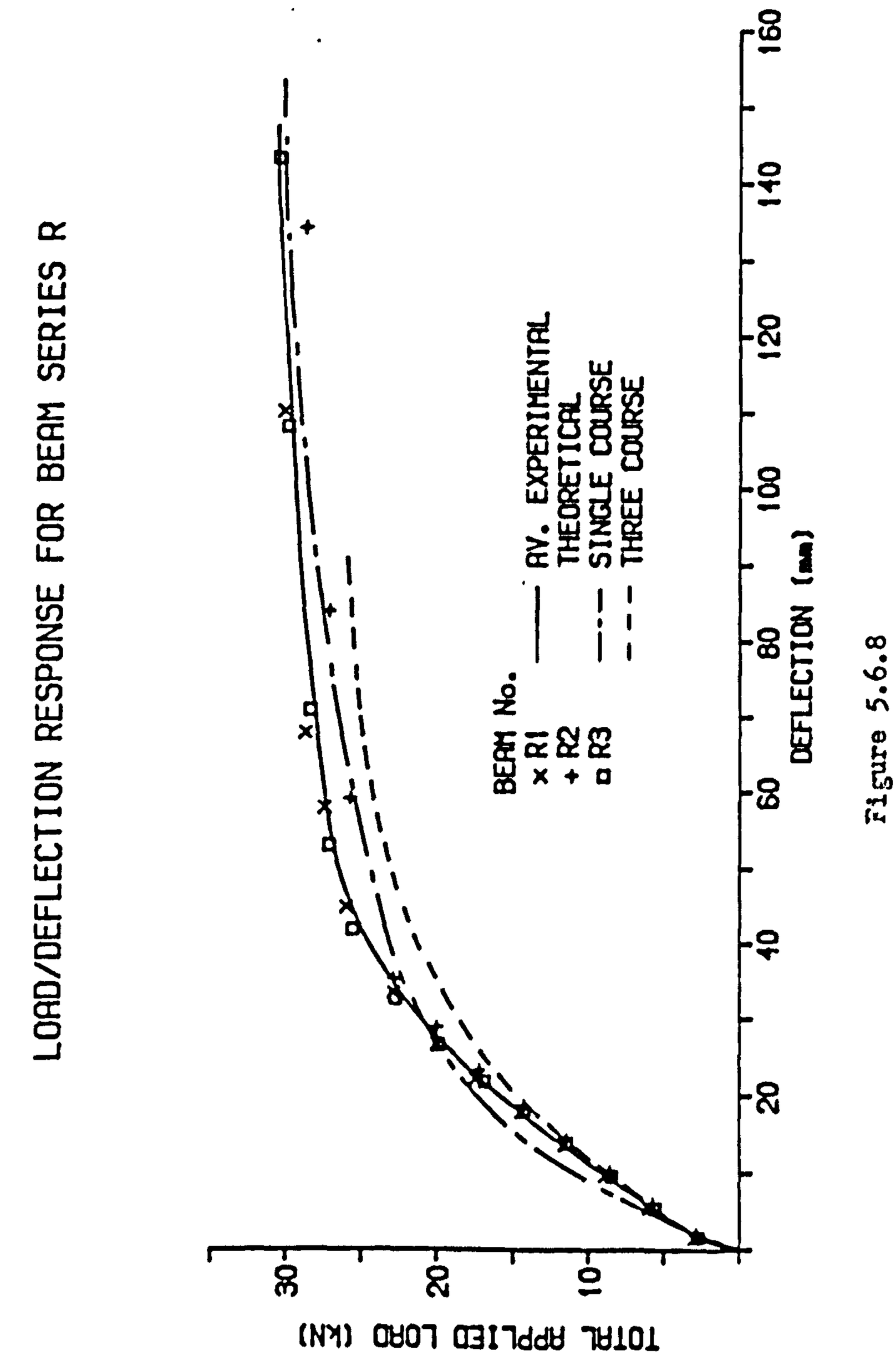
LOAD/DEFLECTION RESPONSE FOR BEAM SERIES R
TOTAL APPLIED LOAD (kN)
DEFLECTION (mm)
0
10
20
30
40
60
80
100
120
140
160
BEAM No.
R1
R2
R3
AV. EXPERIMENTAL
THEORETICAL
SINGLE COURSE
THREE COURSE

Figure 5.6.8

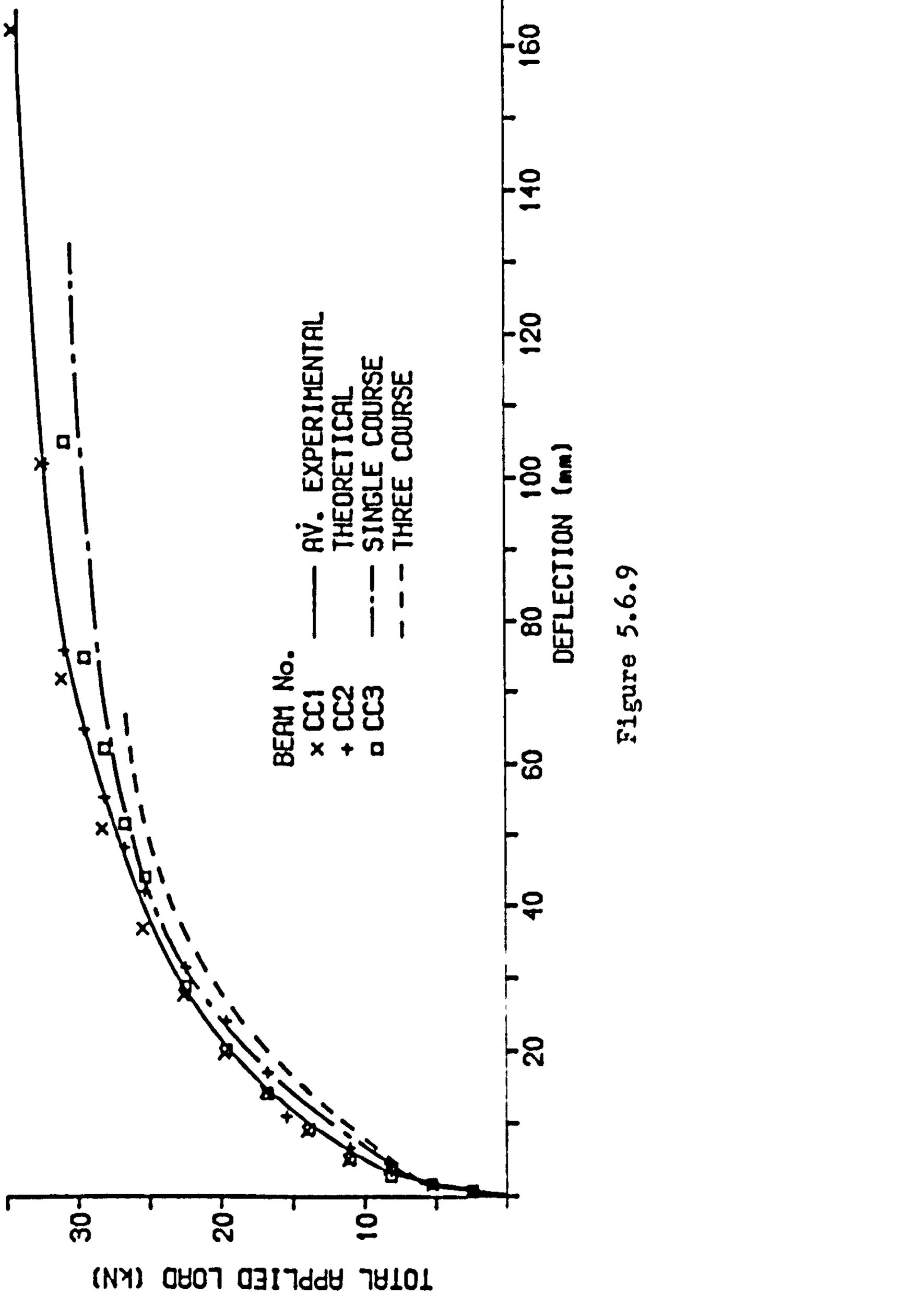
LOAD/DEFLECTION RESPONSE FOR BEAM SERIES CC
TOTAL APPLIED LOAD (kN)
DEFLECTION (mm)
BEAM No.
x CC1
+ CC2
□ CC3
— AV. EXPERIMENTAL
THEORETICAL
— SINGLE COURSE
- - THREE COURSE

Figure 5.6.9

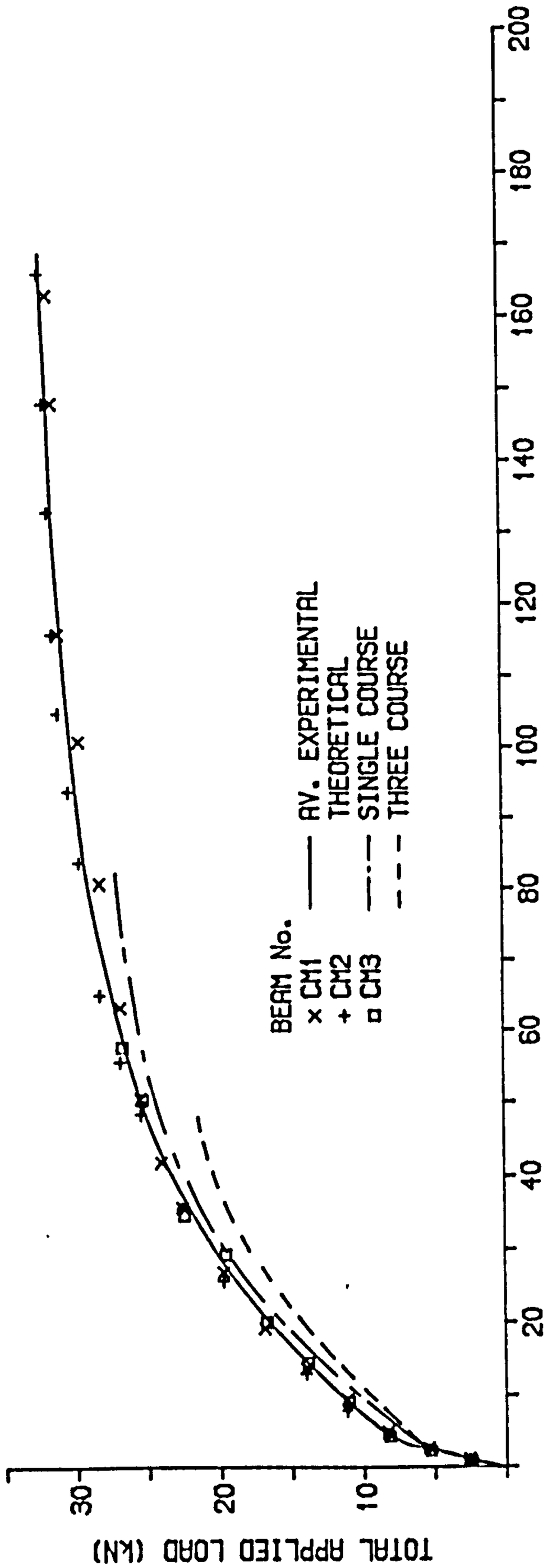
LOAD/DEFLECTION RESPONSE FOR BEAM SERIES CM
BEAM No.
× CM1
+ CM2
□ CM3
—— AV. EXPERIMENTAL
—— THEORETICAL
—·— SINGLE COURSE
– – – THREE COURSE
TOTAL APPLIED LOAD (kN)
DEFLECTION (mm)
0
10
20
30
40
60
80
100
120
140
160
180
200

Figure 5.6.10

LOAD/DEFLECTION RESPONSE FOR BEAM SERIES CL

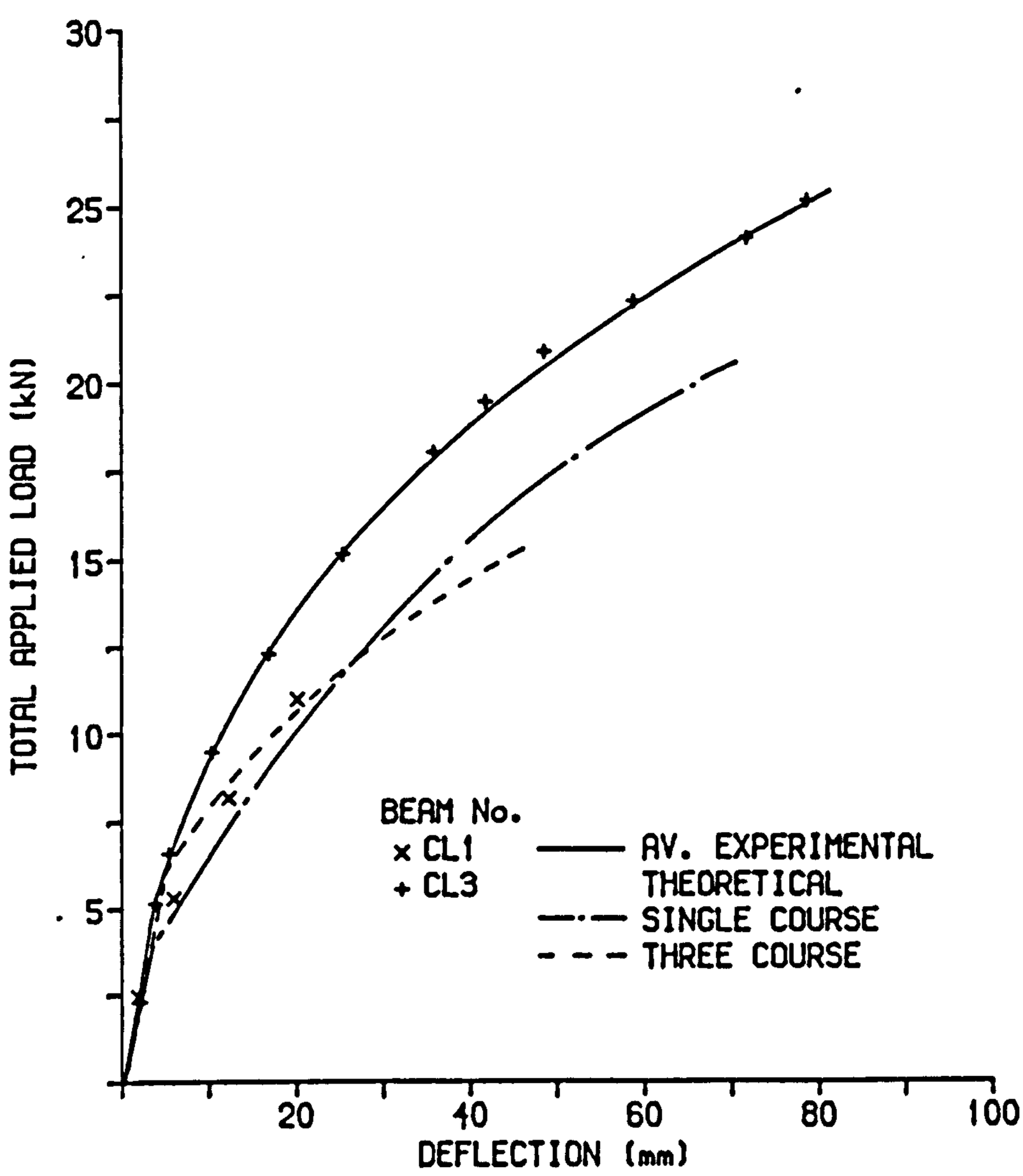

Figure 5.6.11

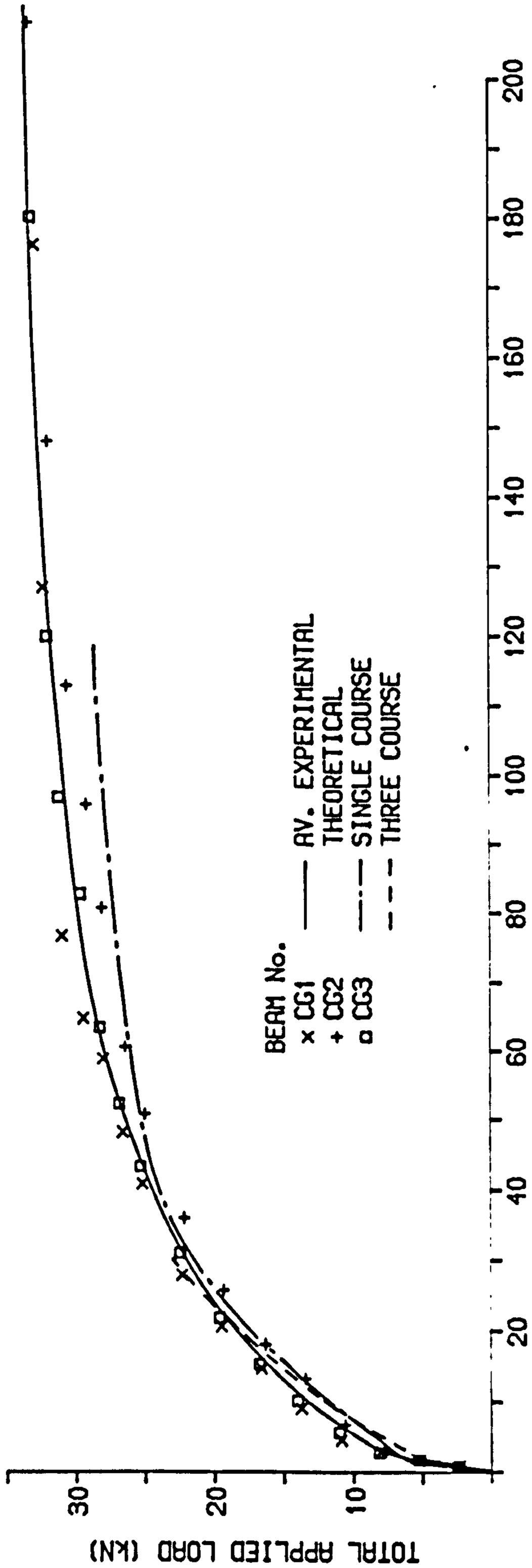
LOAD/DEFLECTION RESPONSE FOR BEAM SERIES CG
TOTAL APPLIED LOAD (kN)
DEFLECTION (mm)
BEAM No.
× CG1
+ CG2
□ CG3
— AV. EXPERIMENTAL
THEORETICAL
-·-·- SINGLE COURSE
- - - THREE COURSE
10
20
30
40
60
80
100
120
140
160
180
200

Figure 5.6.12

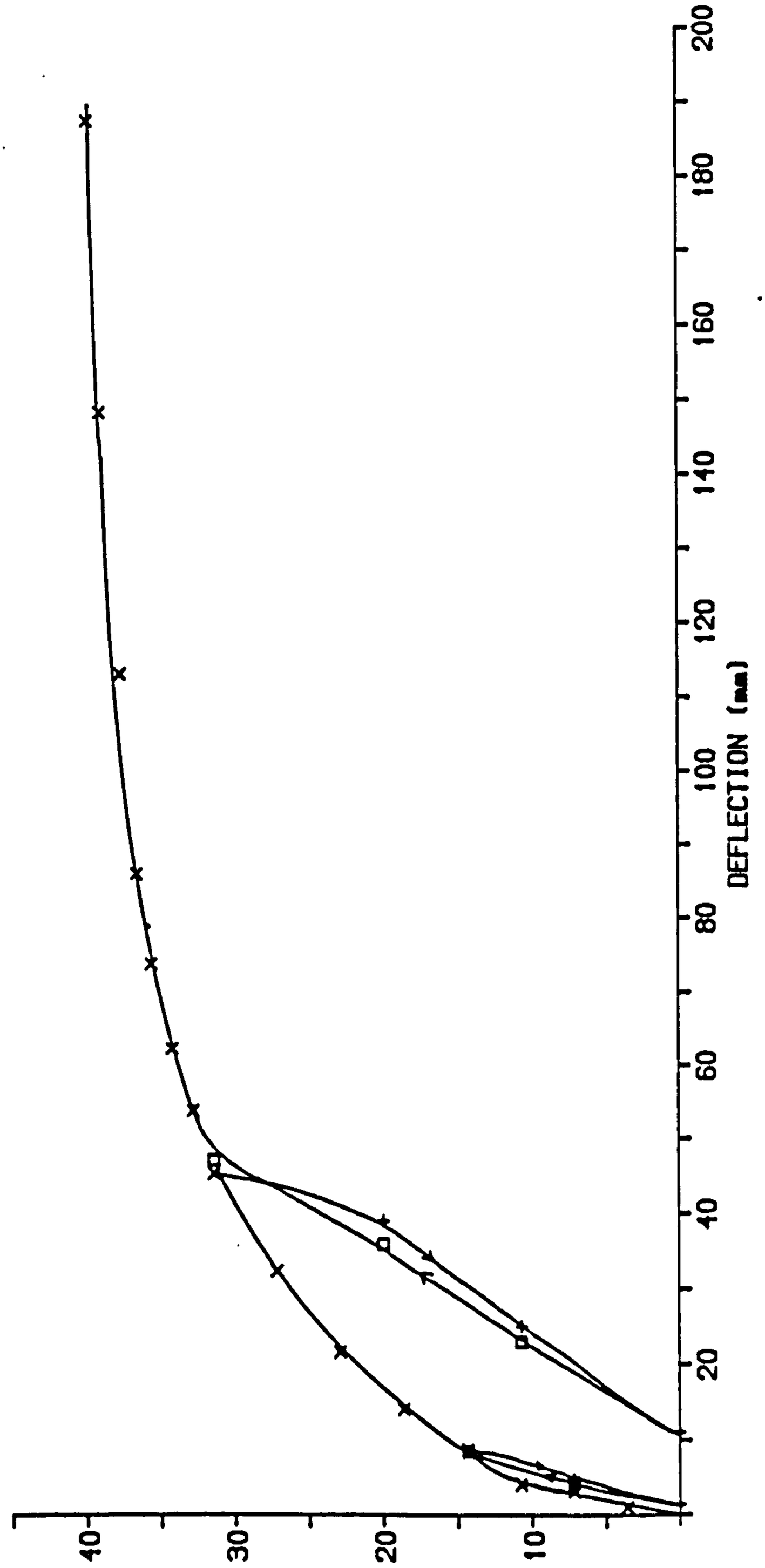
LOAD/DEFLECTION RESPONSE FOR BEAM B3
TOTAL APPLIED LOAD (kN)
10
20
30
40
DEFLECTION (mm)
20
40
60
80
100
120
140
160
180
200

Figure 5.6.13

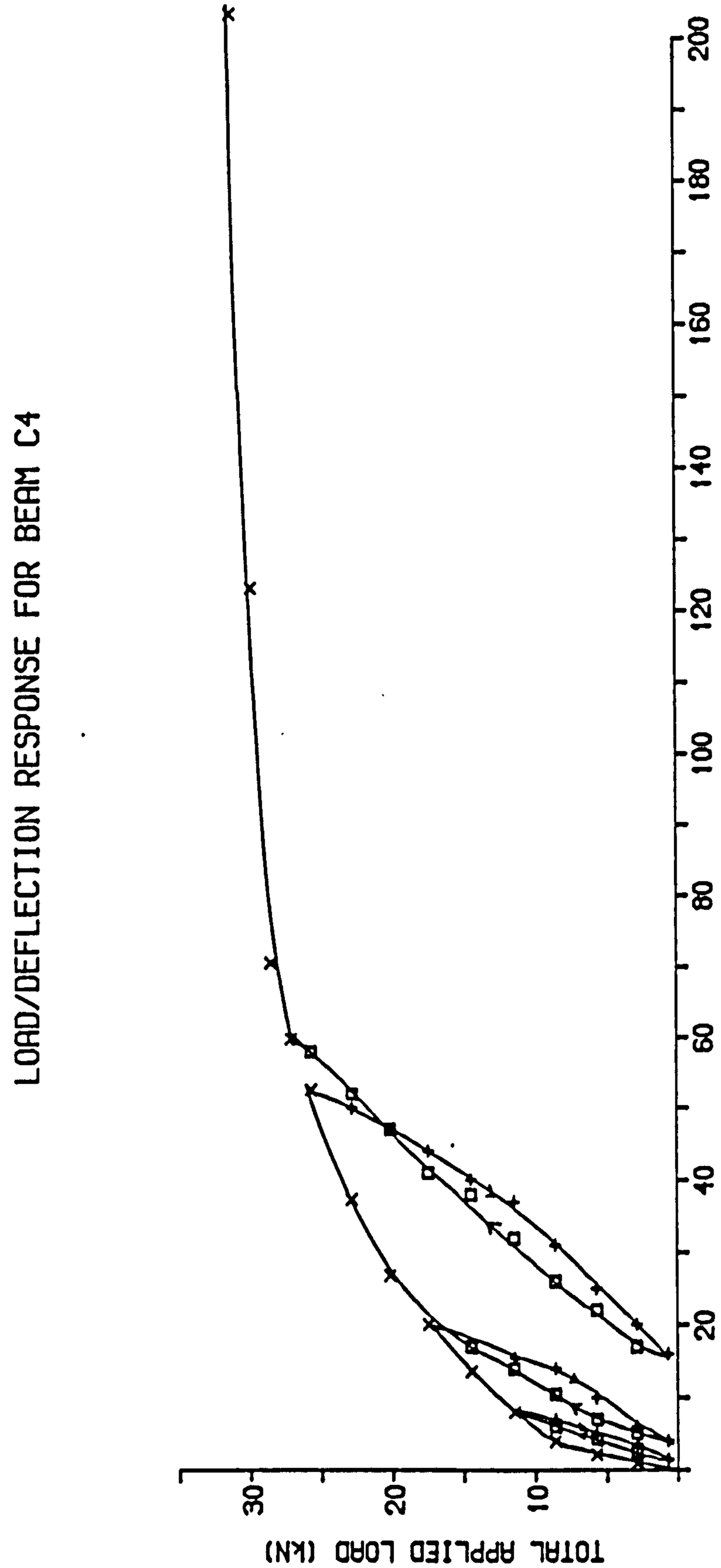
LOAD/DEFLECTION RESPONSE FOR BEAM C4
TOTAL APPLIED LOAD (kN)
DEFLECTION (mm)
0
20
40
60
80
100
120
140
160
180
200
10
20
30

Figure 5.6.14

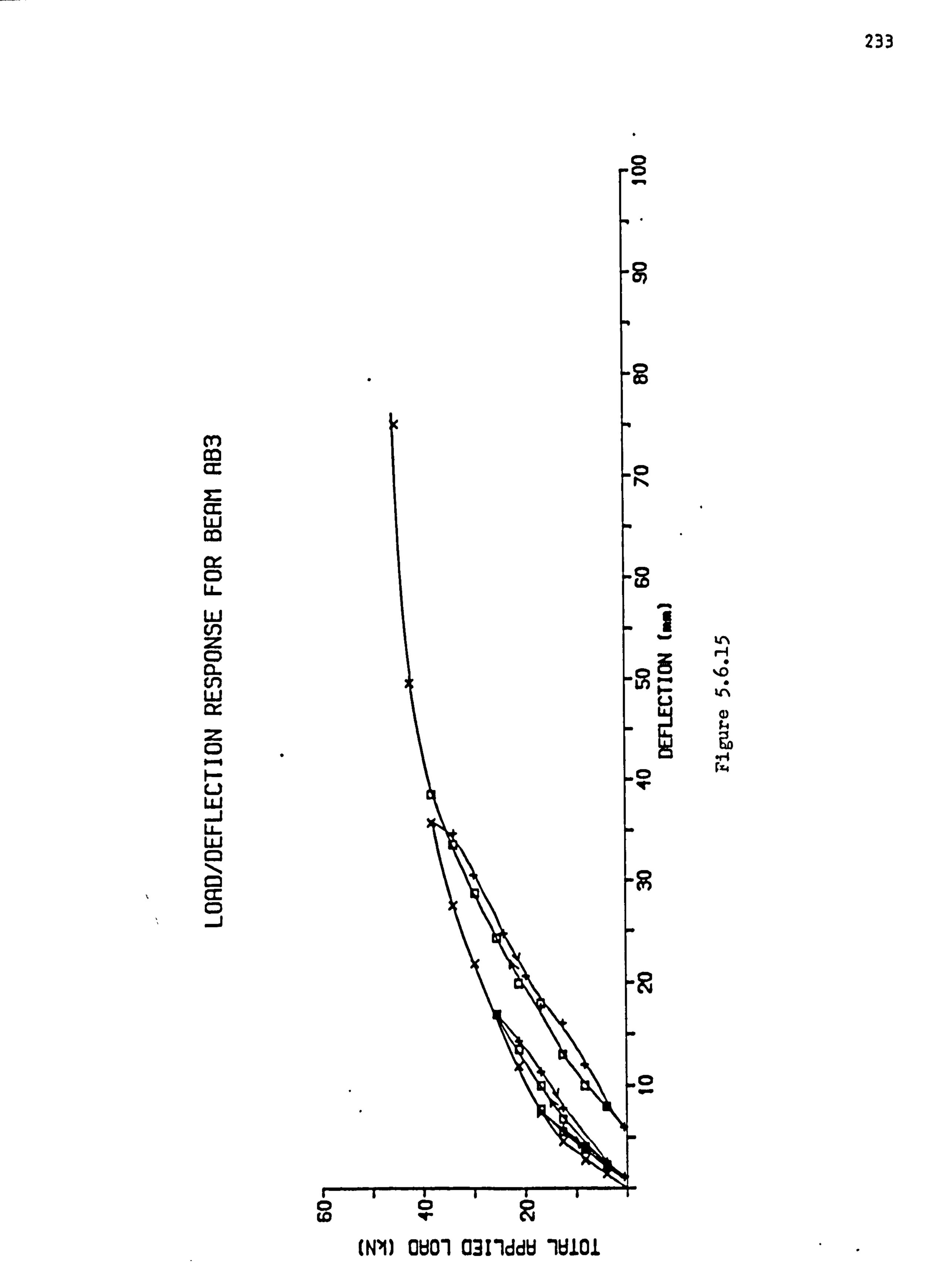
LOAD/DEFLECTION RESPONSE FOR BEAM AB3
TOTAL APPLIED LOAD (kN)
DEFLECTION (mm)
60
40
20
10
20
30
40
50
60
70
80
90
100

Figure 5.6.15

concrete. During the formative stages of loading after cracking whilst the tensile reinforcement behaved elastically the beams exhibited at least 95% recovery in deflection. Once the non-tensioned steel had yielded and so the load/deflection response had entered the third phase a considerable residual deflection was observed, figures 5.6.13 - 5.6.15.

5.6.1 Effect of % area of steel

The individual load/deflection relationships for beam series A (0.47% steel area), B (0.37% steel area) and C (0.31% steel area) are presented in figures 5.6.1 - 5.6.3 respectively. The average experimental curves are presented together for comparison in figure 5.6.16.

The behaviour of each beam with different % area of steel was very similar up to cracking, the deflection was slightly reduced in the beams with the largest steel area due to the increase in stiffness of the uncracked section. The load to cause cracking was unchanged since the % steel area change had no influence upon cracking load.

The post-cracking load/deflection behaviour of all three beam series indicated that they were under-reinforced sections. Immediately after cracking there was large increase in deflection due to the sudden reduction in stiffness, largest deflection always occurring in beam with least steel area. Once the steel yielded excessive deflections occurred for little increase in load, the three curves diverged with further loading until failure.

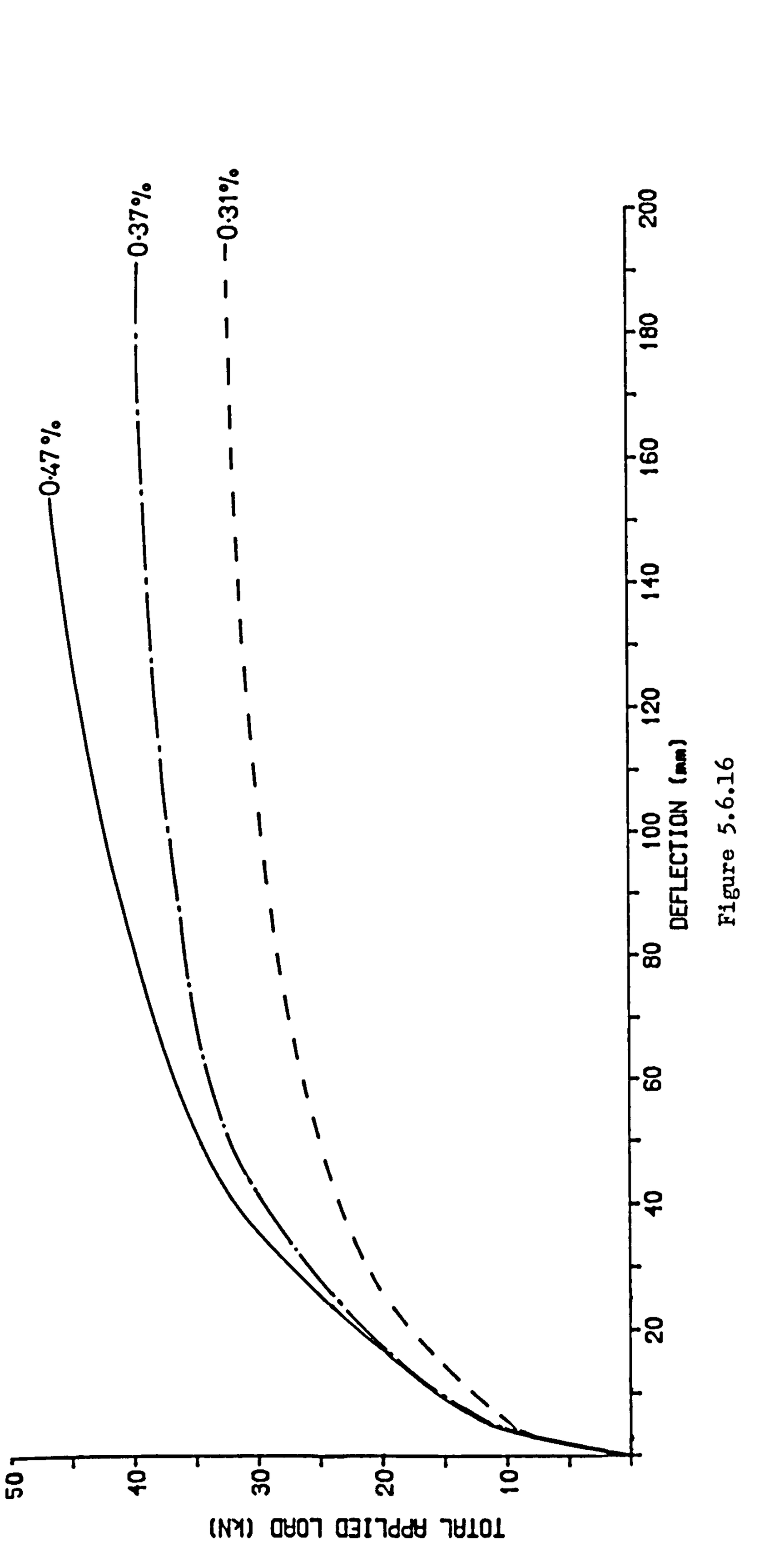
INFLUENCE OF % AREA OF STEEL ON LOAD/DEFLECTION RESPONSE
0·47%
0·37%
0·31%
TOTAL APPLIED LOAD (kN)
10
20
30
40
50
DEFLECTION (mm)
20
40
60
80
100
120
140
160
180
200

Figure 5.6.16

The reduction in steel area caused the stress in the reinforcement to increase in the cracked section in order to sustain equal load. This caused an increase in the compressive strains and reduction in the neutral axis depth and so increase in curvature and thus deflection.

For the purposes of this discussion the serviceability limit state of deflection was taken as span/250[15], or 24.8 mm. The load required to reach this limit varied considerably depending upon the steel area of the beam. In beam series A, B and C the load required was 26 kN, 24 kN and 19 kN respectively, or compared with beam series A an 8% and 27% reduction in maximum service loading for beam series B and C respectively.

5.6.2 Effect of prestressing force

The load/deflection responses for beam series AA and AB are shown in figures 5.6.4 and 5.6.5 respectively. The effect of a 26% reduction in prestressing force upon load/deflection is illustrated by comparison of the average experimental curves in figure 5.6.17a. As the deflection was measured only under applied loading the curves commence at the origin and no comparison of the hogging due to the prestress was possible. From zero load up to cracking the load/deflection responses were identical, no change in the beam stiffness of the uncracked section for a reduction in the prestressing force.

The most obvious effect of a reduction in the prestressing

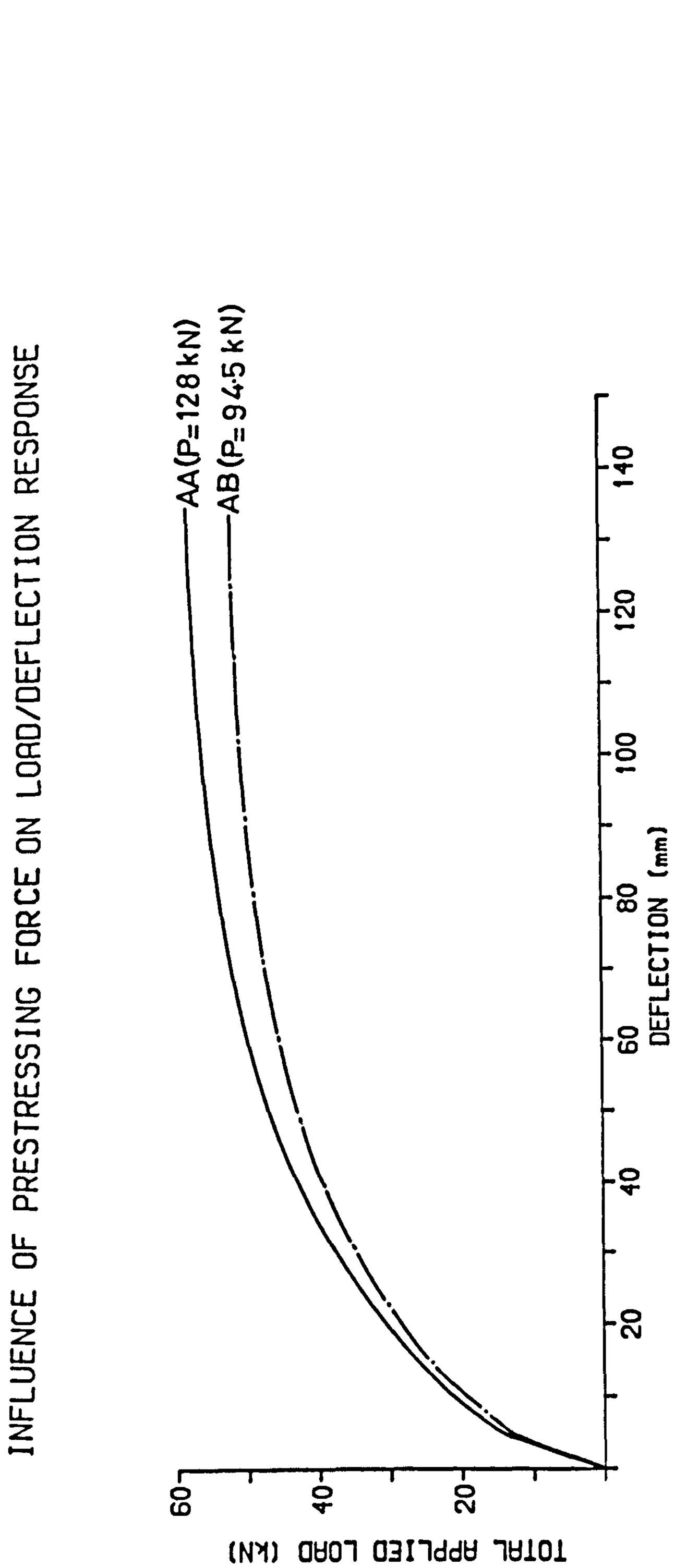

Figure 5.6.17a

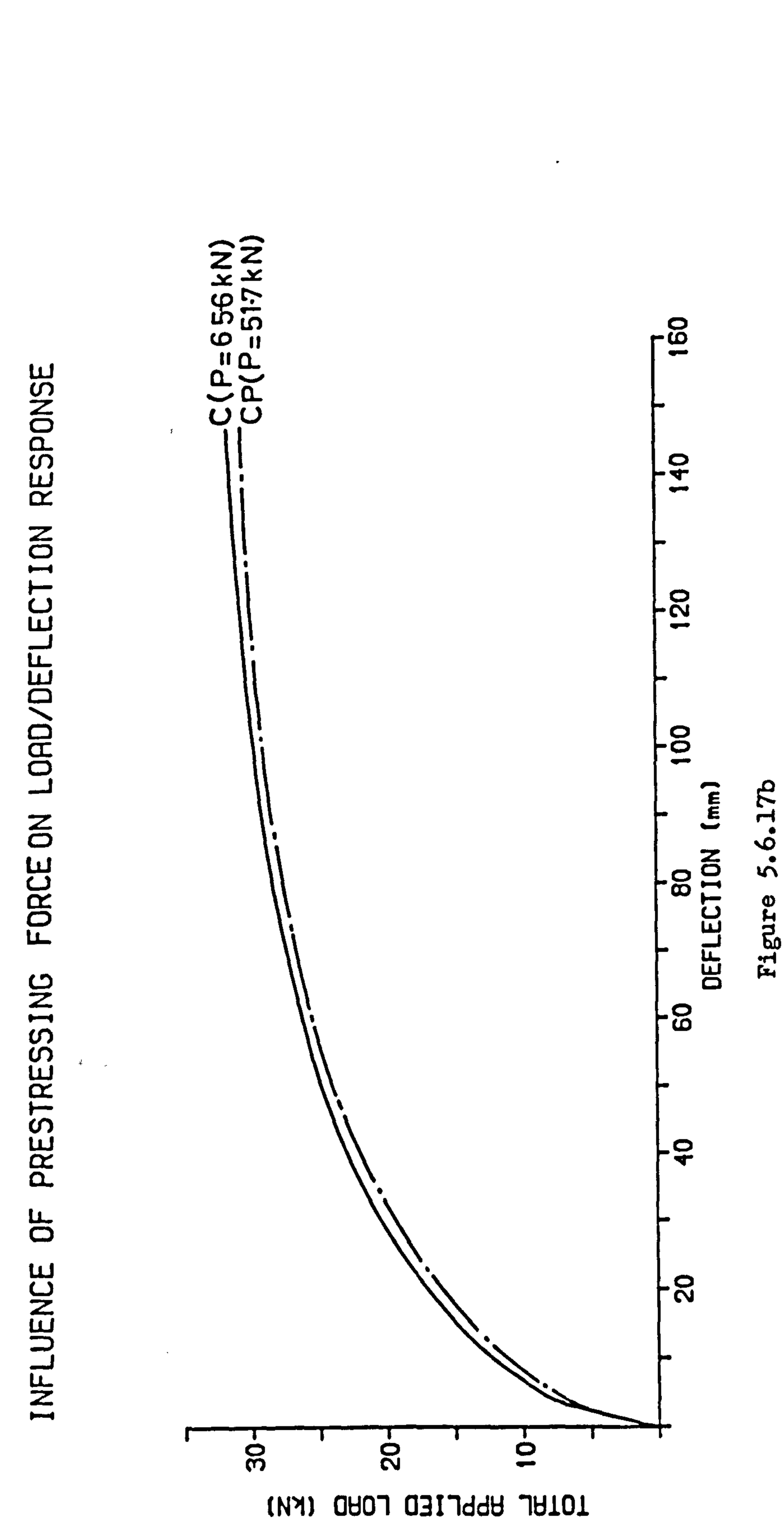

Figure 5.6.17b

force was the reduction in the load required for cracking, figure 5.6.17a. Beyond cracking the deflection of the beams with least pretress, AB1-AB3, was greatly increased in comparison with beams AA1-AA3. The reduction in stiffness caused by cracking occurred earlier in beams AB1-AB3 and consequently for all loads up to failure the stiffness was least and deflection greatest in these beams. Immediately after cracking whilst the reinforcement was elastic the load/deflection responses were approximately parallel and the rate of increase in deflection was similar.

Similar behaviour was exhibited by beams series CP when compared to beam series C, figure 5.6.17b. As the total level of prestress was less than for beam series AA and AB a 21% reduction in the prestressing force had a less significant effect upon the cracking load and hence the curves follow more of a similar path up to failure.

5.6.3 Effect of partial prestressing ratio

The load/deflection responses for test beam series C, P and R are illustrated in figures 5.6.3, 5.6.7 and 5.6.8 respectively. Typical test results are also compared with the load/deflection response of the fully prestressed brickwork beams[9] in figure 5.6.18.

The fully prestressed brickwork beams used in the comparison were taken form Pedreschi's study of fully prestressed brickwork beams[9]. Beams 'B1-B6' (as defined by Pedreschi) were used in the study. The section of the fully prestressed beams were very similar

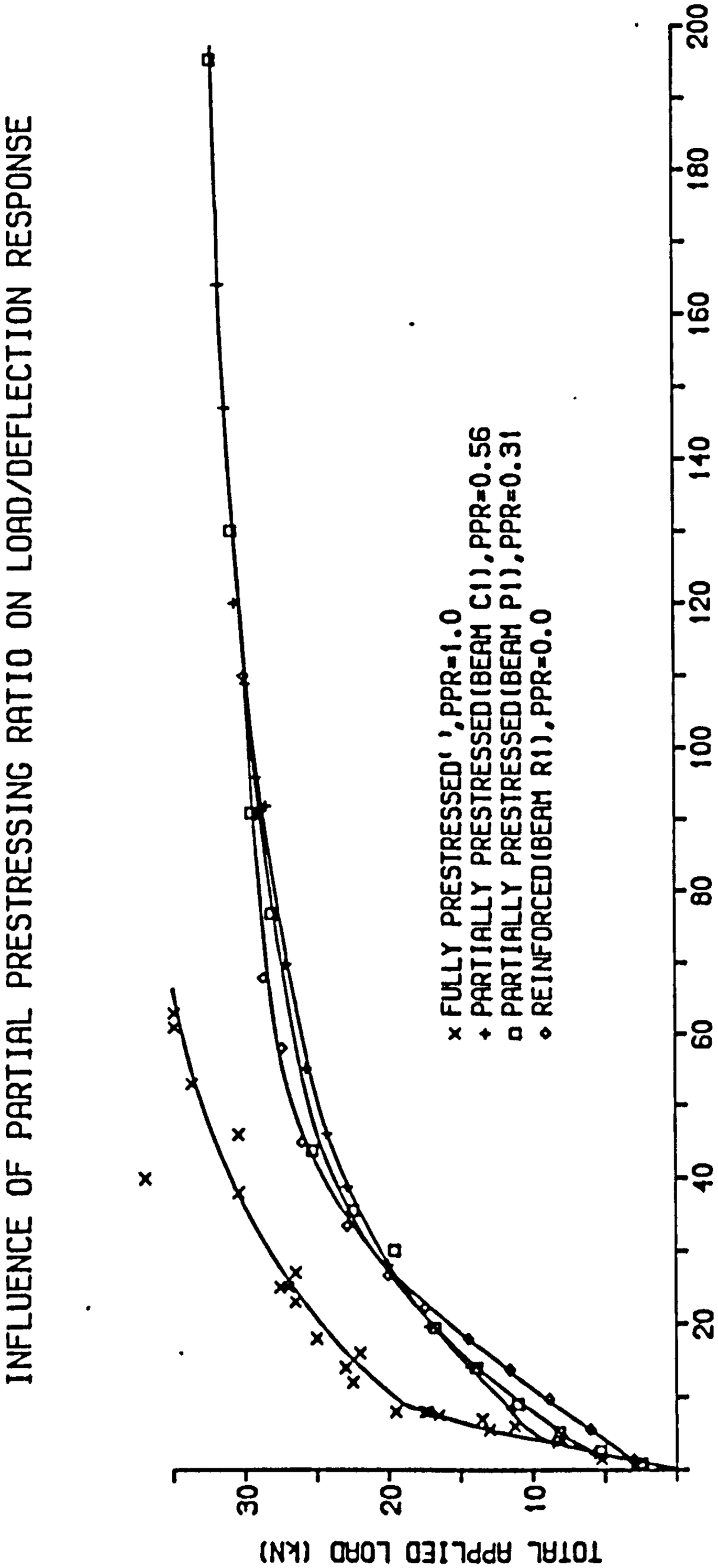
INFLUENCE OF PARTIAL PRESTRESSING RATIO ON LOAD/DEFLECTION RESPONSE
TOTAL APPLIED LOAD (kN)
DEFLECTION (mm)
× FULLY PRESTRESSED' ',PPR=1.0
✦ PARTIALLY PRESTRESSED(BEAM C1),PPR=0.56
□ PARTIALLY PRESTRESSED(BEAM P1),PPR=0.31
◇ REINFORCED(BEAM R1),PPR=0.0
10
20
30
20
40
60
80
100
120
140
160
180
200

Figure 5.6.18

to the partially prestressed beams except that the duct was restricted to the fourth course only. The beams were built of high strength bricks spanning 6200 mm, average prestressing force after losses was 133 kN and area of prestressing steel of 144 mm^2 was placed at the lower 'kern' limit.

As deflection was measured for applied loading only the curves commence at the origin and consequently the curves follow the same response up to cracking since the stiffness of the uncracked section was similar for all beams.The cracking load corresponded to the relative prestressing forces, first cracking in the reinforced beams and highest load for the fully prestressed beams. Subsequent to cracking deflection was greatest in the reinfoced beam and least in the fully prestressed.

The deflection of the partially prestressed brickwork beams lies between the boundaries represented by the fully prestressed and reinforced brickwork beams. Prior to cracking the slope of the load/deflection relationship for each beam type was equal. With increasing load each beam type in turn cracks and so the deflection at any particular load was greatest in the beams with least prestress. For example at a load of 12.8 kN (corresponding to average cracking load of the fully prestressed beams) the deflection due to the applied load for partial prestressing ratio (PPR) equal to 1, fully prestressed, 0.56, series C, 0.33, series P and 0.0, series R reinforced, was 4.5, 12.5, 14.0 and 17.0 mm respectively. By prestressing the deflection has been reduced by up to 74%. The rate of increase with further loading after cracking was less for the beams with largest areas of non-tensioned steel due to the extra

stiffness of the section resulting from the non-tensioned reinforcement. Therefore by appropriate selection of the level of prestress the deflection of any brickwork beam may be controlled to within the limits defined by the reinforced and fully prestressed beams.

5.6.4 Effect of brick strength

The load/deflection relationships for the high, medium and low strength brick beams are shown in figures 5.6.3, 5.6.10 and 5.6.11 respectively and the average experimental results are compared in figure 5.6.19.

Comparing the high and medium strength brick beams, the characteristics of each curve were very similar up to cracking but the post-cracking deflection of the medium strength beams indicated up to a 20% increase in deflection with respect to the high strength brick beams. This was caused by the reduced stiffness of the beam section resulting from a 25% reduction in the brick strength. Failure of the medium strength brick beams occurred at a lower load and consequently the load/deflection curve ceases prior to that of the high strength brick beams.

Comparing the high and low strength brick beams, series CP and CL, indicates a significant increase in deflection caused by a 78% reduction in compressive strength. Throughout the loading history the deflection of the low strength brick beams was consistently larger than that of the high strength beams. Although the slope of each graph was similar the two diverge until failure of

INFLUENCE OF BRICK STRENGTH ON LOAD/DEFLECTION RESPONSE

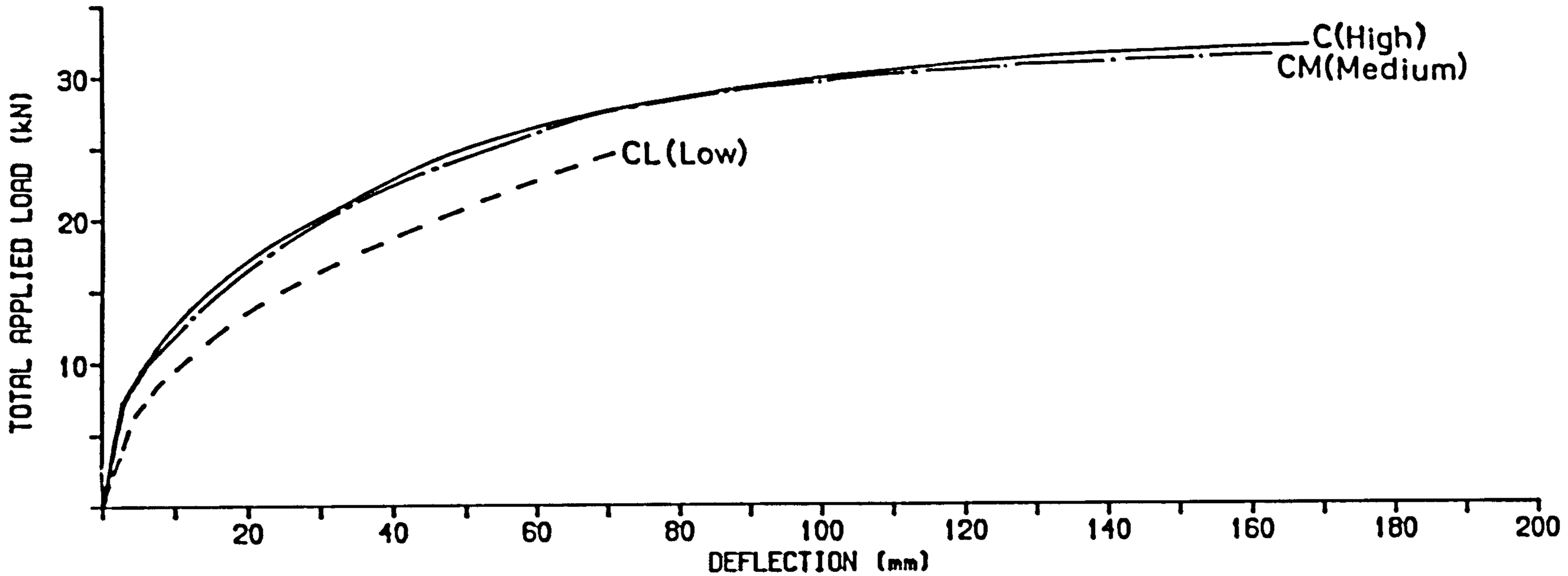

Figure 5.6.19

the low strength beams at an ultimate load 23% lower than that of beam series CP. For example at a total applied load of 9 kN the deflections were 7 and 16 mm respectively for high and low strength brick beams, an increase in delfection of 129%. At a loading of 18 kN the respective deflections were 17.5 and 51.5 mm, a difference of 194%. The load corresponding to serviceability limit state of deflection, 24.8 mm (span/250[15]), the high strength brick beams were able to sustain 23 kN whereas the low strength only 12.2 kN, a reduction in load of 47%.

5.6.5 Effect of mortar grade

In figures 5.6.3 and 5.6.12 respectively the load/deflection repsonses for beams built from grade I and II mortar are presented. The average experimental results also compared in figure 5.6.20. The change in mortar grade did not significantly effect the material properties of the brickwork, chapter 3, and consequently the deflections were similar, slightly less in the grade II beams due to marginal increase in prestressing force.

5.6.6 Comparison of experimental and theoretical load/deflection relationships

The experimental load/deflection responses are compared with theoretical predictions using the direct method in figures 5.6.1 - 5.6.12. The theoretical load/deflection response was predicted from the average moment-curvature relationship, including the effects of tension-stiffening, as outlined in chapter 6. Since deflection is a second order integral of curvature the discussion is limited here

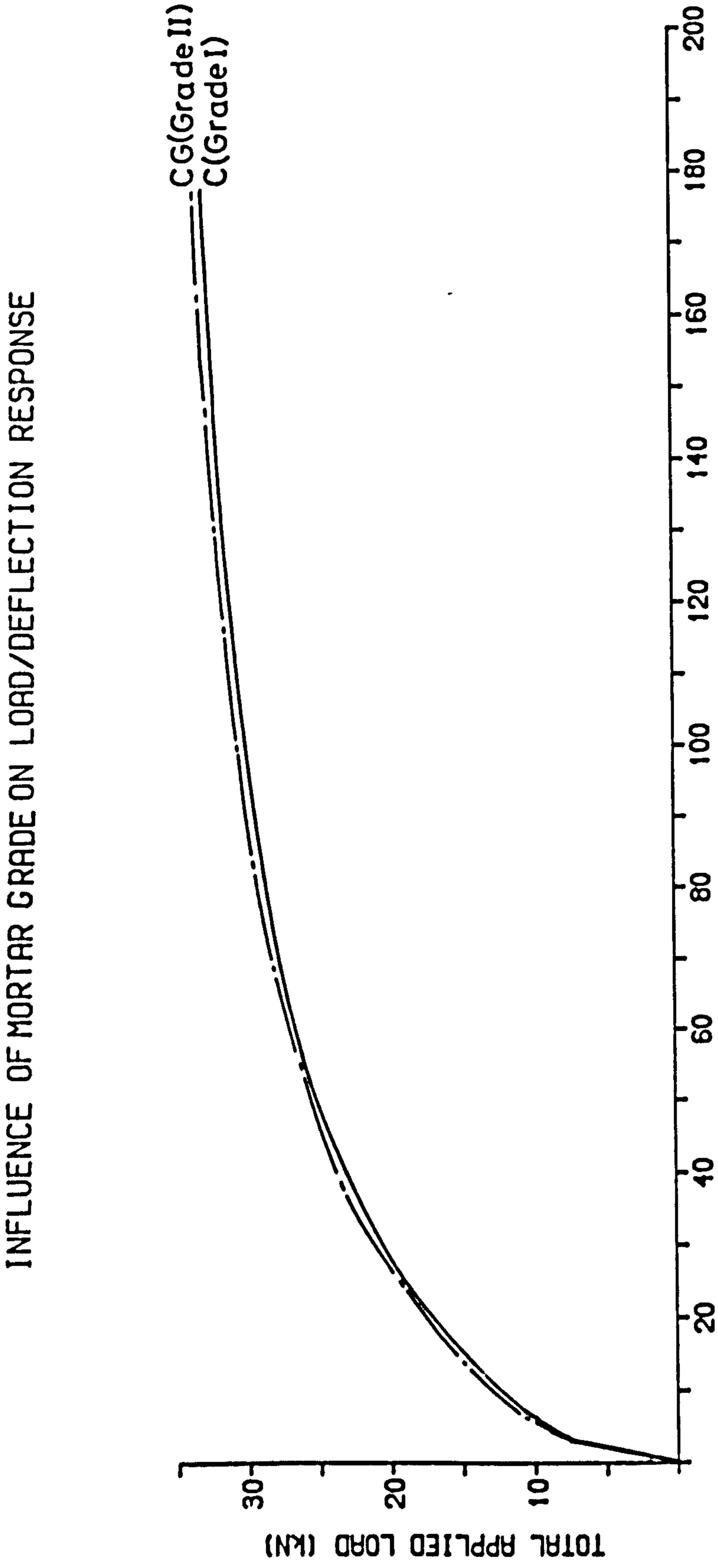
INFLUENCE OF MORTAR GRADE ON LOAD/DEFLECTION RESPONSE
CG(Grade II)
C(Grade I)
TOTAL APPLIED LOAD (kN)
30
20
10
0
20
40
60
80
100
120
140
160
180
200
DEFLECTION (mm)

Figure 5.6.20

since the theory was also compared with the experimental moment-curvature relationships in section 5.5.

5.6.6.1 Theoretical load/deflection using the direct method

The single course prisms provided the most accurate estimate of the load/deflection relationships in all cases. With the exception of the low strength brick beams, figure 5.6.11, the theory was generally accurate to within 10% and therefore showing excellent agreement. The single course prisms were the most accurate throughout the loading history, from zero up to failure. This therefore confirms earlier work that the single course prism properties were the best representation for the compression zone behaviour of the partially prestressed brickwork beams.

Initially the predicted deflection using three course prism properties showed good agreement with experimental results. However, approaching failure the theory grossly over-estimated the deflection due to under-estimation of the moment. Throughout loading the three course prism over-estimated deflection and therefore was safe.

Brickwork properties provided by the single course prisms provided throughout the best estimate of deflection and therefore most accurate representation of compression zone behaviour of the beams.

In most design calculations the maximum, generally mid-span, deflection is of most concern. But excessive deflection in the shear span of the beam may interfere with service fittings and so require

investigation. Measurements of deflection at the 1/4 points of the span were taken in all test beams, typical load/deflection responses are compared with theoretical predictions in figures 5.6.21 and 5.6.22.

As expected the general shape was similar to that of the mid-span load/deflection relationships. The single course prisms provide accurate estimations of the average experimental results. Since the single course prisms accurately predicted the moment-curvature reltionships this was to be expected.

5.6.6.2 Deflection predicted inaccordance with BS 5628 Part 2.

The direct method using the actual non-linear stress/strain curves for the materials was very accurate but may be too rigorous for design purposes. Therfore it may be of general interest to use the 'strength of materials' approach[30] implied by BS 5628 Part 2[15] to predict the deflection and compare it with the experimental results. The characteristic compressive strengths given by the code were used, partial safety factors were taken as equal to one for serviceability calculations.

The experimental load/deflection responses for three of test beams were compared with the predicted deflection in figure 5.6.23 - 5.6.25. The code greatly over-estimated the deflection for all beams and all loads up to failure. As discussed in section 5.4 the characteristic compressive strength for brickwork given by the code was very conservative. The modulus of elasticity based on clause 19.1.17 will be lower than that the experimental value and hence, the

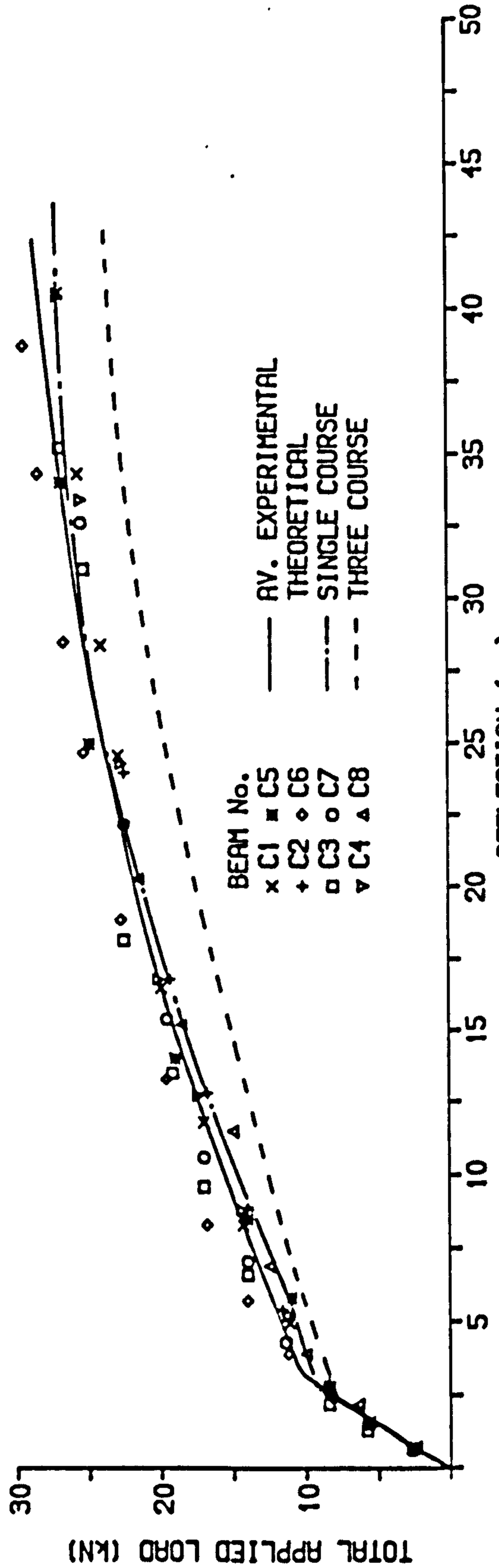
LOAD/DEFLECTION RESPONSE AT 1/4 POINT FOR BEAM SERIES C
BEAM No.
C1 C5
C2 C6
C3 C7
C4 C8
AV. EXPERIMENTAL
THEORETICAL
SINGLE COURSE
THREE COURSE
TOTAL APPLIED LOAD (kN)
DEFLECTION (mm)

Figure 5.6.21

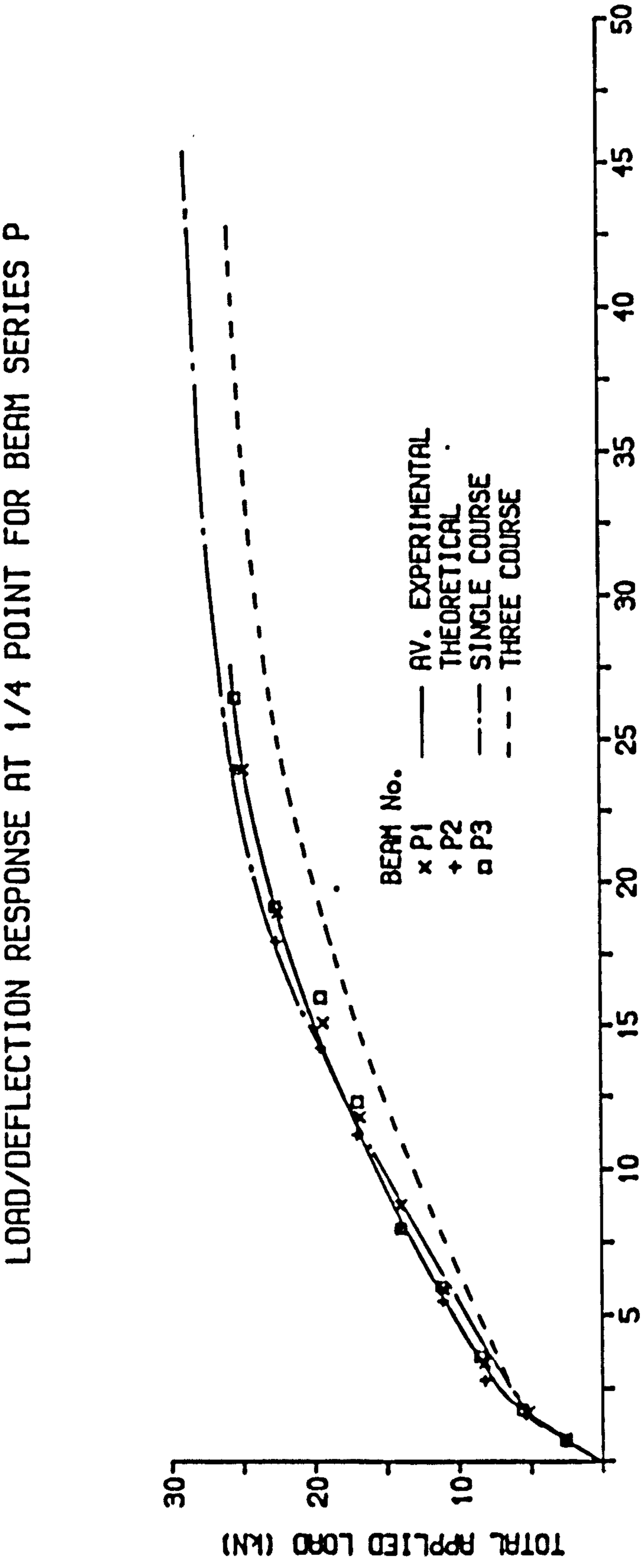
LOAD/DEFLECTION RESPONSE AT 1/4 POINT FOR BEAM SERIES P
BEAM No.
× P1
+ P2
□ P3
—— AV. EXPERIMENTAL
THEORETICAL
—·— SINGLE COURSE
- - - THREE COURSE
TOTAL APPLIED LOAD (kN)
DEFLECTION (mm)
0
5
10
15
20
25
30
35
40
45
50

Figure 5.6.22

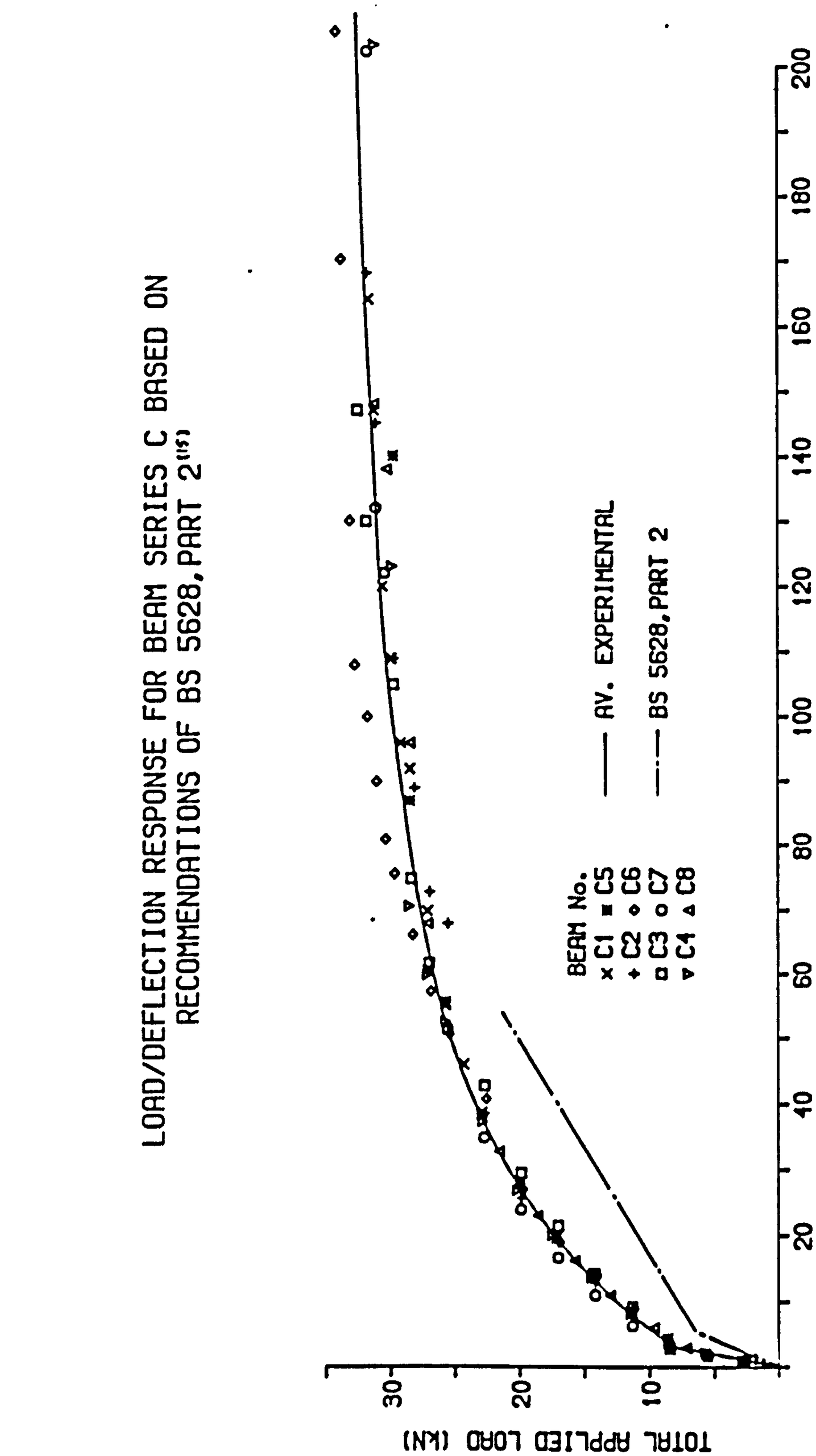
LOAD/DEFLECTION RESPONSE FOR BEAM SERIES C BASED ON RECOMMENDATIONS OF BS 5628, PART 2(5)
TOTAL APPLIED LOAD (kN)
DEFLECTION (mm)
BEAM No.
C1 C5
C2 C6
C3 C7
C4 C8
AV. EXPERIMENTAL
BS 5628, PART 2
0
20
40
60
80
100
120
140
160
180
200
10
20
30

Figure 5.6.23

LOAD/DEFLECTION RESPONSE FOR BEAM SERIES AA BASED ON RECOMMENDATIONS OF BS 5628, PART 2[15]

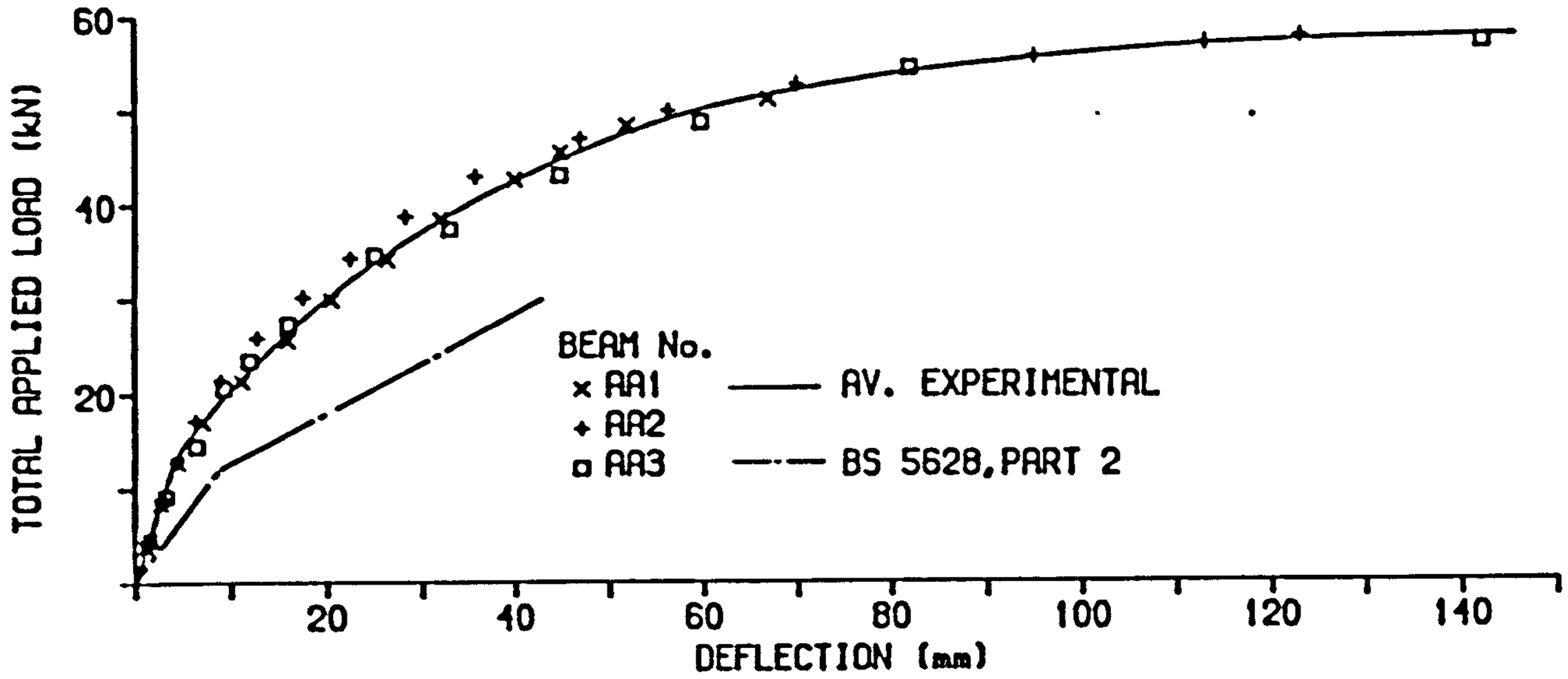

Figure 5.6.24

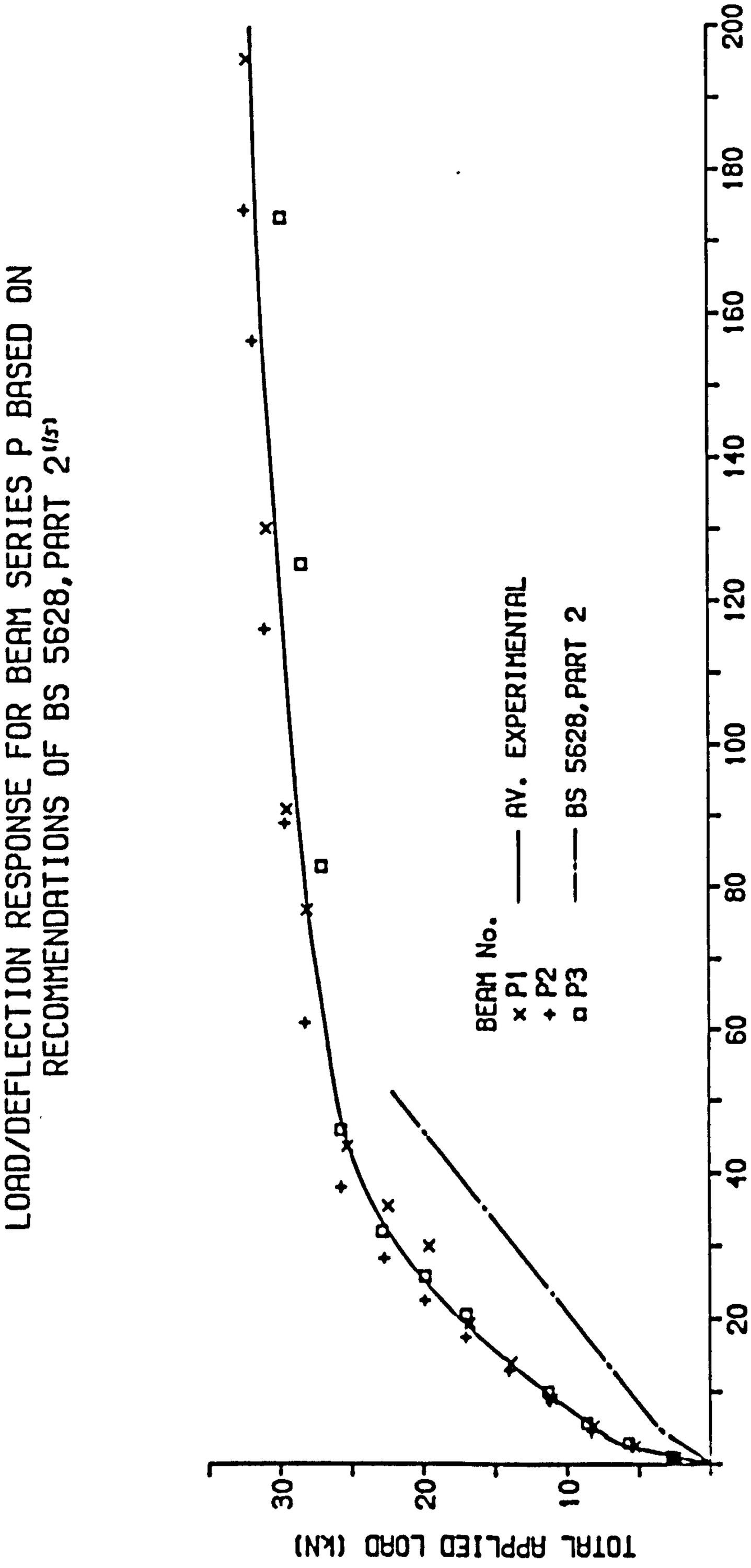
LOAD/DEFLECTION RESPONSE FOR BEAM SERIES P BASED ON
RECOMMENDATIONS OF BS 5628, PART 2 (1st)
BEAM No.
× P1 —— AV. EXPERIMENTAL
+ P2
□ P3 —— BS 5628, PART 2
DEFLECTION (mm)
TOTAL APPLIED LOAD (kN)
0
20
40
60
80
100
120
140
160
180
200
10
20
30

Figure 5.6.25

code gave a very conservative estimate of the deflection.

5.7 SUMMARY AND CONCLUSIONS

All forty-one beams tested were under-reinforced. Thirty-seven beams failed in tension, of which a secondary shear failure occurred in twelve of the beams. Only four beams failed in shear, which may attributed to the weak bond that had devloped at the time of testing between the bricks and either concrete or mortar.

On the basis of this study the following conclusions can be drawn:

1. The method proposed, incorporating the experimentally derived non-linear material properties, accurately modelled the ultimate limit state and load/deflection behaviour of the partially prestressed brickwork beams. The method is also equally applicable to both reinforced and fully prestressed brickwork beam sections. The material properties of the single course brickwork prism provided the most accurate model of the compressive behaviour of the brickwork beams.

2. The ultimate moments of the partially prestressed brickwork beams predicted in accordance with the recommendations of BS 5628 Part 2, 1985 under-estimated the experimental values.

3. Prior to yielding of the tensile steel the partially prestressed brickwork beams exhibited almost complete recovery of deflection upon removal of the applied load.

4. An increase in the area of non-tensioned steel causes an increase in the ultimate flexural moment of partially prestressed brickwork beams. The stiffness of both the uncracked and cracked sections are increased by an increase in the steel area and therefore leads to a reduction in the deformation of the beam in comparison with a similar beam with a reduced steel area.

5. Increases in prestressing force increases the effective shear resistance of a section. Primary or secondary shear failures may be avoided and hence the moment capacity is increased. Other than increasing the shear strength of a section the prestressing force has little significant effect upon ultimate flexural moment. A reduction in prestressing force decreases the cracking moment and hence causes larger deformation in comparison with a similar beam with an increased prestressing force.

6. Increasing the partial prestressing ratio of a section reduces the deformation , due to an increase in the load to cause cracking. By appropriate selection of the partial prestressing ratio the deformation of a brickwork beam may be controlled to within the limits defined by the reinforced and fully prestressed sections.

7. A 100% increase in the cover to the non-tensioned steel had little significant effect upon the ultimate moment or load/deflection response of the partially prestressed brickwork beams.

8. In under-reinforced sections a significant change in brick strength had little effect upon ultimate moment. A reduction in brick strength reduces the stiffness of the beam section and consequently causes an increase in the deflection.

9. The mortar grade has little influence upon the behaviour of partially prestressed brickwork beams.

10. The deflection predicted inaccordance with the recommendations of BS 5628 Part 2 1985 greatly over-estimated the actual deflections of the experimental test beams.

CHAPTER 6

TENSION-STIFFENING AND CRACKING OF PARTIALLY PRESTRESSED BRICKWORK BEAMS

6.1 INTRODUCTION

In chapter 4 a theoretical method was outlined to determine the moment-curvature relationship of a partially prestressed brickwork beam across a flexural crack from cracking up to ultimate moment. However, the curvature across a crack may be considerably larger than the average curvature of the beam due to the tension-stiffening of the uncracked sections between the cracks. When predicting the load/deflection response of the whole beam it is necessary to use the average moment-curvature relationship to avoid over-estimation of the deformation. This chapter presents a method with which to calculate the tension-stiffening effect of partially prestressed brickwork beams and so adjust the curvature across a crack to obtain the average curvature. The theoretical predictions are compared with a number of experimental results for the average curvature, the experimental results for the maximum curvature (across a crack) were presented and discussed in chapter 5.

Depending upon the environmental conditions crack widths up to 0.2 mm are allowed in class 3 prestressed concrete members[36]. In the past much research has been conducted in order to develop methods for accurate crack width prediction in partially prestressed concrete beams[65-70]. However, prior to this work no comparable research had been done in the case of partially prestressed brickwork beams. This lack of data must have influenced the drafting of the current British code of practice for reinforced and prestressed masonry, BS 5628 Part 2[15], and consequently the serviceability limit state of cracking is not considered for prestressed masonry. In design prestressed brickwork is, by implication, expected to

remain uncracked throughout its lifetime.

In the majority of design situations there are no reasons why cracking should be prevented in prestressed brickwork. From the practical viewpoints of both corrosion and aesthetics the limit state values used by the concrete code should be equally applicable to reinforced and prestressed brickwork.

Two methods are proposed for predicting the crack widths of partially prestressed brickwork beams. The first method utilises the non-linear material properties and is a logical extension of the direct method adopted to derive the moment-curvature relationship. Alternatively a simpler approach incorporating the fictitious tensile stress of the brickwork is also presented which may prove more suited for design.

The effects of % area of steel, prestressing force, partial prestressing ratio, cover to non-tensioned steel, brick strength and mortar grade on the cracking behaviour of partially prestressed brickwork beams are discussed in detail. The experimental results are also compared with the predicted values for average and maximum crack width.

6.2 TENSION-STIFFENING AND AVERAGE CURVATURE

In section 4.2.2.3 a method was developed to predict the moment-curvature relationship of a partially prestressed brickwork beam from cracking up to ultimate moment, the curvature was given by:

$$\phi = \frac{\varepsilon_1 + \varepsilon_s}{d_s} \qquad (6.2.1)$$

The predicted curvature was that across a flexural crack and made no account of the tension-stiffening effect of the brickwork and concrete between the cracks.

At a cracked section the stress in the tensile reinforcement will be greater than that away from a crack due to transfer of stress through bond between the reinforcement and concrete, figure 6.2.1. The average curvature of the partially prestressed beam will, therefore, be less than that predicted by equation 6.2.1 in which the maximum steel strain is used. The average curvature is, therefore found by substituting the average steel strain for the maximum steel strain in equation 6.2.1.

A number of researchers[71,72] have proposed expressions for concrete beams to derive the average steel strain by applying a reduction to the maximum strain at a crack.

A constant reduction in steel strain was suggested by Beeby et al[71] for reinforced and partially prestressed concrete beams, thus:

$$\varepsilon_{sm} = \varepsilon_s - \left\{\frac{4b.d}{A_s}\right\} 10^{-6} \qquad (6.2.2)$$

Rao and Subrahmanyam[72] proposed that the tension stiffening effect reduced as the applied moment increased. Comparing experimental measurements of strain with those predicted by a cracked section analysis they developed the following expression:

$$\varepsilon_{sm} = \varepsilon_s - 0.18\left(\frac{f_{scr}}{f_s}\right)\frac{fr\ b\ d}{E_s A_s} \qquad (6.2.3)$$

where f_{scr}/f_s is the ratio of the steel stress at a crack at first cracking to the stress in the steel with further loading.

Pedreschi[9] developed the method proposed by Rao et al[72] to derive an expression for the mean additional strain in the tensile reinforcement of a post-tensioned brickwork beam given by:

$$\varepsilon_{sm} = \varepsilon_s - \left[1 - 0.97\frac{f_{scr}}{f_s}\right]\frac{f_r\ b\ d}{E_s A_s} \qquad (6.2.4)$$

The derivation of the expression differed from that used by Rao et al since the mean additional strain was considered and only experimental measurements were used to develop the relationship. Equation 6.2.4 is contrary to that developed by Rao et al, equation 6.2.3, since it states that the tension-stiffening effect increases with applied moment.

The method devised by Rao[72] was adopted and further developed to derive an expression for the tension-stiffening effect of partially prestressed brickwork beams using the experimental measurements of steel strain.

6.2.1 Theoretical derivation

The partially prestressed brickwork beam section used in this work contained two separate layers of tensile steel with differing material properties. In order to accommodate the

theoretical method, which assumes only a single layer of tensile reinforcement, the steel was assumed to consist of one layer with an effective steel area of A_{se}, where:

$$A_{se} = A_{ps} + \frac{A_s f_{sy}}{f_{psy}} \qquad (6.2.5)$$

at an effective depth of:

$$d_e = \left(\frac{A_{ps} d_{ps} + \frac{A_s f_{sy}}{f_{psy}} d_s}{A_{se}} \right) \qquad (6.2.6)$$

Figure 6.2.2 presents the distribution of tensile stresses in the reinforcement of a cracked beam. The variation of steel stresses between the cracked and uncracked section is due to the bond stresses between the steel and concrete. However, the actual distribution of bond stresses is extremely difficult to determine. Therefore considering equilibrium at a section midway between cracks:

$$a_0 \frac{s_m}{2} \tau_b = A_{se}(f_{se} - f'_{se}) \qquad (6.2.7)$$

The difference in steel strain is:

$$\varepsilon_{sea} - \varepsilon'_{sea} = \frac{(f_{se} - f'_{se})}{E_s} \qquad (6.2.8)$$

and so the mean additional strain is:

$$\varepsilon_{seam} = \varepsilon_{sea} - C_0 \frac{(f_{se} - f'_{se})}{E_s} \qquad (6.2.9)$$

STRESS DISTRIBUTION OVER DEPTH OF CRACKED AND MIDSECTION BETWEEN CRACKS

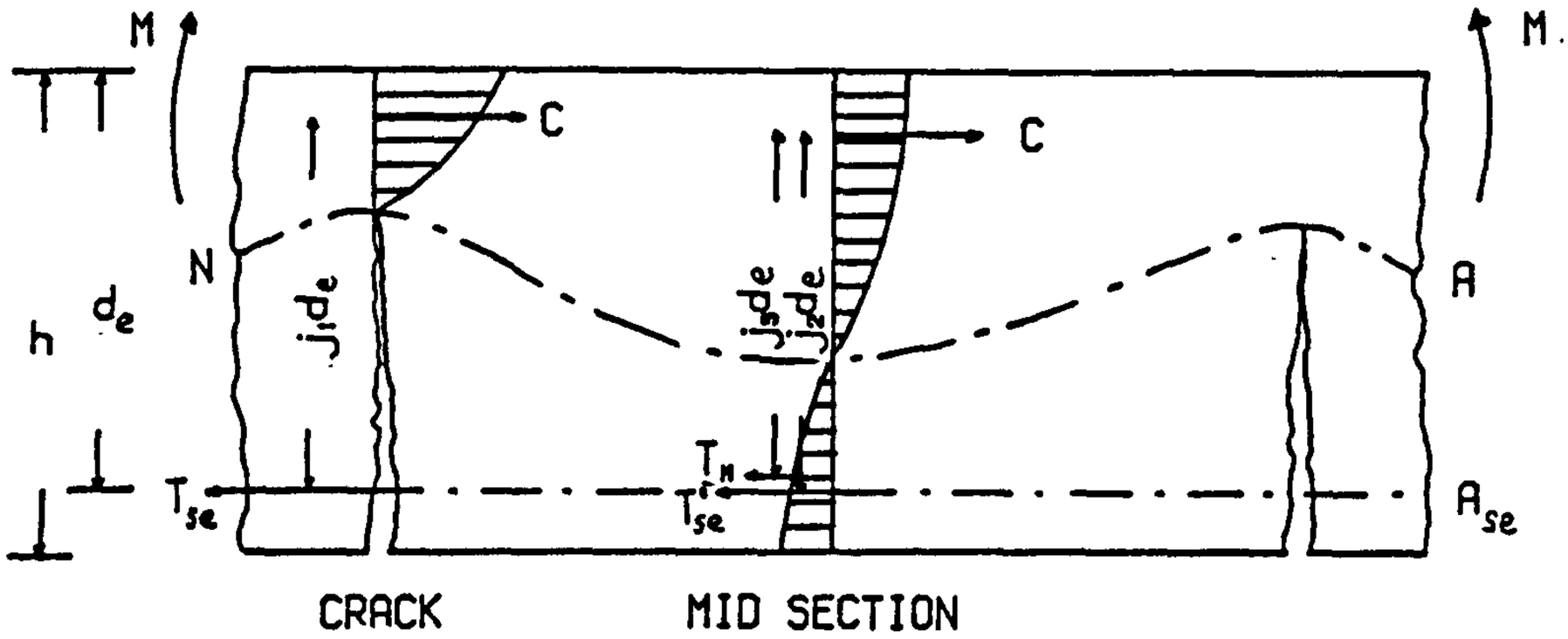

Figure 6.2.1

TENSILE AND BOND STRESS DISTRIBUTION ALONG THE REINFORCEMENT

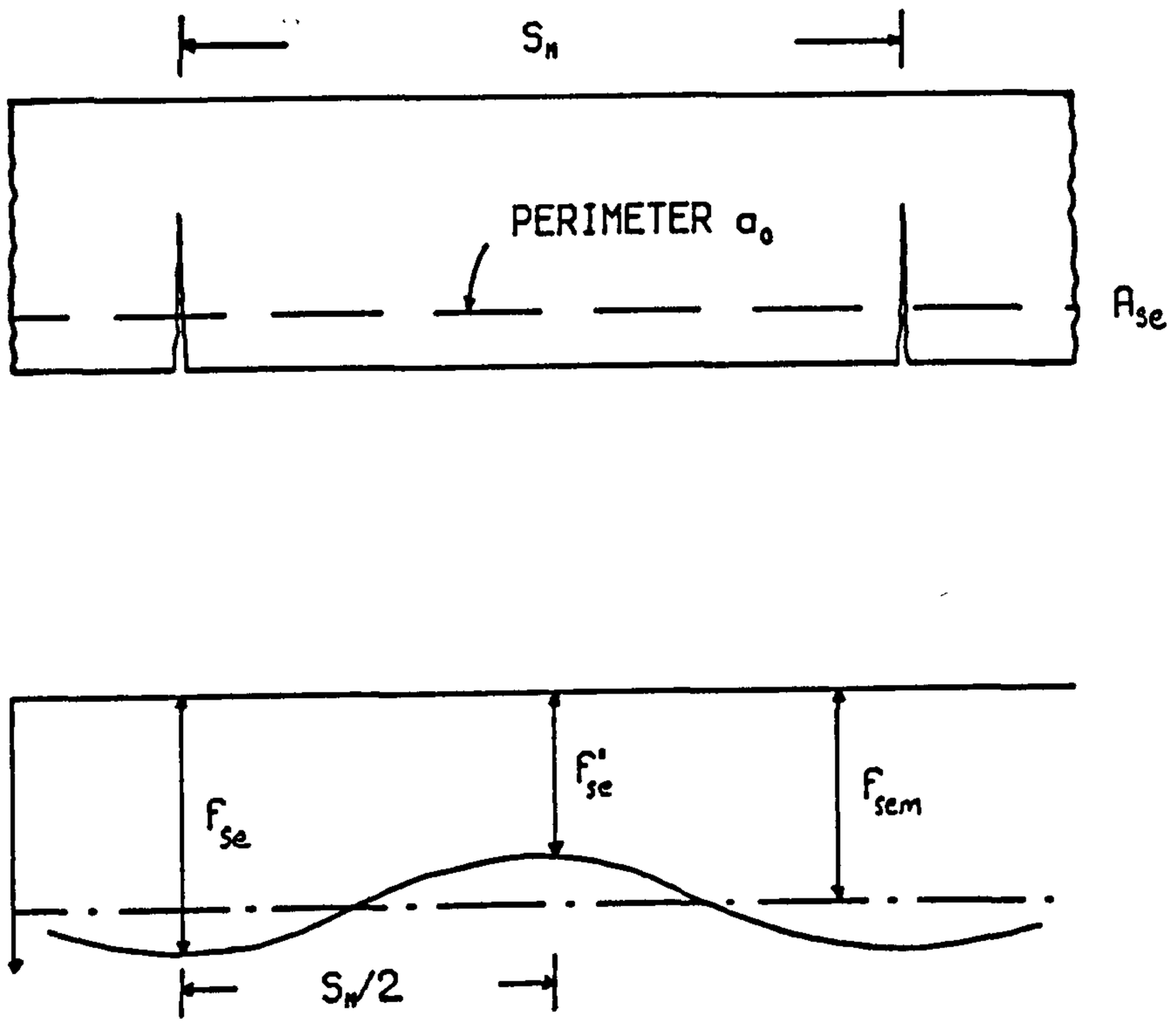

VARIATION OF STEEL STRESS

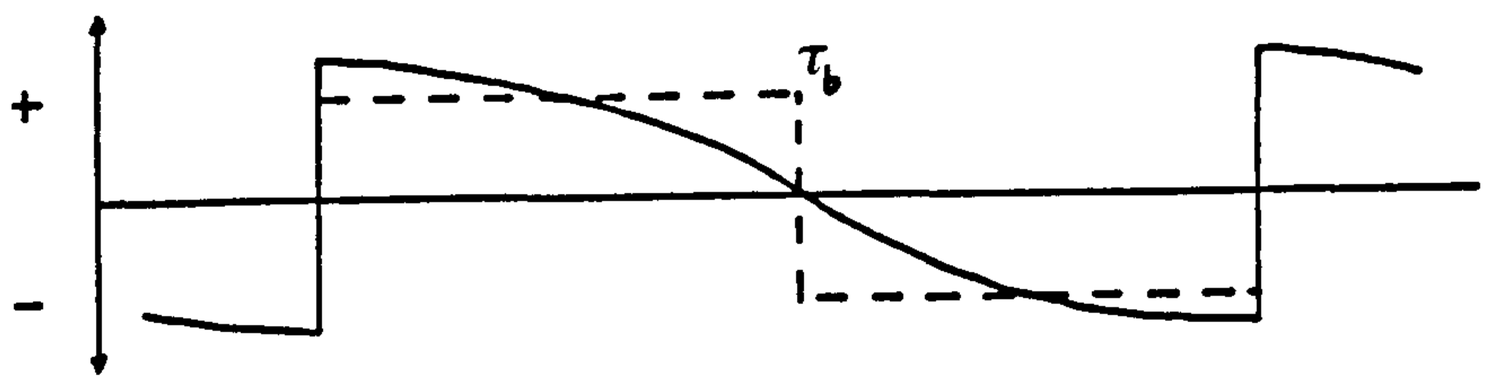

VARIATION OF BOND STRESS

Figure 6.2.2

where C_0 = bond factor.

The resisting moment within the constant moment zone at a crack must equal that at a section midway between two cracks, thus:

$$A_{se}\, f_{se}\, j_1\, d_e = A_{se}\, f'_{se}\, j_3\, d_e + A_e\, f_{mt}\, j_2\, d_e \qquad (6.2.10)$$

where A_e is the area of beam in tension, $A_e = C_1 b d'$

$f_{mt} = C_2 f_r$

also

$j_3 d_e \simeq j_1 d_e$

Therefore equation 6.2.10 can be rewritten as:

$$(f_{se} - f'_{se}) = C_1 C_2 \frac{j_2}{j_1} \frac{f_r\, b\, d_e}{A_{se}} \qquad (6.2.11)$$

substituting in equation 6.2.9

$$\varepsilon_{seam} = \varepsilon_{sea} - \left(C_0\, C_1\, C_2\, \frac{j_2}{\varepsilon_s\, j_1}\, f_r\, \frac{bde}{A_{se}} \right) \qquad (6.2.12)$$

Putting $K = C_0\, C_1\, C_2\, j_2/j_1$

hence: $$\varepsilon_{seam} = \varepsilon_{sea} - \frac{K\, f_r}{E_s\, \rho} \qquad (6.2.13)$$

where $$\rho = \frac{A_{se}}{bd_e}$$

Rearranging equation 6.2.13, gives the value of:

$$K = (\varepsilon_{sea} - \varepsilon_{seam}) \frac{E_s \rho}{f_r} \qquad (6.2.14)$$

However, a value for K is not readily known but may be determined from the experimental measurements of steel strain. The additional strains were determined for the effective depth from strain readings taken on the tensioned and non-tensioned steel. The initial strain due to the prestress was taken as:

$$\varepsilon_{pe} = \frac{P}{A_{se} E_s} \qquad (6.2.15)$$

Figure 6.2.3 presents the experimentally derived relationships between the tension-stiffening coefficient, K, and the degree of cracking, f_{secr}/f_{se}. The equation defining the relationship was found by least squares analysis to be:

$$K = 0.02 + 0.06\left(1-\frac{f_{secr}}{f_{se}}\right) + 0.77\left(1-\frac{f_{secr}}{f_{se}}\right)^2 \qquad (6.2.16)$$

Contrary to previous research[9,72] the relationship for tension-stiffening was non-linear. The work, however, does confirm that previously conducted on fully prestressed brickwork beams [9], i.e. that the tension-stiffening effect increases with moment. The non-linearity of the relationship may have resulted from the non-linear material characteristics of both the steel and brickwork. Once the steel yields the increase in the level of stress was small for large increases in strain and therefore although K, equation 6.2.14, continues to increase with moment, the value of f_{secr}/f_{se} will

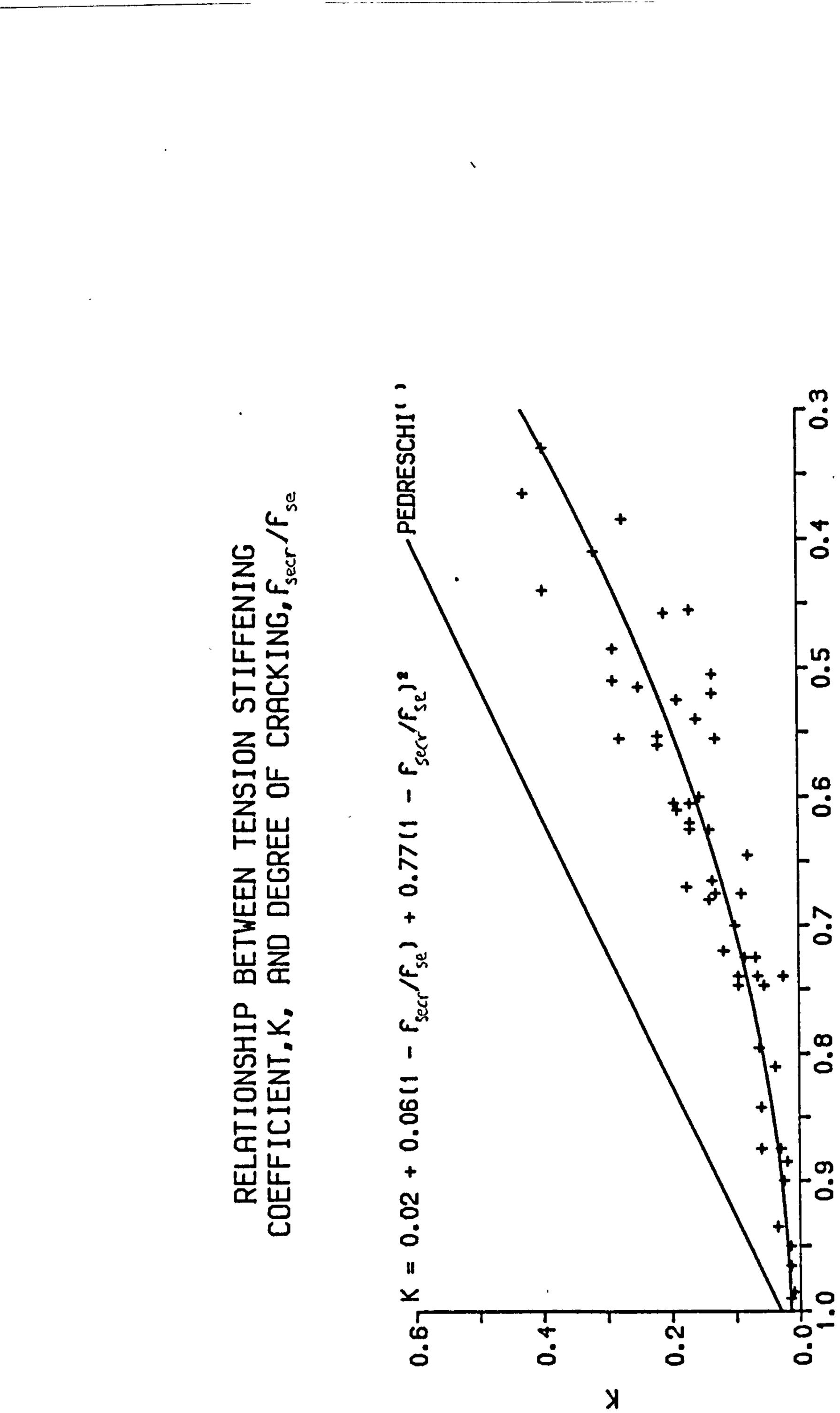
RELATIONSHIP BETWEEN TENSION STIFFENING
COEFFICIENT, K, AND DEGREE OF CRACKING, f_{secr}/f_{se}
$K = 0.02 + 0.06(1 - f_{secr}/f_{se})^2 + 0.77(1 - f_{secr}/f_{se})^8$
PEDRESCHI'
K
.6
.4
.2
.0
0.5
0.6
0.7
0.8
0.9
1.0
f_{secr}/f_{se}

Figure 6.2.3

increase proportionally less and so leading to the non-linear relationship, figure 6.2.3.

The proposed expression is compared in figure 6.2.3 with that proposed by Pedreschi[9], equation 6.2.4. There is a significant difference between the two expressions, the tension-stiffening effect is more pronounced when using the expression for fully prestressed brickwork. The stress distribution between cracks will be influenced by the minimum crack spacing, in brickwork equal to the distance between joints at the soffit of the beam. The minimum crack spacing in the fully prestressed beams was approximately half that of the test beams, this may have influenced the tension-stiffening expression. Since both expressions were derived from experimental measurements of strain taken from the test specimens it was not possible to confirm the effect of the joint spacing. However, it should be noted that the expression proposed by Pedreschi was based on only twelve test results[9], three of which indicated a significant variation with equation 6.2.4.

In calculation of the average curvature the average compressive top fibre strain was assumed to equal that across a crack. The difference was later shown to be small, section 6.2.2, and so likely to have little effect upon the accuracy of the method. The average curvature is given by:

$$\phi_{AV} = \frac{(\varepsilon_1 + \varepsilon_{seam})}{d_e} \qquad (6.2.17)$$

The average moment-curvature relationship is derived by applying equations 6.2.13 and 6.2.16 to the steel strains obtained in

the cracked section analysis, section 4.2.2.3, and re-calculating the curvature using equation 6.2.17.

6.2.2 Experimental average moment-curvature

The measurements of brickwork strain used to determine the average curvature were taken across either 100 or 150 mm gauge lengths. The nature of the cracking, along the mortar joints, and the bonding pattern were such that nearly all of the strain distributions measured in the compression zone corresponded to that of being across a tensile crack. A simple arithmetic mean of the measured curvatures would, therefore, not present an accurate picture of the average curvature. To obtain an accurate value for the experimental average curvature the average measured values for the top fibre strain and additional strain in the reinforcement were substituted into equation 6.2.17.

In a small number of beams the strain profiles were measured at five different sections within the constant moment zone. Figures 6.2.4 and 6.2.5 illustrate typical variations in the neutral axis depth, top fibre strain and curvature in this region. Figures 6.2.4(a) and 6.2.5(a) also show the average neutral axis depth calculated using equation 6.2.18 below, the average compressive strain and additional steel strain were measured.

$$n = \left(\frac{\varepsilon_1}{\varepsilon_1 + \varepsilon_{seam}} \right) d_e \qquad (6.2.18)$$

The average top fibre strain, shown in (b), and average curvature from equation 6.2.17 is also shown in (c). Curvature was

VARIATION IN NEUTRAL AXIS DEPTH, TOP FIBRE STRAIN AND CURVATURE FOR BEAM C7

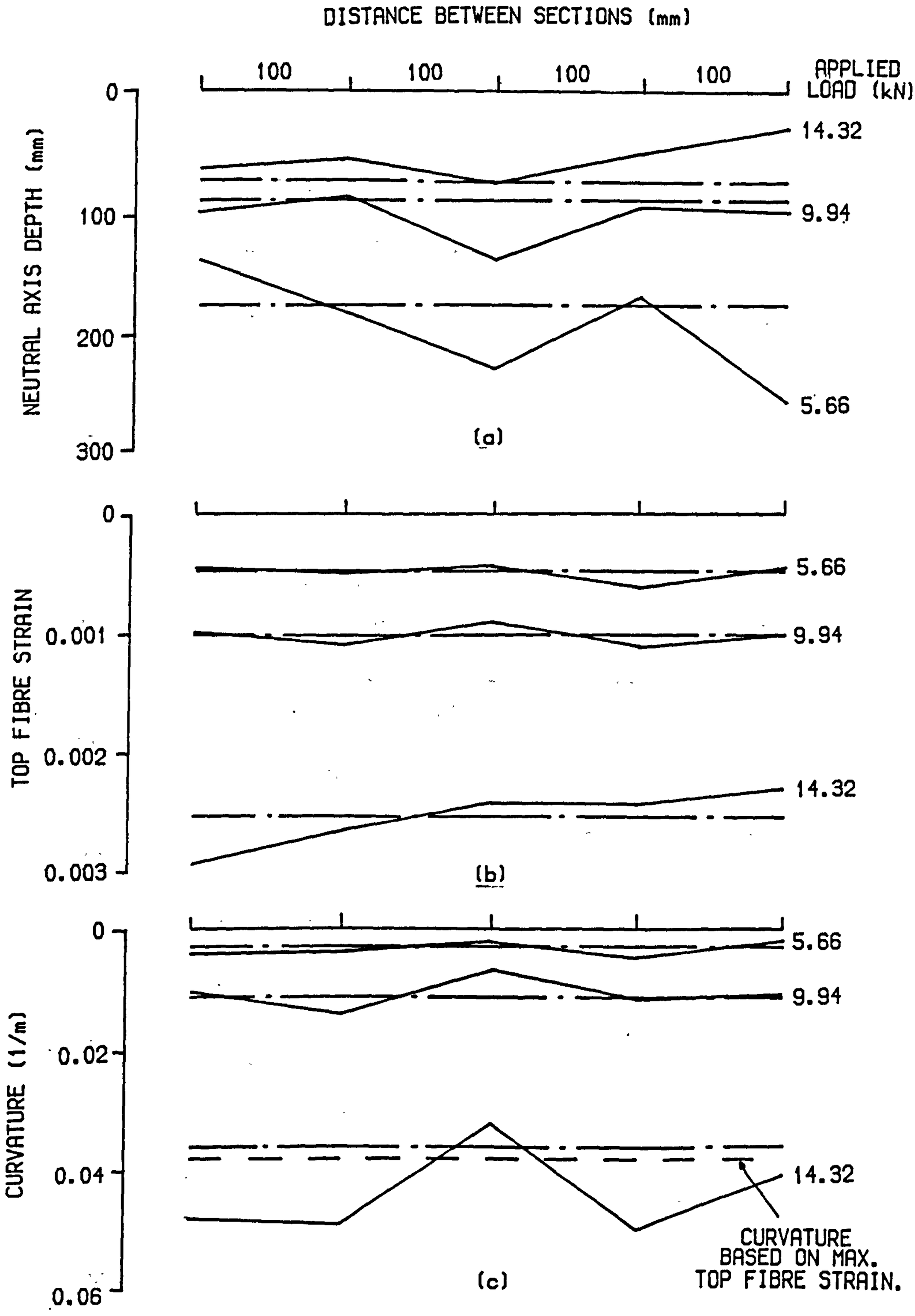

Figure 6.2.4

VARIATION IN NEUTRAL AXIS DEPTH, TOP FIBRE STRAIN AND CURVATURE FOR BEAM C8

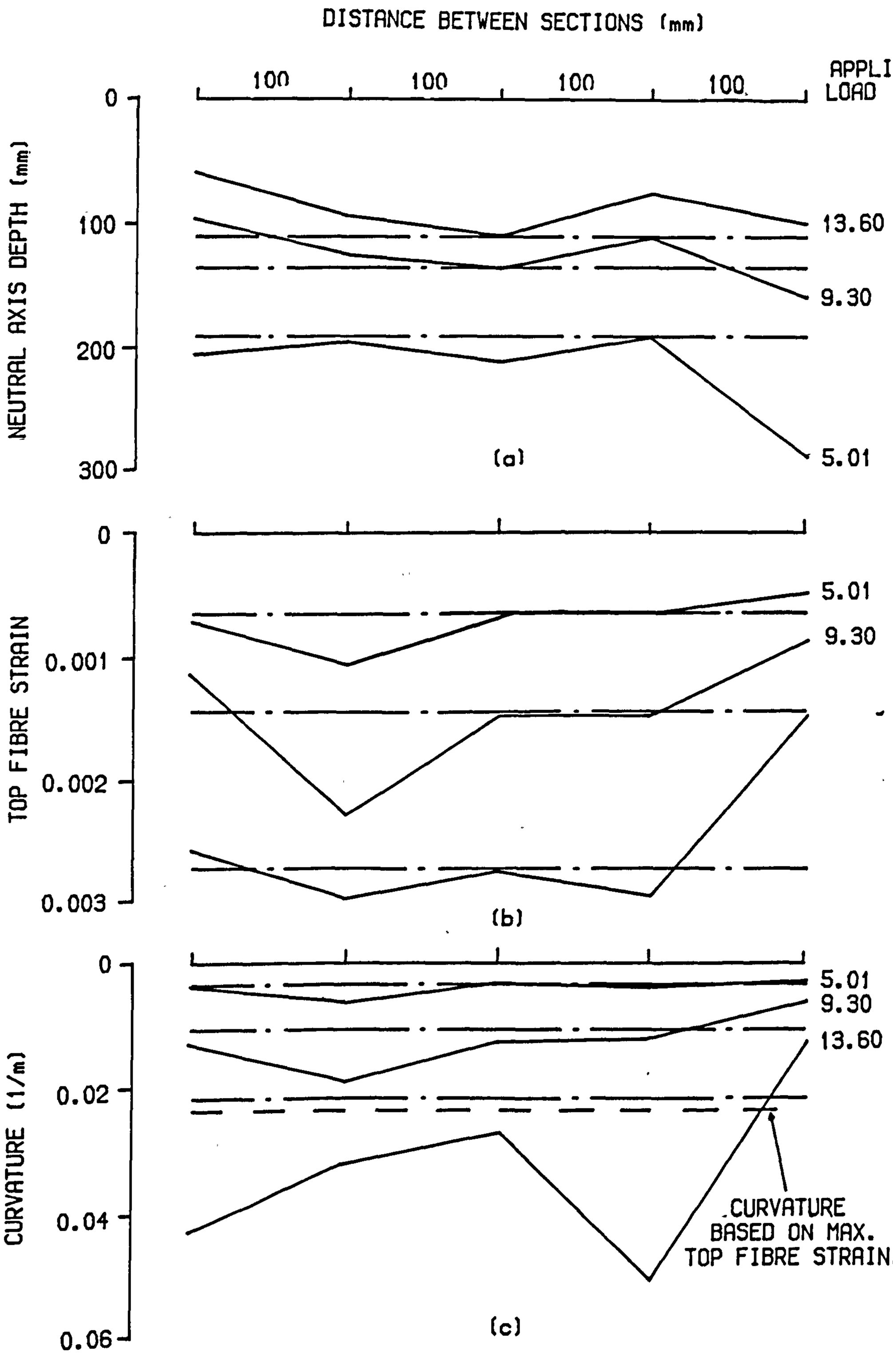

Figure 6.2.5

also calculated using the maximum top fibre strain, the difference of which with the curvature based on average compressive top fibre strain was not greater than 3 - 5%, justifying the assumption made in the theoretical analysis.

The average moment-curvature relationships for a number of the test beams are presented in figures 6.2.6 - 6.2.13. The characteristics of each curve were identical to the corresponding curve of the moment-curvature relationship across a crack, section 5.5. The three phase relationship was exhibited by most beams except those that failed in shear.

The magnitude of the average curvature was less than the corresponding curvature across a crack, figures 5.5.1 - 5.5.12, due to the tension-stiffening effect of the brickwork/concrete. Comparing the moment-curvature relationship across a crack with the corresponding average relationship for all beams show that at cracking the difference in curvature was insignificant. The difference between maximum and average curvature increased with increasing moment, the reduction in maximum curvature due to the tension-stiffening of the brickwork/concrete was by as much as 20 - 25%. The tension-stiffening effect had a significant influence upon behaviour of the beams. The effect was independent of brickwork strength and so similar reductions were exhibited by medium and low strength brick beams as well as the beams built of grade II mortar.

The experimental results are compared with the theoretical method using the axially loaded single course brickwork prism properties. Comparison with the predicted behaviour show a good

AVERAGE MOMENT-CURVATURE RELATIONSHIP FOR BEAM SERIES A

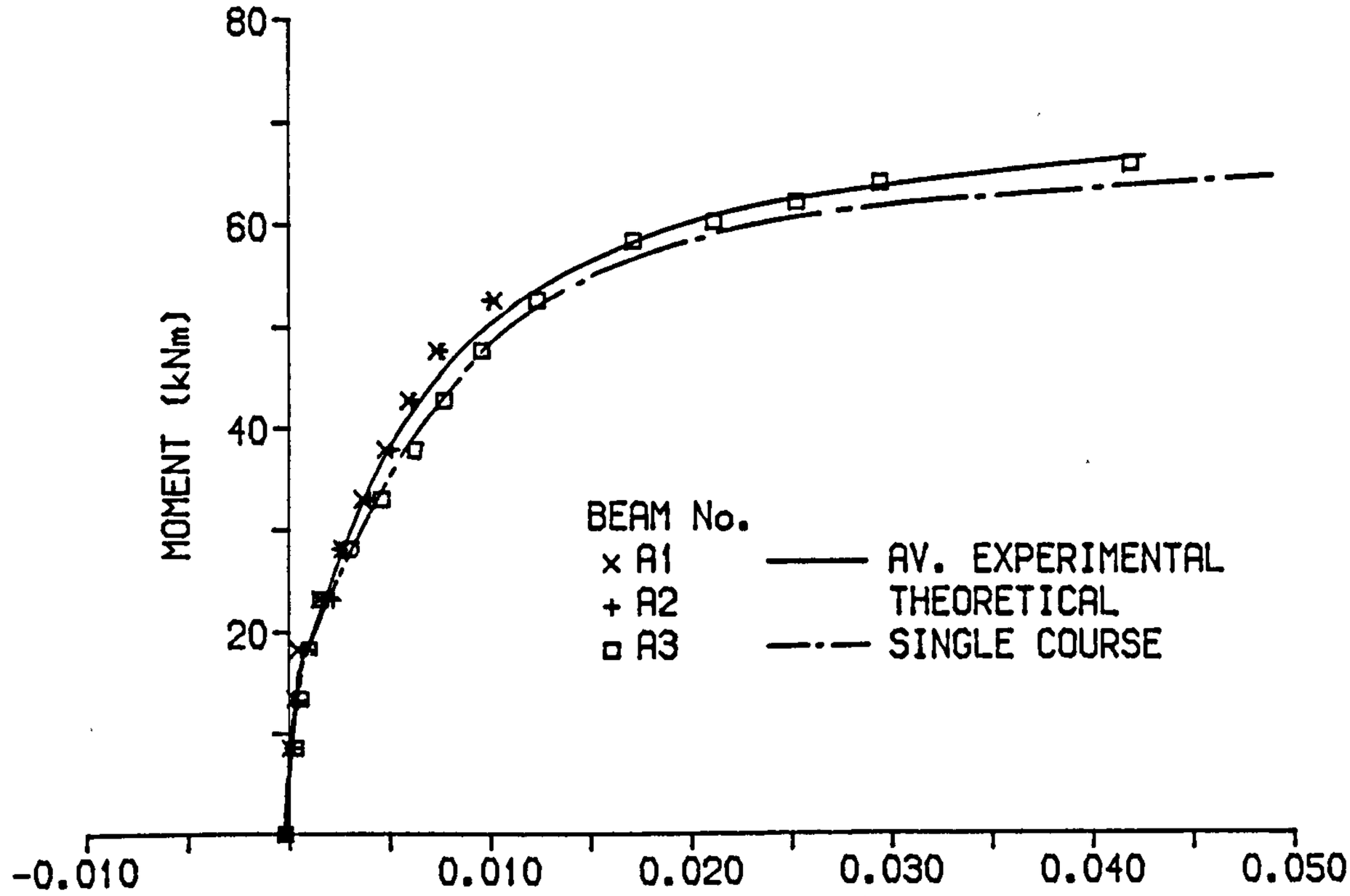

Figure 6.2.6

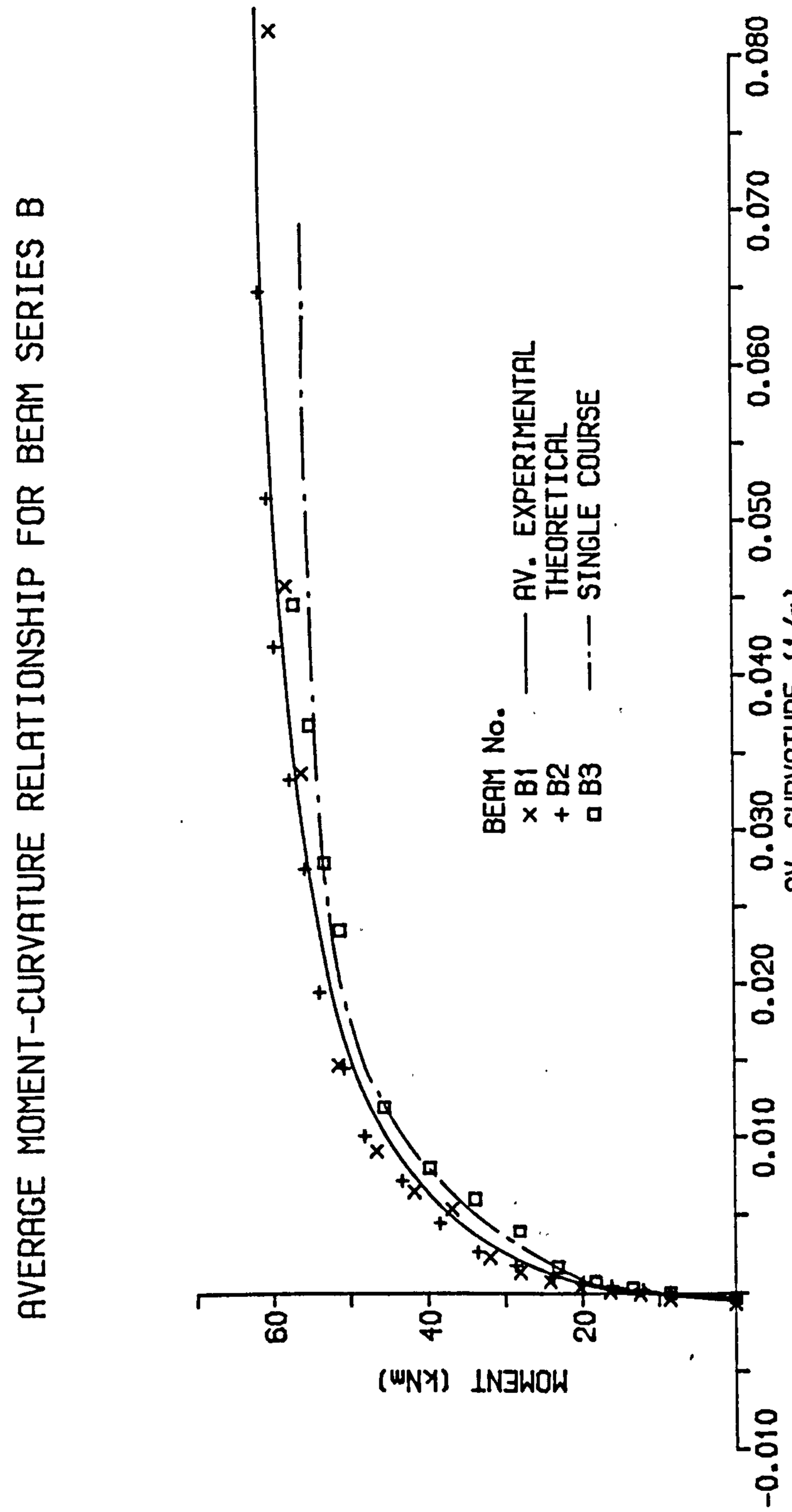
AVERAGE MOMENT-CURVATURE RELATIONSHIP FOR BEAM SERIES B
MOMENT (kNm)
60
40
20
0.010
0.020
0.030
0.040
0.050
0.060
0.070
0.080
AV. CURVATURE (1/m)
BEAM No.
× B1 —— AV. EXPERIMENTAL
+ B2 —— THEORETICAL
□ B3 —·— SINGLE COURSE

Figure 6.2.7

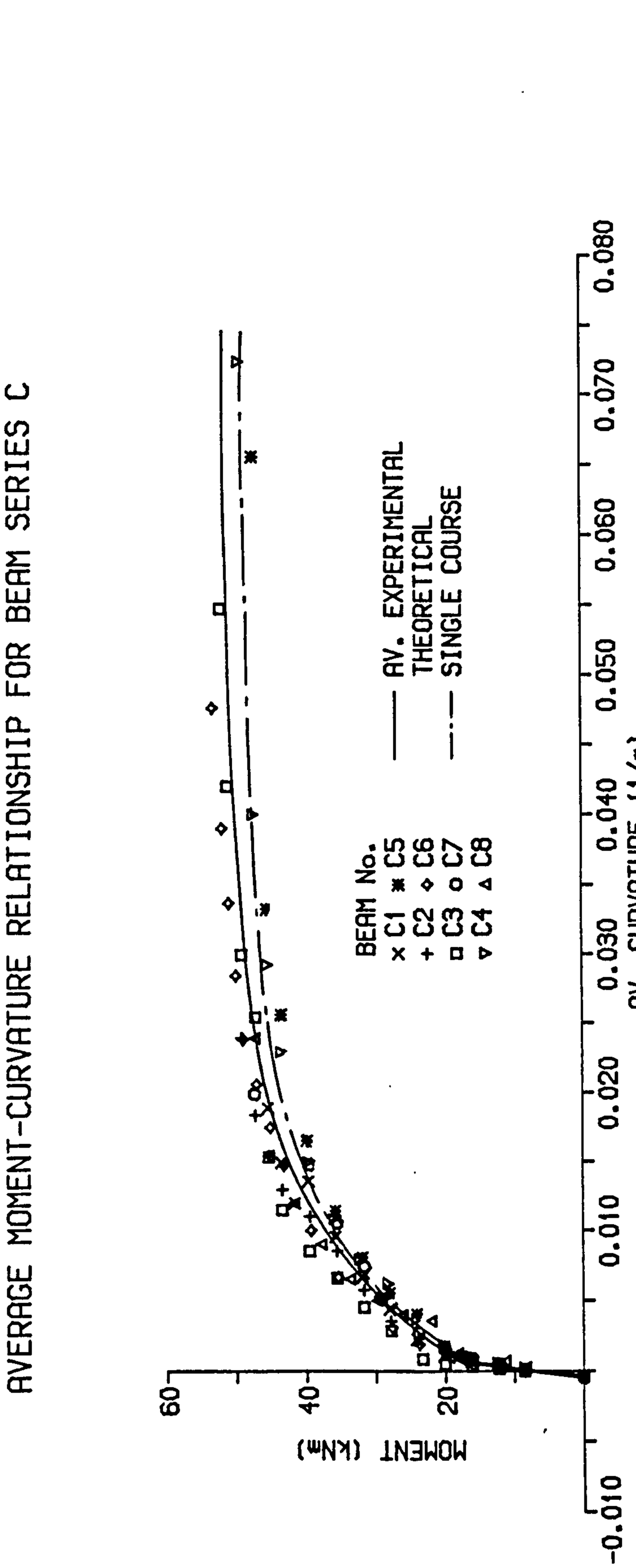
AVERAGE MOMENT-CURVATURE RELATIONSHIP FOR BEAM SERIES C
BEAM No.
× C1 ✱ C5
+ C2 ◇ C6
□ C3 ○ C7
▽ C4 △ C8
—— AV. EXPERIMENTAL
THEORETICAL
—·— SINGLE COURSE
MOMENT (kNm)
60
40
20
0.030
0.040
0.050
0.060
0.070
0.080
0.020
0.010
AV. CURVATURE (1/m)

Figure 6.2.8

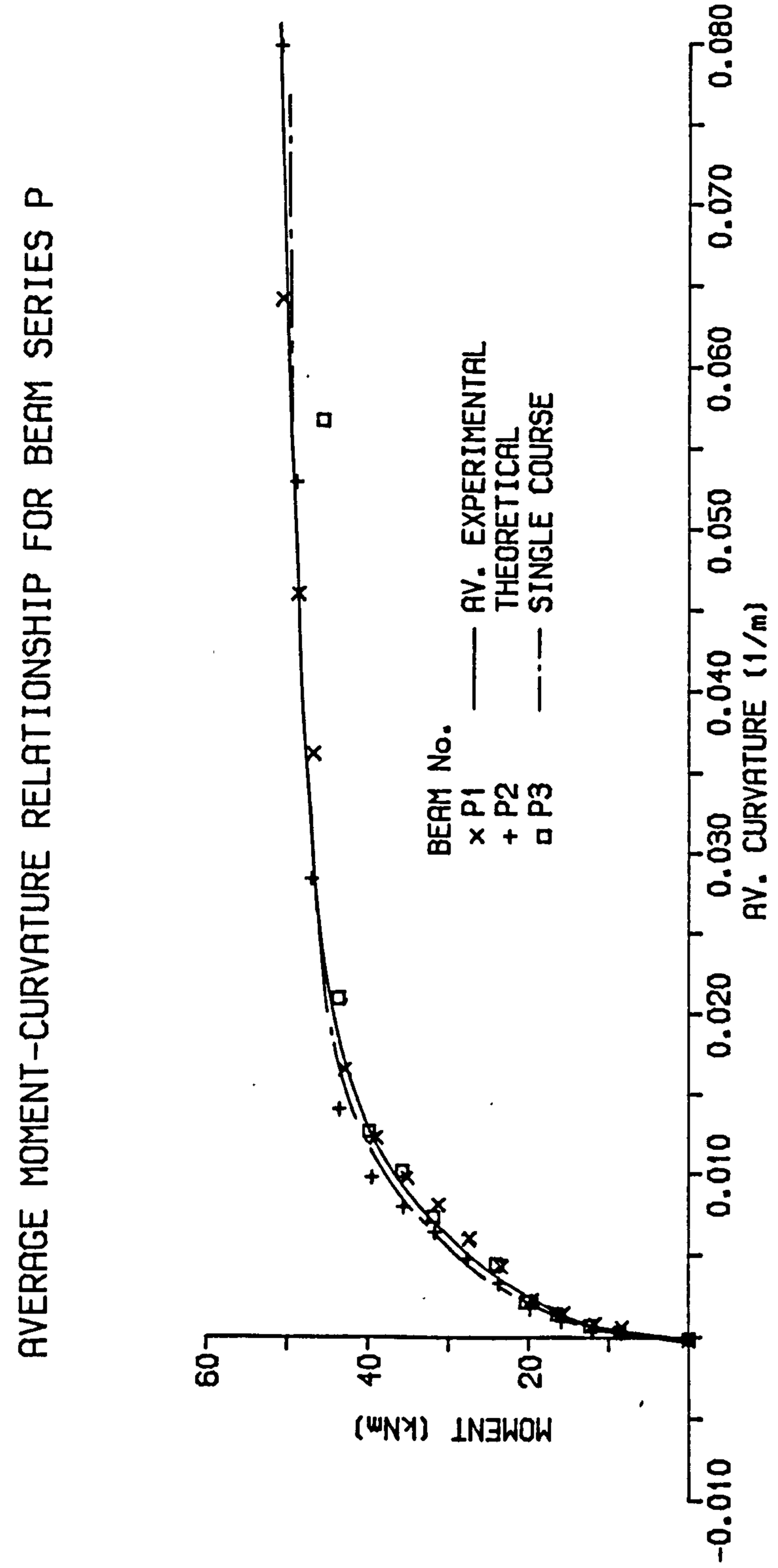
AVERAGE MOMENT-CURVATURE RELATIONSHIP FOR BEAM SERIES P
BEAM No.
× P1
+ P2
□ P3
—— AV. EXPERIMENTAL
THEORETICAL
—·— SINGLE COURSE
MOMENT (kNm)
60
40
20
0.010
0.020
0.030
0.040
0.050
0.060
0.070
0.080
AV. CURVATURE (1/m)

Figure 6.2.9

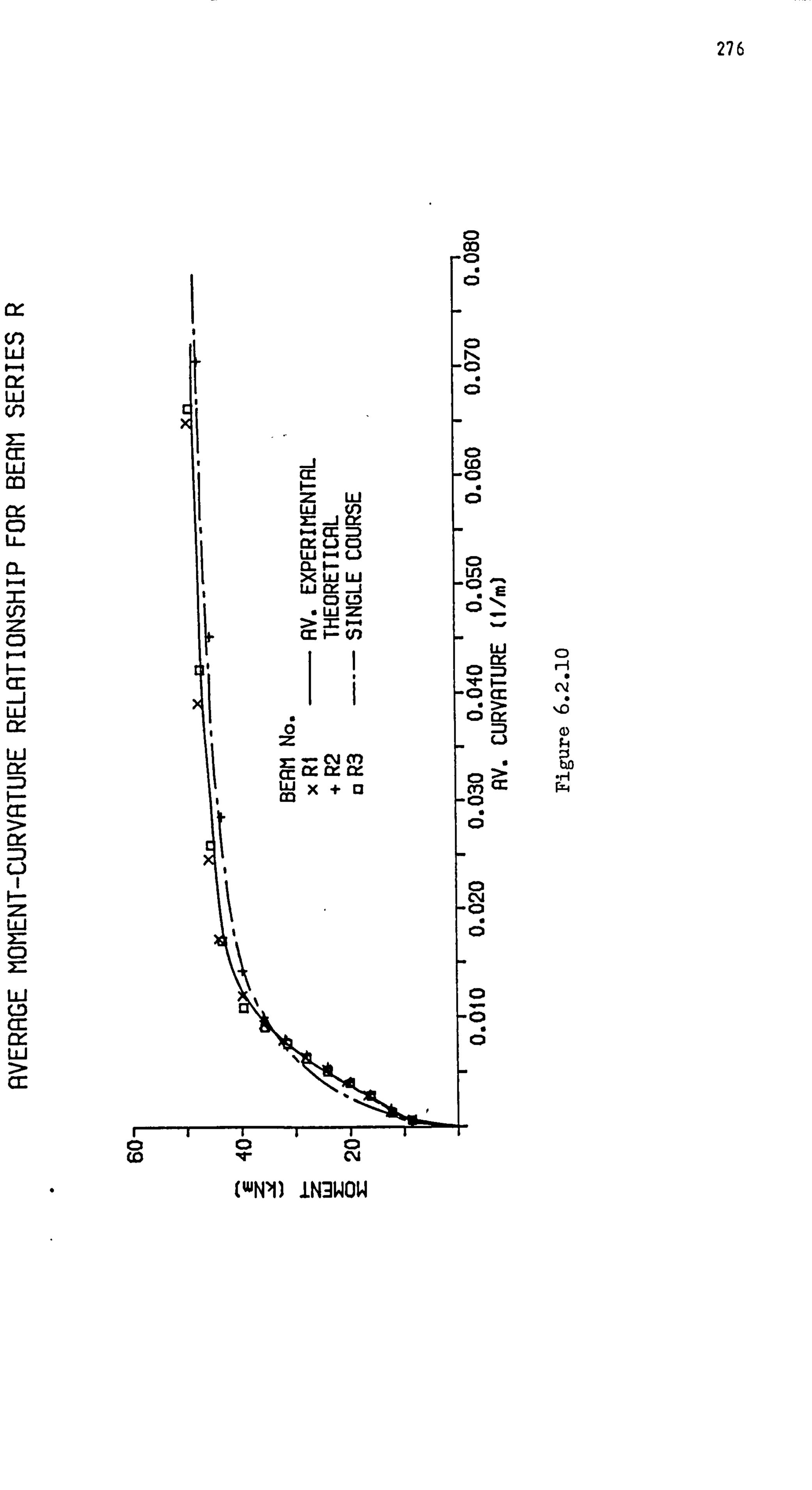
AVERAGE MOMENT-CURVATURE RELATIONSHIP FOR BEAM SERIES R
BEAM No.
× R1
+ R2
□ R3
—— AV. EXPERIMENTAL
THEORETICAL
—·— SINGLE COURSE
MOMENT (kNm)
60
40
20
0.010
0.020
0.030
0.040
0.050
0.060
0.070
0.080
AV. CURVATURE (1/m)

Figure 6.2.10

AVERAGE MOMENT-CURVATURE RELATIONSHIP FOR BEAM SERIES CM

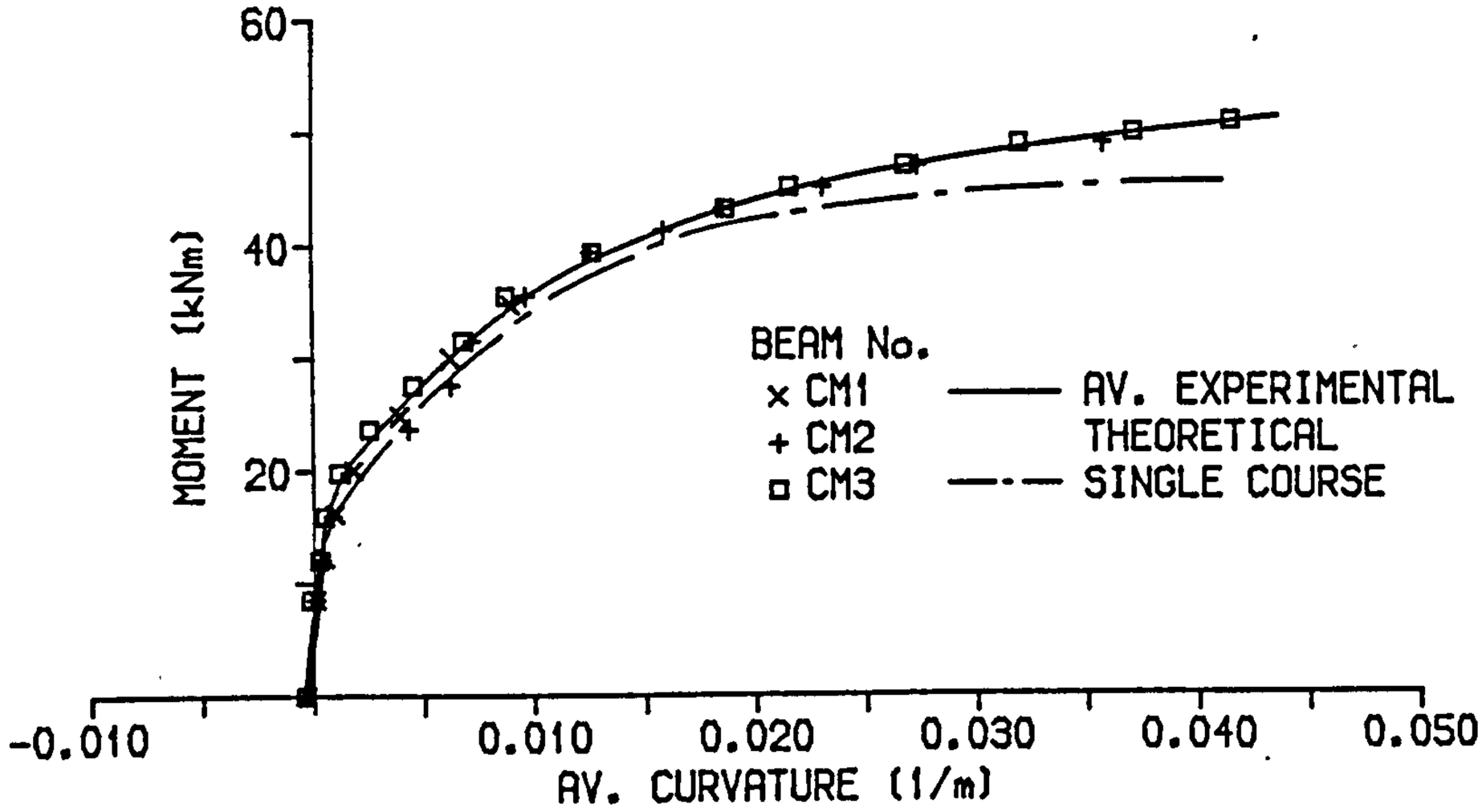

Figure 6.2.11

AVERAGE MOMENT-CURVATURE RELATIONSHIP FOR BEAM SERIES CL

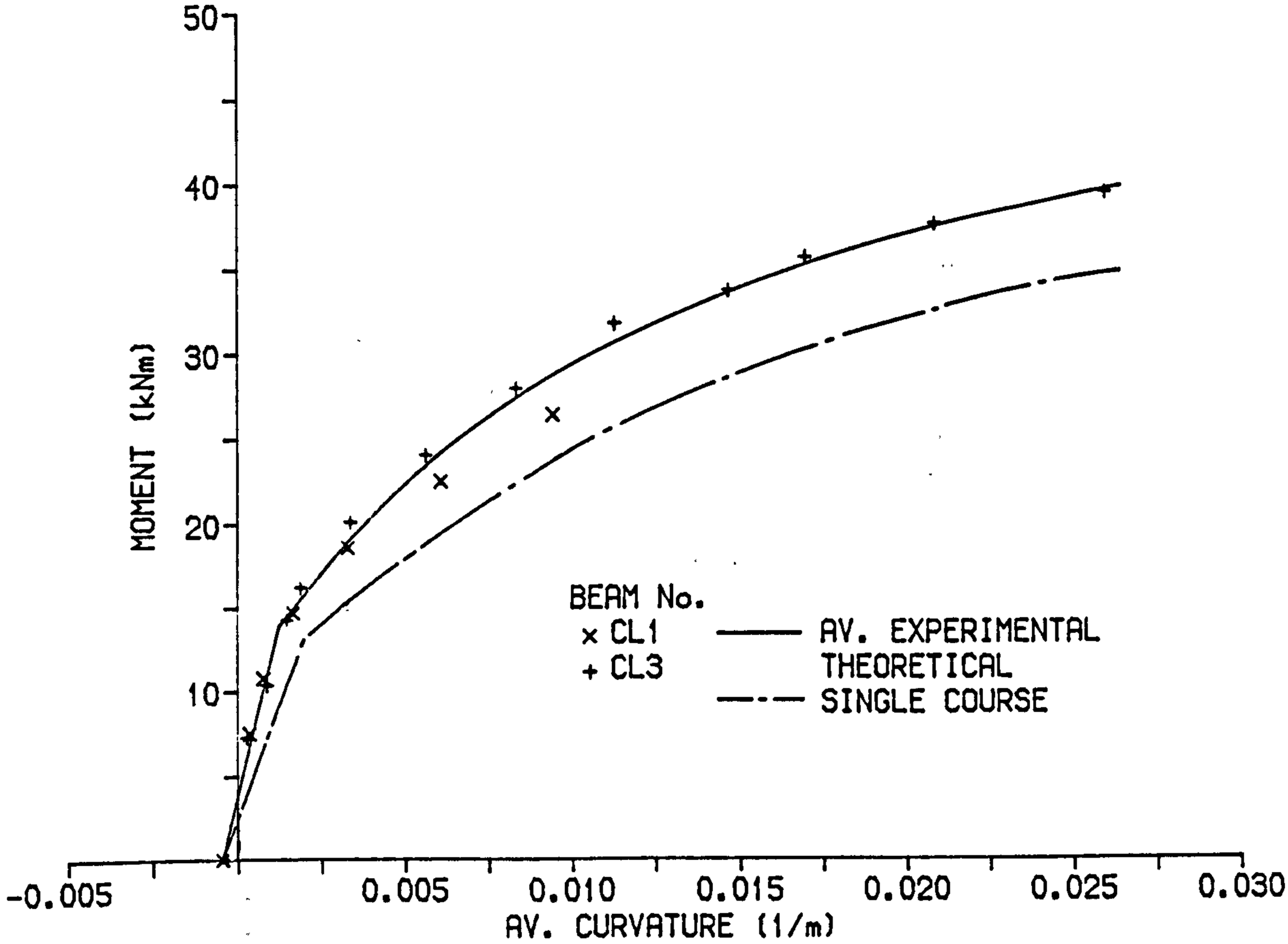

Figure 6.2.12

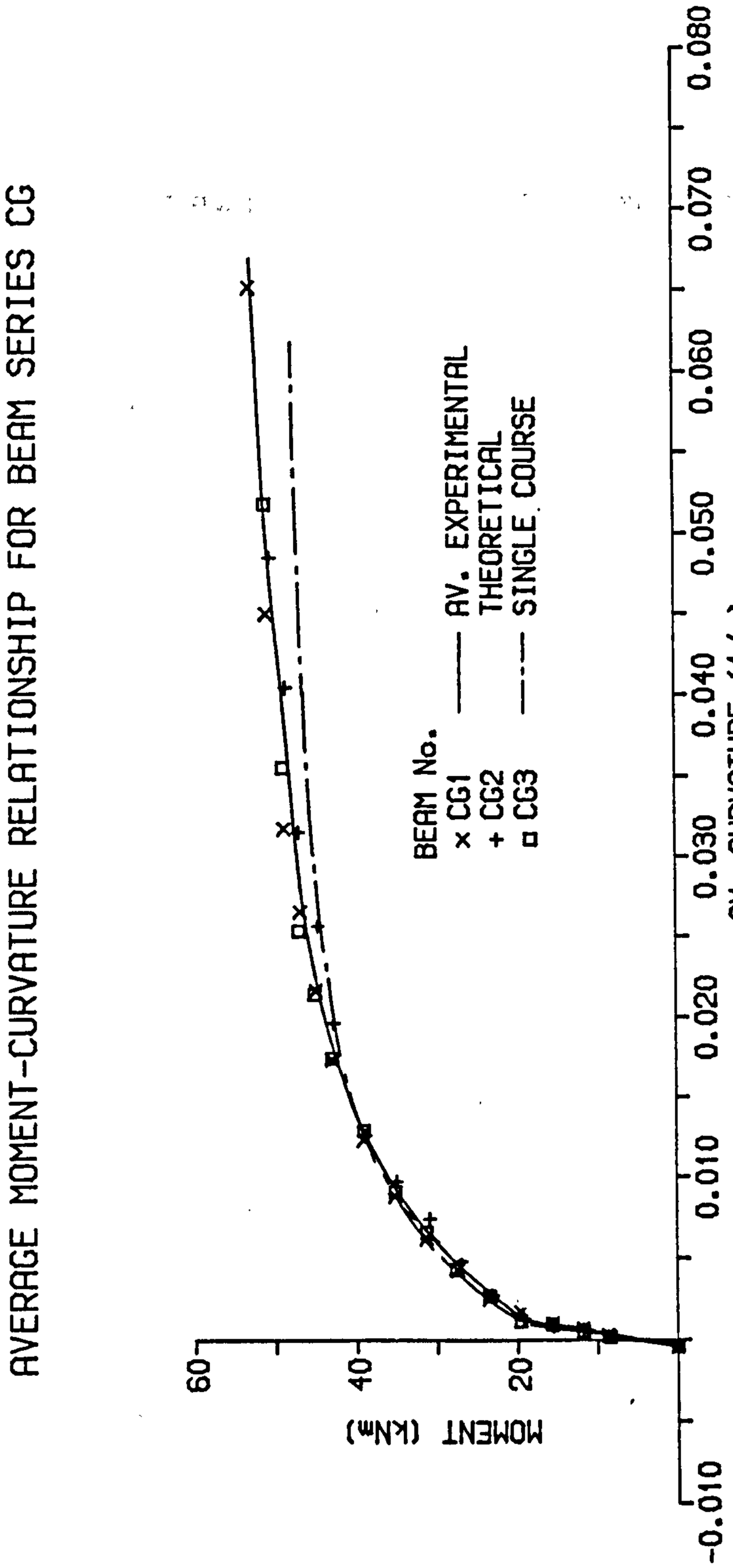
AVERAGE MOMENT-CURVATURE RELATIONSHIP FOR BEAM SERIES CG
BEAM No.
× CG1
+ CG2
□ CG3
—— AV. EXPERIMENTAL
THEORETICAL
—·— SINGLE COURSE
MOMENT (kNm)
60
40
20
0.030
0.040
0.050
0.060
0.070
0.080
AV. CURVATURE (1/m)
0.020
0.010

Figure 6.2.13

correlation for all beams except the low strength brick beams, series CL. Equation 6.2.16, therefore, provides an accurate indication of the tension-stiffening behaviour of the beams tested in this work.

6.3 CRACKING OF PARTIALLY PRESTRESSED BRICKWORK BEAMS

In this section two theoretical methods to predict the cracking in partially prestressed brickwork beams are presented. Firstly the crack widths are predicted from the average strain in the reinforcement, a continuation of the direct method used to predict the moment-curvature and deflection, chapter 4. An alternative method more suited to design, based on the fictitious tensile stresses in the brickwork, is also proposed. The results of a comprehensive series of readings of crack widths taken during testing of the beams are presented and the theoretical predictions are compared.

6.3.1 Theory

The three most widely used methods of predicting the crack widths in partially prestressed concrete are:

(i) methods in which the crack width is related to the stress in steel[65 - 67]

(ii) methods in which the crack widths are related to fictitious tensile stress in the concrete[65,68]

(iii) use of average surface/steel strain [69,71]

Abeles[73] seems to have been the first engineer to relate crack widths to the fictitious tensile stress in the concrete. The fictitious stress is the stress which would develop in the concrete (brickwork) if it were of sufficient strength to remain uncracked. Subsequently a number of authors[65,68] have proposed expressions to predict crack widths in partially prestressed concrete beams based upon this concept. It has also been adopted into the British standard code of practice for structural concrete[36].

The basis of the method using fictitious tensile stress to calculate crack widths is somewhat irrational and the accuracy of the predictions are extremely variable. The main advantage is its simplicity and it is therefore useful in the initial design stages for dimensioning the section and calculating the amount of prestress required.

Krishna Raju et al[68] developed the following expression to predict the crack widths using the fictitious tensile stress after testing a number of partially prestressed concrete beams:

$$w = \frac{R}{p_e} \; c \; fct \qquad (6.3.1)$$

where p_e = percentage of non-tensioned reinforcement and R a factor defining the bond characteristics of the steel. The term p_e was introduced after tests suggested that the area of non-tensioned steel had a significant effect upon the crack widths.

Beeby et al[71] and Desayi[69] proposed that the average crack width may be determined from the average crack spacing and

steel strain, thus:

$$w = S_m \varepsilon_s \qquad (6.3.2)$$

Equation 6.3.2 is not wholly correct since there will be a recovery of strain between the flexural cracks and thereby reducing the average strain. Generally this effect is very small in comparison with the total strain and so is ignored.

Previous research[69] has shown there to be a close correlation between average crack width and average surface strain, the method has been successfully used to predict crack widths of partially prestressed concrete beams.

In the only previous attempt to predict crack widths in either reinforced or prestressed brickwork beams Pedreschi[9] proposed that the average crack widths are given by:

$$w_{av} = (N_j + 0.41)b_j \varepsilon_{smb} \qquad (6.3.3)$$

A good agreement was found between experimental and predicted crack widths. This approach was developed for predicting the crack widths in the partially prestressed brickwork beams.

6.3.1.1 Crack widths based on average strain

Prediction of the crack widths relies upon accurate estimation of the average strain and crack spacing, equation 6.3.2. However, as part of the theoretical prediction of the average

moment-curvature relationship, section 6.2.1, the average additional strain in the reinforcement was calculated and so the problem is reduced to determining the average crack spacing.

Consider a flexural member in which the first crack has occurred, figure 6.3.1, the surface stress will be zero at the crack and will gradually increase until at some distance, S_o, the level of stress will be unaffected by the flexural crack. Since the crack has reduced the surface stress to less than the modulus of rupture a distance of S_o either side of the crack a second crack cannot form within this distance and hence S_o is the minimum crack spacing. If a second crack occurs at a distance greater than $2S_o$ this means that there is sufficient length between the two cracks for a third crack to appear. If, however, the second crack forms at a distance less than $2S_o$ there will be insufficient length for a third crack to appear. The average crack spacing will therefore be between S_o and $2S_o$ and so the problem of determining the crack spacing becomes one of predicting the minimum crack spacing S_o.

In deriving the theory to predict the minimum crack spacing in partially prestressed brickwork beams it is necessary to briefly consider the work conducted on concrete beams. Fundamentally two methods of determining the minimum crack spacing in reinforced concrete members have evolved. The first of these, the 'classical' approach[74], assumes that plane sections remain plane. For this to hold good there is relative displacement or slip between the reinforcement and the concrete. As bond failure has taken place the distribution of bond stresses along the reinforcment is assumed to be a function of the ultimate bond strength. Minimum crack spacing is

CRACK SPACING

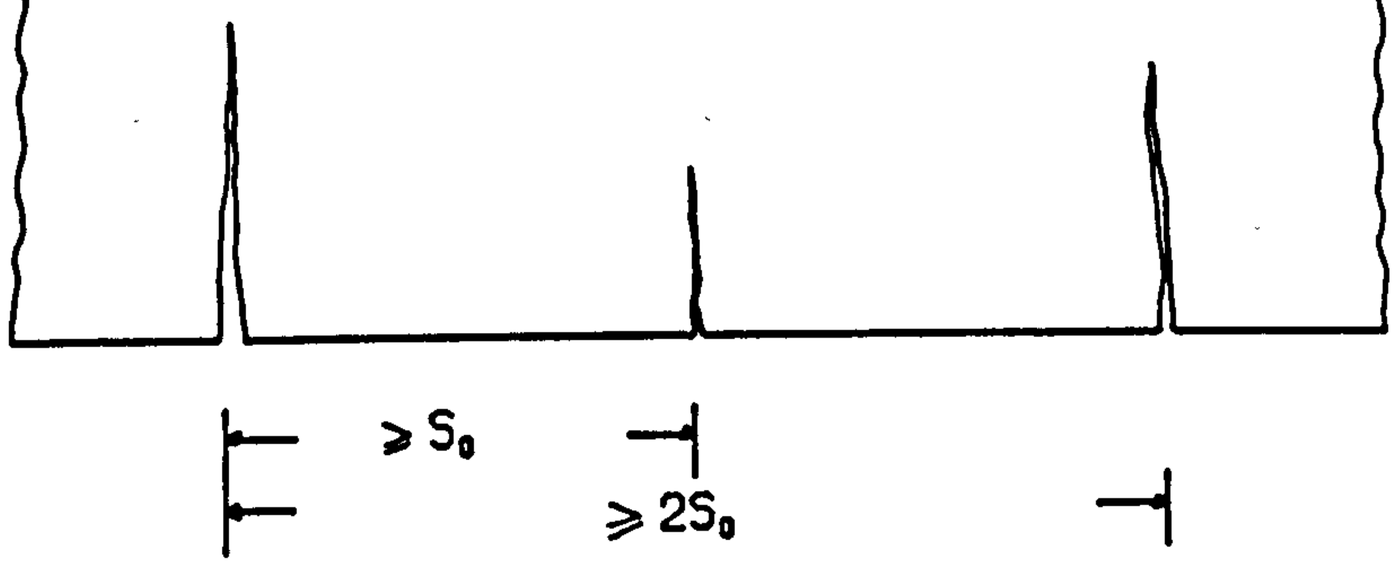

Figure 6.3.1

NO SLIP MECHANISM OF CRACKING:
RELATIONSHIP BETWEEN AND S_0

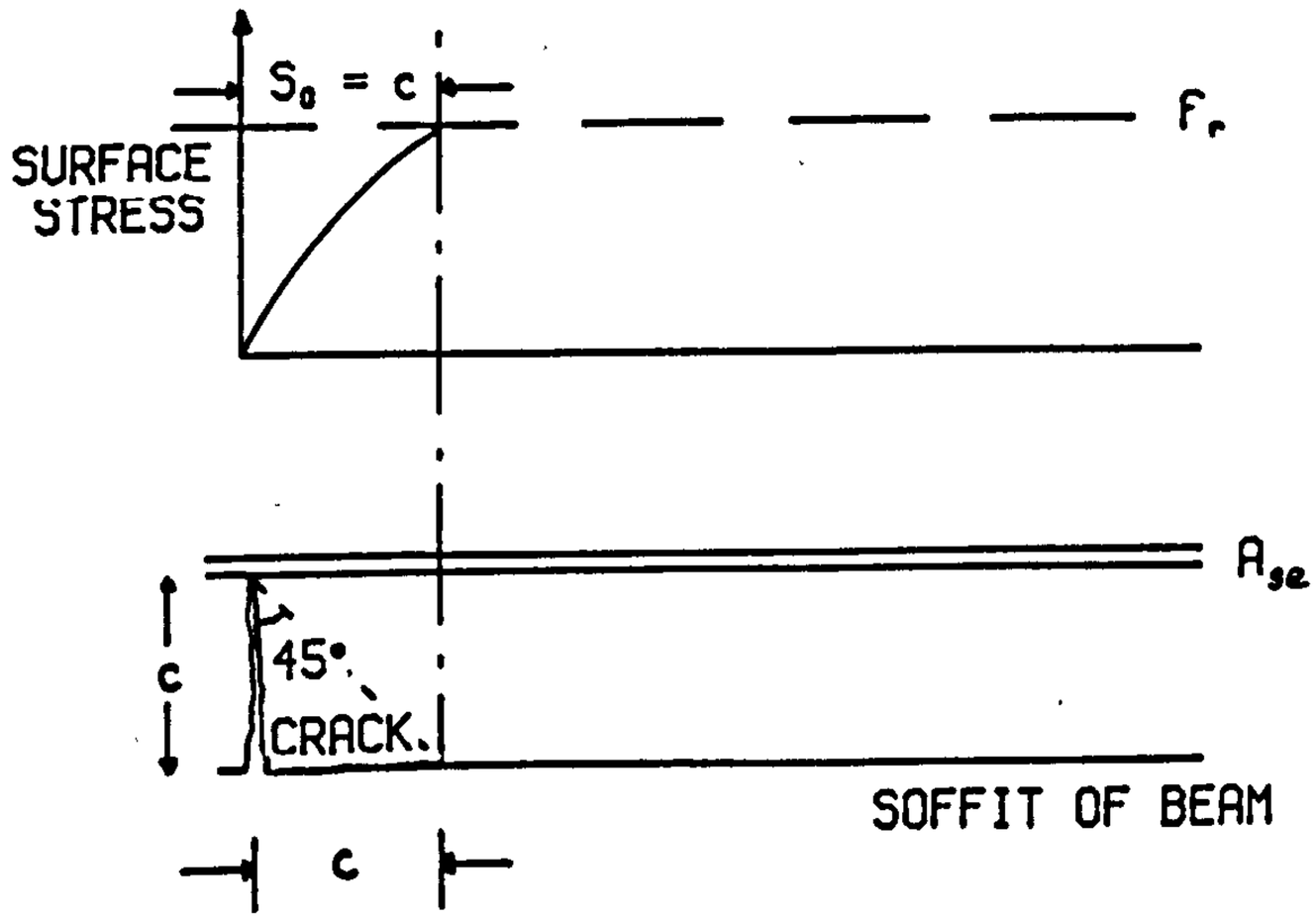

Figure 6.3.2

thus obtained by equating the bond length required to transmit sufficient tensile force from the reinforcement through the bond stresses to overcome the tensile strength of the concrete[67,69]. Problems arise in defining exactly the effective area of concrete which resists the tensile forces, it is usually found from correlation with experimental results.

An alternative method, the 'no-slip' approach[74], is based on assumptions in direct contradiction of the previous method. Plane sections are assumed to no longer remain plane and so bond failure does not occur and hence no-slip. As bond failure has not occurred the crack width at the reinforcement-concrete interface will be zero and maximum at the surface of the concrete. Using elastic theory the minimum crack spacing was shown to be equal to the cover to the reinforcement, figure 6.3.2.

Beeby[75] later proposed that the crack pattern and spacing at any given point results from a combination of both effects. Deformation as per the 'no-slip' theorem must occur since at a crack plane sections do not remain plane, causing a reduction in surface stresses. Some bond failure or slip is likely to occur and will cause a further reduction in stresses and so increasing the minimum crack spacing, S_o. The actual crack spacing is a sum of the two component effects.

The theory described so far has generally been confined to considerations of pure tension members which have been assumed to be equally applicable to the conditions in the soffit of a flexural member. This is not necessarily the case except in very deep beams

and so Beeby[75] introduced further theoretical considerations to account for the behaviour of reinforced concrete beams.

If an axial load is applied with sufficient eccentricity to an unreinforced concrete column tension will be introduced into the section, figure 6.3.3. As the load is gradually increased it will eventually reach a magnitude that will cause cracking of the concrete, but the column will not collapse. Cracking will, however, cause a redistribution of the stresses across the section, figure 6.3.3. The crack will form to an initial height, h_o. Assuming a 45° stress distribution Beeby[75] showed that the distance away from the crack at which the stress distribution was unaffected, crack spacing was equal to h_o. The influence of adding reinforcement to the section would be to increase the neutral axis depth and reduce the initial crack height, not to remove it altogether.

The spacing of the cracks is defined between limits set by the cover and the initial crack height, h_o. Crack spacing at any section will be a combination of the two effects influenced by the degree of bond slip. In very deep beams, where conditions at the soffit are very similar to those of the uniaxial tension specimen, the crack spacing will be controlled by the cover. In shallow sections with a low percentage of tensile reinforcement, such as slabs, the initial crack height will be the controlling influence.

The theory discussed until now has been concerned solely with reinforced concrete members and although the method should be equally applicable to prestressed concrete beams Beeby[71,75] recognised that a problem may arise in defining the initial crack

CRACKING IN AN UNREINFORCED MEMBER

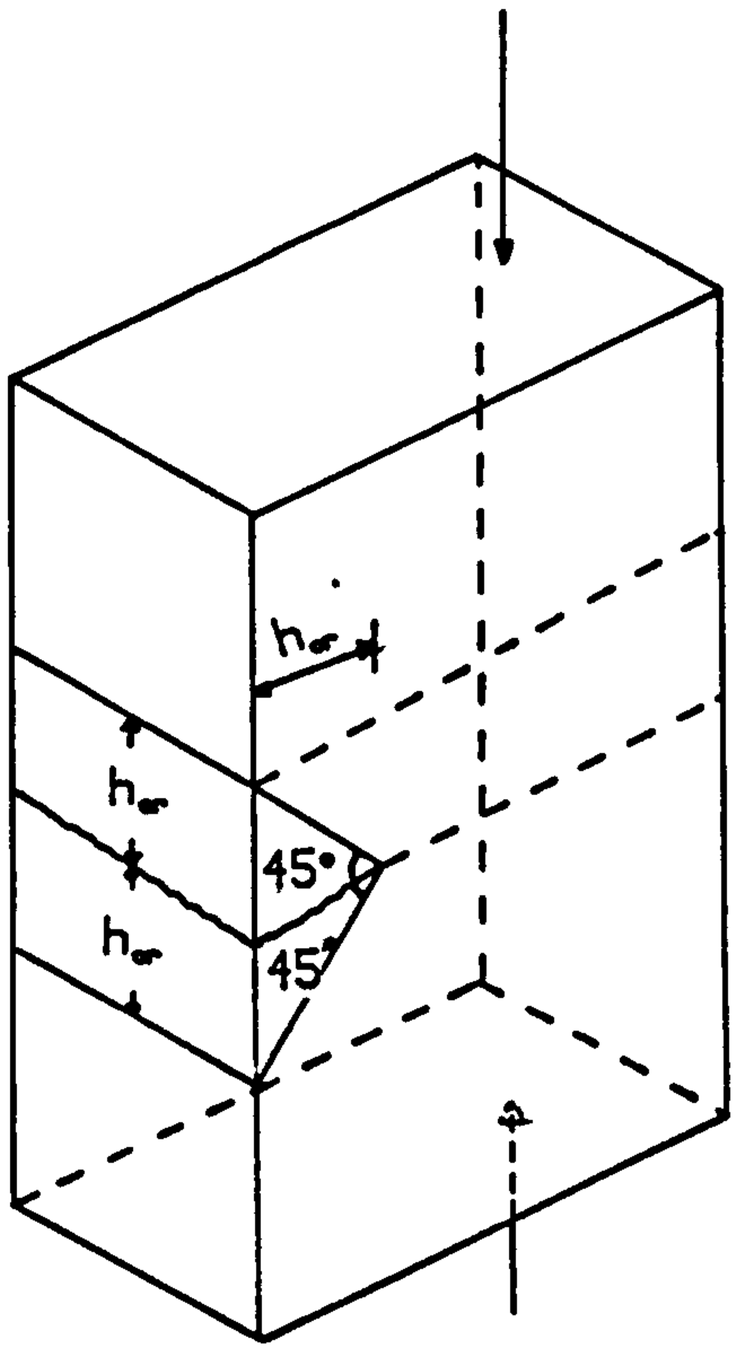

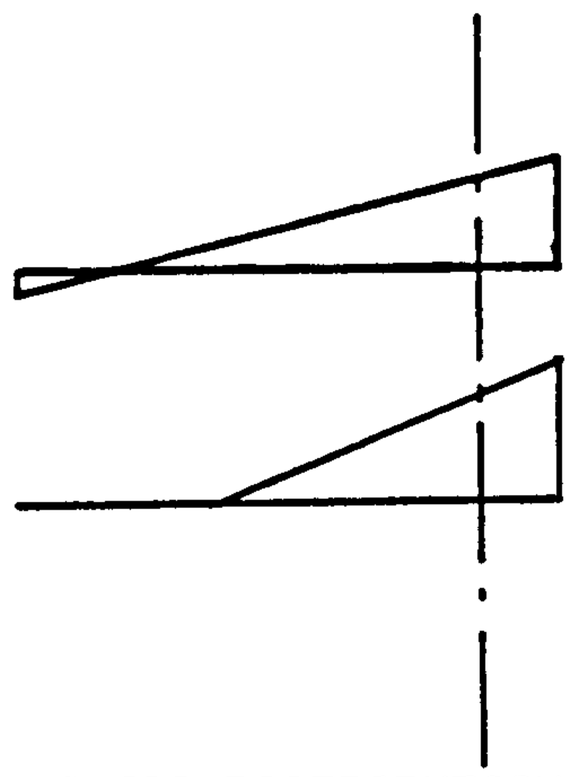

STRESS DISTRIBUTION

Figure 6.3.3

height. In reinforced concrete members an initial crack height immediately after cracking is apparent, figure 6.3.4, beyond this value the crack height does not increase greatly. In partially prestressed concrete beams it is possible for the initial crack height to be completely absent, a variation of crack height with moment as shown in figure 6.3.5. In tests conducted on prestressed concrete beams with unbonded tendons the crack spacing was seen to be dependent upon the height of the cracks and that no initial crack height was present[76]. To overcome this problem and yet maintain the validity and integrity of the theory Beeby[71] proposed that when h_o was not present it should be replaced by a controlling crack height defined by:

$$\partial\left(\frac{h_{cr}}{h}\right) \Big/ \partial\left(\frac{M}{bd^2 fr}\right) = 1 \qquad (6.3.4)$$

Thus when the rate of increase in crack height equals that of the moment the crack height is taken as h_o. Beyond this point the curve will flatten off and hence h_o assumes a similar defining parameter as for reinforced concrete beams.

The cracking behaviour of reinforced and prestressed brickwork beams differs somewhat from concrete. The tensile strength of concrete is relatively uniform along the length of the beam. In brickwork, however, cracking is more likely to occur at the brick/mortar interface where the flexural tensile strength is weakest. The crack spacing will, therefore, be likely to form at intervals coincident with the mortar joints. Cracking may not necessarily occur at every joint but at multiples of the distance between the joints, b_j, figure 6.3.6.

RELATIONSHIP BETWEEN MOMENT AND CRACK HEIGHT FOR REINFORCED CONCRETE BEAM[71]

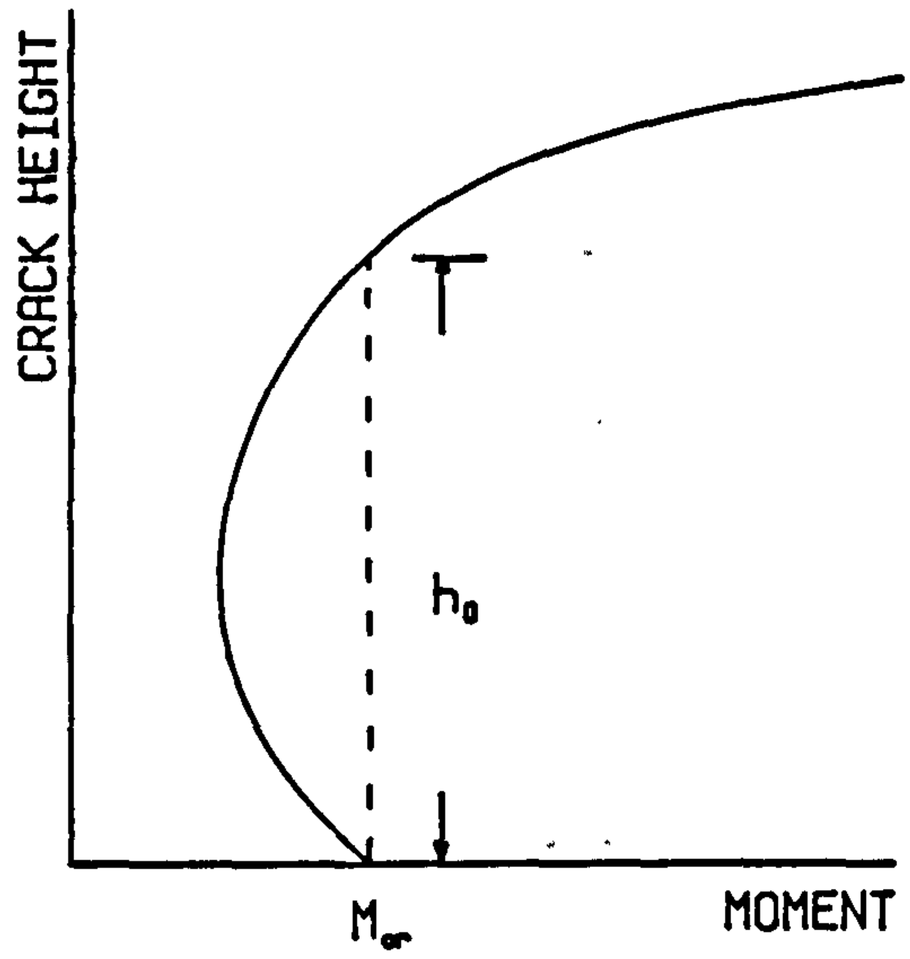

Figure 6.3.4

POSSIBLE RELATIONSHIP BETWEEN MOMENT AND CRACK HEIGHT FOR PRESTRESSED BEAM

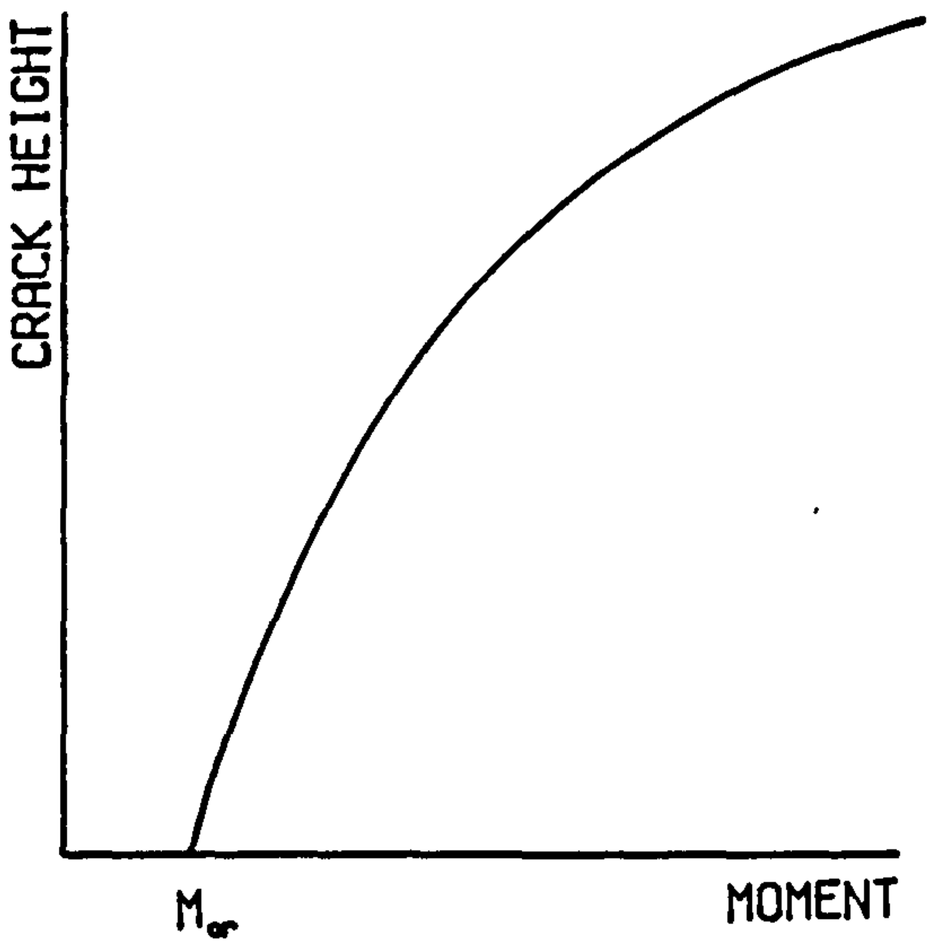

Figure 6.3.5

CRACK SPACING IN BRICKWORK BEAM

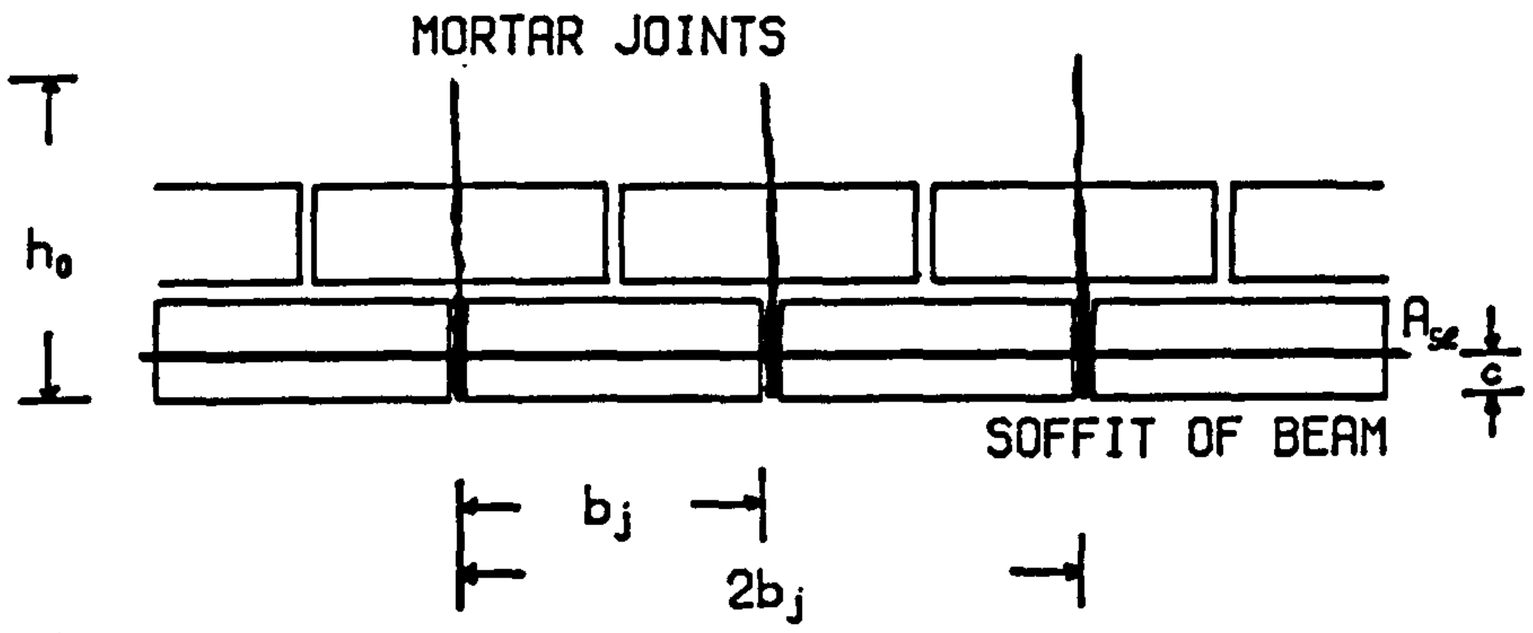

Figure 6.3.6

Average crack spacing will be some multiple of b_j which, as defined by Beeby[75], will be controlled primarily by the limits of the cover and initial, or controlling, crack height. Following this, it is possible to establish criteria for determining the average crack spacing in partially prestressed brickwork beams. For example, when the cover to the reinforcement is greater than b_j the average crack spacing will be greater than b_j and if h_o is greater than $2b_j$ but less than $3b_j$ the average crack spacing will be $2b_j$. If the cover is much less than b_j then the crack spacing will be equal to b_j.

The distance between joints at the soffit of the reinforced and partially prestressed brickwork beams tested was 225 mm throughout. The cover remained constant at 25 mm in all beams except beams CC1 - CC3 where cover was increased to 50 mm. Clearly the theory indicated that the average crack spacing will be equal to b_j, 225 mm, in all beams. Experimental observation in the constant moment zone supports this since in all beams without exception the maximum, average and minimum crack spacing were equal to 225 mm.

Typical experimental crack propagations for test beams are shown in figure 6.3.7. All beams shown were built from high strength bricks but with varying amount of reinforcement and prestress. Initially the cracks occur at the mortar joints and progress up the beams, with further loading cracking occurred through the bricks. At the soffit of the member the crack spacing was equal to 225 mm.

Following the discussion, equation 6.3.2 may be modified and

CRACK PATTERNS

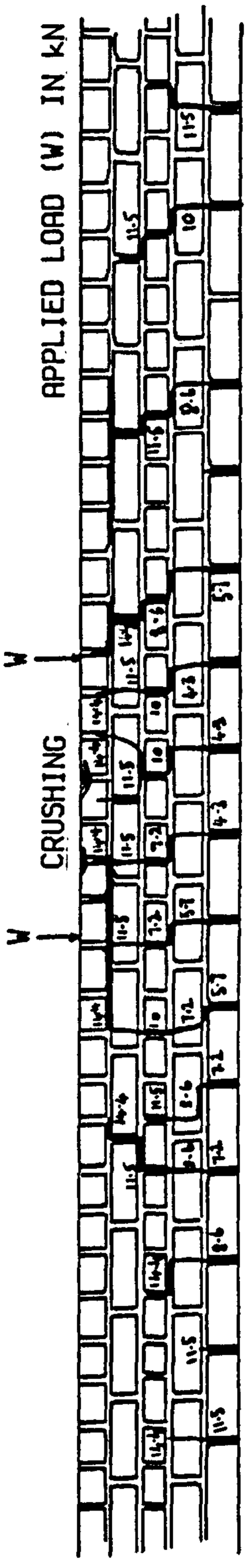

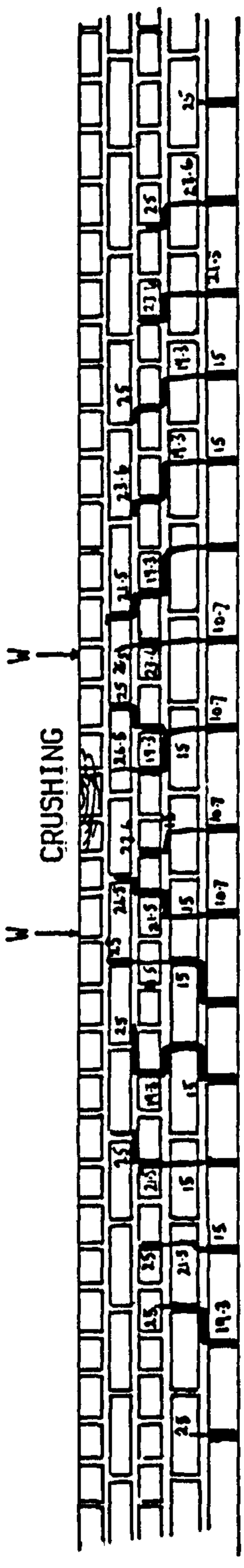

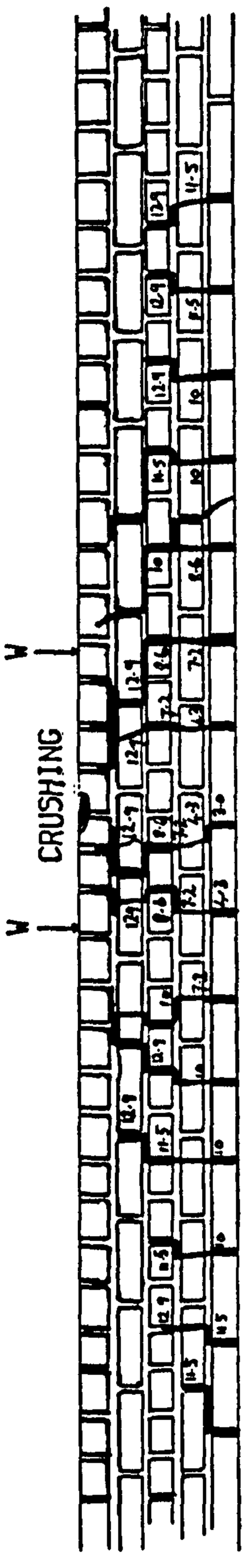

Figure 6.3.7

hence the average crack widths at or near the soffit of the beam can be calculated from:

$$w_{av} = b_j \varepsilon_{smb} \qquad (6.3.5)$$

Comparing this with the expression developed by Pedreschi[9] for fully prestressed brickwork beams, thus:

$$w_{av} = (N_j + 0.41)b_j \varepsilon_{smb} \qquad (6.3.6)$$

where N_j equals the number of joints between cracks.

In equation 6.3.5 N_j equals unity since the crack spacing was constant. Also the constant 0.41 is absent, it accounts for the likelihood of the average crack spacing exceeding the predicted spacing, derived by Pedreschi from comparison with experiments. This term will be zero in equation 6.3.5 as the maximum crack spacing in all beams was equal to the average crack spacing. The inconsistency between equations 6.3.4 and 6.3.5 results from the different bonding patterns, cover to reinforcement and steel percentages. Conditions in the fully prestressed brickwork beams[9] allowed greater flexibility for crack spacing, not all equal to b_j, whereas in the partially prestressed section cracking remained constant at b_j. Clearly further research is required to define a general expression for average crack spacing applicable for all bond patterns, cover and steel areas.

In the analysis to determine the theoretical

moment-curvature relationship the average additional strain in the effective area of tensile reinforcement was calculated. To predict the crack width the strain at the level of cracking considered is required, which can be obtained from:

$$\varepsilon_{smb} = \left(\frac{d_{cr} - n}{d_e - n}\right) \varepsilon_{seam} \qquad (6.3.7)$$

where d_{cr} is depth where cracking is considered. Values for ε_{seam} were obtained from the computational analysis using the single course prism properties.

6.3.1.2 Calculation of crack widths based on the fictitious tensile stress

The experimental relationship between the fictious tensile stress and average crack width is shown in figure 6.3.8. Although there is considerable variation it is apparent that a relationship exists and that it is dependent upon the amount of tensile reinforcement. Similarly the results of fully prestressed brickwork beams[9] are shown in figure 6.3.9 in an attempt to develop a general expression. In order to get a sufficient number of readings crack widths up to 0.5 mm have been considered, although for design purposes it is likely to be unnecessary to consider cracks beyond 0.2 mm.

It is clear from both figures that the percentage area of tensile reinforcement is a variable that requires consideration in the analysis. This would suggest a relationship similar to that developed by Krishna Raju et al[68], equation 6.3.1. The joint

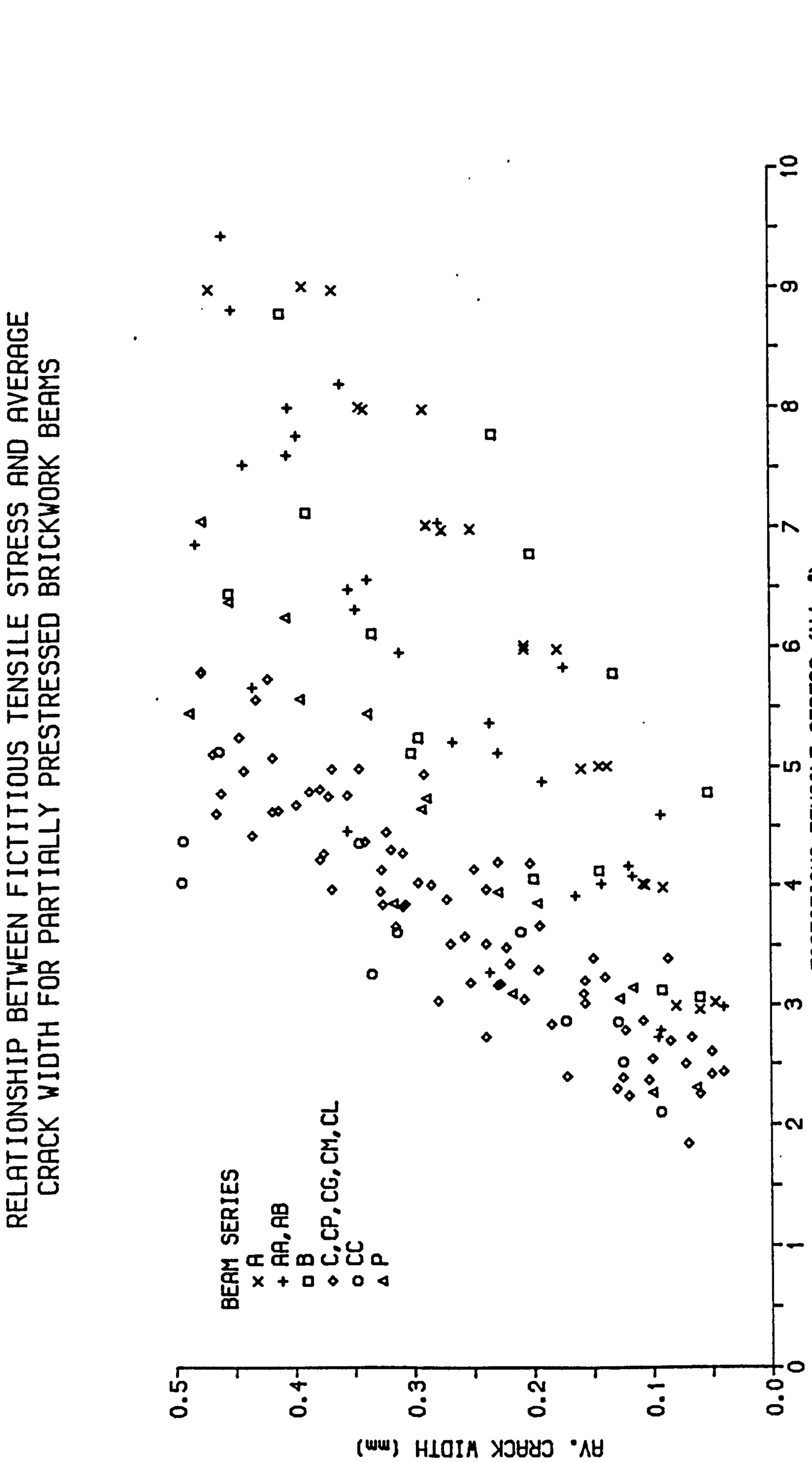
RELATIONSHIP BETWEEN FICTITIOUS TENSILE STRESS AND AVERAGE
CRACK WIDTH FOR PARTIALLY PRESTRESSED BRICKWORK BEAMS
BEAM SERIES
× A
+ AA,AB
□ B
◇ C,CP,CG,CM,CL
○ CC
△ P
FICTITIOUS TENSILE STRESS (N/mm²)
AV. CRACK WIDTH (mm)
0
1
2
3
4
5
6
7
8
9
10
0.0
0.1
0.2
0.3
0.4
0.5

Figure 6.3.8

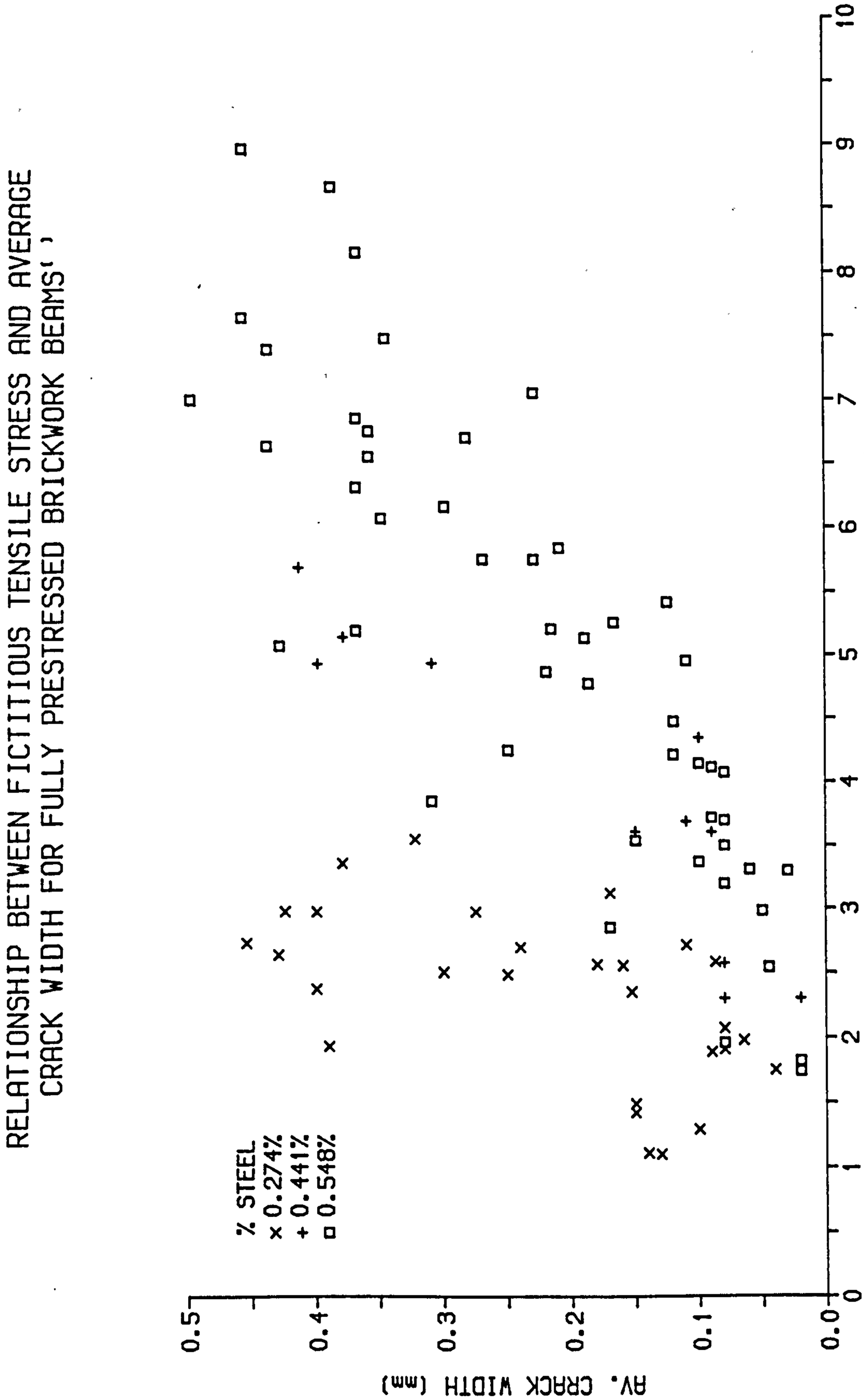
RELATIONSHIP BETWEEN FICTITIOUS TENSILE STRESS AND AVERAGE
CRACK WIDTH FOR FULLY PRESTRESSED BRICKWORK BEAMS'
AV. CRACK WIDTH (mm)
0.0
0.1
0.2
0.3
0.4
0.5
FICTITIOUS TENSILE STRESS (N/mm²)
0
1
2
3
4
5
6
7
8
9
10
% STEEL
× 0.274%
+ 0.441%
□ 0.548%

Figure 6.3.9

spacing seems to be a controlling factor in brickwork, section 6.3.1, hence it has been used instead of cover as in prestressed concrete.

Figure 6.3.10 shows the relationship between average crack width and the fictitious tensile stress, f_{ct}, multiplied by joint spacing, b_j, and divided by the percentage area of tensile reinforcement. The scatter is considerably reduced and there seems a much clearer and distinct linear relationship between average crack width and fictitious tensile stress for both fully and partially prestressed brickwork beams. Although the relationship between average crack width and fictitious tensile stress is similar the slope of the lines for fully and partially prestressed beams are different. Applying a least squares analysis to the test results the following empirical expression was produced:

$$w_{av} = \frac{k_1(f_{ct} - f_r)b_j}{\rho_s} \qquad (6.3.8)$$

where $k_1 = 132 \times 10^{-6}$ mm^2/N for partially prestressed (deformed bars)

$k_1 = 420 \times 10^{-6}$ mm^2/N for fully prestressed (prestressing tendons)

The introduction of the modulus of rupture, f_r, into the expression is a logical extension since it is clear that cracking will not occur until the modulus of rupture is exceeded.

Similar research[65] conducted on prestressed concrete attributed the difference in the slope, k_1, to the different properties of the tensile reinforcement closest to the soffit of the beam, strand, deformed bar or mild steel. In prestressed brickwork

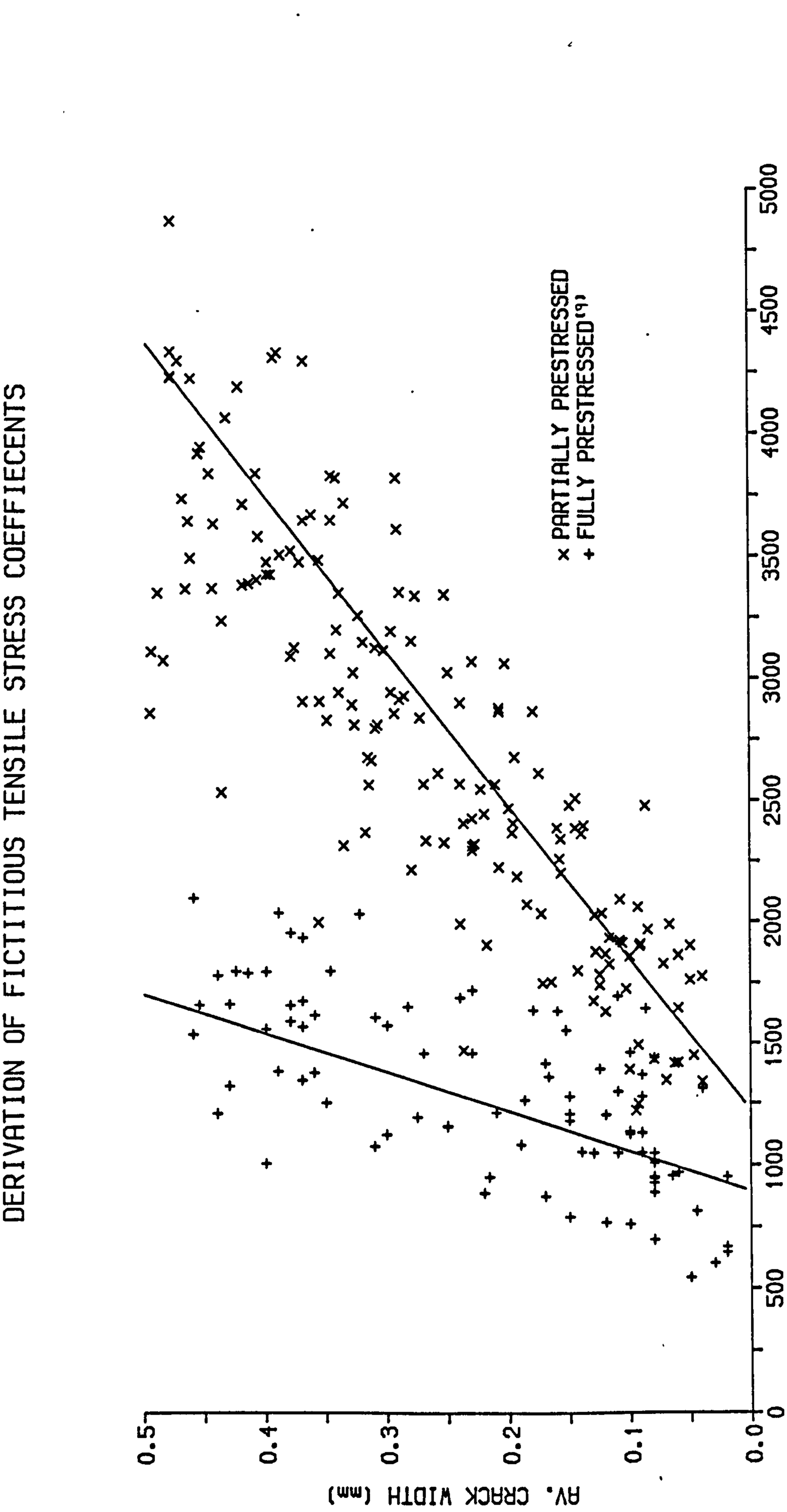
DERIVATION OF FICTITIOUS TENSILE STRESS COEFFICIENTS
× PARTIALLY PRESTRESSED
+ FULLY PRESTRESSED
0.0
0.1
0.2
0.3
0.4
0.5
0
500
1000
1500
2000
2500
3000
3500
4000
4500
5000
fct.bj / ρs (N/mm)
AV. CRACK WIDTH (mm)

Figure 6.3.10

the difference may also have been caused by a change in cover, however, the data presently available does not allow this to be confirmed.

6.3.2 Experimental results and discussion

The experimental relationships between moment and average crack width are shown in figures 6.3.11 - 6.3.22. The values presented for the crack widths are the arithmetic mean of all readings taken in the constant moment zone at each load increment. In all beams, except beam series A, the crack widths were measured using both a microscope at 25 mm above the soffit and vernier calipers at 5 mm above the soffit. The results presented are, when possible, those of the vernier calipers since they provided the most accurate indication of cracking at the soffit of each beam.

It is apparent from the results that approaching failure the crack widths had greatly exceeded any likely serviceability limit state criteria. However, it may be necessary to consider cracking at failure since they will provide warning of collapse and so the experimental results are presented up to ultimate moment. The characteristics of each moment-average crack width relationship were similar. Initially the response was 'quasi-linear' at which point the steel behaved elastically even though the brickwork and concrete did not. Once yielding of the tensile reinforcement occurred the cracks increased in width more rapidly until failure, eventually the curve became parallel to the x-axis.

The experimental results are compared with both of the

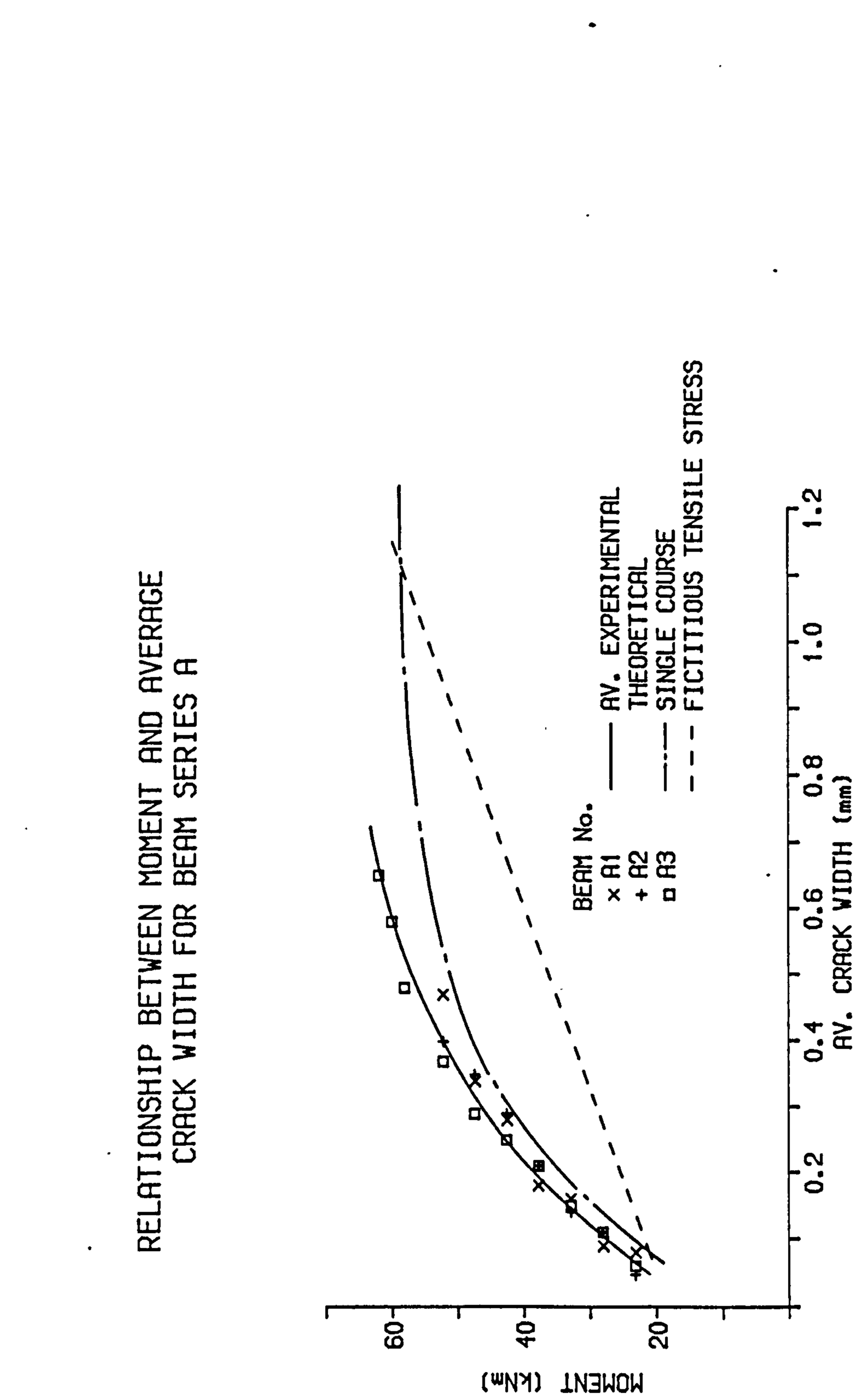
RELATIONSHIP BETWEEN MOMENT AND AVERAGE CRACK WIDTH FOR BEAM SERIES A
MOMENT (kNm)
60
40
20
0.2
0.4
0.6
0.8
1.0
1.2
AV. CRACK WIDTH (mm)
BEAM No.
× A1
+ A2
□ A3
AV. EXPERIMENTAL
THEORETICAL
SINGLE COURSE
FICTITIOUS TENSILE STRESS

Figure 6.3.11

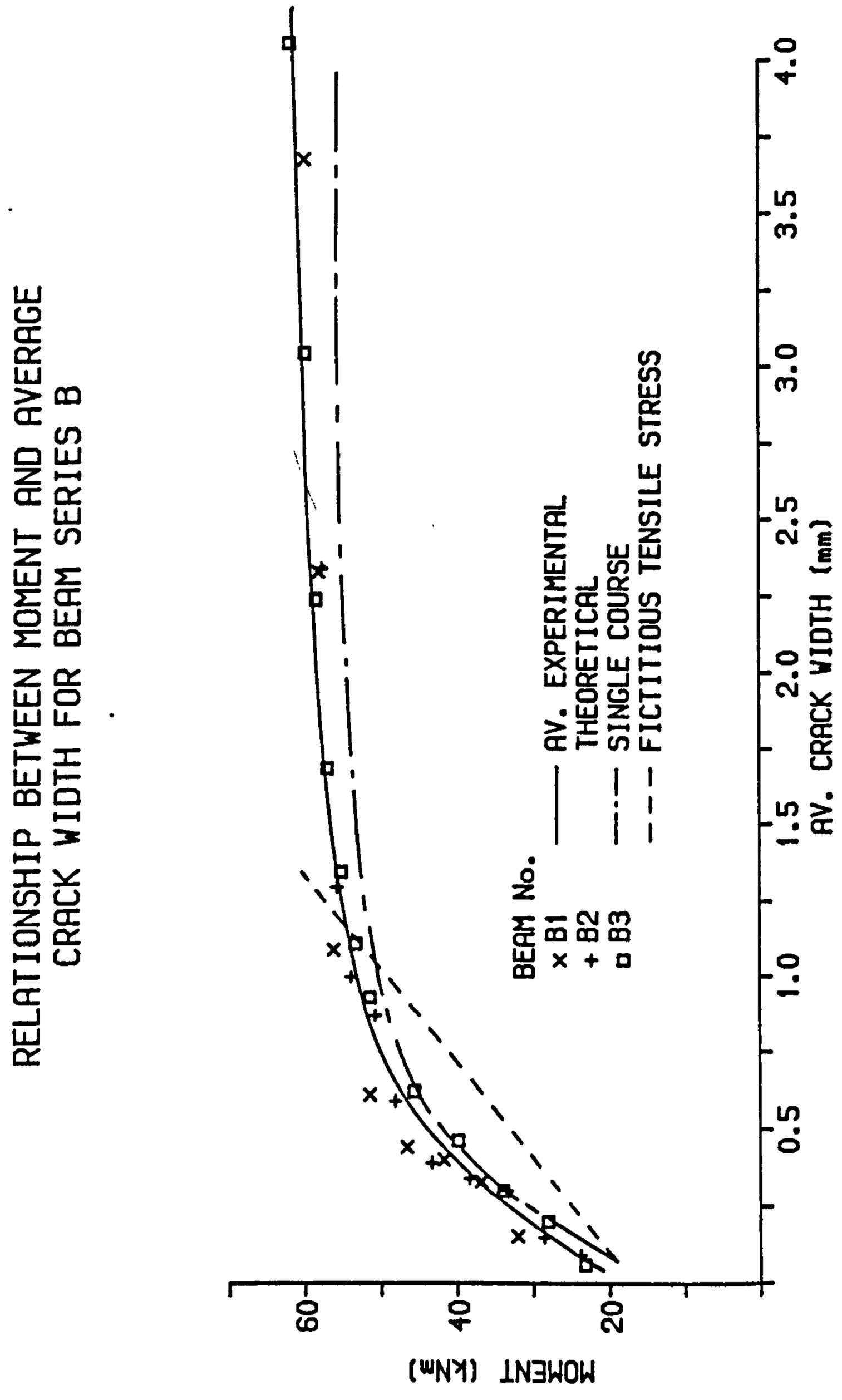
RELATIONSHIP BETWEEN MOMENT AND AVERAGE
CRACK WIDTH FOR BEAM SERIES B
MOMENT (kNm)
60
40
20
AV. CRACK WIDTH (mm)
0.5
1.0
1.5
2.0
2.5
3.0
3.5
4.0
BEAM No.
× B1
+ B2
□ B3
—— AV. EXPERIMENTAL
THEORETICAL
—·— SINGLE COURSE
– – – FICTITIOUS TENSILE STRESS

Figure 6.3.12

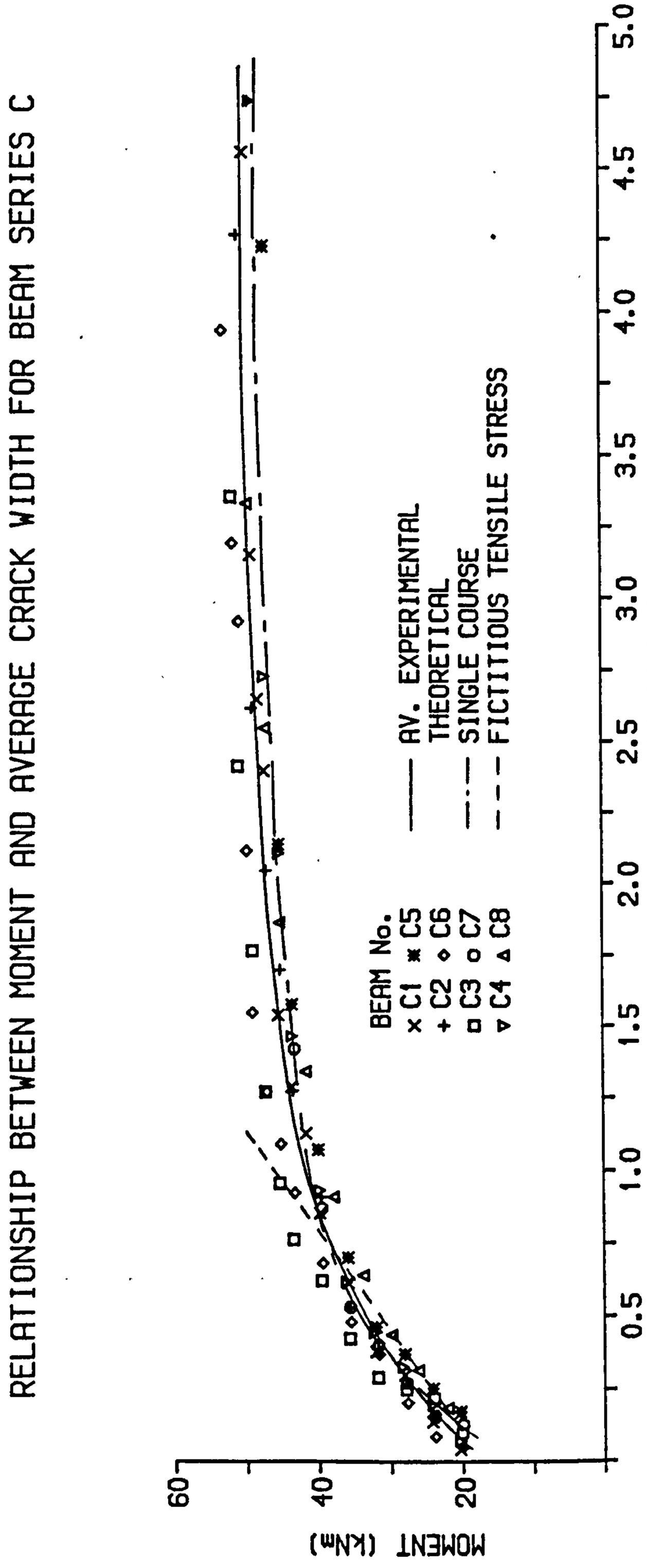
RELATIONSHIP BETWEEN MOMENT AND AVERAGE CRACK WIDTH FOR BEAM SERIES C
MOMENT (kNm)
60
40
20
AV. CRACK WIDTH (mm)
1.0
1.5
2.0
2.5
3.0
3.5
4.0
4.5
5.0
0.5
BEAM No.
× C1 ✱ C5
+ C2 ◇ C6
□ C3 ○ C7
▽ C4 △ C8
—— AV. EXPERIMENTAL
THEORETICAL
—·— SINGLE COURSE
– – – FICTITIOUS TENSILE STRESS

Figure 6.3.13

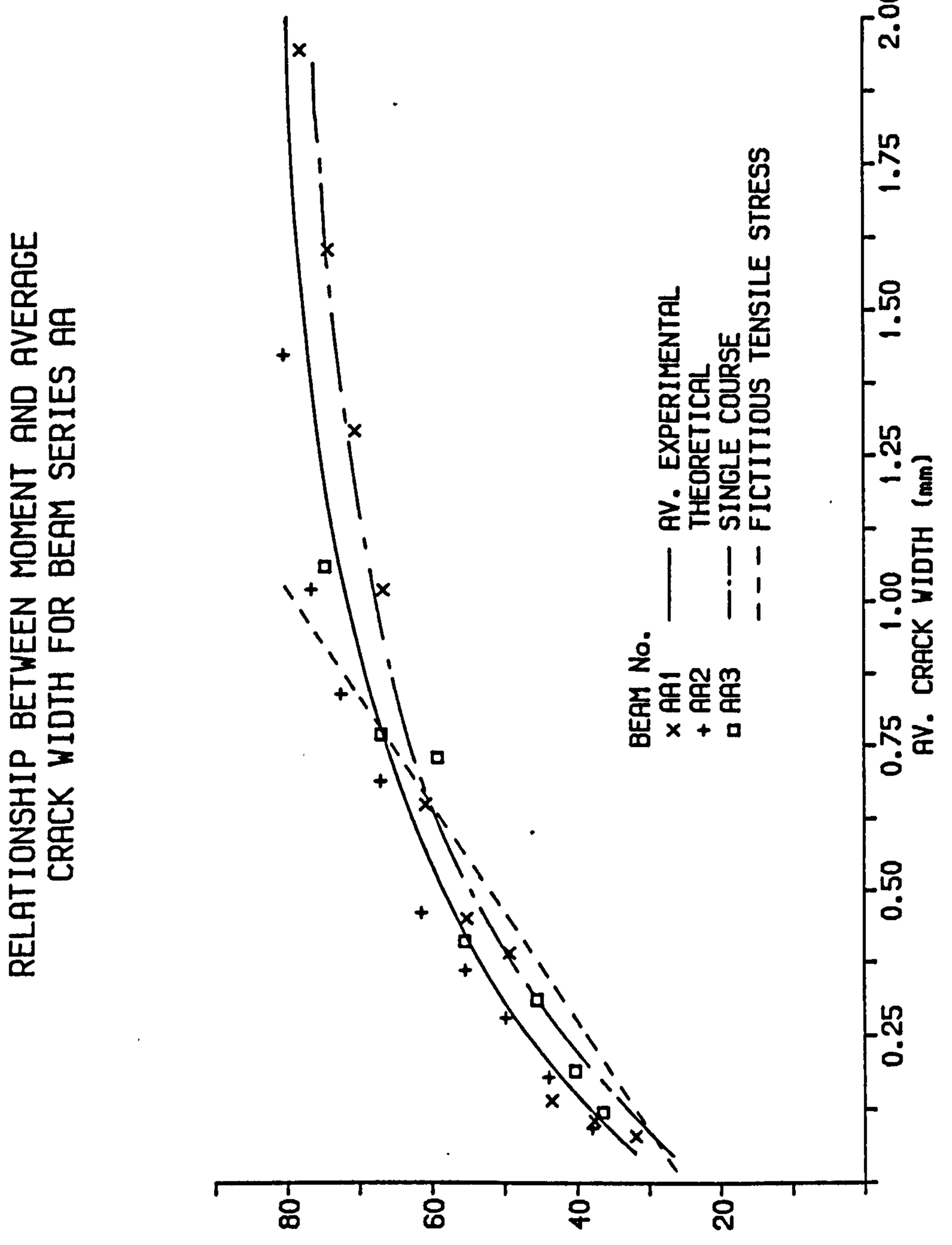
RELATIONSHIP BETWEEN MOMENT AND AVERAGE CRACK WIDTH FOR BEAM SERIES AA
BEAM No.
× AA1
+ AA2
□ AA3
—— AV. EXPERIMENTAL
THEORETICAL
—·— SINGLE COURSE
– – – FICTITIOUS TENSILE STRESS
MOMENT (kNm)
80
60
40
20
AV. CRACK WIDTH (mm)
0.25
0.50
0.75
1.00
1.25
1.50
1.75
2.00

Figure 6.3.14

RELATIONSHIP BETWEEN MOMENT AND AVERAGE CRACK WIDTH FOR BEAM SERIES AB

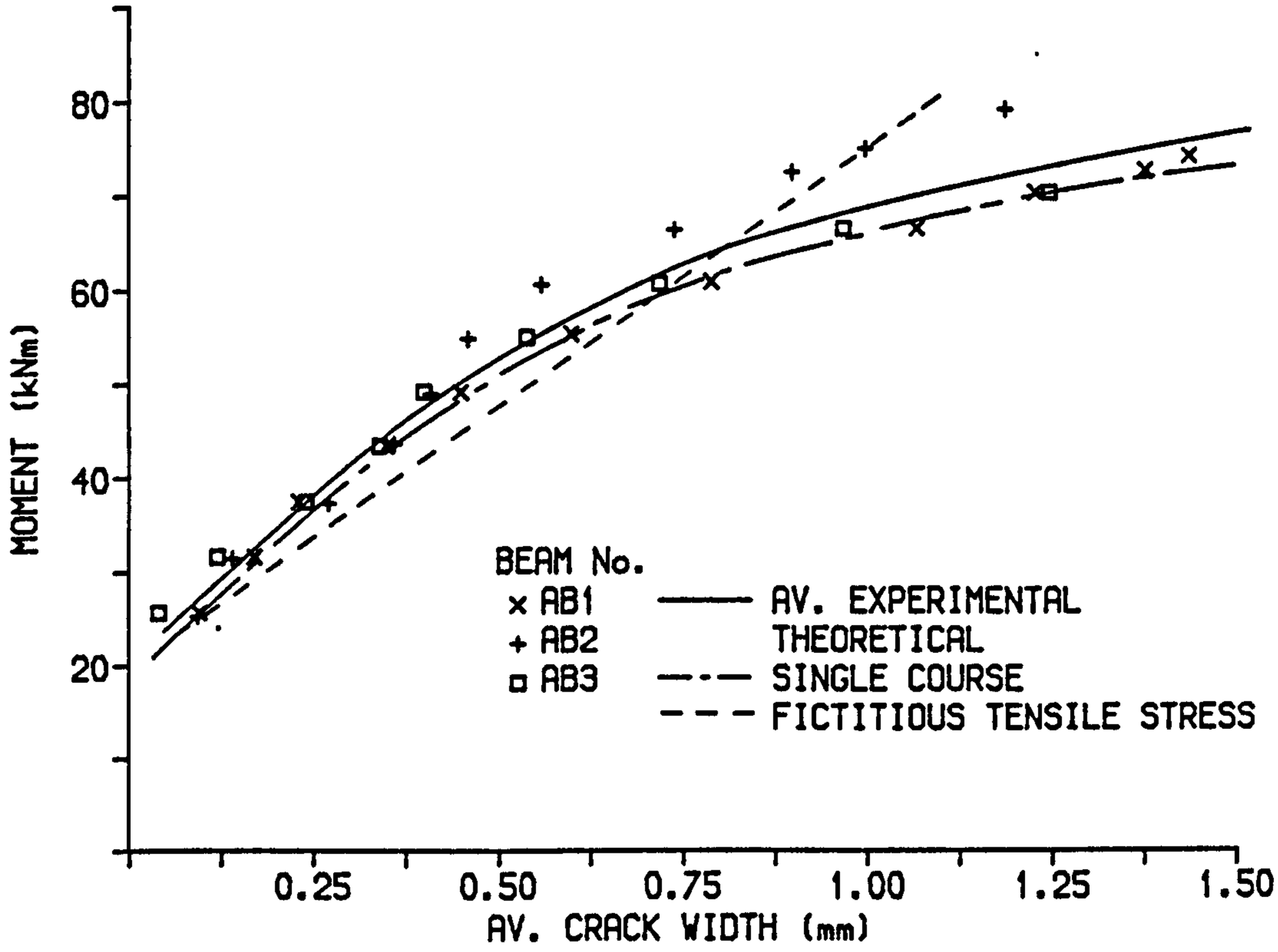

Figure 6.3.15

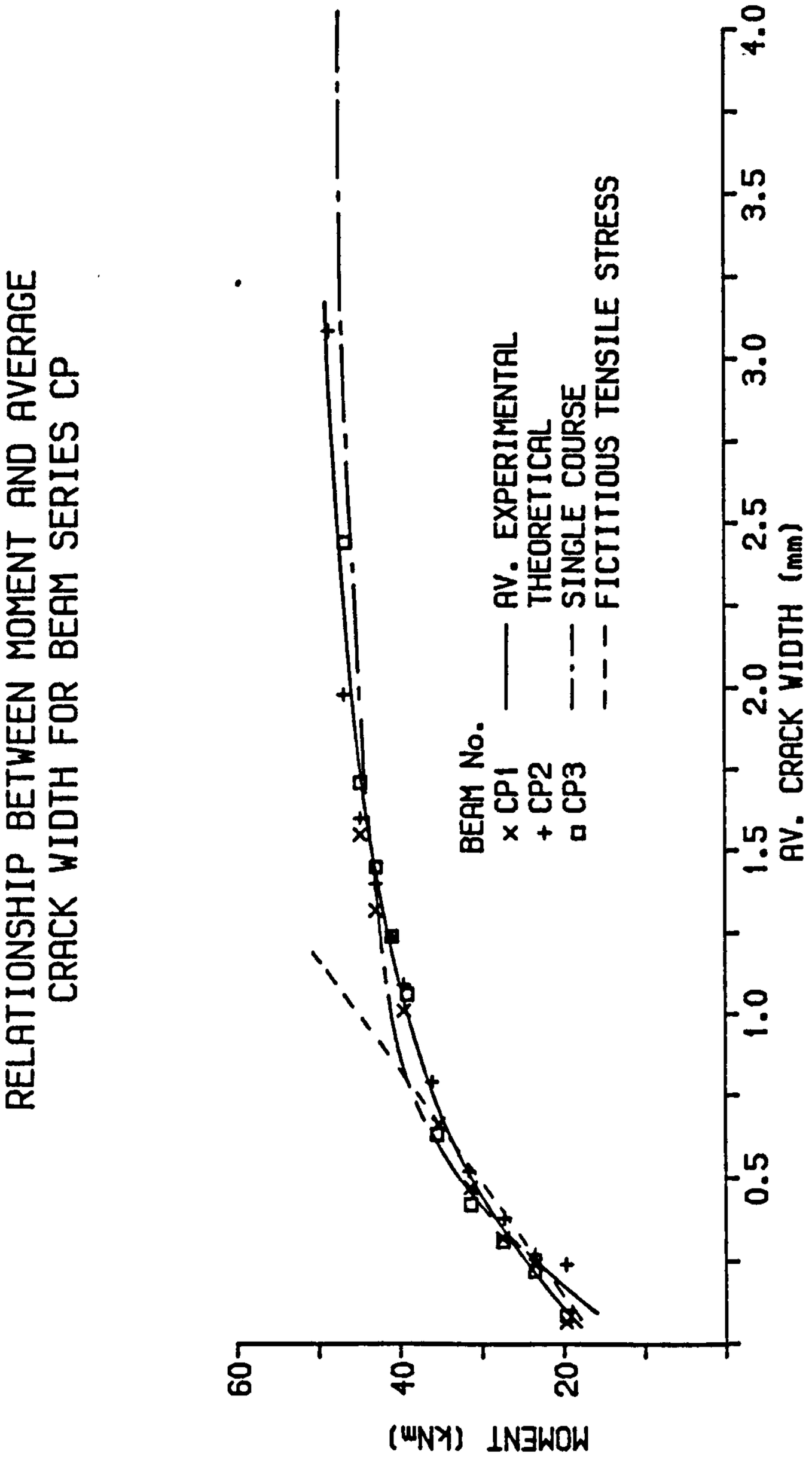
RELATIONSHIP BETWEEN MOMENT AND AVERAGE CRACK WIDTH FOR BEAM SERIES CP
BEAM No.
× CP1
+ CP2
□ CP3
—— AV. EXPERIMENTAL
THEORETICAL
—·— SINGLE COURSE
– – – FICTITIOUS TENSILE STRESS
MOMENT (kNm)
60
40
20
AV. CRACK WIDTH (mm)
0.5
1.0
1.5
2.0
2.5
3.0
3.5
4.0

Figure 6.3.16

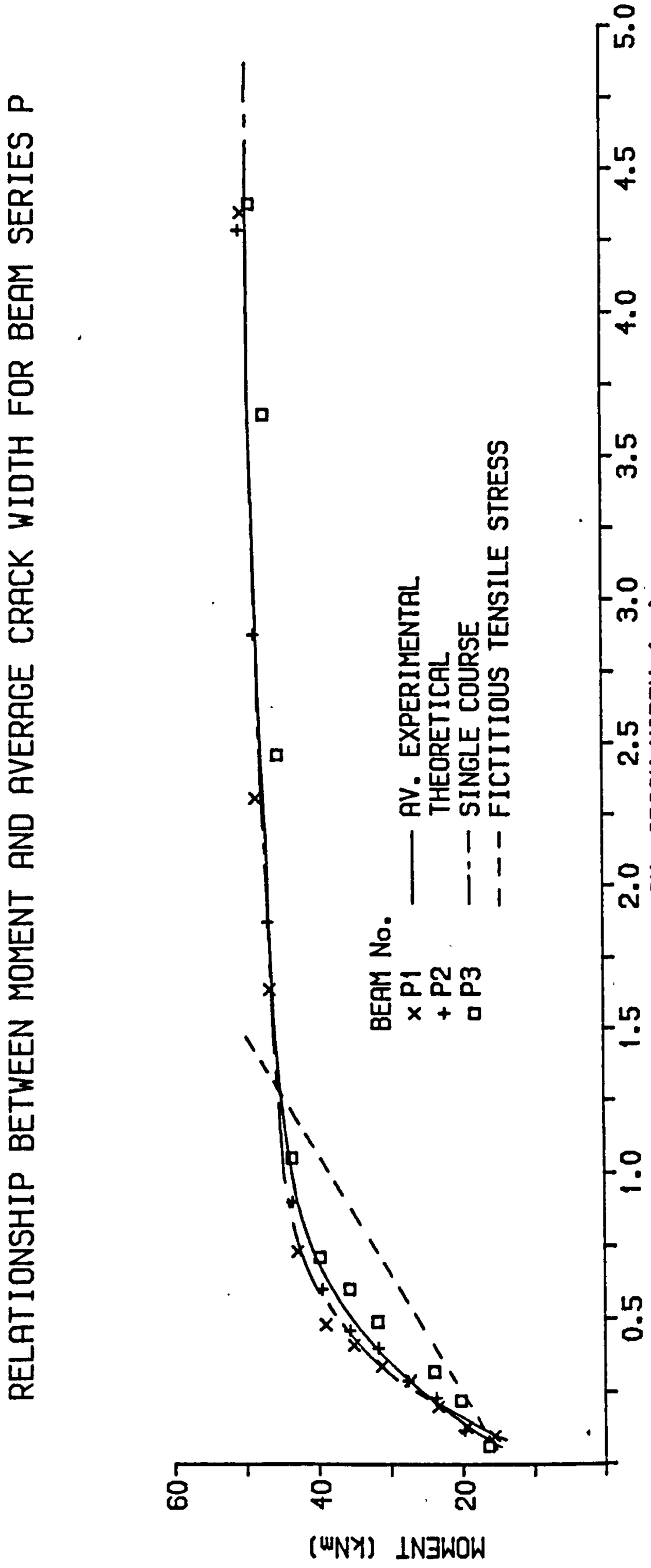
RELATIONSHIP BETWEEN MOMENT AND AVERAGE CRACK WIDTH FOR BEAM SERIES P
MOMENT (kNm)
60
40
20
0.5
1.0
1.5
2.0
2.5
3.0
3.5
4.0
4.5
5.0
AV. CRACK WIDTH (mm)
BEAM No.
× P1
+ P2
□ P3
— AV. EXPERIMENTAL
THEORETICAL
— SINGLE COURSE
-- FICTITIOUS TENSILE STRESS

Figure 6.3.17

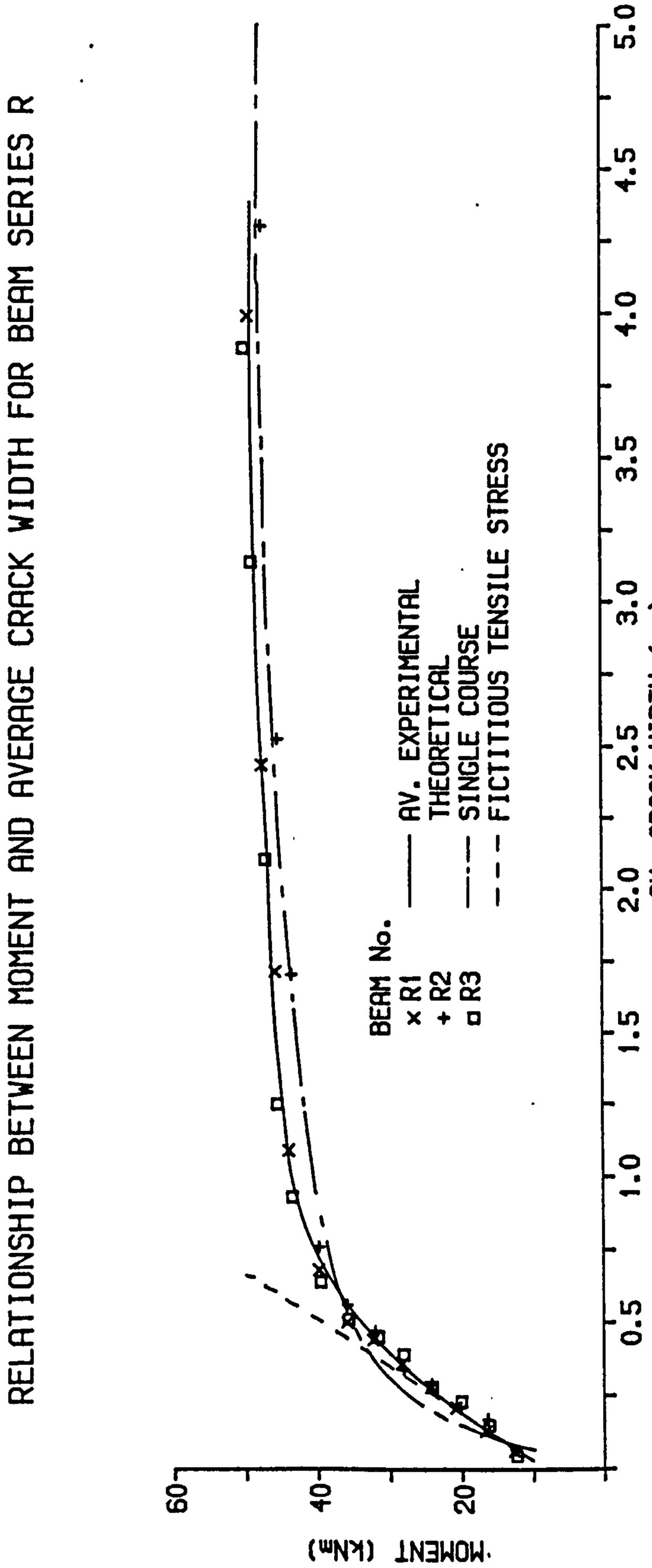
RELATIONSHIP BETWEEN MOMENT AND AVERAGE CRACK WIDTH FOR BEAM SERIES R
MOMENT (kNm)
60
40
20
AV. CRACK WIDTH (mm)
0.5
1.0
1.5
2.0
2.5
3.0
3.5
4.0
4.5
5.0
BEAM No.
× R1
+ R2
□ R3
AV. EXPERIMENTAL
THEORETICAL
SINGLE COURSE
FICTITIOUS TENSILE STRESS

Figure 6.3.18

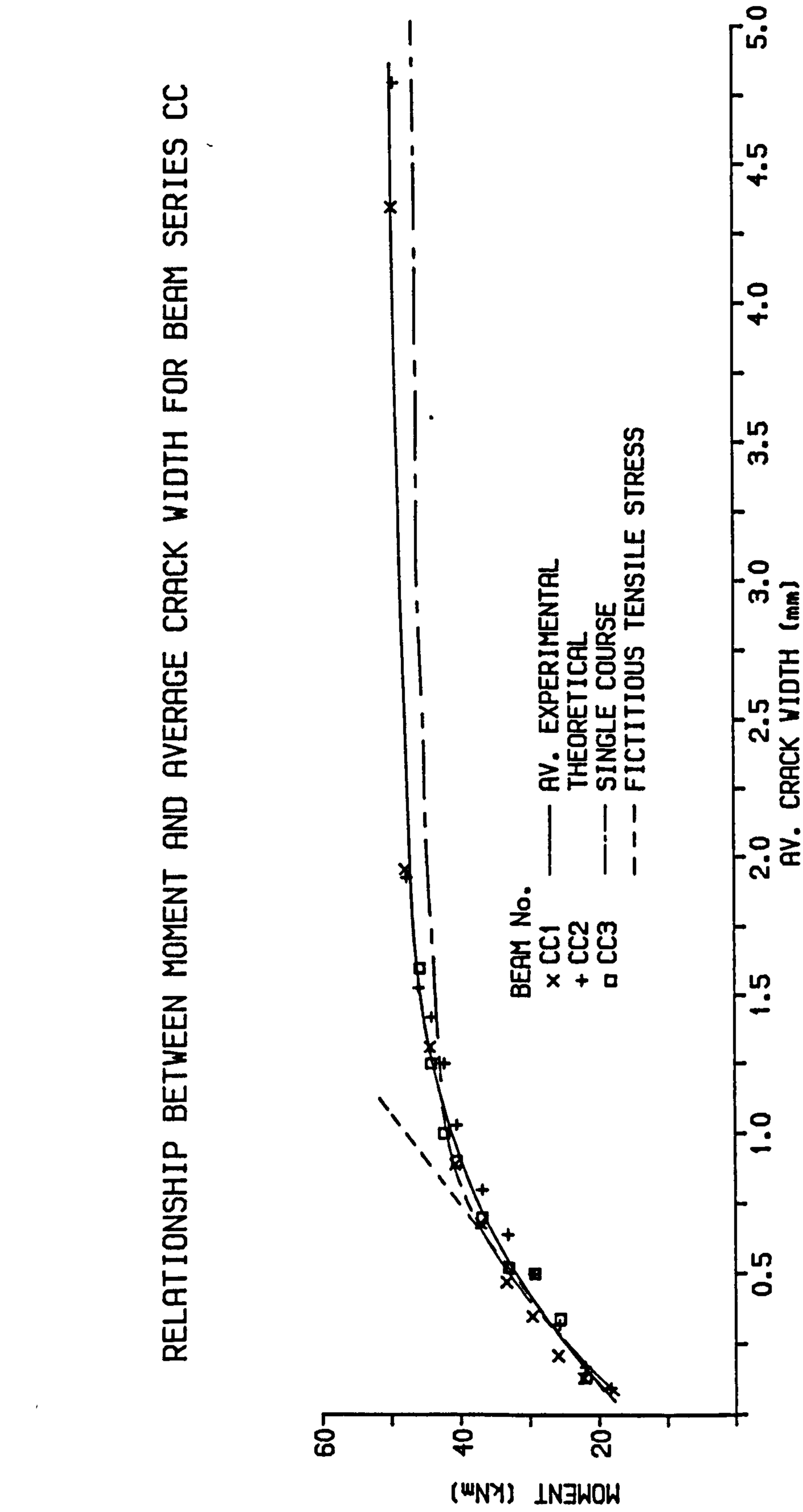
RELATIONSHIP BETWEEN MOMENT AND AVERAGE CRACK WIDTH FOR BEAM SERIES CC
BEAM No.
× CC1
+ CC2
□ CC3
AV. EXPERIMENTAL
THEORETICAL
SINGLE COURSE
FICTITIOUS TENSILE STRESS
MOMENT (kNm)
AV. CRACK WIDTH (mm)
60
40
20
0.5
1.0
1.5
2.0
2.5
3.0
3.5
4.0
4.5
5.0

Figure 6.3.19

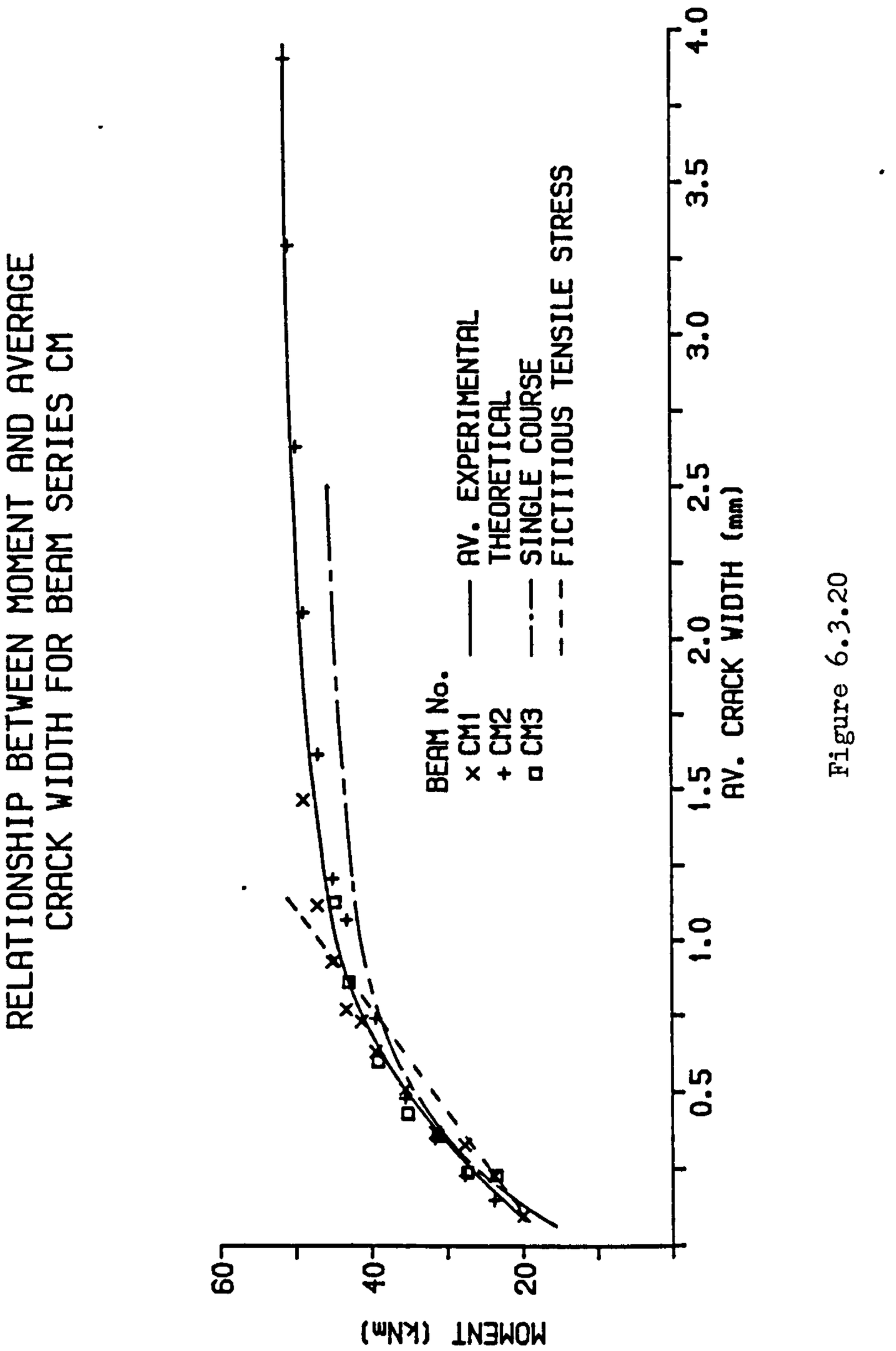
RELATIONSHIP BETWEEN MOMENT AND AVERAGE CRACK WIDTH FOR BEAM SERIES CM
MOMENT (kNm)
60
40
20
AV. CRACK WIDTH (mm)
0.5
1.0
1.5
2.0
2.5
3.0
3.5
4.0
BEAM No.
× CM1
+ CM2
□ CM3
—— AV. EXPERIMENTAL
THEORETICAL
—·— SINGLE COURSE
– – – FICTITIOUS TENSILE STRESS

Figure 6.3.20

RELATIONSHIP BETWEEN MOMENT AND AVERAGE CRACK WIDTH FOR BEAM SERIES CL

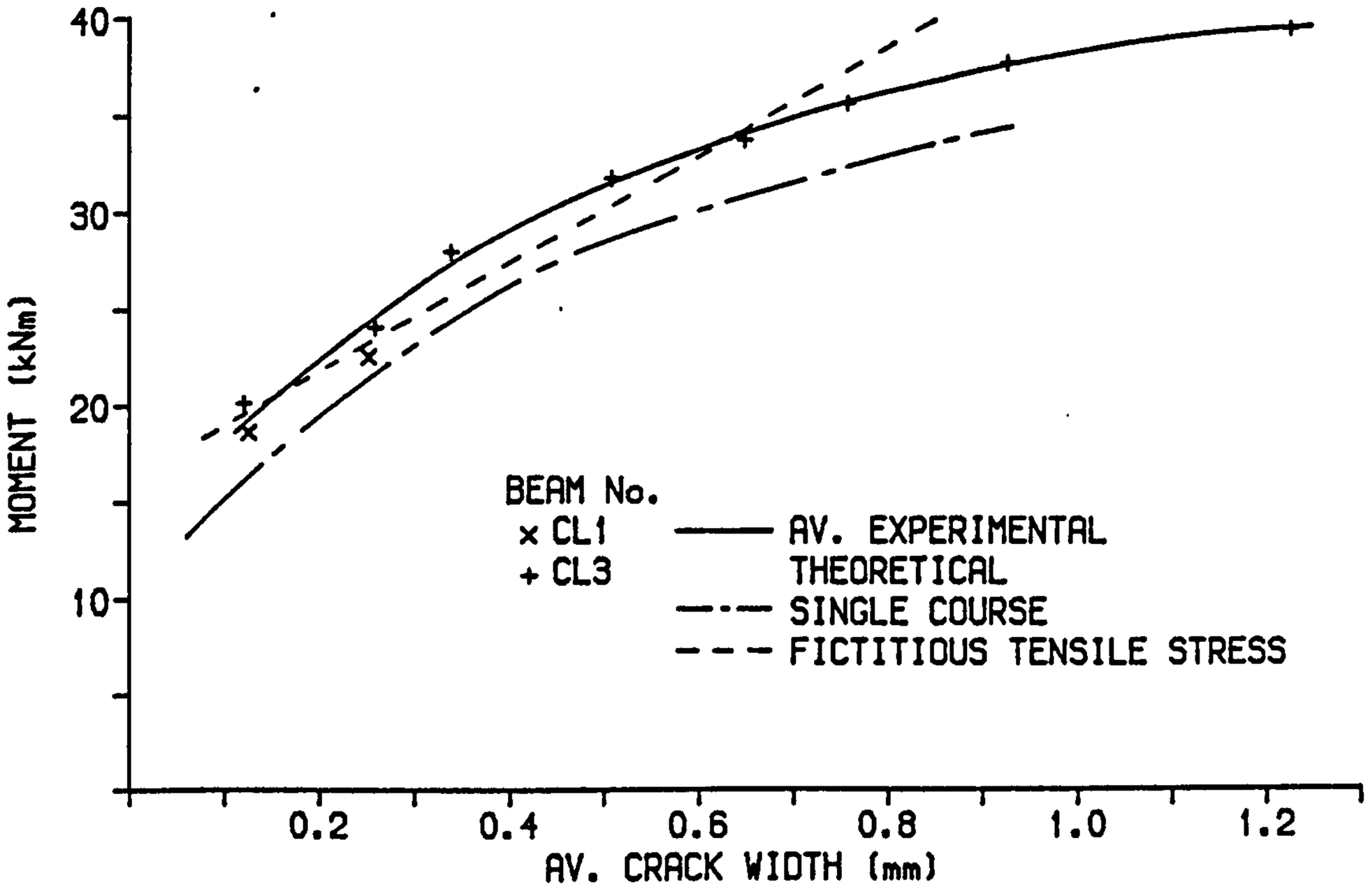

Figure 6.3.21

RELATIONSHIP BETWEEN MOMENT AND AVERAGE CRACK WIDTH FOR BEAM SERIES CL

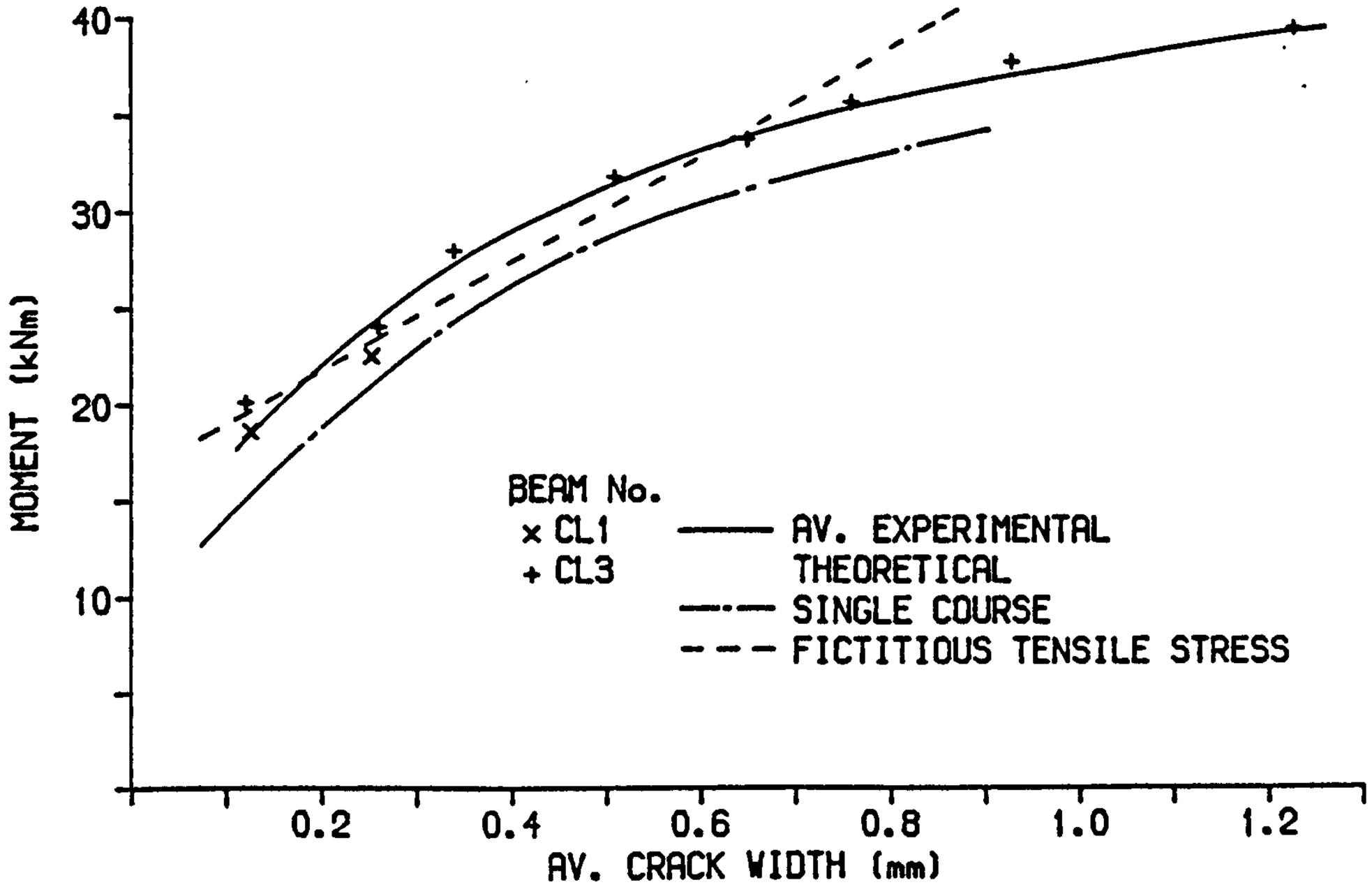

Figure 6.3.21

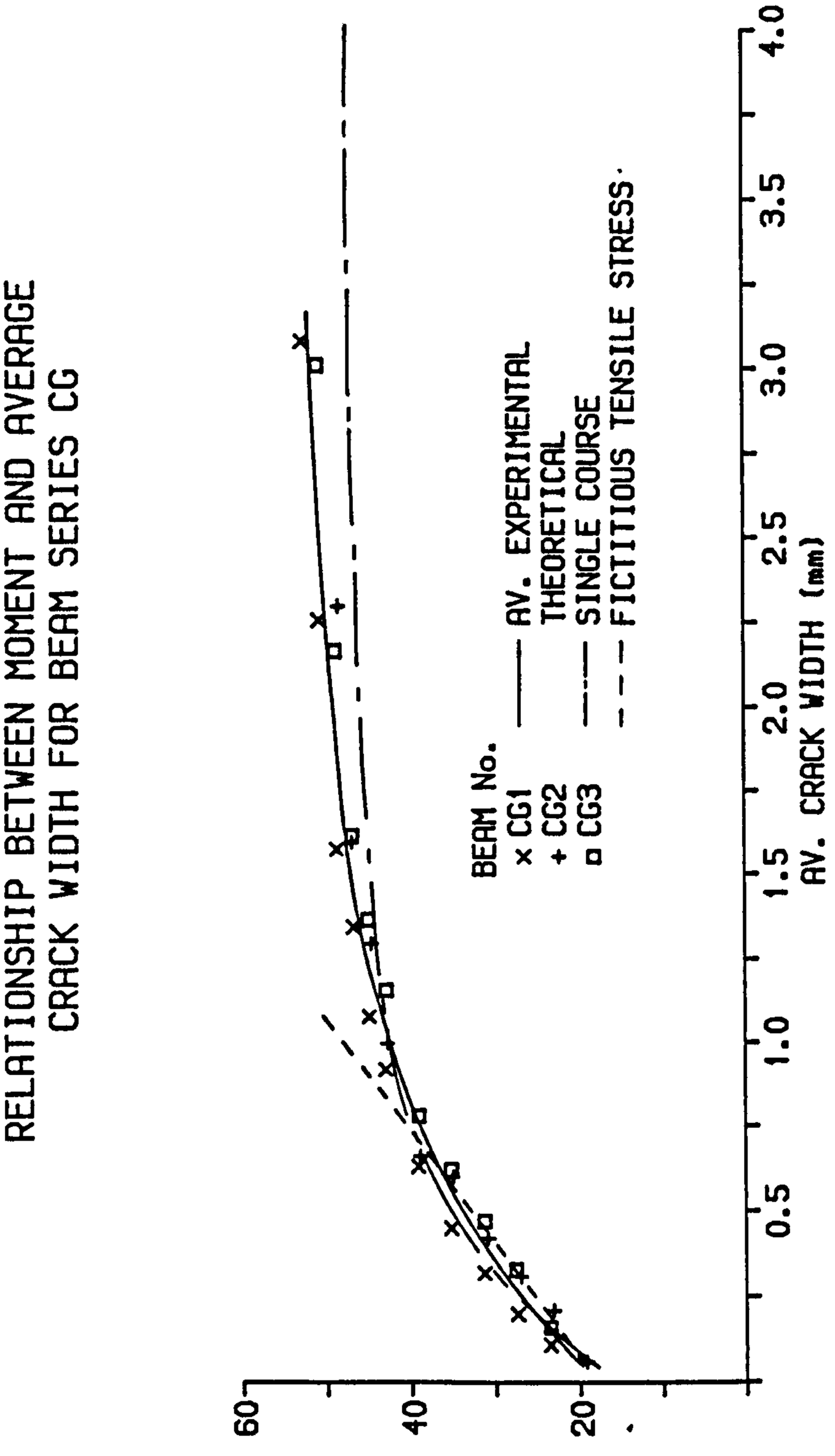
RELATIONSHIP BETWEEN MOMENT AND AVERAGE CRACK WIDTH FOR BEAM SERIES CG
BEAM No.
× CG1
+ CG2
□ CG3
—— AV. EXPERIMENTAL
—— THEORETICAL
—— SINGLE COURSE
- - - FICTITIOUS TENSILE STRESS
MOMENT (kNm)
60
40
20
AV. CRACK WIDTH (mm)
0.5
1.0
1.5
2.0
2.5
3.0
3.5
4.0

Figure 6.3.22

theoretical approaches outlined in section 6.3.1. Crack widths predicted from the average strain, using the properties of the single course brickwork prisms, in all except the low strength brick beams, figure 6.3.21, showed excellent agreement with the experimental results. Previously the single course prisms had provided the best estimates for the curvature and consequently the most accurate estimate of the average additional strain. Although the theory under-predicted ultimate moment, chapter 5, crack widths had by this stage exceeded any likely design serviceability limit state since all beams were under-reinforced. At ultimate the predicted crack widths were sufficiently close to the experimental results for adequate warning of collapse.

The fictitious tensile stress method, equation 6.3.8, over-predicted the average crack widths in all beams up to 80 - 85% of the ultimate moment, beyond this point the method failed to account for yielding of the tensile reinforcement. Generally the estimates were within 20% of the average experimental curve and therefore the fictitious tensile stress approach may prove suitable for design calculations. However, before the fictitious tensile stress method can be applied more widely further studies are required to ascertain the influence of the joint spacing, cover, percentage area of steel and reinforcement type upon equation 6.3.8.

In practice the full service loading may be applied only for relatively short periods and so in design it may be necessary to consider the recovery of the section. Therefore during testing of three beams the applied moment was removed, at between 40 - 80% of the ultimate moment, to study closing of the crack widths. The

relationships between moment and average crack width for beams B3, C4 and AB3 are presented in figures 6.3.23 - 6.3.25.

Prior to yielding of the tensile reinforcement, at between 80 - 85% of the ultimate moment, the cracks exhibited almost complete recovery, residual crack widths in the order of 0.04mm. The residual crack widths may be considered insignificant since cracks of this magnitude in brickwork were not visible to the naked eye and as measurements are made to a tolerance of only 0.02mm it is possible that the cracks had closed completely. Once the tensile reinforcement had exceeded its proof stress the recovery was much less, the residual cracks were visible to the naked eye, ie. greater than 0.2mm.

On the the removing the applied moment full recovery of cracking was not realised until the moment corresponded to that necessary to cause decompression of the prestress. This was because of residual strains in the steel, brickwork and concrete due to the non-elastic behaviour of the materials. Deterioration of bond due to slip in the vicinity of the cracks may have taken place. For closure of the cracks a compressive force will have to be applied to overcome the bond slip at the crack, and therefore recovery was not realised until decompression.

6.3.2.1 Effect of % area of steel

The results of the moment - average crack width relationship for beam series A (0.47% steel area), beam series B (0.37% steel area) and beam series C (0.31% steel area), figures 6.3.11 - 6.3.13,

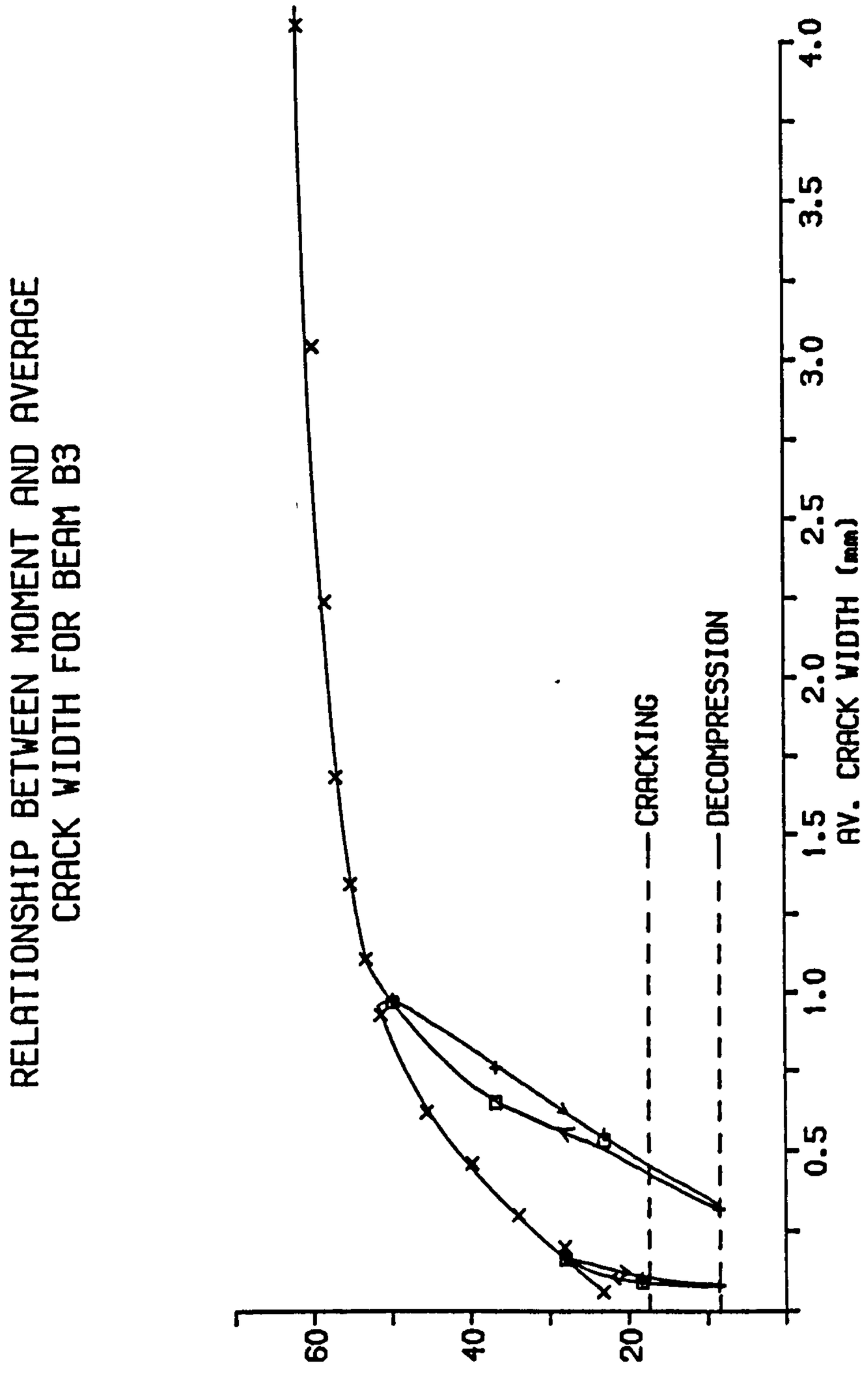
RELATIONSHIP BETWEEN MOMENT AND AVERAGE CRACK WIDTH FOR BEAM B3
MOMENT (kNm)
60
40
20
0.5
1.0
1.5
2.0
2.5
3.0
3.5
4.0
AV. CRACK WIDTH (mm)
C—CRACKING
D—DECOMPRESSION

Figure 6.3.23

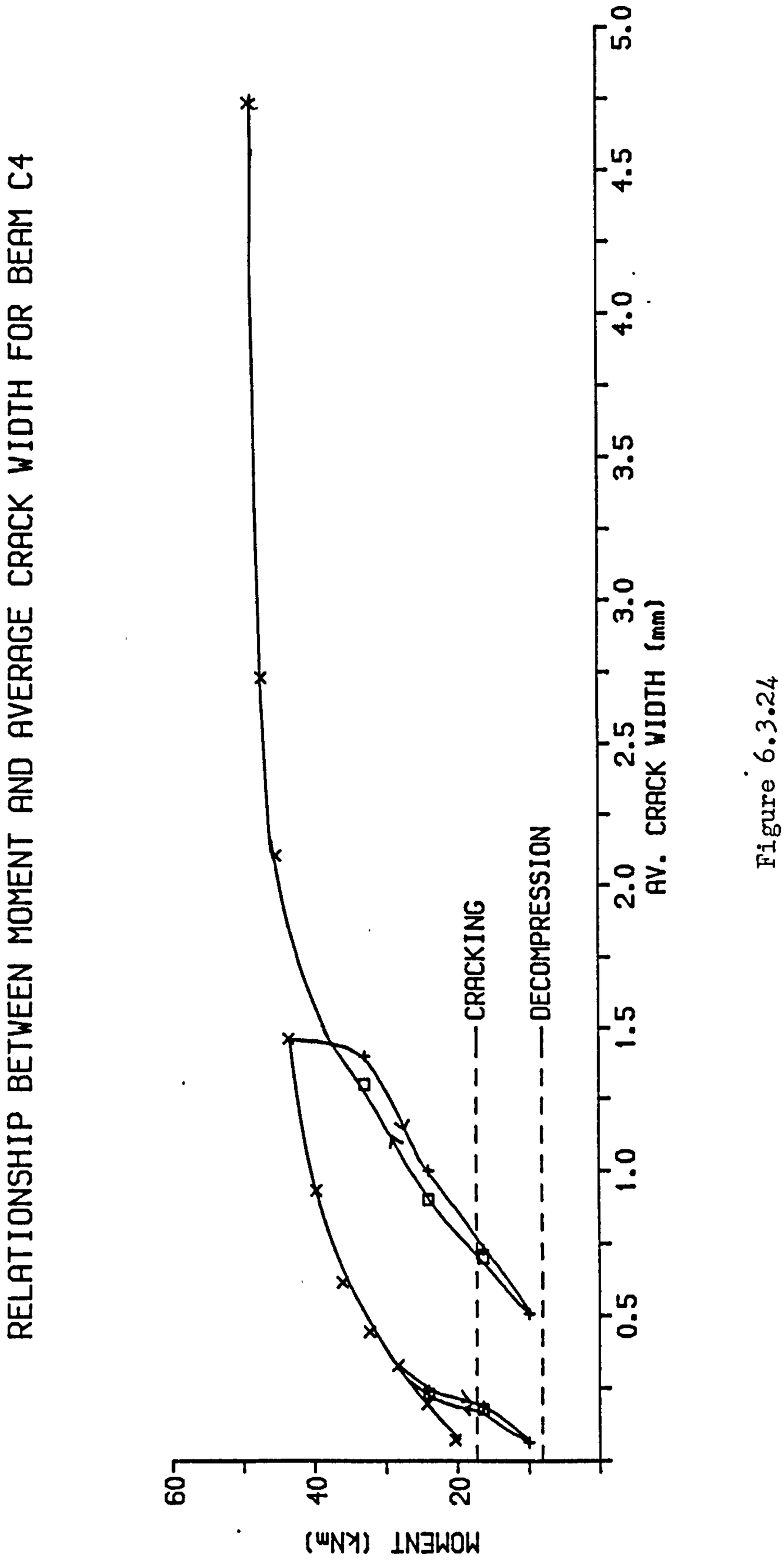
RELATIONSHIP BETWEEN MOMENT AND AVERAGE CRACK WIDTH FOR BEAM C4
MOMENT (kNm)
60
40
20
AV. CRACK WIDTH (mm)
0.5
1.0
1.5
2.0
2.5
3.0
3.5
4.0
4.5
5.0
CRACKING
DECOMPRESSION

Figure 6.3.24

RELATIONSHIP BETWEEN MOMENT AND AVERAGE
CRACK WIDTH FOR BEAM AB3

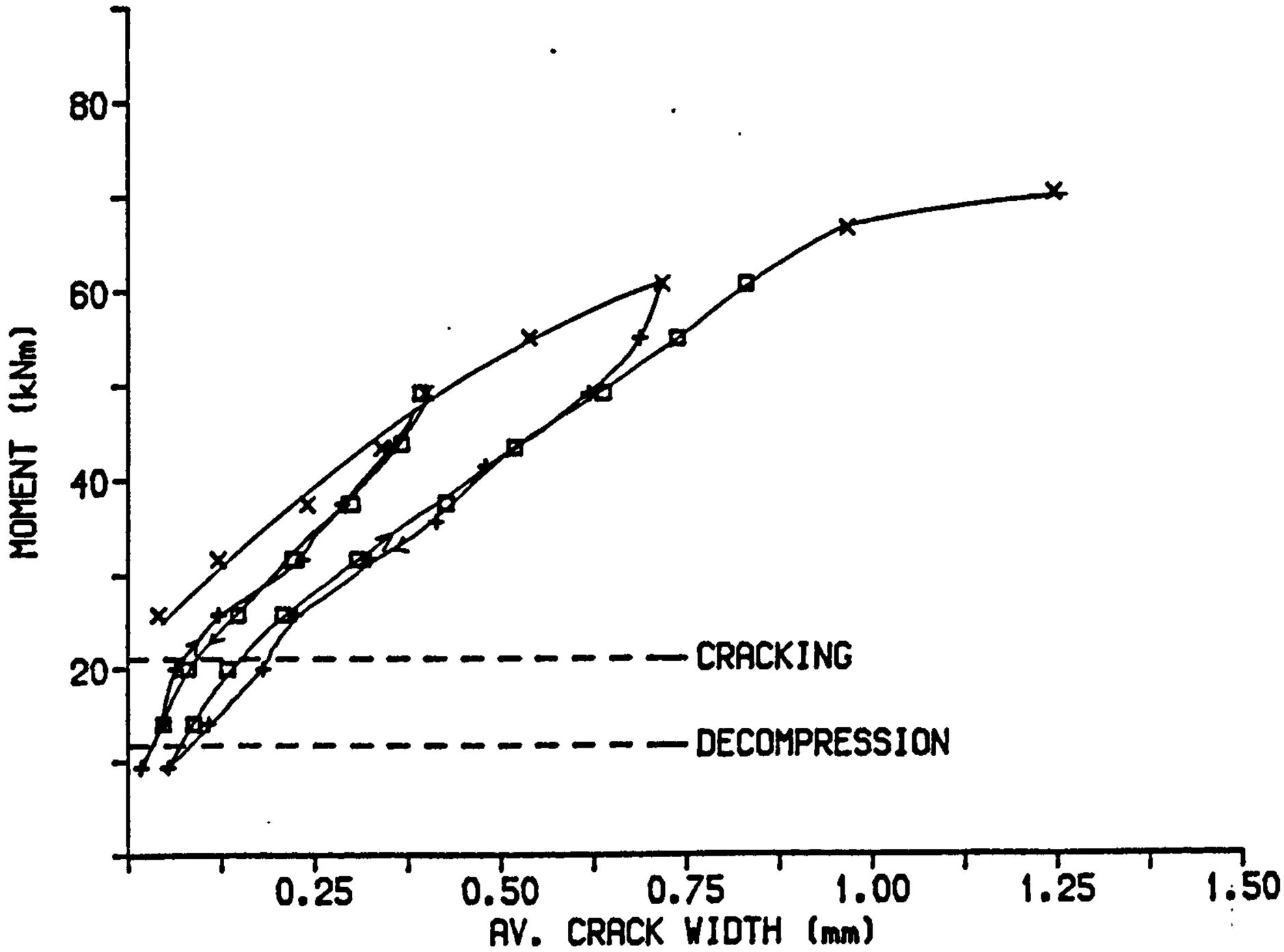

Figure 6.3.25

were collated to determine the influence of the % area of steel on the development of cracking in partially prestressed brickwork beams, figure 6.3.26. The brick strength and average prestressing force in all three beam series were maintained constant.

A reduction in the % area of steel caused an increase in the average crack width, figure 6.3.26. The experimental relationships diverged with increasing moment from cracking up to ultimate moment. For an applied moment of 40 kNm, the commencement of yielding of the non-tensioned reinforcement in beam series C (figure 5.2.5b), the percentage increase in crack width compared to beam series A was 80% for series B and 260% for series C, figure 6.3.26. The increase in the crack widths was due to a decrease in stiffness of the section, in order to sustain an equal moment the steel stress and crack widths in a section with smaller steel area will be increased. As the crack spacing was constant in all beams from equation 6.3.5 it can be seen that the increase in cracking was due to an increase in tensile strain at the soffit of the beam caused by the reduction in % area of steel.

6.3.2.2 Effect of prestressing force

The influence of the prestressing force on the development of crack widths in partially prestressed brickwork beams may be considered by comparing the experimental results for beam series AA and series AB, figures 6.3.14, 6.3.15 and 6.3.27. While all other cross-sectional properties remained constant beams AB1-3 showed a 26% decrease in the average prestressing force after all losses, table 5.2.1.

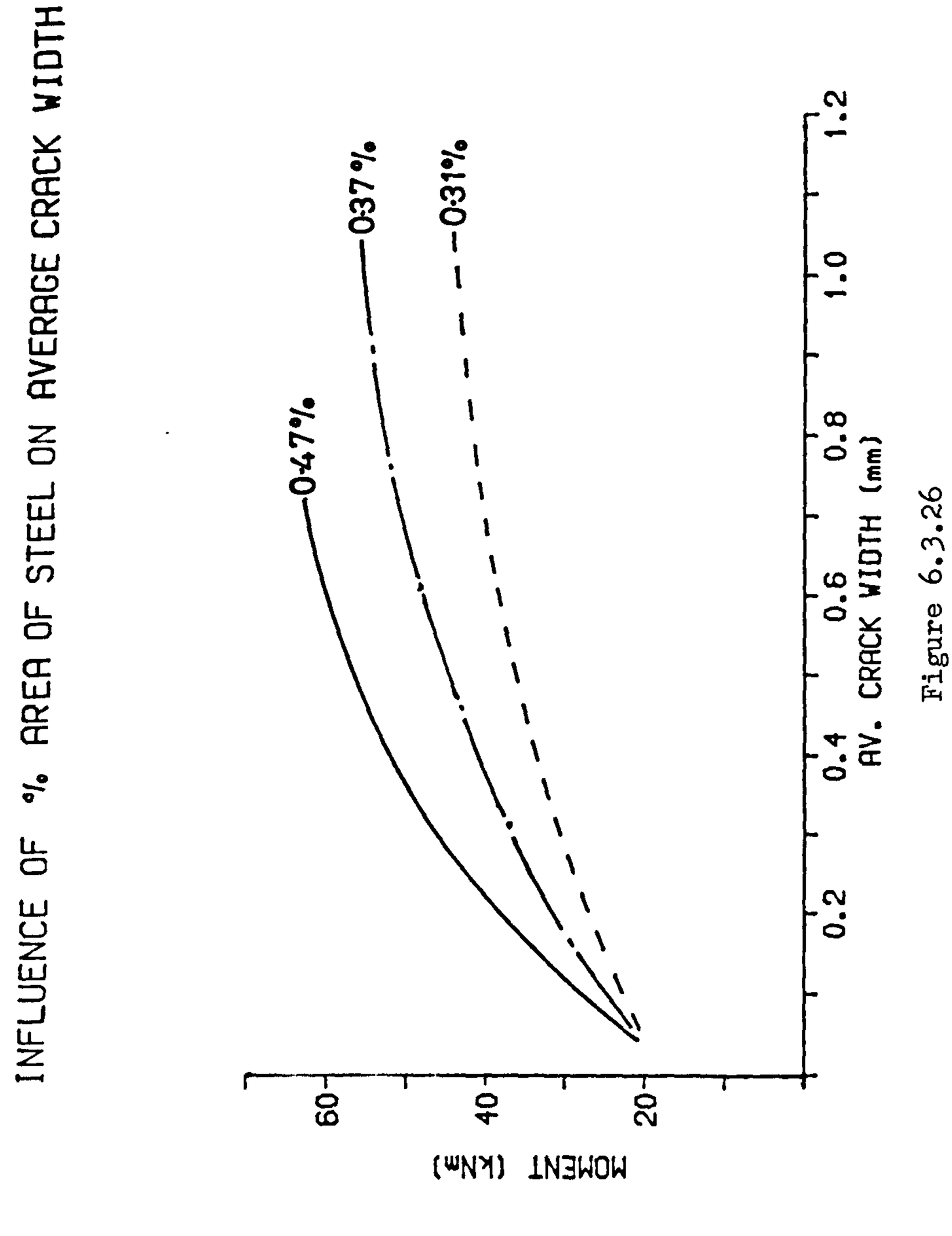
INFLUENCE OF % AREA OF STEEL ON AVERAGE CRACK WIDTH
0·47%
0·37%
0·31%
MOMENT (kNm)
60
40
20
0.2
0.4
0.6
0.8
1.0
1.2
AV. CRACK WIDTH (mm)

Figure 6.3.26

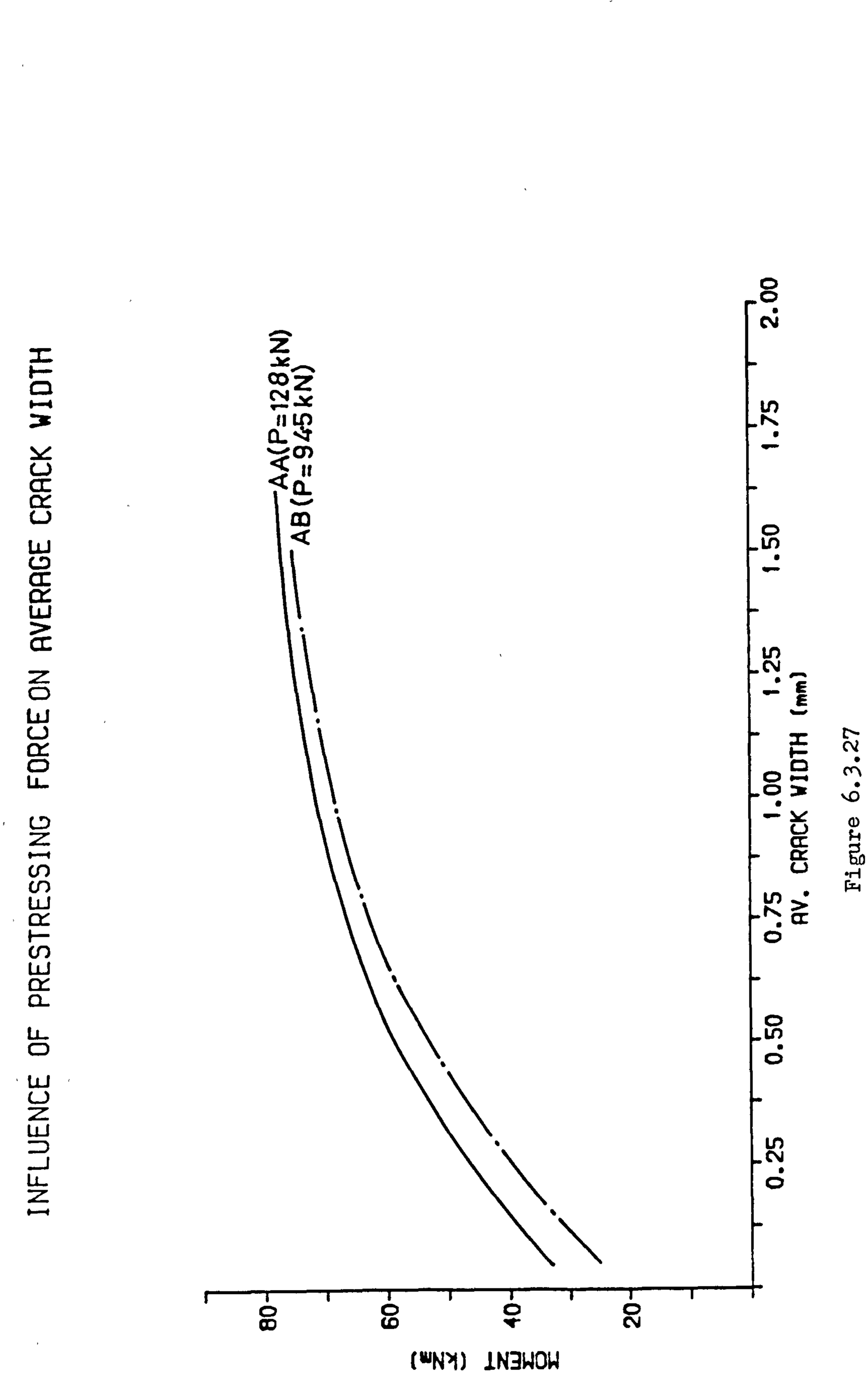
INFLUENCE OF PRESTRESSING FORCE ON AVERAGE CRACK WIDTH
AA(P=1128kN)
AB(P=945kN)
MOMENT (kNm)
80
60
40
20
0.25
0.50
0.75
1.00
1.25
1.50
1.75
2.00
AV. CRACK WIDTH (mm)

Figure 6.3.27

A reduction in the prestressing force resulted in a decrease in the cracking moment and so an increase in the internal stresses and hence crack widths. Compared to beam series AA the crack widths for series AB have increased, up to yielding of the steel, by approximately 0.1 mm (figure 6.3.27), the crack width in beam series AB when the moment equalled the average cracking moment of beams AA1 - AA3.

6.3.2.3 Effect of partial prestressing ratio

In figures 6.3.13, 6.3.17 and 6.3.18 the moment-average crack width relationship for beams with varying partial prestressing ratios 0.56, 0.31 and 0 are presented. Typical relationships are also illustrated in figure 6.3.28 together with the average moment-crack width response for fully prestressed brickwork beams 'B1 - B6'[9], partial prestressing ratio equal to unity. Crack widths in the test beams were measured at approximately 5 mm above the soffit whereas the measurements taken by Pedreschi were made at 25 mm above the soffit. The values shown in figure 6.3.28 for the fully prestressed brickwork beams have been adjusted to give a better picture of the comparative behaviour. It is noticed that the bonding pattern of the fully prestressed beams differs from that of the test beams along the bottom course, thereby influencing the possible crack spacing. A comparison was possible since the experimental crack spacing observed in the fully prestressed beams was equal to that of the test beams , i.e. approximately 225 mm.

Cracking will commence initially in the beams with the least prestressing force and so in the early stages of loading crack widths

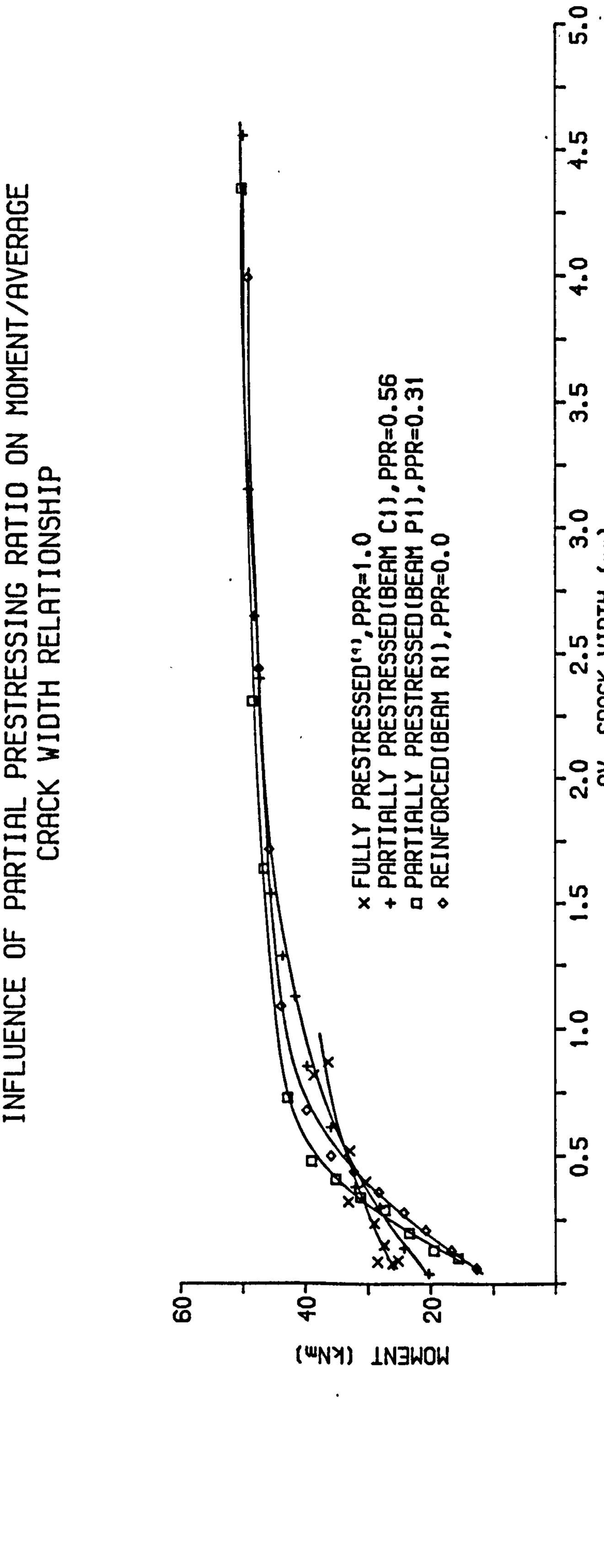
INFLUENCE OF PARTIAL PRESTRESSING RATIO ON MOMENT/AVERAGE CRACK WIDTH RELATIONSHIP
MOMENT (kNm)
AV. CRACK WIDTH (mm)
60
40
20
0.5
1.0
1.5
2.0
2.5
3.0
3.5
4.0
4.5
5.0
× FULLY PRESTRESSED(1),PPR=1.0
+ PARTIALLY PRESTRESSED(BEAM C1),PPR=0.56
□ PARTIALLY PRESTRESSED(BEAM P1),PPR=0.31
◇ REINFORCED(BEAM R1),PPR=0.0

Figure 6.3.28

will be greatest in those beams. The moment-average crack width response for beam series P and series R show an initial linear stage, the slope of which is steepest in the reinforced brickwork beam series R due to the increased area of non-tensioned steel close to the soffit of the beam and hence increased stiffness. It should be noted that during this initial stage the two beams with most prestress were uncracked. Although the crack widths in beam series P and series R had exceeded 0.2 mm beam series C and the fully prestressed beams were yet to crack and hence prestressing improved the crack control characteristics considerably. After cracking of the beams with a higher PPR the curve of the average experimental results is much flatter than that of the beams with lower PPR. There is a larger increase in crack widths for small increase in moment, this was due to reduction in area of non-tensioned steel close to the soffit leading to a reduction in stiffness. Generally the crack widths were largest in the reinforced brickwork beams and least in the fully prestressed, for all levels of moment leading up to failure, the partially prestressed brickwork beams being between the two extremes. Once the tensile reinforcment had yielded and the beams approached failure the curves were almost identical with very large crack widths giving adequate warning of collapse in all beams.

In the design of a beam a primary concern is the serviceability limit state of cracking, taken as 0.2 mm for this discussion, BS 8110[36]. The moments corresponding to this limit were 29 kNm, fully prestressed, 21.5 kNm, beam series C, 16.5 kNm, series P, and 14.3 kNm for the reinforced beam, series R. By prestressing the serviceability limit state moment had been increased from 14.3 to 29 kNm, or by 103%. Comparing the moments at 0.2 mm

with the corresponding ultimate moments for each beam the following factors of safety were obtained, fully prestressed 1.82, series C 2.49, series P 3.33, and 3.55 for the reinforced. Although all of these values were acceptable the beams with higher partial prestressing ratio provide the most satisfactory solution.

6.3.2.4 Effect of cover to non-tensioned steel

The effect of an increase in cover to non-tensioned steel from 25 to 50 mm may be studied by comparing the experimental results for beam series C (figure 6.3.13) and series CC (figure 6.3.19). The average experimental curves are compared in figure 6.3.29. The large variation in experimental results makes exact comparison impossible. An increase in cover of 100% increased the crack widths by between 10 and 20%. This was caused by the reduction in stiffness of the cracked section due to the reduction in effective depth of the non-tensioned steel, thus causing greater strains at the soffit of the beam.

Unlike in reinforced or prestressed concrete beams where the cover is a major variable due to its influence upon the average crack spacing, the crack spacing of the partially prestressed brickwork remained constant, section 6.3.1.1, and so cover in the test beams has a much smaller influence. If, however, the bonding pattern and cover is such that the cover is greater than b_j then a variation in cover may influence crack spacing and therefore the crack widths.

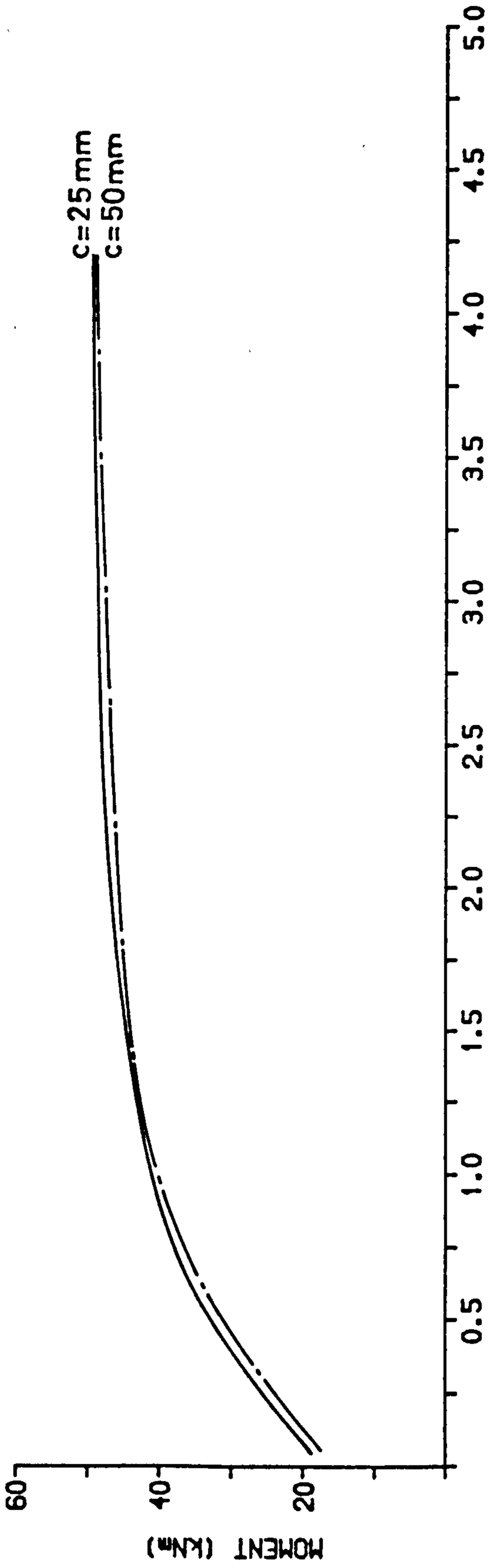
INFLUENCE OF COVER ON AVERAGE CRACK WIDTH
c=25mm
c=50mm
5.0
4.5
4.0
3.5
3.0
2.5
2.0
1.5
1.0
0.5
AV. CRACK WIDTH (mm)
60
40
20
MOMENT (kNm)

Figure 6.3.29

6.3.2.5 Effect of brick strength

The individual experimental relationships between average crack width and moment are shown for the high strength brick beams C1 - C8 and medium strength brick beams CM1 - CM3 in figures 6.3.13 and 6.3.20 respectively. A comparison of the average experimental curves for the high and medium strength brick beams are shown in figure 6.3.30. A reduction in the on-bed brick strength from 96.6 N/mm^2 (high) to 72.3 N/mm^2 (medium) clearly had little influence upon the cracking behaviour. However, a comparison of the high and low strength brick beams in figure 6.3.30 shows a slight increase in the average crack widths of the low strength brick beams for a corresponding reduction in the on-bed brick strength of 78%.

6.3.2.6 Effect of mortar grade

The average experimental curves for beam series C, grade I mortar, and beam series CG, grade II mortar, are compared in figure 6.3.31. The properties of the cross-section remained relatively unchanged by a reduction in mortar strength and therefore the development of average crack widths with moment was unchanged. The very slight decrease in the crack widths for beam series CG was due to a marginal increase in the average prestressing force compared to that of beam series C.

6.3.2.7 Maximum crack widths

The analysis has so far been confined to the consideration of the average crack widths, but in design it is the likelihood of

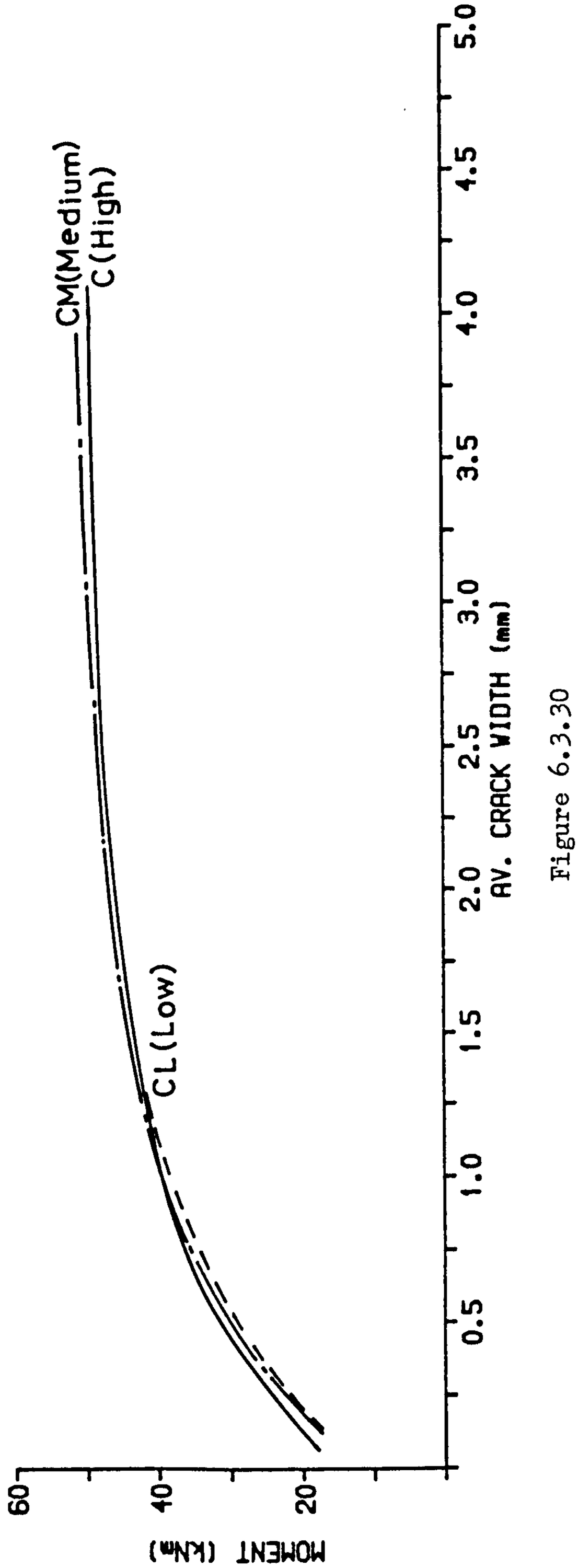
INFLUENCE OF BRICK STRENGTH ON AVERAGE CRACK WIDTH
CM(Medium)
C(High)
CL(Low)
MOMENT (kNm)
60
40
20
0.5
1.0
1.5
2.0
2.5
3.0
3.5
4.0
4.5
5.0
AV. CRACK WIDTH (mm)

Figure 6.3.30

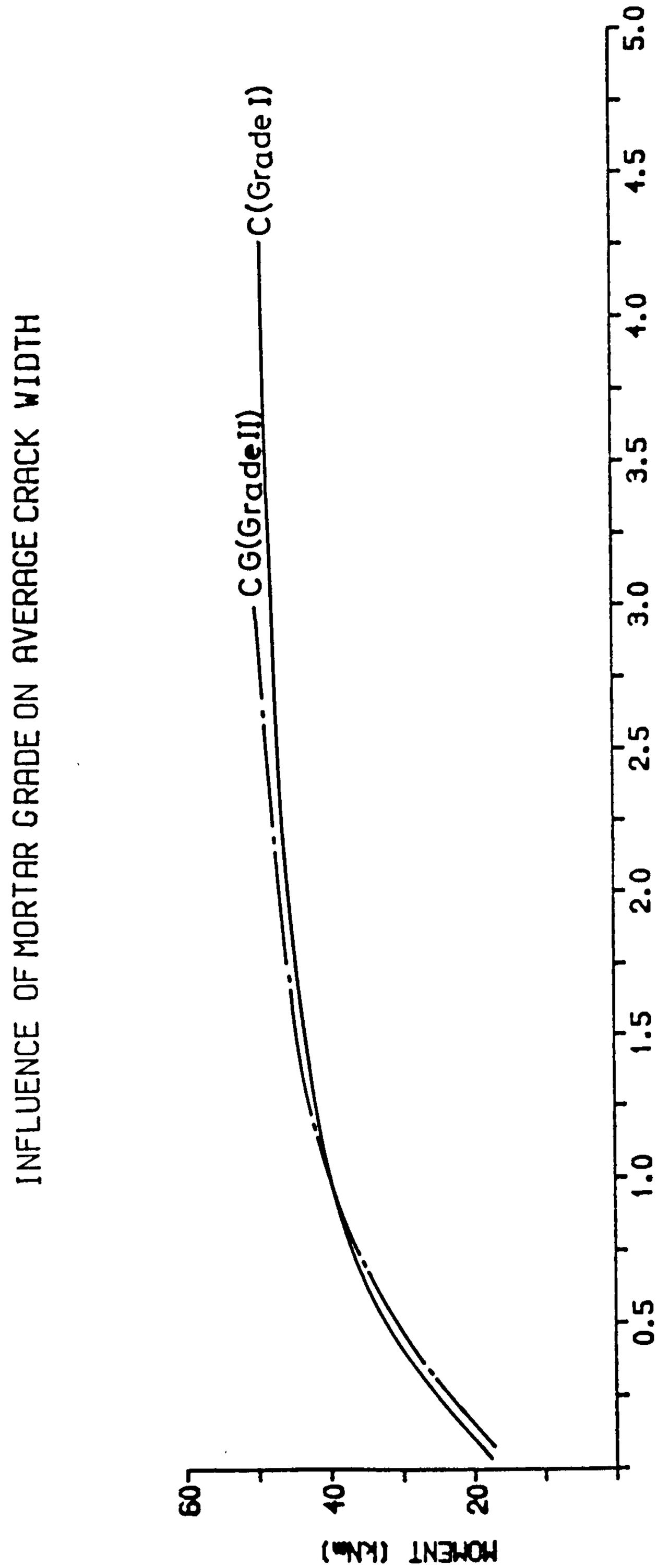
INFLUENCE OF MORTAR GRADE ON AVERAGE CRACK WIDTH
C G(Grade II)
C
MOMENT (kNm)
60
40
20
0.5
1.0
1.5
2.0
AV. CRACK WIDTH (mm)
2.5
3.0
3.5
4.0
4.5
5.0

Figure 6.3.31

the maximum crack width in a beam exceeding the limit state criteria that is of most concern. Previous research carried out on partially prestressed concrete beams has either tried to establish a statistical relationship between average and maximum crack widths[77] or attempted to calculate the maximum crack width by assuming to correlate it to a maximum crack spacing[69]. In the case of partially prestressed beams the crack spacing remained constant and hence the former approach was adopted.

Figure 6.3.32 presents a histogram of the experimental results for all the test beams indicating the frequency with which the maximum exceeded the mean crack width by a given amount. The maximum crack width was most often between 1.3 and 1.4 times the average, 69% of results lie between 1 and 1.5 times the average. Most importantly the 95% confidence limit, in which only 5% of the results were exceeded, equalled to twice the average crack width, thus:

$$w_{max} = 2 \cdot w_{av} \qquad (6.3.9)$$

Rewriting equations 6.3.5 and 6.3.8 in terms of maximum crack widths:

$$w_{max} = 2 \cdot b_j \cdot \varepsilon_{smb} \qquad (6.3.10)$$

and

$$w_{max} = \frac{2 \cdot K(f_{ct} - f_r)b_j}{\rho_s} \qquad (6.3.11)$$

In figure 6.3.33 the relationship between moment and maximum crack width presented for beam series C. The predicted values provide safe estimates, equation 6.3.10 based on average surface

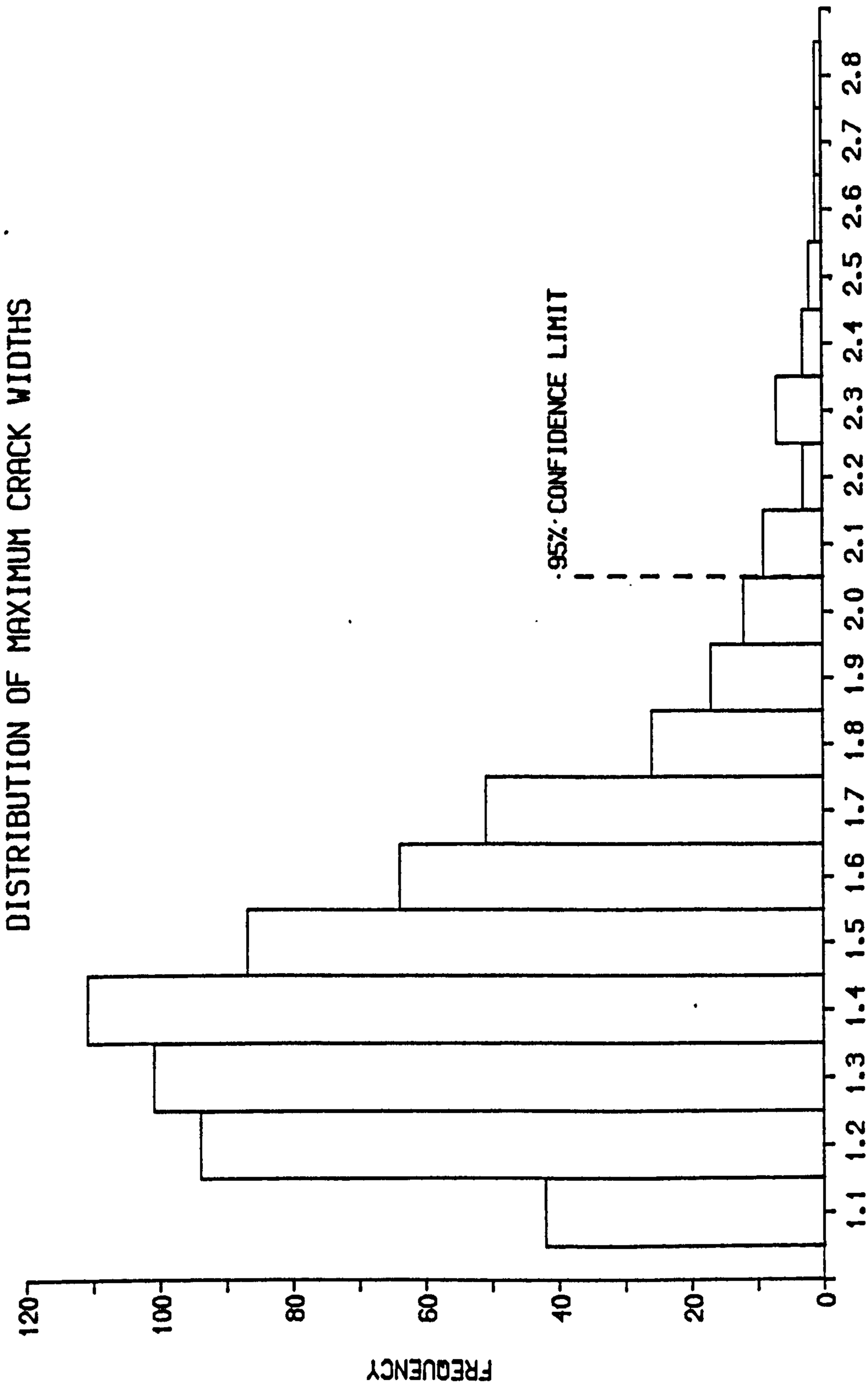
DISTRIBUTION OF MAXIMUM CRACK WIDTHS
95% CONFIDENCE LIMIT
MAX. CRACK WIDTH/AV. CRACK WIDTH
1.1 1.2 1.3 1.4 1.5 1.6 1.7 1.8 1.9 2.0 2.1 2.2 2.3 2.4 2.5 2.6 2.7 2.8
0 20 40 60 80 100 120
FREQUENCY

Figure 6.3.32

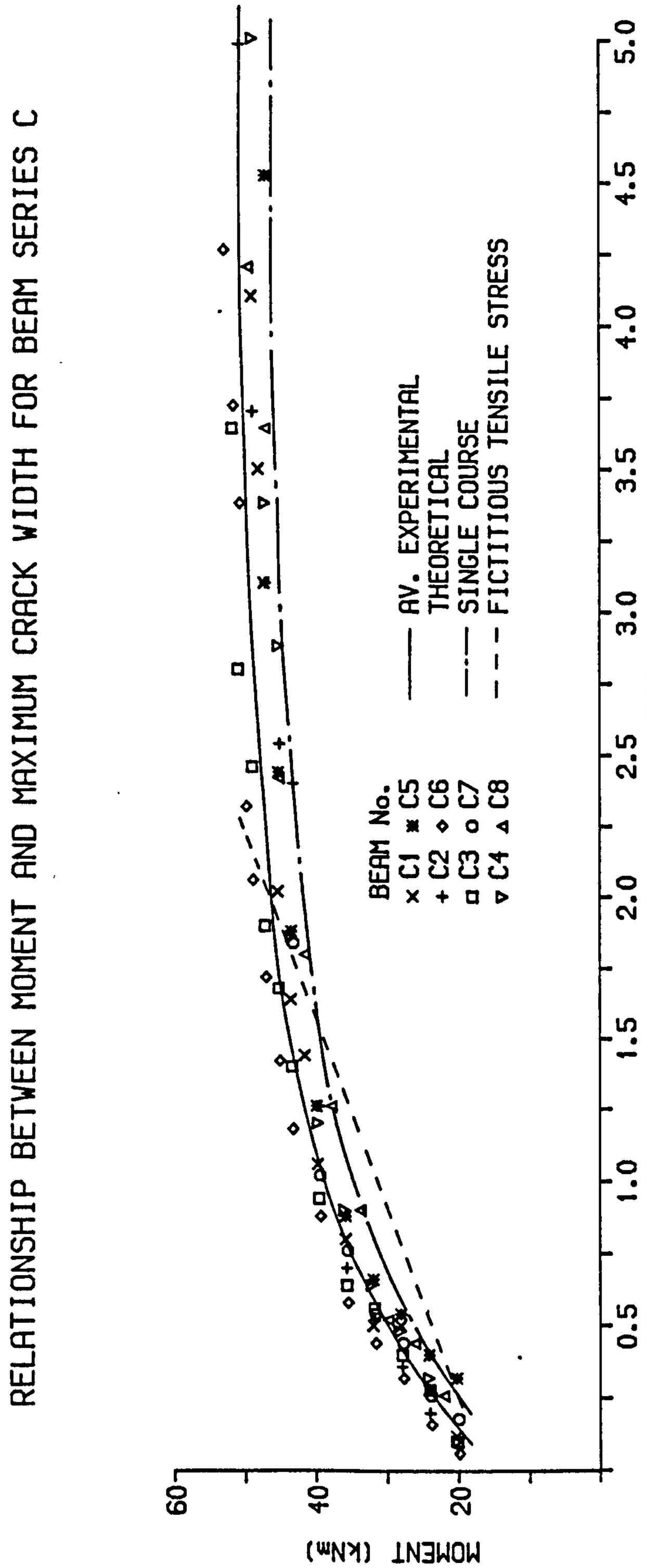
RELATIONSHIP BETWEEN MOMENT AND MAXIMUM CRACK WIDTH FOR BEAM SERIES C
MOMENT (kNm)
60
40
20
MAXIMUM CRACK WIDTH (mm)
0.5
1.0
1.5
2.0
2.5
3.0
3.5
4.0
4.5
5.0
BEAM No.
× C1
✱ C5
+ C2
◇ C6
□ C3
○ C7
▽ C4
△ C8
—— AV. EXPERIMENTAL
THEORETICAL
—·— SINGLE COURSE
– – – FICTITIOUS TENSILE STRESS

Figure 6.3.33

strain giving the closest correlation with experimental results.

6.4 SUMMARY AND CONCLUSIONS

1. The direct method proposed, incorporating the experimentally derived non-linear material properties and tension stiffening effect accurately predicted the average moment-curvature and crack widths of the partially prestressed brickwork beams.

2. The relationship between the tension-stiffening coefficient, K, and degree of cracking, f_{secr/f_s}, was non-linear. Tension-stiffening significantly reduced the curvature of partially prestressed brickwork beams.

3. The fictitious tensile stress approach incorporating variables such as the percentage of tensile reinforcement and joint distance provided reasonable estimates of the average crack widths in the initial stages of loading.

4. The percentage of tensile reinforcement has an important influence on the magnitude of the average crack widths. An increase in the area of non-tensioned steel close to the soffit of the beam reduced the crack widths.

5. A reduction in the prestressing force increased the crack widths at all loads after cracking in comparison with a similar beam with increased prestressing force.

6. By varying the partial prestressing ratio the cracking characteristics of brickwork beams may be controlled, within the limits defined by the fully prestressed brickwork beam (PPR=1) and the reinforced brickwork beam (PPR=0), to suit design requirements.

7. Cover to the non-tensioned steel, brick strength and mortar grade had little influence on the cracking characteristics of partially prestressed brickwork.

CHAPTER 7

CONCLUSIONS

7.1 SUMMARY AND CONCLUSIONS

In this study a total of forty-one full-scale partially prestressed brickwork beams were tested. The influence of the % area of steel, prestressing force, partial prestressing ratio, cover to the non-tensioned steel, brick strength and mortar grade on the ultimate moment, load/deflection and cracking behaviour of partially prestressed brickwork beams was studied experimentally. An interactive computer programme, incorporating the non-linear behaviour of the materials, was developed which predicts the structural behaviour of the beams up to failure. An expression relating the average crack width to the fictitious tensile stress in the brickwork was also proposed.

On the basis of this study the following conclusions can be drawn:

1. An increase in the % area of steel increases the ultimate flexural moment of partially prestressed brickwork beams. An increase in the % area of steel also reduces both the deflection and crack widths of a beam in comparison with a beam with similar effective prestressing force and brick strength but with reduced steel area.

2. The prestressing force has little direct influence on the ultimate flexural moment of under-reinforced partially prestressed brickwork beams. The deflection and crack widths of a beam are increased with a reduction in prestressing force.

3. By appropriate selection of the partial prestressing ratio the deformation and cracking of a brickwork beam can be controlled to within the limits defined by the reinforced and fully prestressed sections.

4. An increase in the cover to the non-tensioned steel decreases the ultimate flexural moment but has little effect upon the crack widths of the partially prestressed brickwork beams tested in this investigation.

5. For under-reinforced beams a reduction in the brick and mortar strength has little influence on the ultimate moment. A reduction in brick strength increases deflection, but has little influence upon the cracking characteristics. The mortar grade had little effect on the deflection and cracking behaviour of the partially prestressed brickwork beams tested in this investigation.

6. The moment-curvature and load/deflection relationships exhibited a distinctive three phase format. Prior to yielding of the tensile reinforcement the partially prestressed brickwork beams illustrated almost complete recovery of both deflection and cracking upon removal of the applied load.

7. The direct method proposed, incorporating the non-linear material properties, accurately predicted the load/deflection response and cracking of the partially

prestressed brickwork beams. The compressive properties for brickwork given by the single course brickwork prisms provided the best model of compression zone behaviour of the partially prestressed brickwork beams prior to and at ultimate.

8. The fictitious tensile stress approach incorporating variables such as the % area of steel and joint distance provided reasonable estimations of the average crack widths and may be used for the crack width calculation in the design of such beams.

9. The ultimate moments and deflections of the partially prestressed brickwork beams predicted in accordance with BS 5628 Part 2, 1985, over estimated the experimental moments.

7.2 SUGGESTIONS FOR FURTHER RESEARCH

In this investigation a number of partially prestressed brickwork beams were tested and a theoretical method, using non-linear material properties, to predict ultimate moment, deformation and cracking was proposed and successfully applied to the test beams. The crack widths were also estimated with a method using fictitious tensile stress in the brickwork and incorporating variables such as percentage of tensile reinforcement and joint distance. However, before the methods are more generally applicable further tests need to be conducted in the areas outlined below.

The present experimental programme was limited to a study of flexural behaviour of partially prestressed brickwork beams under short-term loading. It is necessary also to consider the shear behaviour and response of beams under dynamic loading conditions.

The suggestions for further research are listed as follows:

1. Experimental tests are required to be conducted on beams built using differing bond patterns, therefore requiring a varied format of brickwork prism.

2. Experiments indicated that the joint spacing at the soffit of the beam influenced the tension-stiffening expression and the equations for crack width prediction. A number of tests are required in which the joint spacing at soffit of the beam, cover and percentage area of steel are varied to study further the cracking behaviour of partially prestressed brickwork beams.

3. Previous tests conducted on partially prestressed concrete beams have indicated that a precompression is introduced into the non-tensioned steel due to the prestress of the section. Although this effect was limited in the test beams further tests are required to study the effect in detail and under what circumstances it is likely to be significant. Experiments also required into broader field of prestress losses, the variables influencing losses and hence to develop a theoretical analysis to predict the losses.

4. The shear behaviour of partially prestressed brickwork beams needs to be considered both experimentally and theoretically.

5. The partially prestressed beam section offers improved ductility compared to the fully prestressed section and so better dynamic, seismic, loading characteristics. These potential advantages offered by partially prestressed brickwork should be considered.

R E F E R E N C E S

1 BAKER (L R): 'The flexural action of masonry structures under lateral load'. Ph.D., Deakin University, Australia, 1981.

2 SCHNEIDER (R R) and DICKEY (W L): 'Reinforced Masonry Design'. Publ. Prentice-Hall, New Jersey, 1980.

3 BRITISH STANDARDS INSTITUTE: British Standard code of practice for use of masonry, Part 1. Structural use of unreinforced masonry. BS 5628, Part 1, 1978.

4 PLUMMER (H C) and BLUME (J A): 'Reinforced Brick Masonry and Lateral Force Design'. Publ. Structural Clay Products Ltd, Washington DC, 1953.

5 HASELTINE (B A) and TUTT (J N): 'Brickwork retaining walls'. Publ. The Brick Development Association, Westerham Press, 1979.

6 THE INSTITUTION OF STRUCTURAL ENGINEERS: 'Reinforced and prestressed masonry'. Publ. Institution of Structural Engineers, London, July 1981.

7 SINHA (B P): 'Reinforced grouted cavity brickwork'. Building Research and Practice, July/August 1982, pp 226 - 243.

8 SUTER (G T) and HENDRY (A W): 'Shear strength of reinforced brickwork beams'. The Structural Engineer, June 1975, No. 6, Volume 53, pp 249 - 253.

9 PEDRESCHI (R F): 'A Study of the Behaviour of Post-tensioned Brickwork Beams'. Ph.D., Department of Civil Engineering and Building Science, The University of Edinburgh, 1983.

10 ABELES (P W): 'An Introduction to Prestressed Concrete, Volume 1'. Publ. Concrete Pulications Ltd, London, 1964.

11 RAMASWAMY (G S): 'Modern Prestressed Concrete Design'. Publ. Pitman, London, 1976.

12 WILLIAMS (E O L) and PHIPPS (M E): 'The Bending Behaviour of Prestressed Masonry Box Beams at Ultimate'. Proceedings of the 6th International Brick Masonry Conference, Edited by Laterconsult. Rome, 1982, pp 981 - 992.

13 ROBSON (I J), HULSE (R), AMBROSE (R J) and MORTON (J): 'Performance of Post-tensioned Brickwork Beams under Service and Ultimate Load Conditions'. Proceedings of the 3rd Canadian Masonry Conference, Edited by J Longworth and J Warwaruk. Edmonton, Canada, June 1983, paper no. 14.

14 GARWOOD (T G): 'The Construction and Test Performance of Four Prestressed Brickwork Beams'. The Eighth International Symposium on Loadbearing brickwork, London, 1983.

15 BRITISH STANDARDS INSTITUTE: British Standard Code of Practice for Use of masonry, Part 2. Structural use of reinforced and prestressed masonry, BS 5628, Part 2, 1985.

16 CONCRETE SOCIETY TECHNICAL REPORT No 23: Partial prestressing. Report of a Concrete Society Working Party. Publ. Concrete Society, London, 1983.

17 THOMAS (K): 'Current post-tensioned and prestressed brickwork and ceramics in Great Britain'. Designing Engineering and Constructing with Masonry Products. Edited by F B Johnson. Gulf, Houston, Texas, 1969, pp 285 - 301.

18 GADEGBEKU (C B K): 'A Study of the Magnitude and Distribution of the Stresses in the end-block of a Post-tensioned Concrete Beam'. Ph.D., Rutgers University, New Jersey, 1980.

19 MEHTA (K C) and FINCHER (D): 'Structural Behaviour of Pretensioned Prestressed Masonry Beams'. Proceedings of the 2nd International Brick Masonry Conference, Edited by H W H West and K Speed. Stoke-on-Trent, BCRA, 1971, pp 215-219.

20 CURTIN (W G) and PHIPPS (M E): 'Prestressed Masonry Diapragm Walls'. Proceedings of the 6th International Brick Masonry Conference, Edited by Laterconsult. Rome 1982, pp 971 - 980.

21 ROUMANI (N) and PHIPPS (M E): 'The Shear Strength of Prestressed Brickwork I-Sections'. Eighth International Symposium of Loadbearing Brickwork, London 1983.

22 ROUMANI (N) and PHIPPS (M E): 'The Shear Strength of Prestressed Brickwork I and T Sections'. Proceedings of the 7th International Brick Masonry Conference, Edited by T McNeilly and J C Scrivener. Melbourne, Australia, 1985. Vol 2, pp 1001 - 1014.

23 MONTAGUE (T I) and PHIPPS (M E): 'The Behaviour of Post-tensioned Masonry in Flexure and Shear'. International Symposium on Reinforced and Prestressed Masonry, Edinburgh, 1984. (In press)

24 ROBSON (I J), AMBROSE (R J), HULSE (R) and MORTON (J): 'Post-Tensioned Prestressed Brickwork Beams'. The Eighth International Symposium on Loadbearing Brickwork, London, 1983.

25 PEDRESCHI (R F) and SINHA (B P): 'Development and investigation of the ultimate load behaviour of post-tensioned brickwork beams'. The Structural Engineer, Vol. 60B, No. 3, September 1982, pp 63 - 67.

26 PEDRESCHI (R F) and SINHA (B P): 'Deformation and cracking of post-tensioned brickwork beams'. The Structural Engineer, Vol. 63B, No. 4, December 1985, pp 93 - 99.

27 WALKER (P) and SINHA (B P): 'Behaviour of Partially Prestressed Brickwork Beams'. Proceedings of the 7th International Brick Masonry Conference, Edited by T McNeilly and J C Schrivener, Melbourne, Australia, 1985, pp 1015 - 1029.

28 GARWOOD (T G): 'A Comparison of the Behaviour of Reinforced, Prestressed and Partially Prestressed Brickwork Beams'. Proceedings of the First International Masonry Conference. Held by The British Masonry Society, London, December, 1986.

29 LENCZNER (D): 'Loss of Prestress in Post-tensioned Brickwork Walls and Columns'. Proceedings of the Eighth International Symposium on Loadbearing Brickwork, London, 1983.

30 LENCZNER (D) and DAVIES (P): 'Loss of Prestress in Post-tensioned Brickwork Walls and Columns'. International Symposium on Reinforced and Prestressed Masonry, Edinburgh, 1984. (In press)

31 LENCZNER (D): 'The Loss of Prestress in Post-tensioned Brick Masonry Members'. Masonry International, Number 5, July 1985, pp 9 - 12.

32 NEIL (J A): 'Post-tensioned Brickwork'. Clay Products Technical Bureau. Technical note, Volume 1, no. 9, 1966.

33 FOSTER (D): 'Design and Construction of a Prestressed Brickwork Water Tank'. Proceedings of the 2nd International Brick Masonry Conference, Edited by H W H West and K Speed. Stoke-on-Trent, BCRA, 1971.

34 CURTIN (W G), BECK (J K), SHAW (G) and POPE (L S): 'Post-tensioned, Free Cantilever Diaphragm Wall Project'. Proceedings of the 6th International Brick Masonry Conference, Edited by Laterconsult. Rome, 1982, pp 1645 - 1656.

35 BRADSHAW (R E), DRINKWATER (J) and BELL (S E): 'A Multi-purpose Farm Building Incorporating Prestressed Brickwork Diaphragm Walling'. Loadbearing brickwork(7). Proceedings of the British Ceramic Society, Edited by H W H West. No 30, September 1982, pp 308 - 315.

36 BRITISH STANDARDS INSTITUTE: British Standard Structural Use of Concrete, Part 1. Code of practice for design and construction. BS 8110, Part 1, 1985.

37 NAAMAN (A E) and SIRIAKSORN (A): 'Serviceability Based Design of Partially Prestressed Beams, Part 1: Analytic Formulation'. Journal of the Prestressed Concrete Institute, volume 24, no.2, March/April, 1979, pp 64 - 89.

38 BRITISH STANDARDS INSTITUTE: British Standard Specification for Clay bricks, BS 3921, 1985.

39 LENCZNER (D) and FOSTER (D): 'Strength and Deformation of Brickwork Prisms in Three Directions'. Proceedings of the 5th International Brick Masonry Conference. Edited by J A White. Washington, USA, 1979, pp 49 - 55.

40 PAGE (A W) and MARSHALL(R): 'The Influence of Brick and Brickwork Prism Aspect Ratio on the Evaluation of Compressive Strength'. Proceedings of the 7th International Brick Masonry Conference, Edited by T McNeilly and J C Scrivener. Melbourne, Australia, 1985, Vol 1, pp 653 - 664.

41 PEDRESCHI (R F) and SINHA (B P): 'The Stress/Strain Relationship of Brickwork'. Proceedings of the 6th International Brick Masonry Conference, Edited by Laterconsult. Rome, 1982, pp 321 - 335.

42 HODGKINSON (H R) and DAVIES (S): 'The Stress Strain Relationships of Brickwork when stressed in Directions other than Normal to the Bed Face'. Proceedings of the 6th International Brick Masonry Conference, Edited by Laterconsult. Rome, 1982, pp 290 - 299.

43 BRITISH STANDARDS INSTITUTE: British Standard Specification for Ordinary and Rapid-hardening Portland Cement. BS 12, 1978.

44 BRITISH STANDARDS INSTITUTE: Specification for building limes. BS 890, 1976.

45 BRITISH STANDARDS INSTITUTE: Specification for building sands from natural sources. BS 1200, 1976.

46 BRITISH STANDARDS INSTITUTE: British Standard Specification for aggregates from natural sources for concrete. BS 892, 1983.

47 BRITISH STANDARDS INSTITUTE: British Standard Structural use of concrete. Part 2. Code of practice for special circumstances. B2 8110, Part 2, 1985.

48 BRITISH STANDARDS INSTITUTE. Specification for high tensile steel wire and strand for the prestressing of concrete. BS 5896, 1980.

49 BRITISH STANDARDS INSTITUTE: Specification for hot rolled steel bars for the reinforcement of concrete. BS 4449, 1978.

50 BRITISH STANDARDS INSTITUTE. Methods for tensile testing of metals. Part 2 Steel (General) BS 18, 1971.

51 TURNSEK (V) and CACOVIC (F): 'Some Experimental Results on the Strength of Brick Masonry Walls'. Proceedings of the 2nd International Brick Masonry Conference, Edited by H W H West and K Speed, BCRA, Stoke-on-Trent, 1971, pp 149 - 156.

52 WALKER (P) and SINHA (B P): 'Compressive Strength of Brickwork on Edge under Axial and Eccentric Loading'. Masonry International, No. 6, December 1985, pp 1 - 8.

53 POWELL (B) and HODGKINSON (H R): 'The Determination of Stress/Strain Relationship of Brickwork'. Proceedings of the 4th International Brick Masonry Conference, Brugges, 1976, paper 2.a.5.

54 POPOVICS (S): 'A Review of the Stress-Strain Relationships for Concrete'. Journal of American Concrete Institute, Volume 67, 1970, pp 243 - 247.

55 HENDRY (A W): 'Structural Brickwork'. Publ. The Macmillan Press, London, 1982.

56 BEARD (R): 'A Theoretical Analysis of Reinforced Brickwork in Bending'. Load-bearing Brickwork (7). Proceedings of the British Ceramic Society, Edited by H W H West. No. 30, September 1982, pp 272 - 282.

57 SINHA (B P): 'An ultimate load-analysis of brickwork flexural members'. International Journal of Masonry Construction, Volume 1, no. 4, 1981, pp 151 - 155.

58 SINHA (B P): 'Ultimate load anaylsis of reinforced brick beams'. BCRA Seminar on Theory of Masonry Structures, July 1980.

59 SINHA (B P) and PEDRESCHI (R F): 'Compressive strength and some elastic properties of brickwork'. International Journal of Masonry Construction, Volume 3, No. 1, 1983, pp 19 - 25.

60 BURNS (N H): 'Moment Curvature Relationships for Partially Prestressed Concrete Beams'. Journal of the Prestressed Concrete Institute, Volume 9, 1964, pp 52 - 63.

61 WARWARUK (J), SOZEN (M A) and SEISS (C P): 'Investigation of Prestressed Concrete for Highway Bridges; Part III, Strength and Behaviour in Flexure of Prestressed Concrete Beams'. University of Illinois Bulletin, no 464, 1962.

62 GHALI (A) and NEVILLE (A M): 'Structural Analysis: A Unified Classical and Matrix Approach'. Publ. Chapman and Hall, London, 1971.

63 KONG (F K) and EVANS (R H): 'Reinforced and Prestressed Concrete'. 2nd Edition. Publ. Van Norstrand Reinhold, 1980.

64 THURLIMANN (B A): 'A Case for Partial Prestressing'. Structural Concrete Symposium, Toronto, May 1971. Department of Civil Engineering, University of Toronto, pp 253 - 301.

65 BENNETT (E W) and CHANDRASEKHAR (C S): 'Calculation of the width of cracks in Class 3 prestressed beams'. Proceedings of the Institution of Civil Engineers, Vol 49, July 1971, pp 333 - 346.

66 BENNET (E W) and VEERASUBRAMANIAN (N): 'Behaviour of Non-rectangular Beams With Limited Prestress After Flexural Cracking'. Journal of the American Concrete Institute, Title no 69-48, September 1972, pp 533 - 542.

67 NAWY (E G): 'Flexural Cracking Behaviour of Pretensioned and Post-tensioned Beams: The State of the Art'. Journal of American Concrete Institute, Title No 82-84, Nov/Dec 1985, pp 890 - 900.

68 KRISHNA RAJU (N), BASVARAJAIAH (B S) and AHAMED KUTTY (U C): 'Flexural Behaviour of Pretensioned Concrete Beams with Limited Prestress'. Building Science, Vol 8, 1973, pp 179 - 185.

69 DESAYI (P): 'A method for determining the spacing and width of cracks in partially prestressed concrete beams'. Proceedings of the Institution of Civil Engineers, Vol 59, September 1975, pp 411 - 428.

70 MEIER (S W) and GERGELY (P): 'Flexural Crack Widths in Prestressed Concrete Beams'. Proceedings of A.S.C.E., Vol 107, ST2, February 1981, pp 429 - 433.

71 BEEBY (A W), KEYDER (E) and TAYLOR (H P J): 'Cracking and Deformations of Partially Prestressed Concrete Beams'. Cement and Concrete Association Technical Report 465 Publication 42.465, 1972.

72 SRINIVASA RAO (P) and SUBRAHMANYAM (B V): 'Trisegmental Moment-Curvature Relations for Reinforced Concrete Members'. Journal of the American Concrete Institute, Total No 70-39, May 1973, pp 346 - 357.

73 BENNET (E W): 'Partial Prestressing - A Historical Overview'. Journal of the Prestressed Concrete Institute, Vol 29, Sept - Oct 1984, pp 105 - 117.

74 BASE (G D), READ (J B), BEEBY (A W) and TAYLOR (H P J): 'Crack control in concrete beams'. CERA, Research Report No 6, Cement and Concrete Association, 1966.

75 BEEBY (A W): 'The prediction of crack widths in hardened concrete'. The Structural Engineer, Vol 57A, No 1, January 1979, pp 9 - 17.

76 BEEBY (A W): 'An Investigation of Cracking in Slabs Spanning One Way'. Cement and Concrete Association Technical Report 433, April 1970.

77 PARAMESWARAN (V S), ANNAMALAI (G) and RAMASWAMY (G S): 'Theoretical and Experimental Investigations on the Flexural Behaviour of Class 3 Beams'. Paper presented at the Seventh Congress of the FIP, New York, 28 - 30, May, 1974.

APPENDIX A

INTERACTIVE COMPUTER PROGRAMME

A1 DESCRIPTION OF PROGRAMME

An interactive computer programme was written to predict the moment-curvature relationship, ultimate moment, deflection and crack widths for a rectangular reinforced, fully or partially prestressed brickwork or concrete beam section. The direct method of analysis was used, as outlined in chapter 4. A rectangular concrete cavity has been incorporated into the brickwork section, it may be at any depth and size, such that the section varies between the extremes of being all brickwork or all concrete.

The deflection of the beam is calculated both with and without considering the effects of dead load and hence is directly applicable to experimental test results. Three different types of loading most commonly used in experimental work on flexural members can be adopted with the computations, namely single point load, 2 point loads and uniformly distributed loading acting symmetrically over part or all of the beam. The beam is considered to be simply supported.

A2 DATA REQUIREMENTS

Input of data is carried interactively, a number of default values and error messages are present. A comprehensive list of the data requirements is as follows:-

- Breadth of section (mm)
- Height of section (mm)

- Distance from top of section to top and bottom of cavity (mm) and breadth of cavity (mm)
- Compressive strength of brickwork and/or concrete (N/mm^2)
- Ultimate compressive strain of brickwork or concrete [default = 0.35%]
- Modulus of rupture (N/mm^2) [default for brickwork = 1.0 N/mm^2, concrete = fcu/10]
- Stress/strain properties of brickwork and concrete, coefficients for third degree polynomial [default values; for brickwork stress/strain curves in chapter 3, for concrete stress/strain curves in BS 8110 Part 2 1985]
- Area of steel (N/mm^2), layer 1 and 2.
- Depth of steel (mm), layer 1 and 2
- Prestressing force (kN), layer 1 and 2
- Stress/strain properties of steel, layer 1 and 2, coefficients of tri-linear relationship and ultimate tensile strength [default values]
- Span (mm)
- Loading arrangement; single point, 2 point load or udl
- Dead weight (kN/m)
- Crack width prediction and spacing (mm), depth of cracking (mm) [default values].

```
10 DIM MOM(25),CURV(25),DIFF(19,19),BMAT(19),DEFL(19),DIFFT(19,19)
20 DIM DNARRY(25),MOMENT(25),COFF(4),CURVE(25),STRST(25),SPND2(30)
30 DIM FLOAD(40),DEFLEX(40),STRN1(2),STRN2(2),ESTELS(25),STRANS(25)
40 DIM SMOM(5),CURVEP(5),STRST2(25),HCON(19),KCON(19),D(25)
50 DIM DLL(20),DDWT(20),PLODL(20)
60 PRINT"    This program predicts the moment-curvature,deflection,ultimate"
70 PRINT"moment and average crack widths for a rectangular reinforced,fully"
80 PRINT"or partially prestressed brickwork or concrete beam section.A direct"
90 PRINT"method is used in which at each given strain profile the internal"
100 PRINT"forces are equated using the idealised experimental stress/strain"
110 PRINT"relationships for the materials.The applied loading is considered in"
120 PRINT"three stages;"
130 PRINT"                (i)  prestressing"
140 PRINT"                (ii) prestressing to cracking"
150 PRINT"                (iii)post cracking to ultimate"
160 PRINT"The tension-stiffening effect of the brickwork/concrete is also"
170 PRINT"considered.The deflection is calculated with and without considering"
180 PRINT"the effects of the dead load and hence are directly applicable to"
190 PRINT"experimental results.Three different types of loading most commonly"
200 PRINT"used in experimental work on flexural members can be adopted into the"
210 PRINT"computations,namely two point loads,single central point load and"
220 PRINT"uniformly distributed loading. The beam is considered to be simply"
230 PRINT"supported."
240 PRINT"    Input of data is in free format and unless otherwise stated all"
250 PRINT"values are positive.The program contains a number of default values"
260 PRINT"allowing the maximum ease of calculation."
270 PRINT"                                                                    "
280 PRINT"Continue (y/n)";:INPUT Q$
290 IF Q$="y" OR Q$="Y" GOTO 310
300 END
310 PRINT "The section may be either brickwork, concrete or a composite"
320 PRINT "Input number corresponding to section required"
330 PRINT "1.Brickwork or brickwork/concrete composite"
340 PRINT "2.Concrete"
350 INPUT FACTOR1
360 IF FACTOR1<1 OR FACTOR1>2 GOTO 310
370 IF FACTOR1=2 GOTO 820
380 PRINT "Breadth of section (mm)";:INPUT BREDTH
390 PRINT "Depth of section (mm)";:INPUT DEPTH
400 PRINT "Properties of brickwork"
410 PRINT "Compressive strength of brickwork (N/mm2)";:INPUT STRSMX
420 PRINT "Ultimate compressive strain"
430 PRINT "Default;ult compr strain=0.0035.OK(y/n)";:INPUT ANS10$
440 IF ANS10$="y" OR ANS10$="Y" THEN STRMX=.0035
450 IF ANS10$="y" OR ANS10$="Y" GOTO 490
460 PRINT "ult compr strain ";:INPUT STRMX
470 IF STRMX>.01 THEN PRINT "Check value for ult strain"
480 IF STRMX>.01 GOTO 420
490 PRINT "Modulus of rupture,default=1.5N/mm2.OK (y/n)?";:INPUT AR$
500 IF AR$="y" OR AR$="Y" GOTO 560
510 PRINT "Modulus of rupture (N/mm2)";:INPUT RMOD
520 IF RMOD<STRSMX GOTO 570
530 PRINT "Modulus of rupture greater than compr. strength ?.Retry"
540 GOTO 510
550 GOTO 570
560 RMOD=1.5
570 PRINT "Stress/strain relationship of brickwork is expressed in the"
580 PRINT "form of a third degree polynomial,such that;"
590 PRINT "f/fm=X1(e/em)+X2(e/em)(e/em)+X3(e/em)(e/em)(e/em)"
600 PRINT "Where f=compr. stress,fm=compr. strength,e=strain and"
610 PRINT "em=ult. compr. strain"
620 PRINT "Default;X1=2.118,X2=-1.788,X3=0.661"
630 PRINT "OK (y/n)";:INPUT ANS$
640 IF ANS$="y" OR ANS$="Y" GOTO 690
650 PRINT "X1";:INPUT COFF(1)
660 PRINT "X2 (-ve)";:INPUT COFF(2)
670 PRINT "X3";:INPUT COFF(3)
680 GOTO 720
690 COFF(1)=2.118
700 COFF(2)=-1.778
710 COFF(3)=.661
720 PRINT "Concrete infill (y/n)";:INPUT A$
730 IF A$="n" OR A$="Y" THEN STRMXC=STRMX
740 IF A$="n" OR A$="N" GOTO 1230
750 FACTOR2=2
760 PRINT "Distance from top of section to top of"
770 PRINT "concrete cavity (mm)";:INPUT D1
780 PRINT "Distance from top section to bottom of"
790 PRINT "concrete cavity (mm)";:INPUT D2
800 PRINT "Breadth of concrete cavity (mm)";:INPUT BCON
810 IF FACTOR1<>2 GOTO 940
```

```
820 PRINT "The section is concrete only"
830 PRINT "Breadth (mm)";:INPUT BCON
840 PRINT "Depth (mm)";:INPUT D2
850 PRINT "Ult compr strain for concrete,default=0.0035.OK (y/n)";:INPUT B$
860 IF B$="y" OR D$="Y" GOTO 890
870 PRINT "Ult compr strain ";:INPUT STRMXC
880 GOTO 900
890 STRMXC=.0035
900 PRINT "Modulus of rupture,default=compr strength/10.0.OK (y/n)";:INPUT C$
910 IF C$="y" OR C$="Y" GOTO 930
920 PRINT "Modulus of rupture";:INPUT RMOD
930 D1=0!
940 PRINT "Cube crushing strength of concrete (N/mm2)";:INPUT STRSMC
950 IF C$="y" OR C$="Y" THEN RMOD=STRSMC/10!
960 PRINT "The default stress/strain relationship for concrete is that given "
970 PRINT "by BS 8110, Part 2, 1985. However, the user may specify the stress/"
980 PRINT "strain curve in terms of either a second or third degree polynomial"
990 PRINT "Do you wish to use the code defined curve?, (y/n)";:INPUT CCODE$
1000 IF CCODE$="Y" OR CCODE$="y" GOTO 1050
1010 PRINT "Stress/strain relationship to be defined by user as second or third"
1020 PRINT "polynomial, as for brickwork. If second degree polynomial required"
1030 PRINT "then specify X3=0.Input X1,X2,X3";: INPUT CX1,CX2,CX3
1040 GOTO 1070
1050 YCONC=5.5*(SQR(STRSMC))
1060 CONCK=3*YCONC/STRSMC
1070 IF FACTOR1=2 THEN BREDTH=BCON
1080 IF FACTOR1=2 THEN DEPTH=D2
1090 IF FACTOR1=2 THEN STRSMX=STRSMC
1100 IF FACTOR1=2 THEN FACTOR2=2
1110 IF D1>D2 OR D2>DEPTH GOTO 1140
1120 IF BCON>BREDTH GOTO 1190
1130 GOTO 1240
1140 PRINT "Check values for depth of concrete since depth of "
1150 PRINT "cavity is greater than depth of section or depth to"
1160 PRINT "top of cavity is greater than distance to bottom of cavity???!!!"
1170 PRINT "Retry"
1180 GOTO 760
1190 PRINT "Check value for breadth of concrete cavity since it greater"
1200 PRINT "than the breadth of the section???"
1210 PRINT "Retry"
1220 GOTO 760
1230 BCON=0!
1240 PRINT "This program allows the tensile reinforcement to be placed"
1250 PRINT "at two separate depths.If a prestress force is applied to"
1260 PRINT "only one area of the reinforcement then it should be applied"
1270 PRINT "to the first"
1280 PRINT "Area of steel1 (mm2)";:INPUT ASTL1
1290 PRINT "Effective depth (mm)";:INPUT EFFD1
1300 PRINT "Prestress force (kN)";:INPUT PRSTR1
1310 PRINT "Area of steel2 (mm2)";:INPUT ASTL2
1320 IF ASTL2=0! GOTO 1430
1330 PRINT "Effective depth (mm)";:INPUT EFFD2
1340 IF EFFD2<EFFD1 GOTO 1370
1350 IF EFFD1>DEPTH OR EFFD2>DEPTH GOTO 1400
1360 GOTO 1420
1370 PRINT "Depth of steel2 should be greater than that of steel1"
1380 PRINT "Retry"
1390 GOTO 1280
1400 PRINT "Depth of steel greater than depth of section ?????,Retry"
1410 GOTO 1290
1420 PRINT "Prestress force (kN)";:INPUT PRSTR2
1430 PRINT "The stress/strain properties of the reinforcement are"
1440 PRINT "expressed in tri-linear form"
1450 PRINT "Steel1"
1460 PRINT "Default values are as follows;"
1470 PRINT "strain1=0.0072"
1480 PRINT "strain2=0.012"
1490 PRINT "E1=214000 N/mm2"
1500 PRINT "E2=22900 N/mm2"
1510 PRINT "E3=2300 N/mm2"
1520 PRINT "Ult tensile strength=1708"
1530 PRINT "OK (y/n)";:INPUT ANS1$
1540 IF ANS1$="y" OR ANS1$="Y" GOTO 1760
1550 PRINT "strain1";:INPUT STRN1(1)
1560 PRINT "strain2";:INPUT STRN2(1)
1570 PRINT "E1";:INPUT EMOD
1580 PRINT "E2";:INPUT EMODA
1590 PRINT "E3";:INPUT EMODB
1600 PRINT "Ult tensile strength";:INPUT ULT1
1610 IF STRN1(1)>STRN2(1) THEN PRINT "strain1 greater than strain2?"
1620 IF STRN1(1)>STRN2(1) GOTO 1550
```

```
1630 IF EMODA>EMOD OR EMODB>EMOD THEN PRINT "Either E2 or E3 > E1 ??"
1640 IF EMODA>EMOD OR EMODB>EMOD GOTO 1570
1650 IF EMODB>EMODA THEN PRINT "E3 greater than E2 ???"
1660 IF EMODB>EMODA GOTO 1580
1670 STRESS1=STRN1(1)*EMOD
1680 STRESS2=((STRN2(1)-STRN1(1))*EMODA)+STRESS1
1690 IF STRESS1>ULT1 GOTO 1720
1700 IF STRESS2>ULT1 GOTO 1720
1710 GOTO 1820
1720 PRINT "Ult tensile strength less than stress specified in"
1730 PRINT "stress/strain relationship ??"
1740 GOTO 1550
1750 GOTO 1830
1760 STRN1(1)=.0072
1770 STRN2(1)=.012
1780 EMOD=214000!
1790 EMODA=22900!
1800 EMODB=2300!
1810 ULT1=1708
1820 IF ASTL2=0! GOTO 2190
1830 PRINT "Steel2"
1840 PRINT "Default values are as follows;"
1850 PRINT "strain1=0.002"
1860 PRINT "strain2=0.0043"
1870 PRINT "E1=200000 N/mm2"
1880 PRINT "E2=32600 N/mm2"
1890 PRINT "E3=6000 N/mm2"
1900 PRINT "Ultimate tensile strength=670 N/mm2"
1910 PRINT "OK (y/n)";:INPUT ANS2$
1920 IF ANS2$="y" OR ANS2$="Y" GOTO 2130
1930 PRINT "strain1";:INPUT STRN1(2)
1940 PRINT "strain2";:INPUT STRN2(2)
1950 PRINT "E1";:INPUT EMODS
1960 PRINT "E2";:INPUT EMODSA
1970 PRINT "E3";:INPUT EMODSB
1980 PRINT "Ult tensile strength";:INPUT ULT2
1990 IF STRN1(2)>STRN2(2) THEN PRINT "strain1 > strain2 ???"
2000 IF STRN1(2)>STRN2(2) GOTO 1930
2010 IF EMODSA>EMODS OR EMODSB>EMODS THEN PRINT"either E2 or E3>E1??"
2020 IF EMODSA>EMODS OR EMODSB>EMODS GOTO 1950
2030 IF EMODSB>EMODSA THEN PRINT "E3>E2 ???"
2040 IF EMODSB>EMODSA GOTO 1950
2050 STRESS1=STRN1(2)*EMODS
2060 STRESS2=((STRN2(2)-STRN1(2))*EMODSA)+STRESS1
2070 IF STRESS1>ULT2 GOTO 2100
2080 IF STRESS2>ULT2 GOTO 2100
2090 GOTO 2190
2100 PRINT "Ult strength less than stress specified in stress"
2110 PRINT "/strain relationship ???"
2120 GOTO 1930
2130 STRN1(2)=.002
2140 STRN2(2)=.0043
2150 EMODS=200000!
2160 EMODSA=32600!
2170 EMODSB=6000!
2180 ULT2=670
2190 PRINT "Span (mm)";:INPUT SPAN
2200 PRINT "Input number corresponding to loading required"
2210 PRINT "0.two point loads"
2220 PRINT "1.single central point load"
2230 PRINT "2.U.D.L."
2240 INPUT BMDFACT
2250 IF BMDFACT>2 GOTO 2200
2260 IF BMDFACT=0 GOTO 2290
2270 IF BMDFACT=2 GOTO 2350
2280 GOTO 2430
2290 PRINT "Distance between load points (mm)";:INPUT BAP
2300 IF BAP>SPAN THEN PRINT "Dist. between load points > span ?"
2310 IF BAP>SPAN GOTO 2330
2320 GOTO 2340
2330 GOTO 2290
2340 GOTO 2430
2350 PRINT "Symmetrical udl,such that AA equals distance from support"
2360 PRINT "to start of udl and BB is the distance over which the"
2370 PRINT "udl acts"
2380 PRINT "AA (mm)";:INPUT AA
2390 PRINT "BB (mm)";:INPUT BB
2400 ALENT=(2*AA)+BB
2410 IF ALENT>SPAN THEN PRINT "Dist specified by AA and BB > span ???"
2420 IF ALENT>SPAN GOTO 2380
2430 PRINT "Dead weight (kN/m)";:INPUT DWT
```

```
2440 PRINT "Calculation of crack widths is based upon average strain"
2450 PRINT "and spacing of cracks,i.e."
2460 PRINT "acw = esm . spacing"
2470 PRINT "where acw=av. crack width"
2480 PRINT "       esm=av. strain at level of crack"
2490 PRINT " The crack spacing in brickwork equals the distance"
2500 PRINT "between joints at the soffit or some multiple of that distance."
2510 PRINT "When entering the crack spacing for brickwork either the joint"
2520 PRINT "spacing or a multiple of the joint spacing should be entered."
2530 PRINT "NOTE: Crack width prediction is applicable to concrete, however"
2540 PRINT "since the crack spacing is less uniform than in brickwork the"
2550 PRINT "accuracy of the predictions may be reduced. The expected average"
2560 PRINT "crack spacing should be entered for concrete beams."
2570 PRINT "Input crack spacing (mm)";:INPUT DISTJ
2580 PRINT "Level at which crack widths are to be calculated,default=soffit"
2590 PRINT "OK (y/n)";:INPUT P$
2600 IF P$="y" OR P$="Y" GOTO 2630
2610 PRINT "Input level of crack widths (mm)";:INPUT DEPCRK
2620 GOTO 2640
2630 DEPCRK=DEPTH
2640 PRINT"Do you wish tension-stiffening to be taken into account?"
2650 PRINT"yes or no?";:INPUT PETE$
2660 IF PETE$="y" OR PETE$="Y" THEN LTS=1
2670 IF FACTOR1=2 GOTO 2720
2680 LPRINT"Breadth(mm)="BREDTH"Depth(mm)="DEPTH
2690 LPRINT "Compr. strength of brickwork (N/mm2)="STRSMX
2700 LPRINT "Ult compr strain="STRMX
2710 LPRINT "Modulus of rupture (N/mm2)="RMOD
2720 LPRINT "Prestress in steel1(kN)=" PRSTR1 "Prestress in steel2(kN)="PRSTR2
2730 LPRINT "Depth to steel1 (mm)="EFFD1
2740 LPRINT "Depth to steel2 (mm)="EFFD2
2750 LPRINT "Area of steel1(mm2)=" ASTL1 "Area of steel2(mm2)=" ASTL2
2760 READ NLD,NDV,NMOM,KLM
2770 READ ANDV,ANLD
2780 LPRINT "Span (mm)="SPAN
2790 IF BMDFACT=0 GOTO 2830
2800 IF BMDFACT=1 GOTO 2850
2810 LPRINT "AA="AA"BB="BB
2820 GOTO 2850
2830 LPRINT "Jack space (mm)="BAP
2840 IF FACTOR1=2 GOTO 2880
2850 LPRINT "COEFFICIENTS OF STRESS/STRAIN"
2860 LPRINT COFF(1),COFF(2),COFF(3),COFF(4)
2870 LPRINT "STEEL1"
2880 LPRINT "strain1      strain2      E1(N/mm2)      E2(N/mm2)      E3(N/mm2)"
2890 LPRINT STRN1(1),STRN2(1),EMOD,EMODA,EMODB
2900 LPRINT "STEEL2"
2910 LPRINT "strain1      strain2      E1(N/mm2)      E2(N/mm2)      E3(N/mm2)"
2920 LPRINT STRN1(2),STRN2(2),EMODS,EMODSA,EMODSB
2930 LPRINT "Ultimate tensile strength (N/mm2) steel1=" ULT1
2940 LPRINT "Ultimate tensile strength(N/mm2)steel2=" ULT2
2950 IF A$="n" OR A$="N" GOTO 3000
2960 LPRINT "Breadth of concrete section/infill (mm) ="BCON
2970 LPRINT"Depth to top of conc.(mm)="D1"Depth to bottom of conc.(mm)="D2
2980 LPRINT "Compr. strength of concrete (N/mm2)="STRSMC
2990 IF FACTOR1=2 THEN LPRINT"Ult compr. strain ="STRMXC
3000 LPRINT "Dead weight (kN/m)="DWT
3010 LPRINT "Average crack spacing (mm) =" DISTJ
3020 LPRINT "Distance from top of section to level of cracks(mm)="DEPCRK
3030 IF CCODE$="Y" OR CCODE$="y" GOTO 3070
3040 IF A$="N" OR A$="n" GOTO 3070
3050 LPRINT "Properties of user defined stress/strain curve for concrete"
3060 LPRINT "X1="CX1"X2="CX2"X3="CX3
3070 PRINT "Confirm data input correct (y/n)?";:INPUT ANS3$
3080 IF ANS3$="n" OR ANS3$="N" GOTO 310
3090 YLLBRIC=.74*LOG(STRSMX)
3100 YBRIC=1308*EXP(YLLBRIC)
3110 YCONC=5500*(SQR(STRSMC))
3120 IF FACTOR1=2 THEN YBRIC=YCONC
3130 IF FACTOR1=2 THEN STRSMX=STRSMC
3140 IF FACTOR1=2 THEN BREDTH=0!
3150 IF FACTOR1=2 THEN STRMX=STRMXC
3160 IF FACTOR1=1 THEN STRMXC=.0035
3170 IF FACTOR1=1 AND D1=0! THEN STRMXC=STRMX
3180 FOR II=1 TO 25
3190 MOM(II)=0!
3200 CURV(II)=0!
3210 NEXT II
3220 GOSUB 4440
3230 GOSUB 6920
3240 BENMOM=MOMENT(20)/1000000£
```

```
3250 LPRINT "ULT. BENDING MOMENT="BENMOM "KNM"
3260 IJ=25-NAIL
3270 FOR I=1 TO IJ
3280 MOM(I)=MOM(I)/1000000£
3290 NEXT I
3300 IM=24-NAIL
3310 FOR I=1 TO IM
3320 K=I+1
3330 IF MOM(I)<MOM(K) GOTO 3350
3340 MOM(I)=MOM(K)-.01
3350 NEXT I
3360 LPRINT "COMPLETE MOMENT-CURVATURE RELATIONSHIP"
3370 LPRINT"WITH TENSION STIFFENING"
3380 LPRINT"Moment(kNm)    Curvature(1/mm)"
3390 FOR IK=1 TO IJ
3400 LPRINT MOM(IK),CURV(IK)
3410 NEXT IK
3420 SPN=SPAN/ANDV
3430 NDV2=(NDV+1)/2
3440 SPND1=0!
3450 FOR J=1 TO NDV2
3460 SPND1=SPND1+SPN
3470 SPND2(J)=SPND1
3480 NEXT J
3490 SPN2=SPN*SPN
3500 SSPN=(SPAN-BAP)/2'
3510 DWTS=DWT*SPAN/1000'
3520 DWTMAX=DWTS*SPAN/8000!
3530 IF BMDFACT=1 GOTO 3570
3540 IF BMDFACT=2 GOTO 3590
3550 ULOAD=((BENMOM-DWTMAX)/SSPN)*2000'
3560 GOTO 3630
3570 ULOAD=((BENMOM-DWTMAX)/SPAN)*4000!
3580 GOTO 3630
3590 ZZ=BB/2!
3600 TERM1=BB*AA*(BB+(2*AA))/(2*SPAN)
3610 TERM2=ZZ*(BB-ZZ)/2!
3620 ULOAD=((BENMOM-DWTMAX)*BB/(TERM1+TERM2))*1000!
3630 LPRINT "DEAD WEIGHT (KN)=" DWTS
3640 LPRINT "ULT LIVE LOAD (KN)=" ULOAD
3650 LPRINT "LOAD" "DEFLECTION"
3660 LPRINT "PROFILE FROM SUPPORT"
3670 FOR I=1 TO NDV2
3680 D(I)=SPND2(I)
3690 NEXT I
3700 LPRINT "KN",D(1),D(2),D(3),D(4),D(5),D(6),D(7),D(8),D(9),D(10)
3710 NCUR=(NMOM-1)-NAIL
3720 SPN=SPAN/ANDV
3730 NDIV=NDV+1
3740 SPNTWO=SPN/2'
3750 REM 1ST LOAD INCREMENTS
3760 IF BMDFACT<>0' GOTO 3790
3770 PLOD=ULOAD/(2!*ANLD)
3780 GOTO 3800
3790 PLOD=ULOAD/ANLD
3800 PLODA=PLOD
3810 KL=0
3820 JM=1
3830 SPND=SPN
3840 DEFLT=0!
3850 K=1
3860 SST=SSPN+BAP
3870 REM CALCULATE BM AT EACH NODEPOINT
3880 DWTMOM=DWT*((SPAN*SPND)-(SPND*SPND))/2000000£
3890 IF BMDFACT<>0 GOTO 3910
3900 GOTO 3930
3910 GOSUB 9140
3920 GOTO 4000
3930 IF SPND>SSPN AND SPND<SST GOTO 3970
3940 IF SPND>SST GOTO 3990
3950 BM=((SPND*PLOD)/1000!)+DWTMOM
3960 GOTO 4000
3970 BM=((PLOD*SSPN)/1000!)+DWTMOM
3980 GOTO 4000
3990 BM=((PLOD/1000!)*(SPAN-SPND))+DWTMOM
4000 SPND2(K)=SPND
4010 SPND=SPND+SPN
4020 REM CALCULATE CURVATURE
4030 FOR I=1 TO NCUR
4040 IL=I+1
4050 IF BM<MOM(1) GOTO 4080
```

```
4060 IF BM>MOM(I) AND BM<MOM(IL) GOTO 4110
4070 GOTO 4140
4080 FACT=BM/MOM(1)
4090 CURT=FACT*CURV(1)
4100 GOTO 4150
4110 FACT=(BM-MOM(I))/(MOM(IL)-MOM(I))
4120 CURT=CURV(I)+(FACT*(CURV(IL)-CURV(I)))
4130 GOTO 4150
4140 NEXT I
4150 BMAT(K)=CURT*SPN2
4160 K=K+1
4170 IF K=NDIV GOTO 4190
4180 GOTO 3870
4190 KL=KL+1
4200 GOSUB 8920
4210 FOR I=1 TO NDV2
4220 D(I)=DEFL(I)
4230 DLL(JM)=D(10)
4240 PLODL(JM)=PLOD
4250 NEXT I
4260 IF PLOD=0! GOTO 4350
4270 TPLOD=PLOD+DWTS
4280 LPRINT TPLOD,D(1),D(2),D(3),D(4),D(5),D(6),D(7),D(8),D(9),D(10)
4290 PLOD=PLODA+PLOD
4300 JM=JM+1
4310 IF KL=NLD GOTO 4330
4320 GOTO 3830
4330 PLOD=0!
4340 GOTO 3830
4350 DDWT(10)=D(10)
4360 LPRINT "DEFLECTION DUE TO DEAD WEIGHT (mm)"DDWT(10)
4370 LPRINT "LIVE LOAD/DEFLECTION"
4380 LPRINT "L.LOAD (kN)","DEFLECTION (mm)"
4390 FOR JM=1 TO NLD
4400 DLL(JM)=DLL(JM)-DDWT(10)
4410 LPRINT PLODL(JM),DLL(JM)
4420 NEXT JM
4430 END
4440 REM SUBROUTINE TO CALCULATE PRESTRESS EFFECTS
4450 REM CALCULATE SECTION PROPERTIES
4460 IF FACTOR2<>2 GOTO 4630
4470 BREDTH1=((YCONC/YBRIC)*BCON)+(BREDTH-BCON)
4480 IF BREDTH=0! THEN BREDTH1=BCON
4490 AREA=(BREDTH*D1)+((D2-D1)*BREDTH1)
4500 CENTR1=(BREDTH*D1)*(D1/2!)
4510 CENTR=(CENTR1+(((D2-D1)*BREDTH1)*((D2-D1)/2!+D1)))/AREA
4520 AMOMI1=BREDTH*(CENTR*CENTR*CENTR+((D1-CENTR)*(D1-CENTR)*(D1-CENTR)))
4530 AMOMI2=(DEPTH-CENTR)*(DEPTH-CENTR)*(DEPTH-CENTR)
4540 AMOMI3=(D1-CENTR)*(D1-CENTR)*(D1-CENTR)
4550 AMOMI=(AMOMI1+BREDTH1*(AMOMI2-AMOMI3))/3!
4560 IF BREDTH<>0! GOTO 4580
4570 AMOMI=BREDTH1*DEPTH*DEPTH*DEPTH/12!
4580 ZZM=AMOMI/CENTR
4590 ZZM1=AMOMI/(DEPTH-CENTR)
4600 ECCEN1=EFFD1-CENTR
4610 ECCEN2=EFFD2-CENTR
4620 GOTO 4720
4630 DEPTHS=DEPTH*DEPTH
4640 AREA=DEPTH*BREDTH
4650 ZZM=(BREDTH*DEPTHS)/6!
4660 ZZM1=ZZM
4670 AMOMI=(BREDTH*DEPTHS*DEPTH)/12!
4680 ECCEN1=EFFD1-(DEPTH/2!)
4690 ECCEN2=EFFD2-(DEPTH/2!)
4700 REM PROPERTIES OF TRANSFORMED UNCRACKED SECTION
4710 REM MODULAR RATIOS
4720 RM=(EMOD*STRMX)*(1.9/STRSMX)
4730 REM CENTROID OF SECTION
4740 IF FACTOR2=2 GOTO 4770
4750 DOM=(AREA+(RM*(ASTL1+ASTL2)))
4760 CENTR=((AREA*(DEPTH/2!))+(RM*ASTL1*EFFD1)+(RM*ASTL2*EFFD2))/DOM
4770 REM CALCULATES PRESTRESS EFFECTS
4780 AXIAL1=(PRSTR1/AREA)*1000!
4790 AXIAL2=(PRSTR2/AREA)*1000!
4800 BEND1=(1000!*PRSTR1*ECCEN1)/ZZM
4810 BEND2=(1000!*PRSTR2*ECCEN2)/ZZM
4820 BEND11=(1000!*PRSTR1*ECCEN1)/ZZM1
4830 BEND22=(1000!*PRSTR2*ECCEN2)/ZZM1
4840 SIGMAC=(AXIAL1+AXIAL2)-(BEND1+BEND2)
4850 SIGMAT=(AXIAL1+AXIAL2)+(BEND11+BEND22)
```

```
4870 IF ASTL2=0! GOTO 4900
4880 PRSTN2=(PRSTR2*1000!)/(ASTL2*EMOD)
4890 GOTO 4910
4900 PRSTN2=0!
4910 LPRINT "PRESTRESS STRAINS=" PRSTN1,PRSTN2
4920 RMBC=YCONC/YBRIC
4930 IF FACTOR1=2 GOTO 4970
4940 GEOFACT=BREDTH/((BREDTH-BCON)+(BCON*RMBC))
4950 ERUP=(RMOD*GEOFACT)/(STRSMX*1.9)
4960 GOTO 4980
4970 ERUP=RMOD/(STRSMC*2!)
4980 REM CALCULATE DISTRIBUTION OF PRESTRESS
4990 IF PRSTR1=0! GOTO 5010
5000 RESULT=((EFFD1*PRSTR1)+(EFFD2*PRSTR2))/(PRSTR1+PRSTR2)
5010 ELAST=1.9
5020 END1=SIGMAC/(ELAST*STRSMX)
5030 END2=SIGMAT/(ELAST*STRSMX)
5040 IF SIGMAC<0! GOTO 5110
5050 REM STRAINS WITHIN KERN OF PRESTRESS
5060 EGRAD=(END2-END1)/20!
5070 ALAYER=DEPTH/20!
5080 DSTRNI=EGRAD/2!
5090 GOTO 5190
5100 REM PRESTRESS OUTSIDE KERN
5110 RATIO=SIGMAC/SIGMAT
5120 DCOM=DEPTH/(1+(-1!*RATIO))
5130 EGRAD=END2/20!
5140 EN=END1
5150 END1=0!
5160 DTCOM=DEPTH-DCOM
5170 DSTRNI=DTCOM+(EGRAD/2')
5180 ALAYER=DCOM/20!
5190 EDIV=EGRAD
5200 EDIVS=EDIV/2'
5210 REM 1ST LAYER STRAINS
5220 COMPT=0!
5230 K=1
5240 IF K=21 GOTO 5450
5250 ELAY=END1+EDIVS
5260 ELAY1=(ELAY*STRMX)/STRMXC
5270 IF DSTRNI>D2 GOTO 5290
5280 IF DSTRNI>=D1 GOTO 5320
5290 STRS=(COFF(1)*ELAY)+(COFF(2)*ELAY*ELAY)+(COFF(3)*ELAY*ELAY*ELAY)
5300 COMP=(STRS*ALAYER)*(STRSMX*BREDTH)
5310 GOTO 5400
5320 STRS=(COFF(1)*ELAY)+(COFF(2)*ELAY*ELAY)+(COFF(3)*ELAY*ELAY*ELAY)
5330 IF CCODE$="Y" OR CCODE$="y" GOTO 5360
5340 STRSC=.8*((CX1*ELAY1)+(CX2*ELAY1*ELAY1)+(CX3*ELAY1*ELAY1*ELAY1))
5350 GOTO 5380
5360 ELAY1=ELAY*STRMX/(.0022)
5370 STRSC=.8*(((ELAY1*CONCK)-(ELAY1*ELAY1))/(1!+((CONCK-2!)*ELAY1)))
5380 COMPP=(STRS*ALAYER)*(STRSMX*(BREDTH-BCON))
5390 COMP=((STRSC*ALAYER)*(STRSMC*BCON))+COMPP
5400 COMPT=COMPT+COMP
5410 EDIVS=EDIVS+EDIV
5420 DSTRNI=DSTRNI+ALAYER
5430 K=K+1
5440 GOTO 5240
5450 REM COMPARE C AND T
5460 IF PRSTR1=0! GOTO 5630
5470 RAT=COMPT/((PRSTR1+PRSTR2)*1000!)
5480 IF RAT<1.02 AND RAT>.98 GOTO 5510
5490 ELAST=RAT*ELAST
5500 GOTO 5020
5510 ENDT=END1
5520 IF END1=0! THEN ENDT=EN
5530 ENDTACT=ENDT*STRMX
5540 END2ACT=END2*STRMX
5550 LPRINT "STRAINS DUE TO PRESTRESS"ENDTACT,END2ACT
5560 PRECURV=(STRMX*(END2+ENDT))/DEPTH
5570 LPRINT "CURVATURE DUE TO PRESTRESS" PRECURV
5580 REM STRAIN TO CAUSE CRACKING
5590 E1=END2
5600 IF PRSTR1=0! GOTO 5630
5610 ECRAC=END2+ERUP
5620 GOTO 5650
5630 ECRAC =ERUP
5640 GOTO 6670
5650 EINT=0!
5660 EINC=ECRAC/5!
5670 ENT=END1
```

```
5680 EINCT=0!
5690 END22=END2
5700 LL=0
5710 ECRACACT=ECRAC*STRMX
5720 LPRINT "TENSILE STRAIN TO CAUSE CRACKING"ECRACACT
5730 EINCST=EINC*STRMX
5740 DT=CENTR
5750 ESTINC=0!
5760 LL=LL+1
5770 EINT=EINC+EINT
5780 EINCT=EINCT+EINC
5790 IF LL=6 GOTO 6640
5800 END2=END22-EINCT
5810 REM CALCULATE STRAINS AND FORCES IN STEEL
5820 STEEL1=(EINCT*STRMX)*((EFFD1-DT)/(DEPTH-DT))
5830 STEEL2=(EINCT*STRMX)*((EFFD2-DT)/(DEPTH-DT))
5840 TF1=ASTL1*(EMOD*(STEEL1+PRSTN1))
5850 TF2=ASTL2*(EMODS*(STEEL2+PRSTN2))
5860 TFORCE=TF1+TF2
5870 EINTT=EINT
5880 REM STRAINS IN BRICKWORK
5890 END1=ENT+EINTT
5900 IF END1<0! GOTO 5990
5910 IF END2<0! GOTO 6080
5920 EGRAD=(END2-END1)/20!
5930 ENR=END1
5940 ALAYER=DEPTH/20!
5950 DCOM=DEPTH
5960 DSTRNI=EGRAD/2!
5970 GAP=0!
5980 GOTO 6150
5990 RATIO=END1/END2
6000 DCOM=DEPTH/(1+(-1!*RATIO))
6010 EGRAD=END2/20!
6020 GAP=0!
6030 ALAYER=DCOM/20!
6040 DTCOM=DEPTH-DCOM
6050 DSTRNI=DTCOM+(EGRAD/2!)
6060 ENR=0!
6070 GOTO 6150
6080 RATIO=END2/END1
6090 DCOM=DEPTH/(1+(-1!*RATIO))
6100 ENR=END1
6110 EGRAD=(-1!*END1)/20!
6120 ALAYER=DCOM/20!
6130 GAP=DEPTH-DCOM
6140 DSTRNI=-.5*EGRAD
6150 ALEV=ALAYER/2!
6160 ALEVS=ALAYER
6170 EDIV=EGRAD
6180 EDIVS=EDIV/2!
6190 REM 1ST LAYER STRAINS
6200 TMOMT=0!
6210 COMPT=0!
6220 K=1
6230 IF K=21 GOTO 6480
6240 ELAY=ENR+EDIVS
6250 ELAY1=(ELAY*STRMX)/STRMXC
6260 IF DSTRNI>D2 GOTO 6280
6270 IF DSTRNI>=D1 GOTO 6310
6280 STRS=(COFF(1)*ELAY)+(COFF(2)*ELAY*ELAY)+(COFF(3)*ELAY*ELAY*ELAY)
6290 COMP=(STRS*ALAYER)*(STRSMX*BREDTH)
6300 GOTO 6390
6310 STRS=(COFF(1)*ELAY)+(COFF(2)*ELAY*ELAY)+(COFF(3)*FLAY*ELAY*ELAY)
6320 IF CCODE$="Y" OR CCODE$="y" GOTO 6350
6330 STRSC=.8*((CX1*ELAY1)+(CX2*ELAY1*ELAY1)+(CX3*ELAY1*ELAY1*FLAY1))
6340 GOTO 6370
6350 ELAY1=ELAY*STRMX/(.0022)
6360 STRSC=.8*(((ELAY1*CONCK)-(ELAY1*ELAY1))/(1!+((CONCK-2!)*ELAY1)))
6370 COMPP=(STRS*ALAYER)*(STRSMX*(BREDTH-BCON))
6380 COMP=((STRSC*ALAYER)*(STRSMC*BCON))+COMPP
6390 COMPT=COMPT+COMP
6400 ALEVR=(DCOM-ALEV)+GAP
6410 DSTRNI=DSTRNI+ALAYER
6420 K=K+1
6430 TMOM=COMP*ALEVR
6440 TMOMT=TMOMT+TMOM
6450 EDIVS=EDIVS+EDIV
6460 ALEV=ALEV+ALEVS
6470 GOTO 6230
6480 REM COMPARE C AND T
```

```
6490 IF BREDTH=0! THEN BREDTH=BCON
6500 TFORCE=TFORCE+((GAP*BREDTH)*(RMOD/2!))
6510 CT=COMPT/TFORCE
6520 IF CT<1.05 AND CT>.95 GOTO 6580
6530 CT=(COMPT*2')/(COMPT+TFORCE)
6540 DT=DT/CT
6550 EINT=(EINCT*DT)/(DEPTH-DT)
6560 GOTO 5820
6570 REM LEVERARM
6580 ALEVRM=TMOMT/COMPT
6590 TBRIC=GAP*GAP*BREDTH*RMOD/6!
6600 TEN=(TF1*(DEPTH-EFFD1))+(TF2*(DEPTH-EFFD2))+TBRIC
6610 SMOM(LL)=(ALEVRM*COMPT)-TEN
6620 CURVEP(LL)=((END1-END2)*STRMX)/DEPTH
6630 GOTO 5760
6640 LPRINT"MOMENT-CURVATURE RELATIONSHIP UP TO CRACKING"
6650 LPRINT "MOMENT(NMM)","CURVATURE(1/MM)"
6660 IF FRSTR1<>0! GOTO 6800
6670 AMI=BREDTH*(DEPTH*DEPTH)*(DEPTH/12')
6680 IF FACTOR2=2 THEN AMI=AMOMI
6690 CRKMOM=RMOD*(AMI/CENTR)
6700 ECRAC5=(STRMX*ECRAC)/5!
6710 CKMOM5=CRKMOM/5!
6720 CRK=0!
6730 ERC=0'
6740 FOR L=1 TO 5
6750 CRK=CRK+CKMOM5
6760 ERC=ERC+ECRAC5
6770 CURVEP(L)=ERC/(DEPTH-CENTR)
6780 SMOM(L)=CRK
6790 NEXT L
6800 FOR L=1 TO 5
6810 MOM(L)=MOM(L)+SMOM(L)
6820 CURV(L)=CURVEP(L)
6830 LPRINT SMOM(L),CURVEP(L)
6840 NEXT L
6850 L=5
6860 LPRINT "CRACKING MOMENT" SMOM(L)
6870 CRKMOM=SMOM(L)
6880 STRAIN=ECRAC*STRMX
6890 LPRINT "STRAIN" STRAIN
6900 IF FACTOR1=2 THEN BREDTH=0'
6910 RETURN
6920 REM THIS ROUTINE CALCULATES THE MOMENT-CURVATURE
6930 STRAIN=STRAIN*2!
6940 STRANT=STRAIN
6950 DNA=EFFD1*.7
6960 IF FRSTR1=0! THEN GOTO 7040
6970 IF ENDTACT>0! THEN GOTO 7020
6980 EPSTX=ENDTACT*DEPTH/(END2ACT-ENDTACT)
6990 EPSTEL1=END2ACT*(EFFD1-EPSTX)/(DEPTH-EPSTX)
7000 EPSTEL2=END2ACT*(EFFD2-EPSTX)/(DEPTH-EPSTX)
7010 GOTO 7040
7020 EPSTEL1=(((END2ACT-ENDTACT)/DEPTH)*EFFD1)+ENDTACT
7030 EPSTEL2=(((END2ACT-ENDTACT)/DEPTH)*EFFD2)+ENDTACT
7040 I=0
7050 J=0
7060 FPY=(EMOD*STRN1(1))+(EMODA*(STRN2(1)-STRN1(1)))
7070 FY=(EMODS*STRN1(2))+(EMODSA*(STRN2(2)-STRN1(2)))
7080 IF FY=0! THEN ASTLE=0!
7090 IF FY=0! GOTO 7110
7100 ASTLE=ASTL2*(FY/FPY)
7110 EFFDR=((ASTL1*EFFD1)+(ASTLE*EFFD2))/(ASTL1+ASTLE)
7120 IF FACTOR1=2 THEN BREDTH=BCON
7130 PSTL=(ASTL1+ASTLE)/(EFFDR*BREDTH)
7140 IF FACTOR1=2 THEN BREDTH=0!
7150 IF J=0 GOTO 7170
7160 STRAIN=STRAIN+STRINC
7170 IF J=0 THEN STRAIN=STRANT
7180 IF J=20 GOTO 8230
7190 REM CALC STRAIN IN STEEL
7200 XDEPH1=EFFD1-DNA
7210 ESTELT=STRAIN*(XDEPH1/DNA)
7220 ESTEL1=ABS(ESTFLT)
7230 XDEPH2=EFFD2-DNA
7240 IF ASTL2=0! THEN XDEPH2=0!
7250 ESTELA=STRAIN*(XDEPH2/DNA)
7260 ESTEL2=ABS(ESTELA)
7270 STRN3=STRN2(1)-STRN1(1)
7280 STRN31=STRN2(2)-STRN1(2)
```

```
7300 ESTEL2=ESTEL2+PRSTN2+EPSTEL2
7310 ESTL1=ESTEL1-STRN1(1)
7320 ESTL2=ESTEL2-STRN1(2)
7330 ESTLY1=ESTEL1-STRN2(1)
7340 ESTLY2=ESTEL2-STRN2(2)
7350 IF ESTLY1<0! THEN ESTLY1=0!
7360 IF ESTLY2<0! THEN ESTLY2=0!
7370 IF ESTEL1<STRN1(1) THEN EMOD1=0!
7380 IF ESTEL2<STRN1(2) THEN EMOD2=0!
7390 IF ESTEL1<STRN1(1) THEN ESTL1=0!
7400 IF ESTEL2<STRN1(2) THEN ESTL2=0!
7410 IF ESTEL1>STRN1(1) AND ESTEL1<STRN2(1) THEN EMOD1=EMODA
7420 IF ESTEL2>STRN1(2) AND ESTEL2<STRN2(2) THEN EMOD2=EMODSA
7430 IF ESTEL1>STRN2(1) THEN ESTL1=STRN3
7440 IF ESTEL2>STRN2(2) THEN ESTL2=STRN31
7450 IF ESTEL1>STRN1(1) THEN ESTEL1=STRN1(1)
7460 IF ESTEL2>STRN1(2) THEN ESTEL2=STRN1(2)
7470 REM CALCULATE TENSION FORCE
7480 STRSS1=(EMOD*ESTEL1)+(EMODA*ESTL1)+(ESTLY1*EMODB)
7490 STRSS2=(EMODS*ESTEL2)+(EMODSA*ESTL2)+(ESTLY2*EMODSB)
7500 IF STRSS1>ULT1 THEN STRSS1=ULT1
7510 IF STRSS2>ULT2 THEN STRSS2=ULT2
7520 TF1=ASTL1*STRSS1
7530 TF2=ASTL2*STRSS2
7540 TFORCE=TF1+TF2
7550 UFORCE=(ASTL1*ULT1)+(ASTL2*ULT2)
7560 IF TFORCE>UFORCE THEN TFORCE=UFORCE
7570 REM CALC COMP FORCE
7580 STRANM=STRAIN/STRMX
7590 ALAYER=DNA/50!
7600 EGRAD=STRANM/50!
7610 EDIVS=EGRAD
7620 EDIV=EGRAD/2!
7630 DSTRNI=EDIV
7640 ALEV=ALAYER/2!
7650 TMOMT=0!
7660 COMPT=0!
7670 K=1
7680 REM LAYER STRAINS
7690 K=K+1
7700 IF K=51 GOTO 7950
7710 ELAY=STRANM-EDIV
7720 ELAY1=(ELAY*STRMX)/STRMXC
7730 IF DSTRNI>D2 GOTO 7750
7740 IF DSTRNI>=D1 GOTO 7780
7750 STRS=(COFF(1)*ELAY)+(COFF(2)*ELAY*ELAY)+(COFF(3)*ELAY*ELAY*ELAY)
7760 COMP=(STRS*ALAYER)*(STRSMX*BREDTH)
7770 GOTO 7860
7780 STRS=(COFF(1)*ELAY)+(COFF(2)*ELAY*ELAY)+(COFF(3)*ELAY*ELAY*ELAY)
7790 IF CCODE$="Y" OR CCODE$="y" GOTO 7820
7800 STRSC=.8*((CX1*ELAY1)+(CX2*ELAY1*ELAY1)+(CX3*ELAY1*ELAY1*ELAY1))
7810 GOTO 7840
7820 ELAY1=ELAY*STRMX/(.0022)
7830 STRSC=.8*(((ELAY1*CONCK)-(ELAY1*ELAY1))/(1!+((CONCK-2!)*ELAY1)))
7840 COMPP=(STRS*ALAYER)*(STRSMX*(BREDTH-BCON))
7850 COMP=((STRSC*ALAYER)*(STRSMC*BCON))+COMPP
7860 COMPT=COMPT+COMP
7870 ALEVR=DNA-ALEV
7880 ALEV=ALEV+ALAYER
7890 EDIV=EDIV+EGRAD
7900 TMOM=COMP*ALEVR
7910 TMOMT=TMOMT+TMOM
7920 DSTRNI=DSTRNI+ALAYER
7930 GOTO 7690
7940 REM COMPRESSION AND TENSION FORCES
7950 DIVIS=COMPT/TFORCE
7960 IF DIVIS>.99 AND DIVIS<1.01 GOTO 8000
7970 DELTA1=((COMPT+TFORCE)/(2!*COMPT))*DNA
7980 DNA=DELTA1
7990 GOTO 7200
8000 REM CALCULATE CENTROID OF COMP. FORCE
8010 CENTOD=TMOMT/COMPT
8020 ALEVR1=EFFD1-(DNA-CENTOD)
8030 ALEVR2=EFFD2-(DNA-CENTOD)
8040 REM CALC MOMENT
8050 IF J>0 GOTO 8120
8060 REM COMPOARE APPLIED MOMENT WITH CRACKING MOMENT
8070 CMOM=(ALEVR1*TF1)+(ALEVR2*TF2)
8080 COMMOM=CMOM/CRKMOM
8090 IF COMMOM<1.03 AND COMMOM>.97 GOTO 8120
8100 STRAIN=STRAIN/COMMOM
```

```
8110 GOTO 7200
8120 J=J+1
8130 IF J>1 GOTO 8150
8140 STRINC=(STRMX-STRAIN)/19!
8150 MOMENT(J)=(ALEVR1*TF1)+(ALEVR2*TF2)
8160 STRST(J)=STRSS1
8170 STRST2(J)=STRSS2
8180 STRANS(J)=STRAIN
8190 ESTELS(J)=ESTEL1+ESTLY1+ESTL1
8200 CURVE(J)=(STRANS(J)+ESTELS(J)-PRSTN1)/EFFD1
8210 DNARRY(J)=DNA
8220 IF STRAIN<STRMX GOTO 7160
8230 LPRINT "MOMENT CURVATURE RELATIONSHIP ACROSS CRACK AFTER CRACKING"
8240 LPRINT"Moment(Nmm)   Curvature(1/mm) N.A.Depth(mm) S.Stress1   S.Stress2  Compr. strain"
8250 FOR II=1 TO 20
8260 LPRINT MOMENT(II),CURVE(II),DNARRY(II),STRST(II),STRST2(II),STRANS(II)
8270 NEXT II
8280 NAIL=0
8290 FOR K=1 TO 20
8300 IF MOMENT(K)>CRKMOM GOTO 8330
8310 NAIL=NAIL+1
8320 NEXT K
8330 REM TENSION STIFFENING,STRAIN IN STEEL AFTER CRACKING
8340 ESTEL=ESTELS(1)
8350 FSCR=STRST(1)
8360 LPRINT "STEEL STRESS & STRAIN AFTER CRACKING" FSCR,ESTEL
8370 REM ADJUST CURVATURES TO ALLOW FOR TENSION STIFFENING
8380 LPRINT "PSTL" PSTL
8390 LPRINT "AV. ADDITIONAL    AV. CRACK     MOMENT"
8400 LPRINT"STRAIN IN STEEL    WIDTH(mm)      Nmm"
8410 FOR M=1 TO 20
8420 ESTLS=ESTELS(M)-PRSTN1
8430 REM CALCULATE TENSION STIFFENING COEFFIECENT K
8440 ESCR1=((EFFDR-DNARRY(1))/(EFFD1-DNARRY(1)))*(ESTEL-PRSTN1)
8450 PRESTRESS=1000!*((PRSTR1+PRSTR2)/(ASTL1+ASTLE))
8460 PRESTRAIN=PRESTRESS/EMOD
8470 ESCR1=ESCR1+PRESTRAIN
8480 IF ESCR1>STRN1(1) AND ESCR1>STRN2(1) GOTO 8540
8490 IF ESCR1>STRN1(1) GOTO 8520
8500 FSCR1=(EMOD*ESCR1)
8510 GOTO 8550
8520 FSCR1=(EMOD*STRN1(1))+(EMODA*(ESCR1-STRN1(1)))
8530 GOTO 8550
8540 FSCR1=FPY+(EMODB*(ESCR1-STRN2(1)))
8550 ESTLSE=((EFFDR-DNARRY(M))/(EFFD1-DNARRY(M)))*ESTLS
8560 ESTLSE=ESTLSE+PRESTRAIN
8570 IF ESTLSE>STRN1(1) AND ESTLSE>STRN2(1) GOTO 8630
8580 IF ESTLSE>STRN1(1) GOTO 8610
8590 STRST1=EMOD*ESTLSE
8600 GOTO 8640
8610 STRST1=(EMOD*STRN1(1))+(EMODA*(ESTLSE-STRN1(1)))
8620 GOTO 8640
8630 STRST1=FPY+(EMODB*(ESTLSE-STRN2(1)))
8640 XXX=1-(FSCR1/STRST1)
8650 TK=.02+(.06*XXX)+(.77*XXX*XXX)
8660 ESTLSE=ESTLSE-PRESTRAIN
8670 ESME=ESTLSE-(TK*(RMOD/(200000!*PSTL)))
8680 IF ESME<0! THEN ESME=ESTLSE
8690 ECRM=ESME*((DEPCRK-DNARRY(M))/(EFFDR-DNARRY(M)))
8700 ACW=ECRM*DISTJ
8710 IF ESME<0! THEN ESME=ESTLSE
8720 IF LTS=1 GOTO 8760
8730 ESME=ESTLSE
8740 ECRM=ESME*((DEPCRK-DNARRY(M))/(EFFDR-DNARRY(M)))
8750 ACW=ECRM*DISTJ
8760 LPRINT ESME,ACW,MOMENT(M)
8770 CURVE(M)=(STRANS(M)+ESME)/EFFDR
8780 NEXT M
8790 FOR L=1 TO 20
8800 IF L<=NAIL GOTO 8840
8810 LL=L-NAIL
8820 MOMENT(LL)=MOMENT(L)
8830 CURVE(LL)=CURVE(L)
8840 NEXT L
8850 IK=20-NAIL
8860 FOR II=1 TO IK
8870 KK=5+II
8880 MOM(KK)=MOM(KK)+MOMENT(II)
8890 CURV(KK)=CURV(KK)+CURVE(II)
8900 NEXT II
8910 RETURN
```

```
8920 REM CALCULATION OF DEFLECTIONS
8930 I=1
8940 HCON(I)=BMAT(I)/2!
8950 KCON(I)=.5
8960 I=2
8970 J=I-1
8980 HCON(I)=(BMAT(I)+HCON(J))/(2-KCON(J))
8990 KCON(I)=1/(2-KCON(J))
9000 I=I+1
9010 IF I=NDV GOTO 9030
9020 GOTO 8970
9030 I=NDV
9040 J=I-1
9050 DEFL(I)=(BMAT(I)+HCON(J))/(2-KCON(J))
9060 I=NDV-1
9070 J=I-1
9080 K=I+1
9090 DEFL(I)=(BMAT(I)+HCON(J)+DEFL(K))/(2-KCON(J))
9100 I=I-1
9110 IF I=0 GOTO 9130
9120 GOTO 9070
9130 RETURN
9140 REM SUBROUTINE FOR BEND MOM DIAG
9150 IF BMDFACT=2 GOTO 9230
9160 SPAN2=SPAN/2!
9170 PLOD2=PLOD/2!
9180 IF SPND>SPAN2 GOTO 9210
9190 BM=(PLOD2*SPND/1000!)+DWTMOM
9200 GOTO 9350
9210 BM=(((PLOD2*SPND)-(PLOD*(SPND-SPAN2)))/1000!)+DWTMOM
9220 GOTO 9350
9230 UPLOD=PLOD/(1000!*BB)
9240 SST=AA+BB
9250 IF SPND>AA AND SPND<SST GOTO 9290
9260 IF SPND>SST GOTO 9330
9270 BM=(BB*SPND*UPLOD*(BB+(2*AA))/(2*SPAN))=DWTMOM
9280 GOTO 9350
9290 BM1=BB*AA*UPLOD*(BB+(2*AA))/(2*SPAN)
9300 ZZ1=SPND-AA
9310 BM=((UPLOD*ZZ1*(BB-ZZ1)/2!)+BM1)+DWTMOM
9320 GOTO 9350
9330 SPND10=SPAN-SPND)
9340 BM=(BB*SPND10*UPLOD*(BB+(2*AA))/(2*SPAN))+DWTMOM
9350 RETURN
9360 DATA 10,19,25,12
9370 DATA 20,10
9380 DATA 22,18
```

APPENDIX B

PUBLISHED PAPERS

PUBLISHED PAPERS

The following papers were published, during the course of this investigation, by the author in collaboration with Dr. B. P. Sinha.

PROCEEDINGS OF THE 7th INTERNATIONAL BRICK MASONRY CONFERENCE, Melbourne, Australia, 1985. Ed by T McNeilly and J C Scrivner, Vol 2, pp 1015 - 1031.

MASONRY INTERNATIONAL, Nº 6, December 1985, Ed by Hendry (A W). "Compressive strength of brickwork on edge under axial and eccentric loading".

CIB 86 Symposium, Sept 1986, Washington. "A Comparative Study of reinforced, fully and partially prestressed brickwork beams".

PROCEEDINGS OF THE 7th INTERNATIONAL BRICK MASONRY CONFERENCE

MELBOURNE, AUSTRALIA

17-20 FEBRUARY 1985

Editors: Tom McNeilly
John C. Scrivener

Conference Organisers: Brick Development Research Institute
Department of Architecture & Building, University of Melbourne.

BEHAVIOUR OF PARTIALLY PRESTRESSED BRICKWORK BEAMS

P. Walker, B.Sc., Research Assistant

B.P. Sinha, B.Sc., Ph.D., MICE, FIStruct.E., F.I.E., Lecturer
Department of Civil Engineering & Building Science, University of Edinburgh, Scotland.

ABSTRACT The paper summarises the result of an investigation on the behaviour of full-scale partially prestressed brickwork beams. 10 full-scale beams of span 6.2 m were tested to study the ultimate moment, the moment-deformation relationship, and mode of failure. The variables considered were the percentage of steel and brick strength. The experimental ultimate moment and moment-deformation relationship are compared with theoretical analysis using the material properties obtained from the brickwork prism tests.

INTRODUCTION

The technique of prestressing is generally associated with concrete. Prestressed concrete has established itself as a major structural material, which is used widely in the construction industry. The principle of prestressing which is so widely used for concrete can also be applied to brickwork. Recently, a comprehensive research program (1) has been carried out to study the behaviour of fully prestressed brickwork beams. From this investigation it is very clear that the brickwork can be fully prestressed, but the transfer stress has to be kept low to prevent splitting in the anchorage zone. In addition, the prestressing steel has to be kept at 'kern' limit to avoid the development of tensile stresses due to prestressing. As a result of this constraint, the width of the crack may be much larger than allowed for a class 3 prestressed concrete member [2] at service load. The width of the crack can be controlled by 'partial prestressing'. Partial prestressing of a section is achieved in two ways: i) either by reducing the level of initial prestress applied to the entire tensile reinforcement required for ultimate load, or ii) by prestressing part of the tensile reinforcement to a maximum allowable stress level and leaving the rest non-stressed [3]. As no work has been done so far in this field, a comprehensive investigation of the behaviour of partially prestressed brickwork beam was undertaken to study the effects of the following variables:

i) percentage of steel
ii) ratio of prestressing steel to ordinary reinforcement
iii) mortar strength or grade 1:¼:3 and 1:½:4½ (Cement: Lime:Sand).
iv) brick strength

on ultimate moment, deflection and cracking.

This paper only summarises the result of the preliminary investigation on 10-full-scale partially prestressed brickwork beams.

MATERIALS

Mortar: A 1:¼:3 (Cement:Lime:Sand) mix by volume was used throughout the construction of the beams. The average compressive strength of the mortar for each individual beam is given in Table 2.

Concrete: A 1:2½:2 (Cement:Sand:Pea gravel) mix was used for all the beams except 5 and 6. The mix used for the beams 5 and 6 was 1:2 (Cement:Sand).

In both mixes a plasticiser (Conbex) was used to reduce the effects of shrinkage and to shorten the setting time. Three 100 mm cubes were cast during each concreting operation and tested at 7 days. The average compressive strength of the concrete is given in Table 2 for each of the test specimens.

Bricks: 3-hole perforated bricks were used throughout the test programme. The average compressive strength of high and medium strength bricks was 82.0 N/mm^2 and 58.9 N/mm^2 respectively.

Prestressing Reinforcement: 10.9 mm diameter, stabilised steel strand was used for prestressing. The average ultimate stress was 1708 N/mm^2, with 0.2% proof stress of 1640 N/mm^2. The modulus of elasticity was 214 kN/mm^2.

Non-stressed Reinforcement: 12 mm diameter, high strength deformed bars were used throughout, with an ultimate stress of 670 N/mm^2, a yield stress of 535 N/mm^2 and Young's Modulus 200 kN/mm^2.

The stress-strain relationship of prestressing steel and reinforcement was idealised in tri-linear form as shown in Fig. 1 and 2 for theoretical analysis.

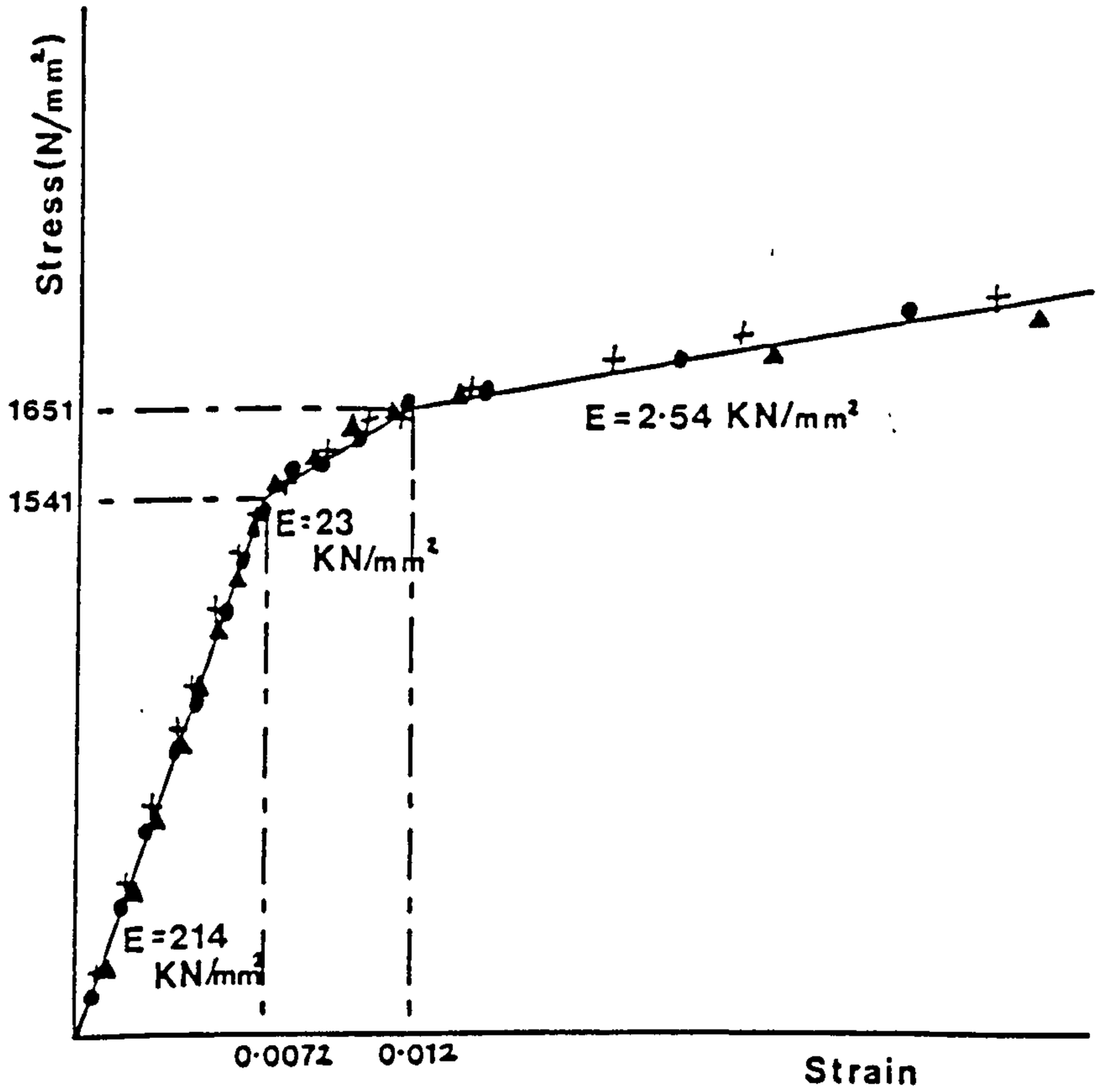

Fig. 1 Idealised tri-linear stress/strain relationship for prestressing steel

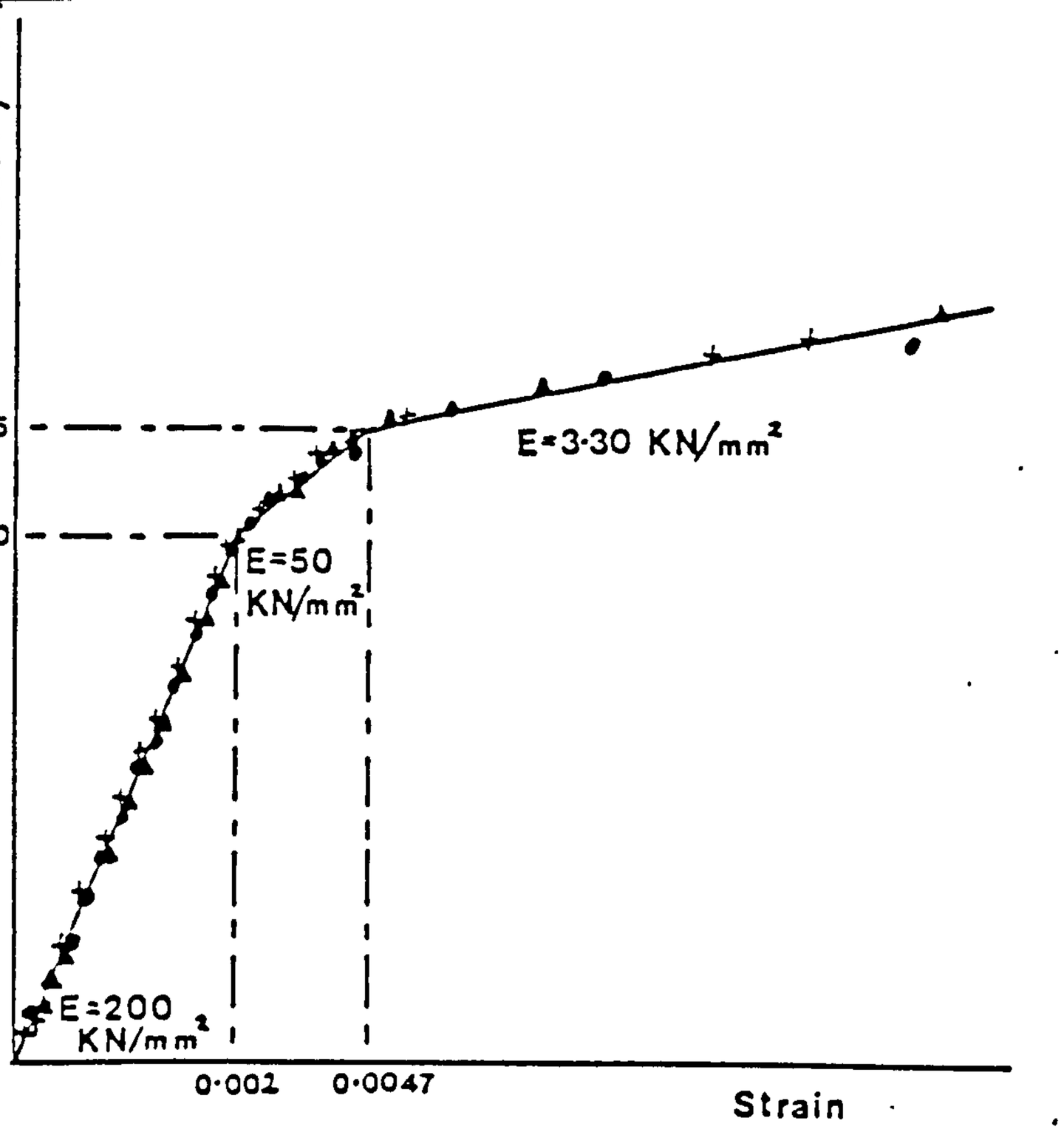

Fig. 2 Idealised tri-linear stress/strain relationship for reinforcement

PROPERTIES OF BRICKWORK

Brickwork prism specimen: The strength and stress-strain relationship, are both required for theoretical analysis. Two types of prisms as shown in Fig. 3 were selected to obtain the strength and material properties of the brick-work. Prism B represents the top three courses of the brickwork resisting the compressive force developed in the beam during early stages of loading. During the testing of the beam, it was observed that the cracks developed after the neutralisation of the prestress and penetrated deeper than the level of prestressing steel. As a result, only the topmost course of brickwork resisted the compressive force, hence single course prism was also tested to obtain the strength and material properties. The test results are given in Table 1.

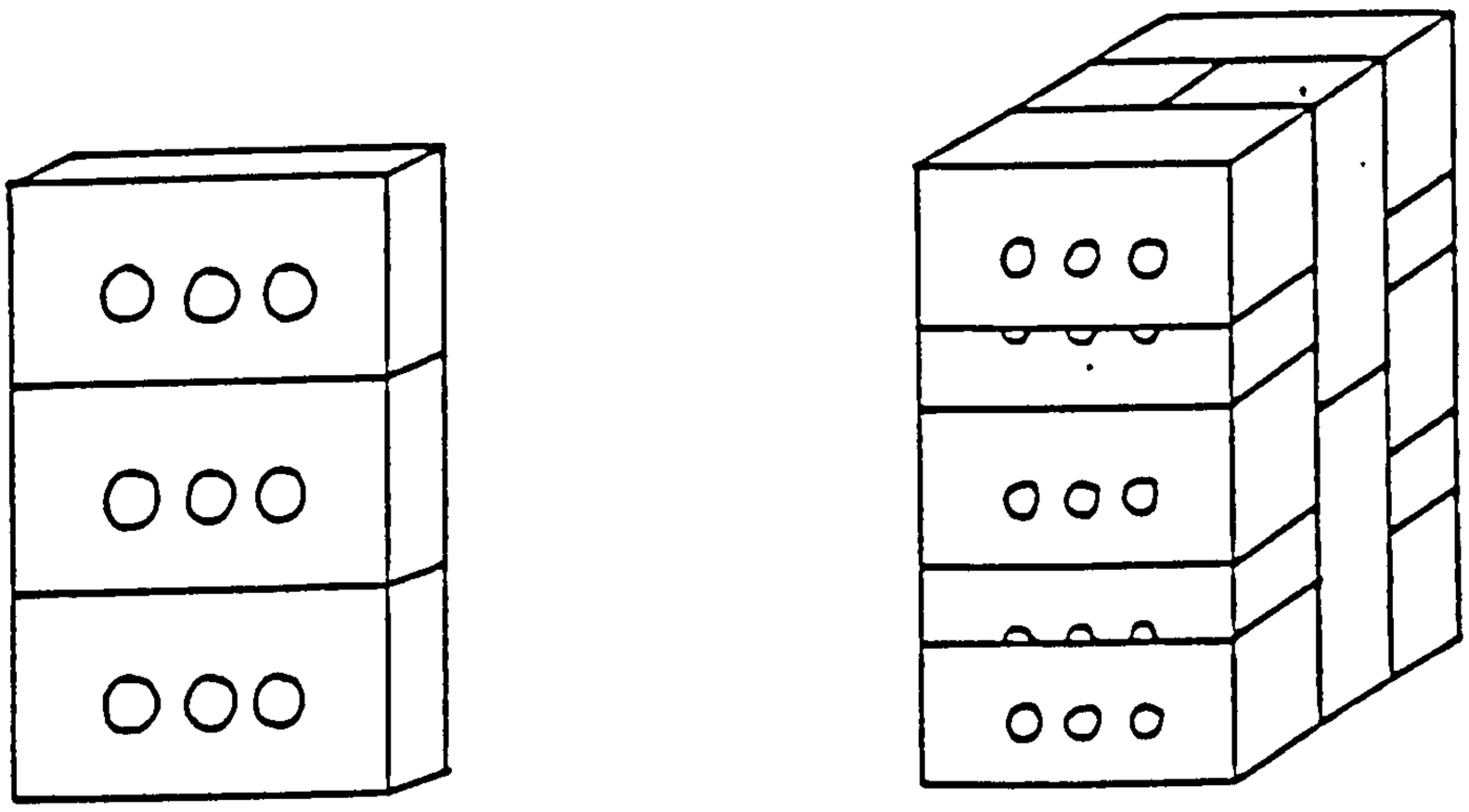

Single Course
Prism Type A

Three Course
Prism Type B

Fig. 3 Brickwork Prisms

Brick Strength N/mm^2	Mortar grade	Prism type	Test No.	Ultimate Compressive Strength N/mm^2 Test Results	Ultimate Compressive Strength N/mm^2 Average	Ultimate Compressive Strain x 10^{-5} Test Results	Ultimate Compressive Strain x 10^{-5} Average
82.0	1:¼:3	Single Course	1	28.9	28.8	305	292
			2	24.2		261	
			3	29.9		313	
			4	30.0		281	
			5	31.8		337	
			6	28.0		255	
82.0	1:¼:3	Three Course	1	16.6	19.4	189	213
			2	19.2		196	
			3	21.5		211	
			4	23.6		257	
			5	17.5		224	
			6	18.0		201	
58.9	1:¼:3	Three Course	1	10.8	11.8	253	270
			2	13.9		294	
			3	10.8		264	

Table 1 Properties of Brickwork Prisms

Stress-strain relationship: Both types of brickwork prisms were tested under uni-axial compression and the resulting strain was measured with a 'demec' gauge. The experimental stress-strain relationship was mathematically idealised and the relationship was obtained by a third-degree polynomial (Fig. 4) of the form:

$$f/f_m = 1.95(\varepsilon/\varepsilon_m) - 1.24(\varepsilon/\varepsilon_m)^2 + 0.29(\varepsilon/\varepsilon_m)^3$$

The equation was very similar to the one proposed earlier [4] . From the stress-strain relationship, the stress block factors $\lambda_1 = 0.63$ and $\lambda_2 = 0.37$ were obtained.

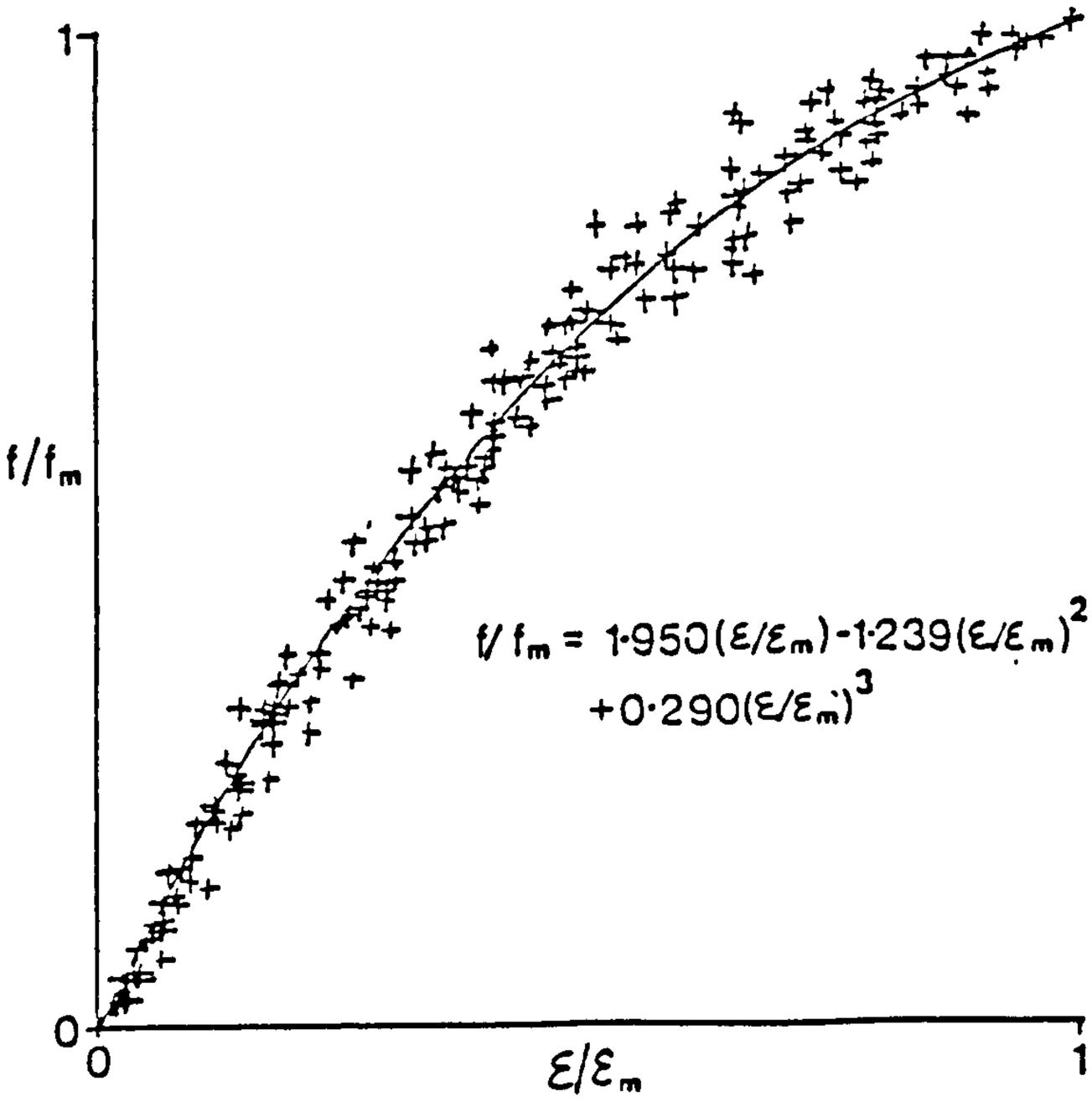

Fig. 4 Non-dimensional stress/strain relationships for brickwork

CHOICE OF BRICKWORK SECTION FOR PARTIALLY PRESTRESSED BEAMS

Any development in brickwork to be of practical use, needs to take into account the available skill and the available shape of the unit. Ignoring these two major constraints may lead to constructional difficulties associated with useless costly development. In addition the section must offer certain other competitive advantages over other forms of construction such as:

i) effective utilisation of as much ceramics as possible

ii) ease of grouting

iii) provision of cavity for placement of the reinforcements at required depth

iv) elimination of formwork

Keeping these in mind, the section developed for the beam is shown in Fig.5 . The top three courses of the beam were built in normal English bond and the bottom two courses receiving the reinforcement was formed by splitting the bricks lengthwise and placing them flush with the face. The cavity allowed positioning of the prestressing steel at the 'kern' limit and the non-stressed reinforcement at any suitable depth. The area of the cavity to be filled with concrete was 18% approximately of the total cross-sectional area.

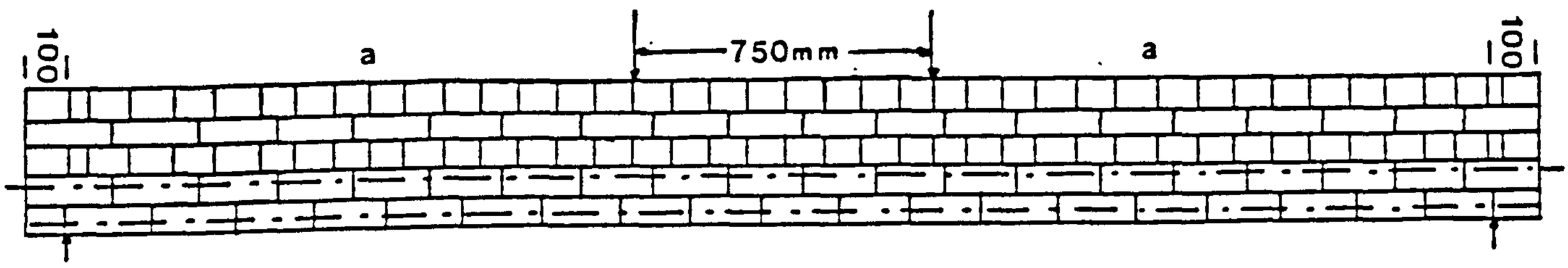

BEAM EVELATION

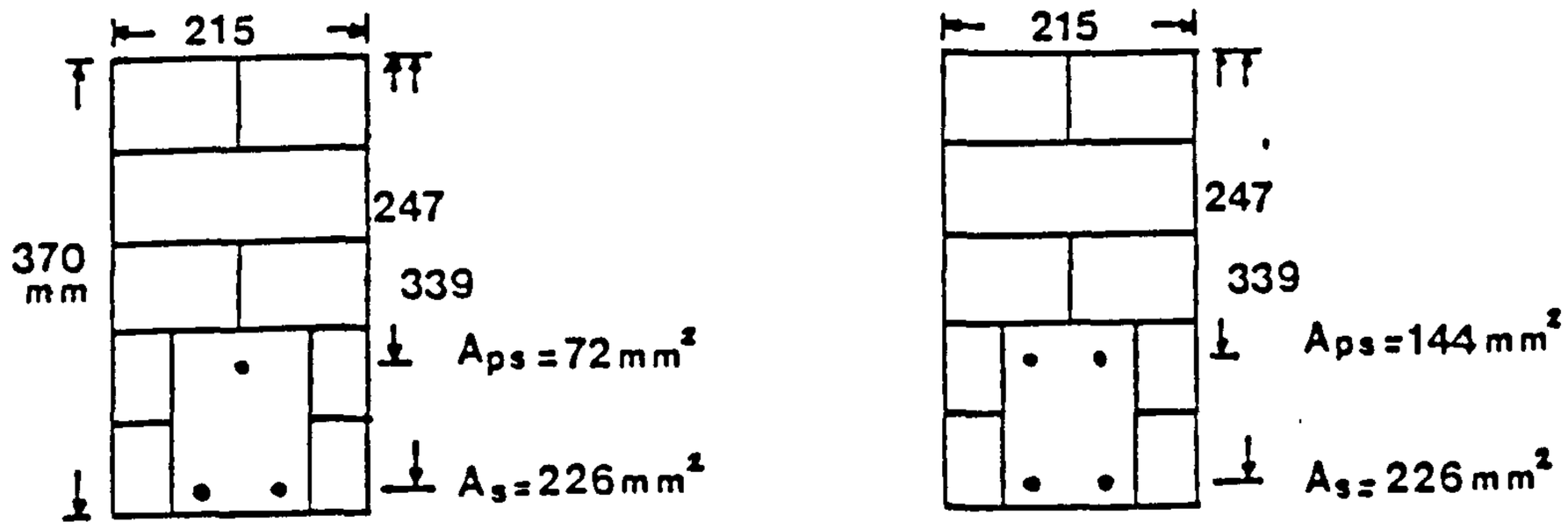

Section
Beams 1-8
p=0.47%

Section
Beams 9-10
p=0.61%

Fig. 5 Beam elevation, brick bonding arrangement and sections

CONSTRUCTION OF THE BEAMS

All test beams were built on the floor of the laboratory by an experienced bricklayer. To prevent horizontal splitting of the bedjoints the ends of the beams were reinforced with 6 mm mild steel rods to resist the anchorage forces which develop in the 'lead in length'.

The beams were cured for 21 days before post-tensioning. 25 mm thick mild steel anchorage plates were attached to the beams. The beams were prestressed to 70% of the tendon's ultimate strength. Immediately after prestressing, the non-stressed steel was put in position and then the concrete was poured to fill the cavity. The beams were tested after 7 days of concreting.

The amount of prestressing steel and non stressed-steel for various beams are shown in Fig. 5.

TEST ARRANGEMENTS AND INSTRUMENTATION

The test set-up is shown in Fig. 6. The test rig (Fig. 7) provided pin and roller support. Load was applied by jacks connected to a hydraulic pump. The loads at the jacking point were measured with load-cells connected to a pen-chart recorder. Strains up to failure were measured in the constant moment zone at various depths of the beams by a 'demec gauge'. Steel strains were measured by the electrical resistance gauges. Crack width and depth were also recorded at each load interval. Central deflection of each beam was measured with dial gauges reading to 0.02 mm.

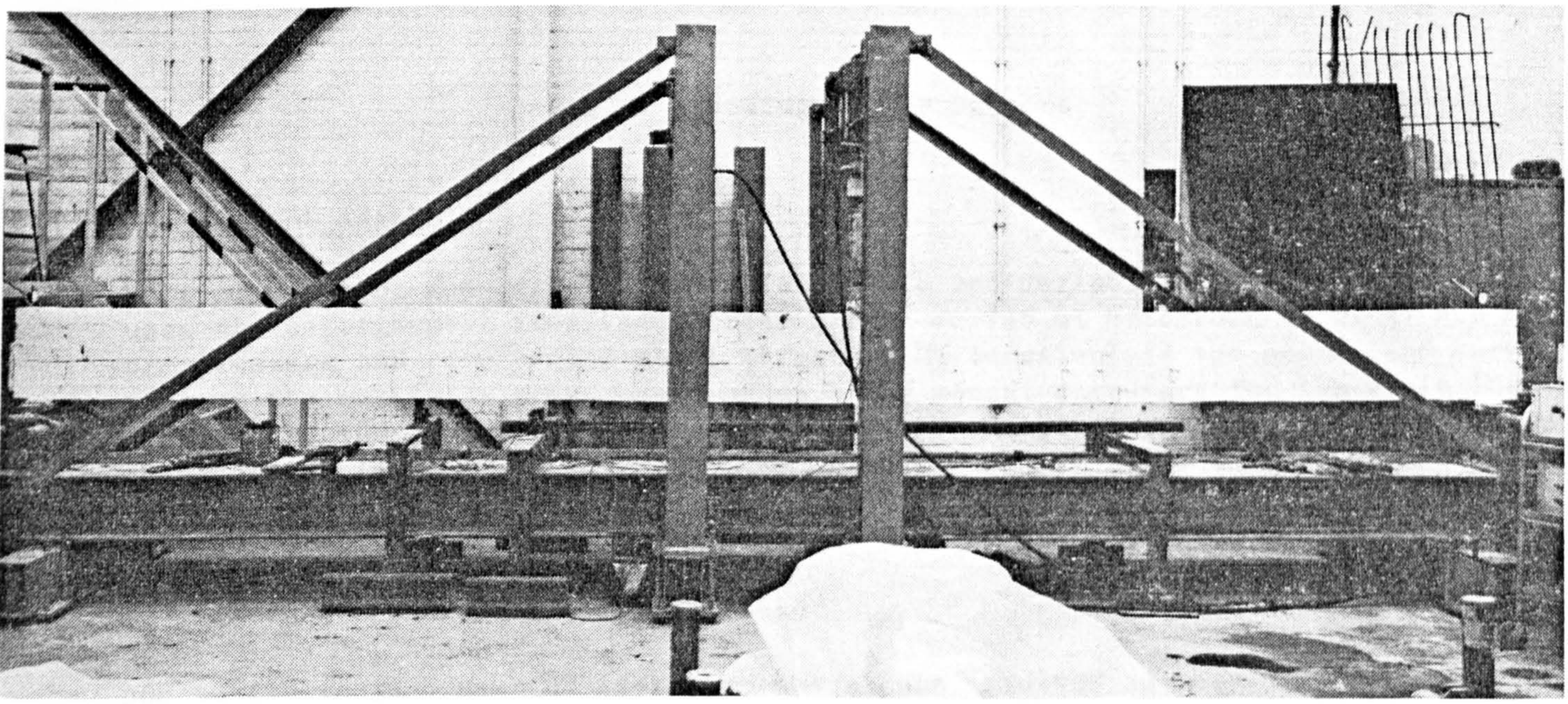

Fig. 6 Test set-up, showing the failure of a beam in shear

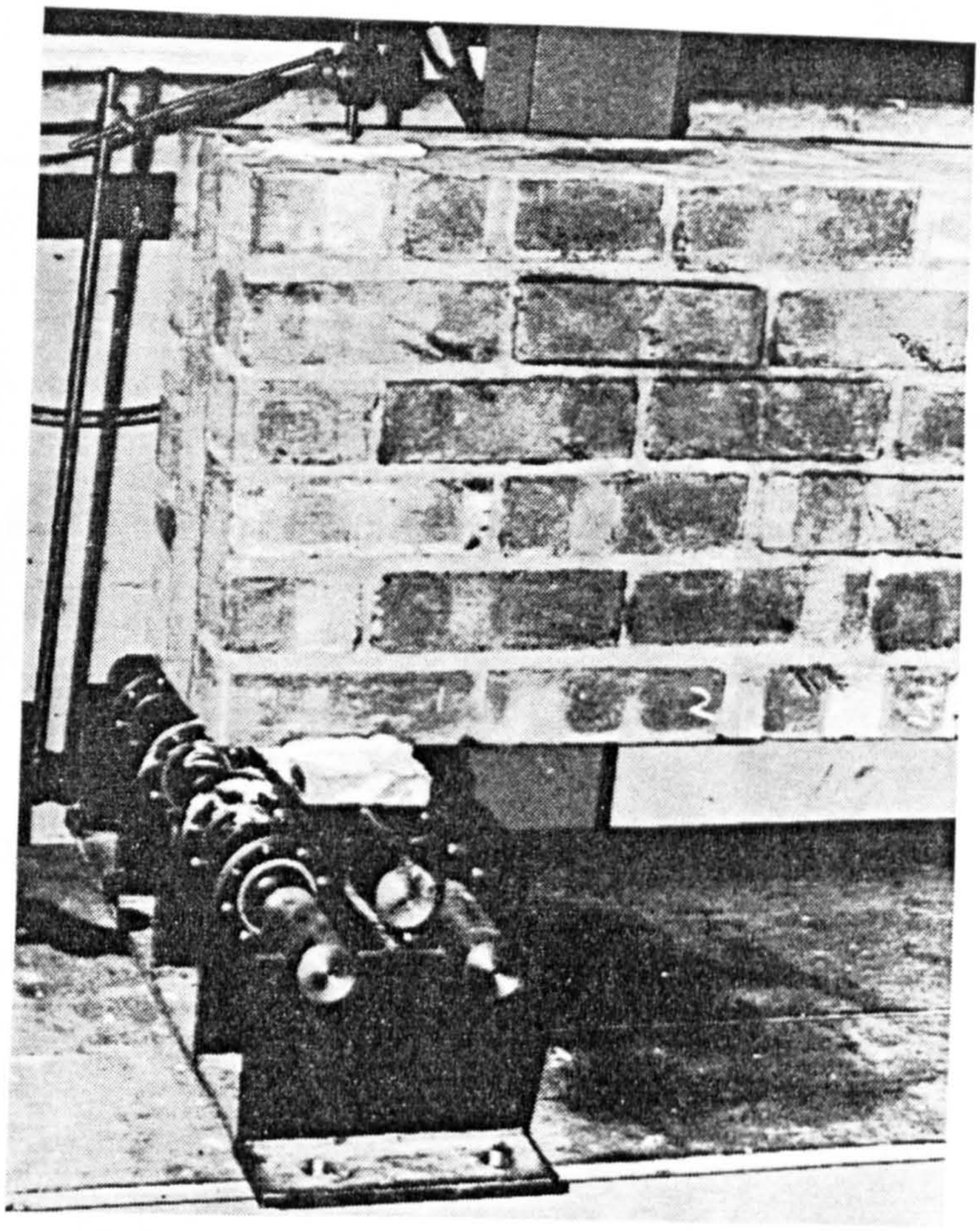

Fig. 7 Showing Roller Support

THEORETICAL ANALYSIS

Determination of moment-curvature relationship and deflection: This direct method uses the experimental idealised stress-strain curves of brickwork (Fig. 4) and both prestressing and reinforcing steel (Figs 1 & 2) to calculate the moment and curvature of the partially prestressed beams. The moment-curvature for the whole loading history is used to calculate the deflection. The applied loading is considered in three stages (1,5):

i) prestressing
ii) prestressing to cracking
iii) post cracking to ultimate load

Due to the large number of iterative operations involved in obtaining the moment-curvature relationship and deflection of the beam, a computer program was written to cope with these. The detailed derivation of this method is given elsewhere [1].

Calculation of ultimate-moment of resistance: The moment of resistance of the beam was also calculated from the stress block in addition to the direct method of calculation described above. At the time of failure, in any beam, the prestressing force is completely neutralised in maximum moment zone and the behaviour of partially prestressed beams then will be very akin to a reinforced brickwork beam.

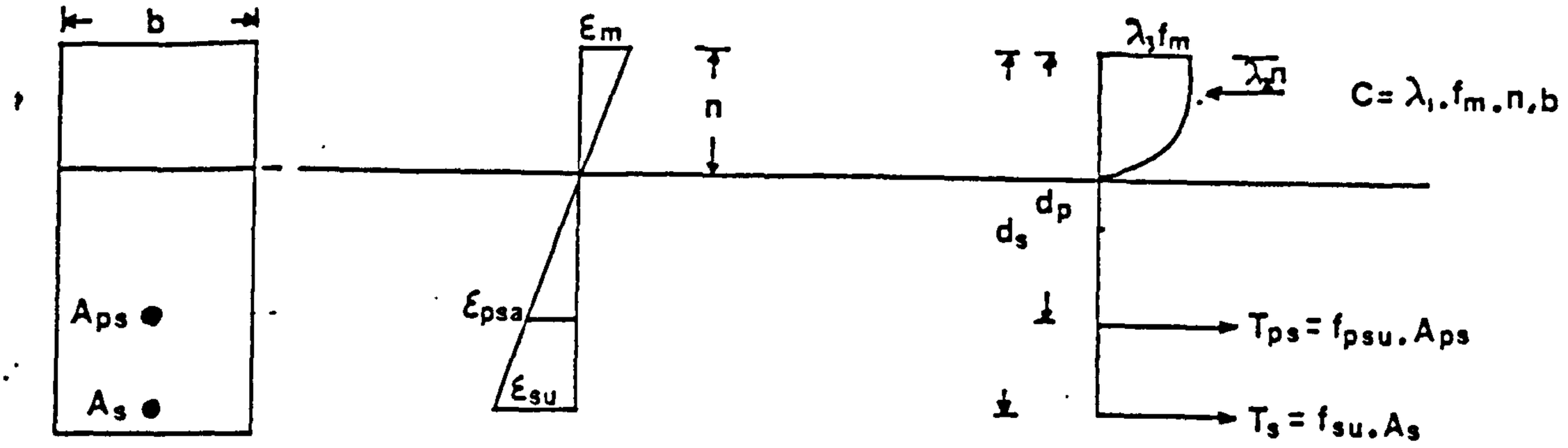

Fig. 8a Beam Section

Fig. 8b Strain Distribution at Failure

Fig. 8c Stress distribution at Failure

From Fig. 7 the total force of compression (6,7) and tension will be given by:

$$F_c = \lambda_1 . b . n . f_m \qquad -(i) \; ; \quad \text{since } \lambda_3 = 1 \; (7)$$

$$F_t = A_{ps} f_{psu} + f_{su} . A_s \qquad -(ii)$$

$$F_c = F_t \qquad -(iii)$$

$$n = \frac{A_{ps} . f_{psu} + A_s f_{su}}{\lambda_1 . b . f_m}$$

$$\varepsilon_{psu} = \varepsilon_{sp} + \varepsilon_{psa} \qquad -(iv)$$

where ε_{psa} = strain due to applied load

ε_{sp} = strain due to prestress

Assuming full bond between the steel and concrete at failure, the strains in the prestressing and non-stressed reinforcement respectively are given by:

$$\varepsilon_{psa} = \varepsilon_m . \frac{(d_p - n)}{n} \qquad -(v)$$

$$\varepsilon_{su} = \varepsilon_m (\frac{d_s - n}{n}) \qquad -(vi)$$

where ε_m is the ultimate strain derived from the brickwork prisms test.

Once ε_{psu} and ε_{su} are known, f_{psu} and f_{su} may be obtained from the respective stress-strain relationships for the steel. This method for the calculation of ultimate moment involves a process of trial and error to calculate n, such that $F_c = F_t$.

Once this is satisfied, moment is given by:

$$M_{su} = f_{psu} . A_{ps} [d_p - \lambda_2 . n] + f_{su} . A_s [d_s - \lambda_2 n] \qquad -(vi)$$

The theoretical moment thus calculated was compared with the experimental results in Table 3.

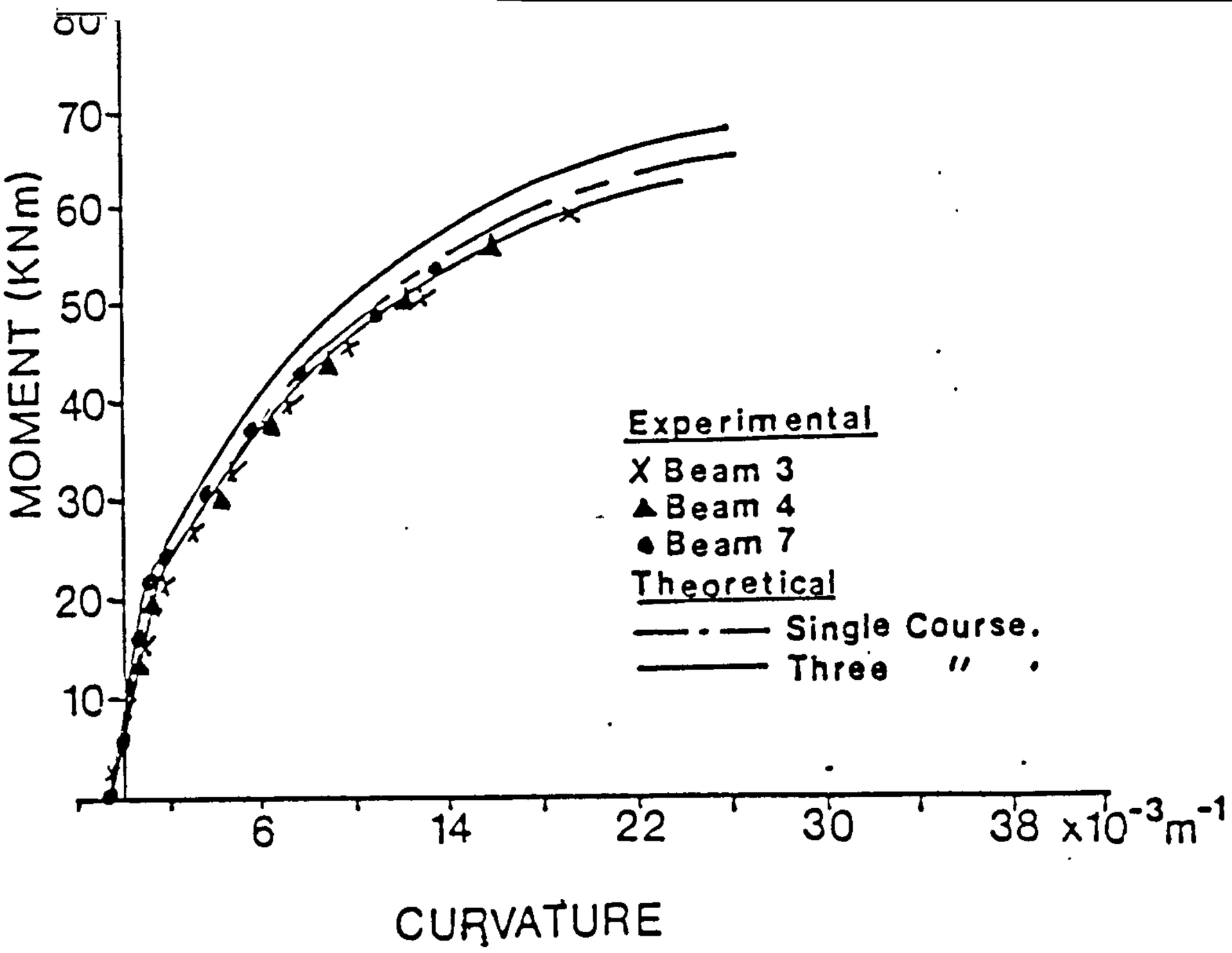

Fig. 10 Moment-curvature relationship for beams of 0.47% steel

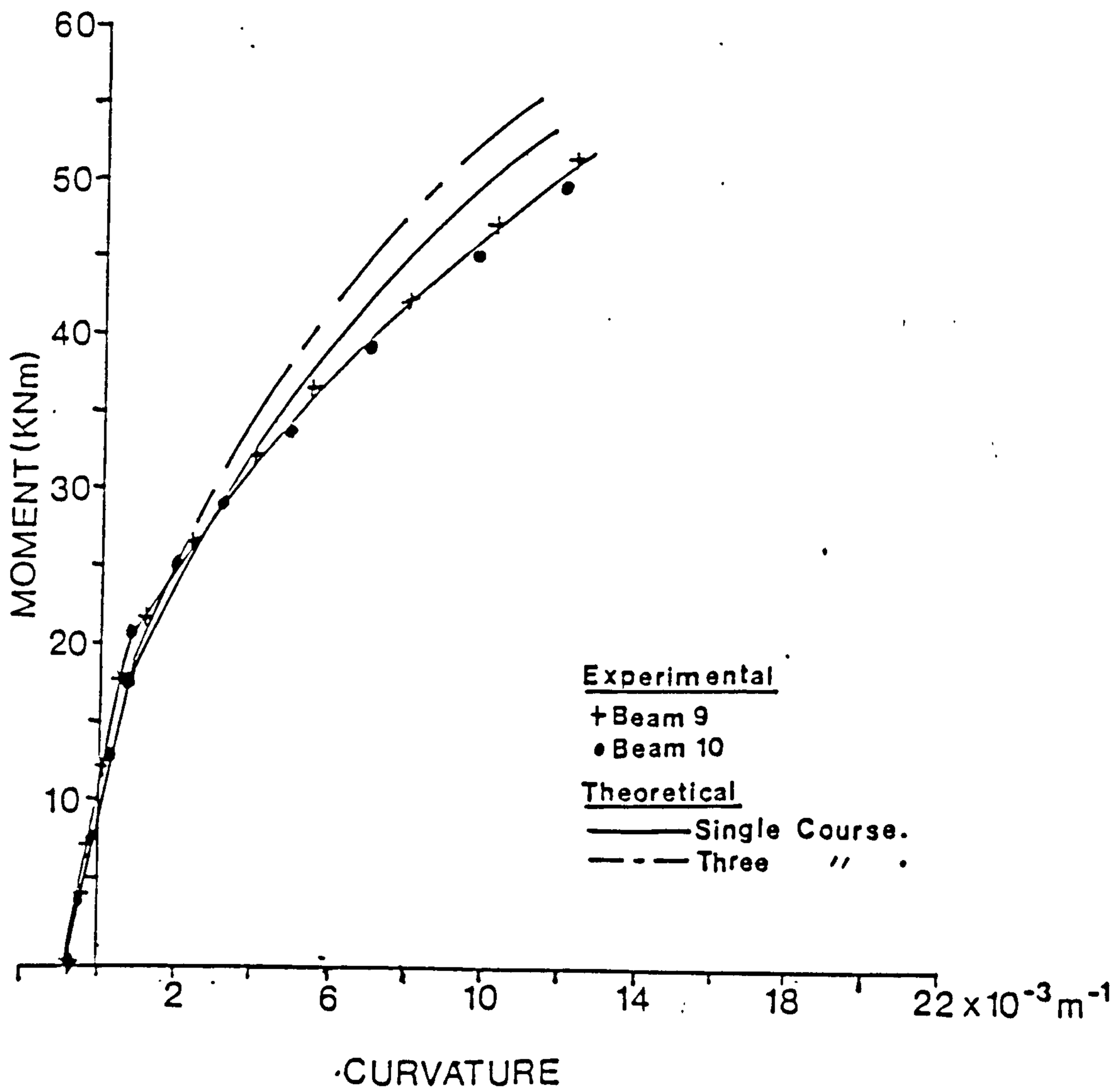

Fig. 11 Moment-curvature relationship for beams of 0.61% steel.

RESULTS AND DISCUSSION

The test results for all the beams and their mode of failure is given in Table 2.

Moment-Curvature Relationship: Typical moment-curvature relationship for the tested beams are shown in figures 9 to 11, the beams (figs.9,10) with a 0.47% of steel which failed in flexure show three distinct phases: linear up to cracking, cracking up to yield stress of steel and post yield phase when it becomes parallel to x-axis. The beams with 0.47% and 0.61% steel area which failed prematurely due to shear, the third phase was completely absent (fig.11).

As expected, the curvature for the beams 9-10 with higher percentage of steel (0.61%) was lower than for beams 1-4 with percentage of steel equal to 0.47.

From figs 9-11, it can be seen that there is very good agreement between the experimental and theoretical values of m-ϕ derived by direct method from both types of brick prisms, but the single course prism results giving slightly better agreement.

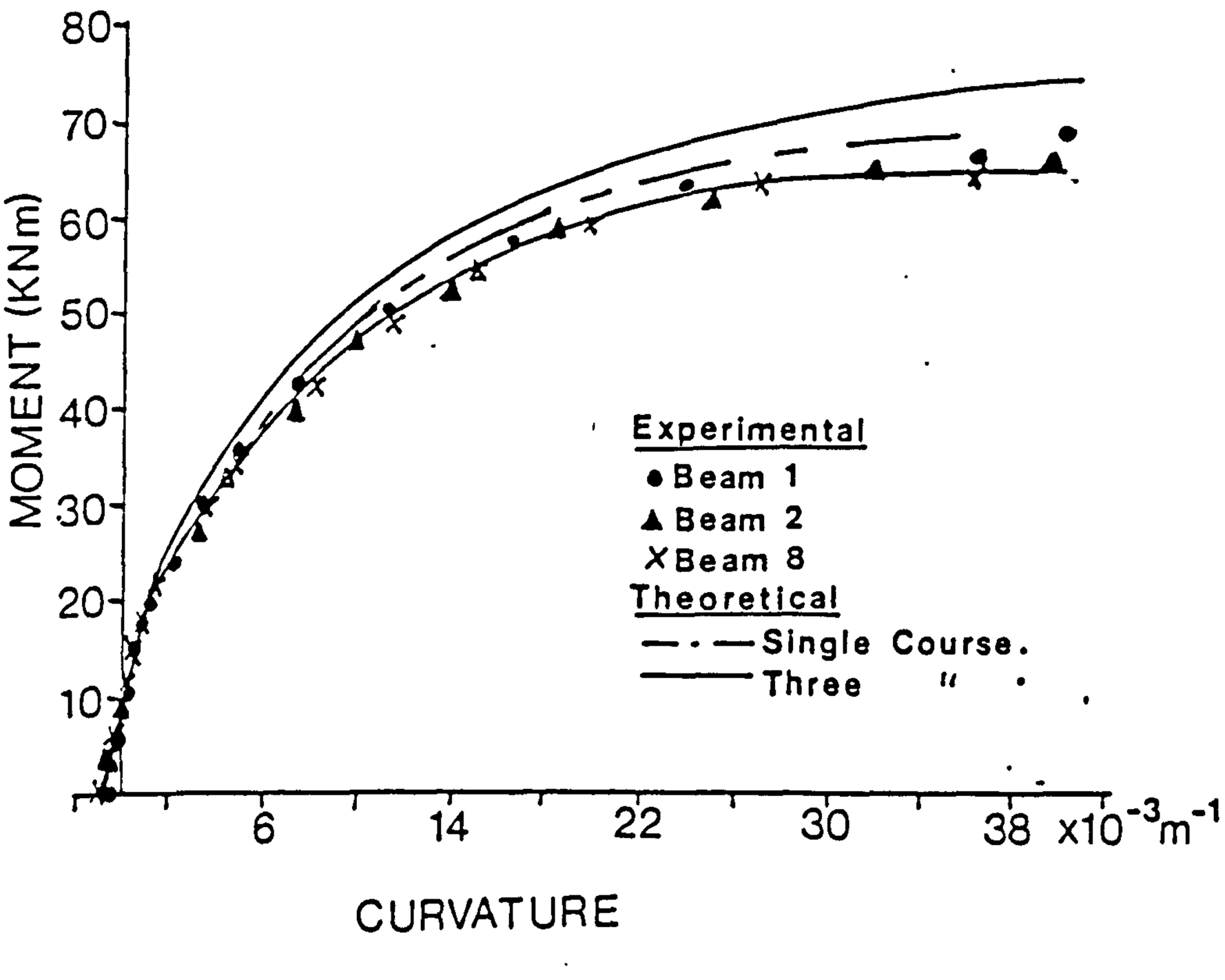

Fig. 9 Moment-curvature relationship for beams of 0.47% steel

Deflection: Figs 12, 13 and 14 show typical moment-deflection relationships for the tested beams, Fig. 11 indicating three distinct phases as with the moment-curvature relationship. Comparing the predicted deflections with those experimentally derived the agreement is good, especially for the deflections using the results of the single course prism tests.

The recovery of deflection after release of the load was between 23 and 46% for beams failing in shear.

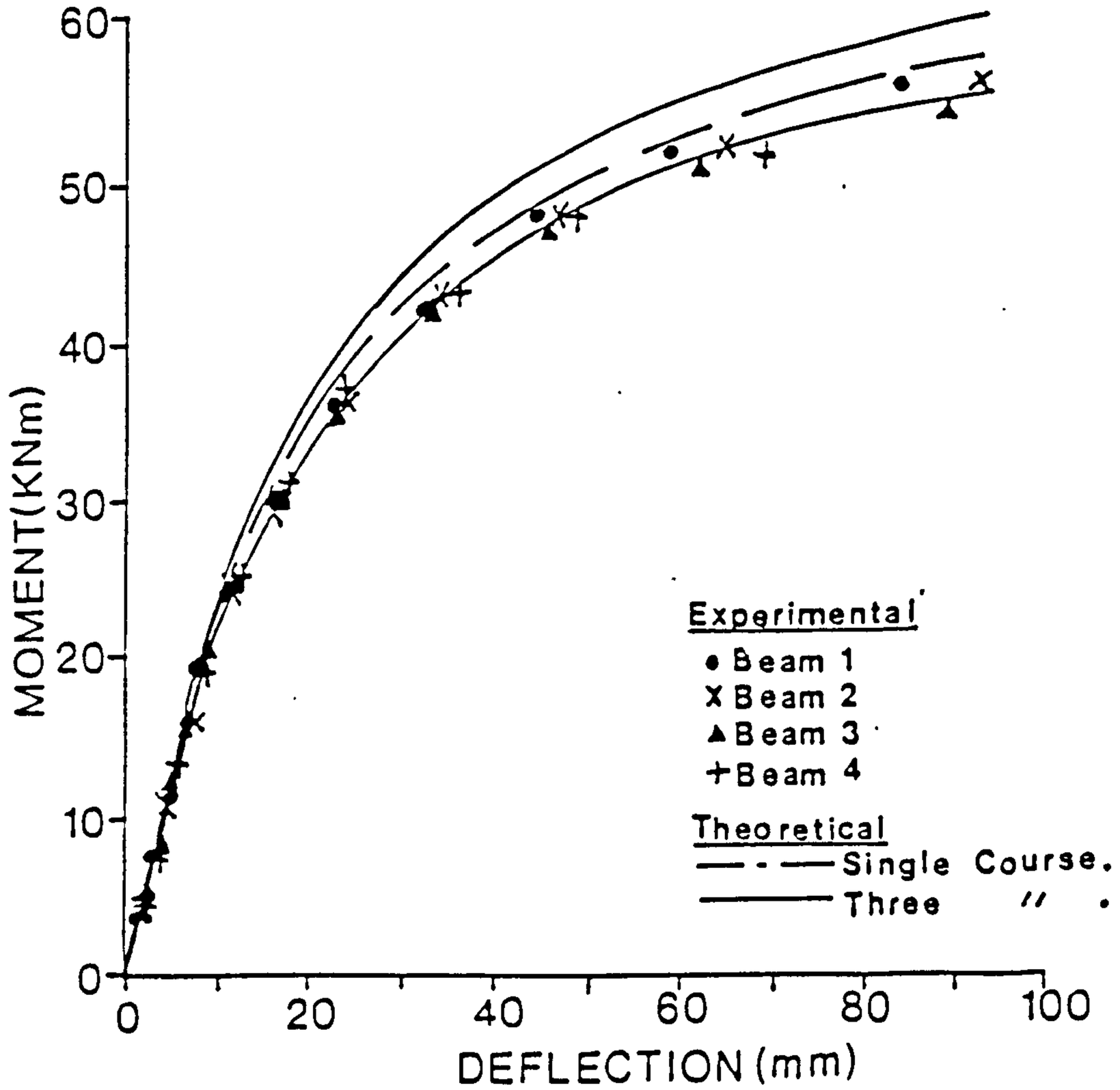

Fig. 12 Moment-deflection relationship for beams of 0.47% steel, span 6.2m.

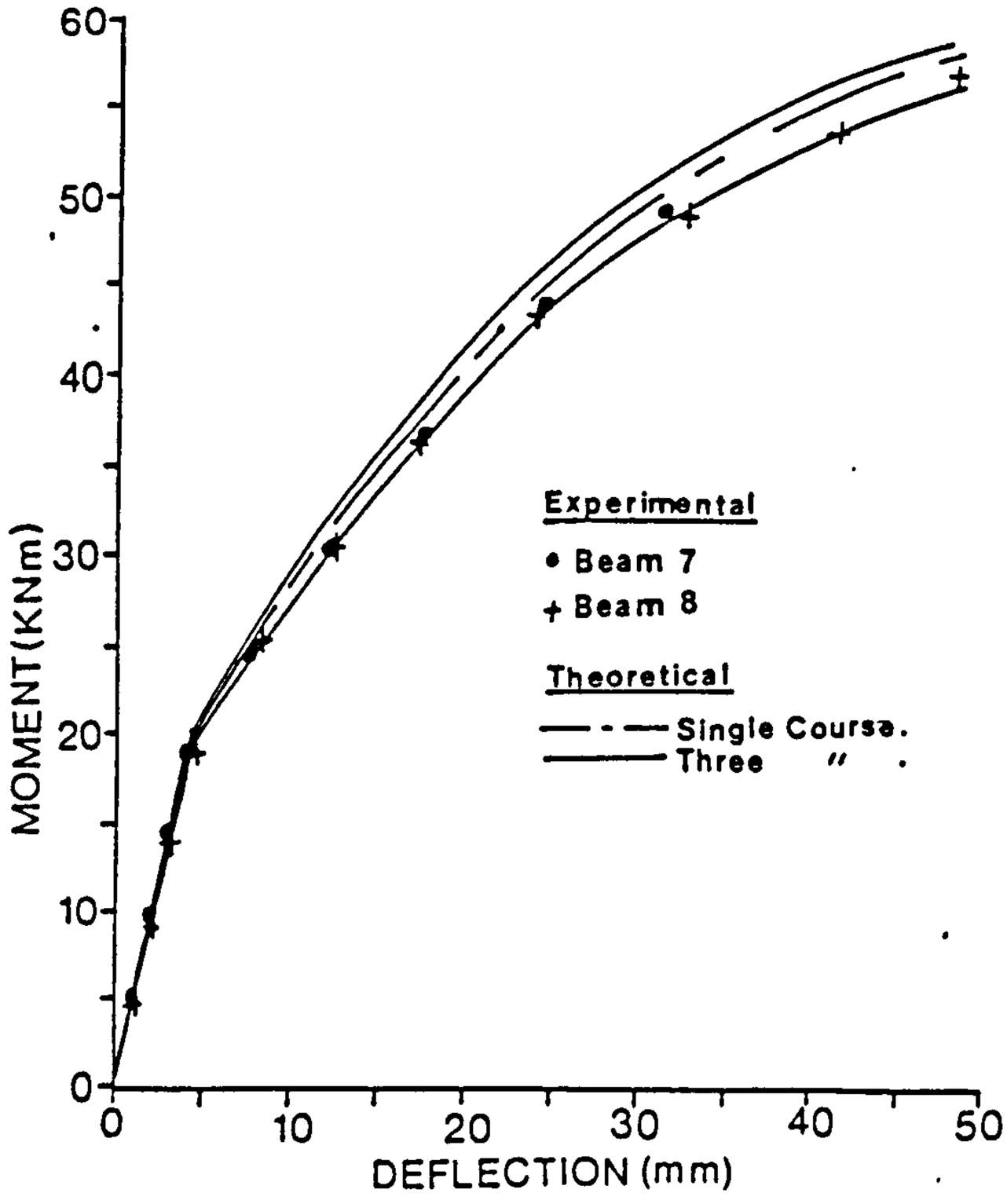

Fig. 13 Moment-deflection relationship for 0.47% steel, span 5.2 m

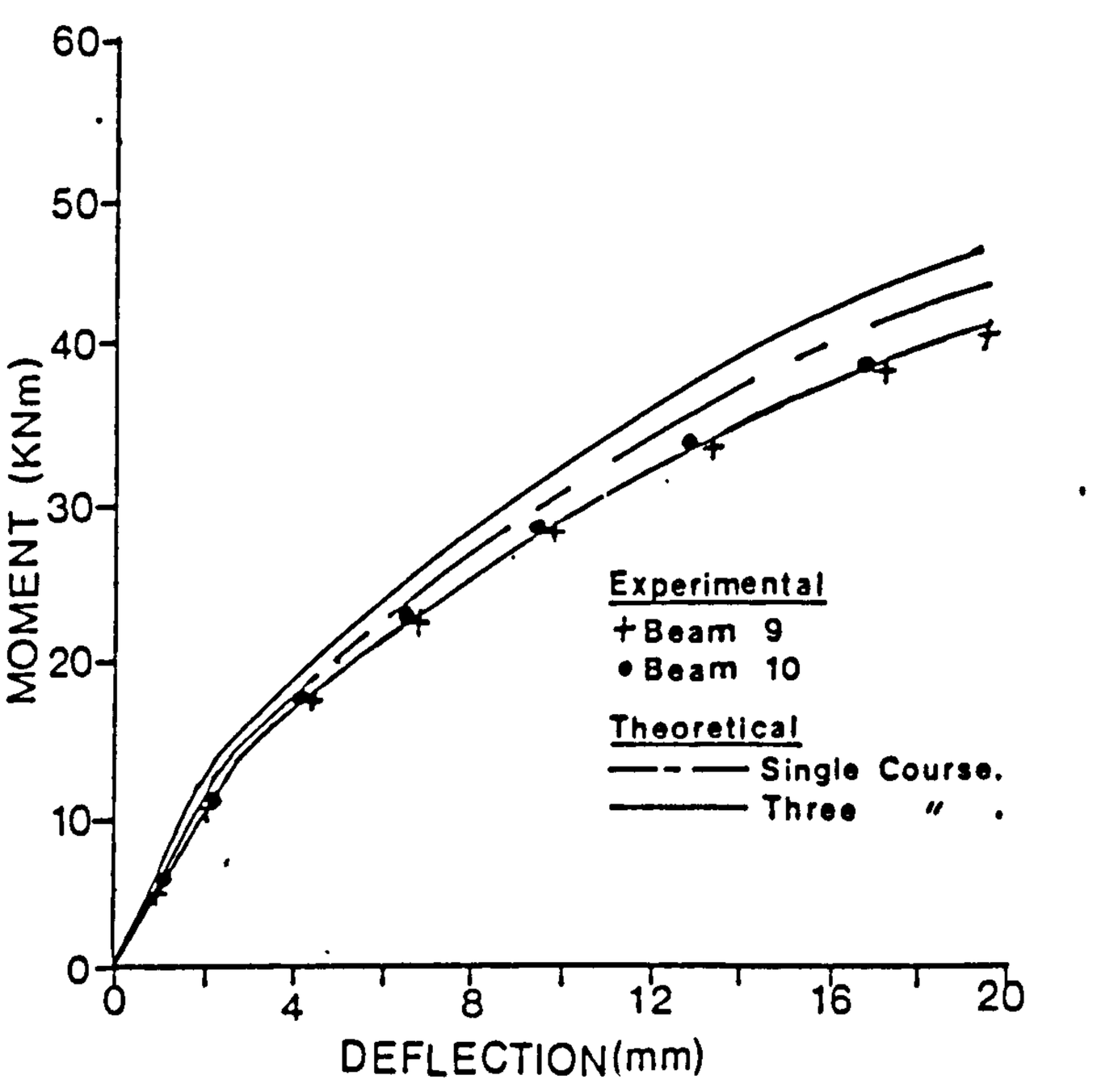

Fig. 14 Moment-deflection relationship for beams of 0.61% steel, span 5.2 m

Beam	Brick Strength N/mm^2	Mortar Strength N/mm^2	Grout Strength N/mm^2	Span m	Effective Prestress kN	Experimental Ultimate Moment kNm	Ultimate Shear Stress, V_u.* N/mm^2	Failure Mode
1	82.0	25.8	25.8	6.2	70.4	67.60	0.39	Tension
2	82.0	23.2	24.7	6.2	68.2	66.70	0.39	Tension
3	82.0	16.9	19.8	6.2	68.5	61.33	0.36	Shear
4	82.0	19.8	21.7	6.2	67.8	58.13	0.34	Shear
5	58.9	24.9	25.3	6.2	66.8	59.43	0.35	Tension
6	58.9	29.9	36.5	6.2	66.8	59.43	0.35	Tension
7	82.0	17.0	21.4	5.2	66.9	52.30	0.31	Shear
8	82.0	30.7	21.2	5.2	69.3	73.09	0.42	Tension
9	82.0	26.9	-	5.2	69.9	59.25	0.36	Shear
10	82.0	35.1	21.4	5.2	67.7	44.42	0.31	Shear

*$V_u = \frac{V}{bd}$. Ultimate shear stress is calculated as the loading at failure, irrespective of the failure mode.

Table 2 Summary of Beam Test Results

Ultimate Moment and Mode of Failure: Beams 1, 2 and 8 (p = 0.47%) of the high strength brick all failed in tension, with yielding of the steel reinforcement leading to crushing of the brickwork (average ultimate moment = 69.1 kNm). Other beams 3, 4 and 7 in this series failed in shear, with a reduction in average ultimate moment of 17% (Table 2). The shear failures of these beams occurred with longitudinal splitting along the concrete/brickwork interface from the support to the loading point (Fig. 6).

The medium strength brick beams 5 and 6 both failed in tension (table 2) with a 14% reduction in ultimate moment compared with the average moment of the high strength brickwork beams failing in tension.

Shear failure occurred with shear cracks propagating from the support along the concrete/brickwork interface to the loading point (fig. 6) all the shear failures occurring suddenly with no warning. But unlike reinforced brickwork there was no 'total' collapse and the beams were still able to carry some load after failure.

Table 3 compares the experimentally and theoretically derived ultimate moment. The experimental results of beams which failed in flexure are only compared with the theory, since it assumes the crushing of the compression zone at ultimate failure. From table 3 it can be seen that the methods presented predict the moments to a very satisfactory degree of accuracy. Thus using either method presented the ultimate moment of a partially prestressed brickwork may be calculated.

Beam No.	Experimental Ultimate Moment, kNm	Moment predicted using stress block factors				Moment predicted by direct method			
		SINGLE COURSE		THREE COURSE		SINGLE COURSE		THREE COURSE	
		kNm	Exp./theo.	kNm	Exp./theo.	kNm	Exp./Theo.	kNm	Exp./Theo.
1	67.6	66.8	1.01	61.1	1.11	73.6	0.92	68.2	0.99
2	66.7	66.8	0.99	61.1	1.09	73.6	0.91	68.2	0.98
5	59.4	-	-	54.0	1.10	-	-	53.3	1.12
6	59.4	-	-	54.0	1.10	-	-	53.3	1.12
8	73.1	66.8	1.09	61.1	1.20	73.6	0.99	68.2	1.07

Table 3 Comparison of experimental and theoretical ultimate moments

SUMMARY AND CONCLUSIONS

i) The section used in this investigation proved satisfactory and no problems were encountered in prestressing, concreting and handling of the specimens.

ii) The ultimate moment of a partially prestressed brickwork beam can reliably be predicted by the methods proposed in this paper.

iii) The direct method proposed in this paper which takes the non-linear behaviour of materials into account predicts accurately the load deflection relationships of the partially prestressed brickwork beams up to failure.

REFERENCES

1. PEDRESCHI, R.F. "A study of the behaviour of post-tensioned brickwork beams", Ph.D., Thesis, Department of Civil Engineering and Building Science, University of Edinburgh, 1983.

2. BRITISH STANDARDS INSTITUTION, 'The Structural Use of Concrete", CP 110, London 1972.

3. THE CONCRETE SOCIETY, 'Partial Prestressing', Concrete Society Technical Report, No.23, May 1983.

4. PEDRESCHI, R.F., and SINHA, B.P., 'The stress/strain relationship of brickwork', Sixth International Brick Masonry Conference, Rome, 1983 pp 321-334.

5. BURNS, N.H., 'Moment-Curvature Relationships for partially prestressed concrete beams', Journal of the Prestressed Concrete Institute, Vol.9, 1964, pp 52-63.

6. PEDRESCHI, R.F., and SINHA, B.P., 'Developement and investigation of the ultimate load behaviour of post-tensioned brickwork beams", The Structural Engineer, Vol. 60B, No.3, 1982, pp. 63-67.

7. SINHA, B.P., "An ultimate load-analysis of reinforced brickwork flexural members", International Journal of Masonry Construction, 1, No.4, 1981, pp 151-156.

NOTATION

a	Shear span
b	Breadth of beam section
d_p	Depth of prestressing steel
d_s	Depth of non-stressed steel
f_m	Ultimate compressive strength of brickwork
f_{psu}	Stress in prestressing steel at failure
f_{su}	Stress in 'non-stressed'steel at failure
n	Neutral axis depth
A_{ps}	Area of prestressing steel
A_s	Area of non-stressed steel
E	Young's Modulus
F_c	Compressive force at failure
F_t	Tensile force at failure
M_u	Ultimate bending moment
ε_m	Ultimate compressive strain of masonry
ε_{psa}	Strain in prestressing due to prestress
ε_{pse}	Strain in prestressing steel at failure due to applied loading
ε_{psu}	Strain in prestress steel at failure
ε_{su}	Strain in 'non-stressed' steel at failure
λ, λ_2	Stress block factors

ACKNOWLEDGEMENT

The work described in this paper is financially sponsored by the Science and Engineering Research Council, U.K. and the Structural Clay Products Ltd., St. Neots, U.K.

Number 6
December, 1985

Masonry International

Compressive Strength of Brickwork on Edge under Axial and Eccentric Loading

P. Walker, B.Sc.,
Department of Civil Engineering and Building Science, University of Edinburgh

B.P. Sinha, B.Sc., Ph.D., CENG, MICE, FIStructE, FIE(INDIA)
Department of Civil Engineering and Building Science, University of Edinburgh

The paper summarises the results of tests in 74 brickwork prisms subjected to axial and eccentric loading in the direction other than bed-joint. Two grades of mortar and three different bricks were used. The stress-strain relationships obtained under axial compression are used to determine the magnitude and distribution of stress under eccentric loading. The experimental results are compared with BS 5628 and with other investigations.

INTRODUCTION

The load carrying capacity of eccentrically loaded brickwork in the direction of the bed-joint has been studied by various research workers (1,2,3,4). These investigations centred on establishing the magnification factor, k, defined as the ratio of apparent maximum compressive strength under eccentric loading to axial compressive strength. The maximum compressive strength under combined bending and direct stress was obtained by either considering the brickwork as a linear elastic material with no tensile strength or by equating the load-carrying capacity using conventional stress blocks such as rectangular or parabolic. No attempt has been made to establish the strain gradient to actual failure stress under eccentric loading, which is very important for the design of flexural members. In addition, in reinforced and prestressed brickwork, the stress may be applied in directions other than bed-joint direction, for which no data is available. Therefore an investigation was undertaken to study the behaviour of brickwork under axial and eccentric loading applied in a direction other than normal to the bed-joint.

SCOPE OF INVESTIGATION

In this investigation, the following variables were considered:

(i) Brick strength: low, medium and high strength brick

(ii) Mortar grade: Grade 1 and Grade 2

(iii) Axial and eccentric loading: the eccentricity was limited to t/6 only.

The height of the prism was kept low ($^{h}/_{d}$ =5.08) so that the secondary effect of loading on strength was negligible. The stress/strain relationship was obtained from axially loaded prisms. The relationship thus obtained was used to derive the magnitude and distribution of stress along the width of the prism using the measured strains.

MATERIALS

Bricks

Three different types of 3-hole perforated bricks were used throughout, varying from high to low strength. Compressive strength and water absorption tests were carried out in accordance with BS 3921 (6); the results are presented in Table 1.

Mortar

Grade I, 1:1/4:3 (cement:lime:sand) and Grade II, 1/½/4½ (cement:lime:sand) mortar mixes were used. The average compressive strength of the mortars for each prism is given in Tables 2 and 3.

Brickwork Prisms

The brickwork test specimen used in this investigation is shown in Figure 1 with nominal dimensions 335 x 215 x 65mm. All test specimens are built by an experienced bricklayer and cured under polythene for 28 days prior to testing.

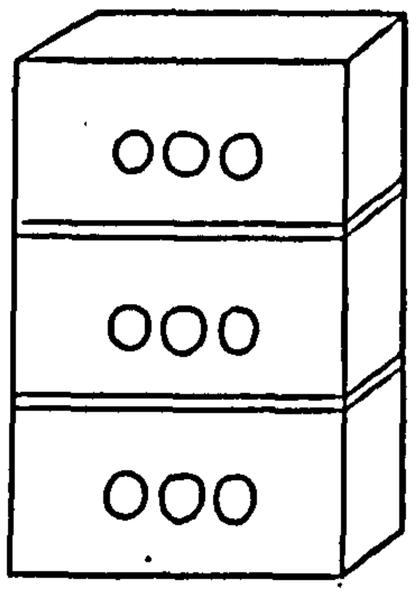

Figure 1. Brickwork Test Specimens

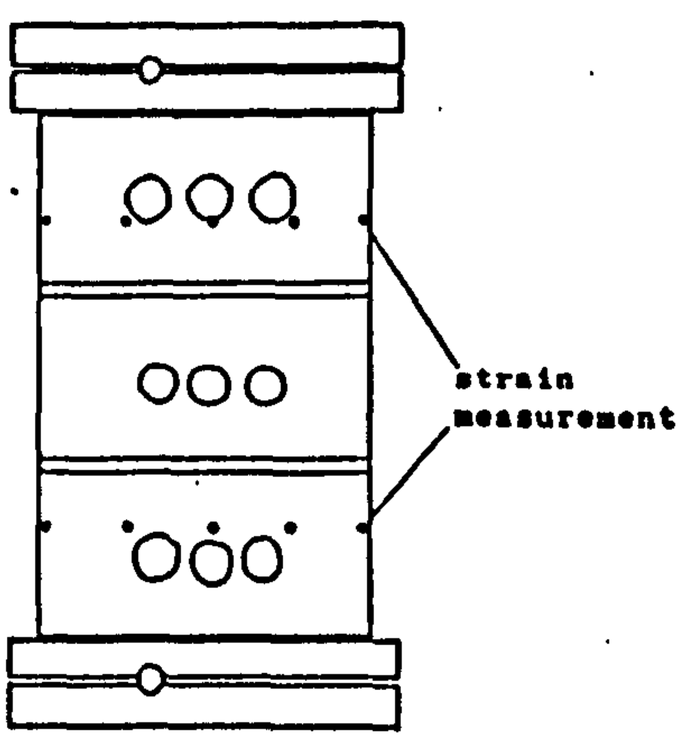

Figure 2. Test Set-up for Eccentrically Loaded Prisms

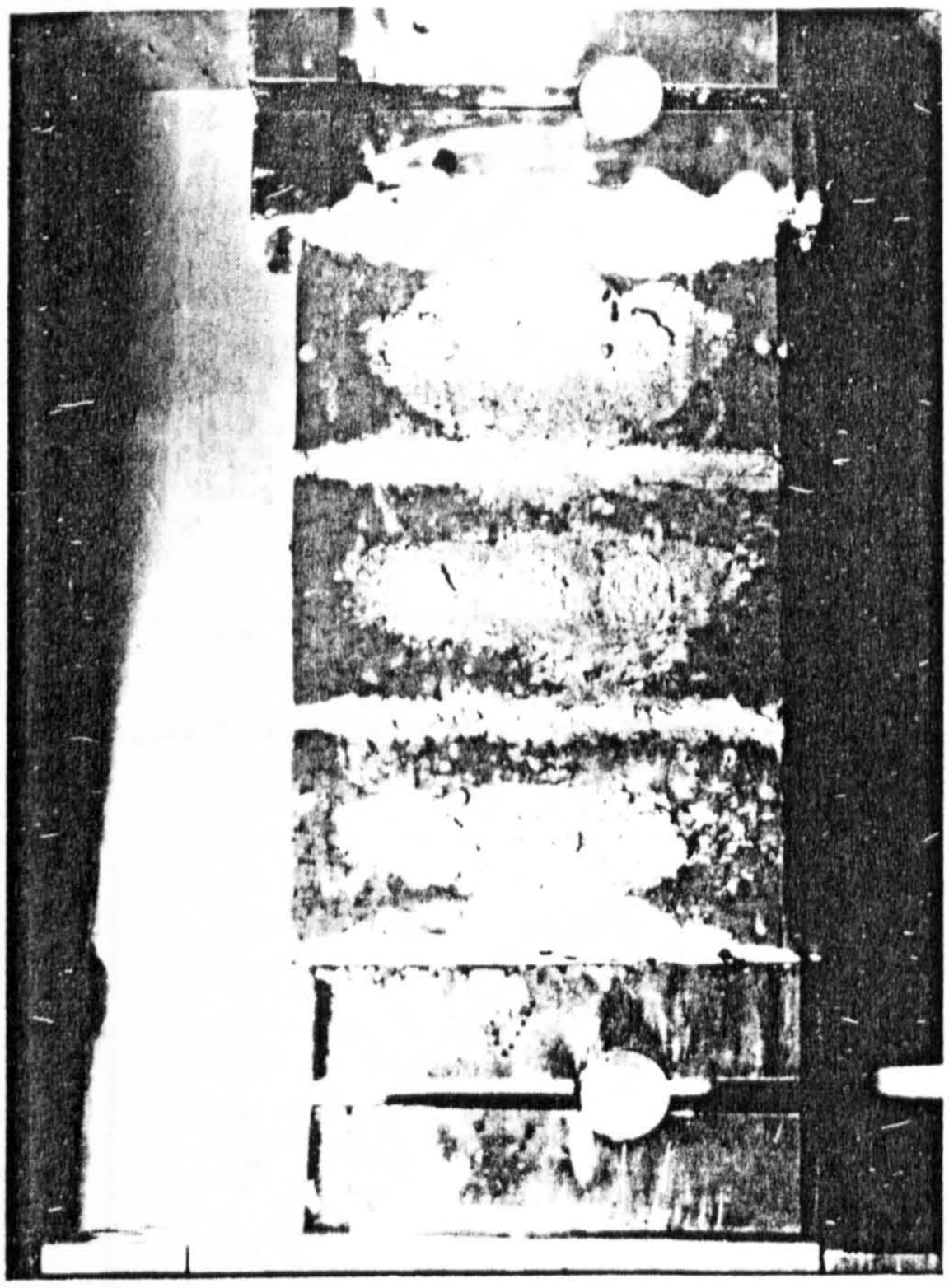

Figure 3 - Test Set-up of Eccentrically Loaded Prisms

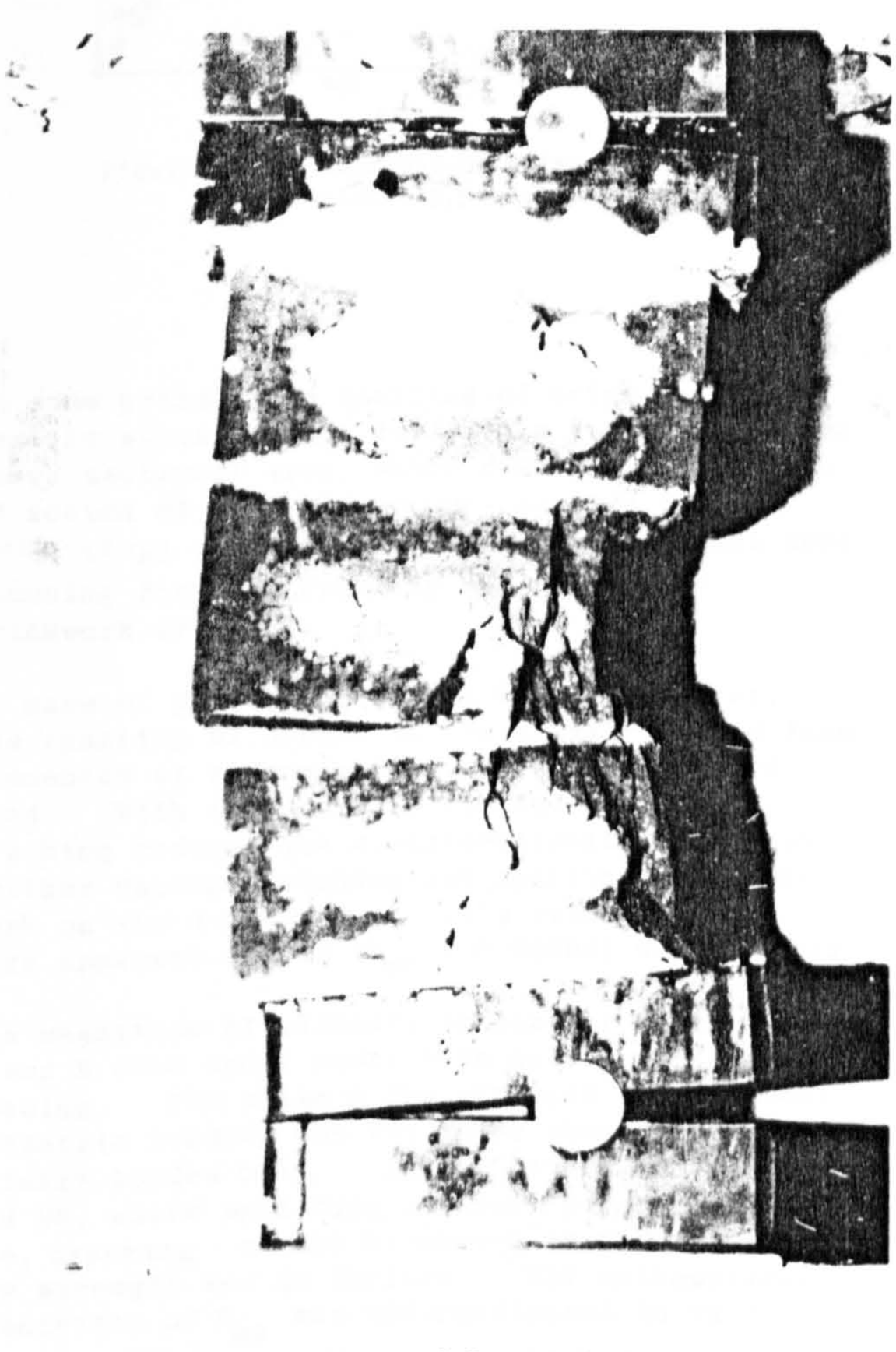

Figure 4 - Typical Failure of Eccentrically Loaded Prism Series DE

Test Procedure

Prior to testing, the axially loaded prisms were capped and levelled using a rich mortar mix. To ensure an even distribution of applied load 3mm plyboard sheets were also placed between the test specimen and loading platens. The set up for the eccentrically loaded prisms is shown in Figs. 2 and 3. The set up was so arranged that the line of action of the load was at an eccentricity of $t/6$.

Strain measurements were taken at positions across the width of the section using a 'Demec' strain gauge at regular intervals of loading. Tables 2 and 3 contain a summary of the test results for ultimate compressive strain.

EXPERIMENTAL RESULTS AND DISCUSSION

Mode of Failure

Vertical splitting of the bricks occurred at between 85-95% of the ultimate load in all of the axially loaded prisms and in the eccentrically loaded prisms built with Class I mortar. Splitting of the bricks was at the centre of the axially loaded prisms and along the line of action of the load in the eccentrically loaded brickwork.

Failure of the eccentrically loaded brickwork prisms built with Class II mortar was preceeded by crushing of the brickwork on the compression face and tensile splitting along the brick/mortar interface at the opposite side. Eventual collapse was caused by explosive spalling of the brickwork on the more heavily loaded face (Fig. 4).

Strain Measurements

Strains were measured at various stages of loading up to 88-95% of the failure load for both axial and eccentrically loaded prisms. The values for ultimate strain (Tables 2 and 3) were mathematically extrapolated from the experimental

load (stress)/strain relationships since it was not possible to measure the strain at failure.

The experimental stress/strain relationships for the axially loaded prisms were mathematically idealised in the form of a non-dimensional third degree polynominal (Figs 5-8), such that:

$$f/f_m = X_1 (\varepsilon/\varepsilon_m) - X_2 (\varepsilon/\varepsilon_m)^2 + X_3 (\varepsilon/\varepsilon_m)^3 \quad (1)$$

Values for X_1, X_2 and X_3 for each prism type are given in Table 4. Except for low strength brick, the value of the three constants were very similar to those derived by Pedreschi and Sinha (7).

Before cracking, in all eccentrically loaded prisms, the strain distribution was linear starting with maximum towards the loaded face reducing to zero on furthest face (Figs 9-12); a characteristic of loading at $t/6$.

Upon cracking of the brickwork, the distribution of strain across the width was no longer represented by a single strain gradient: the gradient from the extreme loaded face towards the loaded end changed. Thus the relationship became bi-linear.

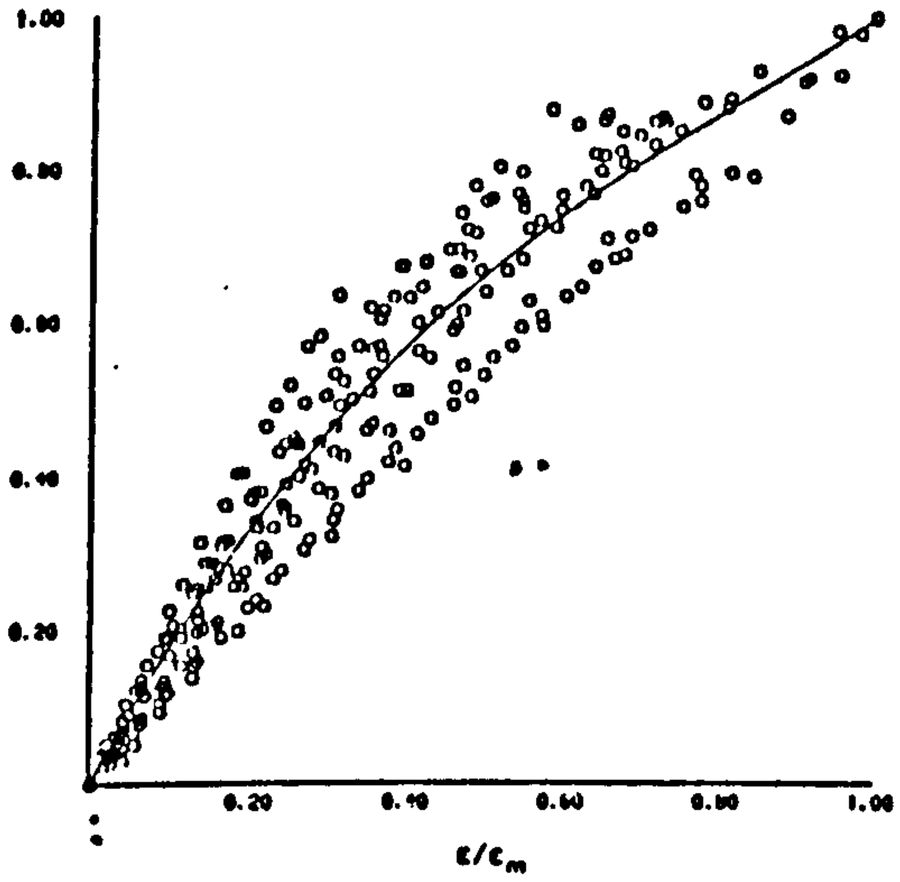

Figure 5. Non-Dimensional Stress/Strain Relationship, Prism Series A

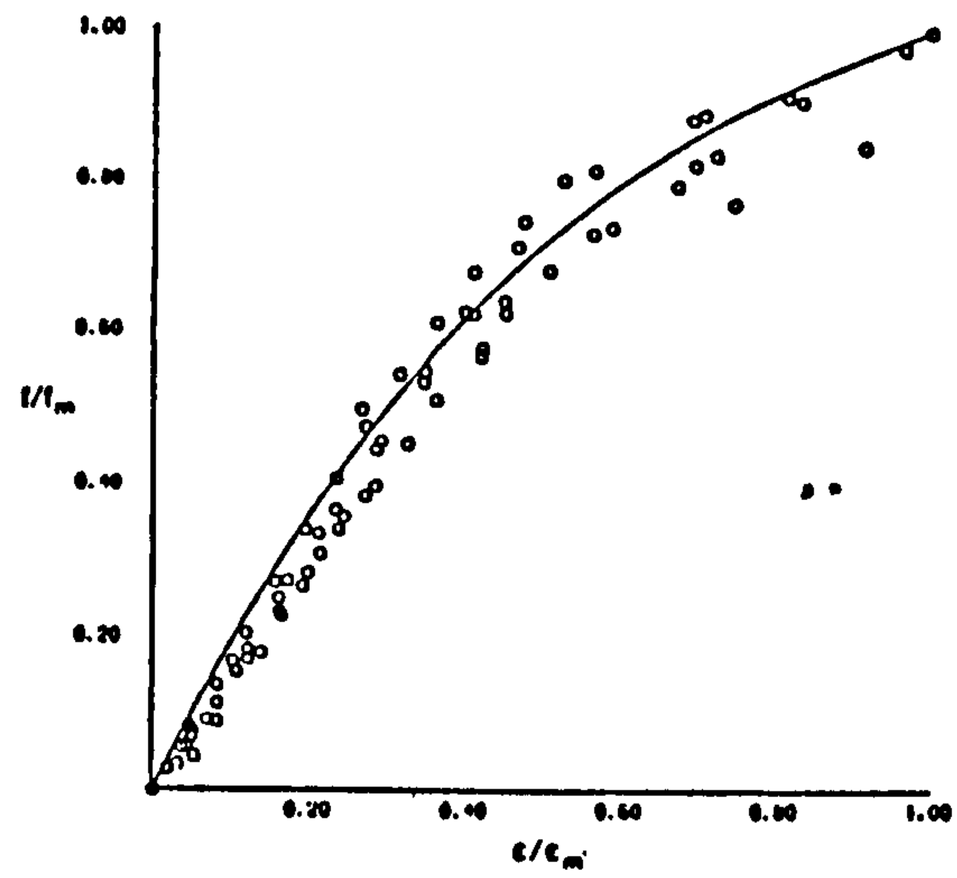

Figure 6. Non-Dimensional Stress/Strain Relationship, Prism Series B

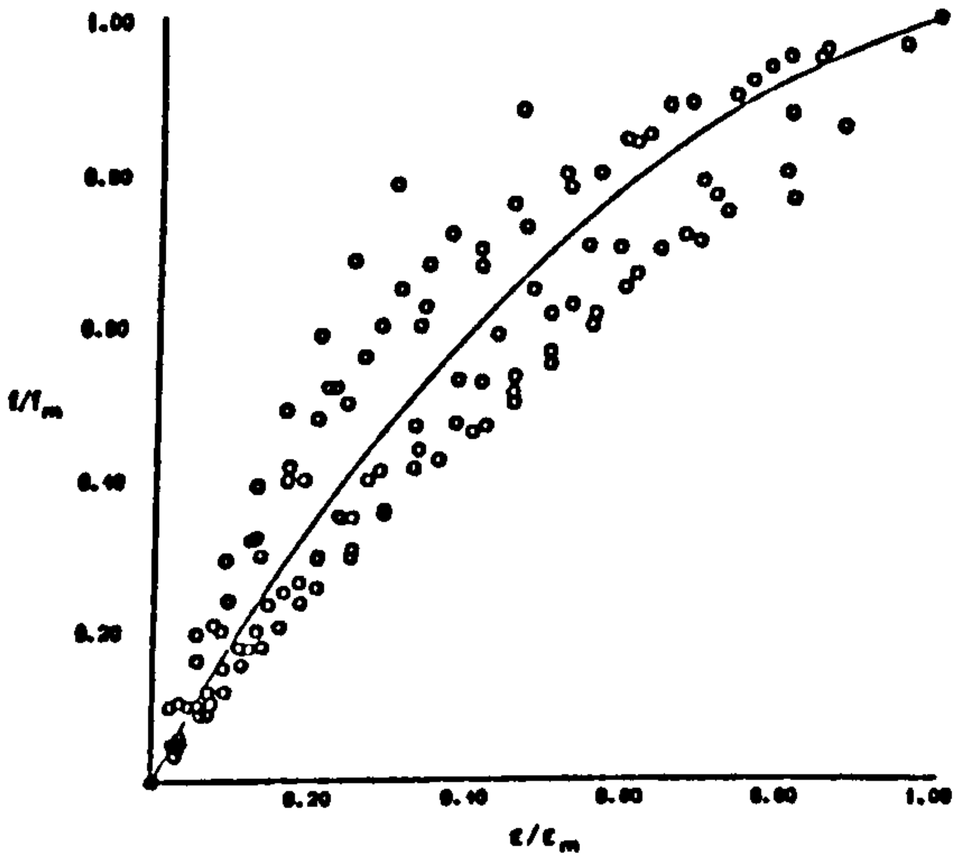

Figure 7. Non -Dimensional Stress/Strain Relationship, Prism Series C

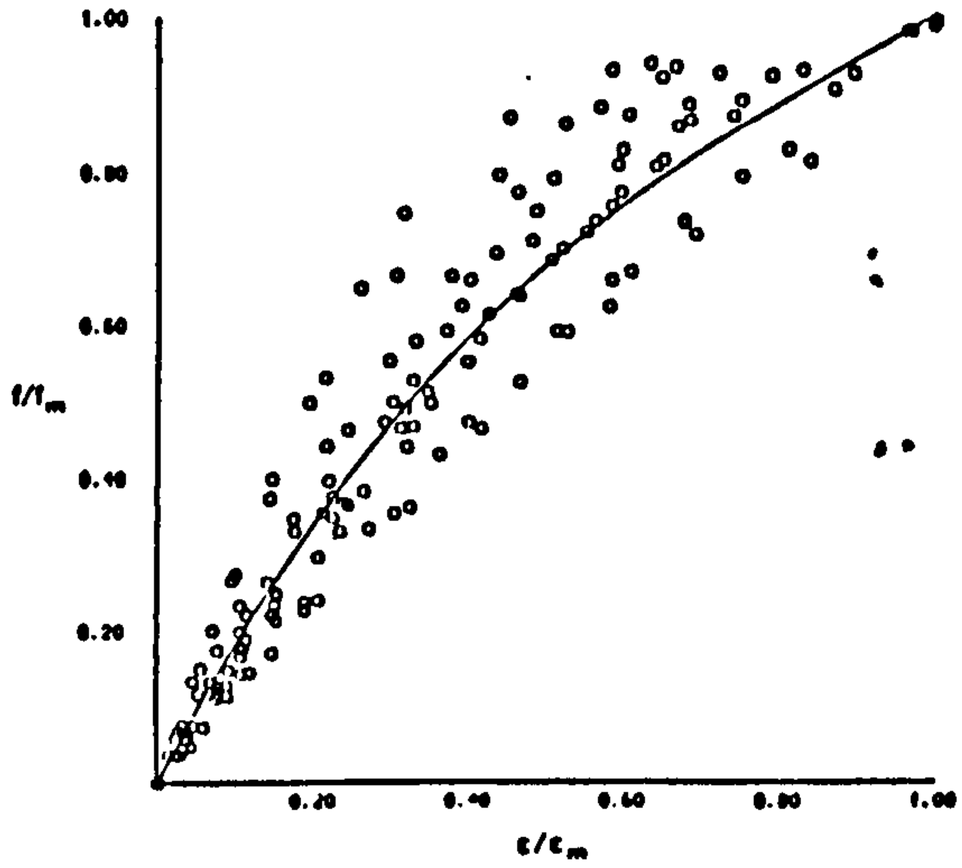

Figure 8. Non-Dimensional Stress/Strain Relationship, Prism Series D

In some prisms, the spalling of brickwork on heavily stressed side led to the reduction of the cross sectional area, which resulted in the line of action of the load acting outside the 'Kern' ($t/6$) causing tension in opposite face thus inducing flexural cracking and failure of brickwork (Fig 13).

In case of prisms built with Grade II mortar, the spalling of mortar on the heavily loaded face commenced at approximately 75% of the failure load. With increasing load, the flexural cracking reduces the cross-sectional area, thus further causing crushing and spalling of brick-work on the loaded face. As a result, a very high apparent strain (ε_{me} = 0.00694) was recorded.

The magnitude of ultimate strain for prism series A and B were equal under both axial and eccentric loading. For prism C the ultimate strain under eccentric loading was 37% lower than for the axially loaded case. Unlike prism series AE and BE, where splitting occurred prior to failure, cracking of the brickwork in the prisms of low strength was at failure. The mathematical prediction of ε_{me} was underestimated in this case.

STRESS DISTRIBUTION PRIOR TO AND AT ULTIMATE LOAD

Using the experimentally derived stress/strain relationship for the axially loaded brickwork prisms and from the experimental strain gradient, the compressive stress distributions at ultimate and before (55% of ultimate) for eccentrically loaded prisms were obtained (Table 5 and Figs 14-16). The stress blocks (Figs 14-16) represent the best least-square fit for the result of each prism series. There appears to be very good agreement between experimental and calculated load both prior to and at ultimate load for all prisms, but for the low strength brickwork at ultimate. This is due to under-tensile region of the series AE and BE prisms have been ignored at ultimate because of the small width (less than 5mm) over which tensile strain developed. The failure load will be overestimated by 0.2% due to this.

Earlier researchers (3) have concluded that the maximum compressive strength of eccentrically loaded brickwork is 10-20% higher compared to axially loaded prism. This apparent increase in maximum stress has been calculated from the experimental failure load assuming rectangular or

parabolic stress blocks. From Tables 2 and 3 it is clear that the maximum compressive stress developed in the eccentrically loaded prism is equal to the ultimate strength (f_m) derived under axial loading. Therefore, 10-20% increase proposed in stress may be attributed to the inaccuracy in the assumption rather than real increase in the failure stress.

From the stress block for the Grade II mortar, eccentrically loaded prism (Fig 16) it is clear that at failure only 80% of the section is resisting the compressive load. Crushing of the brickwork has reduced the overall effective width of the section and thereby changing the eccentricity.

By taking moments about the line of action of the load (centre of gravity of the stress block) it was possible to determine the width of the cross-section that had crushed, 5mm, the effective width of the section 210mm, and therefore the eccentricity of the applied load, $^{e}/_{t} = {}^{1}/_{5.1}$.

COMPARISON OF EXPERIMENTAL RESULTS WITH OTHER TEST RESULTS AND WITH BS 5628

In Figure 17 the reduction in capacity of eccentrically loaded prisms in terms of axial load has been plotted for various eccentricity ratios ($e/_t$) using the stress block derived experimentally.

Although the present test was limited to $^{t}/_{6}$, the capacity reduction was obtained from the non-linear stress block neglecting the portion of the prism in tension for other eccentricities which agrees well with the results of other investigators (1,2,8).

The results of this and all other investigations were compared in Figure 17 with BS 5628 and it appears that the Code overestimates the value of capacity reduction factor thus allowing higher load for eccentrically loaded prisms than obtained in the experiments. BS 5628 assumes that for $^{e}/_{t}$ = 0 to 0.05 the capacity reduction factor remains unchanged, which means that the failure load for axially and eccentrically loaded prisms of low slenderness ratio (up to 8) will be unaffected by eccentricity. A rectangular stress block with a constant stress of $1.1f_k$ under ultimate load condition has been assumed giving the value of capacity reduction factor as:

$$\beta = 1.1\ [1-2^{e}{}_{m}/_{t}] \qquad (2)$$

The above equation represents a straight line (Fig 17) giving a value of 1.1 at zero eccentricity and zero at $^{e}/_{t} = \frac{1}{2}$. From Fig 17 it appears that there is no justification for using the factor 1.1. However, the stress blocks shown in Figs 14 and 16 can be replaced by a simplified equivalent rectangular stress block

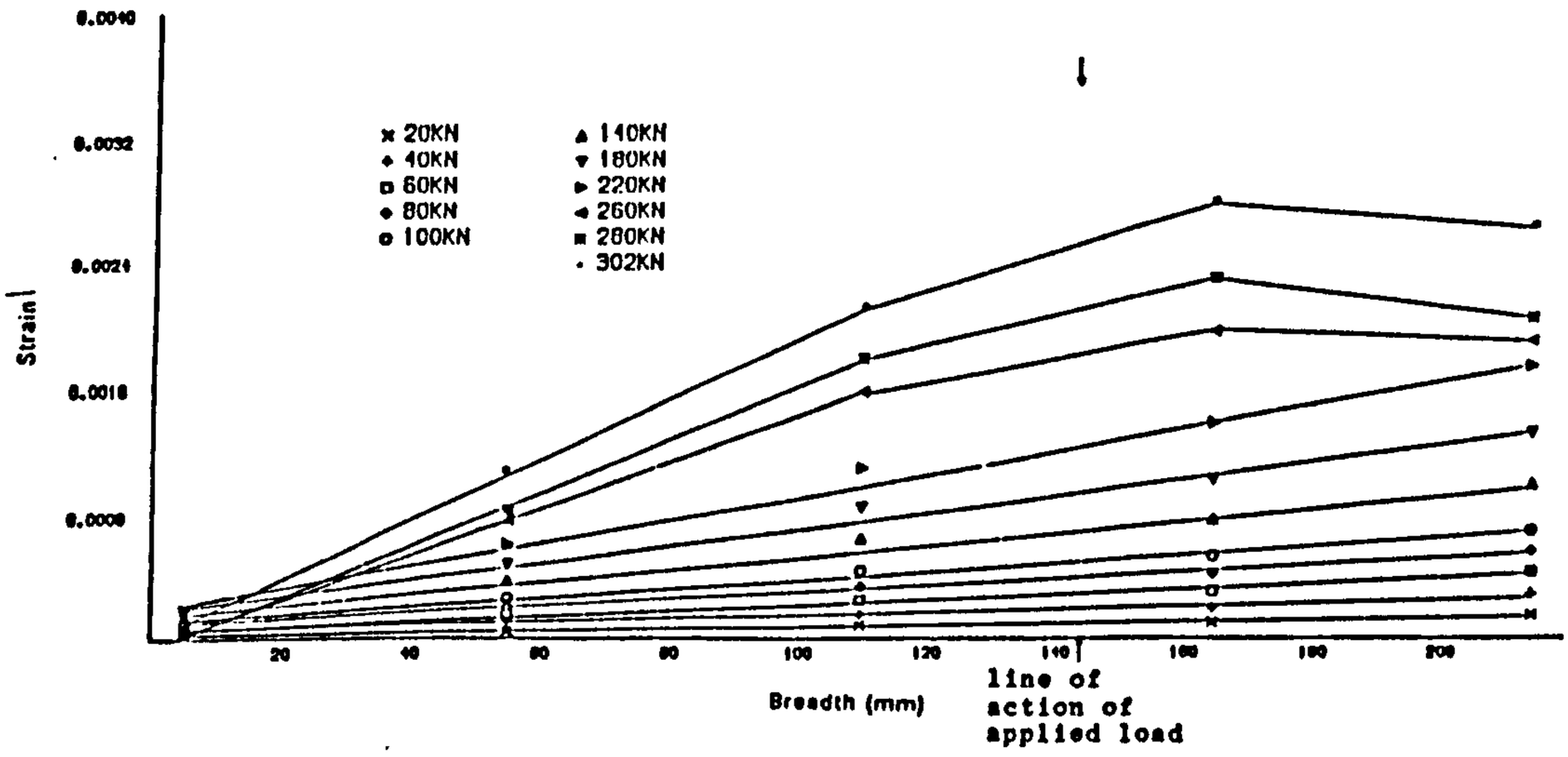

Figure 9. Typical Strain Distribution for Prism Series AE

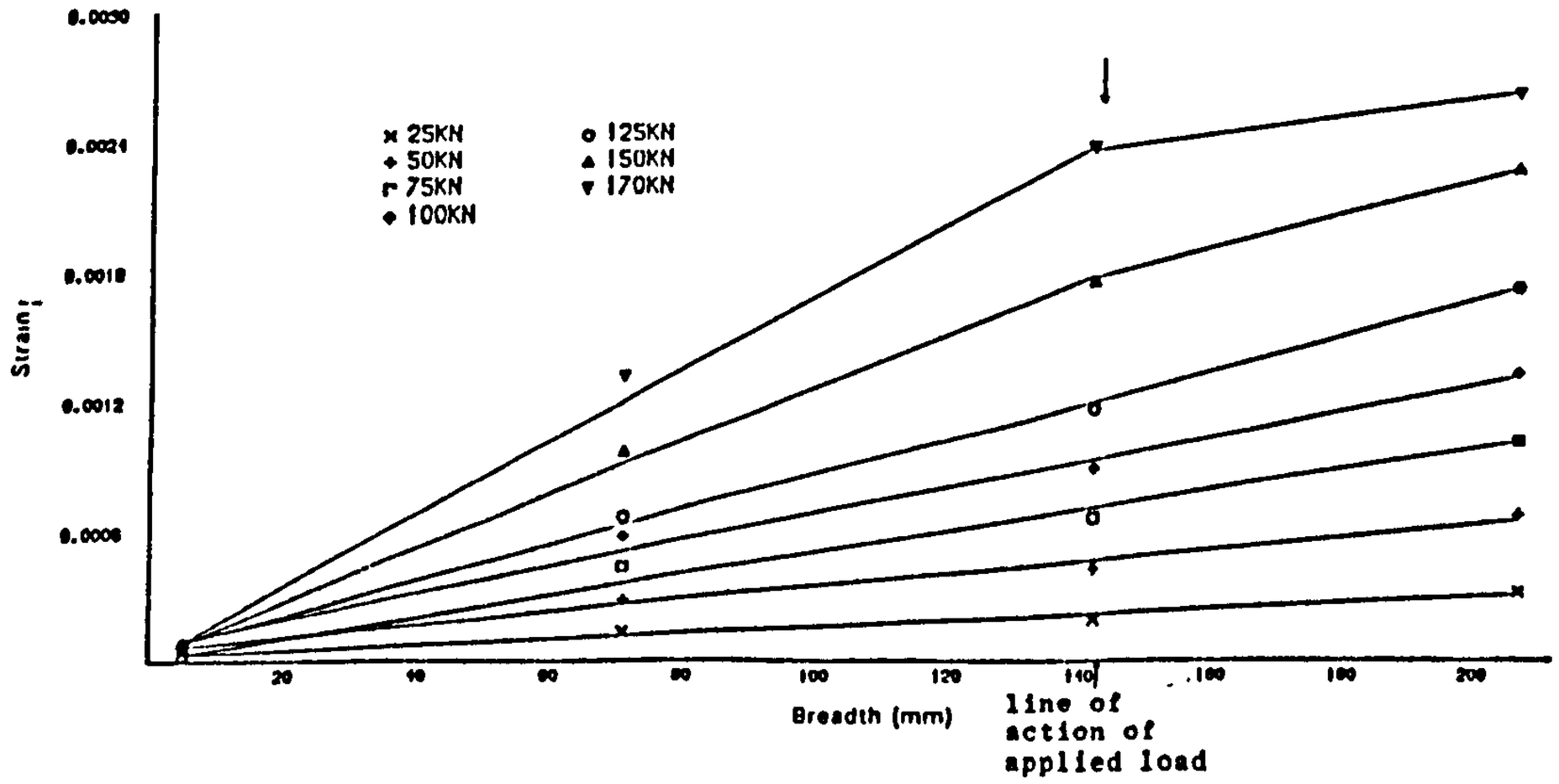

Figure 10. Typical Strain Distribution for Prism Series BE

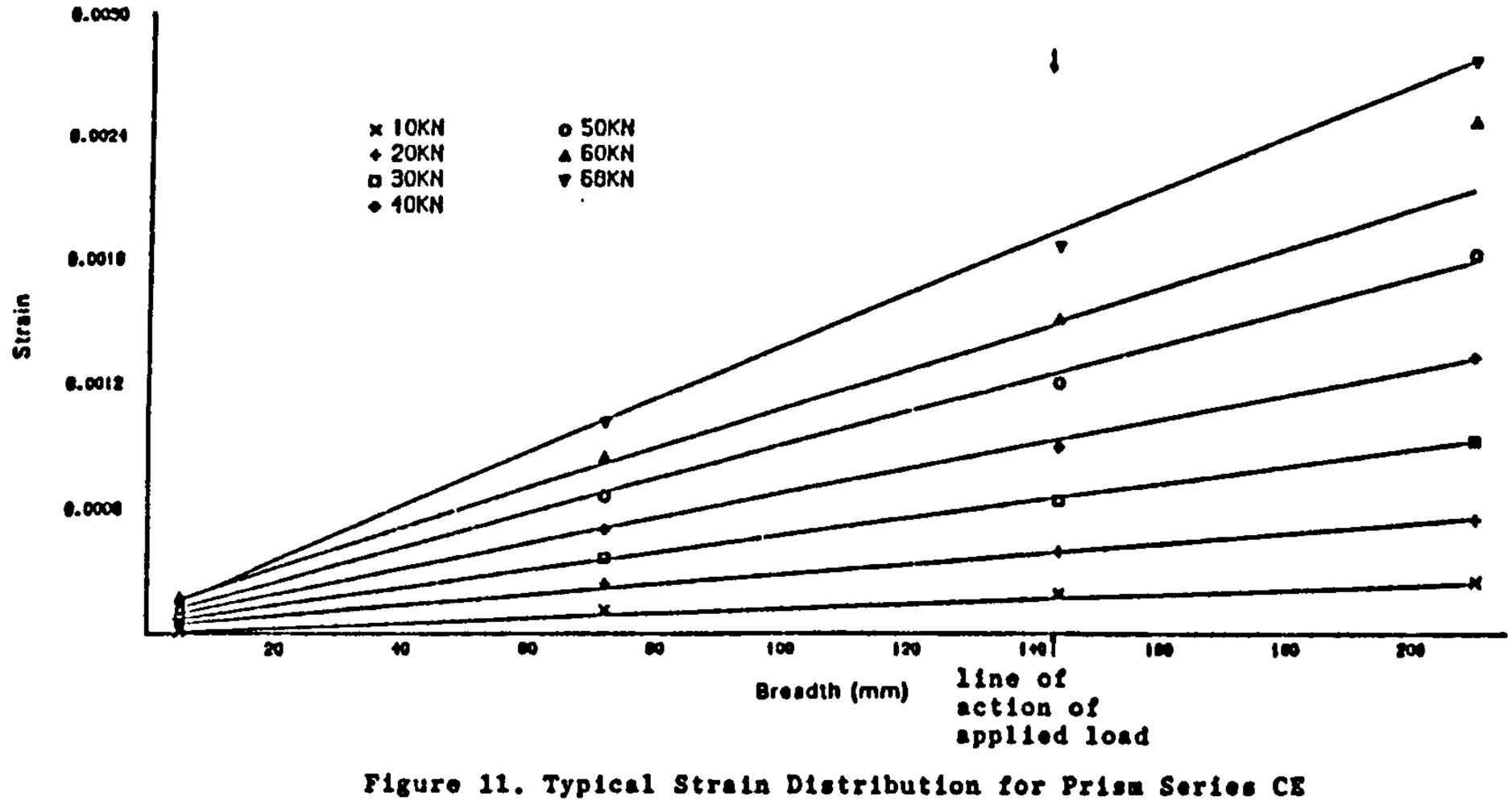

Figure 11. Typical Strain Distribution for Prism Series CE

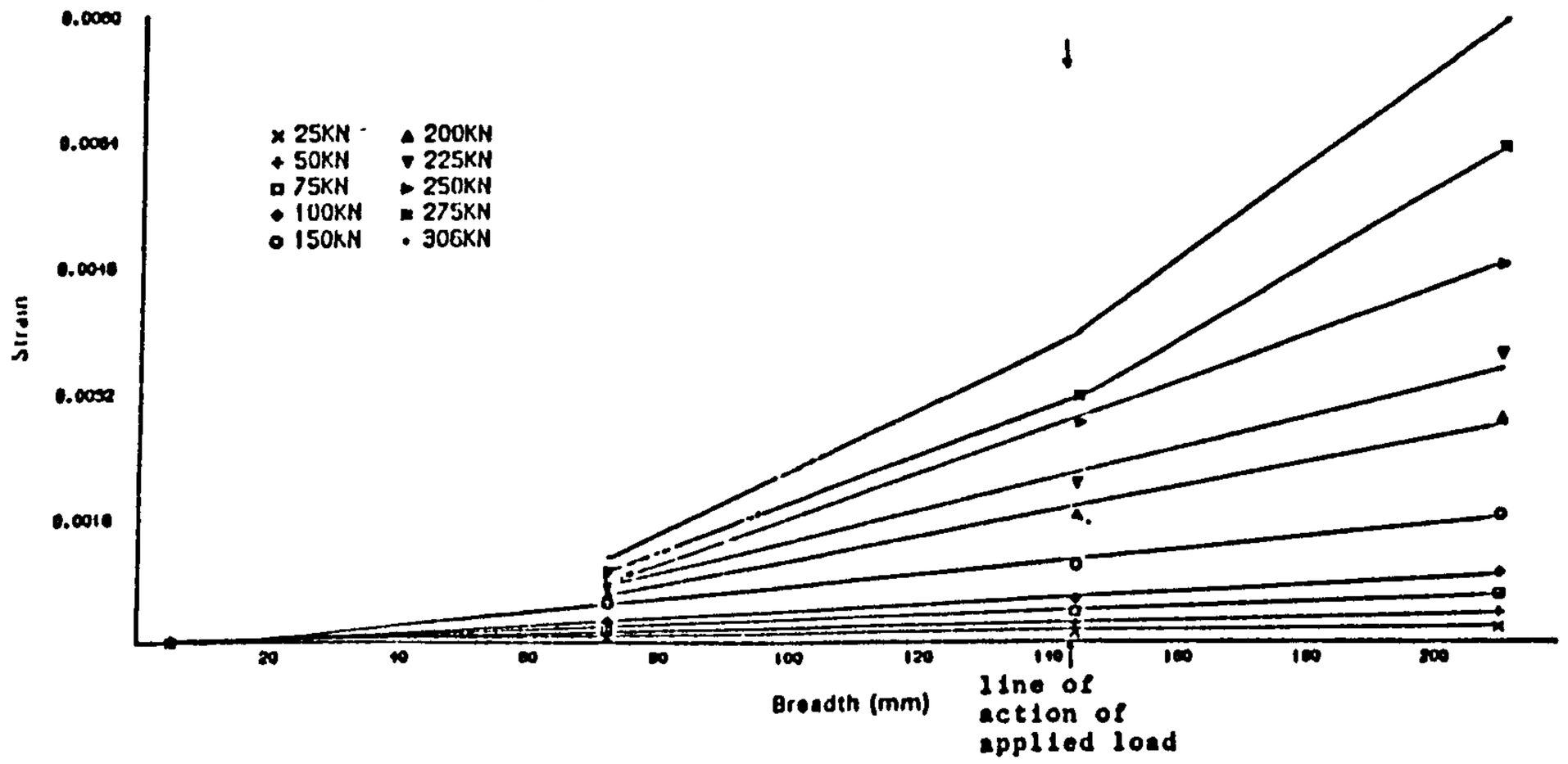

Figure 12. Typical Strain Distribution for Prism Series DC

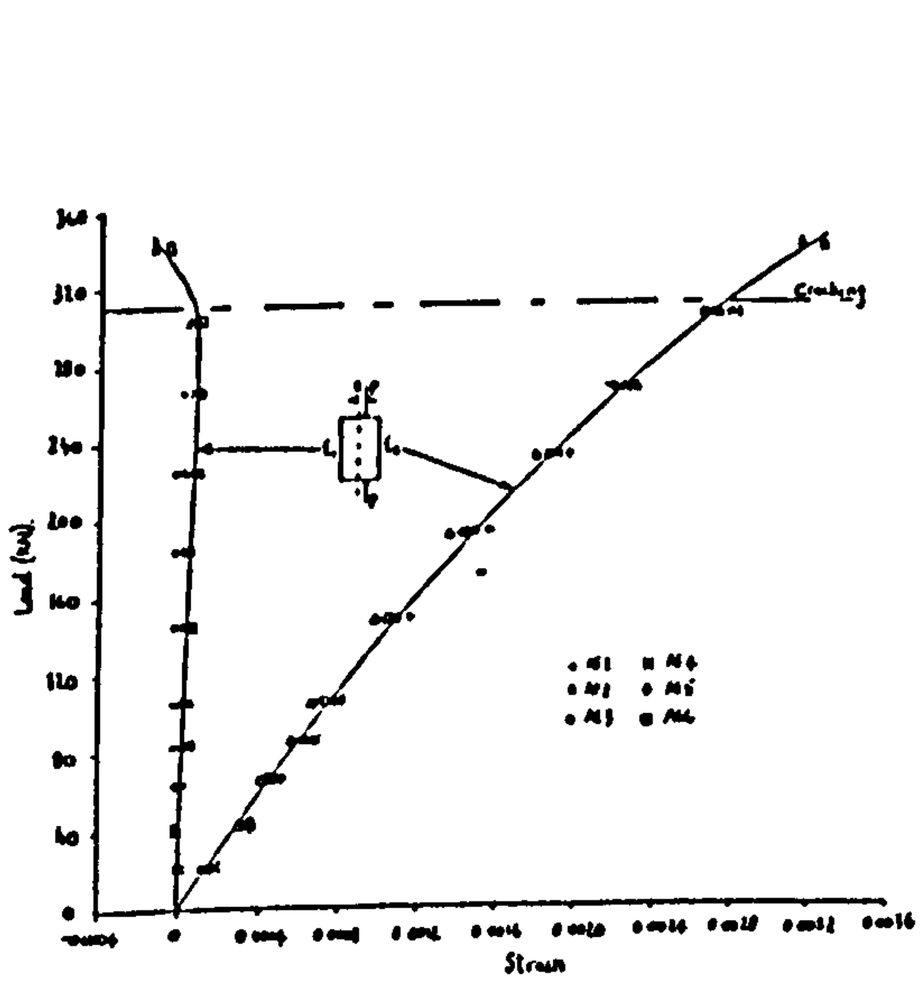

Figure 13. Typical Load-strain Relationships for Eccentrically Loaded Prism

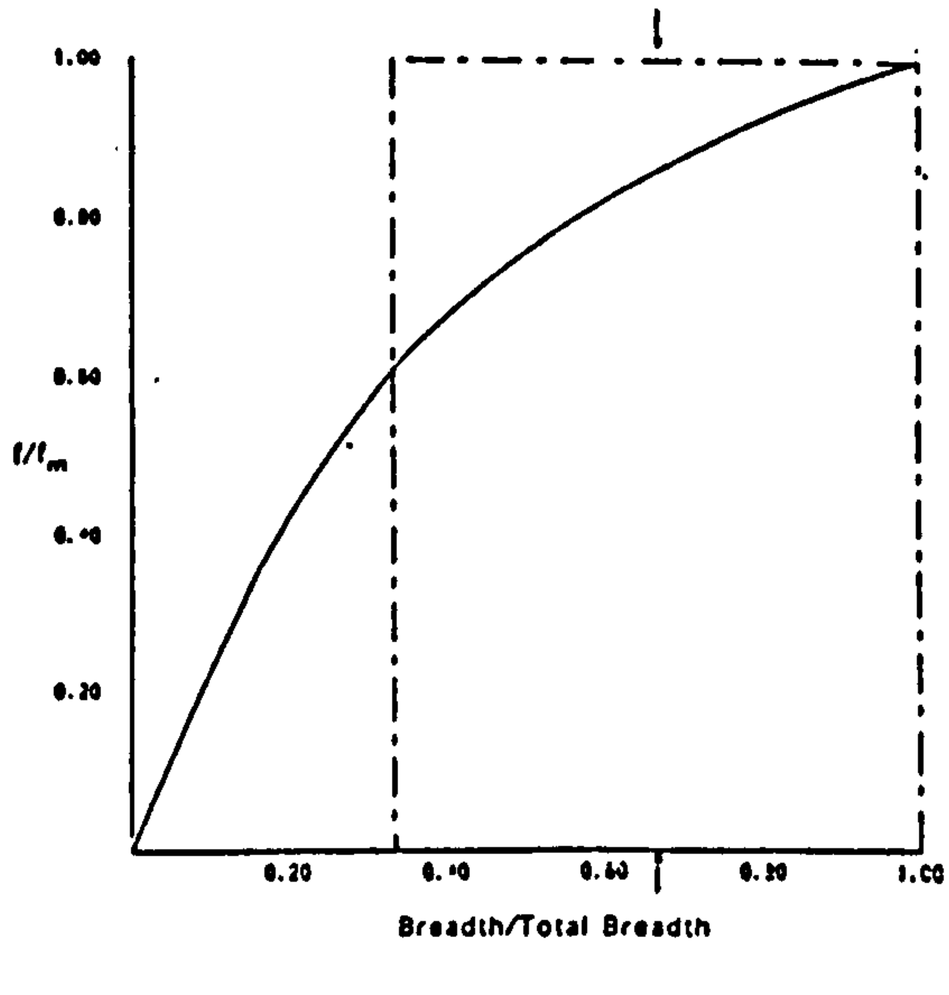

Figure 14. Average Stress Block at Failure for Prism Series AE and BE

with a constant value of ultimate compressive strength which gives the values of:

$$\beta = 1 \times [1-2^{e}/_{t}] \qquad (3)$$

The result of this modification is shown in Fig 17. A very good correlation is obtained between the experimental results and the proposed modification. This modification gives the same linear relationship between capacity reduction factor and $^{e}/_{t}$, which was obtained by stress block obtained from strain gradient.

CONCLUSIONS

1. The load carrying capacity or stress prior to or at ultimate for eccentrically loaded brickwork prisms can be predicted by assuming a linear strain distribution along the width of the section; and by using the actual non-linear stress-strain relationship obtained under axial loading.

2. The maximum stress developed at the time of failure of eccentrically loaded brickwork prisms stressed in directions other than normal to the bed-joint and built with different grades of mortar and brick strength appears to be the same as the ultimate stress in axial compression

3. The British Standard Code of Practice (BS 5628) overestimates the capacity reduction factor due to the use of a rectangular stress block with constant stress multiplied by a factor of 1.1. Although the shape of the actual stress block is different, the simplified rectangular stress block may be used for design provided that the multiplication factor for stress is modified to unity as proposed in this paper.

REFERENCES

[1] Maurenbrecher, A.H.P., "Compressive strength of eccentrically loaded masonry prisms", 3rd Canadian Masonry Symposium, Edmonton, 1983.

[2] Drysdale, R.C. and Hamid, A.A., "Effect of eccentricity of the compressive strenght of brickwork", Proc. British Ceramic Society, No. 30, Sept., 1982, pp. 140-148.

[3] Tunnsek, V and Cacovic, F., "Some experimental results on the strength of brick masonry walls", SIMBAC, pp. 149-156.

[4] Haller P., "Load capacity of brick masonry", Designing Engineering and Construction with Masonry Products, Gulf Publishing Co., Texas, 1969, pp. 129-149.

[5] British Standard Institution, BS 5628, "Code of Practice for Use of Masonry, Part 1, Structural use of unreinforced masonry", 1978, London.

[6] BSI, "Clay Bricks and Blocks",1974, London.

[7] Pedreschi,R.F. and Sinha, B.P., "Compressive strength and some elastic properties of brickwork, Int. Journal of Masonry Construction, Vol. 3, No. 1, 1983, pp. 19-25

[8] Fattel, S.G. and Catteneo, L.E. "Structural performance of masonry walls under compression and flexure", National Bureau of Washinton, Building Science Series 73, 1976.

NOTATION

e	eccentricity of applied load
f	compressive stress
f_m	axial compressive strength of brickwork
f_{me}	eccentric compressive strenght of brickwork
P	compressive load
P_o	axial compressive load at failure
P_e	eccentric compressive load at failure
t	width of brickwork section
t'	width in compression for loading outside Kern
X_1, X_2, X_3	coefficients of stress/strain relationship
ε	compressive strain
ε_m	axial ult. compressive strain
ε_{me}	eccentric ult. compressive strain
ε_1	maximum compressive strain in eccentrically loaded brickwork at loading P
ε_2	minimum compressive or maximum tensile strain in eccentrically loaded brickwork at loading P

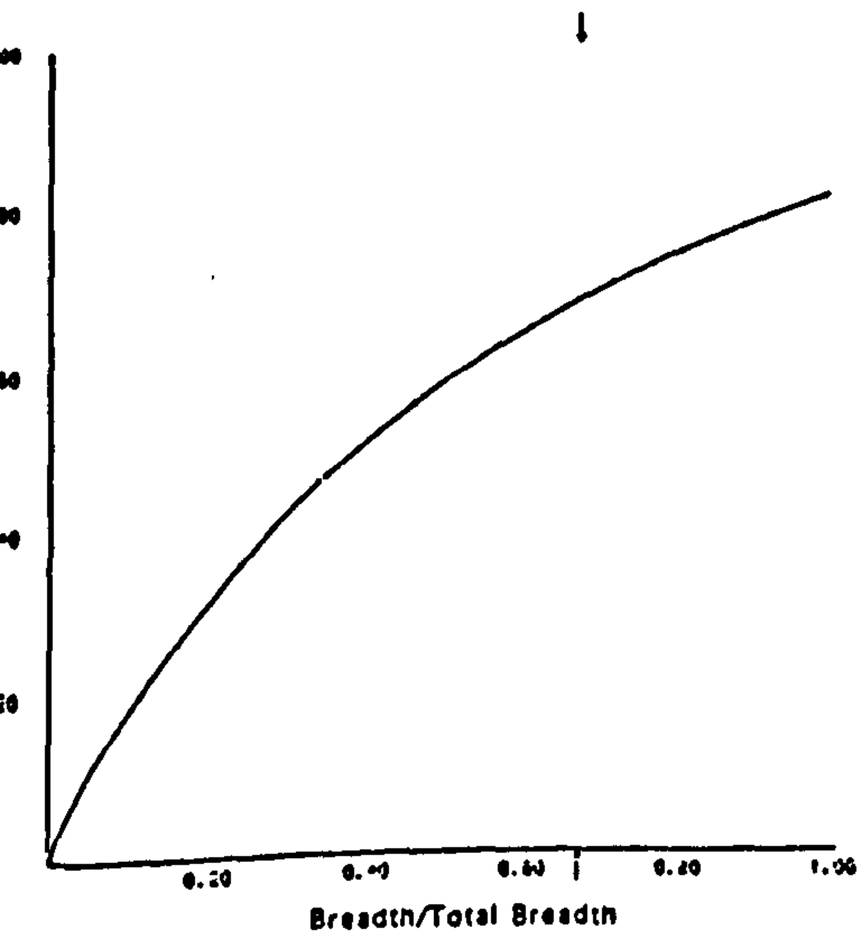

Figure 15. Stress Block at Failure for Prism Series CE

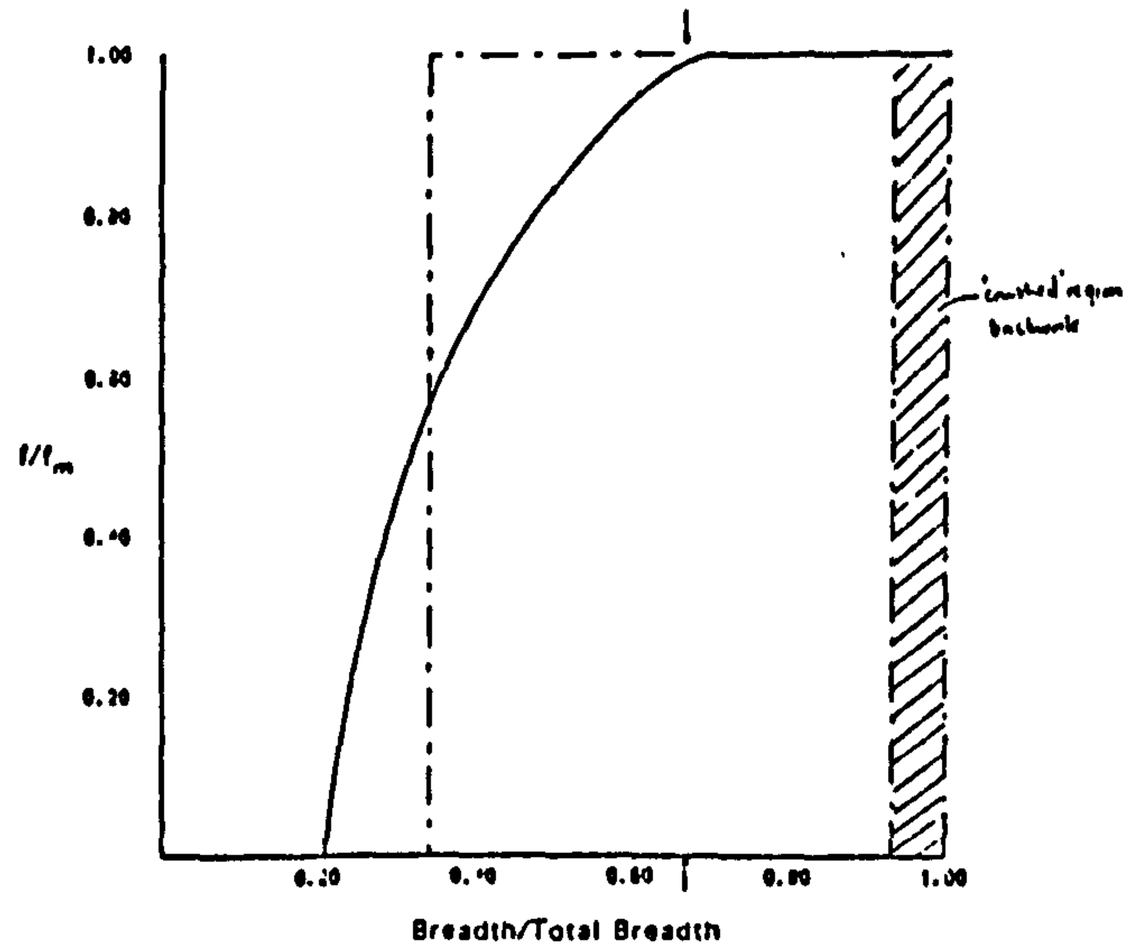

Figure 16. Stress Block at Failure for Prism Series DE

Table 1 Properties of Bricks

Brick Type	Compressive Strength			Absorption
	Loading Duration	Average (N/mm²)	Coeff. Var. %	% by wt. (5hr.)
High	Bed	96.58	11.8	4.40
	Edge	53.52	10.1	
Medium	Bed	72.25	13.8	8.77
	Edge	23.51	11.3	
Low	Bed	19.69	15.1	26.34
	Edge	7.05	24.7	

TABLE 2

Results of Axially Loaded Prism Tests

Brick Strength N/mm²	Prism No.	Mortar Str. N/mm²	Ult. Load P_o kN	Compr. Str. f_m N/mm2	Ult Strain ϵ_m
19.7	C1	19.9	87.5	6.17	0.00411
	C2	17.5	101	7.12	0.00651
	C3	19.9	105	7.38	0.00492
	C4	17.2	88	6.21	0.00429
	C5	25.2	97	6.86	0.00481
	C6	19.5	105	7.40	0.00482
	C7	19.5	125	8.81	0.00574
	C8	20.5	117	8.23	0.00273
	C9	20.5	103	7.26	0.00493
Average		20.0	103	7.27	0.00476
Coeff. of Variation		11.5%		11.8%	22.1%
96.6	D1	7.3	472	33.18	0.00306
	D2	8.6	427	30.02	0.00211
	D3	6.6	283	19.90	0.00225
	D4	7.8	450	31.61	0.00294
	D5	7.8	439	30.77	0.00218
	D6	7.8	420	29.50	0.00236
	D7	7.8	405	28.45	0.00288
	D8	7.8	450	31.61	0.00383
	D9	7.8	400	28.10	0.00470
	D10	7.5	405	28.48	0.00320
	D11	7.5	431	30.27	0.00301
	D12	7.5	380	26.73	0.00328
	D13	7.5	382	26.83	0.00470
	D14	7.5	438	30.77	0.00380
	D15	7.5	428	30.05	0.00328
Average		7.6	417	29.31	0.00318
Coeff. of Variation		5.5%		10.5%	25.4%

Brick Strength N/mm²	Prism No.	Mortar Str. N/mm²	Ult. Load P_o kN	Compr. Str. f_m N/mm2	Ult Strain ϵ_m
96.6	A1	27.8	427	30.02	0.00313
	A2	16.9	412	28.97	0.00373
	A3	19.8	453	31.83	0.00370
	A4	16.3	427	29.86	0.00315
	A5	19.5	406	28.49	0.00384
	A6	17.9	500	35.12	0.00327
	A7	20.1	403	28.32	0.00472
	A8	19.2	597	41.90	0.00376
	A9	19.9	674	47.31	0,00314
	A10	16.4	636	44.67	0.00347
	A11	19.1	377	26.48	0.00314
	A12	16.1	500	35.14	0.00410
	A13	21.4	452	31.76	0.00380
	A14	21.4	487	34.19	0.00250
	A15	19.0	467	32.78	-
	A16	19.0	550	38.62	0.00365
	A17	19.0	515	36.18	0.00340
	A18	19.3	351	24.67	0.00379
	A19	19.3	392	27.51	0.00396
	A20	19.3	516	36.23	0.00340
Average		19.3	477	33.50	0.00356
Coeff.of Variation		12.9%		18.1%	13.3%
72.3	B1	19.1	274	19.91	0.00260
	B2	19.6	344	24.99	0.00280
	B3	21.3	217	15.77	0.00310
	B4	18.9	289	21.01	0.00308
	B5	20.5	259	18.78	0.00330
	B6	20.5	239	17.33	0.00262
Average		19.9	271	19.63	0.00292
Coeff.of Variation		4.7%		16.4%	9.8%

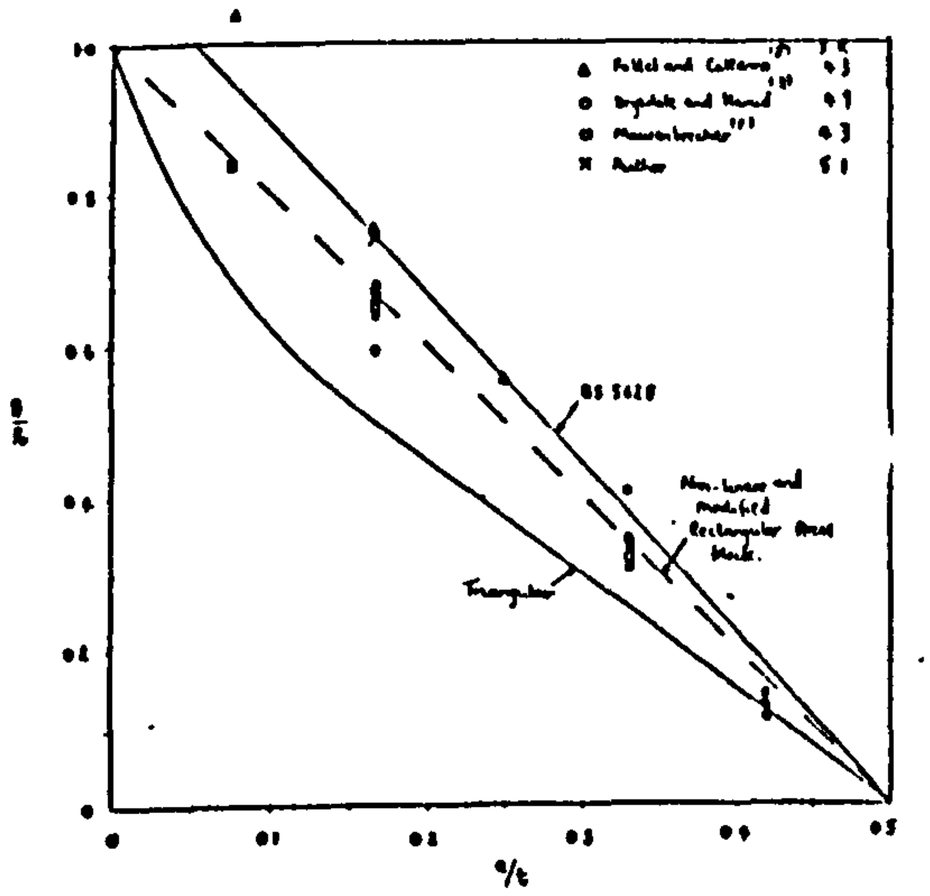

Figure 17. Effect of Eccentricity on Ultimate Load Capacity of Brickwork Prisms

TABLE 3

Results of Eccentrically Loaded Prism Tests

Brick Strength N/mm²	Prism No.	Mortar Strength N/mm²	Ult. Load P_e kN	Ult. Strain ε_{ae}	Compr. Strength f_{ae} N/mm²
96.6	AE1	19.3	294	0.00412	33.50
	AE2		302	0.00284	28.29
	AE3		318	0.00339	32.86
	AE4		336	0.00304	30.79
	AE5		376	0.00283	33.50
	AE6		309	0.00351	33.50
Average Coeff. of Variation			323 9.4%	0.00342 15.8%	32.58
72.3	BE1	20.5	195	0.00272	19.19
	BE2		174	0.00324	19.83
	BE3		190	0.00253	18.64
	BE4		208	0.00288	19.63
	BE5		170	0.00268	18.92
	BE6		170	0.00263	18.83
Average Coeff. of Variation			181 7.8%	0.00294 17.7%	19.83
19.7	CE1	20.5	85.5	0.00364	8.23
	CE2		68.5	0.00231	5.34
	CE3		77.0	0.00256	5.55
	CE4		88.5	0.00316	5.94
	CE5		68.0	0.00279	5.71
	CE6		80.0	0.00362	6.21
Average Coeff. of Variation			78.0 10.9%	0.00301 18.3%	5.83 8.2%
96.6	DE1	7.5	276	0.00695	29.31
	DE2		296	0.00660	29.31
	DE3		273	0.00685	29.31
	DE4		306	0.00820	29.31
	DE5		276	0.00661	29.31
	DE6		269	0.00540	29.31
Average Coeff. of Variation			293 5.2%	0.00694 9.4%	29.31

Table 4 Properties of Stress/Strain Relationships

Brick Type	Mortar Grade	X_1	X_2	X_3
High	1:1/4:3	1.958	1.596	0.636
Medium	1:1/4:3	2.094	1.556	0.466
Low	1:1/4:3	2.868	3.665	1.804
High	1:½:4½	2.005	1.566	0.565

Table 5 Comparison of Experimental and Predicted Loading of Eccentrically Loaded Prisms

Prism Type	Ultimate Load			0.55 x Ultimate Load	
	Expt. Load (kN)	Non-Linear Stress Block(kN)	BS 5628 (kN)	Expt. Load (kN)	Non-Linear Stress Block(kN)
AE	323	308	343	180	175.4
BE	181	194	201	100	103.1
CE	78	58	75	40	37.9
DE	283	295	300	150	165.3

CIB-80

Advancing Building Technology

Proceedings of the 10th Triennial Congress of the International Council for Building Research, Studies and Documentation

Volume 6 of 11

Translating Research into Practice

Performance and Durability of Materia

Building Assemblies/Components

A COMPARATIVE STUDY OF REINFORCED, FULLY AND PARTIALLY PRESTRESSED BRICKWORK BEAMS

P. Walker, B.Sc., & B.P. Sinha, B.Sc., Ph.D., MICE, FIStruct.E., FIE.

Department of Civil Engineering and Building Science
University of Edinburgh
King's Buildings, Edinburgh.

KEYWORDS

Beams, Brickwork, Prestressed, Reinforcement

ABSTRACT

Brickwork is very strong in compression, but very weak in tension. As a result, it cannot be used as a flexural member such as a beam, which carries the load predominantly due to bending; resulting in both tension and compression throughout the section. There are ways of countering this low tensile strength by using reinforcement or by prestressing or by a combination of both as in the case of partial prestressing, so that it can be used economically and effectively as a flexural member. With increasing pressure on finite resources, one has to look for cheaper alternatives to high energy input materials like steel and concrete, which are used, at present, for flexural members. Instead the flexural member built from brickwork may replace them, at least in the housing and public building sectors of both developed and developing countries. The brickwork beam, which does not require formwork nor the degree of sophistication needed for other materials may prove cheaper and viable in such a situation. Therefore, an R & D programme was undertaken to examine the behaviour of of such beams up to failure.

This paper summarises the results of tests on 12 full-scale reinforced prestressed and partially prestressed brickwork beams which were built and tested to study the load-deformation relationship up to failure. The experimental results were compared with the theoretical results. The theoretical results were obtained by using the non-linear properties of brickwork and steel.

Une Etude Comparative des Poutres en Briques Armées, Précontraintes et Partiellement Précontraintes.

P. Walker et B.P. Sinha

Université et d'Edimbourg, Ecosse.

Mots - clés

Poutres, Briques, Précontraintes, Armature.

Sommaire

Le briquetage est très résistant à la compression mais peu résistant à la traction. Par conséquent, on ne peut pas s'en servit comme membre flexible tel qu'une poutre, qui supporte la charge grace siotout a la flexion, ce qui produit á la fois la traction et la compression dans toute la section.

On peut compenser cette faible résistance à la traction en se servant de l'armature ou de la précontrainte ou d'une combinaison des deux, telle que la précontrainte partielle, afin de l'employer de façon économique et efficace comme membre flexible. A une époque où les ressources finies sout de plus en plus recherchées, il faut trouver des matériaux dont la production consomme moins d'énergie que l'acier ou le béton dout on se sert actuellement comme membres flexibles. On pourrait les remplacer par les poutres en briques, au moins dands les secteurs de la construction des logements et des travaux public dans les pays developpés aussi bien que dans les pays en voie de développement. La poutre en brique, qui n'a besoin ni de coffrage ni du degré de sophistication exigé par d'autres matériaux, pourait se révéler moins chere et viable dans cette situation. Donc on a entrepris des travaux de recherche et de développement afin d'examines le comportement de les poutres jusqu'à la defaillance.

Cette communication résume les résultats des expériences effectuées sur 12 poutres en briques de grandeur naturelle armées, préconstraintes et partiellement précontraintes, construites et essayées pour étudier le rapport charge-déformation jusqui'à la défaillance. Les résultats des expériences furent compare's avec les résultats théoriques. On a obtenu les résultats théoriques en se servant des propriétés non-linéaires de la brique et de l'acier .

INTRODUCTION

In many developing countries brickwork is the only indigenous material used for the construction of houses. To span openings reinforced concrete or steel is used. These materials are not only expensive but in short supply in these countries. With an acute housing shortage and constraint upon resources it is essential that cheaper alternatives should be tried. Reinforced or prestressed brickwork beams or slabs may offer a cheaper alternative for spanning openings. While utilising a labour intensive, widely available material, reinforced and prestressed brickwork flexural members do not require the sophisticated techniques involved with other conventional materials. Hence an investigation was undertaken at Edinburgh University to study the comparative behaviour of reinforced, partially and fully prestressed beams subjected to lateral loading.

The techniques of reinforcing[1] or full prestressing[2] have been successfully applied to brickwork beams, however partial prestressing has received little attention. Partial prestressing of a section is achieved by prestressing only part of the tensile reinforcement to a maximum allowable limit and leaving the rest non-tensioned[3]. Reinforced and fully prestressed members where either all of the reinforcement is non-tensioned or all the reinforcement is fully prestressed.

MATERIALS All materials used in the test programme conformed to relevant British Standard.

MORTAR A 1:1/4:3 (Cement:lime:sand) mix by volume was used. 100mm cubes were taken, the average compressive strength of the mortar at 28 days for each beam is given in Table 1.

GROUT For beam series A a grout mix of 1:2 (Cement:Sand) by volume was used. A concrete mix of 1:2½:2 (Cement:sand:pea gravel) was used in beam series B,C and D.

A plasticiser, 'Conbex', was added to the mixes to reduce the effect of shrinkage and shorten the setting time. 100mm cubes were taken during each grouting operation and tested at 7 days. The average compressive strength of the grout for each beam is given in Table 1.

BRICKS 3-hole perforated class B engineering bricks were used. The average compressive strength in the bed-joint direction was 96.6 N/mm^2.

REINFORCEMENT

7 wire stabilised steel strand was used for prestressing, average ultimate stress, f_{pu} = 1700 N/mm^2 and a 0.2% proof stress, f_{py} = 1640 N/mm^2.

High stress deformed bars were used for the non-stressed reinforcement, average ultimate stress, f_{su} = 670 N/mm^2 and a 0.2% proof stress, f_{sy} = 470 N/mm^2.

The experimental stress/strain relationships of the steel were idealised in tri-linear form[4] for use in subsequent theoretical predictions.

BRICKWORK PROPERTIES

COMPRESSIVE STRENGTH AND STRESS/STRAIN RELATIONSHIP

An understanding of the stress/strain characteristics of the brickwork are necessary for accurate predictions of the behaviour of brickwork beams. The ultimate compressive strength and stress/strain properties of brickwork were obtained from the prism illustrated in fig.1, which represents the top course (compression zone) of the brickwork beam section.

Twenty prisms were loaded in uniaxial compression and measurements of strain were taken at increments of loading up to failure using a 'demec' gauge. The average compressive strenght (f_m) was 33.5N/mm² and the ultimate strain(ε_m) was 0.00356.

The experimental stress/strain relationships were mathematically idealised in the form of a third degree polynomial, such that:

$$f/f_m = x_1(\varepsilon/\varepsilon_m) - x_2(\varepsilon/\varepsilon_m)^2 + x_3(\varepsilon/\varepsilon_m)^3 \qquad (1)$$

where $x_1 = 1.96$, $x_2 = 1.60$ and $x_3 = 0.64$

The stress block factors, $\lambda_1 = 0.61$ and $\lambda_2 = 0.37$ are given by:

$$\lambda_1 = \int_0^1 [x_1(\varepsilon/\varepsilon_m) - x_2(\varepsilon/\varepsilon_m)^2 + x_3(\varepsilon/\varepsilon_m)^3]\, d(\varepsilon/\varepsilon_m) \qquad (2)$$

$$\lambda_2 = 1 - \frac{\int_0^1 [(\varepsilon/\varepsilon_m)\{x_1(\varepsilon/\varepsilon_m) - x_2(\varepsilon/\varepsilon_m)^2 + x_3(\varepsilon/\varepsilon_m)^3\}]\, d(\varepsilon/\varepsilon_m)}{\lambda_1} \qquad (3)$$

CONSTRUCTION OF THE BEAMS AND TESTING PROCEDURE

The section used for the reinforced and partially prestressed brickwork beams is shown in fig.1. The section used for the fully prestressed[2] brickwork beams and the development of these sections are dealt with elsewhere[4,5].

All test beams were built 'upside down' on the floor of the laboratory by an experienced bricklayer. They were allowed to cure for 21 days before pre-stressing. The tendon and non-stressed reinforcement were placed in the cavity and 25mm thick mild steel plates were attached to the ends of the beams. The tendons were stressed to 70% of their ultimate strength, after stressing the cavity was grouted. For the reinforced beams the cavity was grouted at 21 days. The beams were cured for a further 7 days prior to testing. All beams were designed for approximately the same ultimate moment.

The beams were tested in a two point loading rig (fig.2) which provided a pin and roller support (simply supported) over a span of 6.2m. Loading was

applied by hydraulic jacks and measured using load cells connected to a digital volt meter and pen chart recorder. The load was applied incrementally up to failure. At each loading brickwork strains in the constant moment zone at various depths were recorded using a 'demec' gauge. Steel strains were measured using electrical resistance strain gauges. Central deflection was measured with a dial gauge reading to 0.01mm.

EXPERIMENTAL RESULTS AND DISCUSSION

MODE OF FAILURE

Both the fully and partially prestressed brickwork beams exhibited typical flexural failures characteristic of an under-reinforced section, yielding of the tensile reinforcement leading to crushing of the brickwork in compression (fig.3). In the partially prestressed brickwork beams yielding of the non-tensioned reinforcement occurred at a moment equal to 75% of the ultimate, the prestressing steel yielded at approximately 90% of the ultimate moment. The maximum strain in both types of reinforcement at failure was approximately 2%. The tensioned steel in the fully prestressed beams (series A) reached its proof stress at 95% of the failure moment.

The maximum steel strain in the reinforced brickwork beam (series D) at failure was 1%, indicating that the steel had yielded even though failure was due to secondary shear. Inclined flexural cracks in the shear span propagated along the brick/mortar interface to the loading point, eventual failure occurred suddenly without warning (fig.4). Therefore by prestressing flexural cracking is delayed and hence the effective shear resistance of the section is increased and secondary shear failure is avoided.

CRACKING AND ULTIMATE MOMENT

CRACKING MOMENT

As soon as the extreme tensile fibre stress exceeded the flexural strength of the brickwork, visible cracking appeared in the reinforced brickwork beams, and the initial cracks penetrated to a height of 150-200mm. The average cracking moment was 9.3kNm (Table 1). Prestressing enhanced the performance of the beams by raising the threshold of the cracking moment, first cracking appeared in the fully prestressed beams at an average moment of 26kNm (Table 1), an increase of 280%. The cracking moment of the partially prestressed beams ranged between 13.7 and 17.4kNm depending upon the level of pre-compression, an increase of 147% and 187% in comparison with the reinforced brickwork beams. The initial crack height in all the prestressed members was approximately 100mm. Therefore, the onset and initial height of flexural cracks in brickwork beams can be controlled by prestressing.

ULTIMATE MOMENT

All beams were designed as under-reinforced and to fail at a similar ultimate moment. The experimental results are presented in Table 1. Although, all beams were designed for similar ultimate moment the reinforced brickwork beams exhibited a decrease in failure moment of up to 10% due to the premature secondary shear failure. By delaying flexural cracking and thereby increasing the effective shear resistance of the section the full flexural capacity was realised in the prestressed brickwork beams.

The test results are compared in Table 1 with a theoretical approach which

utilises the actual stress/strain relationships of the materials, developed and described in detail elsewhere(2). For the fully and partially prestressed brickwork beams the theory generally underpredicts the ultimate moment although this difference is less than 10%. The theoretical prediction of the ultimate moment for the reinforced brickwork beams overestimates in comparison with the test result due to the secondary shear failure, even though the stress in the reinforcement had exceeded the proof stress. The calculation of ultimate moment assumes that the maximum compressive strain in the brickwork at failure is equal to 0.356%, compressive stress 33.5N/mm², whereas the maximum compressive strain measured at failure was only 0.28%, compressive stress equal to 28.9kN/mm². Once the reinforcement has yielded there is little increase in stress with strain, and so in order to balance a tensile force similar to that at failure at a stress of only 28.9N/mm² the depth of the compression zone will be greater than at ultimate, thereby reducing the lever arm and hence the ultimate moment.

MOMENT-CURVATURE AND LOAD-DEFLECTION

The experimental results for average moment-curvature and load-deflection are presented in figs. 5 & 6 respectively. The experimental curvatures were obtained from the brickwork strain readings taken in the constant moment zone, curvature equal to the slope of the strain profile at each loading.

Also in figs. 5 & 6 the experimental points are compared with theoretical relationships for moment-curvature and load-deflection. The method used was developed by Pedreschi(2) to predict the moment-curvature and load-deflection relationships of fully prestressed brickwork beams. It utilised the experimental idealised stress/strain relationship(4) for the prestressing and reinforcing steels. Although the theory was developed for fully prestressed beams there is excellent agreement with the predicted and experimental values for all test beams, and therefore is equally applicable to either reinforced, fully prestressed or partially prestressed brickwork beams.

In fig.5 there is an initial negative curvature caused by the prestress, the higher the prestress the larger the curvature. Upon loading the moment-curvature relationship has three distinct phases:

(i) linear up to cracking
(ii) cracking up to yielding of the steel, and
(iii) post-yield phase where it eventually becomes parallel to x-axis

The load-deflection curves (fig.6) show similar characteristics to the moment-curvature relationships. Unlike the moment-curvature relationships the load-deflection curves all start from the origin since it was not possible to measure the deflection due to self weight and so the load-deflection corresponds to applied loading.

The deformation of the partially prestressed brickwork beams lies between the boundaries represented by the fully prestressed and reinforced brickwork beams (figs.5,6). Prior to cracking the slope of the moment-curvature and load-deflection relationships for each type of beam was equal. With increasing loading each beam cracks and so the deflection at any particular loading will be greatest in the beams with the least prestress. For example at a bending moment of 26kNm the deflection due to applied load for beam series A,B,C and D was 4.5, 12.5, 14.0 and 17.0mm respectively. By prestressing the deflection has

been reduced by 74% for beam series A, 26% for series B and 18% for series C in comparison with the reinforced brickwork beams. The rate of increase in deformation with further loading was less for the beams with the largest areas of non-tensioned reinforcement, due to the extra stiffness of the section resulting from the non-tensioned steel. Therefore by appropriate selection of the level of prestress the deflection of any brickwork beam may be controlled to within the limits defined by the reinforced and fully prestressed beams.

The average moment and deflection for each beam type at a measured maximum crack width of 0.2mm is given in Table 1. By prestressing, the deflection in comparison with the reinforced brickwork beams has been reduced by 26% in the fully prestressed beam and by between 6% and 10% in the partially prestressed beams. Conversely the moment has increased by up to a factor of 2, from 14.3kNm to 29.0kNm, depending upon the level of prestress. The deflection of all four types of beam satisfies the serviceability limit state of deflection of span/250[6] (24.8mm) and hence for design the limit state of cracking becomes the controlling factor. The factor of safety, ratio of ultimate moment to the moment at a maximum of crack width is 0.2mm, for the reinforced brickwork beam is 3.55. For the fully prestressed and the partially prestressed beams the factor of safety is 1.82, 2.49 for series B and 3.33 for series C respectively. Although the safety factor is adequate for all beams the prestressed brickwork beams provide the most economical use of the materials by raising the magnitude of the moment at the serviceability limit state and therefore keeping the factor of safety to a minimum.

SUMMARY AND CONCLUSION

(i) Prestressing increases the cracking moment of a brickwork beam, hence cracking can be avoided under service loading by suitably prestressing the section.

(ii) All test beams were under-reinforced and designed to reach same ultimate moment, but the reinforced beams primarily failed due to yielding of steel leading to secondary shear failure. This resulted in 10% reduction in the ultimate moment compared to the fully and partially prestressed beams. Thus prestressing enhances the effective shear capacity of the beam.

(iii) The ultimate moment, moment-curvature and load-deflection relationships of reinforced, fully and partially prestressed brickwork beams can be accurately predicted using the experimentally idealised stress/strain relationships for the brickwork, prestressing and reinforcing steels.

(iv) The deflection of a brickwork beam can be controlled to within the limits defined by the fully prestressed and reinforced brickwork beams by appropriate selection of the level of the prestress. The deflection is least in the fully prestressed brickwork beam and greatest in the reinforced brickwork beam for all loads up to failure.

REFERENCES

1. Sinha, B.P., "An ultimate load-analysis of reinforced flexural members", International Journal of Masonry Construction, 1, No. 4, 1981, pp 151-156.

2. Pedreschi, R.F., "A study of the behaviour of post-tensioned brickwork beams", Ph.D. Thesis, Dept. of Civil Engineering and Building Science, University of Edinburgh, 1983.

3. The Concrete Society, "Partial Prestressing", Concrete Society Technical Report, No. 23, May 1983.

4. Walker, P and Sinha, B.P., "Behaviour of Partially Prestressed Brickwork Beams", Seventh International Brick Masonry Conference, Melbourne, Australia, Feb. 1985.

5. Pedreschi, R.F. and Sinha, B.P., "Development and investigation of the ultimate load behaviour of post-tensioned brickwork beams", The Structural Engineer, Vol.60B, No. 3, 1982, pp 63-67.

6. BS 5628, Code of practice for use of masonry, Part 2, Structural use of reinforced and prestressed masonry, BSI, 1985.

Table 1 Summary of Beam Test Results

Beam No.	Strength N/mm^2		Effective Prestress kN	Moment kNm			$\frac{M_{ult}}{M_{th}}$	Moment at 0.2mm crack kNm	Deflection at 0.2mm crack (mm)
	Mortar	Grout		Cracking	Ult.Expt. M_{ult}	Theory M_{th}			
A1	15.8	17.8	133	26.1	52.9	54.3	0.97		
A2	15.8	17.8	115	23.7	56.4	54.3	1.04	29.0	7.1
A3	16.6	13.4	152	28.2	58.8	54.3	1.08		
B1	19.2	27.5	67	17.4	52.8	50.4	1.05		
B2	19.9	20.0	67	17.4	53.2	50.4	1.06	21.5	8.6
B3	16.4	26.1	61	16.7	54.6	50.4	1.09		
C1	19.9	20.3	36	13.9	56.6	54.9	1.03		
C2	20.1	25.2	35	13.7	55.3	54.9	1.01	16.5	9.0
C3	17.4	20.6	42	14.6	52.9	54.9	0.96		
D1	16.9	23.0	-	9.3	52.2	53.9	0.97		
D2	19.7	18.8	-	9.3	48.9	53.9	0.91	14.3	9.6
D3	21.8	17.5	-	9.3	51.3	53.9	0.95		

A1 to A3 - Fully Prestressed

B1 to B3 & C1 to C3 - Partially Prestressed

D1 to D3 - Reinforced

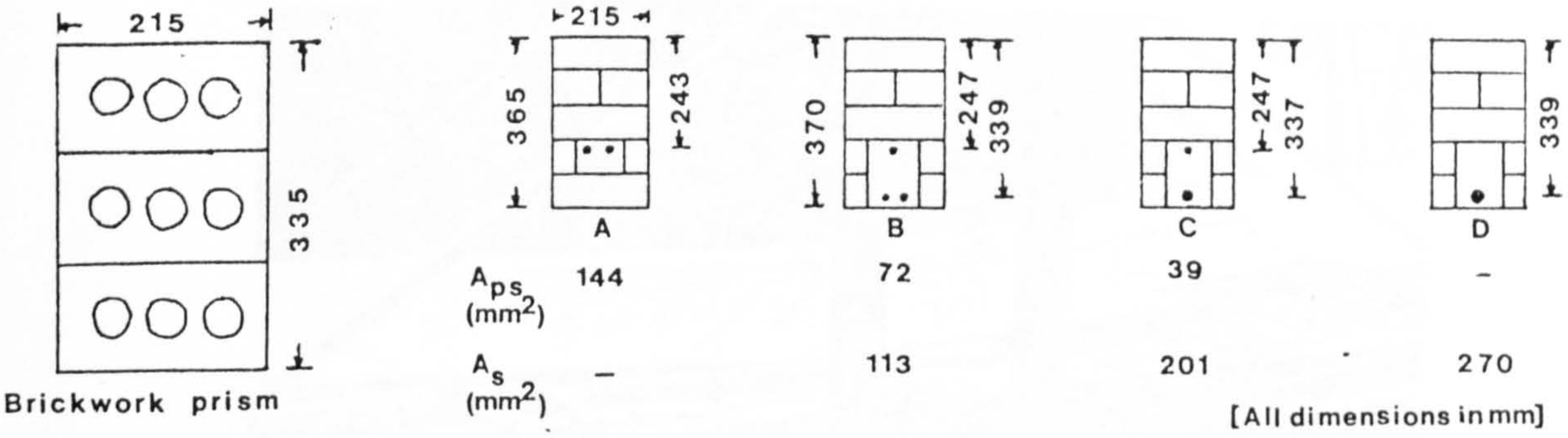

Fig.1 Brickwork Prism and Details of Beam Sections

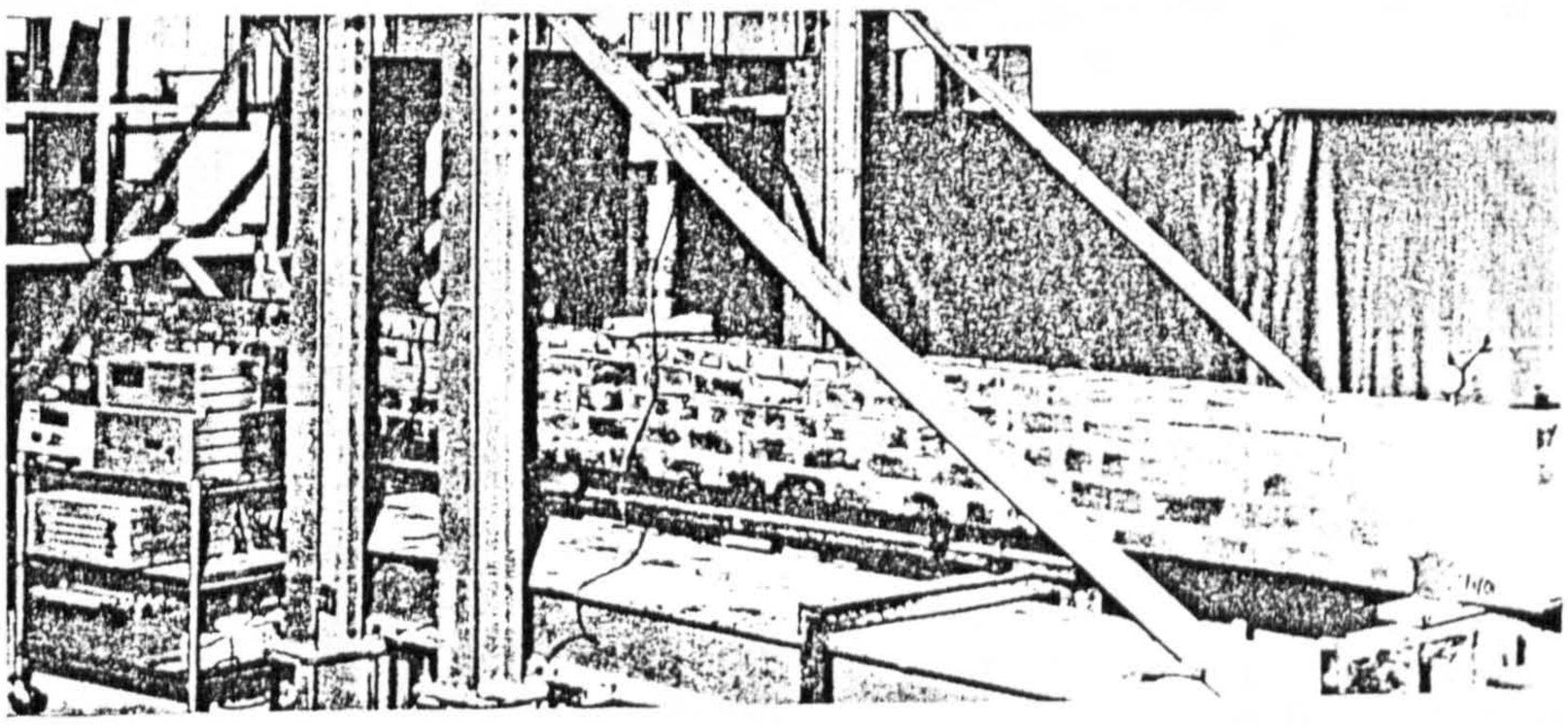

Fig.2 Test set-up

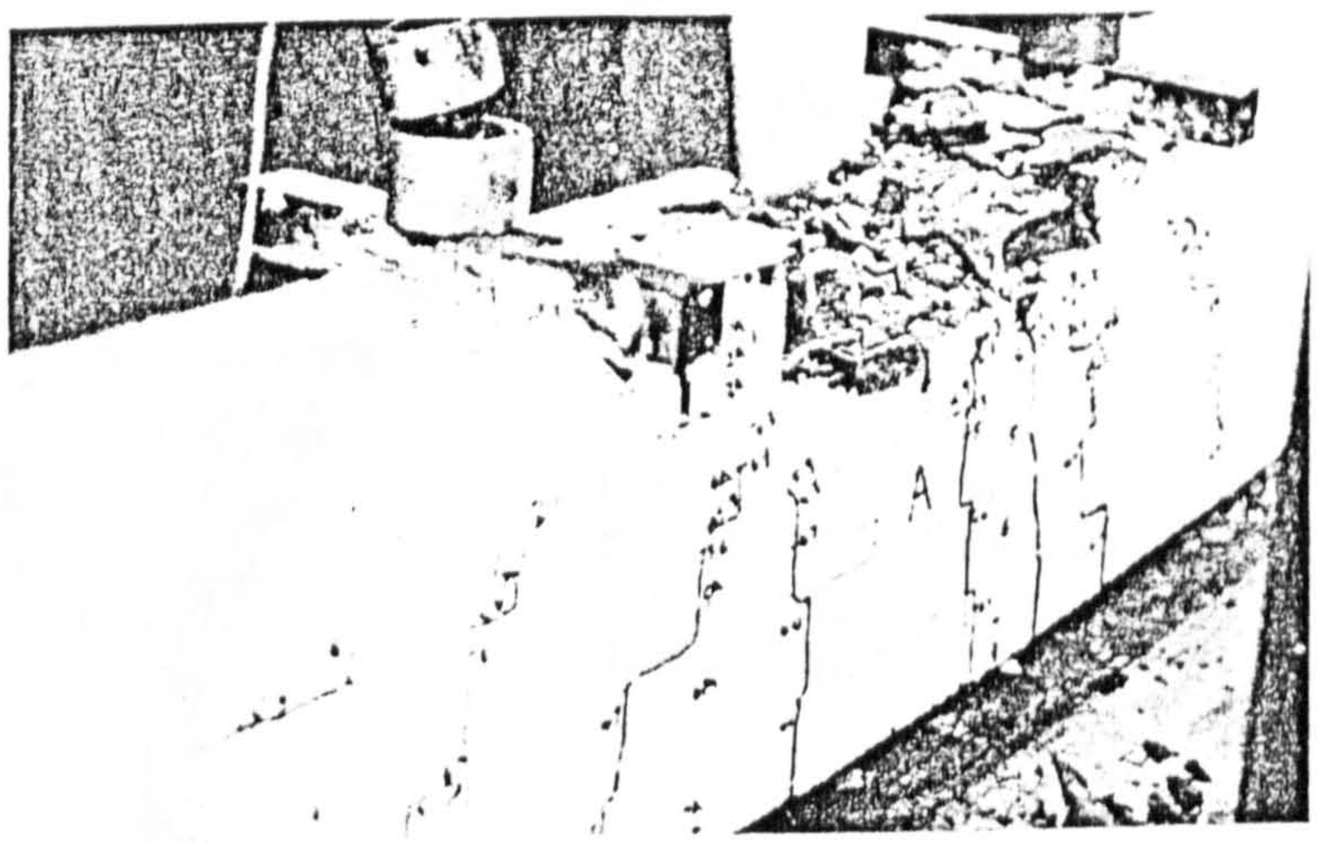

Fig.3 Typical Flexural failure of fully and partially prestressed brickwork beams

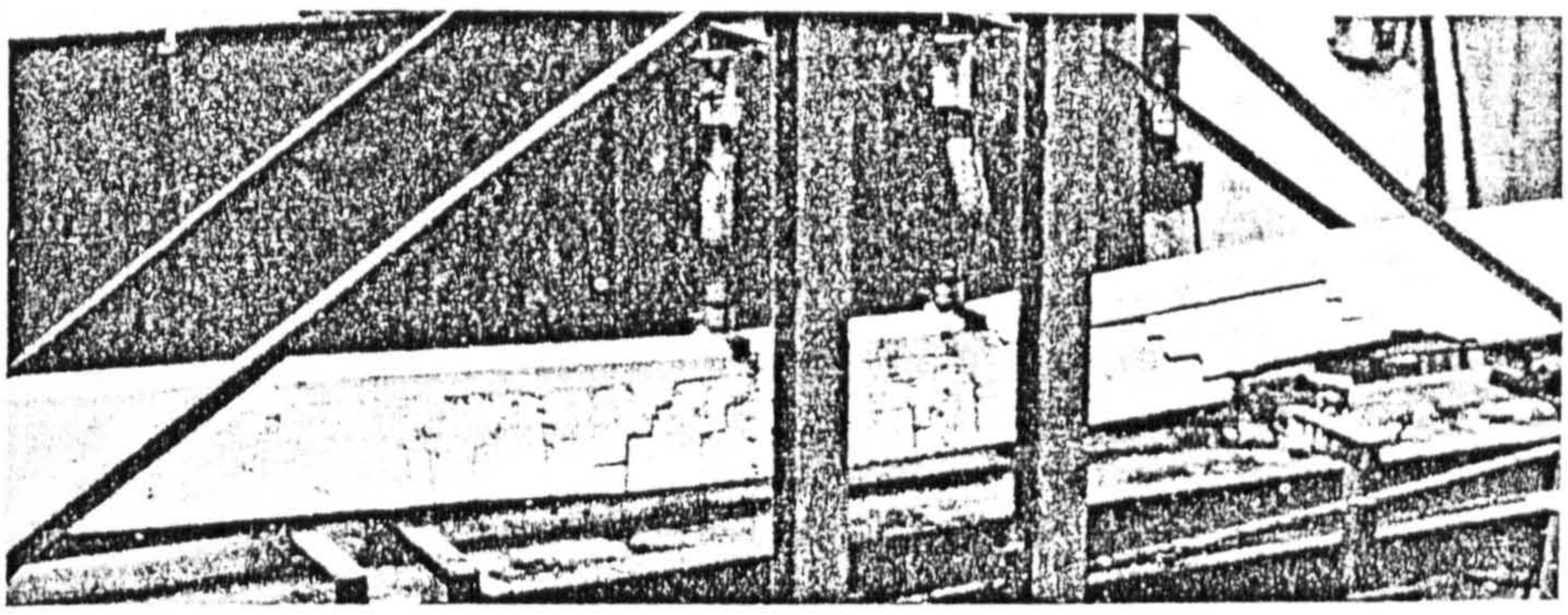

Fig.4 Typical secondary shear failure of reinforced brickwork beams

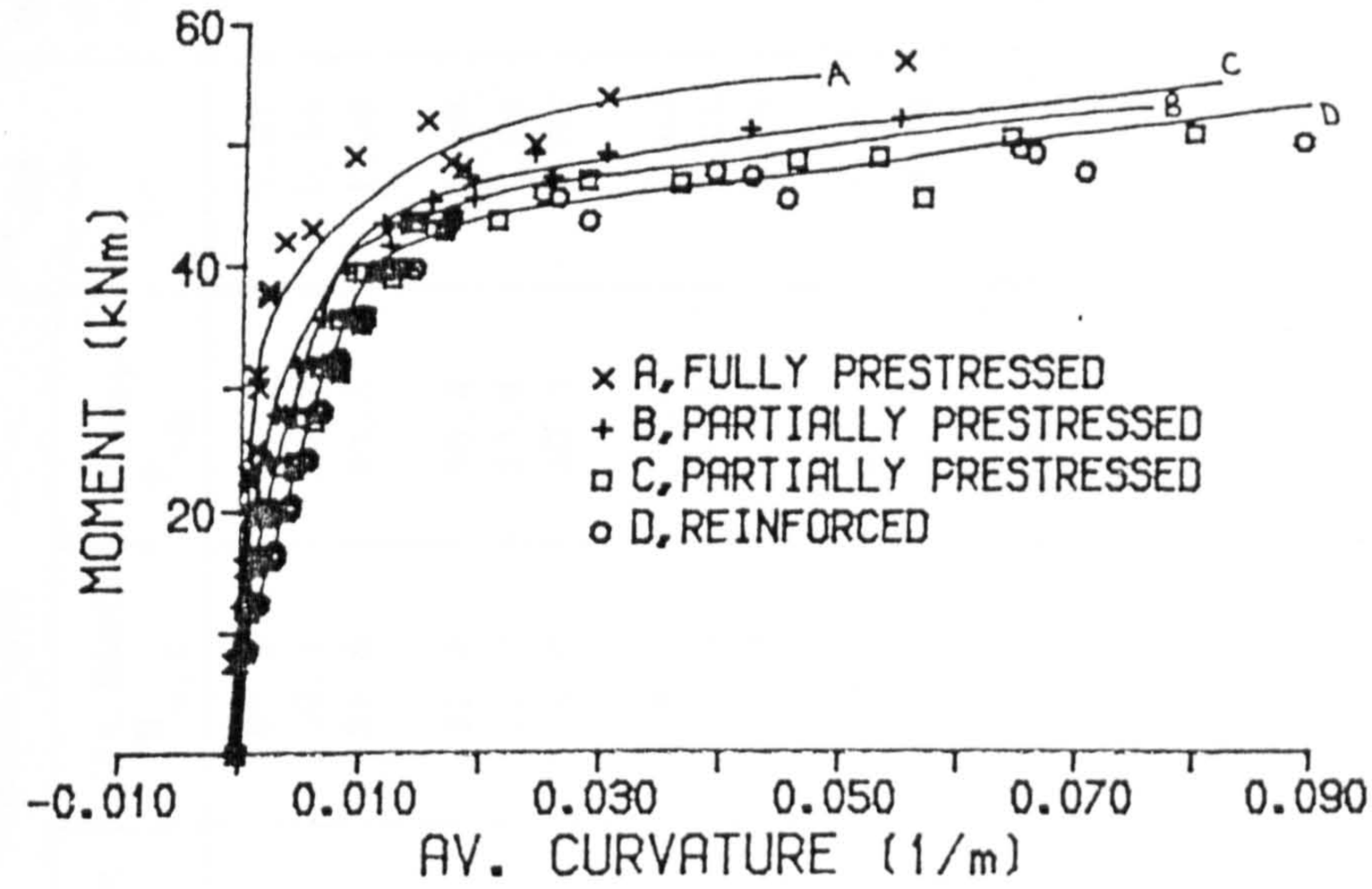

Fig.5 Moment-curvature relationships for test beams

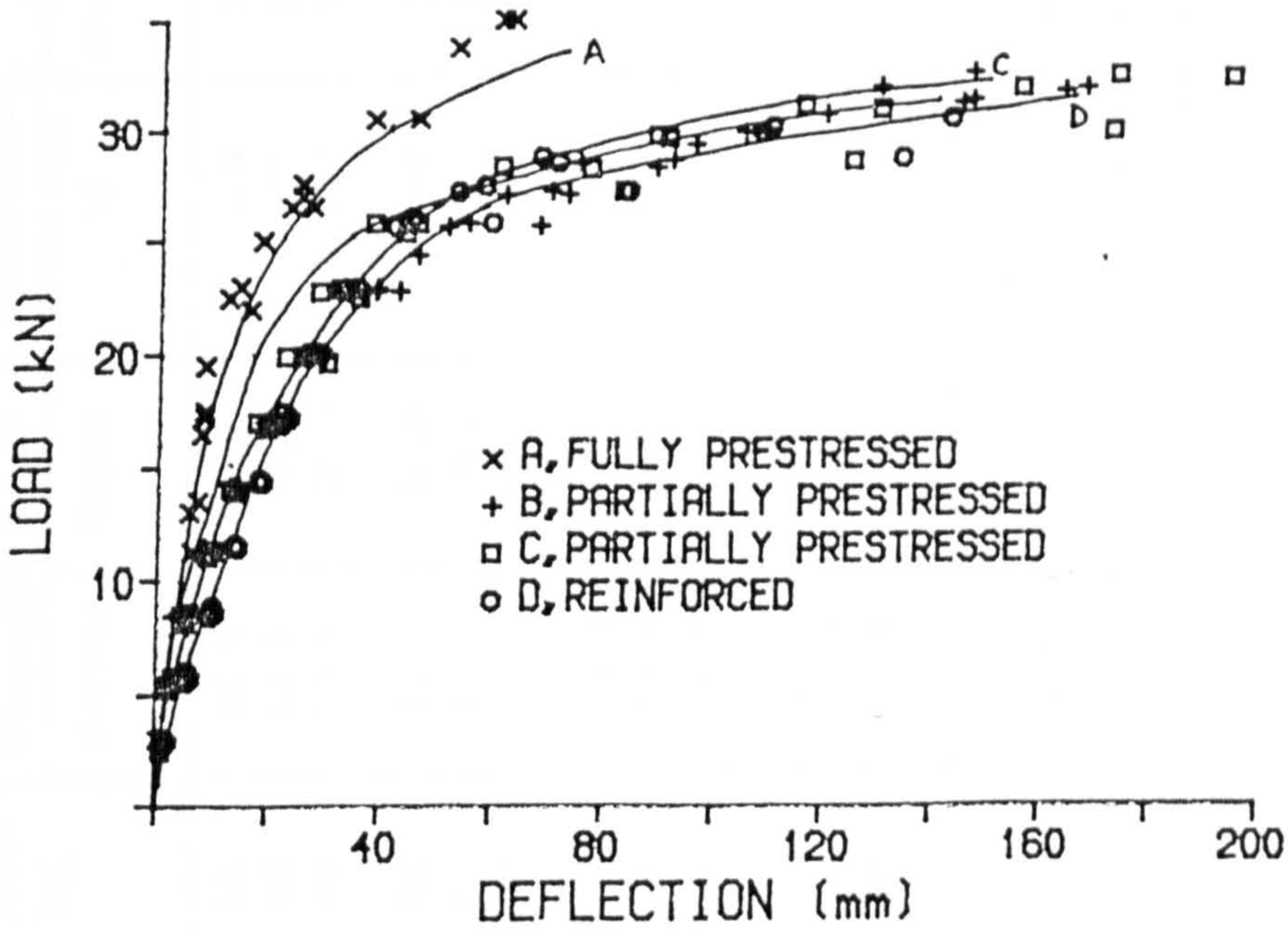

Fig.6 Load-deflection relationships for test beams

Table 1 Summary of Beam Test Results

Beam No.	Strength N/mm^2		Effective Prestress kN	Moment kNm			$\frac{M_{ult}}{M_{th}}$	Moment at 0.2mm crack kNm	Deflection at 0.2mm crack (mm)
	Mortar	Grout		Cracking	Ult. Expt. M_{ult}	Theory M_{th}			
A1	15.8	17.8	133	26.1	52.9	54.3	0.97		
A2	15.8	17.8	115	23.7	56.4	54.3	1.04	29.0	7.1
A3	16.6	13.4	152	28.2	58.8	54.3	1.08		
B1	19.2	27.5	67	17.4	52.8	50.4	1.05		
B2	19.9	20.0	67	17.4	53.2	50.4	1.06	21.5	8.6
B3	16.4	26.1	61	16.7	54.6	50.4	1.09		
C1	19.9	20.3	36	13.9	56.6	54.9	1.03		
C2	20.1	25.2	35	13.7	55.3	54.9	1.01	16.5	9.0
C3	17.4	20.6	42	14.6	52.9	54.9	0.96		
D1	16.9	23.0	-	9.3	52.2	53.9	0.97		
D2	19.7	18.8	-	9.3	48.9	53.9	0.91	14.3	9.6
D3	21.8	17.5	-	9.3	51.3	53.9	0.95		

A1 to A3 - Fully Prestressed

B1 to B3 & C1 to C3 - Partially Prestressed

D1 to D3 - Reinforced